



U.S. Department of Transportation  
Federal Highway Administration

Publication No. FHWA-NHI-15-004  
October 2014

## **NHI Course No. 130093 and 130093A**

---

# **LRFD Seismic Analysis and Design of Bridges Reference Manual**

### **Developed following:**

**AASHTO LRFD Bridge Design Specifications 6th Ed., 2013 Interim**

**AASHTO Guide Specifications for LRFD Seismic Bridge Design, 2nd Ed., 2014 interim**

**AASHTO Guide Specifications for Seismic Isolation Design, 2010**



NATIONAL HIGHWAY INSTITUTE

*Training Solutions for Transportation Excellence*



## **NOTICE**

The contents of this report reflect the views of the authors, who are responsible for the facts and accuracy of the data presented herein. The contents do not necessarily reflect policy of the Department of Transportation. This report does not constitute a standard, specification, or regulation. The United States Government does not endorse products or manufacturers. Trade or manufacturer's names appear herein only because they are considered essential to the object of this document.

**Technical Report Documentation Page**

1. Report No. FHWA NHI-15-004	2. Government Accession No.	3. Recipient's Catalog No.	
4. Title and Subtitle LRFD SEISMIC ANALYSIS AND DESIGN OF BRIDGES REFERENCE MANUAL NHI COURSE NO. 130093 AND 130093A		5. Report Date October 2014	
		6. Performing Organization Code	
7. Principal Investigator(s): See Acknowledgements for Authors and Contributors M. Lee Marsh <sup>1</sup> , PhD, P.E., Ian G. Buckle <sup>2</sup> , PhD, and Edward Kavazanjian, Jr. <sup>3</sup> , PhD, P.E.		8. Performing Organization Report No.	
9. Performing Organization Name and Address Parsons Brinckerhoff, Inc. One Penn Plaza, New York, NY 10119  <sup>1</sup> BergerABAM, Inc., Federal Way, WA 98003 <sup>2</sup> University of Nevada, Reno, NV 89557 <sup>3</sup> Arizona State University, Tempe, AZ 85287		10. Work Unit No. (TRAIS)	
		11. Contract or Grant No.  DTFH61-11-D-00047-T12001	
12. Sponsoring Agency Name and Address National Highway Institute U.S. Department of Transportation Federal Highway Administration, Washington, D.C. 20590		13. Type of Report and Period Covered	
		14. Sponsoring Agency Code	
15. Supplementary Notes  <i>FHWA COR: Louisa Ward</i> <i>FHWA Task Manager: Wen-huei (Phillip) Yen, PhD, PE</i> <i>FHWA Technical Reviewers: Wen-huei (Phillip) Yen, PhD, PE; Derrell Manceaux, PE; and Jamal Elkaissi, PE</i> <i>Contractor Project Manager: C. Jeremy Hung, PE</i> <i>This manual is an update of the original version prepared by Parsons Brinckerhoff, Inc. in 2011 with Co-Principal Investigators M. Lee Marsh, Ian G. Buckle, Roy A. Imbsen, and Edward Kavazanjian, Jr.</i>			
16. Abstract  This manual is intended to provide a technical resource for bridge engineers responsible for seismic analysis and design. It serves as a reference manual for use with the 5-day National Highway Institute (NHI) 130093 course "LRFD Seismic Analysis and Design of Bridges", and the 3-day 130093A course "Displacement-Based LRFD Seismic Analysis and Design of Bridges". The manual covers fundamental topics such as engineering seismology; seismic and geotechnical hazards; structural dynamics (SDOF and MDOF); and methods for modeling and analyzing bridges subject to earthquake ground motions. It also presents the principles of capacity design; applications of capacity design to piers, foundations, superstructures and connections; and discusses the requirements and recommendations of the seismic provision in each of the AASHTO LRFD Bridge Design Specifications and AASHTO Guide Specifications for LRFD Seismic Bridge Design, and their common features. Lastly, the manual addresses seismic isolation design in accordance with AASHTO Guide Specifications for Seismic Isolation Design, and retrofitting strategies in accordance with the 2006 FHWA Seismic Retrofitting Manual for Highway Structures.			
17. Key Words  Seismic design, analysis, bridges, earthquakes, structural dynamics, bridge modeling, force-based design, displacement-based design, capacity design, piers, foundations, superstructures, seismic isolation, seismic retrofit.		18. Distribution Statement  No restrictions.	
19. Security Classif. (of this report)	20. Security Classif. (of this page)	21. No. of Pages	22. Price
UNCLASSIFIED	UNCLASSIFIED	608	

## CONVERSION FACTORS

Approximate Conversions to SI Units			Approximate Conversions from SI Units		
When you know	Multiply by	To find	When you know	Multiply by	To find
(a) Length					
inch	25.4	millimeter	millimeter	0.039	inch
foot	0.305	meter	meter	3.28	foot
yard	0.914	meter	meter	1.09	yard
mile	1.61	kilometer	kilometer	0.621	mile
(b) Area					
square inches	645.2	square millimeters	square millimeters	0.0016	square inches
square feet	0.093	square meters	square meters	10.764	square feet
acres	0.405	hectares	hectares	2.47	acres
square miles	2.59	square kilometers	square kilometers	0.386	square miles
(c) Volume					
fluid ounces	29.57	milliliters	milliliters	0.034	fluid ounces
gallons	3.785	liters	liters	0.264	gallons
cubic feet	0.028	cubic meters	cubic meters	35.32	cubic feet
cubic yards	0.765	cubic meters	cubic meters	1.308	cubic yards
(d) Mass					
ounces	28.35	grams	grams	0.035	ounces
pounds	0.454	kilograms	kilograms	2.205	pounds
short tons (2000 lb)	0.907	megagrams (tonne)	megagrams (tonne)	1.102	short tons (2000 lb)
(e) Force					
pound	4.448	Newton	Newton	0.2248	pound
(f) Pressure, Stress, Modulus of Elasticity					
pounds per square foot	47.88	Pascals	Pascals	0.021	pounds per square foot
pounds per square inch	6.895	kiloPascals	kiloPascals	0.145	pounds per square inch
(g) Density					
pounds per cubic foot	16.019	kilograms per cubic meter	kilograms per cubic meter	0.0624	pounds per cubic foot
(h) Temperature					
Fahrenheit temperature(°F)	5/9(°F- 32)	Celsius temperature(°C)	Celsius temperature(°C)	9/5(°C)+ 32	Fahrenheit temperature(°F)

Notes: 1) The primary metric (SI) units used in civil engineering are meter (m), kilogram (kg), second(s), newton (N) and pascal (Pa=N/m<sup>2</sup>).

2) In a "soft" conversion, an English measurement is mathematically converted to its exact metric equivalent.

3) In a "hard" conversion, a new rounded metric number is created that is convenient to work with and remember.

## PREFACE

This reference manual is an update of the original version prepared by Parsons Brinckerhoff, Inc. in 2011 with Co-Principal Investigators M. Lee Marsh, Ian G. Buckle, Roy A. Imbsen, and Edward Kavazanjian, Jr. It presents the theory and practice of seismic analysis, design, and retrofit of highway bridges in ten chapters. It also provides the background and underlying concepts behind the recently adopted AASHTO LRFD Bridge Design Specifications (2013) and Seismic Guide Specification (2014 Interim) and explains in detail the seismic design provisions in these specifications. The manual is used in conjunction with National Highway Institute training courses 130093 “LRFD Seismic Analysis and Design of Bridges” and 130093A “Displacement Based LRFD Seismic Analysis and Design of Bridges”. Topics covered in each chapter are as follows:

Chapters 2 and 3 describe the characterization of seismic loads for use in design, first by defining the ground motion hazard in the U.S., including site amplification effects (Chapter 2), and then by discussing other geotechnical hazards such as soil liquefaction and fault rupture (Chapter 3).

Basic principles of seismic design are introduced in Chapter 4. These principles are fundamental to good design regardless of the code or specification selected for the design of a bridge. Chapter 5 presents methods for the calculation of seismic demands including both forces and displacements. Methods for modeling a bridge for use in these calculations, ranging from simple to complex, are also discussed.

Chapter 6 describes the inelastic behavior of bridges once they yield during strong shaking and explains how a plastic mechanism is established, thereby limiting internal forces. Chapter 7 then explains the design of those elements of the structure that are chosen to yield, to withstand the expected plastic deformations. This chapter also describes the protection of the remaining elements in the bridge against yielding or failure. In addition, both the Force-Based and Displacement-Based Methods are described. Chapter 8 outlines the seismic provisions of both the AASHTO *LRFD Bridge Design Specifications* (2013) and the AASHTO *Guide Specifications for LRFD Seismic Bridge Design* (2014) and explains in detail the implementation of capacity design as required by these specifications. To improve the readability of the text, these two specifications are cited in this Manual as the *LRFD Specifications* and *Guide Specifications* respectively

Chapter 9 provides an introduction to seismic isolation design, which corresponds to Global Strategy Type 3 in the *Guide Specifications*. The material in this chapter is consistent with the provisions in the AASHTO *Guide Specifications for Seismic Isolation Design* (20104). Finally, Chapter 10 gives an introduction to the seismic retrofitting of bridges. This material extends the application of capacity design principles to existing bridges, while recognizing that it is not always possible to fully apply these principles to such structures. This chapter summarizes the methodology and approach given in the FHWA *Seismic Retrofitting Manual for Highway Structures: Part 1-Bridges* (2006).

## ACKNOWLEDGMENTS

This Reference Manual is an update of the original version prepared by Parsons Brinckerhoff, Inc. in 2011 with Co-Principal Investigators M. Lee Marsh, Ian G. Buckle, Roy A. Imbsen, and Edward Kavazanjian, Jr. It provides the technical background for the National Highway Institute (NHI) Course 130093 titled *LRFD Seismic Analysis and Design of Bridges*, and 130093A titled *Displacement-Based LRFD Seismic Analysis and Design of Bridges* developed by the Parsons Brinckerhoff (PB) team.

This reference manual is updated by Lee Marsh, Ian Buckle, and Edward Kavazanjian, Jr. It addresses both force-based and displacement-based design methods, and discusses the requirements and recommendations of the seismic provisions in both the AASHTO *LRFD Bridge Design Specifications* (2013) and the AASHTO *Guide Specifications for LRFD Seismic Bridge Design* (2014). The manual also reviews the principles and practice of seismic isolation in accordance with the AASHTO *Guide Specifications for Isolation Design* (2010) and the FHWA/MCEER Special Publication on *Seismic Isolation of Highway Bridges* (Buckle et. al., 2006). Lastly, the manual presents a procedure for evaluating and upgrading the seismic resistance of existing highway bridges based on the FHWA *Seismic Retrofitting Manual for Highway Structures* (2006).

The Principal Investigators would like to especially acknowledge the continuing support of Louisa Ward, NHI Program Manager, Wen-huei (Phillip) Yen, FHWA Task Manger, and the reviews and recommendations provided by the following individuals for this update and the original 2011 version:

- Fadel Alameddine, Ph.D., P.E. Caltrans
- Leslie Daugherty, P.E. Alaska DOT
- Jerry A. DiMaggio, P.E. Jerry A. DiMaggio Consulting, LLC
- Jamal Elkaissi, PE FHWA
- Reggie Holt, P.E. FHWA
- Tim Huff, P.E. Tennessee DOT,
- Firas I. S. Ibrahim, Ph.D., P.E. FHWA
- Roy A. Imbsen, P.E., D. Engr. Imbsen Consulting
- Derrell Manceaux, P.E. FHWA
- Silas Nichols, P.E. FHWA
- Thomas K. Saad, P.E. FHWA
- Daniel H. Tobias, Ph.D., P.E. Illinois DOT,
- Jaw-Nan Joe Wang, Ph.D., P.E. Parsons Brinckerhoff

In addition, the Principal Investigators wish to extend their gratitude for the support provided by a number of professionals at Parsons Brinckerhoff, BergerABAM, and the University of Nevada, Reno. including Tessie Urtubia and Douglas Edwins at Parsons Brinckerhoff for their assistance.

## TABLE OF CONTENTS

<b>LIST OF FIGURES</b> .....	<b>x</b>
------------------------------	----------

<b>LIST OF TABLES</b> .....	<b>xvi</b>
-----------------------------	------------

<b>CHAPTER 1 - INTRODUCTION</b> .....	<b>1-1</b>
---------------------------------------	------------

1.1	GENERAL .....	1-1
1.2	BRIDGE PERFORMANCE IN RECENT EARTHQUAKES AND DEVELOPMENT OF AASHTO SPECIFICATIONS.....	1-3
1.3	SEISMIC DESIGN PHILOSOPHY .....	1-11
1.4	ROAD MAP FOR SEISMIC DESIGN .....	1-14
1.5	CAPACITY DESIGN PRINCIPLES .....	1-15
1.5.1	Demand vs. Capacity.....	1-16
1.5.2	Capacity-Protected Design .....	1-17
1.5.3	Design Methodologies.....	1-18
1.5.3.1	Force-Based Method .....	1-19
1.5.3.2	Displacement -Based Method .....	1-20
1.6	SCOPE OF MANUAL .....	1-21

<b>CHAPTER 2 – GROUND MOTION HAZARDS</b> .....	<b>2-1</b>
--	------------

2.1	GENERAL .....	2-1
2.2	SEISMIC HAZARD ANALYSIS .....	2-3
2.2.1	Seismic Source Identification.....	2-3
2.2.2	Magnitude-Recurrence Relationships.....	2-4
2.2.3	Ground Motion Prediction Relationships .....	2-7
2.2.4	Uniform Hazard Spectra.....	2-10
2.2.5	De-aggregation of Design Earthquake, Magnitude and Distance.....	2-14
2.2.6	Probabilistic versus Deterministic Analysis Methods .....	2-16
2.3	HAZARD LEVELS AND RETURN PERIODS .....	2-19
2.3.1	Selection of Return Period.....	2-19
2.4	CHARACTERIZATION OF HORIZONTAL GROUND MOTIONS .....	2-24
2.4.1	Acceleration Response Spectra vs Displacement Spectra .....	2-24
2.4.2	Near-Fault (Near-Field) Effects.....	2-24
2.4.3	Local Site Effects .....	2-25
2.5	USE OF AASHTO/USGS DESIGN HAZARD MAPS .....	2-27
2.5.1	Deviation of AASHTO Seismic Coefficient Spectra .....	2-29
2.5.2	Site Class Definitions .....	2-29
2.5.3	Site Factors.....	2-30
2.6	SITE-SPECIFIC RESPONSE SPECTRA FOR HORIZONTAL GROUND MOTIONS .....	2-41
2.7	VERTICAL GROUND MOTION RESPONSE SPECTRA .....	2-43
2.8	ACCELERATION TIME HISTORIES .....	2-44
2.9	SPATIAL VARIABILITY OF GROUND MOTIONS.....	2-46

2.10	SUMMARY .....	2-49
<b>CHAPTER 3 – GEOTECHNICAL HAZARDS .....</b>		<b>3-1</b>
3.1	GENERAL .....	3-1
3.2	SOIL LIQUEFACTION HAZARD .....	3-1
3.2.1	Hazard Description and Initial Screening.....	3-1
3.2.2	Liquefaction Design Requirements .....	3-5
3.2.3	Earthquake Ground Motions Parameters for Liquefaction Analysis .....	3-5
3.2.4	Procedures for Liquefaction Evaluation .....	3-7
3.3	LIQUEFACTION INDUCED GROUND DEFORMATIONS.....	3-18
3.3.1	Post Liquefaction Shear Strength .....	3-18
3.3.2	Flow Failures.....	3-19
3.3.3	Lateral Spreading Displacement Evaluations.....	3-21
3.4	LIQUEFACTION IMPACTS ON DEEP FOUNDATIONS .....	3-25
3.4.1	Liquefaction Impacts on Vertical and Lateral Resistance .....	3-25
3.4.2	Liquefaction Impacts on Vertical and Lateral Loads.....	3-26
3.5	SOIL SETTLEMENT HAZARD.....	3-27
3.5.1	Hazard Description and Initial Screening.....	3-27
3.5.2	Procedure for Settlement Evaluation of Unsaturated Cohesionless Soils.....	3-28
3.5.3	Procedure for Post-Earthquake Settlement of Liquefied Soils .....	3-33
3.6	SEISMIC SLOPE INSTABILITY HAZARD .....	3-34
3.6.1	Hazard Description and Initial Screening.....	3-35
3.6.2	Slope Instability and Displacement Estimates.....	3-35
3.7	SURFACE FAULT RUPTURE HAZARD .....	3-37
3.7.1	Hazard Description and Initial Screening.....	3-37
3.7.2	Fault Rupture Characteristics and Displacement Estimates .....	3-41
3.8	SUMMARY .....	3-43
<b>CHAPTER 4 – PRINCIPLES OF SEISMIC DESIGN .....</b>		<b>4-1</b>
4.1	GENERAL .....	4-1
4.2	STRUCTURAL FORM.....	4-4
4.2.1	Basic Requirements.....	4-4
4.2.2	Load Paths .....	4-6
4.2.2.1	Dynamic Equilibrium.....	4-7
4.2.2.2	Lateral Load Paths in Bridges .....	4-11
4.2.3	Simplicity, Integrity, and Symmetry .....	4-17
4.2.3.1	Balanced Stiffness and Frame Geometry .....	4-17
4.2.3.2	Skew and Curvature .....	4-19
4.2.3.3	Articulation, Restrainers, and Support Length .....	4-20
4.2.3.4	Summary .....	4-21
4.2.4	Acceptable and Unacceptable Structural Form .....	4-21
4.3	EARTHQUAKE RESISTING SYSTEMS AND GLOBAL DESIGN STRATEGIES .....	4-28
4.3.1	Earthquake Resisting Systems.....	4-28
4.3.2	Global Design Strategies.....	4-29
4.3.3	Essentially Elastic Substructure with Elastic Superstructure.....	4-30
4.3.4	Ductile Substructure with Essentially Elastic Superstructure.....	4-31
4.3.5	Essentially Elastic Substructure with Ductile Superstructure.....	4-31

4.3.6	Elastic Superstructure and Elastic Substructure with Fusing Interface .....	4-33
4.4	SUMMARY .....	4-34
<b>CHAPTER 5 – DEMAND ANALYSIS.....</b>		<b>5-1</b>
5.1	GENERAL .....	5-1
5.1.1	Bridge Structural Dynamics .....	5-2
5.1.1.1	Single-Degree-of-Freedom Behavior .....	5-2
5.1.1.2	Multi-Degree-of-Freedom Behavior .....	5-5
5.1.2	Elastic and Nonlinear Behavior .....	5-13
5.1.3	Summary and Limitations of Analysis Methods .....	5-14
5.2	ELASTIC ANALYSIS METHODS.....	5-14
5.2.1	General .....	5-14
5.2.2	Uniform Load Method.....	5-14
5.2.3	Single-Mode Spectral Analysis Method.....	5-19
5.2.4	Multi-Mode Spectral Analysis Method .....	5-23
5.2.5	Time History Method .....	5-28
5.2.5.1	Newmark’s Procedure for Time History Solutions of Linear Single Degree-of-Freedom Systems.....	5-28
5.2.5.2	Newmark’s Procedure for Time History Solutions of Linear Multi-Degree-of-Freedom Systems.....	5-29
5.3	NONLINEAR ANALYSIS METHODS.....	5-30
5.3.1	Nonlinear Static Methods.....	5-30
5.3.1.1	Structure Capacity/Demand (Pushover) Method.....	5-31
5.3.1.1.1	Approach.....	5-31
5.3.1.1.2	Displacement Capacity Evaluation .....	5-31
5.3.1.1.3	Demands .....	5-32
5.3.1.1.4	Procedure .....	5-32
5.3.1.1.5	Restrictions .....	5-34
5.3.1.2	Capacity / Demand Spectrum Method .....	5-34
5.3.1.2.1	Modified Acceleration Response Spectrum.....	5-34
5.3.1.2.2	Capacity / Demand Spectrum.....	5-36
5.3.1.2.3	Calculation of Bridge Response.....	5-37
5.3.2	Nonlinear Dynamic Methods .....	5-38
5.3.2.1	Basic Step-by-Step Numerical Integration Procedure (Newmark’s Procedure).....	5-39
5.3.2.2	Fast Nonlinear Analysis Procedure (Wilson’s Approach).....	5-39
5.4	ANALYSIS METHODS FOR IMPOSED SUPPORT DISPLACEMENTS.....	5-41
5.4.1	Elastic Method for Multiple Support Excitation .....	5-41
5.4.2	Elastic Method for Statically Imposed Support Displacements .....	5-44
5.5	ANALYSIS METHODS FOR SOIL-FOUNDATION-STRUCTURE INTERACTION .....	5-45
5.5.1	General .....	5-45
5.5.2	Shallow Footings.....	5-46
5.5.3	Piles .....	5-46
5.6	MODELING RECOMMENDATIONS FOR BRIDGE STRUCTURES .....	5-48
5.6.1	General .....	5-48
5.6.2	Distribution of Mass.....	5-50
5.6.3	Distribution of Stiffness and Modeling of Structural Members and Connections.....	5-51
5.6.4	Distribution of Stiffness and Modeling of Substructures and Abutments .....	5-51
5.6.5	Modeling of In-span hinges and Expansion Joints .....	5-53
5.6.6	Modeling of Bridge Superstructures, Skew and Curved Geometry .....	5-54
5.6.7	Modeling of Bridges with Imposed Support Displacements .....	5-54
5.6.8	Modeling of Bridges with Partially Submerged Members .....	5-55

5.6.9	Representation of Damping .....	5-55
5.7	SUMMARY .....	5-56
<b>CHAPTER 6 – BEHAVIOR OF INELASTIC BRIDGES.....</b>		<b>6-1</b>
6.1	GENERAL .....	6-1
6.2	MEASURED BEHAVIOR OF INELASTIC RESPONSE.....	6-2
6.2.1	General .....	6-2
6.2.2	Circular and Rectangular Tied Reinforced Concrete Columns .....	6-3
6.2.3	Columns with Interlocking Hoops or Spirals .....	6-12
6.2.4	Flared Columns .....	6-15
6.2.5	Pier Walls .....	6-19
6.2.6	Shear Keys.....	6-22
6.3	METHODS OF ESTIMATING BRIDGE RESPONSE USING ELASTIC ANALYSIS .....	6-25
6.3.1	Estimating Inelastic Response Using Elastic Analysis.....	6-25
6.3.2	Estimation of Response Between Adjacent Frames .....	6-29
6.4	CALCULATION OF INELASTIC RESPONSE .....	6-31
6.4.1	General .....	6-31
6.4.2	Nominal and Expected Strength .....	6-31
6.4.3	Overstrength.....	6-34
6.4.4	Cross-Sectional Analysis.....	6-35
6.4.5	Material Requirements and Properties .....	6-39
6.4.5.1	Reinforcing Steel.....	6-39
6.4.5.2	Prestressing Steel.....	6-41
6.4.5.3	Concrete .....	6-43
6.4.5.4	Structural Steel .....	6-46
6.4.5.5	Welding Requirements for Structural Steel.....	6-47
6.4.6	System Strength and Deformation.....	6-47
6.4.6.1	Determination of System Strength .....	6-47
6.4.6.2	Determination and Assessment of System Deformation Capacity .....	6-49
6.4.6.3	Deformation Capacity of Reinforced Concrete Members .....	6-49
6.5	SYSTEM DEFORMATION CAPACITY OF STEEL SUBSTRUCTURES .....	6-60
6.5.1	General .....	6-60
6.5.2	Local Buckling .....	6-62
6.5.3	Over-all Member Buckling.....	6-65
6.5.4	Connections.....	6-65
6.6	ESTIMATION OF INELASTIC RESPONSE .....	6-67
6.6.1	Damage of Bridge Columns .....	6-67
6.6.2	Performance of Bridge Columns .....	6-68
6.7	SUMMARY .....	6-75
<b>CHAPTER 7 – SEISMIC DESIGN METHODS .....</b>		<b>7-1</b>
7.1	GENERAL .....	7-1
7.1.1	Methods of Linearization for Design.....	7-3
7.1.2	Seismic Load Combinations.....	7-6
7.2	FORCE-BASED DESIGN METHOD .....	7-8
7.3	DISPLACEMENT-BASED DESIGN METHOD.....	7-12
7.4	COMPARISON OF THE TWO DESIGN METHODS .....	7-15

7.5	CAPACITY DESIGN OF PIERS.....	7-16
7.5.1	Member Actions for Single- and Multi-Column Piers Using Capacity Design Principles.....	7-16
7.5.2	Capacity Protection of Reinforced Concrete Columns.....	7-18
7.5.3	Capacity Protection of Steel Columns and Moment-Resisting Steel Frames.....	7-24
7.5.4	Capacity Protection of Cap Beams.....	7-25
7.5.5	Flexural Design and Capacity Protection of Reinforced Concrete Wall Piers.....	7-26
7.5.6	Capacity Protection of Beam-Column Joints.....	7-27
7.6	CAPACITY DESIGN OF FOUNDATIONS AND ABUTMENTS.....	7-30
7.6.1	Member Actions in Foundations and Abutments Using Capacity Design Principles.....	7-31
7.6.1.1	Overstrength Plastic Mechanism Forces.....	7-31
7.6.1.2	Elastic Analysis and Load Combinations.....	7-32
7.6.1.3	Effect of Structural Form and Earthquake Resisting Elements (EREs) on the Desired Behavior.....	7-33
7.6.1.4	Fusing Elements.....	7-33
7.6.2	Capacity Protection of Foundations.....	7-34
7.6.2.1	Resistance Components.....	7-35
7.6.2.2	Developing Foundation Free-Body Diagrams (FBDs).....	7-36
7.6.2.3	Failure Modes / Structural.....	7-38
7.6.2.4	Soil Deformations and Reconciliation with Modeling.....	7-42
7.6.2.5	Other Load Interaction Effects.....	7-43
7.6.3	Capacity Protection of Abutments.....	7-44
7.6.3.1	Use of Abutments in Analytical Demand Model.....	7-44
7.6.3.2	Developing Abutment Free Body Diagrams.....	7-46
7.6.3.3	Failure Modes / Structural.....	7-47
7.6.3.4	Soil Deformations and Reconciliation with Modeling.....	7-48
7.6.4	Exceptions to Capacity-Protected Design of Foundations and Abutments.....	7-48
7.6.4.1	Definition of Exceptions.....	7-49
7.6.4.2	Developing Design Forces and Design Criteria.....	7-49
7.6.5	Liquefaction Design Requirements with Softened/Weakened Ground.....	7-50
7.6.5.1	Soil Resistance Becomes the Load.....	7-51
7.7	CAPACITY DESIGN OF SUPERSTRUCTURES AND CONNECTIONS.....	7-53
7.7.1	Capacity Protection of Superstructures.....	7-56
7.7.1.1	Developing Free-Body Diagrams (FBDs) for Forces at Piers.....	7-56
7.7.1.2	Developing Free-Body Diagrams (FBDs) for Forces in Superstructure as a Whole.....	7-59
7.7.2	Design of Ductile End Diaphragms.....	7-60
7.7.3	Capacity Protection of Bearings, Restrainers and Shear Keys.....	7-61
7.8	DISPLACEMENT CAPACITY OF BRIDGE STRUCTURES.....	7-62
7.8.1	Minimum Support Lengths.....	7-63
7.8.2	P-Δ Effects.....	7-64
7.9	SUMMARY.....	7-67

**CHAPTER 8 – AASHTO SEISMIC DESIGN SPECIFICATIONS.....8-1**

8.1	GENERAL.....	8-1
8.2	COMMON FEATURES OF AASHTO LRFD AND GUIDE SPECIFICATIONS.....	8-6
8.2.1	Determine Seismic Input.....	8-6
8.2.2	Establish Design Procedures.....	8-7
8.2.2.1	Performance (Seismic Zones and Seismic Design Categories).....	8-8
8.2.3	Identify the Earthquake Resisting System and Global Design Strategy.....	8-9
8.2.4	Demand Analysis.....	8-9
8.2.4.1	Loading.....	8-10
8.2.4.2	Directional Combinations.....	8-12

8.2.4.3	Analytical Model Appropriate for the Selected Design Strategy .....	8-13
8.2.4.4	Demand Analysis .....	8-14
8.2.4.4.1	Equivalent Static Analysis .....	8-14
8.2.4.4.2	Elastic Dynamic Analysis .....	8-15
8.2.5	Design and Check the Earthquake Resisting Elements .....	8-15
8.2.5.1	Support Lengths .....	8-16
8.2.5.2	Minimum Force and Displacement Design for Single-Span .....	8-19
8.2.5.3	Bridges in Seismic Zone 1 and SDC A .....	8-20
8.2.6	Liquefaction .....	8-22
8.2.7	Capacity Protection .....	8-22
8.2.7.1	Overstrength Forces .....	8-22
8.2.8	Capacity Protected Elements .....	8-24
8.2.8.1	Columns and Piers.....	8-25
8.2.8.2	Superstructures.....	8-25
8.2.8.3	Foundations .....	8-26
8.3	<b>AASHTO LRFD SPECIFICATIONS .....</b>	<b>8-26</b>
8.3.1	Determine Seismic Input .....	8-27
8.3.2	Establish Design Procedures .....	8-27
8.3.3	Identify the Earthquake Resisting System and Global Design Strategy .....	8-27
8.3.4	Demand Analysis .....	8-27
8.3.5	Design and Check the Earthquake Resisting Elements .....	8-28
8.3.6	Design Procedures Using Response Modification Factors.....	8-28
8.3.7	Bridges in Seismic Zone 2.....	8-28
8.3.7.1	Bridges in Seismic Zones 3 and 4 .....	8-31
8.3.7.2	Show Forces and Displacements of Overall System Acceptable .....	8-34
8.3.8	Capacity Protection of the Remaining Elements .....	8-37
8.3.8.1	Strength .....	8-37
8.3.8.2	Overstrength Forces .....	8-39
8.3.8.3	Wall Pier Design Forces.....	8-41
8.3.8.4	Foundation Design Forces.....	8-41
8.4	<b>AASHTO LRFD GUIDE SPECIFICATIONS.....</b>	<b>8-42</b>
8.4.1	Determine Seismic Input .....	8-43
8.4.2	Establish Design Procedures .....	8-44
8.4.3	Identify the Earthquake Resisting System and Global Design Strategy .....	8-44
8.4.3.1	Seismic Design Categories.....	8-44
8.4.3.1.1	Partitioning.....	8-45
8.4.3.2	Earthquake Resisting Elements and Systems .....	8-45
8.4.4	Demand Analysis .....	8-46
8.4.4.1	Model of Selected Design Strategy .....	8-46
8.4.5	Design and Check the Earthquake Resisting Elements .....	8-48
8.4.5.1	Show Forces and Displacements of Overall System Acceptable .....	8-48
8.4.5.2	General Design Requirements.....	8-51
8.4.5.3	P- $\Delta$ Capacity Requirement for SDC C and D.....	8-54
8.4.6	Capacity Protection of the Remaining Elements .....	8-57
8.4.6.1	Overstrength Forces .....	8-57
8.4.6.2	Capacity Protection Force Requirements for SDC B, C and D.....	8-58
8.4.6.3	Force Design of Steel Components .....	8-58
8.4.6.4	Ductile Moment Resisting Frames and Single Column Steel Structures for SDC C and D...	8-59
8.4.6.5	Concrete Filled Steel Pipe Substructure for SDC C and D .....	8-60
8.5	<b>SUMMARY .....</b>	<b>8-60</b>
<b>CHAPTER 9 – SEISMIC ISOLATION .....</b>		<b>9-1</b>

9.1	GENERAL .....	9-1
9.1.1	Basic Principles .....	9-1
9.1.1.1	Flexibility .....	9-2
9.1.1.2	Energy Dissipation .....	9-3
9.1.1.3	Rigidity Under Service Loads .....	9-5
9.1.2	Seismic Isolators.....	9-5
9.1.3	Bridge and Site Suitability.....	9-8
9.1.3.1	Superstructure Weight.....	9-8
9.1.3.2	Soft Soil Sites.....	9-8
9.1.3.3	Flexible Substructures .....	9-9
9.2	APPLICATIONS.....	9-10
9.2.1	Early Applications.....	9-10
9.2.1.1	South Rangitikei River Rail Bridge.....	9-10
9.2.1.2	Sierra Point Overhead .....	9-11
9.2.2	Recent Applications .....	9-12
9.2.3	Performance of Isolated Bridges in Recent Earthquakes.....	9-18
9.3	ANALYSIS .....	9-18
9.3.1	Simplified Method.....	9-19
9.3.1.1	Assumptions .....	9-19
9.3.1.2	Basic Equations for Bridges with Stiff Substructures .....	9-20
9.3.1.2.1	Effective Stiffness .....	9-20
9.3.1.2.2	Effective Period.....	9-20
9.3.1.2.3	Equivalent Viscous Damping Ratio .....	9-20
9.3.1.2.4	Superstructure Displacement .....	9-21
9.3.1.2.5	Total Base Shear and individual Isolator Forces.....	9-22
9.3.1.3	Procedure for Bridges with Stiff Substructures.....	9-22
9.3.1.4	Basic Equations for Bridges with Flexible Substructures .....	9-23
9.3.1.4.1	Effective Stiffness of Bridge with Flexible Substructures .....	9-23
9.3.1.4.2	Substructure and Isolator Forces.....	9-24
9.3.1.5	Procedure for Bridges with Flexible Substructures.....	9-25
9.3.2	Single and Multimode Spectral Analysis Methods .....	9-26
9.3.3	Time History Method .....	9-27
9.4	DESIGN .....	9-28
9.4.1	Design of Isolated Bridge Substructures and Foundations.....	9-28
9.4.2	Design Properties of Isolation Systems .....	9-28
9.4.2.1	Minima and Maxima .....	9-28
9.4.2.2	System Property Modification Factors ( $\lambda$ -factors).....	9-29
9.4.2.3	System Property Adjustment Factors .....	9-30
9.4.3	Minimum Restoring Force Capability.....	9-30
9.4.4	Uplift, Restrainers and Tensile Capacity.....	9-32
9.4.5	Clearances .....	9-32
9.4.6	Vertical Load Stability .....	9-33
9.4.7	Non-Seismic Requirements .....	9-33
9.5	ELASTOMERIC ISOLATORS .....	9-33
9.5.1	Lead Rubber Isolators .....	9-34
9.5.1.1	Mechanical Characteristics of Lead-Rubber Isolators.....	9-35
9.5.1.2	Strain Limits in Rubber .....	9-38
9.5.1.2.1	Compressive Strains.....	9-38
9.5.1.2.2	Shear Strains .....	9-38
9.5.1.3	Stability of Lead-Rubber Isolators .....	9-39
9.5.1.3.1	Stability in Undeformed State.....	9-39
9.5.1.3.2	Stability in Deformed State.....	9-40
9.5.1.4	Stiffness Properties of Lead-Rubber Isolators.....	9-42

9.5.2	Properties of Natural Rubber.....	9-43
9.5.2.1	Elastic Modulus, $E$ .....	9-43
9.5.2.2	Bulk Modulus, $\kappa$ .....	9-44
9.5.2.3	Shear Modulus, $G$ .....	9-44
9.5.2.4	Hardness.....	9-44
9.5.2.5	Ultimate Strength and Elongation-at-Break.....	9-45
9.5.2.6	Fillers.....	9-45
9.5.2.7	Hysteresis.....	9-46
9.5.2.8	Temperature Effects.....	9-46
9.5.2.9	Oxygen, Sunlight and Ozone.....	9-47
9.5.2.10	Chemical Degradation.....	9-47
9.5.3	Properties of Lead.....	9-47
9.5.4	Effects of Variability of Properties, Aging, Temperature and Load History.....	9-48
9.5.4.1	Variability of Properties.....	9-48
9.5.4.2	Aging.....	9-48
9.5.4.3	Temperature.....	9-49
9.5.4.3.1	Heating During Cyclic Movement.....	9-50
9.5.4.3.2	Effect of Ambient Temperature.....	9-50
9.5.4.4	Loading History.....	9-52
9.5.5	System Property Modification Factors for Elastomeric Isolators.....	9-54
9.6	SLIDING ISOLATORS.....	9-56
9.6.1	Concave Friction Isolators.....	9-60
9.6.1.1	Mechanical Characteristics of Concave Friction Isolators.....	9-61
9.6.1.1.1	Formulation of Isolator Behavior.....	9-62
9.6.2	Eradquake Isolators.....	9-64
9.6.2.1	Mechanical Characteristics of Eradquake Isolators.....	9-64
9.6.2.1.1	Formulation of Bearing Behavior.....	9-65
9.6.3	Design of Sliding Isolators.....	9-66
9.6.4	Frictional Properties of Sliding Isolators.....	9-68
9.6.5	Effects of Variability of Properties, Aging, Temperature, and Load History.....	9-71
9.6.5.1	Variability of Properties.....	9-72
9.6.5.2	Aging.....	9-72
9.6.5.3	Temperature.....	9-74
9.6.5.3.1	Heating During Cyclic Movement.....	9-74
9.6.5.3.2	Effect of Ambient Temperature.....	9-74
9.6.5.4	Loading History.....	9-76
9.6.6	System Property Modification Factors for Sliding Isolators.....	9-76
9.7	EXAMPLES.....	9-78
9.8	TESTING ISOLATION HARDWARE.....	9-86
9.9	SUMMARY.....	9-87
<b>CHAPTER 10</b>	<b>.....</b>	<b>10-1</b>
10.1	GENERAL.....	10-1
10.2	BACKGROUND.....	10-2
10.3	PHILOSOPHY.....	10-6
10.4	SEISMIC PERFORMANCE CRITERIA.....	10-8
10.4.1	Performance Levels.....	10-8
10.4.2	Earthquake Ground Motion Levels.....	10-10
10.4.3	Bridge Importance.....	10-10
10.4.4	Anticipated Service Life.....	10-11

10.4.5	Selection of Performance Level .....	10-13
10.4.6	Retrofitting Process for Dual Level Ground Motions .....	10-13
10.4.7	Exempt Bridges .....	10-15
10.5	SEISMIC HAZARD LEVELS .....	10-15
10.6	PERFORMANCE-BASED SEISMIC RETROFIT CATEGORIES.....	10-17
10.7	RETROFITTING PROCESS FOR LOWER LEVEL GROUND MOTION.....	10-20
10.7.1	Screening and Prioritization for the Lower Level Ground Motion.....	10-21
10.7.2	Evaluation for the Lower Level Ground Motion.....	10-23
10.7.3	Retrofitting for the Lower level Ground Motion.....	10-24
10.8	RETROFITTING PROCESS FOR UPPER LEVEL GROUND MOTION .....	10-24
10.9	MINIMUM REQUIREMENTS FOR UPPER LEVEL GROUND MOTION .....	10-27
10.10	SCREENING AND PRIORITIZATION FOR UPPER LEVEL GROUND MOTION.....	10-27
10.10.1	General .....	10-27
10.10.2	Factors to be Considered.....	10-29
10.10.3	Seismic Vulnerability Rating Methods.....	10-31
10.10.3.1	Minimum Screening Requirements.....	10-33
10.10.3.2	Seismic Inventory of Bridges.....	10-33
10.10.4	Indices Method.....	10-33
10.10.5	Expected Damage Methods.....	10-35
10.11	METHODS FOR EVALUATION OF UPPER LEVEL GROUND MOTION .....	10-37
10.12	RETROFIT STRATEGIES FOR UPPER LEVEL GROUND MOTION .....	10-41
10.12.1	General .....	10-41
10.12.2	Retrofit Strategy Selection .....	10-41
10.12.2.1	Objective of Retrofitting and Acceptable Damage.....	10-41
10.12.2.2	Cost Considerations of Seismic Retrofit .....	10-42
10.12.2.3	Other Considerations and Non-seismic Issues .....	10-44
10.12.2.4	Identification and Evaluation a Retrofit Strategy .....	10-45
10.12.2.5	Do-nothing and Full-replacement Options .....	10-47
10.12.3	Seismic Retrofit Approaches.....	10-48
10.12.3.1	General.....	10-48
10.12.3.2	Strengthening .....	10-48
10.12.3.3	Improvement of Displacement Capacity .....	10-49
10.12.3.4	Force Limitation.....	10-49
10.12.3.5	Response Modification.....	10-50
10.12.3.6	Site Remediation by Ground Improvement.....	10-51
10.12.3.7	Acceptance or Control of Damage to Specific Components .....	10-51
10.12.3.8	Partial Replacement.....	10-52
10.13	RETROFIT MEASURES FOR UPPER LEVEL GROUND MOTION .....	10-52
10.13.1	General .....	10-52
10.13.2	Seismic Retrofit Matrix .....	10-61
10.14	SUMMARY .....	10-65
<b>CHAPTER 11 - REFERENCES.....</b>		<b>11-1</b>

## LIST OF FIGURES

Figure 1-1	Four Historic Earthquakes of Similar Magnitude Showing Larger Felt Areas in the Central and Eastern U.S. than in the West.....	1-2
Figure 1-2	USGS National Seismic Hazard Map (2008) for Conterminous U.S. for Seismic Design Coefficient at One Second Period ( $= S_A/g$ ) for 7% Probability of Exceedance in 75 years (1,000 year Return Period) and Competent Soil (the B/C boundary) .....	1-2
Figure 1-3	Examples of Unseated Spans due to Insufficient Support Length.....	1-4
Figure 1-4	Examples of Superstructure Damage due to Inadequate Load Path .....	1-5
Figure 1-5	Examples of Column and Pier Damage due to Lack of Ductile Detailing .....	1-6
Figure 1-6	Examples of Structural Damage due to Ground Failure .....	1-7
Figure 1-7	Elastic Performance .....	1-11
Figure 1-8	Inelastic Performance .....	1-11
Figure 1-9	Maximum Elastic and Inelastic Displacements .....	1-12
Figure 1-10	Cost Implications of Performance-Based Design .....	1-13
Figure 1-11	Chain Analogy for Capacity-Protected Design (after Paulay and Priestley, 1992) .....	1-16
Figure 1-12	Calculation of Design Force Level and Displacement Demand in Force-Based Method .....	1-18
Figure 1-13	Calculation of Design Force Level and Displacement Demand in Displacement-Based Method .....	1-19
Figure 2-1	Steps in Probabilistic Seismic Hazard Analysis .....	2-2
Figure 2-2	Geometry of Seismic Sources in Seismic Hazard Analysis.....	2-3
Figure 2-3	Example of PHGA Attenuation Relationship for Strike-Slip Earthquakes and Soil Sites. (Boore, Joyner, and Fumal, 1997).....	2-9
Figure 2-4	Boundary Defining WUS and CEUS Seismic Hazard Regions Based on Change in Attenuation Relationship (Based on USGS National Seismic Hazard Map, 2002 Edition.) .....	2-10
Figure 2-5	Comparison Between Spectral Curves for the WUS and CEUS Hazard Regions; a) Acceleration Spectra for $M = 6.5$ , and $R = 20\text{km}$ ; b) Displacement Spectra for $M = 6.5$ and $R = 20\text{km}$ .....	2-11
Figure 2-6	Seismic Hazard Curve for Site in Southern California: Individual Contributions and Total Hazard from Three Faults .....	2-12
Figure 2-7	Magnitude Deaggregation for Augusta, GA, at 1.0 sec Period for a 2,500-year .....	2-17
Figure 2-8	Influence of Rupture Directivity on Velocity Time Histories Recorded at the Lucerne and Joshua Tree Sites During the 1992 Landers Earthquake (Somerville et al., 1997).....	2-26
Figure 2-9	Seismic Coefficient Design Spectrum Constructed with the Three-Point Method.....	2-29
Figure 2-10	USGS Acceleration Response Spectrum and the AASHTO Seismic Coefficient Design Spectrum for a Rock Site in Memphis, Tennessee 1,000-yr Return Period (7% PE in 75 Years).....	2-30
Figure 2-11	Initiation Screen for USGS Web Application.....	2-33
Figure 2-12	Summary Screen from USGS Web Site Application.....	2-34
Figure 2-13	Initiation Screen for the USGS/AASHTO Ground Motion Program .....	2-36
Figure 2-14	Screen No. 2: Site Location, Design Hazard Level, $PGA$ , $S_s$ and $SI$ for Rock Site (Site Class B).....	2-36
Figure 2-15	Screen No. 3: Table of Site Factors $F_{pga}$ , $F_a$ and $F_v$ for Bridge Site (Site Class C)....	2-37
Figure 2-16	Screen No. 4: $A_s$ , $SD_s$ and $SDI$ for Bridge Site (Site Class C).....	2-37
Figure 2-17	Screen No. 5: Spectral Values for Acceleration and Displacement for Site Class B ('Map Spectrum' Option) .....	2-38
Figure 2-18	Screen No. 6: Spectral Values for Acceleration and Displacement for Site Class C ('Design Spectrum' Option) .....	2-39

Figure 2-19	Screen No. 7: Display Option 1 ('Map Spectrum' $S_a$ vs $T$ ) and Drop-Down Menu for Other Options.....	2-39
Figure 2-20	Screen No. 8: Display Option 5 (All $S_a$ vs. $T$ Spectra) .....	2-40
Figure 2-21	Screen No. 9: Display Option 6 (All $S_a$ vs. $S_d$ Spectra) .....	2-40
Figure 2-22	Coherency Function for Horizontal Component Motion (Abrahamson, 1992).....	2-47
Figure 2-23	Coherency Function for Vertical Component Motion (Abrahamson, 1992) .....	2-48
Figure 3-1	Simplified Base Curve Recommended for Determination of CRR from SPT Data for Magnitude 7.5 Along with Empirical Liquefaction Data .....	3-11
Figure 3-2	Magnitude Scaling Factors Derived by Various Investigators .....	3-12
Figure 3-3	CPT Liquefaction Resistance Chart (Robertson and Wride, 1998).....	3-14
Figure 3-4	Shear Wave Velocity Liquefaction Resistance Chart (Andrus and Stokoe, 2000).....	3-15
Figure 3-5	Soil Flexibility Factor ( $r_d$ ) Versus Depth as Developed by Seed and Idriss (1971) with Added Mean Value Lines .....	3-16
Figure 3-6	Example of a Liquefaction Triggering Analysis for a Single SPT Boring (Idriss and Boulanger, 2008) .....	3-17
Figure 3-7	Correlation between the Undrained Residual Strength Ratio, $S_r/\sigma'_{vo}$ and a) standardized normalized SPT blow count, $(N1)_{60}$ and b) normalized CPT tip resistance, $q_{c1}$ (Olson and Johnson, 2008) .....	3-20
Figure 3-8	Landing Road Bridge Lateral Spread (after Berrill et al., 1997) .....	3-22
Figure 3-9	Site and Damage Characteristics for a Precast Concrete Pile Subjected to a Lateral Spread in the Kobe Earthquake (after Tokimatsu and Asaka, 1998).....	3-22
Figure 3-10	Newmark Sliding Block Analysis.....	3-23
Figure 3-11	Plot for Determination of Earthquake-induced Shear Strain in Sand Deposits (Tokimatsu and Seed, 1987).....	3-30
Figure 3-12	Relationship between Volumetric Strain, Cyclic Shear Strain, and Penetration Resistance for Unsaturated Sands (Tokimatsu and Seed, 1987).....	3-31
Figure 3-13	Computation of Settlement for 50-ft Deep Sand Layer .....	3-32
Figure 3-14	Curves for Estimation of Post-liquefaction Volumetric Strain using SPT Data and Cyclic Stress Ratio for $M_w$ 7.5 Earthquakes (Tokimatsu and Seed, 1987) .....	3-34
Figure 3-15	Types of Earthquake Faults .....	3-39
Figure 3-16	Relationship between Maximum Surface Fault Displacement and Earthquake Moment Magnitude (Wells and Coppersmith, 1994).....	3-42
Figure 4-1	Chain Analogy for Capacity Design (after Paulay and Priestley, 1992).....	4-3
Figure 4-2	Force-Displacement Relationships for Elastic and Ductile Systems .....	4-5
Figure 4-3	Equilibrium of Forces on Single-Degree-of-Freedom (SDOF) Structure.....	4-8
Figure 4-4	Influence of Ground Excitation .....	4-9
Figure 4-5	Lateral Moments Induced in a Two-Column Bent .....	4-12
Figure 4-6	Lateral Load Path of a Two-Span Bridge Under Transverse Seismic Loading .....	4-13
Figure 4-7	Superstructure Bending and Relative Lateral Load Distribution in Two-Span Continuous Bridge .....	4-13
Figure 4-8	Transverse Deformation of Superstructure for Two-Span Non-Continuous Bridge .....	4-15
Figure 4-9	Lateral Load Path of a Two-Span Bridge Under Longitudinal Seismic Loading .....	4-16
Figure 4-10	Different Longitudinal Behavior for Stub and Seat Abutments .....	4-16
Figure 4-11	Balanced Frame Stiffness and Geometry (adapted from Caltrans, 2013).....	4-18
Figure 4-12	Isolation Casings (Keever, 2008, Yashinsky and Karshenas, 2003).....	4-19
Figure 4-13	Type 1 - Ductile Substructure and Elastic Superstructure .....	4-32
Figure 4-14	Type 2 - Elastic Substructure with Ductile Superstructure .....	4-33
Figure 4-15	Type 3 - Elastic Substructure and Superstructure with a Fusing Interface .....	4-34
Figure 5-1	Two-Span Bridge Subject to Longitudinal Earthquake Ground Motion .....	5-2
Figure 5-2	Plan View of a Span with Mass Assigned to Quarter Points and Corresponding Transverse Displacement Degrees-of-Freedom.....	5-7

Figure 5-3	Transverse and Longitudinal Loading, $p_0$ , and Displacement, $v_s(x)$ .....	5-22
Figure 5-4	Capacity / Demand Spectrum .....	5-36
Figure 5-5	Range of Common Bridge Models from Simple Stick Linear Models to Finite Element Three-Dimensional Models .....	5-49
Figure 6-1	Poorly Confined Column in 1971 San Fernando Earthquake.....	6-4
Figure 6-2	Poorly Confined Column with Lap Spliced Longitudinal Reinforcement at the base (Priestley, Seible and Chai, 1992).....	6-5
Figure 6-3	Stress vs. Strain Curve for Unconfined and Confined Concrete.....	6-6
Figure 6-4	Poisson's Effect on Confined Concrete Columns in Compression.....	6-6
Figure 6-5	Examples of Effective Confinement (after Paulay and Priestley, 1992) .....	6-7
Figure 6-6	Hysteretic Behavior of Poorly and Well Confined Square Reinforced Concrete Columns .....	6-8
Figure 6-7	Shear Failure of a Column in the 1971 San Fernando Earthquake .....	6-9
Figure 6-8	Single Column Lateral Reinforcement in Plastic Hinge Zone Region .....	6-11
Figure 6-9	Multi-Column Lateral Reinforcement in Plastic Hinge Region .....	6-11
Figure 6-10	Interlocking Spirals Column Section (WSDOT, 2014) .....	6-13
Figure 6-11	Interlocking Spirals with Crossties (Correal, Saiidi, and Sanders, 2004).....	6-13
Figure 6-12	Flexurally Controlled Interlocking Spiral Test Results (McLean and Buckingham, 1994) .....	6-14
Figure 6-13	Shear Controlled Interlocking Spiral Test Results (McLean and Buckingham, 1994)..	6-14
Figure 6-14	Damage to Integral Flared Columns in the 1994 Northridge Earthquake (Nada, Sanders, and Saiidi, 2003).....	6-16
Figure 6-15	Damage to Isolated Flared Columns with 2 inch Soffit Gaps (Sanchez, Seible, and ....	6-18
Figure 6-16	Detail of Reinforcement in Isolated Flared Column (Nada, Sanders, and Saiidi, 2003)	6-18
Figure 6-17	Load Versus Top Displacement of Strong Axis Pier Wall (Haroun et.al., 1993).....	6-21
Figure 6-18	Force Displacement Envelope of Pier Wall Hysteresis Loops (Haroun et.al., 1994)....	6-21
Figure 6-19	Lateral Pier Wall Reinforcement within the Plastic Region (Caltrans, 1999) .....	6-22
Figure 6-20	Load Displacement Curve for an Interior Shear Key (Megally et. al., 2002).....	6-24
Figure 6-21	Shear Key Damage Levels (Megally et. al., 2002) .....	6-25
Figure 6-22	Comparison of Response for Linear Elastic and Inelastic Bilinear Systems .....	6-28
Figure 6-23	Adjustment for Estimating Inelastic Displacements (ATC-49, 2003).....	6-28
Figure 6-24	Relative Seismic Displacement vs. Period Ratio .....	6-31
Figure 6-25	Sample Distribution of A615 Grade 60 Steel Yield Strength (after Mirza and MacGregor, 1979) .....	6-32
Figure 6-26	Ratio of Maximum Flexural Strength to the Nominal Strength for Circular Cross Sections (after Priestley, Seible and Calvi, 1996) .....	6-33
Figure 6-27	Moment-Curvature Relationship (Caltrans, 2013).....	6-36
Figure 6-28	Moment-Curvature Sectional Analysis.....	6-37
Figure 6-29	Stress-Strain Curve for Mild Reinforcing Steel (Caltrans, 2013).....	6-40
Figure 6-30	Stress-Strain Model for Monotonic Loading of Confined and Unconfined Concrete (Mander et. al., 1988).....	6-44
Figure 6-31	Definition of Parameters for Rectangular Sections (after Mander et al., 1988).....	6-45
Figure 6-32	Plastic Hinging Mechanism for a Cantilever Column .....	6-51
Figure 6-33	Plastic Hinge Stages.....	6-52
Figure 6-34	Five Regions of Expected Performance and Damage for Steel .....	6-61
Figure 6-35	Areas of Potential Inelastic Deformations in Steel Substructure .....	6-62
Figure 6-36	Column Performance Identification Curves .....	6-69
Figure 6-37	Ductile Performance Damage Levels .....	6-69
Figure 6-38	Brittle Performance Damage Level .....	6-70
Figure 6-39	Drift Capacity for Reinforced Concrete Spalling from Berry and Eberhard (Imbsen, 2006).....	6-71

Figure 6-40	Plots Showing the Calculated Drift Capacity vs. D/H for the Columns of Table 6-6 ...	6-72
Figure 6-41	Plot Showing the Determination of the Drift Capacity for a Low Seismic Zone (Imbsen, 2006) .....	6-73
Figure 6-42	Plot Showing the Determination of the Drift Capacity for a Moderate Seismic Zone (Imbsen, 2006) .....	6-74
Figure 7-1	Transverse Seismic Forces.....	7-5
Figure 7-2	Frame Elevation.....	7-5
Figure 7-3	Composite Force-Displacement Curves .....	7-6
Figure 7-4	Force-Based Method for Lateral System Force vs. Displacement.....	7-9
Figure 7-5	Capacity Design of Bridges Using Overstrength.....	7-17
Figure 7-6	Concrete Column Shear Degradation Models (Net of Axial Effects).....	7-19
Figure 7-7	Contribution of Column and/or Cap Beam Axial Force to Shear Strength .....	7-22
Figure 7-8	Single Spiral Transverse Reinforcement (AASHTO, 2014).....	7-22
Figure 7-9	Column Interlocking Spiral Details (AASHTO, 2014) .....	7-23
Figure 7-10	Column Tie Details (AASHTO, 2009) .....	7-23
Figure 7-11	Column Tie Details (AASHTO, 2009) .....	7-23
Figure 7-12	Joint Shear Deformation in a Two Column Bent.....	7-29
Figure 7-13	Reinforcement Elongation and Slip Deformation in a Two-Column Bent.....	7-29
Figure 7-14	Joint Classification for Rotational Capacity .....	7-30
Figure 7-15	Types of Deep Foundations Used for Bridges.....	7-35
Figure 7-16	Spread Footing and Pile Cap Failure Modes (FHWA, 1995).....	7-40
Figure 7-17	Types of Abutments.....	7-47
Figure 7-18	Three Common Superstructure-to-Substructure Configurations .....	7-55
Figure 7-19	Effective Superstructure Width (AASHTO, 2014).....	7-57
Figure 7-20	External Shear Key for Box Girder Bridge.....	7-61
Figure 7-21	Effect of P- $\Delta$ on a Single-Column Pier (after Priestley et. al., 1996).....	7-65
Figure 7-22	P- $\Delta$ Effect on Cyclic Response (after Priestley et. al., 1996) .....	7-66
Figure 8-1	Seismic Capacity using <i>LRFD Specifications (LS)</i> and <i>Guide Specifications (GS)</i> .....	8-6
Figure 8-2	Confinement Requirements using <i>LRFD Specifications (LS)</i> and <i>Guide Specifications (GS)</i> .....	8-6
Figure 8-3	Support Length, <i>N</i> .....	8-18
Figure 8-4	Single-Span Bridge – Minimum Design Forces .....	8-21
Figure 8-5	Zone 1 and SDC A – Design Forces for Acceleration Coefficient $A_s < 0.05$ .....	8-22
Figure 8-6	Zone 1 and SDC A – Design Forces for Acceleration Coefficient $A_s \geq 0.05$ .....	8-22
Figure 8-7	Zone 2 – Seismic Design Forces.....	8-31
Figure 8-8	Zone 3 and 4 – Column Design Forces for the Application of the Modified Design Forces and the Inelastic Hinging Forces.....	8-33
Figure 8-9	Zone 3 and 4 – Footing Design Forces for the Application of the Modified Design Forces and the Inelastic Hinging Forces.....	8-34
Figure 8-10	Zone 3 and 4 – Design Forces for Connections .....	8-34
Figure 8-11	Dynamic Analysis Modeling Technique (AASHTO, 2014).....	8-48
Figure 8-12	Idealized Load – Deflection Curve of a Bridge .....	8-51
Figure 8-13	Effects of Foundation Flexibility on the Force-Deflection Relation for a Single Column Pier (Caltrans, 2013) .....	8-56
Figure 9-1	Deformations in Conventional and Isolated Bridges During Strong Ground Shaking (Buckle et. al., 2006).....	9-4
Figure 9-2	Effect of Period Shift Due to Isolator Flexibility on Bridge Response.....	9-5
Figure 9-3	Bilinear Representation of Typical Isolator Hysteresis Loop (AASHTO, 2010) .....	9-6
Figure 9-4	Effect of Damping on Bridge Response (Buckle et.al., 2006).....	9-7
Figure 9-5	Three Types of Seismic Isolator Commonly Used in the United States for Protection of Highway Bridges (Buckle et. al., 2006).....	9-9

Figure 9-6	South Rangitikei River Rail Bridge, Mangaweka, New Zealand (Buckle et. al., 2006)	9-12
Figure 9-7	Sierra Point Overhead US 101 Near San Francisco (Buckle et. al., 2006)	9-14
Figure 9-8	Lead-Rubber Isolators Being Installed in the JFK Airport Light Rail Viaduct, NY	9-17
Figure 9-9	Concave Friction Bearings Being Installed in the Benicia-Martinez Bridge, CA	9-18
Figure 9-10	Plan and Elevation of Corinth Canal Highway Bridges (Buckle et. al., 2006)	9-19
Figure 9-11	Idealized Deformations in an Isolated Bridge with Flexible Substructures (AASHTO, 2010)	9-27
Figure 9-12	Cross section of Typical Lead-Rubber Isolator (Buckle et. al., 2006)	9-36
Figure 9-13	Shear Deformation in a Lead Rubber Isolator (Buckle et. al., 2006)	9-37
Figure 9-14	Overlap Area, $A_o$ , Between Top-Bonded and Bottom-Bonded Areas of Elastomer in a Displaced Elastomeric Isolator (AASHTO, 2010)	9-43
Figure 9-15	Time-Dependent Low-Temperature Behavior of Elastomers (Buckle et.al., 2006)	9-53
Figure 9-16	Force-Displacement Relation of an Elastomeric Isolator at 68 <sup>0</sup> F (top) and -4 <sup>0</sup> F (bottom) (Buckle et.al., 2006)	9-53
Figure 9-17	Force-Displacement Relation of a Lead-Rubber Isolator at 68 <sup>0</sup> F (top) and -4 <sup>0</sup> F (bottom) (Buckle et.al., 2006)	9-54
Figure 9-18	Force-Displacement Relation for a Virgin (Unscragged) High-Damping Elastomeric Isolator (Buckle et. al., 2006)	9-55
Figure 9-19	Values of the Scragging $\lambda$ -Factor for Elastomeric Isolators (Buckle et. al., 2006)	9-58
Figure 9-20	Flat Sliding Bearings: (a) Pot bearing, (b) Disc bearing, (c) Ball and socket (spherical) bearing (Buckle et. al., 2006)	9-59
Figure 9-21	Elasto-Plastic Yielding Steel Device Used in Combination with Lubricated Sliding Isolators in Bridges (Buckle et.al., 2006)	9-60
Figure 9-22	Eradquake Isolator (Buckle et.al., 2006)	9-61
Figure 9-23	Concave Friction Isolator (Buckle et.al., 2006)	9-61
Figure 9-24	Concave Friction Isolator, Mississippi River Bridge, Ontario, Canada	9-62
Figure 9-25	Section and Plan, Concave Friction Isolator, Mississippi River Bridge, Ontario, Canada (Buckle et.al., 2006)	9-63
Figure 9-26	Forces Acting in Concave Friction Isolator when Sliding to Right - Not to Scale (Buckle et. al., 2006)	9-64
Figure 9-27	Idealized Force-Displacement Hysteretic Behavior of a Concave Friction Isolator (Buckle et.al., 2006)	9-65
Figure 9-28	Coefficient of Sliding Friction of Unfilled PTFE-Polished Stainless Steel Interfaces - Surface Roughness 1.2 $\mu$ in Ra; Ambient Temperature about 68 <sup>0</sup> F (Buckle et.al., 2006)	9-72
Figure 9-29	Coefficient of Friction of Unfilled PTFE-Polished Stainless Steel Interfaces as a Function of Temperature (Buckle et.al., 2006)	9-72
Figure 9-30	Effect of Cumulative Movement (Travel) on Sliding Coefficient of Friction of unfilled PTFE in Contact with Polished Stainless Steel (Buckle et. al., 2006)	9-73
Figure 9-31	Effect of Surface Roughness of Stainless Steel on the Sliding Coefficient of Friction of Unfilled PTFE (Buckle et.al., 2006)	9-74
Figure 9-32	Effect of Temperature on the Frictional Properties of PTFE-Polished Stainless Steel Interfaces (Buckle et. al., 2006)	9-77
Figure 9-33	Normalized Force-Displacement Relation of a Flat Sliding Isolator at 70 <sup>0</sup> F (top) and	9-77
Figure 10-1	Overview of the Retrofitting Process for Highway Bridges (FHWA, 2006)	10-3
Figure 10-2	Conceptual Relationship Between Relative Effort, Increasing Hazard and Performance Level (FHWA, 2006)	10-8
Figure 10-3	Retrofit Process for Dual Level Earthquake Ground Motions (FHWA, 2006)	10-16
Figure 10-4	Determination of Seismic Retrofit Category (FHWA, 2006)	10-19

Figure 10-5	Seismic Retrofitting Process for Highway Bridges Subject to Upper Level Ground Motion (FHWA, 2006) .....	10-25
Figure 10-6	Relative Effort to Retrofit (a) ‘Standard’ and (b) ‘Essential’ Bridges with Varying Service Life and Hazard Level (FHWA, 2006). .....	10-26
Figure 10-7	Screening and Prioritization Process (FHWA, 2006) .....	10-28
Figure 10-8	Evaluation Methods for Existing Bridges Showing Relationship Between Demand Analysis and Capacity Assessment (FHWA, 2006) .....	10-39
Figure 10-9	Identification and Evaluation of a Retrofit Strategy (FHWA, 2006).....	10-46
Figure 10-10(a)	Restrainers at Piers for Steel Girders (top and bottom) and Concrete Girders (upper center) .....	10-54
Figure 10-10(b)	Bearing Strengthening and Replacement: Bearing Replacement with Elastomeric Pad (upper left), Improving Stability of Rocker Bearing (upper right), and Anchor Bolt Replacement (lower left) .....	10-55
Figure 10-10(c)	Superstructure Strengthening: Cross Brace Strengthening (top), Making Simple Spans Continuous (center), and Seat Extension at Intermediate Hinge (bottom) .....	10-56
Figure 10-10(d)	Lead-Rubber Isolator (top), Friction-Pendulum Isolator (center), and Installation of Friction Pendulum Isolator on I-40 Crossing Mississippi River, Memphis (bottom)..	10-57
Figure 10-10(e)	Steel Jackets for Concrete Columns (top) and Installation on Hernando Desoto Bridge, I-40 Retrofit, photo R.A. Imbsen (bottom).....	10-58
Figure 10-10(f)	Infilled Walls for Concrete Piers (top) and Installation on West Lake Sammish Parkway, I-90 Retrofit, photo L.M. Marsh (bottom) .....	10-59
Figure 10-10(g)	Footing Overlay with Piled Extension (top) and Installation on Hernando-Desoto Bridge, I-40 Retrofit, photo R.A. Imbsen (center and bottom).....	10-60
Figure 10-10(h)	Vibro-Replacement Site Remediation .....	10-61



## LIST OF TABLES

Table 1-1	Learning from Earthquakes.....	1-7
Table 1-2	AASHTO Specifications Timeline .....	1-8
Table 2-1	Magnitude Deaggregation for Bakersfield, California, .....	2-16
Table 2-2	Performance- Based Seismic Design Criteria for Transportation Facilities (NCHRP, 2001) .....	2-21
Table 2-3	NEHRP Site Classification System .....	2-31
Table 2-4	Values of $F_{pga}$ and $F_a$ as Function of Site Class and.....	2-32
Table 2-5	Values of $F_v$ as a Function of Site Class and .....	2-32
Table 3-1	Seismic Design Categories AS DEFINED by AASHTO (2014) .....	3-4
Table 3-2	Influence of Earthquake Magnitude on Volumetric Strain Ratio for Dry Sands (after Tokimatsu and Seed, 1987).....	3-31
Table 3-3	Computation of Settlement for Deposit of Dry Sand.....	3-32
Table 4-1	Permissible Earthquake Resisting Elements .....	4-23
Table 4-2	Permissible Earthquake Resisting Elements that Require Owner’s Approval.....	4-25
Table 4-3	Earthquake Resisting Elements not Recommended for New Bridges .....	4-27
Table 4-4	Permissible Earthquake Resisting Systems .....	4-30
Table 5-1	Methods OF Analysis .....	5-15
Table 5-2	Restrictions on the Application of the Uniform Load and Single Mode Spectral Methods (AASHTO, 2013, AASHTO 2014) .....	5-16
Table 5-3	Numerical Integration Procedure for Linear SDOF Bridges .....	5-29
Table 5-4	Numerical Integration Procedure for Linear MDOF Bridges.....	5-30
Table 5-5	Effective Viscous Damping Ratios and Damping Factors.....	5-35
Table 5-6	Basic Numerical Integration Procedure for Nonlinear MDOF Bridges.....	5-40
Table 5-7	Component Rigidities .....	5-52
Table 6-1	Procedure for Calculating Moment-Curvature .....	6-38
Table 6-2	Properties of Reinforcing Steel.....	6-42
Table 6-3	Expected Yield Stress versus Nominal Yield Stress for Steel (AASHTO, 2009) .....	6-47
Table 6-4	Values of Plastic Curvature Corresponding to Various Limit States in Reinforced Concrete Columns and Beams, FHWA (2006).....	6-55
Table 6-5	Limiting Width-Thickness Ratios.....	6-63
Table 6-6	Analytical Data Base Column Parameters .....	6-72
Table 7-1	General Steps for Seismic Design.....	7-2
Table 7-2	Force-Based Method – General Approach.....	7-10
Table 7-3	Displacement-Based Method – General Approach.....	7-12
Table 7-4	Approach for Capacity Design of Foundations.....	7-31
Table 7-5	Approach for Designing Foundations for Seismic Loading .....	7-42
Table 7-6	Approach for Designing Foundations Subject to Liquefaction - No Lateral Movement Expected.....	7-51
Table 7-7	Approach for Designing Foundations Subject to Liquefaction - Lateral Flow or Spreading Kinematic Loading Case.....	7-53
Table 8-1	General Steps for Seismic Design.....	8-3
Table 8-2	Seismic Partitions for Both Specifications .....	8-8
Table 8-3	Features to Consider for Software .....	8-10
Table 8-4	Load Combinations and Load Factors .....	8-11
Table 8-5	Percentage N by Zone and Acceleration Coefficient $A_s$ , LRFD Specifications.....	8-17
Table 8-6	Percentage N by Zone and Acceleration Coefficient $A_s$ , Guide Specifications .....	8-18
Table 8-7	Response Modification Factors – Substructures .....	8-29
Table 8-8	Response Modification Factors – Connections.....	8-29

Table 8-9	Recommended Overstrength Values for Materials Properties (appendix B3, AASHTO, 2007).....	8-39
Table 8-10	Requirements by Seismic Design Category.....	8-45
Table 9-1	States with More Than Ten Isolated Bridges.....	9-13
Table 9-2	Bridge Applications by Isolator Type.....	9-14
Table 9-3	Examples of Bridges with Large Isolators.....	9-14
Table 9-4	System Property Adjustment Factors.....	9-30
Table 9-5	Hardness and Moduli for a Conventional Rubber Compound <sup>1</sup> .....	9-45
Table 9-6	Maximum Values for Temperature $\lambda$ -Factors for Elastomeric Isolators, $\lambda_{max,T}$ (AASHTO, 2010).....	9-55
Table 9-7	Maximum Values for Aging $\lambda$ -Factors for Elastomeric Isolators, $\lambda_{max,a}$ (AASHTO,2010).....	9-55
Table 9-8	Maximum Values for Scragging $\lambda$ -Factors for Elastomeric Isolators, $\lambda_{max,scrag}$ (AASHTO, 2010).....	9-56
Table 9-9	Maximum Values for Temperature $\lambda$ -Factors for Sliding Isolators ( $\lambda_{max,t}$ ) (AASHTO, 2010).....	9-77
Table 9-10	Maximum Values for Aging $\lambda$ -Factors for Sliding Isolators ( $\lambda_{max,a}$ ) <sup>1</sup> (AASHTO, 2010).....	9-77
Table 9-11	Maximum Values for Travel and Wear $\lambda$ -Factors for Sliding Isolators ( $\lambda_{max,tr}$ ) (AASHTO, 2010).....	9-77
Table 9-12	Maximum Values for Contamination $\lambda$ -Factors for Sliding Isolators ( $\lambda_{max,c}$ ) (AASHTO, 2010).....	9-78
Table 10-1	Service Life Categories (FHWA, 2006) .....	10-12
Table 10-2	Minimum Performance Levels for Retrofitted Bridges .....	10-14
Table 10-3	Seismic Hazard Level (FHWA, 2006).....	10-17
Table 10-4	Performance-Based Seismic Retrofit Categories (FHWA, 2006) .....	10-18
Table 10-5	Minimum Requirements (FHWA, 2006).....	10-22
Table 10-6	Sample Bridge Seismic Inventory Form (FHWA, 2006). .....	10-34
Table 10-7	Evaluation Methods for Existing Bridges (FHWA, 2006) .....	10-38
Table 10-8	Cost of Various Retrofit Strategies as Percentage of New Construction Costs <sup>1,2</sup> (FHWA, 2006).....	10-43
Table 10-9	Matrix of Seismic Retrofit Approaches and Associated Retrofit Measures (FHWA, 2006). .....	10-62

# CHAPTER 1

## INTRODUCTION

### 1.1 GENERAL

According to the U.S. Geological Survey, at least 40 percent of the United States can expect to experience earthquake ground motions that have the potential to damage highway bridges within their lifetime, unless they are designed specifically to resist these motions.

While earthquakes are often considered to occur only on the west coast, and California in particular, damaging earthquakes are not limited to the western U.S. In fact, some of the strongest earthquakes in the history of the U.S. have occurred in the central and eastern U.S. The Charleston, South Carolina earthquake of 1886 is believed to have been as strong as, if not stronger than, the 1971 San Fernando and 1994 Northridge earthquakes, and there were three high-magnitude earthquakes in the New Madrid seismic zone in the central U.S. in 1811 and 1812, one of which is believed to have been as strong as the 1906 San Francisco earthquake.

Not only do large earthquakes occur in the central and eastern U.S., the motions they generate do not attenuate as quickly as in the west and are felt over very wide areas. As shown in Figure 1-1, the impacted areas of the Charleston (1886) and New Madrid (1811, 1812) earthquakes are considerably greater than for the similar-sized San Francisco (1906) and San Fernando (1971) earthquakes. This fact increases the hazard in the central and eastern U.S. as can be seen from the USGS National Seismic Hazard Map for the conterminous U.S. in Figure 1-2. This map shows the maximum seismic coefficient for a bridge with a return period 1,000 years. This coefficient determines the total lateral earthquake load on a bridge as function of its weight, and values above 20% are known to be damaging unless the bridge has been specifically designed for this load. Thus bridges in the dark gray areas of the map are subject to ground motions that have the potential to damage or collapse bridges.

It will be seen in Figure 1-2, that the seismic coefficients in many areas of the U.S., and particularly on the west coast, are very high (above 1.0). Designing a bridge for these loads is very challenging and with each major earthquake the state-of-the-art of seismic design has evolved.

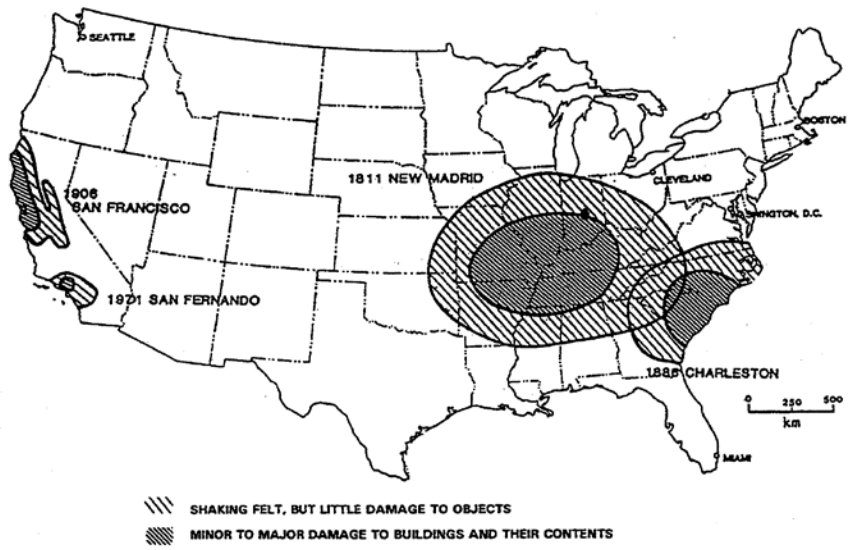


Figure 1-1 Four Historic Earthquakes of Similar Magnitude Showing Larger Felt Areas in the Central and Eastern U.S. than in the West

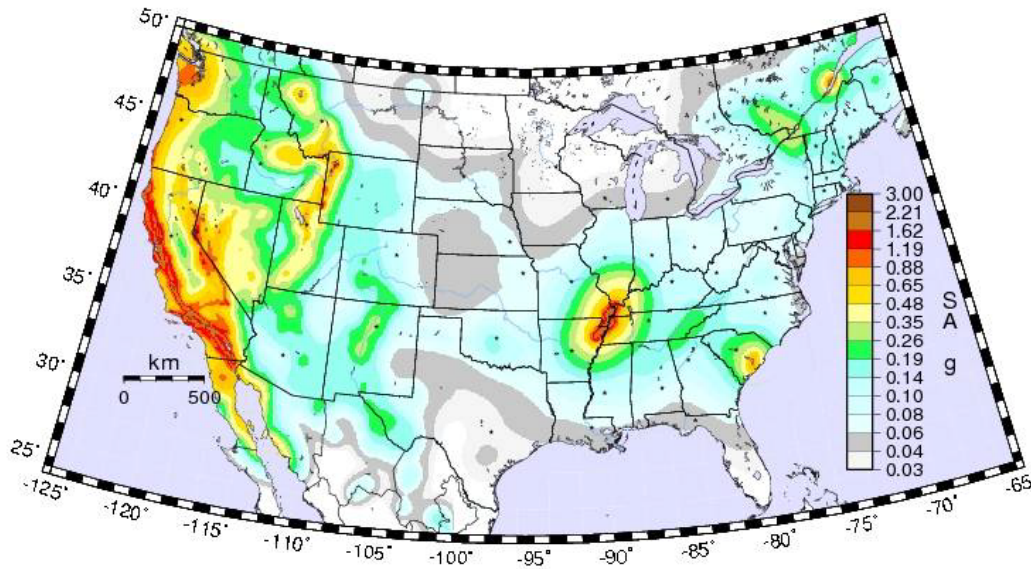


Figure 1-2 USGS National Seismic Hazard Map (2008) for Conterminous U.S. for Seismic Design Coefficient at One Second Period ( $= S_A/g$ ) for 7% Probability of Exceedance in 75 years (1,000 year Return Period) and Competent Soil (the B/C boundary)

In fact each earthquake teaches new lessons and Sec 1.2 summarizes bridge performance in recent earthquakes, lessons learned, and their influence on the development of the AASHTO specifications.

## **1.2 BRIDGE PERFORMANCE IN RECENT EARTHQUAKES AND DEVELOPMENT OF AASHTO SPECIFICATIONS**

Typical damage sustained by highway bridges can be grouped under four headings:

- Unseated spans due to insufficient support lengths,
- Collapse/damage to superstructures due to inadequate load path (e.g. deficient shear keys and cross frames, unbalanced pier stiffnesses),
- Column failure in flexure and shear due to inadequate detailing for ductility, and
- Structural damage due to ground failure, liquefaction, and fault rupture.

Examples of typical damage are given in Figures 1-3 through 1-6 from recent earthquakes in the U.S., Japan, Taiwan and Chile. The lessons learned from these earthquakes have led to major advances in earthquake engineering for bridges. Table 1-1 links these advances to the occurrence of damaging earthquakes.

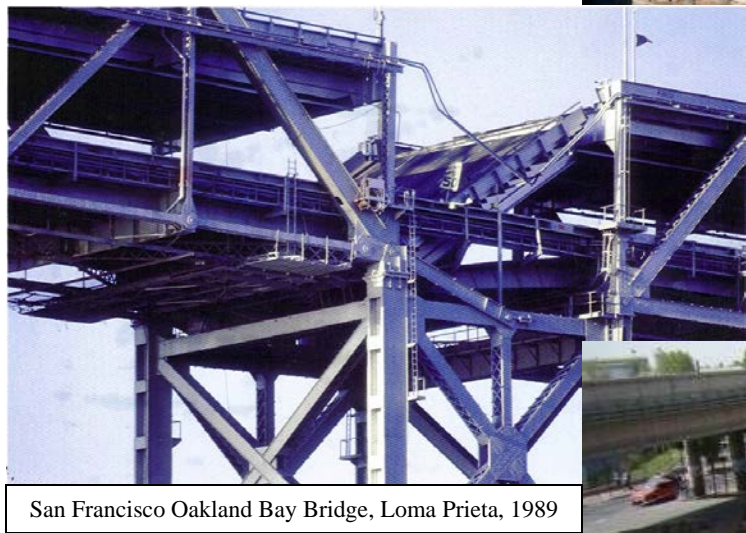


Figure 1-3 Examples of Unseated Spans due to Insufficient Support Length

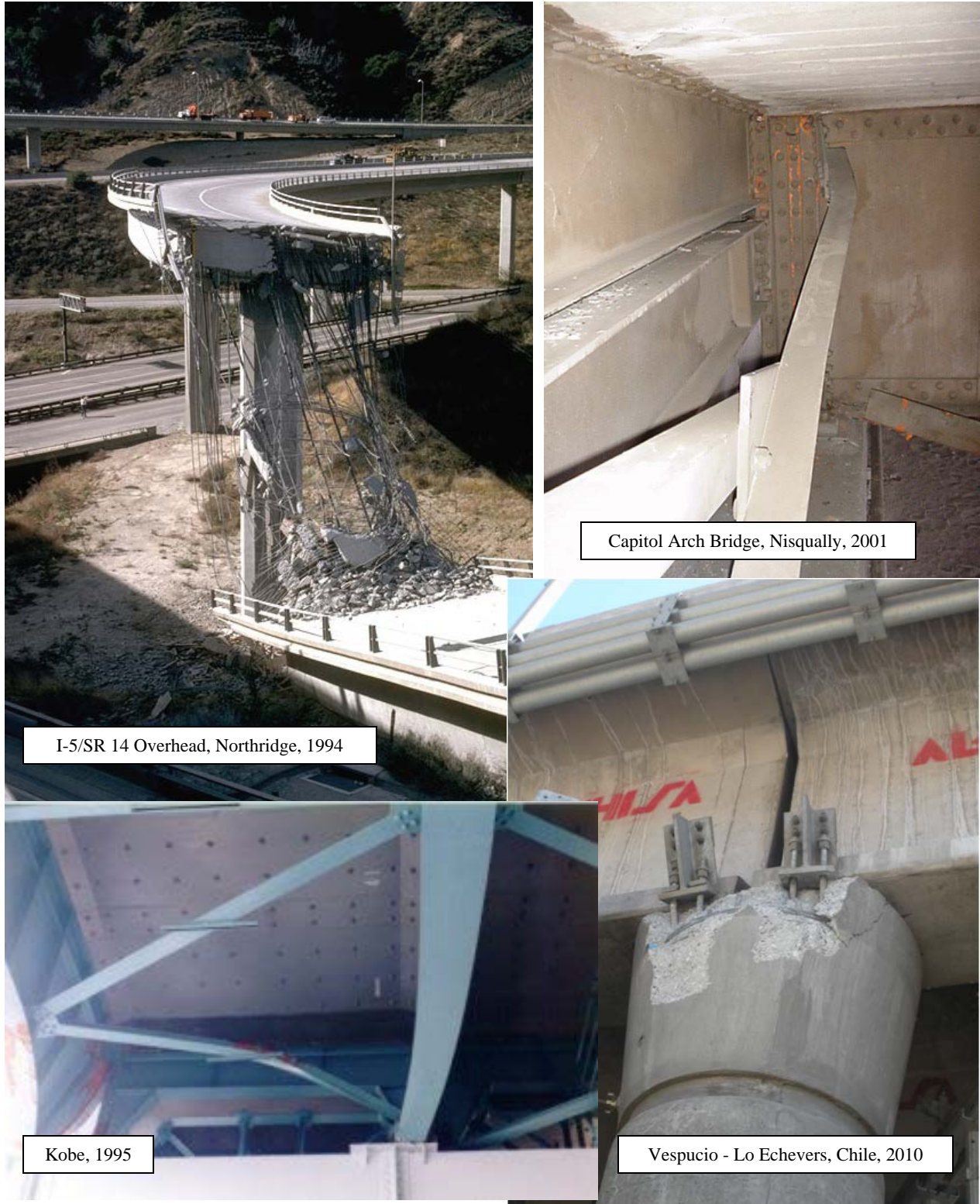


Figure 1-4 Examples of Superstructure Damage due to Inadequate Load Path

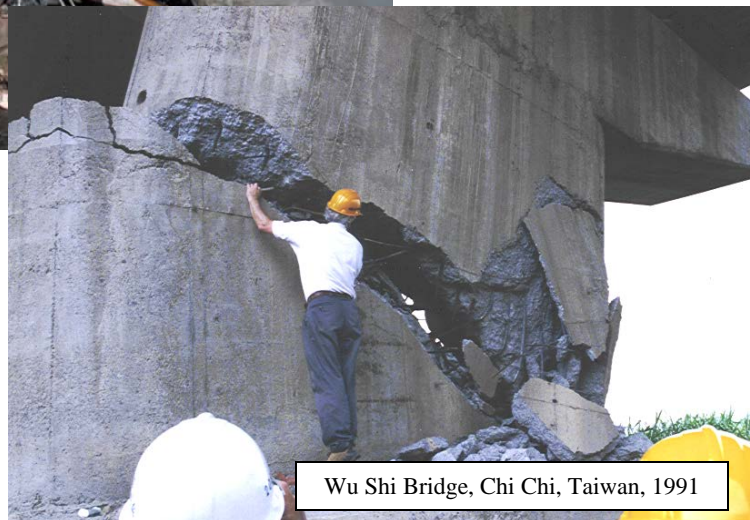
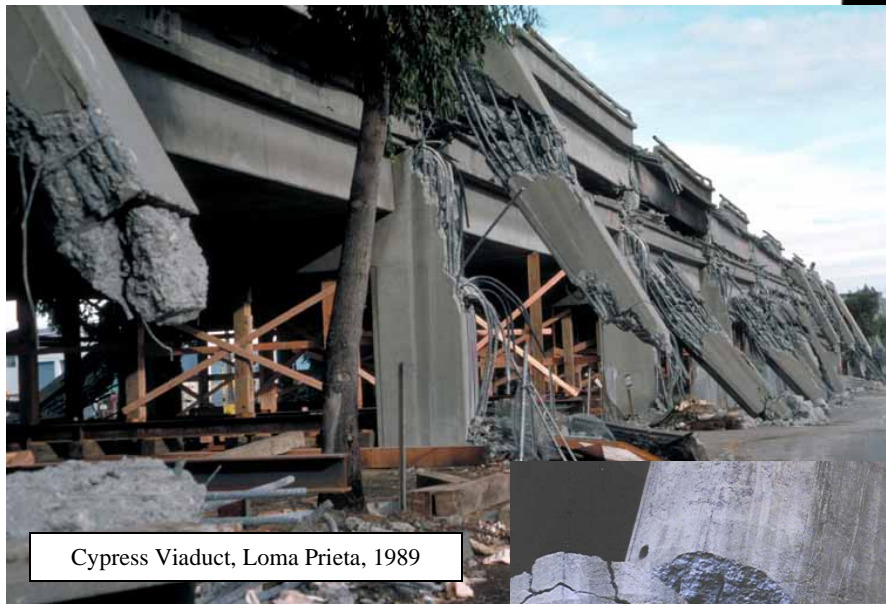


Figure 1-5 Examples of Column and Pier Damage due to Lack of Ductile Detailing



Figure 1-6 Examples of Structural Damage due to Ground Failure

**TABLE 1-1 LEARNING FROM EARTHQUAKES**

Year	Earthquake	Major Lessons	Major Advances
1964	Prince William Sound, AK	Ground failure due to liquefaction, span unseating	Site susceptibility to liquefaction, longer support lengths
1964	Niigata, Japan	Ground failure due to liquefaction, span unseating	Site susceptibility to liquefaction, longer support lengths
1971	San Fernando, CA	Column failure, span unseating	Capacity design, longer support lengths
1989	Loma Prieta, CA	Non-ductile details in older structures, span unseating, soil amplification effects	Restrainers, column jackets, extensive tool box of retrofit measures, revised site amplification factors
1994	Northridge, CA	Adverse load distribution in piers with unbalanced stiffness, unseating in skewed bridges, flared column failures, cross-frame damage in steel plate girder superstructures	Balance pier stiffnesses in multi-span continuous structures, longer support lengths, new details for flared columns, explicit design of load path in plate girder superstructures, displacement-based design
1995	Kobe, Japan	Damage to steel superstructures and bearings, non-ductile response of concrete columns	Increase in minimum connection forces, full scale testing of Japan-designed bridge columns on E-defense shake table in Kobe
2001	Nisqually, WA	Liquefaction, cross-frame damage in steel plate girder superstructures	Site remediation, estimation of lateral flows due to liquefaction, ductile cross frames for plate girder bridges
2008	Wenchuan, China	Span unseating and abutment damage due to rockfalls, curved girder unseating	Stabilize adjacent rock slopes, explicit design of load path in curved bridge superstructures; longer seat lengths
2010	Maule, Chile	Span unseating due to inadequate shear keys, rotation in skewed and non-skewed spans, liquefaction-induced column settlement and shear failures, tsunami-induced scour and column damage	Explicit design of load path in all bridge superstructures including diaphragms and connections; longer support widths for skewed bridges, remediation of liquefiable sites under bridge foundations to minimize settlement and lateral flow
2010, 2011	Christchurch, New Zealand	Liquefaction induced lateral flow damages abutment piles and when resisted can buckle single span bridge superstructures in compression, aggressive retrofitting program reduced extent of bridge damage	Ground improvement under bridge approaches to reduce extent of lateral flow (site remediation), benefits of seismic retrofit program demonstrated
2011	Great East Japan Earthquake, Japan	Bridge damage due to shaking was mainly in bridges not yet retrofitted, or only partially retrofitted. Bridge damage due to tsunami inundation was greater in non-integral bridges	Benefits of seismic retrofit program demonstrated, survival during tsunami inundation is possible if adequate connection provided between super- and sub-structure

The Prince William Sound earthquake near Anchorage, Alaska in 1964 was one of the largest earthquakes to strike anywhere in the world at that time. Significant damage to bridges occurred in the area with many unseated spans, primarily due to liquefaction or its effects. Similarly, the 1964 earthquake in Niigata, Japan dramatically demonstrated the effects of liquefaction. However, it was the 1971 San Fernando earthquake that was a seminal event in U.S. bridge design for seismic effects. Numerous

bridges collapsed or were damaged in this Southern California event, and some of the bridges were either under construction at the time or had been recently completed. This earthquake and the damage it caused prompted an evaluation of U.S. practice in seismic design, which led to the adoption of capacity-based design and the requirement for longer support lengths at abutments and piers.

In 1989 and 1994, damaging earthquakes in California again demonstrated the vulnerability of both new and existing bridges and prompted the move away from force-based design methods in high seismic zones, the development, and eventual adoption, of displacement-based methods.

As shown in Table 1-2 continual improvements to the AASHTO specifications for seismic design have occurred over the years, usually in response to lessons learned from major earthquakes, and the results of research programs funded by Caltrans and FHWA.

**TABLE 1-2 AASHTO SPECIFICATIONS TIMELINE**

Date	AASHTO Specifications
before 1973	AASHTO <i>Standard Specifications</i> required the following for Earthquake Stresses (Art 1.2.20): In regions where earthquakes may be anticipated, $EQ = C \times D$ where EQ = Lateral force applied horizontally D = Dead Load of structure C = 0.02 for structures on material rated at 4 tons or more per sq ft = 0.04 for structures on materials rated less than 4 tons per sq ft = 0.06 for structures on piles
1975	Interim revision of <i>Standard Specifications</i> , based on modified Caltrans design procedures, adopted
1981	ATC-6: <i>Seismic Design Guidelines for Highway Bridges</i> published
1983	ATC-6 Guidelines adopted by AASHTO as <i>Guide Specifications for Seismic Design</i>
1990	AASHTO <i>Guide Specifications</i> adopted as Division I-A of the <i>Standard Specifications</i>
1994	First Edition, <i>LRFD Bridge Design Specifications</i> adopted with seismic provisions derived from Division I-A of <i>Standard Specifications</i>
2003	ATC/MCEER-49: <i>Recommended LRFD Guidelines for the Seismic Design of Highway Bridges</i> published
2008	Interim Fourth Edition, <i>LRFD Bridge Design Specifications</i> adopted with updated seismic provisions
2009	First Edition, <i>Guide Specifications for LRFD Seismic Bridge Design</i> adopted (Displacement-Based Methodology)
2013	Interim Sixth Edition <i>LRFD Bridge Design Specifications</i> adopted with updated seismic provisions
2014	Second Edition <i>Guide Specifications for LRFD Seismic Bridge Design</i> adopted

Prior to 1973 the procedure for the seismic design of bridges was rudimentary by today's standards. A simple lateral force was applied to the structure equal to a specified fraction of the permanent weight of

the bridge. No special detailing or analysis for dynamic effects was required and elastic behavior was assumed. In addition, no allowance was made for the variation in seismic hazard (loading level) that existed across the country.

Following several damaging earthquakes around the Pacific rim and, in particular, the 1971 San Fernando earthquake, major changes to the AASHTO and Caltrans design procedures were undertaken in the 70s. In 1975, Interim Revisions were adopted by AASHTO pending a full review of design philosophy, procedures and detailing for seismic loads. These interims were based on revised procedures that had been developed by Caltrans following the 1971 event. In 1981, the Applied Technology Council published the results of this review along with a proposed set of *Seismic Design Guidelines for Highway Bridges* (Report ATC-6). This landmark document formed the basis of the seismic provisions for bridges in the U.S. for about the next 30 years. In 1983, ATC-6 was adopted as a *Guide Specification* by AASHTO and in 1990 (in response to the 1989 Loma Prieta Earthquake) it was adopted as Division I-A of the AASHTO *Standard Specifications*. In 1994, the first LRFD specifications for bridge design were adopted by AASHTO with seismic provisions derived from Division I-A of the *Standard Specifications*. These provisions in the LRFD specifications were updated in 2008 and remain the basis of seismic design for highway bridges throughout most of the U.S. today. As noted below these provisions are based on a force-based method of design (Sec. 1.5.3), but by the mid 90s there was growing dissatisfaction about the suitability of this methodology, especially for bridges in high seismic zones. In response, a joint venture of ATC and MCEER (Multidisciplinary Center for Earthquake Engineering Research) was formed to develop and publish in 2003 a set of recommendations on performance-based, seismic design of highway bridges based on a displacement-based methodology. These recommendations, along with Caltrans *Seismic Design Criteria*, became the basis for the development and adoption by AASHTO of the *Guide Specifications for LRFD Seismic Bridge Design*, in 2009.

### **1.3 SEISMIC DESIGN PHILOSOPHY**

The current AASHTO philosophy for seismic design has its roots in the answers to three fundamental questions:

1. *Is it possible to design a bridge to remain undamaged during a moderate-to-strong earthquake, as is done for wind, braking, and other lateral loads?*

The answer is not in an economical way. To avoid damage the bridge must respond elastically and very large forces will be developed in the columns and foundations as a result (Figure 1-7). In all but the lowest of seismic regions, these forces will be too large to be resisted economically. Furthermore, there is a small but significant possibility that an earthquake larger than the design earthquake will occur in the lifetime of the bridge and produce even larger forces.

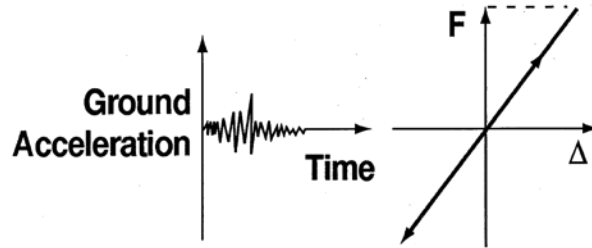


Figure 1-7 Elastic Performance

2. *How can bridges be designed to permit damage and remain safe?*

Bridges can be constructed to behave in a ductile manner under large earthquake loads (Figure 1-8). These ductile damage modes generally involve yielding of various structural members and corresponding plastic deformation in these members. Once yielding occurs, the forces in the bridge cannot exceed those which yield the members, even during very large earthquakes. This fuse-like action can be achieved safely and collapse avoided if the members are designed and detailed for the associated plastic deformations. This is a very powerful concept, because it places a cap on the forces that have to be considered in design, from the connections to the foundations, even for large earthquakes.

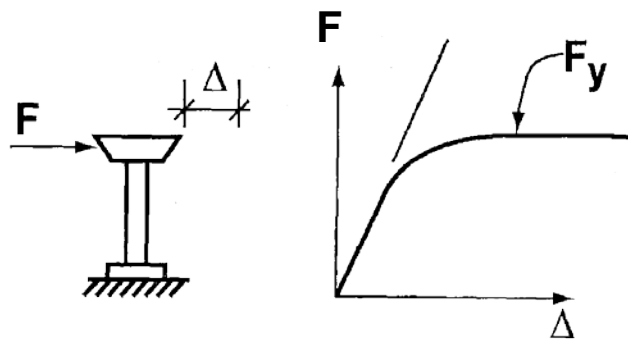


Figure 1-8 Inelastic Performance

3. *How can a bridge that is yielding under dynamic loads be analyzed without undue cost and effort?*

From many rigorous time-history analyses of yielding structures, experience has shown that conventional elastic analysis techniques may be used to adequately predict the maximum displacements in a bridge. In other words, it turns out that for many common bridges, the displacements assuming elastic behavior are about the same as for a yielding bridge i.e.  $\Delta_{\text{Inelastic Max}} = \Delta_{\text{Elastic Max}}$  in Figure 1-9. For some stiff bridges, the yielding structure tends to experience larger displacements and adjustment factors are available to correct for this effect.

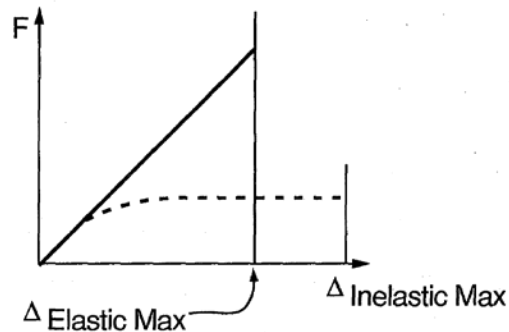


Figure 1-9 Maximum Elastic and Inelastic Displacements

In view of the above, the following design philosophy has been developed and widely accepted for the seismic design of highway bridges:

- Small-to-moderate earthquakes should be resisted within the elastic range of the structural components without significant damage.
- Realistic seismic ground motion intensities should be used to determine the seismic demands on the structural components. These ground motions are generally chosen to have a return period of 1000 years. This is the so-called ‘design earthquake’.
- Exposure to shaking from moderate-to-large earthquakes should not cause collapse of all or part of the bridge. However damage is accepted provided it is ductile in nature, readily detectable and accessible for inspection and subsequent repair if necessary.

This is essentially a ‘no-collapse’ philosophy for seismic design and it has been adopted by many state and federal agencies, not only for bridges but also for public and private buildings. It is widely believed that ‘no-collapse’ will assure ‘life-safety’, which is a fundamental objective of structural codes both in the U.S. and around the world.

However despite the fact that no spans will collapse, the bridge may be damaged to the point of not being usable even by emergency vehicles, and repair costs may exceed the cost of a new bridge. This may be undesirable for certain classes of bridges, such as those that are critically important. As a consequence Performance-Based Design methodologies have been developed which assure higher performance levels at the discretion of the owner. As shown in Figure 1-10, the initial cost of a bridge designed to a higher performance level than collapse prevention (box 'f') can be significant, particularly for earthquakes with longer return periods (box 'a'). But the increment in cost may be small compared to repair/replacement costs and societal/business losses during closure, if the design earthquake occurs in the lifetime of the bridge (compare boxes 'f' and 'd').

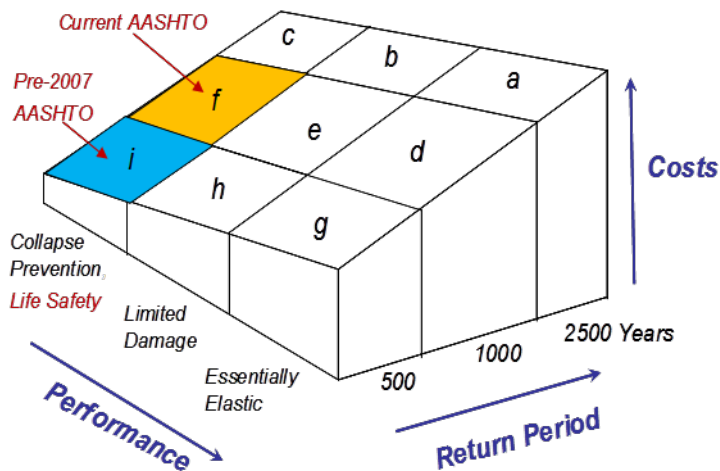


Figure 1-10 Cost Implications of Performance-Based Design

The topic of performance-based seismic design is beyond the scope of this manual, but an overview and detailed treatment may be found in *NCHRP Synthesis 440, Performance-Based Seismic Bridge Design* (Marsh and Stringer, 2013).

## 1.4 ROAD MAP FOR SEISMIC DESIGN

The seismic design process is essentially a three-part process: first, decide the performance level required during the design earthquake (for most bridges this will be the ‘no-collapse’ requirement); second, calculate the demand that the design earthquake places on the bridge; and third, make sure the bridge has the capacity to withstand this demand and satisfy the required performance level (e.g. ‘no-collapse’). The road map for the seismic design of a bridge is therefore as follows:

**PART A: PERFORMANCE LEVEL DETERMINATION**

Step 1: Determine required performance level in consultation with the Owner. In most cases this will simply be the ‘collapse prevention’ requirement.

**PART B: DEMAND ANALYSIS**

Step 2: Determine seismic loads at the bridge site from either national maps of design coefficients or a site-specific seismic hazard assessment exercise.

Step 3: Determine soil conditions at the site and modify seismic loads accordingly.

Step 4: Analyze the bridge for given loads using one of several possible elastic dynamic methods chosen according to the complexity of the bridge. As a minimum, obtain maximum values for forces and displacements. Perform this analysis in each of two orthogonal directions and combine the results to give values for use in design.

**PART C: CAPACITY DESIGN**

Step 5: Select locations in the bridge where yielding will be permitted, i.e., select the plastic hinge mechanism.

Step 6: Design yielding elements to have capacity in excess of the demand from Step 4 without degradation. Detail these locations for ductility.

Step 7: Check the load path through the bridge and protect all components (except the yielding members) against damage. This step is known as ‘capacity protection’.

Steps 5 – 7 are explored further in the following section and all of the above steps are described in greater detail in subsequent chapters.

## **1.5 CAPACITY DESIGN PRINCIPLES**

As noted above, current AASHTO design philosophy accepts the fact that a bridge will be damaged and behave inelastically during the design earthquake (an event with a return period of about 1,000 years). Such behavior is not like that accepted for other load combinations and this is because earthquake loads are so large that to design for them elastically would be prohibitively expensive, except for the most critical of bridges. Damage is therefore explicitly permitted and is expected during the design earthquake. But not all damage is acceptable. Only ductile yielding is permitted and then only in members specifically designed and detailed for such behavior. Brittle failure is not permitted at any time. Ensuring that a

bridge can sustain the magnitude and reversal of earthquake loading without collapse requires design principles and detailing that are different from those required for most other load types.

Designing for earthquake loads therefore requires a somewhat different way of thinking on the part of the designer than for other load cases. Typically, providing additional strength or capacity is thought of as advantageous from a safety perspective, although such practice might make the design more expensive. However, in seismic design there is a need to estimate the maximum forces that can be developed in the structure and design for these forces, so that the appropriate displacement capacity is provided. This means that simply adding more strength in one element, without regard to its impact on other parts of the structural system, is not an appropriate practice for seismic design.

In some geographic locations the seismicity of the area may be low enough that elastic response may be achieved economically.. In such locations, seismic design is relatively simple. However, in many locations the ability of a bridge to deform inelastically and in a ductile manner is a necessity. The use of inelastic response has both an economic and a technical basis. Economically, it is prudent to permit some damage to avoid spending undue resources on responding elastically to an extreme event that has a low likelihood of occurrence. Technically, it is prudent to design structures using fusing action that limits internal forces. This makes the structure less vulnerable to earthquake events that are larger than the design event. This section explains the principles that underpin modern seismic design, which have evolved to ensure this fusing action is effective. This action is known in earthquake engineering as ductile response.

### 1.5.1 Demand vs. Capacity

It is fundamental to the success of capacity design that the demand on a bridge (or any component in the structure) be less than the capacity of the bridge (or the component) to resist that demand. This requirement may be expressed as follows:

$$\frac{Demand}{Capacity} < 1.0 \quad 1-1$$

Since the designer has little choice over the demand, most of the design effort goes into providing sufficient capacity to satisfy Equation 1-1. One notable exception to this approach is the use of seismic isolation to reduce the demand and, as described in Chapter 9, it may then possible to satisfy this equation without exceeding the elastic capacity of the structure.

## 1.5.2 Capacity-Protected Design

The three principles of capacity design were introduced in Steps 5-7 of the road map in Section 1.4, and are repeated below in a slightly expanded format:

1. Choose the structural elements of the bridge that will deform inelastically, form a plastic hinge mechanism and sustain yield under the action of lateral earthquake loading, i.e., identify the yielding elements and calculate their capacities.
2. Design and detail these elements so that they will continue to resist the applied loading with little or no degradation under both continued deformation and reversal of loading, i.e., detail for ductility.
3. Develop a complete load path in the bridge whereby other elements of the structure will not be damaged before the yielding elements reach their maximum resistance ( capacity), and configure the system to provide sufficient deformability so that yielding can occur, i.e., capacity-protect the other elements in the load path.

The capacity design concept can be illustrated using the chain analogy described by Paulay and Priestley (1992) and shown in Figure 1-11. If one link of the chain is ductile and the tensile strength of that link is less than the strength of the other links, which may even be brittle, the chain will exhibit ductile behavior based on the behavior of the one ductile link. However, if any of the brittle links have strengths lower than that of the ductile link, then the chain will exhibit brittle behavior. In the case of a bridge, the entire lateral load path is analogous to the chain, and individual elements, such as columns, foundations, abutments, and superstructure comprise the links in the chain.

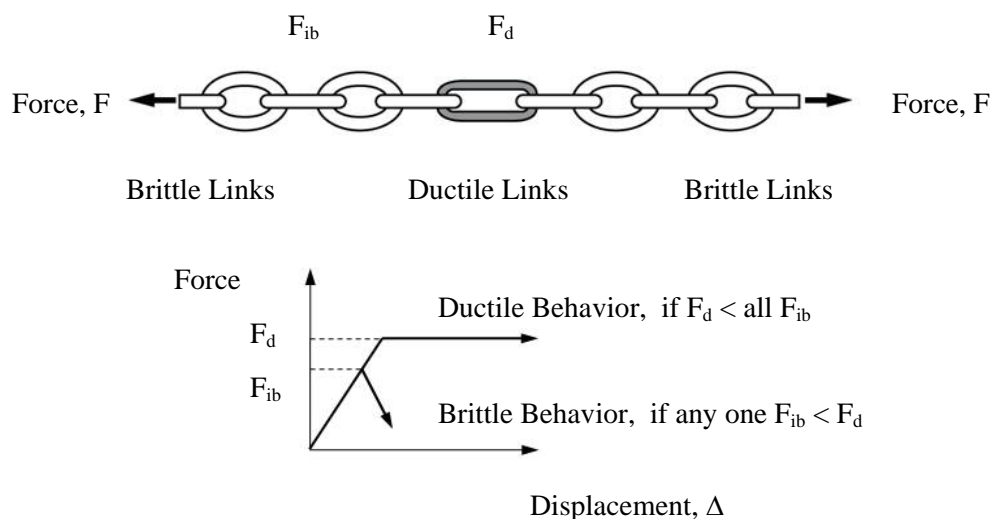


Figure 1-11 Chain Analogy for Capacity-Protected Design (after Paulay and Priestley, 1992)

### 1.5.3 Design Methodologies

Two similar but distinct methodologies have been developed to implement the road map in Section 1.4. These are the Force-Based Method (FBM) and the Displacement-Based Method (DBM).

The underlying philosophy used in both methods is to design a bridge that has, in its entirety, both ductility and deformability with some reserve to resist an earthquake even greater than anticipated in the design. The traditional approach in seismic bridge design has been to select key components that provide the ductility (e.g. columns) - and deformability (e.g. adequate capacity in movement joints) to resist the design level earthquake ground motions. Once these key components are selected, the remaining components are designed to provide a load path and displacements to accommodate the forces and deformations imposed on the selected key components without the remaining components losing their strength. This is known as capacity design approach, and has been part of the AASHTO seismic design approach for many years.

Fundamentally, both methods seek the same end – a capacity-designed structure where certain elements are designed to yield in a ductile manner and all the rest are designed to remain essentially elastic. It is only the method of achieving this result where the two methods differ. In the FBM, response modification factors are used to reduce elastic demand forces to obtain design yield forces in the columns and prescriptive details are then followed to ensure adequate ductility and capacity protection (Figure 1-12). On-the-other hand, in the DBM, the inelastic deformation capacity of the columns designed to satisfy the non-seismic load combinations, are determined explicitly by conducting section analyses and detailing provided to ensure adequate ductility and capacity protection for the elastic demand displacements (Figure 1-13).

Both methods require the conduct of a seismic demand analysis. This process, which is similar in both methods, includes generating a global analytical model, conducting a response analysis and selecting the forces and displacements from the analytical results for use in design of individual bridge components. The complexity of the analytical process is determined by the seismic hazard and the geometry of the bridge. Varying seismic hazard is recognized in both methods. In general, the higher the hazard, the higher the ductility demands and the more rigorous are the requirements for seismic design. In the end, the demand on the bridge must be compared and successfully reconciled against its capacity. This is accomplished for both methods, but in a different fashion for each.

### 1.5.3.1 Force-Based Method

The Force-Based Design Method (FBM) is the method traditionally used by the AASHTO *LRFD Bridge Design Specifications*. The method develops seismic design forces for the yielding elements by dividing the elastic seismic forces obtained from the demand analysis by an appropriate Response Modification Factor ( $R$ ). Inherent in this approach is the expectation that the columns will yield when subjected to the design ground motions at a force level equal to the reduced elastic demand. Graphically, the approach is illustrated in Figure 1-12, where the force,  $F$ , and displacement,  $\Delta$ , are global measures of the bridge response, e.g., total base shear and maximum displacement of the bridge. The elastic response line represents the response of the bridge if no damage and no yielding occur. An elastic analysis is based on such conditions. The maximum force obtained during shaking from an earthquake corresponds to the peak of the elastic plot and would likely be a large force to be resisted. In the FBM, yielding is permitted as shown by the lower bilinear plot, where the yield force ( $F_{yield}$ ) is the peak elastic force ( $F_{elastic}$ ) divided by  $R$ . If the bridge forms its plastic mechanism instantly (rather than progressively, one hinge at a time) and the period of vibration is such that  $\Delta_{demand}$  is equal to  $\Delta_{elastic}$  (the equal displacement rule), then the  $R$ -factor also corresponds to the ductility factor,  $\mu$ , as defined in Equation 1-2.

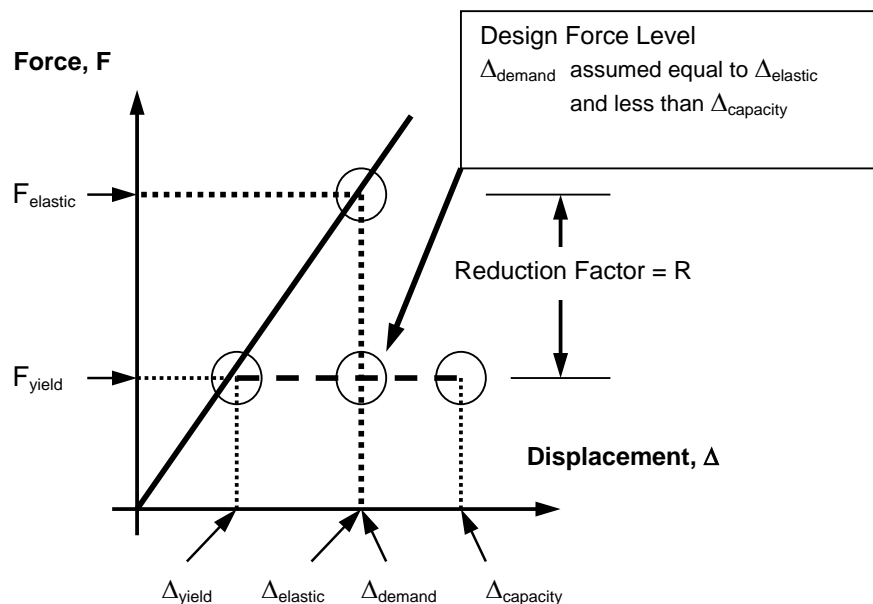


Figure 1-12 Calculation of Design Force Level and Displacement Demand in Force-Based Method

$$\mu = \frac{\Delta_{demand}}{\Delta_{yield}}$$

1-2

Thus, the *R*-factor is often thought of as being synonymous with the ductility factor which is a measure of ductility demand.

### 1.5.3.2 Displacement -Based Method

The Displacement-Based Method (DBM) is the method used in the AASHTO *Guide Specifications for LRFD Seismic Bridge Design*. Fundamentally, it has the same objective as the FBM, but the means are different. The DBM, unlike the FBM, does not calculate a specific design force for the yielding elements. Instead, the designer is free to proportion the yielding system as necessary to ensure that the displacement demand is less than the displacement capacity at each pier, provided that a minimum lateral strength threshold is provided for each pier and that all of the non-seismic load cases are also satisfied. Thus, the designer simply proposes a lateral load system and corresponding element strengths, and then checks to ensure that the displacement capacity is adequate, i.e. that  $\Delta_{capacity} > \Delta_{demand}$ . See Figure 1-13.

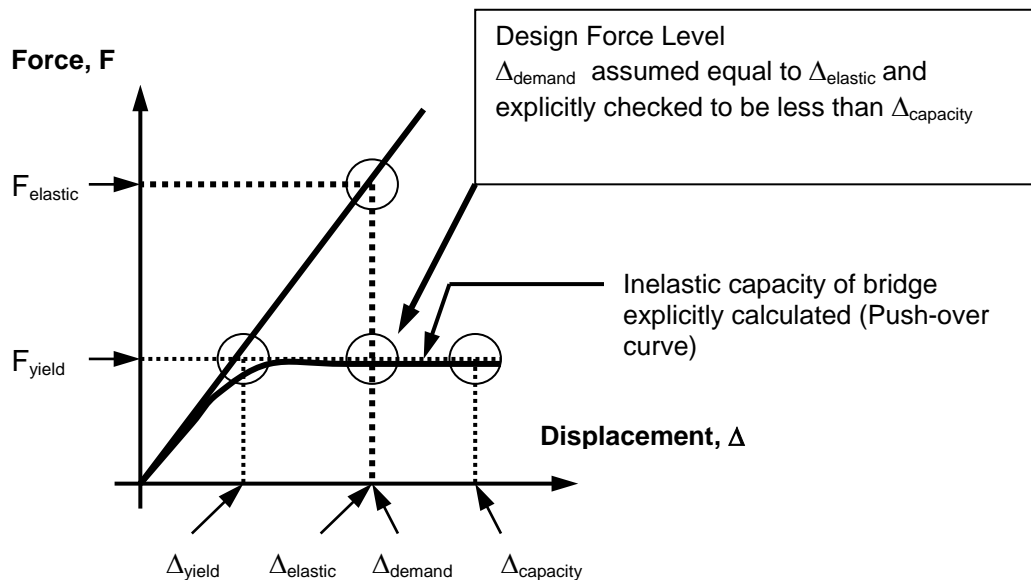


Figure 1-13 Calculation of Design Force Level and Displacement Demand in Displacement-Based Method

The capacity is based on the ductility of the yielding column elements, and may be controlled by both the longitudinal and transverse reinforcement in the columns and the configuration of the substructure (e.g.,

height-to-width aspect ratios of the columns and end fixity). Finally, a direct check of the displacement capacity is made relative to the demand.

## 1.6 SCOPE OF MANUAL

This Manual presents the theory and practice of seismic analysis, design, and retrofit of highway bridges in ten chapters. It also provides the background and underlying concepts behind the AASHTO LRFD specifications for seismic design (AASHTO, 2013, 2014, 2010) and explains in detail the seismic design provisions in these specifications. Topics covered in each chapter are as follows:

Chapters 2 and 3 describe how seismic loads are characterized for use in design, first by defining the ground motion hazard in the U.S., including site amplification effects (Chapter 2), and then by discussing other geotechnical hazards such as soil liquefaction and fault rupture (Chapter 3).

The basic principles of seismic design are introduced in Chapter 4. These principles are fundamental to good seismic design regardless of the code or specification selected for the design of a bridge. Chapter 5 presents methods for the calculation of seismic demands including both forces and displacements. Methods for modeling a bridge for use in these calculations, ranging from simple to complex, are also discussed.

Chapter 6 describes the inelastic behavior of bridges once they yield and explains how the plastic mechanism is established, thereby limiting internal forces. Then Chapter 7 explains how the elements of the structure, that are chosen to yield, are designed to withstand the expected plastic deformations. This chapter also explains how the remaining elements in the structure are protected against yielding or failure. In addition, both the Force-Based and Displacement-Based Methods are described. Chapter 8 outlines the seismic provisions of both the *AASHTO LRFD Bridge Design Specifications* (2013) and the *AASHTO Guide Specifications for LRFD Seismic Bridge Design* (2014) and explains in detail how capacity design is implemented and guided by these specifications. To improve the readability of the text, these two specifications are cited in this Manual as the *LRFD Specifications* and *Guide Specifications* respectively.

Chapter 9 provides an introduction to seismic isolation design, which corresponds to Global Strategy Type 3 in the *Guide Specifications*. The material in this chapter is consistent with the provisions in the *AASHTO Guide Specifications for Seismic Isolation Design* (2010). Finally, Chapter 10 gives an

introduction to the seismic retrofitting of bridges. This material extends the application of capacity design principles to existing bridges, while recognizing that it is not always possible to fully apply these principles to such structures. This chapter summarizes the methodology and approach given in the FHWA *Seismic Retrofitting Manual for Highway Structures: Part 1-Bridges* (2006).



## CHAPTER 2

### GROUND MOTION HAZARDS

#### 2.1 GENERAL

This chapter describes the fundamental principles of seismic hazard analysis, which is a recognized process for determining earthquake ground motions for use in seismic design. Two basic types of seismic hazard analysis (probabilistic and deterministic analysis) are commonly employed in design practice. AASHTO uses a probabilistic approach and in 2007 adopted a 1,000-year return period as the basis for design for ordinary bridges. However, occasionally a different return period, or a deterministic analysis, may provide an appropriate basis upon which to establish design ground motions. Sometimes a deterministic analysis may be warranted to validate or supplement the results of a probabilistic analysis. This chapter discusses the rationale in the selection of design earthquake return period(s) and the relative merits of, and fundamental differences between, the probabilistic and deterministic approaches. In addition, the procedure for obtaining design ground motions in accordance with the AASHTO criteria is presented.

Figure 2-1 outlines the four fundamental steps in a probabilistic seismic hazard analysis. In Step 1 (Seismic Source Identification), the seismic sources capable of generating strong ground motions at the project site(s) are identified and the geometries of these sources (i.e. their location and spatial extent) are defined. In Step 2 (Magnitude-Recurrence), a recurrence relationship describing the rate at which various magnitude earthquakes are expected to occur is assigned to each of the identified seismic sources. Together Steps 1 and 2 may be referred to as ‘seismic source characterization’. In Step 3 (Ground Motion Attenuation), an attenuation relationship (referred to as a ground motion prediction equation, or GMPE, in current practice) is assigned to each seismic source to describe the relationship between the amplitude of the ground motion and distance from the source, i.e., the link between earthquake magnitude, site-to-source distance, and the ground motion parameter of interest. In Step 4 (Probability of Exceedance), the results from the first three steps are combined to produce a curve relating the value of the ground motion parameter of interest at the site(s) of interest to the probability that it will be exceeded in a specified time interval.

Deterministic seismic hazard analysis may also be described as a four step process. However, in a deterministic analysis, Step 2 (Magnitude-Recurrence) is abbreviated by assigning a discrete, deterministic magnitude to each seismic source. The magnitude assigned to each source is generally some sort of maximum expected magnitude. Then, Step 4 consists solely of determining which source from among the sources identified in Step 1 generates the maximum value of the ground motion parameter of interest at the site(s).

Each of the steps described above for the probabilistic and deterministic methods of analysis is discussed in the following sections, along with further discussion of how the deterministic approach differs from the probabilistic approach. Additional explanation of these two approaches is given in the Reference Manual to NHI Course 130094 on 'LRFD Seismic Analysis and Design of Transportation Geotechnical Features and Structural Foundations' (NHI 2011). Selection of the target ground motion level for use in design, characterization of the design ground motions from the results of a probabilistic or deterministic seismic hazard analysis, and details of the procedure for obtaining design ground motions in accordance with the AASHTO probabilistic seismic hazard criteria are also discussed in the following sections.

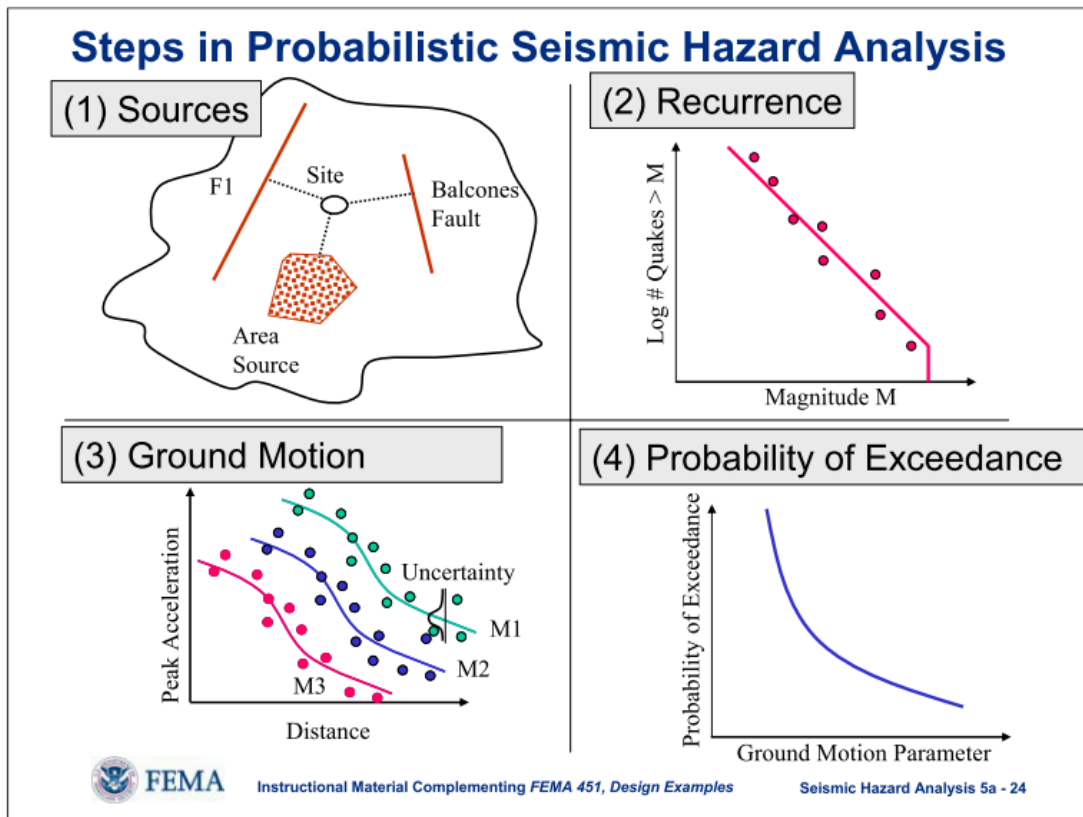


Figure 2-1 Steps in Probabilistic Seismic Hazard Analysis

## 2.2 SEISMIC HAZARD ANALYSIS

### 2.2.1 Seismic Source Identification

The first step in seismic source characterization is to identify the seismic sources capable of generating strong ground motions at the bridge site. An important step in source identification is to develop a model of the geometry of each source. Two basic geometries are generally used for this purpose: area source zones (sometimes discretized into point sources), and fault sources (typically modeled as line sources). Both sources are conceptually illustrated in Figure 2-2.

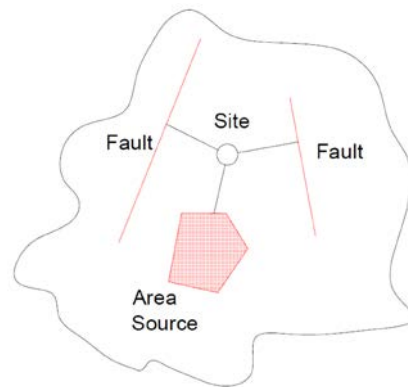


Figure 2-2 Geometry of Seismic Sources in Seismic Hazard Analysis

Well-defined faults are usually modeled as line sources, while area source zones are used to model spatially distributed seismicity. Source geometry also includes the depth beneath the ground surface of the source. In the 1970s and early 1980s, seismic source characterization was typically based on area sources that were defined using historical seismicity data. In many parts of the world, particularly those without known faults, modeling seismic sources using area sources is still standard of practice. In the United States (especially in the western U.S.), faults that have the potential to produce strong ground shaking have generally now been well defined by geological and seismological studies. However, even in regions with well known faults, area sources are commonly included in the source characterization to account for background seismicity and for earthquakes that may occur on faults that have not yet been identified.

In state-of-the-practice seismic hazard analyses (such as those currently used by the USGS), fault sources are treated as planes and area sources are treated as volumes to account for the depth of the seismic activity. Accounting for the three-dimensional nature of seismic sources (i.e. including the depth dimension) is necessary to properly account for the distance between the site and a specific seismic

source. This subject is further discussed in Section 2.2.3 in the discussion on ground motion prediction equations (formerly referred to as attenuation relationships).

### 2.2.2 Magnitude-Recurrence Relationships

After defining the geometry of each seismic source that can contribute to the strong ground shaking at the bridge site, the next step in a seismic hazard analysis identifies the size of the earthquake(s) associated with each seismic source.

In practice, the size of an earthquake is quantified by the *earthquake magnitude*,  $M$ , a measure of the energy released by an earthquake. A variety of different earthquake magnitude scales exist, and the difference among these scales is the way energy content is quantified. Characteristics used to quantify energy content include the local intensity of ground motions, the body waves generated by the earthquake, the surface waves generated by the earthquake, and the strain energy released by the fault rupture. The first earthquake magnitude scale, and the scale commonly cited in media reports and non-technical publications (often incorrectly), is the Richter magnitude scale. *Richter magnitude* is sometimes also referred to as the *local magnitude*, as it is based upon the local intensity of the ground motions, and is designated by the symbol  $M_L$ . While Richter magnitude was the first scale developed to quantify earthquake magnitude, it is generally not used in engineering practice anymore. In the eastern United States, earthquake magnitude was historically measured as a *short period body wave magnitude*,  $m_b$ . However, the long period body wave magnitude,  $m_B$ , was also sometimes used in the central and eastern United States. In California, earthquake magnitude was historically often measured as  $M_L$  or *surface wave magnitude*,  $M_s$ .

Due to the limited strength of near surface geologic materials, some of the historical magnitude scales discussed above tend to reach an asymptotic upper limit (a phenomenon referred to as ‘saturation’). In part to compensate for this phenomenon, and in general to provide a more consistent and logical basis for quantifying the size of earthquakes, the *moment magnitude*,  $M_w$ , scale was developed by seismologists Hanks and Kanamori (1979). The moment magnitude of an earthquake is a measure of the potential energy released by the earthquake.  $M_w$  is proportional to the ‘seismic moment’, defined as a product of the rupture strength of the fault (called ‘material rigidity’ by seismologists and geotechnical engineers), the fault rupture area, and the average dislocation (displacement or ‘slip’) of the rupture surface. *Moment magnitude* has been adopted by the most of the earthquake engineering community as a unifying,

consistent measure of earthquake energy content. For this reason, *moment magnitude* is used in this document to describe earthquake magnitude, unless noted otherwise.

$M_w$  is defined by the following equation:

$$M_w = \frac{2}{3} \log_{10}(M_o) - 10.7 \quad 2-1$$

where  $M_o$  is defined as the 'seismic moment' (dyne-cm), given by the following equation:

$$M_o = \mu \times A \times D \quad 2-2$$

where  $\mu$  is the rupture strength (shear modulus) of the crust (dyne/cm<sup>2</sup>),

$A$  is the area of the fault rupture (cm<sup>2</sup>), and

$D$  is the average displacement (slip) over the rupture surface (cm).

$M_w$  and  $M_o$  both have units of force times length (dyne-cm), or work done, and hence both are direct measures of the energy released by fault rupture during an earthquake.

From Equation 2-1, it can be shown that seismic moment is related to moment magnitude as follows:

$$M_o = 10^{(3/2(M_w + 10.7))} \quad 2-3$$

From Equation 2-3, it can be seen that  $M_o$  is logarithmic quantity, i.e. for each unit increase in moment magnitude,  $M_w$ , the seismic moment,  $M_o$  (energy released by fault rupture), increases by a factor of 31.6. Hence, the energy released by magnitude 6, 7 and 8 earthquakes will be 31.6, 1,000 and 31,623 times greater, respectively, than the energy released by a magnitude 5 earthquake. The additional energy associated with a large magnitude earthquake will not only usually induce stronger shaking at a specific site but will also subject a larger area to strong shaking and cause the duration of strong shaking to be longer.

In both deterministic and probabilistic seismic hazard analyses, the maximum magnitude earthquake that can be generated for each seismic source must be defined. In a deterministic seismic hazard analysis, knowledge of the maximum magnitude, or a characteristic magnitude, for each fault is generally sufficient. In a probabilistic hazard analysis, a magnitude distribution function (i.e. the rate of occurrence

of various magnitude earthquakes, including the maximum magnitude earthquake) needs to be defined in addition to the maximum earthquake. The magnitude distribution function is commonly referred as the magnitude-recurrence relationship and relates earthquake magnitude to the frequency of occurrence, i.e. to the number of earthquakes per year equal to or greater than that magnitude, for a seismic source. The need to define the frequency of occurrence of earthquakes with a magnitude-recurrence relationship is one of the main distinctions between deterministic and probabilistic seismic hazard analyses.

Two different types of magnitude recurrence relationships, a truncated Gutenberg-Richter relationship and a characteristic relationship, are commonly used in probabilistic seismic hazard analyses, often concurrently. Widely used in the 1970s and early 1980s, the Gutenberg-Richter recurrence model is given by the following simple equation:

$$\text{Log}_{10}(n) = a + b \times M_w \quad 2-4$$

where  $n$  is the annual number of earthquakes with magnitude  $M_w$ , and the  $a$  and  $b$  parameters define the recurrence rate based on curve fitting to historical seismicity data.

One limitation of the original Gutenberg-Richter model was that it produced as small but finite number of very large magnitude earthquakes that could unrealistically influence the seismic hazard over large exposure periods. Therefore, in current practice the Gutenberg-Richter model is truncated at a maximum magnitude assigned to the causative fault. The truncated Gutenberg-Richter model (also referred to as the truncated exponential model) works well for large regions (e.g. worldwide seismicity database), but does not do so well for finite fault sources (Swartz and Coppersmith, 1984) and for seismicity data measured over smaller regions during the relatively short time frame of instrumental seismicity (i.e., since 1933, the start of seismicity measurements using scientific instruments). Furthermore, geologic evidence suggests that the truncated exponential model may under-predict the occurrence rate of large magnitude earthquakes on well-defined fault sources, e.g. on the San Andreas Fault in California. Therefore, other means are usually necessary to supplement the truncated exponential recurrence model at the large earthquake end of the magnitude-recurrence relationship.

In current practice, a model referred to as the characteristic earthquake model” is employed to account for the recurrence of large magnitude earthquakes on well known faults as a complement to the truncated exponential model, which is used to account for the smaller magnitude earthquakes. This model is based upon observations that individual faults tend to generate earthquakes of a preferred magnitude due to the

geometry of the fault and the rate of accumulation of stress on the fault due to tectonic forces (i.e. the tectonic slip rate). As a result of this phenomenon, there is a ‘characteristic’ size (magnitude) of earthquake that a fault tends to generate based on the dimension of the fault segment and associated slip rate. In the characteristic model, the occurrence of large earthquakes is assumed to be uniformly distributed over a rather narrow range of characteristic magnitudes, typically within 0.5 to 1.0 magnitude units of the maximum magnitude assigned to the fault. The rate at which earthquakes of the characteristic magnitude occur is based on both geodetic and geologic data, the latter from paleoseismic studies that can cover a much longer history of the earth’s geologic processes than the historic record.

In summary, a composite of the truncated Gutenberg-Richter and characteristic models is often used to describe magnitude-recurrence in seismic hazard analysis. The truncated Gutenberg-Richter model is used to describe the recurrence of small magnitude events based upon instrumental seismicity and the characteristic model is used to describe magnitude recurrence in the large magnitude range based upon geologic data, such as by the fault’s historic slip rate.

### **2.2.3 Ground Motion Prediction Relationships**

The next step in a seismic hazard assessment (after characterizing seismic source geometry and magnitude-recurrence) involves defining the appropriate ground motion prediction equation(s), or GMPE(s), for the strong ground motions. A GMPE, previously referred to as an attenuation relationship, relates the design ground motion shaking parameter(s) of interest (e.g. peak ground acceleration or spectral acceleration as a function of modal period) to a combination of magnitude ( $M$ ) and distance ( $D$ ). As shown in Figure 2-3, a GMPE is typically characterized by a median value and a distribution about the median. The preferred method for developing a GMPE is to base the equation on statistical analysis of strong motion data from historical earthquakes. However, in some tectonic regimes there is not sufficient historical data from which to develop such a relationship. In these cases, empirical and analytical seismological models are employed to supplement the available historical data.

Historical strong motion data show a wide range of scatter, even after reconciling discrepancies due earthquake magnitude, source mechanism, tectonic regime, and site conditions. This variation in ground motion among recorded data occurs even within a single earthquake event. In addition to the intra-event variation, there is also scatter in the data from multiple earthquakes. Thus, it is generally recognized that GMPEs need to reflect the statistical variation (commonly referred as the uncertainty) in the strong

motion data. Hence, relationship GMPE is typically presented in terms of a median relationship with the scatter about the median modeled in terms of a statistical distribution function.

Figure 2-3 presents an example of a common PHGA (Peak Horizontal Ground Acceleration) GMPE along with the historical strong motion data used to develop it. The dots in Figure 2-3 represent the historical data points while the solid lines represent the median values and the dashed lines represent the 95% confidence interval from statistical analysis. The bell-shaped curves in Figure 2-3 show, at 1 km distance, the statistical distribution of predicted ground motion parameter values.

Most current GMPEs assume a log-normal, or Gaussian, distribution functional form to describe the scatter in ground motion attenuation. If the functional form of the distribution is known, the scatter about the median can be characterized simply in terms of the standard deviation or variance of the ground motion parameter. Hence, modern GMPEs are typically defined by an equation for the median value of the ground motion parameter as a function of magnitude and distance plus the standard deviation ( $\sigma$ ) for the specified functional form (the standard deviation may also be a function of magnitude and/or distance). Most current GMPEs provide for prediction of both peak ground acceleration and spectral acceleration at various modal periods. A few GMPEs also provide for predictions for other ground response parameters, e.g. peak ground velocity.

The role the GMPE(s) plays in the outcome of both probabilistic and deterministic seismic hazard analysis cannot be over-emphasized. The state-of-the-art on the subject is constantly evolving: almost every major earthquake leads to a change in the corresponding GMPEs. As the state-of-the-art has progressed, GMPEs have become more complex and greater expertise may become necessary in selecting and implementing the appropriate relationships.

GMPEs are particularly sensitive to tectonic regime. In the United States, tectonic regimes that may be encountered include (1) shallow crustal earthquakes in active tectonic regions, e.g. for the western U.S., (2) subduction zone earthquakes in Alaska and the northwestern U.S., (3) stable continental regions in the central and eastern U.S., and (4) extensional tectonic regions such as those in Nevada and Arizona. Individual GMPE modelers often have different viewpoints about earthquake mechanisms and hence often employ different variables in their specific GMPE.

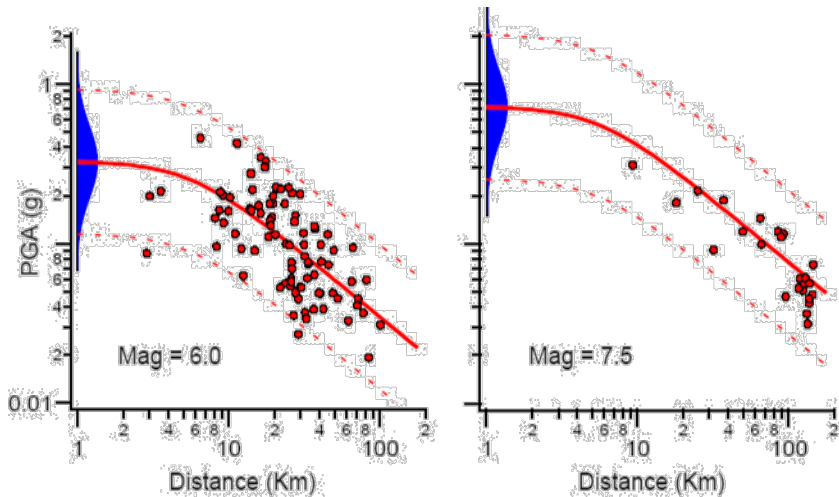
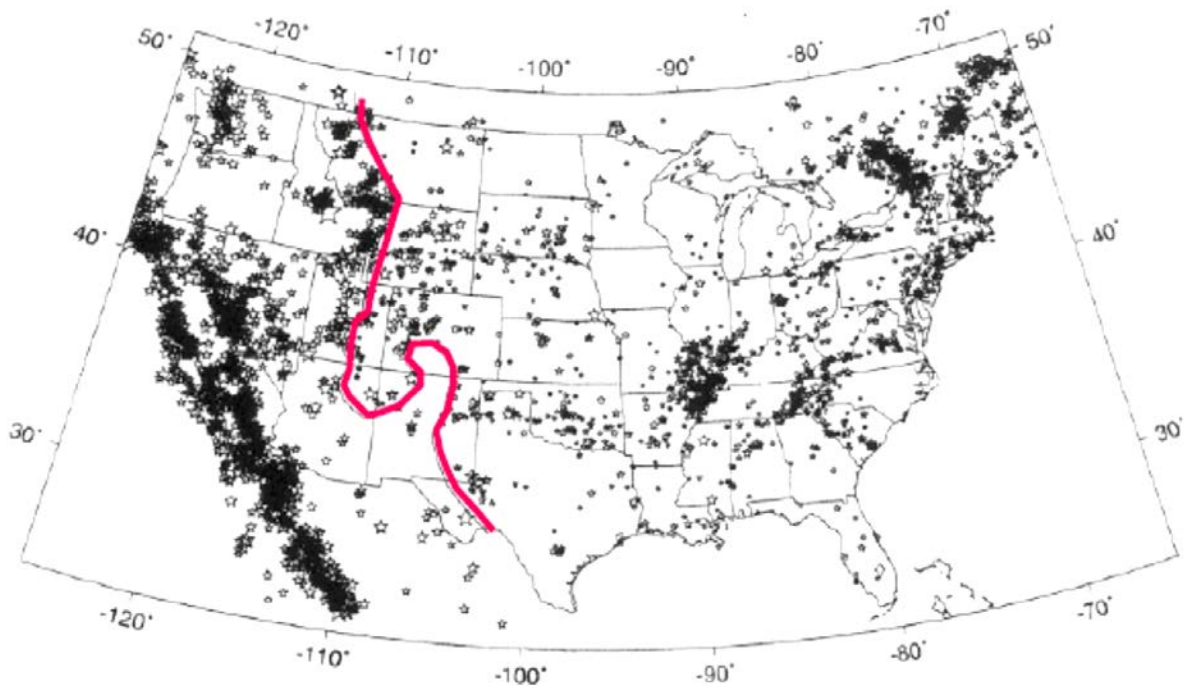


Figure 2-3 Example of PHGA Attenuation Relationship for Strike-Slip Earthquakes and Soil Sites. (Boore, Joyner, and Fumal, 1997)

The current viewpoint among engineering seismologists is that there are fundamental differences in strong motion attenuation between different tectonic regimes such as between the shallow crustal earthquakes in the western U.S. (WUS), subduction zone earthquakes in the WUS, and mid-continent earthquakes in the central and eastern U.S. (CEUS), leading to the adoption of different attenuation models in each of these tectonic regimes. The boundary between WUS and CEUS tectonic regimes is shown in Figure 2-4, approximately lying along the Rocky Mountains. West of this boundary is referred to as the more seismically active WUS region and east of the boundary is the less active CEUS region. In general, ground motions appear to attenuate with distance less rapidly in the CEUS compared to the WUS. However, probabilistic ground shaking levels are higher in the WUS compared to the CEUS due to higher activity rates, especially at longer modal periods (for example, 0.5 seconds or more).

Figure 2-5 compares results from WUS and CEUS GMPEs for a typical Magnitude 6.5 event at 20 km. The CEUS models used to develop this figure include two different analytical models (developed to compensate for the lack of sufficient strong motion data) plus a third model that is a weighted average of the first two models (NUREG, 2001). Figure 2-5a presents a comparison of spectral acceleration curves (i.e. acceleration response spectra normalized by the PGA) and Figure 2-5b presents a comparison of spectral displacement curves from these models. The CEUS spectral curve has a higher amplitude at short modal periods ( $T < 0.1$  sec) while the WUS curve is higher in the potentially more damaging longer period range, the range of periods of importance in most bridge structural designs. At a period of one second, the WUS spectral acceleration is about twice the amplitude of the CEUS acceleration for the same PGA. The WUS spectral amplitude is over 3 times the amplitude of CEUS spectrum at a period of

3 sec, for the same PGA. It is noted that this comparison does not consider the effect of even more intense, long-period motions associated with forward directivity of near-fault ground motions, a phenomenon that can be encountered in the WUS.

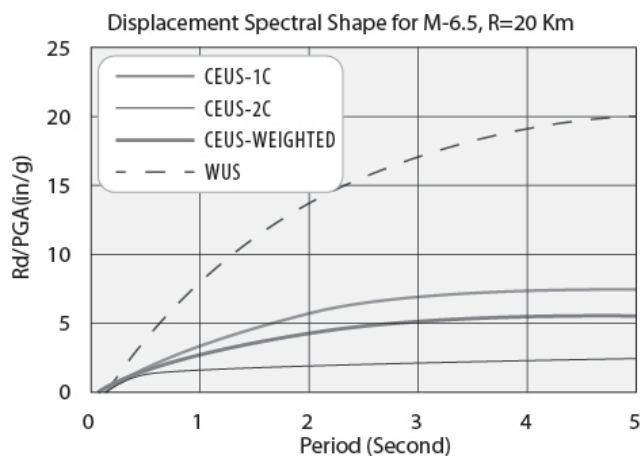


Note: Different attenuation relationships are used for different regions

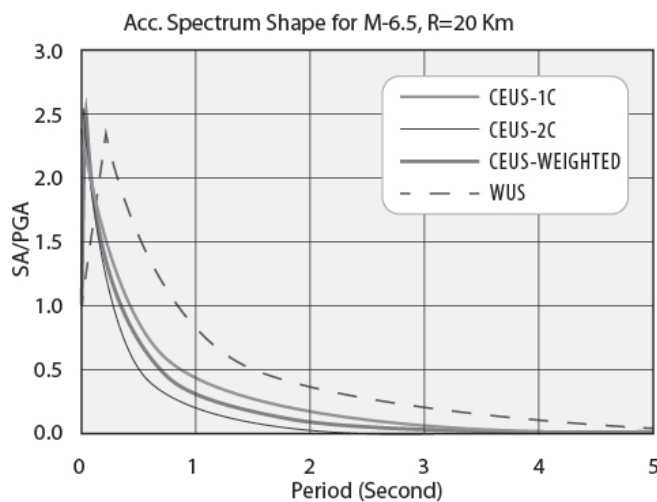
Figure 2-4 Boundary Defining WUS and CEUS Seismic Hazard Regions Based on Change in Attenuation Relationship (Based on USGS National Seismic Hazard Map, 2002 Edition.)

#### 2.2.4 Uniform Hazard Spectra

An essential output from a probabilistic seismic hazard analysis is a plot of the ground motion parameter of interest, say PGA, versus the annual probability of exceeding that parameter. This plot is called a seismic hazard curve. Figure 2-6 shows a plot of PGA versus the annual probability of exceedance seismic hazard curve from the seismic hazard analysis for a site in southern California. The inverse of the annual probability of exceedance (return period in years), is shown on the right vertical axis. The figure shows not only the total probability of exceedance but also the contributions from individual seismic sources. The annual probability of exceedance from each source is summed to give the total hazard curve, e.g. the “All SOURCES” curve in Figure 2-6.



(a)



(b)

Figure 2-5 Comparison Between Spectral Curves for the WUS and CEUS Hazard Regions; a) Acceleration Spectra for M = 6.5, and R = 20km; b) Displacement Spectra for M = 6.5 and R = 20km

A hazard curve such as the one in Figure 2-6 may be used in several ways. For example the level of ground motion with a 10% probability of exceedance in 50 years at this site, i.e. for a return period of 475 years, is 0.55g. (10% exceedance in 50 years is an annual exceedance rate of 0.0021 events per year, or a return period of 475 years). This same curve indicates that if the return period was doubled to approximately 1,000 years the design ground motion would be 0.65g. It can thus be observed that doubling the return period does not double the design ground motion. Likewise if a bridge at this site has

an elastic strength of 0.2g, this capacity will be exceeded about once every 15 years (annual probability of exceedance for this ground motion = 0.07).

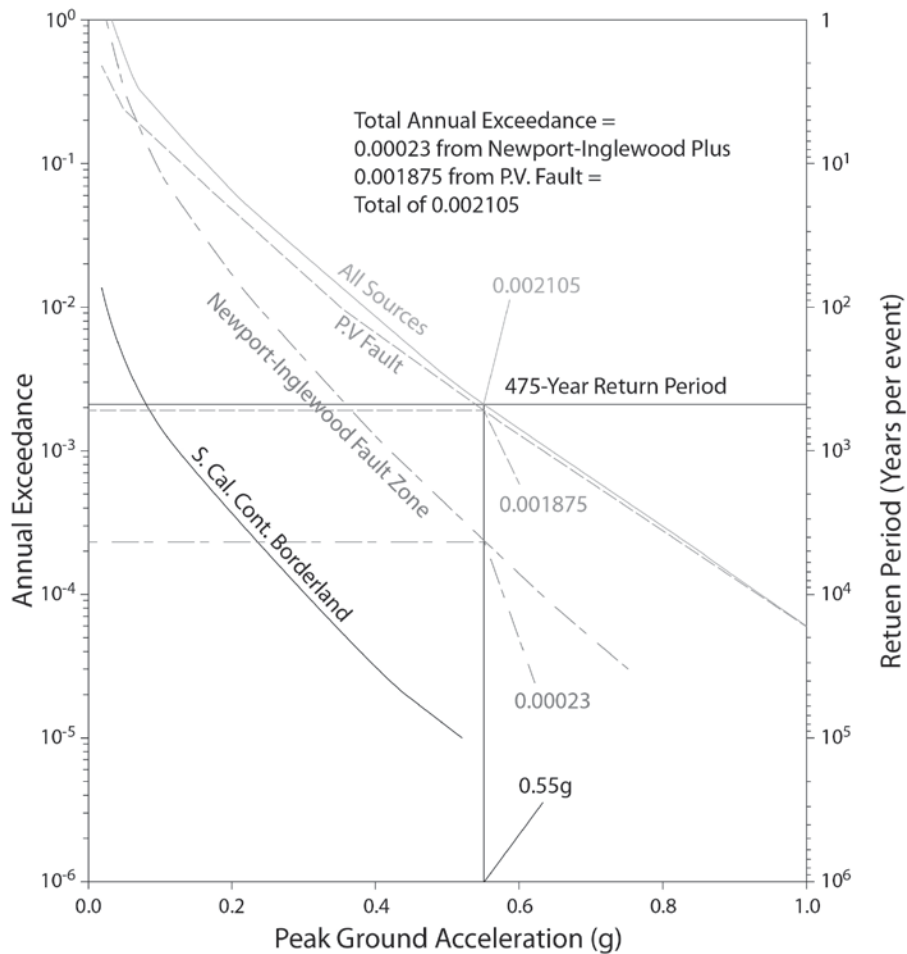


Figure 2-6 Seismic Hazard Curve for Site in Southern California: Individual Contributions and Total Hazard from Three Faults

Similar hazard curves can also be generated for spectral acceleration at selected modal periods. Then, by plotting the spectral acceleration against modal period for a specified exposure period and probability of exceedance, or return period, what is referred to as a uniform hazard response spectra can be extracted from the hazard curves at various return periods. The resulting spectra are called uniform hazard spectra (UHS) because the ground motion parameter at all periods in a given spectrum has the same, consistent hazard level, or return period.

The return period is a fundamental parameter for quantifying the risk assumed in design. The inverse of the return period in years is essentially the annual risk. As noted earlier, AASHTO adopted a 1,000-year

return period in 2007 for the no-collapse design limit state of ordinary bridges, wherein damage is expected to occur during the 1000-yr ground motion, but collapse of one or more spans must be avoided. The annual risk level of 0.001 associated with the 1000-yr return period may be compared to that for other natural hazards, such as extreme weather (floods and high wind) when making decisions regarding the risk level for design. At an annual risk of 0.001 the seismic risk level is lower than the risk level typically employed for flooding and scour, but public reaction following loss of life, damage and business disruption in recent earthquakes (Loma Prieta, 1989, Northridge, 1994, Kobe, 1995, and Chi-chi, 1999) indicates that the public has less tolerance for damage from rapid onset disasters such as earthquakes, even though they are relatively rare, than for other natural hazards. Furthermore, in some circumstances even lower risk levels may be appropriate such as for particularly important bridges. For example, a 1,500 year return period (0.00067 annual risk) was adopted for the design of the new East Bay Spans for the San Francisco Oakland Bay Bridge based upon recommendations from Caltrans' Seismic Advisory Board. Elsewhere, a 2,500-year return period (0.0004 annual risk) has been employed for design of major critical water crossings in the U.S., including the seismic retrofit of several long-span bridges in New York City, the Arthur Ravenal, Jr. Bridge across the Cooper River in Charleston, and the Tacoma-Narrows Second Crossing in Seattle.

While the return period (or annual risk) is a convenient way to interpret the risk associated with the design ground motions, many design engineers prefer to look at the risk over the bridge's design life, sometimes referred to as the exposure period. By assuming that earthquakes occur randomly (mathematically, assuming a Poisson distribution of earthquake in time, i.e. that if an earthquake occurs today, it still has the same chance of occurring tomorrow), the following equation can be used to relate the probability of exceedance,  $P$ , for an exposure period  $t$  to the annual risk  $\gamma$  (the annual probability of exceedance, or the inverse of return period  $R$ ):

$$P = 1 - e^{-\gamma t} \quad 2-5$$

For example, for a return period of 1,000 years,  $\gamma = 0.001$ , the probability of exceedance during a 50-year exposure period ( $t = 50$  year) is about 5%. If the exposure period becomes 75 years (a common assumption for the design life of highway bridges), the probability of exceedance is approximately 7%.

Care must be exercised in choosing the exposure period, or design life, for a bridge. If the design life is too short, the design earthquake ground motion can become so low that it has little chance of representing the ground motion in a real earthquake. Also, while a design life of 50 years is commonly assumed for

economic analysis of many engineered structures, this rarely represents the true exposure period for a transportation facility, especially for more critical structures. For example, the Manhattan Bridge in New York City was opened to traffic in 1909. The bridge has now been in service for about 100 years, probably much longer than its intended design life. But it is inconceivable that this bridge would be demolished today and chances are that, with routine maintenance, it will be in service for at least another 50 years. However, if one becomes too rigorous in treating the exposure period as the design life of a critical structure, the probabilistic design ground motions may become exceedingly high, in some cases significantly greater than the median value of the maximum magnitude earthquake for the site. For this reason, some seismic codes and design specifications place a deterministic cap on the level of ground motions used in design. AASHTO has adopted an exposure period of 75 years for ordinary bridges. The 1000-yr return period used in design corresponds to a probability of exceedance of 7 percent over this 75-year exposure period.

### **2.2.5 De-aggregation of Design Earthquake, Magnitude and Distance**

While the uniform hazard spectrum (UHS) is the most common means of characterizing the seismic hazard for use in design, some structural and many geotechnical analyses require additional information about the design earthquake that is associated with the UHS, e.g. the earthquake magnitude. For this purpose, the UHS can be decomposed into the contributions from each individual seismic source to give the corresponding magnitude and distance combinations. This decomposition process is known as deaggregation. Deaggregation of the seismic hazard enables identification of the magnitude and distance combinations that make the most significant contributions to the seismic hazard. This information is used, for example, when developing acceleration time histories for structural and geotechnical time history analyses. The deaggregated magnitude is also necessary for certain geotechnical analyses, including the evaluation of liquefaction potential and in some geotechnical deformation analyses, where the magnitude parameter plays a significant role because of its direct relationship to the duration of shaking.

The AASHTO specifications do not provide information on deaggregation of the seismic hazard, i.e. on the earthquake magnitude(s) associated with the ground shaking levels. Fortunately, the USGS does provide an interactive application for recovering the deaggregated hazard data associated with the National Seismic Hazard Maps. For consistency, the 2002 deaggregation data for a 975 year return period should be employed with the AASHTO ground motions. This information can be found at

<http://geohazards.usgs.gov/deaggint/2002/>. Deaggregation for other return periods and for the most recent (2008) National Seismic Hazard Maps can also be accessed from this web page. Deaggregation data can be recovered from this site in tabular form, as shown in Table 2-1, and in graphical form, as illustrated in Figure 2-7.

Selecting a representative design earthquake magnitude from the deaggregated magnitude data is complicated, in part because each modal period on a UHS will have a different, unique magnitude deaggregation. The dependence of magnitude deaggregation on modal period occurs because earthquake ground motion attenuation depends upon magnitude and distance, and this dependence is different for every modal period. For example, the spectral acceleration at short periods (including the zero period or peak ground acceleration) tends to attenuate faster than at longer periods. Furthermore, large magnitude earthquakes tend to have more energy at longer modal periods when compared to smaller magnitude events. Therefore, the magnitude deaggregation for shorter periods tend to be biased towards smaller magnitude and closer earthquakes compared to longer periods. Table 2-1 illustrates this effect, presenting the magnitude deaggregation for the seismic hazard at a site in Bakersfield, California, at periods of 0.0 sec (the PGA) and 1.0 sec (a frequency of 1 Hz) for ground motions with a 2% probability of exceedance during a 50-year exposure period, which is the same as a 10% probability of exceedance in 250 years, or a return period of approximately 2,500 years.

Another complicating factor when selecting a design magnitude from deaggregation data is the distributed nature of the magnitude data. Sometimes, the magnitude deaggregation falls in a narrow band, as illustrated by the bold points in Table 2-1 and selection of the dominant magnitude for a given spectral acceleration is relatively straight forward, although it may still depend upon period. However, at other times the magnitude distribution is broadly distributed or multi-modal. Figure 2-7 graphically illustrates the bi-modal distribution of the deaggregated seismic hazard for Augusta, Georgia, at a period of 1 second for a 2,500 year return period. The seismic hazard in this case is split between two major seismic sources of different dominant magnitudes: the M 7.3 Charleston source and the M 8.0 New Madrid source. While the Charleston source contributes a greater percentage to the overall hazard (and is thus identified in the figure as the dominant source), the New Madrid source is potentially more damaging to certain types of structures. The choice of dominant magnitude is therefore not that straight forward and requires engineering judgment. Furthermore, as the site of interest moves, the distribution of the hazard changes and the selection of dominant magnitude may change. For instance, if the site of interest in the example presented in Figure 2.7 moved closer to New Madrid and away from Charleston, the magnitude distribution would become more weighted towards the larger New Madrid event.

**TABLE 2-1 MAGNITUDE DEAGGREGATION FOR BAKERSFIELD, CALIFORNIA,  
FOR A 2,500-YR RETURN PERIOD**

Deaggregated Seismic Hazard										
(a) Case 1. Modal Period = 0.0 s, PGA = 0.4244 g										
Deaggregated Seismic Hazard PE = 2% in 50 years pga										
Bakersfield CA 35.373 deg N 119.018 deg W PGA=0.42440 g										
	M<=	5.0	5.5	6.0	6.5	7.0	7.5	8.0	8.5	9.0
d<=	25.	0.000	18.239	18.339	<b>32.288</b>	18.484	0.000	0.000	0.000	0.000
	50.	0.000	0.019	0.024	0.086	4.200	7.059	0.000	0.000	0.000
	75.	0.000	0.000	0.001	0.006	0.033	0.019	1.154	0.000	0.000
	100.	0.000	0.000	0.000	0.000	0.015	0.008	0.000	0.000	0.000
	125.	0.000	0.000	0.000	0.000	0.009	0.002	0.000	0.000	0.000
	150.	0.000	0.000	0.000	0.000	0.001	0.003	0.000	0.000	0.000
	175.	0.000	0.000	0.000	0.000	0.001	0.000	0.000	0.000	0.000
	200.	0.000	0.000	0.000	0.000	0.007	0.002	0.000	0.000	0.000
(b) Case 2. Modal Period = 1.0 s. SA = 0.38360 g										
Deaggregated Seismic Hazard PE = 2% in 50 years 1hz										
Bakersfield CA 35.373 deg N 119.018 deg W SA= 0.38360 g										
	M<=	5.0	5.5	6.0	6.5	7.0	<b>7.5</b>	<b>8.0</b>	8.5	9.0
d<=	25.	0.000	0.957	2.329	17.096	16.216	<b>0.000</b>	<b>0.000</b>	0.000	0.000
	50.	0.000	0.004	0.019	0.272	12.374	<b>23.708</b>	<b>0.000</b>	0.000	0.000
	75.	0.000	0.000	0.001	0.019	0.254	<b>0.208</b>	<b>26.228</b>	0.000	0.000
	100.	0.000	0.000	0.000	0.001	0.074	0.097	0.000	0.000	0.000
	125.	0.000	0.000	0.000	0.001	0.037	0.016	0.000	0.000	0.000
	150.	0.000	0.000	0.000	0.000	0.006	0.029	0.008	0.000	0.000
	175.	0.000	0.000	0.000	0.000	0.002	0.006	0.000	0.000	0.000
	200.	0.000	0.000	0.000	0.000	0.015	0.025	0.000	0.000	0.000

### 2.2.6 Probabilistic versus Deterministic Analysis Methods

In a deterministic seismic hazard analysis, individual earthquake scenarios (i.e. scenarios of specified earthquake magnitude and distance from the site to the seismic source) are developed for each relevant seismic source and a specified ground motion probability level is selected. By tradition, the probability level is taken to be either (i) the median (i.e. the zero standard deviation), or (ii) the mean-plus-one standard deviation (i.e., the 84-percentile confidence limit) ground motion attenuation level. This level of attenuation is then used to compute the ground motion demand for design. The approach is ‘deterministic’ in the sense that a single-value of each parameter: magnitude, distance, and number of standard deviation, is selected for each scenario.

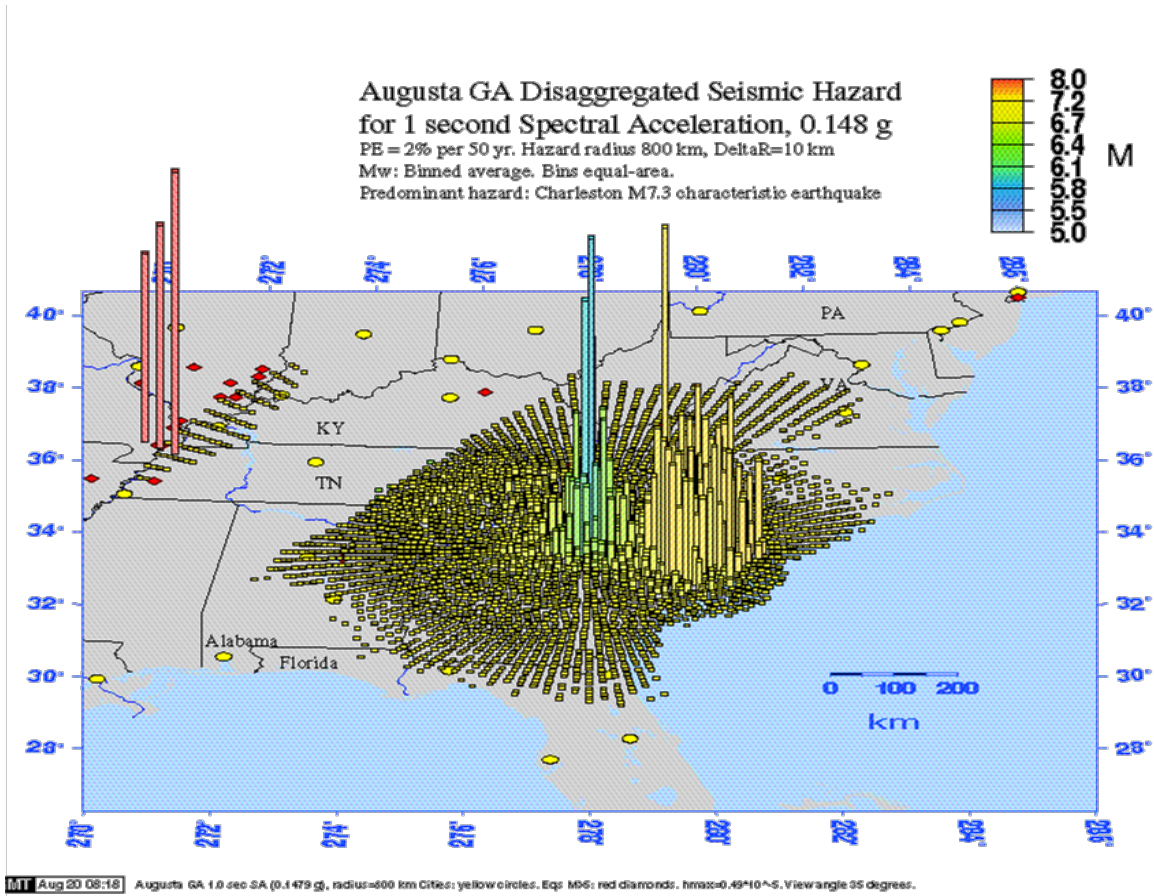


Figure 2-7 Magnitude Deaggregation for Augusta, GA, at 1.0 sec Period for a 2,500-year Return Period: Predominant Hazard is Charleston M7.3 Characteristic Earthquake

In practice, the scenario earthquake is usually some sort of maximum magnitude event, e.g. the maximum magnitude expected in the currently known tectonic framework (sometimes termed the Maximum Considered Earthquake, or MCE) or the maximum magnitude earthquake expected during some specified exposure period (for instance, in a 100-year period). Furthermore, this maximum magnitude event is usually placed at the closest approach of the seismic source to the site, sometimes referred to as the ‘worst case scenario’. However, if the median GMPE is used, as is the current practice for most transportation facilities, the resulting ground motion will not, in fact, be the worst case scenario, as 50% of the earthquakes of the maximum magnitude occurring at that location will produce ground shaking greater than the median value.

In the probabilistic seismic hazard approach, the relative likelihood of all possible and relevant earthquake scenarios (all possible magnitude and location combinations) are considered as well as all possible ground motion probability levels. Therefore, the probabilistic approach incorporates uncertainties with respect to earthquake location, magnitude, and ground motion, producing a weighted average of all possibilities that is a best estimate of the risk associated with seismic activity. For this reason, the probabilistic approach is considered the most appropriate basis for making rational design decisions about risk versus benefit and has been widely adopted by the engineering community for use in establishing design ground motions. However, even after the probabilistic approach has been embraced, a decision still must be made about the appropriate level of risk level to use in design.

For critical engineering facilities, e.g. lifeline bridges, hospitals, nuclear power plants, and high hazard dams, engineers and other decision makers are sometimes uncomfortable with use of a probabilistically-based design level. Oftentimes, the decision makers express a desire to design these critical facilities for the so-called worst case scenario. In such cases, the deterministic approach of employing a Maximum Credible Earthquake is sometimes used. However, as noted above, the deterministic approach may not lead to a worst case ground motion prediction, particularly if the median GMPE is used, due to uncertainties regarding ground motion attenuation. Use of a median plus one standard deviation (84 percentile) ground motion level, as practiced for some critical structures, e.g. high hazard dams and some critical buildings such as hospitals and schools, can provide a higher level of certainty regarding the maximum anticipated ground motions. However, designing to an 84 percentile attenuation basis is not traditionally done by transportation agencies, as it often results in ground motion levels that are extremely costly to design for. In fact, the risk associated with either the median or 84 percentile ground motions from a deterministic seismic hazard analysis is unknown because the analysis only considers uncertainty with respect to ground motion attenuation and does not consider uncertainties with respect to earthquake location, magnitude, or rate of occurrence.

It should also be noted, however, that designing to an arbitrarily high probabilistic design level (i.e. very long return period) can also produce unrealistically high ground motions due to compounding of the uncertainties at low probability levels. One alternative approach that has been used for the design of important facilities to compensate for the deficiencies in both probabilistic and deterministic analyses is to combine these two approaches. For example, Caltrans' seismic peer review panel and the Seismic Advisory Board recommend evaluation of both probabilistic and deterministic ground motion levels (including considering both median and median-plus one standard deviation) when setting the design ground motions for the Toll Bridge Retrofit Program in California.

In a nutshell, it should be recognized, that fundamentally there is relatively little difference in the basic philosophy and calculation methods between deterministic and probabilistic approaches. A probabilistic approach merely can be regarded as an approach providing better defined risk levels in terms of return periods or the annual rate of exceedance for design: information that can then be the basis for design decisions balancing cost versus the calculated risk. The estimated risk for an earthquake from a probabilistic assessment can also be compared to the risk associated with other extreme environmental loading conditions to produce a balanced design. A probabilistic approach also has the merit of being able to distinguish relative contributions to risk from the more active versus less active faults. However, a deterministic hazard approach is simpler than a probabilistic approach and can be conducted by most engineers (probabilistic analyses should preferably be conducted by qualified professionals who specialize in this area of expertise). It is very difficult, and sometimes impossible, to verify probabilistic solutions by independent checks. Furthermore, as noted previously, the results of probabilistic hazard solutions can sometimes be unreasonable, or at least questionable, particularly at very long return periods. It is generally believed prudent to employ deterministic solutions as a sanity check on the results of probabilistic analyses for long return periods. Generally, a median-plus-one standard deviation deterministic hazard solution can be regarded as an upper bound on the results of a probabilistic hazard analysis when designing transportation facilities.

## **2.3 HAZARD LEVELS AND RETURN PERIODS**

### **2.3.1 Selection of Return Period**

The choice of the design ground motion level, whether based upon probabilistic or deterministic analysis, cannot be considered separately from the level of performance specified for the design event. Common performance levels used in design of transportation facilities include protection of life safety and maintenance of function after the event. Keeping a bridge functional after a large earthquake is a more rigorous requirement than simply maintaining life safety and is typically only required for essential or critical facilities, e.g. ‘lifeline’ bridges. Sometimes, facilities may be designed for more than one performance level, with a different ground motion level assigned to each performance level, a practice referred to as performance-based design. As discussed above, the probabilistic seismic hazard approach provides a more rational basis for making risk versus benefit decisions (compared to deterministic analysis) and thus has been generally adopted in practice for use in performance-based design.

Table 2-2 presents a two-level, performance-based, set of design criteria for transportation facilities that were developed for a proposed revision to the AASHTO LRFD seismic design specifications under the sponsorship of the National Cooperative Highway Research Program (NCHRP, 2001). In this approach, two levels of design ground motion (a ‘rare’ earthquake and an ‘expected’ earthquake), are specified for two different performance levels (‘life safety’ for ordinary facilities and ‘operational’ for critical facilities). Performance criteria are specified for each ground motion level and performance level. For instance, in a ‘rare’ earthquake an ordinary facility is expected to suffer significant disruption in service and significant damage (but not loss of life), while a critical facility is expected to remain in service with minimal damage. In the ‘expected’ earthquake, both ordinary and critical facilities are expected to be serviceable after the earthquake, with an ordinary facility suffering minimal damage and a critical facility suffering minimal-to-no damage. In the NCHRP proposed criteria, the ‘rare’ earthquake, was defined as one with a 3% probability of exceedance in 75 years, (corresponding approximately to a 2,500-year return period), while the expected earthquake was one with a 50% probability of exceedance in 75 years, corresponding approximately to a 100-year return period.

AASHTO first adopted a probabilistic approach to seismic design in 1981 with the publication of Guide Specifications for Seismic Design of Bridges (AASHTO, 1981). These specifications were an approved alternative to the seismic provisions in the Standard Specifications for Highway Bridges in use at that time and were based on a 500-year return period seismic hazard map prepared by USGS. In developing the current AASHTO design criteria (AASHTO, 2007), the two-level design approach proposed in the NCHRP study (NCHRP, 2001) was considered to be unjustified for most transportation facilities in the US and was not adopted. Furthermore, when considering the return period for the ‘design’ earthquake (the term used in single-level design) 2,500 years was considered to be too long, too inconsistent with the return periods for other natural hazards, and potentially too costly, especially in the design of foundations. There was also concern that the cost of retrofitting existing bridges designed for a 500-year return period to this new hazard level would be prohibitive.

Nevertheless the arguments for raising the hazard level from 500 yrs were persuasive and in 2007, AASHTO elected to adopt a 1,000-year hazard level for the design of conventional bridges. This hazard level is used in both the revised LRFD Specifications (AASHTO, 2014) and the LRFD Guide Specifications for Seismic Design (AASHTO, 2013). The Guide Specifications were initially developed under NCHRP Project 20-07/193 which showed that the hazard level for the 2,500-year return period corresponds to a shaking level at about the median-plus-one standard deviation level in many parts of U.S. Considering Caltrans practice,

**TABLE 2-2 PERFORMANCE- BASED SEISMIC DESIGN CRITERIA FOR  
TRANSPORTATION FACILITIES (NCHRP, 2001)**

Probability of Exceedance For Design Earthquake Ground Motions <sup>(4)</sup>		Performance Level <sup>(1)</sup>	
		Life Safety	Operation
Rare Earthquake (MCE) 3% PE in 75 years/1.5 mean Deterministic	Service <sup>(2)</sup>	Significant Disruption	Immediate
	Damage <sup>(3)</sup>	Significant	Minimal
Expected Earthquake 50% PE in 75 years	Service	Immediate	Immediate
	Damage	Minimal	Minimal to None

Notes:

(1) Performance Levels

These are defined in terms of their anticipated performance objectives in the upper level earthquake. Life safety in the MCE event means that the bridge should not collapse but partial or complete replacement may be required. Since a dual level design is required the Life Safety performance level will have immediate service and minimal damage for the expected design earthquake. For the operational performance level the intent is that there will be immediate service and minimal damage for both the rare and expected earthquakes.

(2) Service Levels

- *Immediate* – Full access to normal traffic shall be available following an inspection of the bridge.
- *Significant Disruption* – Limited access (reduced lanes, light emergency traffic) may be possible after shoring, however the bridge may need to be replaced.

(3) Damage Levels

- *None* – Evidence of movement may be present but no notable damage.
- *Minimal* – Some visible signs of damage. Minor inelastic response may occur, but post-earthquake damage is limited to narrow flexural cracking in concrete and the onset of yielding in steel. Permanent deformations are not apparent, and any repairs could be made under non-emergency conditions with the exception of superstructure joints.
- *Significant* – Although there is no collapse, permanent offsets may occur and damage consisting of cracking, reinforcement yield, and major spalling of concrete, and extensive yielding and local buckling of steel columns, global and local buckling of steel braces, and cracking in the bridge deck slab at shear studs on the seismic load path is possible. These conditions may require closure to repair the damage. Partial or complete replacement of columns may be required in some cases. For sites with lateral flow due to liquefaction, significant inelastic deformation is permitted in the piles, whereas for all other sites the foundations are capacity-protected and no damage is anticipated. Partial or complete replacement of the columns and piles may be necessary if significant lateral flow occurs. If replacement of columns or other components is to be avoided, the design approaches producing minimal or moderate damage, such as seismic isolation or the control and reparability concept should be assessed.

(4) The upper-level earthquake considered in these provisions is designated the Maximum Considered Earthquake, or MCE. In general, the ground motions on national MCE ground motion maps have a probability of exceedance (PE) of approximately 3% PE in 75 years. However, adjacent to highly active faults, ground motions on MCE maps are bounded deterministically as described above. When bounded deterministically, MCE ground motions are lower than ground motions having 3% PE in 75 years. The performance objective for the expected earthquake is either explicitly included as an essentially elastic design for the 50% PE in 75 year force level or results implicitly from design for the 3% PE in 75 year force level.

which uses median GMPE values for setting the safety level limit state ground motion criteria for ordinary (conventional) bridges, it can be argued that the 2,500-year hazard level is too conservative for ordinary bridges. Hence, one can infer that the AASHTO decision for rejecting the 2,500-year return period and adopting a 1000-yr return period is justified. The NCHRP 20-07/193 study also showed that the return period that best correlated with historical earthquakes in various parts of the country varied widely, ranging from less than 500 years for the seismically active western U.S. to close to 2,000-years in some parts of central and eastern U.S. Thus the selection by AASHTO of a 1,000-year return period is a compromise which can be reconciled against many of the historical earthquakes that have occurred in the central and eastern part of U.S. (on a median attenuation basis).

AASHTO has no explicit requirements for checking bridge performance for more frequently occurring ground motions than those that occur every thousand years, on average. But some owners may desire that certain important bridges will remain functional following more frequently occurring earthquakes such as those with return periods of the order of a hundred years or so. In practice, where owners have chosen to check functionality, the selected return period has varied from project to project, even within the same geographic region. A 72-year return period has been used in California for toll road projects in Orange County, CA, and for designing wharf structures in the Ports of Los Angeles and Long Beach. A 92-year return period has been used for the functional earthquake for the East Bay Spans of the San Francisco Oakland Bay Bridge. However, for major bridge structures in less active seismic states, longer return periods have been used for the functional earthquake. For example, 500 years has been used for the retrofit of the major water crossing bridges in New York City and for design of the new Arthur Ravenal (Cooper River) cable-stayed bridge in Charleston, South Carolina. The decision on whether or not to design for functionality involves balancing the risk of service disruption and the cost of disruption versus the cost associated with additional design and construction/retrofit measures. While this decision is the owners' responsibility, it is the engineer's responsibility to provide the owner with sufficient information with which to make this economic decision and, having made the decision to use a functional level earthquake, to set the functional level earthquake criteria on a project specific basis.

It is noted that the 2006 Edition of the Retrofitting Manual for Highway Structures published by the Federal Highway Administration (FHWA, 2006), recommends dual-level performance criteria when retrofitting bridges. This Manual uses the terms 'upper' and 'lower' level to describe the dual-level ground motions when defining suggested performance criteria and retrofit measures to achieve this performance. The upper level motions have a return period of 1,000 years and the lower level motions have a period of 100 years.

### 2.3.2 Design Events for Various Importance Categories

As discussed above, a 1,000-year return period has been adopted by AASHTO for conventional bridges. However, owners may deviate from the 1,000-year return period ground motion criteria for non-bridge transportation facilities and in some cases for bridges if the situation warrants it. The following are some of the reasons that have been cited for deviation from the AASHTO criteria:

- 1) A longer return period may be justified for critical structures, when (a) an extended duration in loss of operation of the structure would cause an undue cost to the community, such as long-span water crossing structures, or (b) the structure is part of the lifeline route for emergency operations. For these critical structures, especially for complex structural systems, project-specific ground motions and performance criteria should be developed with the assistance of a peer review panel.
- 2) A shorter return period may be justified, if (a) the capital cost to design the structure to the 1,000-year return period is deemed too costly, or (b) in retrofit situations the existing structure has limited remaining operating life, and the bridge is expected to be replaced. It is noted that the FHWA Manual (FHWA, 2006), does not favor a reduction in the return period for older structures. Instead, the minimum level of retrofit is adjusted to account for age, with little or no requirements recommended for a bridge about to be closed or replaced.
- 3) The return period may also be reduced when the 1,000-year return period ground motion is excessive, e.g. when it is higher than a median-plus-one standard deviation of the Maximum Considered Earthquake ground motion. This situation is common in seismically active areas such as some parts of California where the faults have relative short rupture recurrence intervals, in terms of just a few hundred years. For such situations, it is common to place a deterministic cap on the probabilistic ground motions, e.g. the median-plus-one standard deviation MCE design scenario.

## 2.4 CHARACTERIZATION OF HORIZONTAL GROUND MOTIONS

Once the performance criteria have been established, the design ground motions corresponding to the return periods used to define the criteria must be characterized. In general a seismic hazard analysis characterizes these ground motions in terms of acceleration response spectra. It may also be important that the corresponding displacement response spectra are also established, particularly when a displacement-based design approach is used. In addition, the results of a hazard analysis may need to be modified to account for two factors: 1) near fault (near-field) effects; and 2) local site effects due to the presence of soil overburden.

### 2.4.1 Acceleration Response Spectra vs Displacement Spectra

The most common method of seismic design for bridges focuses on providing sufficient strength to resist the earthquake demands. This approach is called a ‘force-based’ approach and it employs acceleration response spectra to calculate the earthquake demands. However, there is a growing trend in bridge design to move away from ‘force-based’ methods to ‘displacement-based’ methods where the focus is on providing sufficient displacement capacity. This approach may employ either acceleration or displacement response spectra to calculate the earthquake demands. A displacement response spectrum may be derived from an acceleration response spectrum using the following equation:

$$S_d = \frac{T^2}{4\pi^2} S_a \quad 2-6$$

where  $S_d$  is spectral displacement,  $S_a$  is spectral acceleration, and  $T$  is period.

The spectral displacement demand from the above equation is the relative displacement between the center of mass of the structure and the point where ground motion is input to the structure.

### 2.4.2 Near-Fault (Near-Field) Effects

Research over the last two decades (e.g. Somerville et al., 1997) has shown that certain combinations of site location, configuration of the seismic source, and direction of fault rupture can result in a significant enhancement to the long period motions at a bridge site. Such motions can be very damaging to certain classes of bridges. Figure 2-8 illustrates the effect of directivity in near-fault ground motions, by comparing velocity time histories from two sites subject to the same earthquake, but in different

directions from the epicenter along the fault. It is seen in this figure that the ground motion recorded at the Lucerne recording station, in the direction of fault rupture propagation relative to the epicenter, is remarkably different from that at the Joshua Tree station, which is in opposite the direction of fault rupture, for the same earthquake (1992  $M_w$  7.2 Landers earthquake in Southern California). The Lucerne record shows a very large velocity pulse, with a peak ground velocity of 53.5 in/s, as compared to the Joshua Tree record, which has much lower peak ground velocity of 16.9 in/s, even though the duration of shaking is much more pronounced in the Joshua Tree record.

Figure 2-8 shows that when a bridge site is located sufficiently near to a fault, and if the earthquake is a forward rupturing event (i.e. the fault ruptures toward the site), ground motion with a very large velocity pulse can occur. Because these kinds of pulses can be very damaging to long-period bridges, it is necessary to take special precautions in these situations. However, methods used to account for these directivity effects vary from project to project, in part because the subject matter is still under research. In particular, the means for quantifying the velocity pulse and relating it to structural response is still a subject of research, although a time history analysis using appropriate time histories is one way this can be accounted for. The need to consider near-fault directivity is, in general, limited to those states with well-defined shallow active faults (e.g. California, Washington, and Utah). Furthermore, only bridge sites within about 10 miles of the rupturing fault need be considered for fault directivity effects.

### **2.4.3 Local Site Effects**

Local soil conditions at a bridge site can have a significant effect on the characteristics of earthquake ground motions and this effect needs to be taken into account when establishing design ground motions. There are, in general, three methods that can be used to account for the influence of local soil conditions:

- 1) use of site factors to modify the results of the seismic hazard analysis to account for local soil conditions
- 2) use of GMPEs to directly account for the local soil conditions in the seismic hazard analysis, and
- 3) use of site response analysis.

Most seismic hazard analyses, and the AASHTO Seismic Hazard Maps, are produced for a ‘rock’ site where the average shear wave velocity within the upper 100 ft of the site profile ranges from 2,500 to 5,000 ft/s. If the shear wave velocity in the upper 100 ft differs from this value, the design response spectra must be modified. Modifications to spectra to account for a different shear wave velocity in the upper 100 ft, i.e. for local site conditions, are discussed in Section 2.5.

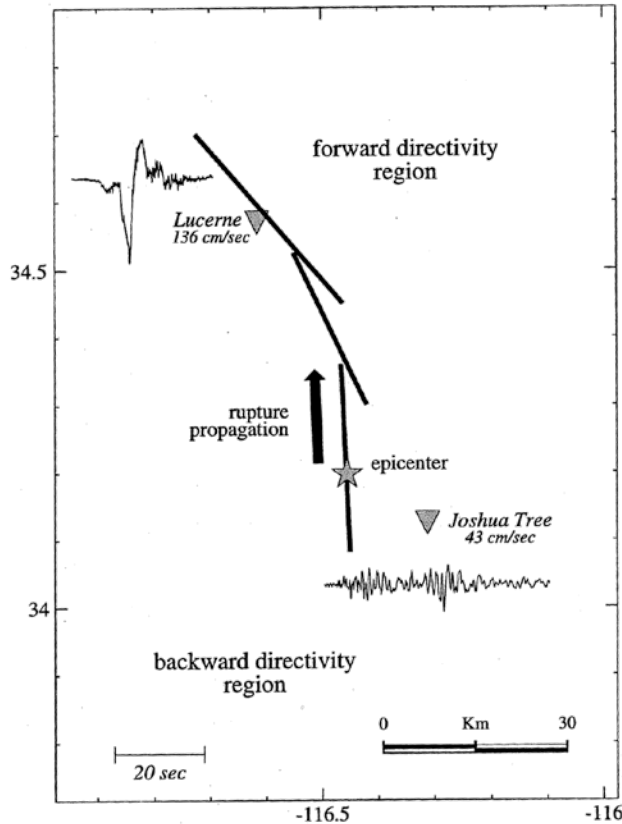


Figure 2-8 Influence of Rupture Directivity on Velocity Time Histories Recorded at the Lucerne and Joshua Tree Sites During the 1992 Landers Earthquake (Somerville et al., 1997)

Until recently, soil site GMPEs were generally considered too crude to properly account for local soil conditions, as they tended to group all soil sites into a single site class. However, a new generation of GMPEs that discriminates among soil sites on the basis of the shear wave velocity in the upper 100 ft have been developed and are now being employed in practice (Abrahamson et. al, 2008). If the seismic hazard analysis is conducted using these relationships no adjustment for local site conditions is necessary. Furthermore, the next generation of seismic hazard maps produced by the US Geological Survey (USGS) under the National Seismic Hazard Mapping Program may employ these relationships to explicitly account for local soil conditions.

The use of site response analysis to account for the influence of local soil conditions on earthquake ground motions is discussed in Section 2.6.

## 2.5 USE OF AASHTO/USGS DESIGN HAZARD MAPS

In most situations, the seismic design of an ordinary bridge is based on the seismic hazard maps developed by the USGS for the 2007 AASHTO specifications. These maps are, in fact, based upon the 2002 National Seismic Hazard Maps produced by USGS. These maps provide rock spectral accelerations at periods of 0.0, 0.2, and 1.0 seconds for a return period of 1,000 years (7% PE in 75 years). Construction of the complete acceleration spectrum for use in structural design of bridges follows in accordance with the procedure given in both the AASHTO LRFD Specifications (2013) and the Seismic Guide Specifications (2014). The FHWA Retrofitting Manual (2006) uses the same maps and procedure.

When the AASHTO seismic design criteria were changed to employ a 1000-yr return period, the National Seismic Hazard Maps developed by the USGS did not include a 1000-yr return period map. Therefore, AASHTO commissioned USGS to develop a 1000-yr return period map using the 2002 National Seismic Hazard Map data. USGS has since produced 1000-yr return period maps and provides them on their web site. In fact, the USGS web site provides interactive options for obtaining seismic hazard data for any desired return period, including the option of using archived data for the 2002 National Seismic Hazard Maps. Therefore, if a response spectrum is required for a different return period, e.g. for 500- or 2500-yr return periods, these data, including data from the 2002 maps and for the most recent maps, are available at <http://earthquake.usgs.gov/hazards/apps/gis/>. As the AASHTO seismic design criteria is fixed at values from the 2002 maps, designers may choose to use the 2002 data for consistency with the AASHTO specifications. However, it may be prudent to also check seismic hazard values using the latest version of the National Seismic Hazard Maps produced by USGS to see how much they have changed since 2002, especially for new construction and important projects.

When the 1000-yr return period maps were developed for AASHTO they were not available online. Therefore, a user-friendly CD was been released by AASHTO which not only contains data for constructing acceleration response spectra for rock sites, but also correction factors for local site conditions. AASHTO seismic hazard data are now directly available from the USGS web site at <http://earthquake.usgs.gov/hazards/designmaps/pdfs/?code=AASHTO&edition=2009>. However, the AASHTO CD may still be in use in some jurisdictions. Examples on how to use the USGS web site and the AASHTO CD are given in Section 2.5.4 and 2.5.5, respectively.

### 2.5.1 Derivation of AASHTO Seismic Coefficient Spectra

For structural analysis, it is common to place a deterministic cap on a probabilistically-derived acceleration spectrum developed from a seismic hazard analysis. This cap truncates the shape of the spectrum in the short period range. Furthermore, the shape of the spectrum in the longer period range may be smoothed and assumed to be inversely proportional to the modal period,  $T$ . Strictly speaking, the resulting plot is no longer an acceleration response spectrum, since it has been modified for design purposes. To make this distinction clear, AASHTO and FHWA refer to this type of spectrum as a ‘seismic coefficient’ spectrum.

An example of this spectrum is shown in Figure 2-9. It is based on the three spectral accelerations ( $PGA$ ,  $SS$  and  $S1$ ) at periods equal to 0.0, 0.2 and 1.0 seconds given by the AASHTO/USGS 1000-yr maps (or CD) for a rock site. Site Factors ( $F_{pga}$ ,  $F_a$ , and  $F_v$ ) are used to adjust this spectrum for local site conditions as explained in Sections 2.5.2 and 2.5.3)

This method of modifying the acceleration response spectrum is employed not only in the AASHTO LRFD and Guide Specifications but also in the recommended seismic design provisions from the National Earthquake Hazard Reduction Program (NEHRP), and has been employed in the International Building Code (IBC) since 2003. The only difference with these various approaches is the return period used to determine the anchoring spectral accelerations. One important difference between this current procedure and previous versions of this procedure involves anchoring the design spectrum at the zero period, corresponding to the mapped  $PGA$ . In previous versions of this procedure, the  $PGA$  was simply assumed to be equal to 0.4 times the spectral acceleration at 0.2 second. In the current procedure, the  $PGA$  is obtained directly from the corresponding seismic hazard map or seismic hazard analysis.

Figure 2-10 compares the acceleration response spectrum developed from the USGS national seismic hazard mapping program data with the seismic coefficient spectrum recommended for design at a rock site in Memphis, Tennessee and a return period of 1,000 years (7% PE in 75 years). As shown in this figure, the major difference between these two types of spectra is the truncation of spectral accelerations at periods of less than 1 second.

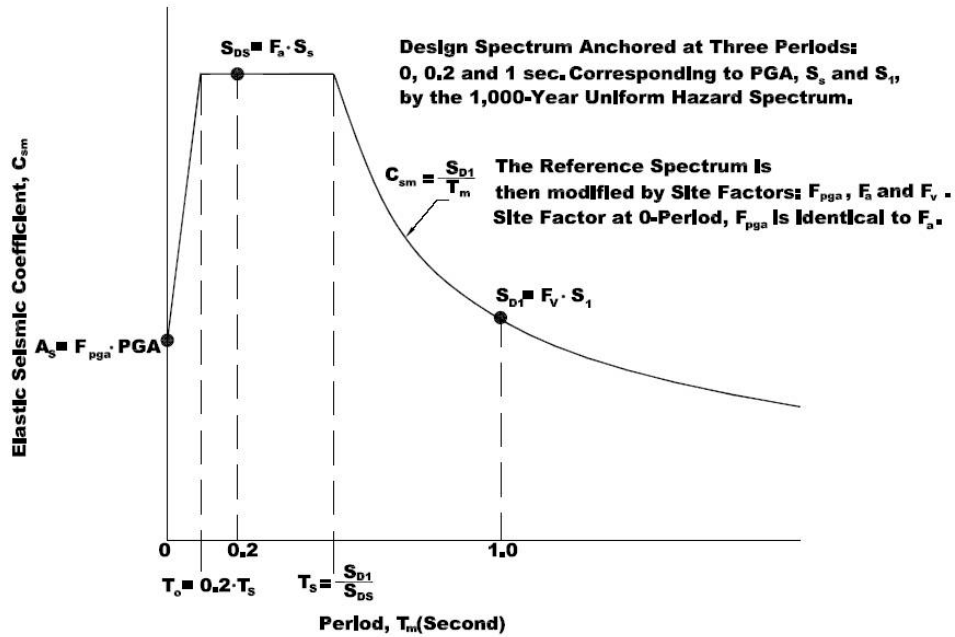


Figure 2-9 Seismic Coefficient Design Spectrum Constructed with the Three-Point Method

### 2.5.2 Site Class Definitions

The use of site factors to account for the influence of local soil conditions on ground motion characteristics is illustrated in Figure 2-9. Using this approach, the anchoring spectral accelerations for the design spectrum, obtained from the AASHTO seismic hazard maps for rock site conditions (often referred to as reference site conditions) are modified by site response factors  $F_{pga}$  (for the 0.0 second period),  $F_a$  (for the 0.2 second period) and  $F_v$  (for the 1.0 second period). The values of  $F_{pga}$ ,  $F_a$  and  $F_v$  depend on both the local soil conditions (i.e. the average shear wave velocity in the upper 100 ft) and the amplitude of the respective spectral accelerations. Local soil conditions are defined on the basis of the average shear wave velocity for the top 100 ft of the site, sometimes referred to as  $V_{s30}$  (the “30” refers to 30 meters, the metric equivalent of 100 feet). Six Site Classes, designated A through F, have been established on the basis of  $V_{s30}$ . These Site Classes, referred to as the NEHRP Site Classes because they were initially established under the NEHRP program, are shown in Table 2-3. Note that for Site Class F, site factors should not be used and a site specific response analysis should be conducted to evaluate the influence of local soil conditions on site response.

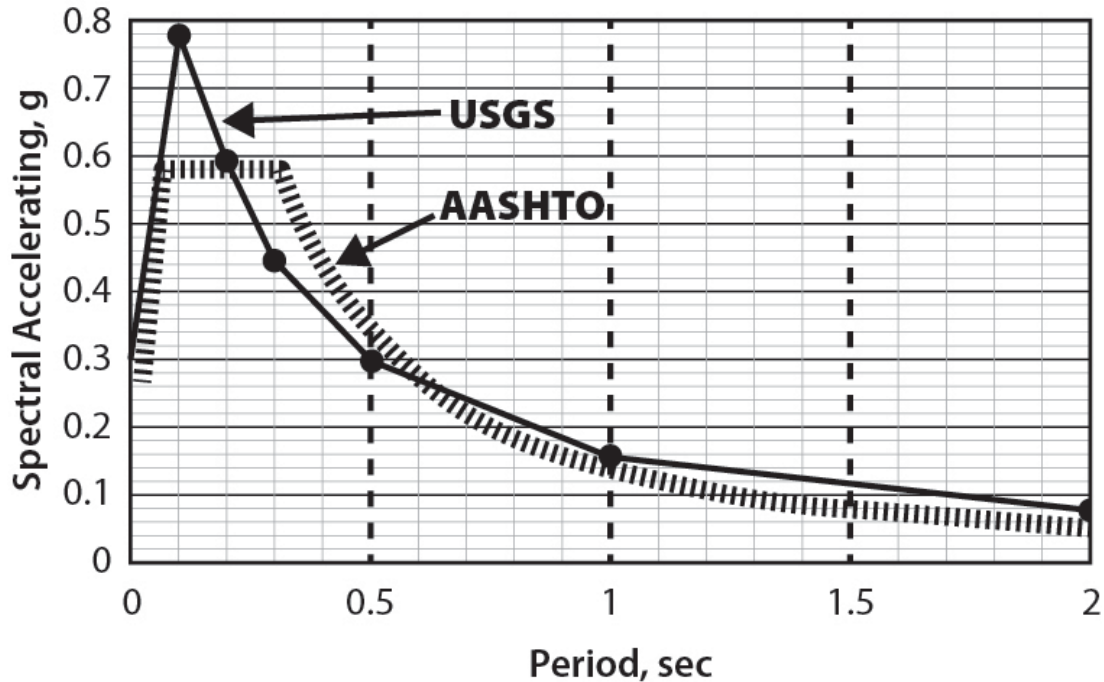


Figure 2-10 USGS Acceleration Response Spectrum and the AASHTO Seismic Coefficient Design Spectrum for a Rock Site in Memphis, Tennessee 1,000-yr Return Period (7% PE in 75 Years)

### 2.5.3 Site Factors

The short- and long-period site factors,  $F_a$  and  $F_v$ , are given in Tables 2-4 and 2-5 respectively. These factors are applied to the 0.2 second and 1 second spectral accelerations respectively, for rock (reference site) conditions (i.e. Site Class B). The factor  $F_{pga}$  used to adjust the zero period spectral acceleration (i.e. the PGA), is also provided in Table 2-4. Note that  $F_{pga}$  is essentially the same as  $F_a$  except that the amplitude ranges for  $F_{pga}$  are 0.4 times the amplitude ranges for  $F_a$ , as noted in Table 2-4. In most cases, these factors are greater than 1.0 (and as great as 3.5 in one case), resulting in an amplification of the spectral accelerations by local soil conditions. But for Site Class A, corresponding to hard, crystalline rock sites (sites with an average shear wave velocity in the top 100 ft in excess of 5,000 ft/s), they are equal to 0.8, resulting in a reduction of the spectral accelerations obtained for the reference rock site from the seismic hazard analysis. It will be seen that for Site Classes C, D and E, these factors decrease as the ground motion increases (higher values of  $S_S$  and  $S_I$ ) and  $F_a$  even becomes less than 1.0 at high amplitudes. This is because, at strong levels of ground shaking, these soils soften considerably (i.e., yield) and lose their ability to amplify the ground motion. As indicated in Tables 2-4 and 2-5, site factors should not be used for Site Class F, and a site specific geotechnical investigation and dynamic response analyses should be conducted to evaluate the influence of local soil conditions on site response.

**TABLE 2-3 NEHRP SITE CLASSIFICATION SYSTEM**

SITE CLASS DEFINITIONS				
SITE CLASS	SOIL PROFILE NAME	AVERAGE PROPERTIES IN TOP 100 feet		
		Soil shear wave velocity, $v_s$ (ft/s)	Standard penetration resistance, $N$ (blows/ft)	Soil undrained shear strength, $s_u$ (psf)
A	Hard rock	$v_s > 5,000$	N/A	N/A
B	Rock	$2,500 < v_s \leq 5,000$	N/A	N/A
C	Very dense soil and soft rock	$1,200 < v_s \leq 2,500$	$N > 50$	$s_u \geq 2,000$
D	Stiff soil profile	$600 < v_s \leq 1,200$	$15 \leq N \leq 50$	$1,000 \leq s_u \leq 2,000$
E	Soft soil profile	$v_s < 600$	$N < 15$	$s_u < 1,000$
E	-	Any profile with more than 10 feet of soft clay having the following characteristics: 1. Plasticity index $PI > 20$ , 2. Moisture content $w \geq 40\%$ and, 3. Undrained shear strength $s_u < 500$ psf		
F	-	Soils requiring site-specific ground motion response evaluations such as: 1. Peats and/or highly organic clays ( $H > 10$ feet of peat and/or highly organic clay where $H$ = thickness of soil) 2. Very high plasticity clays ( $H > 25$ feet with plasticity index $PI > 75$ ) 3. Very thick soft/medium stiff clays ( $H > 120$ feet)		
<p>Exceptions: Where soil properties are not known in sufficient detail to determine the Site Class, a site investigation shall be undertaken sufficient to determine the Site Class. Site Class E or F should not be assumed unless the authority having jurisdiction determines that Site Class E or F could be present at the site or in the event that Site Class E or F is established by geotechnical data.</p>				

**TABLE 2-4 – VALUES OF  $F_{pga}$  and  $F_a$  AS FUNCTION OF SITE CLASS AND MAPPED PEAK GROUND ACCELERATION OR SHORT PERIOD SPECTRAL ACCELERATION COEFFICIENT**

Site Class	Mapped Peak Ground Acceleration or Spectral Response Acceleration Coefficient at Short Periods				
	$PGA \leq 0.10$ $S_S \leq 0.25$	$PGA = 0.20$ $S_S = 0.50$	$PGA = 0.30$ $S_S = 0.75$	$PGA = 0.40$ $S_S = 1.00$	$PGA \geq 0.50$ $S_S \geq 1.25$
A	0.8	0.8	0.8	0.8	0.8
B	1.0	1.0	1.0	1.0	1.0
C	1.2	1.2	1.1	1.0	1.0
D	1.6	1.4	1.2	1.1	1.0
E	2.5	1.7	1.2	0.9	0.9
F	<i>a</i>	<i>a</i>	<i>a</i>	<i>a</i>	<i>a</i>
Notes:	Use straight line interpolation for intermediate values of $S_S$ , where $S_S$ is the spectral acceleration coefficient at 0.2 second obtained from the ground motion maps.				
	<i>a</i> Site-specific geotechnical investigation and dynamic site response analyses should be performed				

**TABLE 2-5 – VALUES OF  $F_v$  AS A FUNCTION OF SITE CLASS AND MAPPED LONG PERIOD SPECTRAL ACCELERATION**

Site Class	Mapped Spectral Response Acceleration Coefficient at 1.0 sec Period				
	$S_l \leq 0.10$	$S_l = 0.20$	$S_l = 0.30$	$S_l = 0.40$	$S_l \geq 0.50$
A	0.8	0.8	0.8	0.8	0.8
B	1.0	1.0	1.0	1.0	1.0
C	1.7	1.6	1.5	1.4	1.3
D	2.4	2.0	1.8	1.6	1.5
E	3.5	3.2	2.8	2.4	2.4
F	<i>a</i>	<i>a</i>	<i>a</i>	A	<i>a</i>
Notes:	Use straight line interpolation for intermediate values of $S_l$ , where $S_l$ is the spectral acceleration at 1.0 second obtained from the ground motion maps.				
	<i>a</i> Site-specific geotechnical investigation and dynamic site response analyses should be performed				

## 2.5.4 Use of the USGS Web Site – Step by Step Procedure

As noted in Section 2.5, AASHTO seismic hazard data is now available directly from the USGS website. The AASHTO seismic hazard maps, including maps for the continental US, Alaska, and Hawaii, can be found at <http://earthquake.usgs.gov/hazards/designmaps/pdfs/?code=AASHTO&edition=2009> and an interactive procedure for establishing the design spectral accelerations and the site-adjusted seismic coefficient spectrum is available on the USGS web site at <http://earthquake.usgs.gov/designmaps/us/application.php>. This section steps through the use of the USGS web site to obtain the AASHTO response spectrum for the San Francisco Oakland Bay Bridge site. Use of the AASHTO CD is illustrated in Section 2.4.5.

The initial screen for the USGS web site application is shown in Figure 2-11. In the drop down box under “Design Code Reference Document,” select “2009 AASHTO.” Then, enter the project title in the “Report Title” box, select the appropriate AASHTO Site Class from the drop down box under “Site Soil Classification” (Site Class D for this example), and enter the site latitude and longitude in their respective boxes, as shown in Figure 2-11. Note that, by convention, site longitude is negative. After entering the data, click on the “Compute Values” box at the bottom center of this screen.

application.php

usgs interactive seismic hazard maps

**USGS**  
science for a changing world

USGS Home  
Contact USGS  
Search USGS

**Earthquake Hazards Program**

Home About Us Contact Us Search

**EARTHQUAKES HAZARDS DATA & PRODUCTS LEARN MONITORING RESEARCH**

Seismic Design Maps & Tools

US Seismic Design Maps

Use the Tool

Documentation & Help

Recent Changes

Worldwide Seismic Design Tool

Use the Tool

Documentation & Help

**U.S. Seismic Design Maps**

For occasional announcements about this web tool, please visit our [U.S. Seismic Design Maps wiki](#).

Application Batch Mode Help

**Design Code Reference Document**  
Consult your local design official if you need help selecting this:  
2009 AASHTO

**Report Title (Optional)**  
This will appear at the top of the generated report.  
SFOBB Example

**Site Soil Classification**  
This is not automatically selected based on site location.  
Site Class D - "Stiff Soil" (Default)

**Site Latitude**  
Decimal degrees for the site location.  
37.814

**Site Longitude**  
Decimal degrees for the site location.  
-122.359

Compute Values

Enter address (optional)

10 km  
5 mi

20.673°N, 122.746°W

Powered by Leaflet — Tiles Courtesy of MapQuest — Data © OpenStreetMap contributors

Figure 2-11 Initiation Screen for USGS Web Application

After clicking on “Compute Values,” the screen shown in Figure 2-12 will appear. The two sets of tabular values on the lower left hand side represent the PGA, short period, and 1 second spectral accelerations for Site Class b reference site conditions (on the left hand side) and as corrected for Site Class (on the right hand side). By clicking on “Detailed Report” in the top right hand side of this screen, a much more detailed report, including the specific site factors employed and the corresponding AASHTO seismic design category is produced that can be used for documentation purposes. Note that by selecting the appropriate document in the first drop down box (the “Design Code Reference Box”) on the initial screen, ground motion values corresponding to the latest version of the National Seismic Hazard Reduction program maps produced by USGS (in this case, the 2009 NEHRP maps) can be obtained.

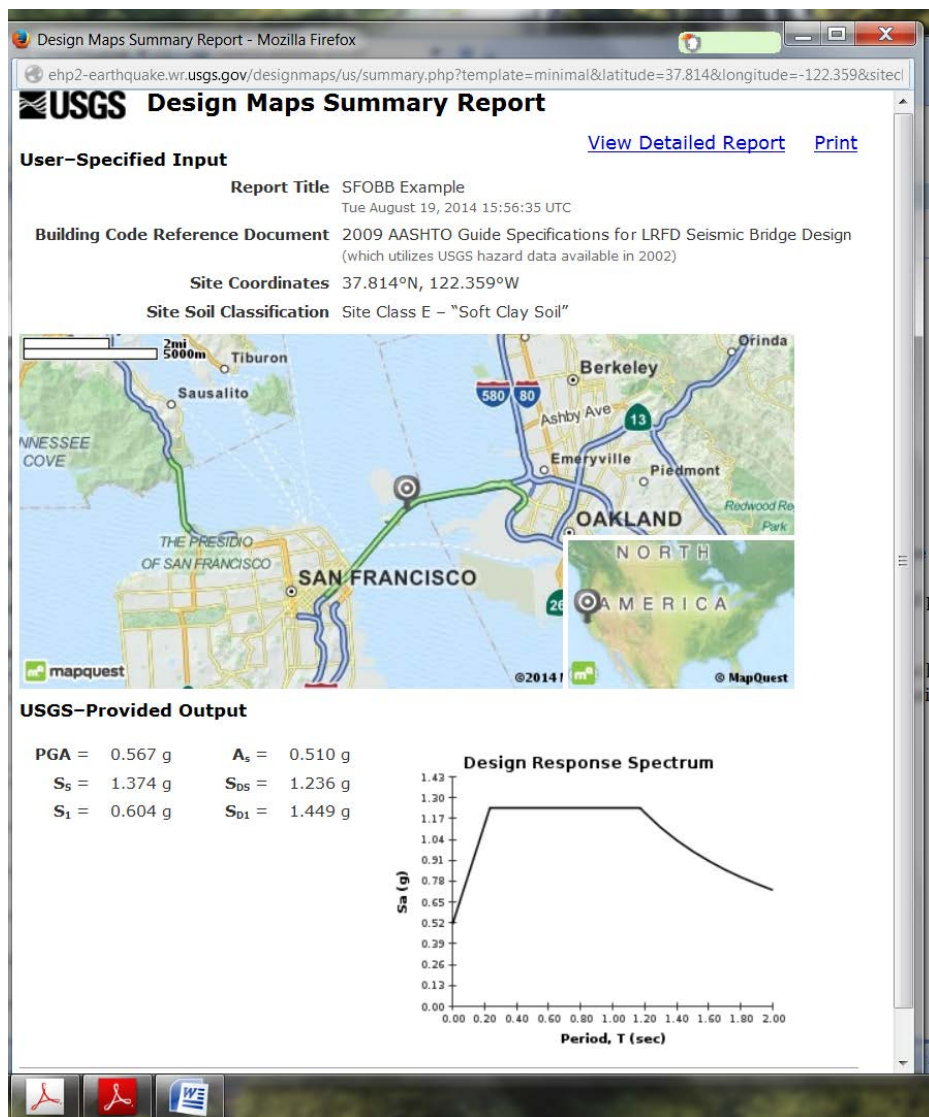


Figure 2-12 Summary Screen from USGS Web Site Application

### 2.5.5 Use of AASHTO CD – Step-by-Step Procedure

As noted in Sec 2.5, a user-friendly CD is available that can also be used to develop the AASHTO 1,000-yr (7% PE in 75 years) design spectrum for a bridge site, including corrections for local site conditions. As some jurisdictions may still use this CD, this section steps through the use of this CD ROM and explains how to obtain response spectra using the site of the San Francisco Oakland Bay Bridge (SFOBB) to illustrate the process. The initial screen for the program is shown in Figure 2-13.

- Step 1: Click the ‘Okay’ button, and display the screen shown in Figure 2-14. Select the geographic region and input the location of the bridge using either latitude/longitude coordinates or zip code. The coordinates shown here (latitude  $37.814^{\circ}$  north and longitude  $-122.359^{\circ}$  west) correspond to the far eastern point of the East Span of the SFOBB at Yerba Buena Island.
- Step 2: Select the desired hazard level (7% PE in 75 yr corresponds to the 1,000-yr return period). Click the ‘Calculate PGA,  $S_s$  and  $S_1$ ’ button, and the program displays the three anchor points for the design spectrum, i.e. the spectral accelerations at 0.0, 0.2, and 1.0 seconds, for a rock site (i.e. Site Class B, a site with an average shear wave velocity in the top 100 ft of between 2,500 and 5,000 ft/s). For the example site, the three anchor points,  $PGA$ ,  $S_s$  and  $S_1$ , are 0.567g, 1.373g, and 0.604g respectively.
- Step 3: Click the ‘Calculate  $A_s$ ,  $SD_s$  and  $SD_1$ ’ button in Screen 2 (Figure 2-14) and display the screen shown in Figure 2-15. Select the appropriate Site Class from the list of NEHRP classes on the left hand side of the screen. In this example, Site Class C is selected and values for the Site Factors are calculated and displayed in the lower left hand corner of the screen. These are  $F_{pga} = 1.0$ ,  $F_a = 1.0$  and  $F_v = 1.3$ .
- Step 4: Click ‘OK’ on Screen 3 (Figure 2-15) and display the screen shown in Figure 2-16. Along with the rock spectral accelerations previously shown ( $PGA$ ,  $S_s$ , and  $S_1$  on Screen 2, Figure 2-14), values for Site Class C are now displayed as  $A_s$ ,  $SD_s$  and  $SD_1$ . At this point, the user has the option of constructing the spectrum for Site Class B, called the ‘Map Spectrum’ (click the ‘Map Spectrum’ button), or the adjusted spectrum for the actual conditions at the site (in this case Site Class C) called the ‘Design Spectrum’ (click the ‘Design Spectrum’ button). If both spectra are required, click both buttons.

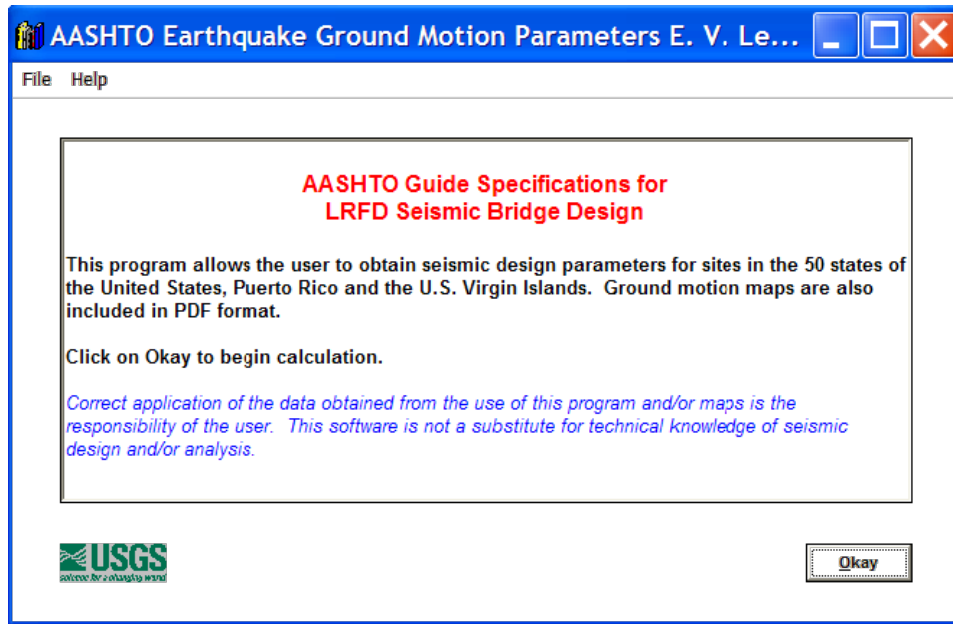


Figure 2-13 Initiation Screen for the USGS/AASHTO Ground Motion Program

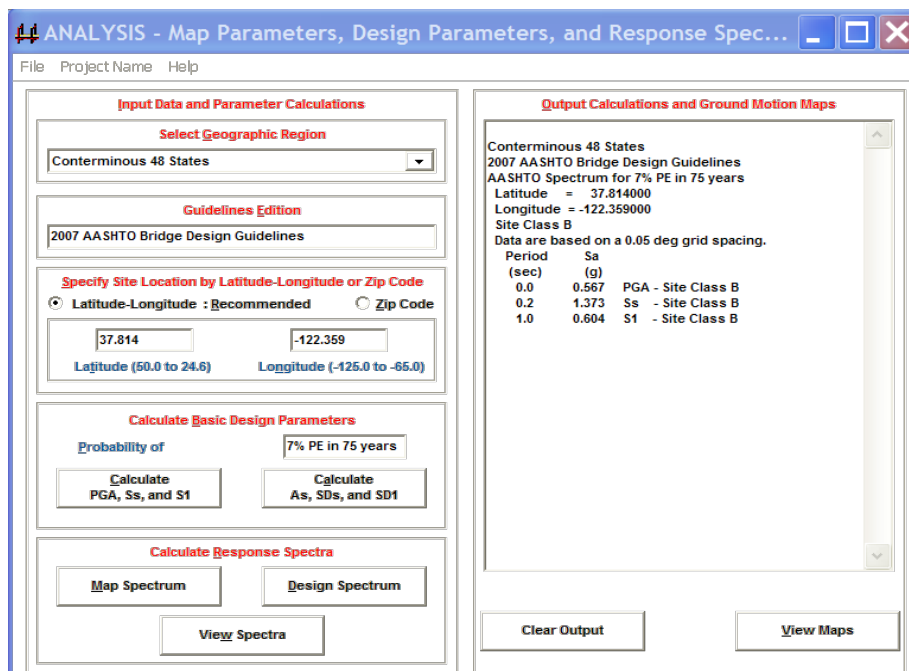


Figure 2-14 Screen No. 2: Site Location, Design Hazard Level,  $PGA$ ,  $S_s$  and  $S_1$  for Rock Site (Site Class B)

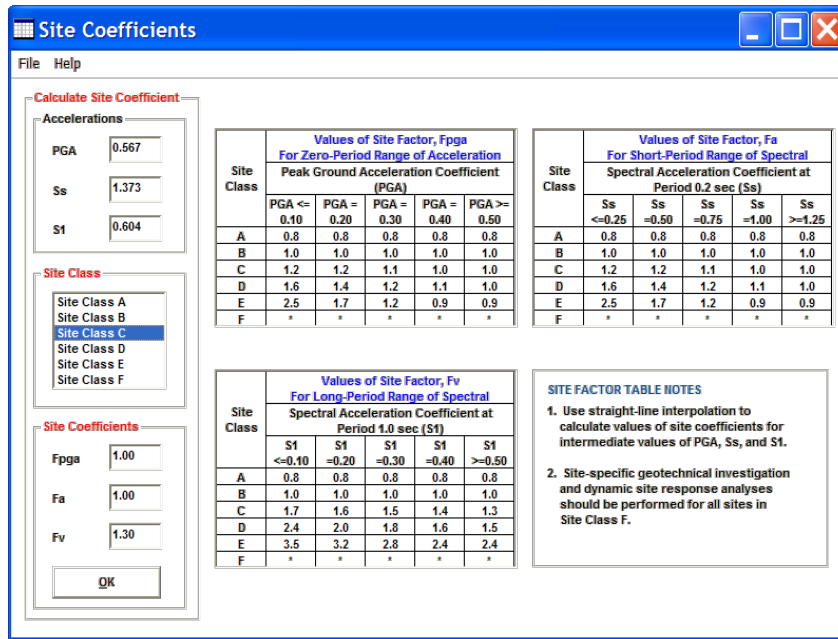


Figure 2-15 Screen No. 3: Table of Site Factors  $F_{pga}$ ,  $F_a$  and  $F_v$  for Bridge Site (Site Class C)

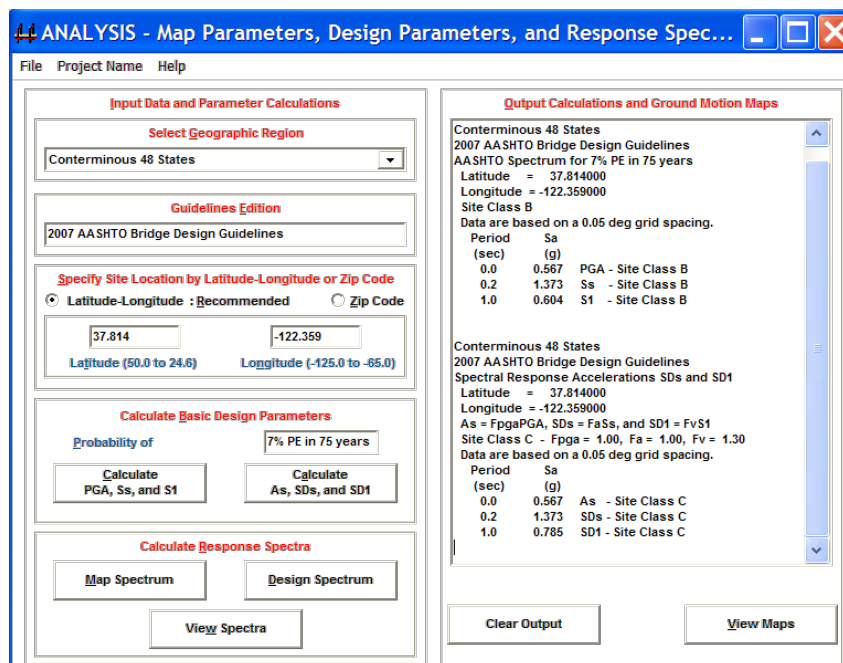


Figure 2-16 Screen No. 4:  $A_s$ ,  $SD_s$  and  $SD_1$  for Bridge Site (Site Class C)

If the 'Map Spectrum' option is chosen (Site Class B), spectral values for both acceleration and displacement are tabulated on the right hand side of Screen 5 (Figure 2-17). If the 'Design Spectrum' option is chosen (Site Class C in this case) spectral values for both acceleration and displacement are tabulated on the right hand side of Screen 6 (Figure 2-18).

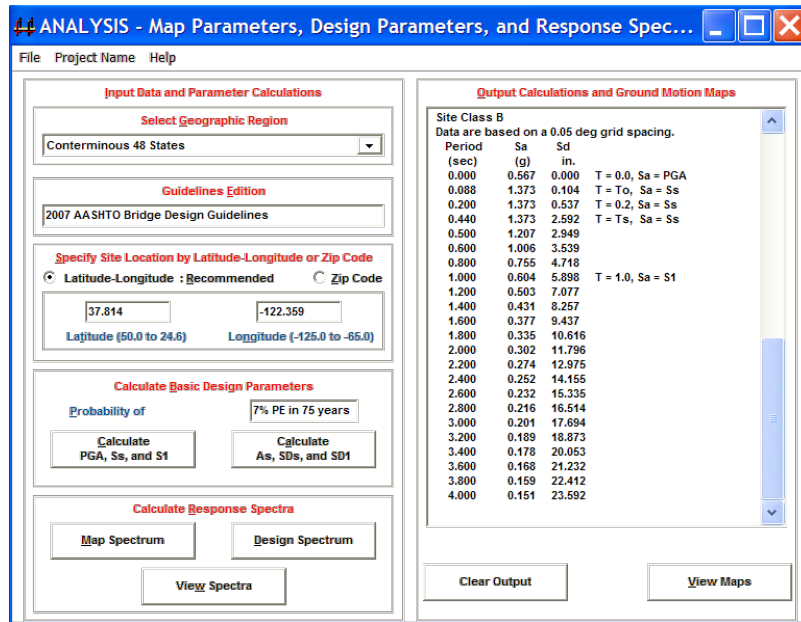


Figure 2-17 Screen No. 5: Spectral Values for Acceleration and Displacement for Site Class B ('Map Spectrum' Option)

Step 5. Click the 'View Spectra' button on Screen 6 (Figure 2-18) to graphically display the Map and Design Spectra. Various options for these plots may be selected from a drop-down menu (Screen 7, Figure 2-19) as listed below:

- 1) Map Spectrum for  $S_a$  vs.  $T$
- 2) Map Spectrum for  $S_a$  vs.  $S_d$  (a plot of spectral acceleration versus spectral displacement)
- 3) Design Spectrum for  $S_a$  vs.  $T$
- 4) Design Spectrum for  $S_a$  vs.  $S_d$  (All  $S_a$  vs.  $T$  Spectra for viewing a comparison between the Map Spectrum and the Design Spectrum), and
- 5) All  $S_a$  vs.  $S_d$  Spectra

Figure 2-19 shows the screen displayed when selecting Option 1 (Map Spectrum for  $S_a$  vs.  $T$ ). Screen displays for Options 5 and 6 are shown in Figures 2-20 and 2-21 respectively.

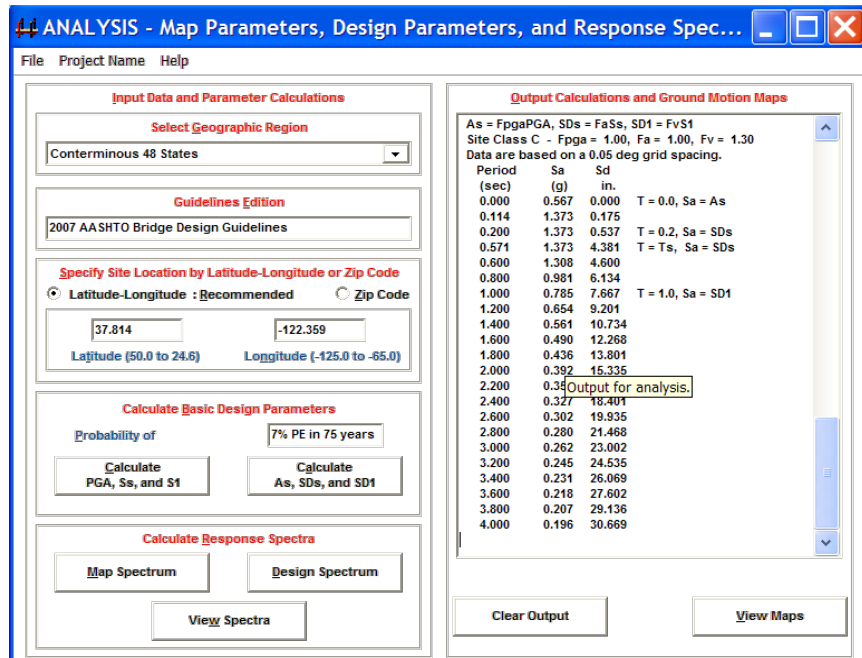


Figure 2-18 Screen No. 6: Spectral Values for Acceleration and Displacement for Site Class C ('Design Spectrum' Option)

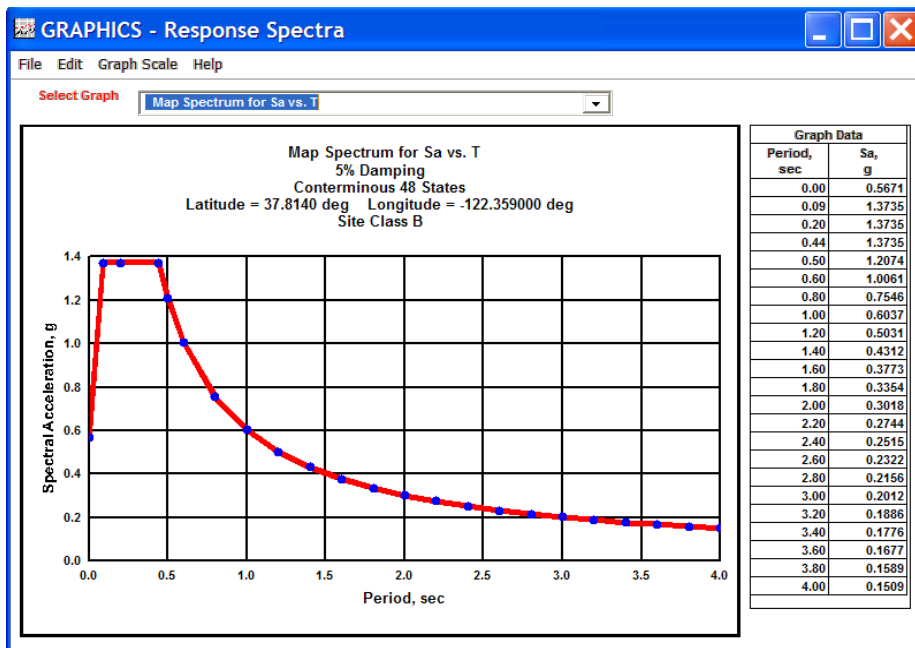


Figure 2-19 Screen No. 7: Display Option 1 ('Map Spectrum' Sa vs T) and Drop-Down Menu for Other Options

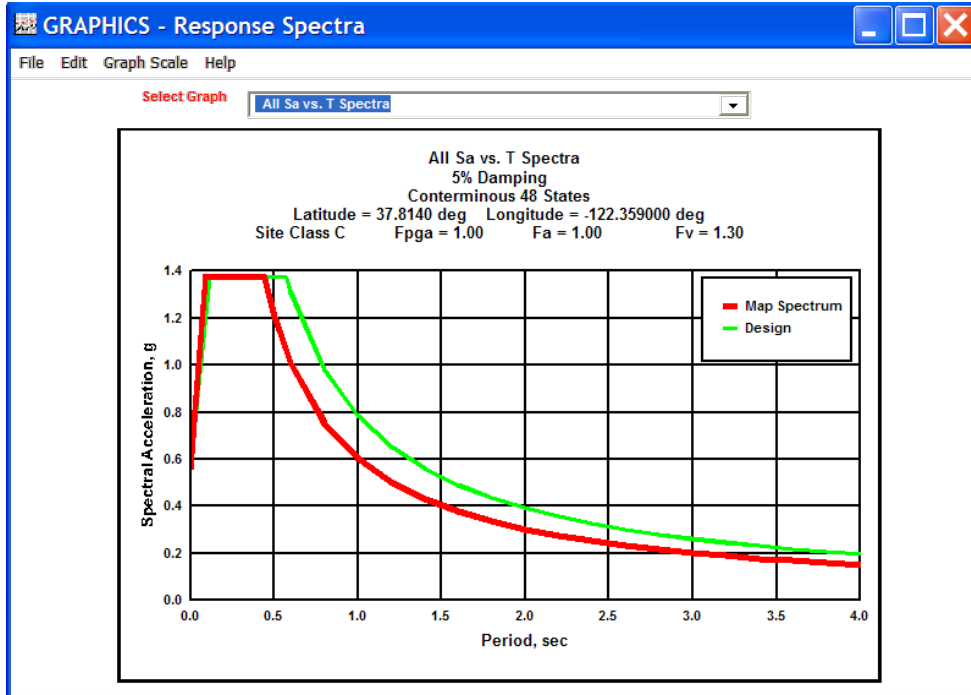


Figure 2-20 Screen No. 8: Display Option 5 (All  $S_a$  vs.  $T$  Spectra)

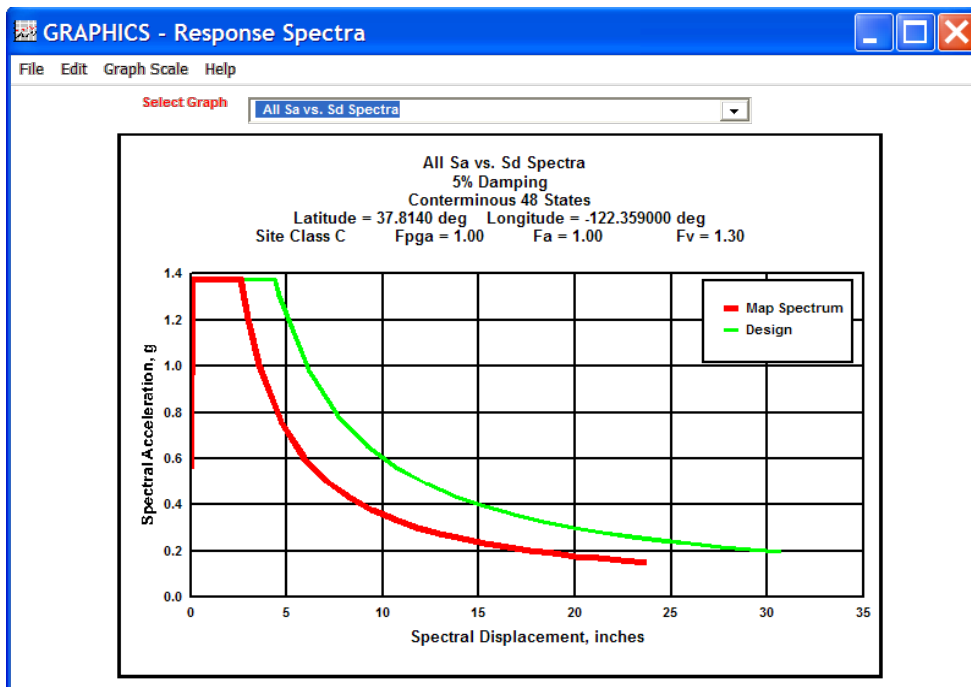


Figure 2-21 Screen No. 9: Display Option 6 (All  $S_a$  vs.  $S_d$  Spectra)

There is a minor error in the plotting of the Site Class-corrected spectrum by the CD software. The value of  $A_s$  used in plotting the spectrum is erroneously calculated as  $F_aPGA$  (rather than as  $F_{PGA}PGA$ ). However, the tabulated value of  $A_s$  is correctly calculated. Even if the value for  $A_s$  from the plotted spectrum is used, this error is minor and should not have any effect of bridge analysis results.

## 2.6 SITE-SPECIFIC RESPONSE SPECTRA FOR HORIZONTAL GROUND MOTIONS

As noted in Sec 2.5.3, site factors  $F_a$  and  $F_v$  are not provided for bridge sites on Site Class F soils. Instead, site-specific geotechnical investigations and dynamic site response analyses are required for these soils. Guidelines are given below for conducting these investigations and site response analyses

The data required to conduct a site response analysis is obtained from site-specific geotechnical investigations and includes borings with sampling, standard penetration tests (SPTs), cone penetrometer tests (CPTs), and/or other subsurface investigative techniques and laboratory soil testing to establish the soil types, properties, layering and the depth to rock or rock-like material. Shear wave velocity is a particularly important parameter in a site response analysis. Shear wave velocities should preferably be measured. However, if direct measurement of shear wave velocity is not possible or impractical, it can be estimated from soil index properties and based upon shear wave velocity data for similar soils in the same area.

Components of a dynamic site response analysis include modeling the soil profile, selecting rock motions as input to the soil profile, analyzing the response of the site to these motions, and interpreting results.

Typically, a one-dimensional soil column extending from the ground surface to bedrock is adequate to capture first-order site response characteristics. However, two- or three-dimensional models may be considered for critical projects when two- or three-dimensional wave propagation effects may be significant (e.g., in basins). The soil layers in a one-dimensional model are characterized by their total unit weights and shear wave velocities (from which low-strain (maximum) shear moduli may be obtained), and by relationships defining the nonlinear shear stress-strain relationships of the soils. The required non-linear property relationships are typically provided in the form of curves that describe the variation of shear modulus with shear strain (modulus reduction curves) and that describe the variation of hysteretic damping with shear strain (damping curves). In a two- or three-dimensional model, compression wave velocities or moduli, and Poisson's ratios may also be required. In an analysis to

estimate the effects of liquefaction on soil site response, the nonlinear soil model must also incorporate the buildup of soil pore water pressures and the consequent reduction in soil stiffness and strength. Typically, modulus reduction curves and damping curves are selected on the basis of published relationships for similar soil. Laboratory tests on site-specific soil samples to establish nonlinear soil characteristics can be considered where published relationships are judged to be inadequate for the types of soils present at the site. The uncertainty in soil properties should be considered especially in the selected maximum shear moduli, modulus reduction and damping curves. Sensitivity analyses should be conducted to evaluate the effects of the uncertainties that are considered most significant on the results of the analyses

Acceleration time histories are usually required as input to the site response model. These time histories should be representative of the horizontal rock motions at the site for the return period under consideration. They preferably should be derived using recorded motions from earthquakes with magnitudes and distances that significantly contribute to the seismic hazard at the site where such records are available. The standard of practice is to use multiple time histories when conducting a site response analysis.

At least three, and preferably seven or more, acceleration time histories should be used to model site response. These time histories will generally be scaled such that the mean spectrum of the input motions conforms to the target response spectrum for the site. Scaling factors are typically limited to between 0.5 and 2.0 to avoid developing unrealistic time histories. The target spectrum is usually taken as the reference site uniform hazard spectrum a probabilistic hazard analysis or a deterministic acceleration response spectrum developed using GMPEs and a characteristic magnitude and site to source distance. The selected time histories are then usually input to the response analysis as ground surface “bedrock” time histories and the program converts them to motions that are input to the bottom of the soil column for the site. Results of the analyses typically include both the acceleration response spectrum and acceleration time histories at the ground surface (or elevation of the foundation footing or pile cap). For a response spectrum analysis, if seven or more acceleration time histories have been used, the resulting response spectra are averaged and the average curve is smoothed to provide the design response spectrum. If less than seven (but at least three) time histories are employed, the maximum spectral accelerations are enveloped with a smooth curve for use in design. Acceleration time histories are discussed further in Section 2.8

Unless a site-specific seismic hazard analysis is carried out to develop the design rock response spectrum at the site, the reference site AASHTO/USGS map spectrum described in Sec 2.5 (Site Class B) can be

used for this purpose. For hard rock sites (Site Class A), the spectrum may be adjusted using the site factors in Tables 2-4 and 2-5. For profiles having great depths of soil above Site Class A or B rock, consideration can be given to defining the base of the soil profile and the input rock motions at a depth where soft rock or very stiff soil of Site Class C is encountered. In such cases, the design rock response spectrum may be taken as the spectrum for Site Class C defined using the site factors in Tables 2-4 and 2-5.

Methods for site-specific site response analysis may be linear and use equivalent linearized properties or explicitly nonlinear. Computer programs used in practice for one-dimensional site response analysis include the equivalent linear program SHAKE (Idriss and Sun, 1992) and nonlinear programs such as DESRA-2, (Lee and Finn, 1978), MARDES (Chang et al., 1991), SUMDES (Li et al., 1992), D-MOD (Matasovic, 1993), TESS (Pyke, 1992), and DESRA-MUSC (Qiu, 1998). If the soil response is highly nonlinear (e.g., the site is subject to very high acceleration levels or underlain by soft clay soils), nonlinear programs may be preferable to equivalent linear programs. As noted previously, sensitivity analyses to evaluate the effect of uncertainties in the soil properties and soil profile should be conducted and considered in developing the design response spectrum.

## **2.7 VERTICAL GROUND MOTION RESPONSE SPECTRA**

The subject of vertical ground motions sometimes leads to heated debates among academics and practicing engineers and an in-depth discussion on this subject is outside the scope of this Manual. Nevertheless a brief discussion of the issues surrounding vertical ground motion is given below.

- 1) Few structural design codes and specifications and essentially no geotechnical design provisions require consideration of vertical ground motions.
- 2) Vertical design spectra are not available from the USGS National Seismic Hazard Mapping program. If vertical motions are to be considered in design, generation of site-specific vertical spectra will be necessary. In general these spectra may be developed from horizontal site-specific spectra as described in the FHWA Retrofit Manual (FHWA, 2006) and in item (3) below.
- 3) For response spectrum analyses, the method of most technical merit for the development of a vertical ground motion spectrum makes use of the magnitude and distance data from the deaggregation of the hazard curve and an appropriate GMPE to develop a period dependent V/H (vertical to horizontal) ground motion spectrum ratio. This V/H function can then be applied to the horizontal design spectrum to generate a target vertical spectrum for design.

- 4) In many situations (particularly for the CEUS) an appropriate GMPE for vertical ground motions may not exist. In these circumstances, the rule of thumb of scaling the horizontal design response spectrum by  $2/3$  can be used to develop a target vertical spectrum for design. However, this rule-of-thumb can break down at high frequencies (i.e., at modal periods less than 0.15 second), especially where the site to seismic source distance is less than 50 km. Use of the  $2/3$  rule-of-thumb procedure for bridges with short fundamental periods and close to active faults is therefore not advised.

It is not clear that one-dimensional wave propagation theory (the most common approach in a site-specific response analysis – see Section 2.6 above) is the proper approach to account for the impact of local soil conditions on vertical ground motions. Experience indicates that modeling the propagation of compression waves using a one-dimensional soil column model usually leads to unrealistic vertical motions, especially at high excitation levels. It is better to rely on empirical adjustments for local soil effects (based on GMPEs), when developing acceleration spectra for vertical ground motions.

## **2.8 ACCELERATION TIME HISTORIES**

While the response spectrum method is the most common method of seismic analysis for conventional bridge design, many geotechnical analyses and some of the more complex structural analyses require the development of a set of acceleration time histories to represent the design earthquake. The process of developing appropriate time histories for these analyses generally starts with establishing the target response spectrum. Then, time histories are developed that are consistent with this spectrum by first selecting a candidate set of appropriate strong motion records (sometimes referred as the startup time histories or seed time histories). These are usually determined by the magnitude and other relevant seismic source characteristics (e.g. source mechanism, duration of strong motion, and energy content) appropriate to the design earthquake and bridge site. After selecting the candidate strong motion records, they are scaled so that the resultant mean spectrum developed from the scaled response spectra closely matches the target response spectrum. Candidate records may also be modified in the time or frequency domain to achieve a match with the target spectrum, resulting in what is referred to as a spectrum compatible time history.

The basic form of seed acceleration time history modification is simple scaling of the acceleration amplitudes in the ground motion record by a constant factor. Scaling of a record by a factor between 0.5

and 2.0 is a non-controversial process and one that is widely accepted. Scaling by factors outside of this range must be done with care and is subject to criticism. The basic problem with matching a natural time history to the target spectrum is that the acceleration response spectrum from a naturally recorded time history has many peaks and valleys. Therefore, a single, scaled time history will generally fit the target spectrum only over a very narrow range of period. Therefore, a suite of scaled time histories is required to encompass the entire target spectrum. As noted previously, a minimum of three, and preferably seven, scaled time histories are therefore employed if scaled natural records are to be used in an analysis. If three time histories are used the maximum of the three responses is used in design. If seven time histories are used the average of the seven responses is used.

Many engineers prefer to use only amplitude scaling for the development of time histories, as opposed to also modifying the records in the time or frequency domain. In this way, the phasing characteristics of the time history record are preserved and the correlation features between the three orthogonal components of ground motion are maintained. However, the number of input time histories required for an analysis can require significant computational effort (particularly if seven sets of three-component time histories are to be used) and present significant practical problems in design applications. To limit the number of time histories for practical reasons, some bridge designers employ spectrum-compatible input time histories. Even for an analysis using spectrum-compatible motions it may be necessary to use only three sets of such motions to achieve a statistically stable result.

There are two basic ways to modify a naturally recorded startup motion to develop a spectrum-compatible motion: (1) time domain adjustment (Lilhan and Tseng, 1988) and (2) frequency domain adjustment (Silva and Lee, 1987). Both approaches have advantages and disadvantages but, in the end, the best way to achieve a spectrum-compatible ground motion is the method that makes the least change to the original startup motion. Further details on this topic are given by Lam et al. (2000).

Startup ground motions for the generation of acceleration time histories can be selected from one of the many available catalogs of recorded earthquake ground motions on the basis of seismic source mechanism, earthquake magnitude, and other earthquake parameters. For the shallow crustal earthquakes common in the Western United States, the Pacific Earthquake Engineering Research Center (PEER) has compiled an extensive database. The PEER database includes over 3000 strong ground motions records from shallow crustal earthquakes in active tectonic regimes throughout the world. The PEER website also includes a powerful tool for selecting and scaling time histories to match a target spectrum. The PEER database and tool for selecting and scaling time histories to match a target spectrum can be found at

[http://peer.berkeley.edu/peer\\_ground\\_motion\\_database](http://peer.berkeley.edu/peer_ground_motion_database) . Another comprehensive catalog of ground motions is that developed by the Nuclear Regulatory Commission for use in design of Nuclear Power Plants (Nureg/CR-6728: Technical Basis for Revision of Regulatory Guidance on Design Ground Motions: Hazard- and Risk Consistent Ground Motion Spectra Guidelines). Nureg/CR-6728 provides a catalog of over 500 sets of three component time history records classified into (1) two tectonic regions: the western US (WUS) and the central and eastern U.S. (CEUS), (2) two site classes: rock and soil sites, and (3) magnitude (M- 5 to 6, M- 6 to 7, and 7+) and distance (R from 0-10, 10-50, 50-100 and >100 km) . Nureg/CR-6728 also includes a set of CD-ROMs containing the time histories. The benefit of this database is that it includes time histories considered appropriate for the CEUS. However, the user should be aware that, due to the lack of recorded data, the CEUS records were developed by modifying WUS records to account for differences in seismic source and crustal properties between the two regions based on seismological modeling.

## 2.9 SPATIAL VARIABILITY OF GROUND MOTIONS

Because transportation systems are lineal systems that extend over large distances, it is sometimes necessary to consider the effect of the spatial variation in typical earthquake ground motions. This may involve analyzing the system (e.g. a long-span bridge, multi-span viaduct, or a tunnel) with input motions that differ from support to support. In such circumstances, time histories of both acceleration and displacement are required at each support.

Several factors contribute to spatial variability of ground motions, including:

- 1) Wave Passage Effects. The wave passage effect is due to non-vertical wave propagation and produces systematic time shifts in the arrival of the seismic waves at each support. This effect can be modeled by applying a time shift to each support time history. Based on field measurements, an apparent wave speed of 8,250 ft/s (2.5 km/s) may be used to calculate this time shift. This velocity is toward the lower end of the range of measured speed, leading to somewhat conservative estimates of the differential motions. Wave passage effects are generally not considered significant in bridges less than 1500 ft long.
- 2) Attenuation over Distance. When the seismic source is close to a long span bridge, the different distances to the various support locations can result in different ground motions at each support due

to the attenuation of the ground motion with distance. Conventional GMPEs may be used to estimate this difference in the ground motion.

- 3) Complex Wave Scattering. Wave propagation can result in spatial incoherency (spatial differences) in both the amplitude and phase of the ground motions. These effects are sometimes referred to as complex wave scattering effects and are observed empirically in the recorded data from closely spaced strong motion instruments. Empirical models for the coherency function for the horizontal and vertical components of ground motion developed by Abrahamson (1992) are shown in Figures 2-22 and 2-23. These plots show that the degree of coherency decreases, and incoherency increases, at higher frequencies and larger spatial distances.

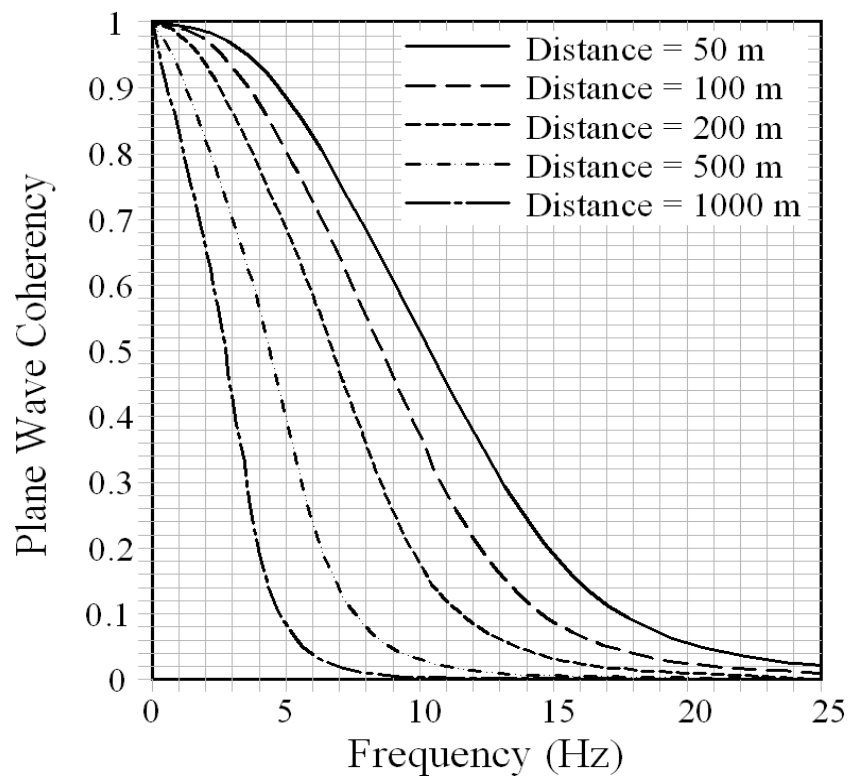


Figure 2-22 Coherency Function for Horizontal Component Motion (Abrahamson, 1992)

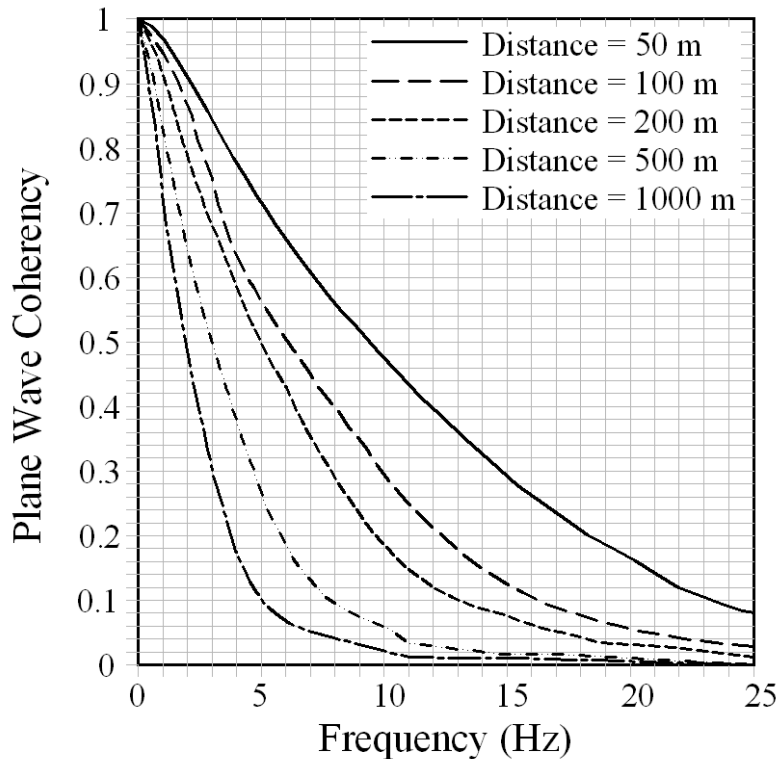


Figure 2-23 Coherency Function for Vertical Component Motion (Abrahamson, 1992)

- 4) Variation due to Local Soil Condition. The variation in soil conditions along the length of a bridge can be significant and lead to large variations in the ground motions at or near the ground surface at the bridge support points (i.e. abutments and intermediate piers). This is perhaps the most significant source of spatially-varying input motions for most bridges. Variations in local soil conditions are generally accounted for by conducting one-dimensional site response analyses for representative soil columns at each support location. The base of each column is subjected to the free-field design ground motions and the difference in soil response at the top of the columns is assumed to represent the variation in ground motions due to local soil conditions. Bridges of almost any length can be susceptible to the effect of soil variability from one end to the other.

Each of the above phenomena can contribute to differences in the ground motions at the supports of a long bridge or tunnel. However, experience has shown that the effect of the first three phenomena is usually very small and may be ignored (with the exception of the wave passage effect on long span structures). The most important factor contributing to differential ground motion is likely to be variability in the soil conditions from support to support. It is most important to include this factor when developing spatially varying, multiple support motions for use in time history analyses. As noted above, both

displacement and acceleration time histories are required to correctly model the response of the bridge, although some computer programs will compute one from the other if both are not available. At the present time, differential motions due to the variability in support motions across the bridge site cannot be accounted for in a response spectrum analysis. Approximate methods that use a modified response spectrum approach, and avoid time history analysis, have been proposed but not yet shown to be reliable.

## **2.10 SUMMARY**

This chapter describes the methods used to assess and characterize strong ground motion for use in seismic design. The fundamental steps in a seismic hazard analysis are described, including seismic source characterization, strong motion attenuation, and prediction of design ground motion parameters. Both probabilistic and deterministic seismic hazard analyses are described and the advantages and disadvantages of these two types of analysis are discussed. The essential products of a probabilistic seismic hazard analysis, including the uniform hazard spectra and the magnitude-distance deaggregation, are described. The selection of ‘rare’ and ‘expected’ earthquakes for performance-based design is discussed along with the basis for the 1,000-yr return period design ground motion used in the current AASHTO seismic design specifications. The procedure for developing the seismic coefficient design spectrum as defined in the AASHTO specifications, including adjustments for local soil conditions, is presented along with a methodology for deriving displacement spectra from acceleration spectra.

Step-by-step procedures are presented for developing the AASHTO 1000-yr return period response spectrum for the design of a conventional bridge from either the USGS web site or the AASHTO design ground motions CD. The importance of a variety of special considerations, including near-field fault directivity effects, vertical ground motions, and the spatial variability in earthquake ground motions, is discussed. The procedures used to select a suite of representative time histories for use in time-domain analysis is presented. Finally, general guidelines are given for conducting site-specific site response analyses, which are required for bridges in Site Class F.



## **CHAPTER 3**

### **GEOTECHNICAL HAZARDS**

#### **3.1 GENERAL**

This chapter describes procedures for the evaluation of earthquake-induced geotechnical hazards at highway bridge sites. These hazards include soil liquefaction, soil settlement, surface fault rupture, and seismic slope instability. In the following sections, these hazards and their potential adverse consequences to highway bridges are described along with procedures for evaluating the hazards. While the consequences of these hazards (e.g., the ground displacements accompanying the hazards) are addressed in this chapter, methods for evaluating the effects of these hazards on the capacity and deformations of the bridge–foundation system as well as measures for mitigating them are described in other chapters of this manual.

A two-part procedure is generally employed for assessing geotechnical seismic hazards. In the first part, a screening-type evaluation is conducted. Generally, this can be accomplished based on a review of available information and field reconnaissance. If the screening criteria are satisfied, the hazard potential is considered to be low and further evaluations of the hazard are not required. If a hazard cannot be screened out, more detailed evaluations, which may require obtaining additional data, are required to assess the hazard and its consequences. In this chapter, guidelines for initial seismic hazard screening are provided and an overview is provided of methods for detailed seismic hazard evaluation. Seismic hazard screening and evaluation should be carried out by engineers and scientists having knowledge of the hazards and experience in evaluating them (e.g. geotechnical engineers competent in seismic design, engineering geologists, and other engineers and scientists as appropriate).

#### **3.2 SOIL LIQUEFACTION HAZARD**

##### **3.2.1 Hazard Description and Initial Screening**

Soil liquefaction is a phenomenon in which a cohesionless soil deposit below the groundwater table loses a substantial amount of strength due to strong earthquake ground shaking. The reason for strength loss is that cohesionless soils tend to compact during earthquake shaking and in a saturated or nearly saturated soil this tendency causes the pore water pressure in the soil to increase. This pore water pressure increase,

in turn, causes a reduction in soil strength and in stiffness. Recently deposited (i.e., geologically young) and relatively loose natural cohesionless soils and uncompacted or poorly compacted cohesionless fills are susceptible to liquefaction. Loose sands and silty sands are particularly susceptible. Loose low plasticity silts and some gravels also have potential for liquefaction. Dense natural soils and well-compacted fills have low susceptibility to liquefaction.

Liquefaction has been perhaps the single most significant cause of geotechnical-related damage to bridges during past earthquakes. Most of this damage has been related to the lateral movement of soil subsequent to liquefaction at bridge abutments. However, cases involving the loss of lateral and vertical bearing support of foundations for bridge piers have also occurred.

The potential consequences of liquefaction can be grouped into the following categories:

1. Flow slides. Flow failures are the most catastrophic form of ground failure that can occur due to liquefaction. These large displacement slides occur when the downslope static (gravity) loads exceed the resistance provided by the low shear strength of the liquefied soils, (i.e. the static factor of safety drops below 1.0 due to liquefaction). These slides can occur even after the ground stops shaking and commonly result in tens of feet of displacement. Further discussion of flow sliding is provided in Section 3.3.2.
2. Lateral spreads. Lateral spreading is the most common form of landslide-type movements accompanying liquefaction. It can occur on very gently sloping ground or under embankments underlain by liquefied soil due to the combined effect of the static (gravity) forces and the seismically induced inertia forces in the soil mass. Lateral movements accumulate during the earthquake whenever the static plus seismically induced shear stresses exceed the strength of liquefied soil. However, once the ground shaking stops, slide movement is arrested, i.e. in a lateral spread, gravity forces alone are not sufficient to cause instability. The resulting lateral movements can range in magnitude from inches to several feet and are typically accompanied by ground cracking with horizontal and vertical offsets. The potential for lateral movements is increased if there is a 'free face,' such as a river channel bounding the slide mass. Lateral spreading can occur beneath a bridge approach fill or highway embankment if the underlying soil liquefies. Lateral spreading can subject bridges supported on shallow foundations to large differential support displacements and can subject deep foundations to large lateral loads and displacements. Further discussion of lateral spreading is provided in Section 3.3.3.

3. Reduction in foundation bearing capacity. The occurrence of liquefaction beneath and/or laterally adjacent to bridge foundations can greatly reduce foundation vertical and/or lateral capacity, resulting in bearing capacity failure, large lateral loads, and associated unacceptable foundation settlements and/or lateral movements.
4. Ground settlement. Even in the absence of flow sliding, lateral spreading, or reduction in foundation bearing capacity due to liquefaction, ground settlements due to soil consolidation can occur as liquefaction-induced excess pore water pressures in the soil dissipate. This consolidation occurs over time after the ground shaking stops, perhaps for as long as several days after the earthquake, and may result in unacceptable settlement and/or differential settlement of foundations located above the liquefied layer. Furthermore, pile foundations extending through liquefied strata into stable ground may be subject to downdrag as soils overlying the liquefied strata settle relative to the piles. However, the magnitudes of total and differential ground movements associated with liquefaction-induced ground settlement are less usually than those associated with flow slides, lateral spreading, or reduction in foundation bearing capacity. Further discussion liquefaction-induced ground settlement is provided in Section 3.4.
5. Increased lateral loads on retaining walls. Liquefaction in the backfill behind a retaining wall, such as an abutment backwall or wingwall, will increase pressures on the wall, potentially leading to wall failure or excessive deformations.

Prior to initiating screening and liquefaction evaluation procedures for soils that are susceptible to liquefaction, a check should be made as to whether liquefaction has occurred at the site (or at locations in the near vicinity of the site with similar geotechnical conditions) during past earthquakes. This check may involve review of the earthquake history of an area and review of published post-earthquake reconnaissance reports. If there is evidence that liquefaction has previously occurred at the site, then the potential for liquefaction cannot be screened out and it must be given further consideration.

In AASHTO, the requirement to conduct an evaluation of liquefaction is a function of the Seismic Zone in the Bridge Design Specifications (AASHTO, 2013) and Seismic Design Category in the Guide Specifications (AASHTO, 2014). Seismic Zones 1 through 4 in the Bridge Design Specifications correspond, respectively, to Seismic Design Categories A through D in the Guide Specification (Seismic Design Categories will be employed in this discussion). Seismic Design Category is based upon the value

of  $S_{D1}$ , the Site Class-corrected spectral acceleration at a period of 1 second for the design ground motion. The Seismic Design Category criteria are presented in Table 3-1.

For Seismic Design Categories A and B, the potential for liquefaction is generally low, as peak ground accelerations are likely to be less than 0.14g and earthquake magnitudes are likely to be less than 6.0. In addition, little potential exists for permanent movement of the ground because of the small size and limited duration of seismic events at these levels. However, where loose to very loose saturated sands are within the subsurface profile such that liquefaction of these soils could impact the stability of the structure, the potential for liquefaction in Seismic Design Category B should be considered.

**TABLE 3-1 SEISMIC DESIGN CATEGORIES AS DEFINED BY AASHTO (2014)**

Value of $S_{D1} = F_v S_1$	Seismic Design Category (SDC)
$S_{D1} < 0.15$	A
$0.15 \leq S_{D1} < 0.30$	B
$0.30 \leq S_{D1} < 0.50$	C
$0.50 \leq S_{D1}$	D

The potential for liquefaction at the higher spectral accelerations corresponding to Seismic Design Categories C and D is higher and careful attention is needed to determine the potential for and consequences of liquefaction at sites with these categories. AASHTO mandates that an evaluation of the potential for and consequences of liquefaction in soils near the surface should be made at sites in Seismic Design Categories C and D if the following two conditions are met:

- The water table is deeper than 50 feet below the existing ground surface or proposed finished grade at the site, whichever is lower (including considerations for seasonal, historic and possible future rises in groundwater level); and
- Sands and low plasticity silts within the upper 75 ft are characterized by one of the following:
  1. The normalized cone penetration resistance  $q_{c1N}$ , is less than or equal to 150;
  2. The normalized and standardized Standard Penetration Test blow count,  $(N_1)_{60}$ , is less than or equal to 25;
  3. The normalized shear wave velocity,  $V_{s1}$ , is less than 660 ft/s;
  4. A geologic unit that has been observed to have liquefied in previous earthquakes is present at the site.

The shear wave velocity criterion and the criterion pertaining to liquefaction of the soil unit in previous earthquakes may also be used to screen gravelly soil at the site for liquefaction potential.

### **3.2.2 Liquefaction Design Requirements**

If the conditions in Section 3.2.1 that require a liquefaction analysis are met, the liquefaction assessment shall consider the following effects of liquefaction:

- Loss in strength in the liquefied layer or layers;
- Liquefaction-induced ground settlement; and
- Flow failures, lateral spreading, and slope instability.

AASHTO also requires that bridges at sites found to be susceptible to liquefaction should be designed for two configurations as follows:

- Assuming no liquefaction occurs, using the ground motions and soil properties appropriate for the non-liquefied condition;
- Assuming that liquefaction has occurred and that the liquefied soil provides the appropriate residual resistance for lateral and axial deep foundation response consistent with liquefied soil conditions using the same design spectrum as that used for the non-liquefied conditions.

### **3.2.3 Earthquake Ground Motions Parameters for Liquefaction Analysis**

To perform analyses of the potential for liquefaction, as well as for some types of analyses of the consequences of liquefaction, an estimate of peak ground acceleration at the site and the associated earthquake magnitude are needed, at a minimum. Earthquake magnitude and earthquake source-to-site distance are also needed for some types of lateral spreading evaluation. The peak ground acceleration can be obtained either by using the AASHTO map-based procedure (i.e. based on The AASHTO ground motion maps and using Site Factors to account for local ground conditions) or a using a site-specific procedure (e.g. a one-dimensional site response analysis), as described in Chapter 2

As discussed in Chapter 2, AASHTO design ground motions are based on a probabilistic approach, except near highly active faults where ground motions are “bounded” deterministically so as not to exceed levels associated with the occurrence of maximum magnitude earthquakes on the faults. When the design ground motions for the bridge are based on a probabilistic approach (i.e., are developed for a certain probability of ground motion exceedance or return period), then it is necessary to deaggregate the peak ground acceleration hazard to determine the “dominant” (or representative) magnitude contributing to the hazard, as described in Chapter 2. The process of deaggregation is required because different seismic sources, earthquake magnitudes, and distances contribute to the probability of exceedance of

ground motions in a probabilistic analysis. The representative earthquake magnitude must be established based upon the magnitude-distance combinations in the deaggregated earthquake hazard and engineering judgment.

Where a deterministic approach is applied to establish the design earthquake, design ground motions are based upon some type of maximum magnitude earthquake occurring on a specific seismic source. It is generally assumed that the earthquake occurs on the source at its closest approach to the site. However, because liquefaction potential depends upon both magnitude and peak ground acceleration, it may not be possible to distinguish between the liquefaction potential of a small magnitude earthquake on a nearby source and a larger magnitude earthquake on a more distant source. Accordingly, in a deterministic analysis one or more earthquake sources and associated magnitudes must be evaluated to determine the most critical event with respect to liquefaction at the site.

AASHTO (2011) does allow for consideration of the effects of pore pressure generation that accompanies liquefaction in establishing design ground motions. Consideration of the effects of pore pressure generation on ground motions requires a site specific response analysis using a non-linear effective stress analysis. Such an analysis should consider the effects of pore pressure dissipation along with pore pressure generation. Use of this approach, described by Matasovic and Hashash (2012), requires considerable skill. The complexity of this approach is such that Owner's approval is mandatory and it is highly advisable that an independent peer review panel composed of members with expertise in this type of analysis review the analysis and its results. Furthermore, under no conditions shall the non-linear effective stress analysis reduce the acceleration response spectrum for the design ground motion to less than two-thirds of the response spectrum for the non-liquefied condition. It also should be noted that occasionally liquefaction may increase spectral accelerations in the long period range, i.e. for spectral periods over about 1-2 second, compared to the non-liquefied case.

### 3.2.4 Procedures for Liquefaction Evaluation

The procedures given below for the evaluation of liquefaction are consistent with the AASHTO specifications and are based on the following source documents:

- Proceedings of the 1996 and 1998 NCEER and MCEER Workshops on evaluating liquefaction resistance (Youd et al., 2001).
- Recommended LRFD guidelines for the seismic design of highway bridges (ATC/MCEER, 2003), and the Guide Specifications for LRFD Seismic Bridge Design (AASHTO, 2014)
- Seismic Retrofitting Manual for Highway Structures: Part 1- Bridges (FHWA, 2006).
- Procedures for implementing guidelines for analyzing and mitigating liquefaction in California (SCEC, 1999).
- LRFD Seismic Analysis and Design of Transportation Geotechnical Features and Structural Foundations (FHWA, 2011)

#### Field Exploration

A number of factors must be considered during the planning and conduct of the field exploration phase of the liquefaction investigation. These include:

- Location of potentially liquefiable soils.
- Location of groundwater level.
- Depth of potential liquefaction.

During the field investigation, the limits of unconsolidated deposits with liquefaction potential should be mapped within and beyond the footprint of the bridge. Typically, this will involve an investigation at each pier location and at a sufficient number of locations away from the approach fill to establish the spatial distribution of the material. The investigation should establish the thickness and consistency of liquefiable deposits from the ground surface to the depth at which liquefaction is not expected to occur.

The groundwater level should be established during the exploration program. If uncertainty exists in the location of the groundwater level, piezometers should be installed during the exploration program. Ideally, the groundwater level should be monitored in the piezometers over a sufficient duration to establish seasonal fluctuations that may be due to rainfall, river runoff, or irrigation.

If the groundwater level fluctuates due to tidal action or seasonal river fluctuations, then the zone of fluctuation will often have a lower degree of saturation than if the soil that is always beneath the groundwater level, making the soil more resistant to liquefaction. Unless the fluctuating ground water level is at a higher elevation for an extended period of time, say weeks at the higher level, it is usually acceptable to use a long-term mean groundwater level as a basis for design.

Field exploration should be conducted to the maximum depth of liquefiable soil. A depth of about 50 ft has often been used as the depth of analysis for the evaluation of liquefaction. However, liquefaction is reported to have occurred to depths in excess of 80 ft during the 1964 Alaska earthquake. For this reason it is recommended that a minimum depth of 80 ft below the existing ground surface or lowest proposed finished grade (whichever is lower) be investigated for liquefaction potential. For deep foundations (e.g. shafts or piles), the depth of investigation should extend to a depth that is a minimum of 20 ft below the lowest expected foundation level (e.g. shaft bottom or pile tip) or 80 ft below the existing ground surface or lowest proposed finished grade, whichever is deeper. However, a liquefaction investigation need not extend below a depth at which only geologic deposits that are clearly non-liquefiable are present.

Two field exploration methods are most commonly used during the evaluation of liquefaction potential: the Standard Penetration Test (SPT) and the Cone Penetrometer Test (CPT). Other methods should be used as required. For example, the measurement of shear wave velocities may be useful in some assessments of liquefaction potential. Shear wave velocity testing is particularly useful in soils not amenable to SPT or CPT testing, e.g. soils with oversized particles that inhibit SPT or CPT testing. A geologic reconnaissance and review of the available geotechnical information for the site should supplement any field investigation.

Information presented in Youd et al. (2001) and SCEC (1999) indicate that the results of SPT explorations are affected by small changes in measurement method. Primarily because of their inherent variability, sensitivity to test procedure, and uncertainty, SPT *N*-values have the potential to provide misleading assessments of liquefaction hazard if the tests are not performed carefully. Furthermore, SPT testing averages the penetration resistance over a significant depth interval (i.e. over at least 18 inches) and may yield only one value every five feet, creating a potential for missing thin layers of liquefiable soil

The CPT method is gaining recognition as the preferred method of evaluating liquefaction potential in many locations. Methods for assessing liquefaction potential from CPT results are given in Youd et al. (2001) and FHWA (2011). The primary advantages of the CPT method are:

- It provides an almost continuous penetration resistance profile that can be used for stratigraphic interpretation, which is particularly important in determining the potential for lateral spreading, lateral flows, and significant differential post-liquefaction settlements.
- Repeatability of the test is very good.
- The test is fast and economical compared to drilling and laboratory testing of soil samples.

The limitations of the CPT method are:

- It does not routinely provide soil samples for laboratory tests.
- It provides interpreted soil behavior types and does not provide the actual soil types in accordance with ASTM Test Methods D 2488 (Visual Classification) or D 2487 (USCS Classification) [ASTM, 1998].
- Tests cannot be performed in gravelly soils and sometimes the presence of hard/dense crusts or layers at shallow depths makes penetration to desired depths difficult.

### Evaluation of Liquefaction Potential

Two basic procedures are used to evaluate the potential for liquefaction at a site. These are:

- A simplified procedure that is based on empirical correlations between soil resistance (e.g. SPT blow count, CPT tip resistance, shear wave velocity) and observations of liquefaction.
- More rigorous numerical modeling.

For most projects, the simplified procedure will be acceptable. However, for some projects, more rigorous modeling using advanced computer codes may be appropriate. Conditions warranting the use of more rigorous methods include:

- Sites where liquefiable soils extend to depths greater than 50 ft.
- Sites that have significant interlaying, particularly where interlayers comprise highly impermeable soils or soft clay layers.
- Sites where the cost of ground remediation methods to mitigate liquefaction is great.

Results of site-specific ground response analyses conducted using these rigorous methods that include pore pressure generation may often result in lower estimates for ground acceleration and shearing stresses within the soil profile because the energy dissipative mechanisms occurring during liquefaction and the effects of pore pressure softening are explicitly considered in this approach. The results of such analyses should not be used in conjunction with the empirical curves employed in the simplified procedure, as the stress ratios in these empirical plots were developed without consideration of these softening effects.

## Simplified Procedure

The most common procedure used in engineering practice for assessment of liquefaction potential is the ‘Simplified Procedure’. This procedure compares the cyclic resistance ratio (CRR, the cyclic shear stress ratio required to induce liquefaction for a cohesionless soil stratum at a given depth) with the earthquake-induced cyclic shear stress ratio (CSR) at that depth from the design earthquake (defined by a peak ground surface acceleration and an associated earthquake magnitude). CRR and CSR are ratios of cyclic shear stress to initial (pre-earthquake) effective overburden pressure on a horizontal plane at a given depth in the soil deposit.

Values of CRR for the Simplified Procedure are generally established from databases for sites where surface manifestations of liquefaction were and were not observed during past earthquakes. Values of the normalized SPT blow count,  $(N_1)_{60}$ , are associated with the predicted CSR in both liquefied and non-liquefied strata. The boundary curve between the sites where liquefaction was observed and sites where liquefaction was not observed defines the CRR -  $(N_1)_{60}$  relationship. The consensus version of the baseline chart defining the CRR -  $(N_1)_{60}$  relationship for magnitude 7.5 earthquakes is shown in Figure 3-1. This chart was established by consensus at the 1996 and 1998 NCEER/MCEER workshops (Youd et al., 2001). As illustrated in Figure 3-1, the determination of the CRR must consider the fines content of the soil. Other factors that affect the CRR include the energy of the hammer (which influences the value of  $(N_1)_{60}$ ), the effective overburden pressure, and the magnitude of the earthquake (Youd et al., 2001).

The effect of earthquake magnitude on CRR is accounted for by applying a magnitude scaling factor (MSF) to the ordinates of Figure 3-1. Recommendations from several different investigators for MSF were considered during the 1996 and 1998 workshops (Youd et al., 2001). The range of magnitude scaling factors considered at the workshops is shown in Figure 3-2. The consensus arrived at in the workshop is that the factors defined by the curve at the lower-bound of the recommended range (cross-hatched area) in Figure 3-2 be used unless different factors can be justified. Note that for magnitudes greater than 7.5, the recommended curve is the second highest curve shown in Figure 3-2.

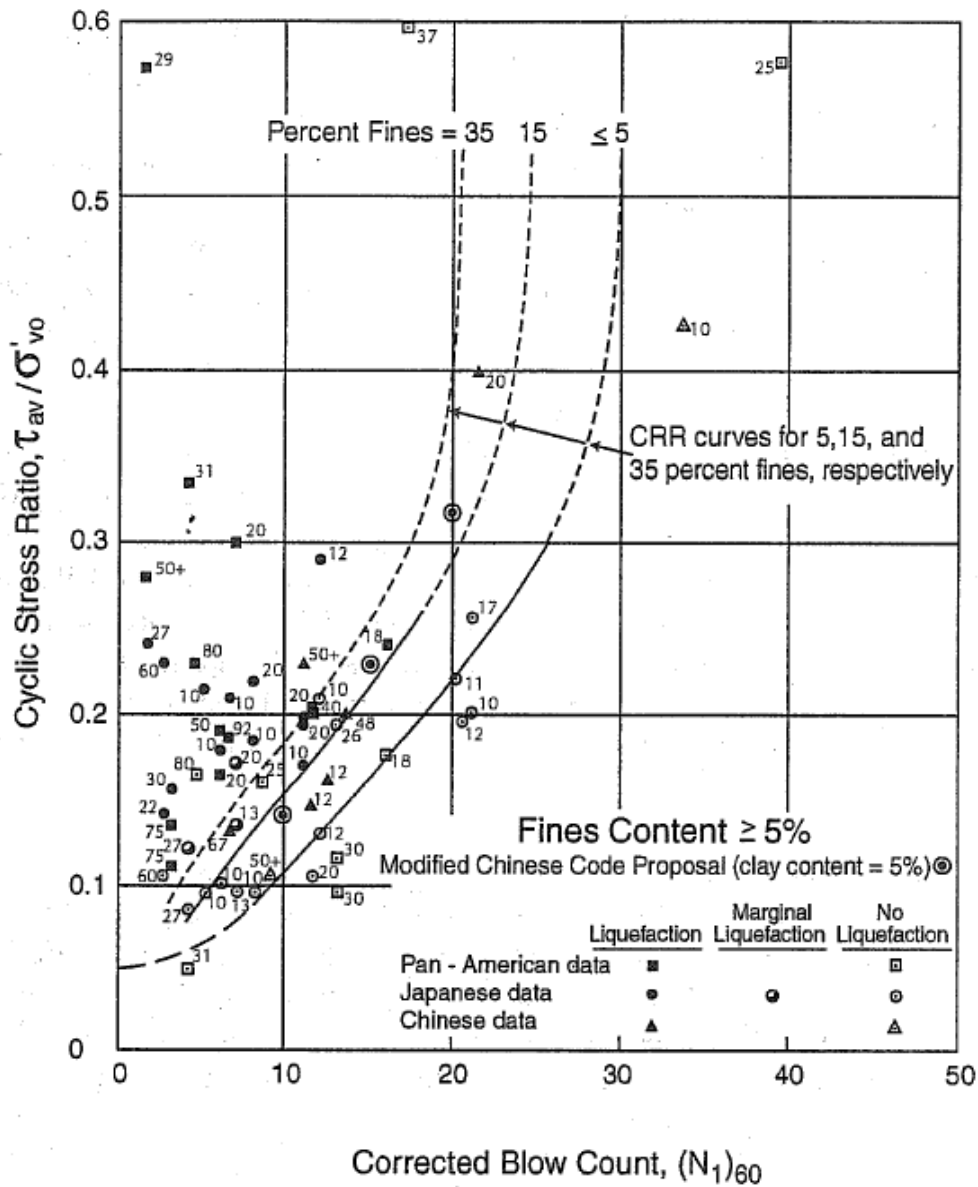


Figure 3-1 Simplified Base Curve Recommended for Determination of CRR from SPT Data for Magnitude 7.5 Along with Empirical Liquefaction Data

Adjustments for changes in water table and overburden condition should be made when conducting a simplified liquefaction analyses. The following text provides guidance on making these adjustments.

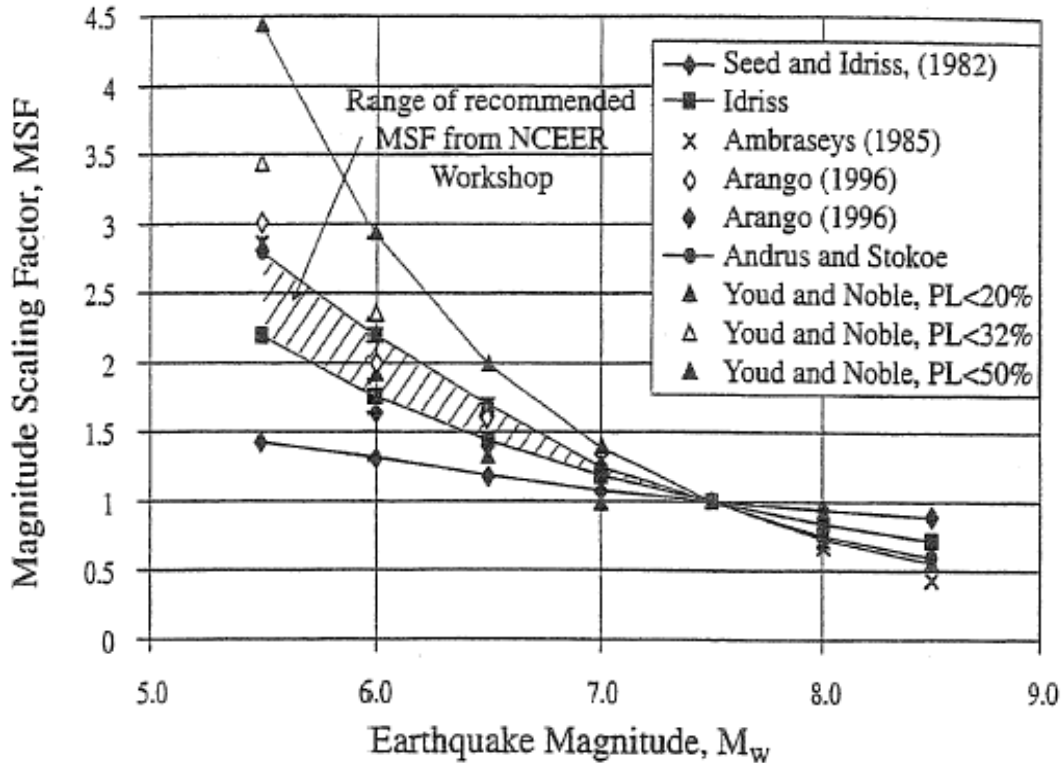


Figure 3-2 Magnitude Scaling Factors Derived by Various Investigators

- Overburden Corrections for Differing Water Table Conditions. To perform analyses of liquefaction potential, liquefaction settlement, seismically induced settlement, and lateral spreading, it is necessary to develop a profile of SPT blow counts that have been normalized using the effective overburden pressure. Normalization factors are presented in Youd et al. (2001). This normalization should be performed using the effective stress profile that existed at the time the SPT testing was performed. These normalized values are then held constant throughout the remainder of the analyses, regardless of whether or not the analyses are performed using higher or lower water-table conditions. Although the possibility exists that softening effects due to soil moistening can influence SPT results if the water table fluctuates, it is commonly assumed that the only effect that changes in the water table have on the results is due to changes in the cyclic stress ratios due to changes in the effective overburden stress.
- Overburden Corrections for Differing Fill Conditions. Approach fills and other increases in overburden pressure should be handled in a manner similar to that described above for changes in

groundwater elevation. It is necessary to develop a profile of the CRR based upon the SPT blow counts that have been normalized using the effective overburden pressure existing before the fill is placed. These normalized values are then held constant throughout the remainder of the analyses, regardless of whether or not the analyses are performed using a higher fill condition.

Figure 3-3 shows the Robertson and Wride chart (Youd et al, 2001) for determining liquefaction strength (CRR) on the basis of  $q_{CIN}$ , the CPT tip resistance corrected for fines content and normalized to an overburden pressure of 1 TSF. The chart, like the SPT chart in Figure 3-1, is only valid for magnitude 7.5 earthquakes. The CPT shows calculated cyclic stress ratios plotted as a function of  $q_{CIN}$  for sites where liquefaction effects were or were not observed following past earthquakes. The curve separating regions of the plot with data indicative of liquefaction from regions indicative of non-liquefaction defines the CRR -  $q_{CIN}$  relationship for magnitude 7.5 events. Procedures for calculating  $q_{CIN}$  from the raw CPT data are presented in Youd et al. (2001).

As for the SPT method, the determination of CRR using the CPT method must account for fines content of the soil, the effective overburden pressure, and the magnitude of the earthquake. Methods to account for fines content and effective overburden pressure are presented in Youd et al. (2001). The comments given above regarding use of normalized (for effective overburden pressure) SPT blow counts in analyses are also valid for use of normalized CPT data. Recommended magnitude scaling factors for CRR are the same for SPT and CPT and are shown in Figure 3-2.

The CRR can also be obtained using shear wave velocity data, as discussed in Youd et al. (2001). The shear wave velocity procedure is useful especially for gravelly soils because of the difficulty of obtaining meaningful SPT blow count or CPT resistance in gravelly soils (due to the large size of gravel particles in comparison to the diameter of the SPT sampler and the tip of the cone penetrometer). Figure 3-4 presents the relationship between CRR and  $V_{S1}$ , the shear wave velocity normalized to an overburden pressure of 1 TSF (Andrus and Stokoe, 2000). Procedures for calculating  $V_{S1}$  are presented in Youd et al. (2001).

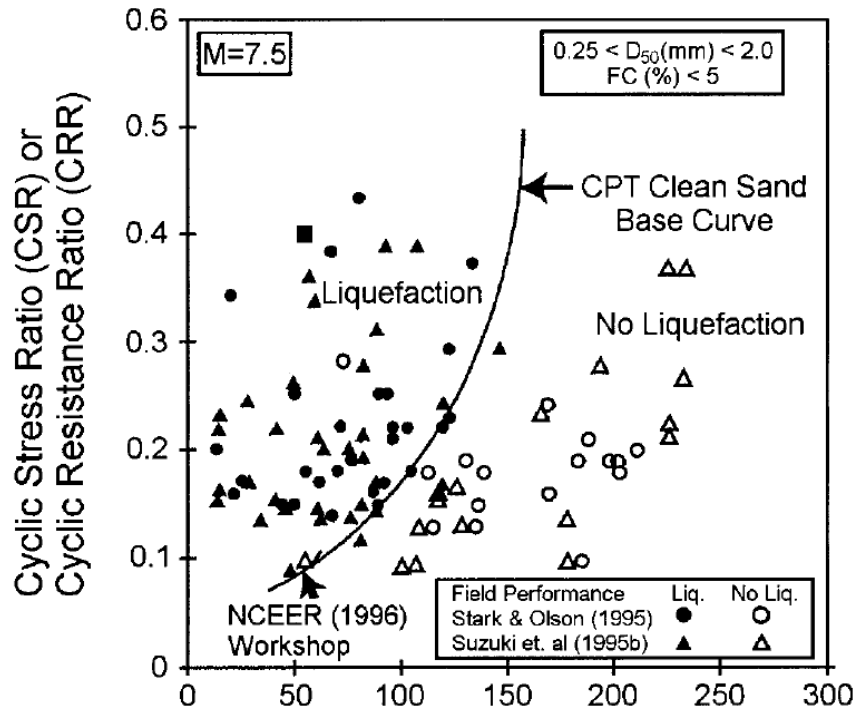


Figure 3-3 CPT Liquefaction Resistance Chart (Robertson and Wride, 1998)

For estimating values of the earthquake-induced cyclic shearing stress ratio, CSR, the MCEER workshop (Youd et al., 2001) recommended essentially no change to the original simplified procedure (Seed and Idriss, 1971) where a mean soil flexibility factor,  $r_d$  (Figure 3-5) is used to define the reduction in CSR with depth. As an alternative to using  $r_d$  charts, a site-specific response analysis of the ground motions can be performed, as discussed below.

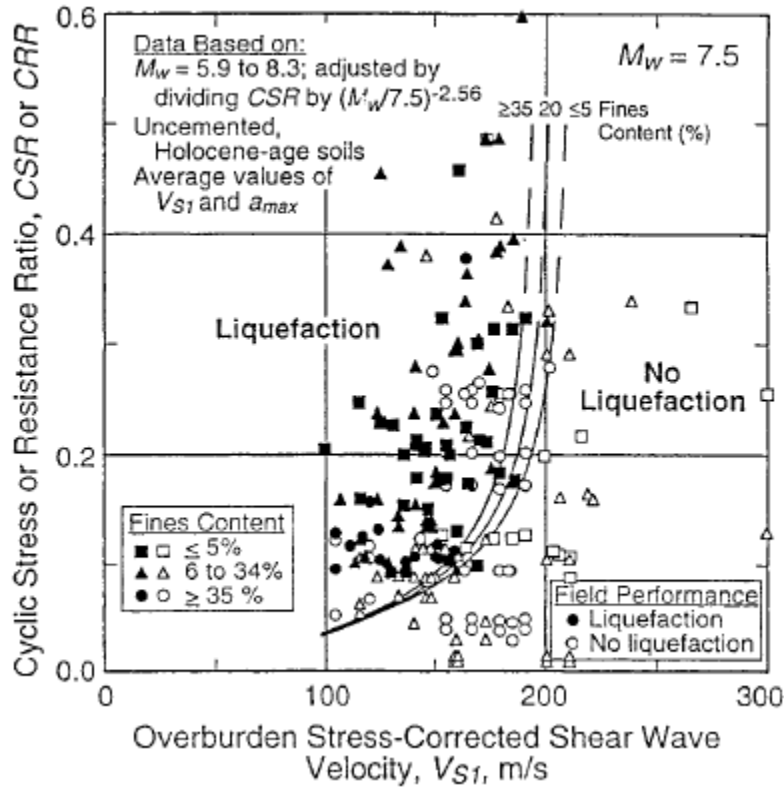


Figure 3-4 Shear Wave Velocity Liquefaction Resistance Chart (Andrus and Stokoe, 2000)

With the Simplified Procedure, CSR is calculated using the following equation:

$$CSR = \left( \frac{\tau_{av}}{\sigma'_{vo}} \right) = 0.65 \left( \frac{a_{max}}{g} \right) \left( \frac{\sigma_{vo}}{\sigma'_{vo}} \right) r_d \quad 3-1$$

- where
- $\left( \frac{\tau_{av}}{\sigma'_{vo}} \right)$  is the average earthquake induced shearing stress divided by the effective overburden stress
  - $a_{max}$  is the peak ground acceleration in units of g (acceleration due to gravity)
  - $\left( \frac{\sigma_{vo}}{\sigma'_{vo}} \right)$  is the ratio of total overburden stress to effective overburden stress
  - $r_d$  is a soil flexibility factor

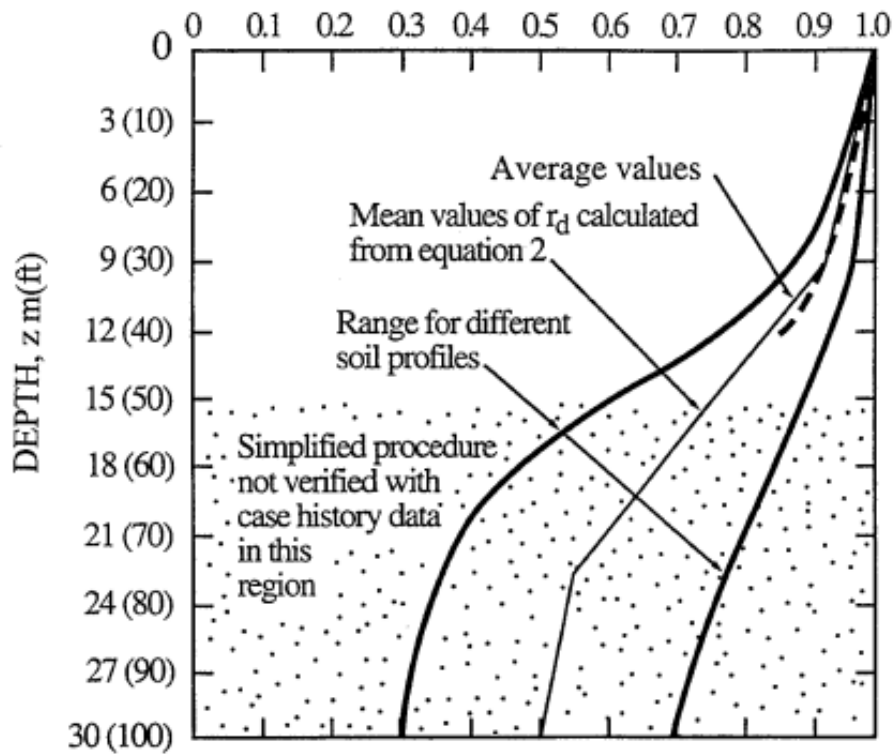


Figure 3-5 Soil Flexibility Factor ( $r_d$ ) Versus Depth as Developed by Seed and Idriss (1971) with Added Mean Value Lines

After values of CRR and CSR are established for a soil stratum at a given depth, the factor of safety (capacity to demand ratio in LRFD) against liquefaction (i.e.  $FS = CRR/CSR$ ) can be computed. The ratio of CRR to CSR should be greater than 1.0 to preclude the development of liquefaction. As the ratio drops below 1.0, the potential for liquefaction increases. An example of a liquefaction triggering analysis for a single SPT boring is shown in Figure 3-6.

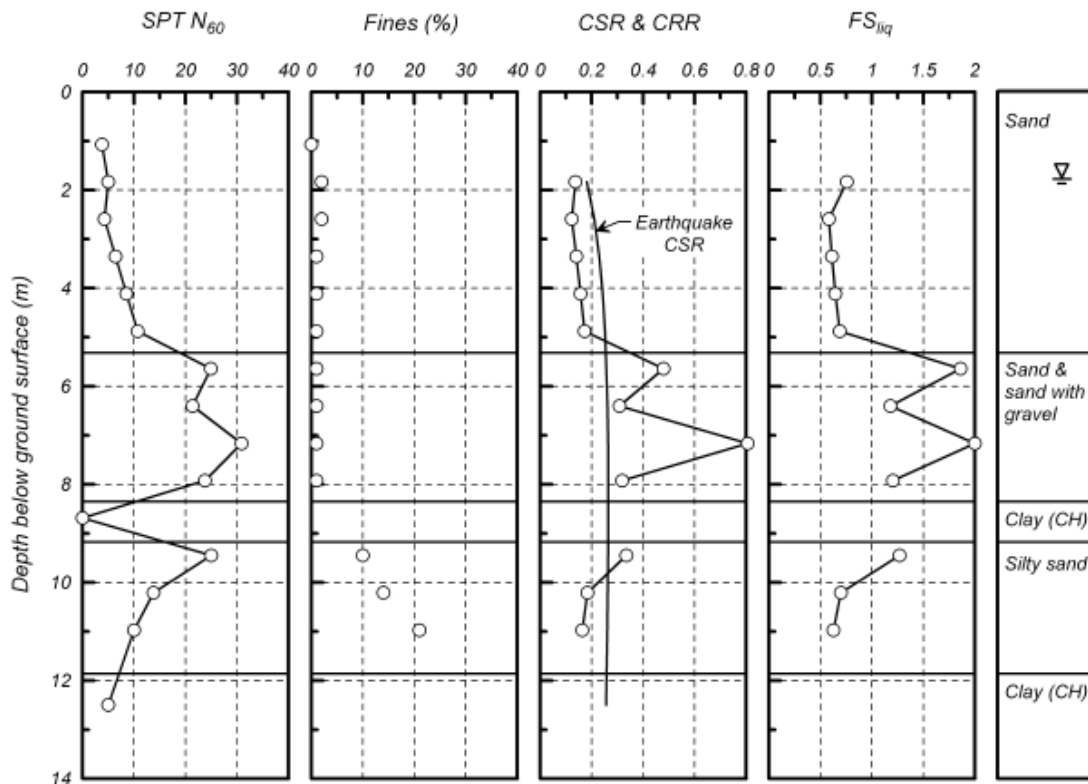


Figure 3-6 Example of a Liquefaction Triggering Analysis for a Single SPT Boring (Idriss and Boulanger, 2008)

### Numerical Modeling

For important projects, the use of equivalent linear or nonlinear site-specific, one-dimensional ground response analyses may be warranted to assess the liquefaction potential at a site. For these analyses, as discussed with respect to site specific site response analyses in Chapter 2, acceleration time histories representative of the seismic hazard at the site are used to define input ground motions at a hypothetical outcrop of rock or firm-ground at the site. The computer program then translates these motions into motions that are applied at the rock/soil interface at depth.

The most common approach to numerical modeling is to use the equivalent linear total stress computer program SHAKE (Idriss and Sun, 1992) to determine the earthquake-induced shearing stresses (i.e. the CSR) at depth for use with the simplified procedure described above, in lieu of using Equation 3-1. Note that, as in Equation 3-1, a factor of 0.65 should be applied to maximum values of CSR obtained using SHAKE to obtain average values of CSR for comparison with CRR values. However, this approach is

subject to criticism, as the plots used to establish the CRR were, for the most part, established using Equation 3-1. However, as long as plots using the mean, or expected, value of  $r_d$  are used with Equation 3-1, the use of SHAKE to obtain a best estimate of the CSR is justifiable.

Another alternative approach to evaluating liquefaction potential involves the use of nonlinear effective stress methods to directly determine developed pore water pressures. In a truly non-linear effective stress site response analysis, nonlinear shear stress-shear strain models (including failure criteria) that replicate hysteretic, degrading soil response and pore pressure development over the time history of earthquake loading are employed. The computer program DESRA2, originally developed by Lee and Finn (1978), was perhaps the first widely recognized nonlinear, effective stress, one-dimensional site response program. Since the development of DESRA2, a number of other nonlinear, effective stress, one-dimensional programs have been developed, including D-MOD 2000 (GeoMotions LLC, 2007), DESRA-MUSC (Martin and Qiu, 2000), and a model in the program FLAC (Itasca, 2006). However, as discussed by Matasovic and Hashash (2012), these non-linear models are more commonly used to assess site response and the use of these models to assess liquefaction potential is not generally accepted at the present time. Furthermore, interpretation of the results of these programs can be very subjective. For instance, if multiple histories are used (as required by ASHTO for time domain analyses) and liquefaction is predicted for some but not all time histories, is liquefaction assumed to occur in the design event?

Non-linear site response analyses should not be used as an alternative to Equation 3-1 for determining the CSR. As the CRR plots were developed based upon equivalent linear analysis, use of a non-linear analysis to determine the CSR is incompatible with these plots.

### **3.3 LIQUEFACTION INDUCED GROUND DEFORMATIONS**

#### **3.3.1 Post Liquefaction Shear Strength**

Perhaps the most serious consequence of liquefaction in the field occurs when the post-liquefaction shear strength of the soil, often referred to as the residual strength, is insufficient to maintain stability of a slope or supported embankment under the post-earthquake static loading. For these cases, a so-called flow slide will occur, leading to uncontrolled large deformations. Deformations will continue until the deformed geometry is statically stable.

Empirical approaches for estimating values of the post liquefaction (residual) shear strength,  $S_r$ , have been developed by back-analyses of liquefaction induced flow slides as first presented by Seed (1987). Widely used relationships in current practice include those developed by Olsen and Johnson (2008), shown in Figure 3-7, and Idriss and Boulanger (2007).

Olson and Johnson (2008) state that they used the average of CPT tip resistance normalization procedures suggested by Jamiolkowski et al. (1985) and Tatsuoka et al. (1990) to evaluate the normalized CPT tip resistance,  $q_{c1}$ , as shown in Figure 3-7. However, for practical purposes the following normalization equation presented in Mayne (2007) can be used:

$$q_{c1} = q_t / (\sigma'_{vo} - \sigma_{atm})^{0.5} \quad 3-2$$

where  $\sigma'_{atm}$  is atmospheric pressure (96 kPa)

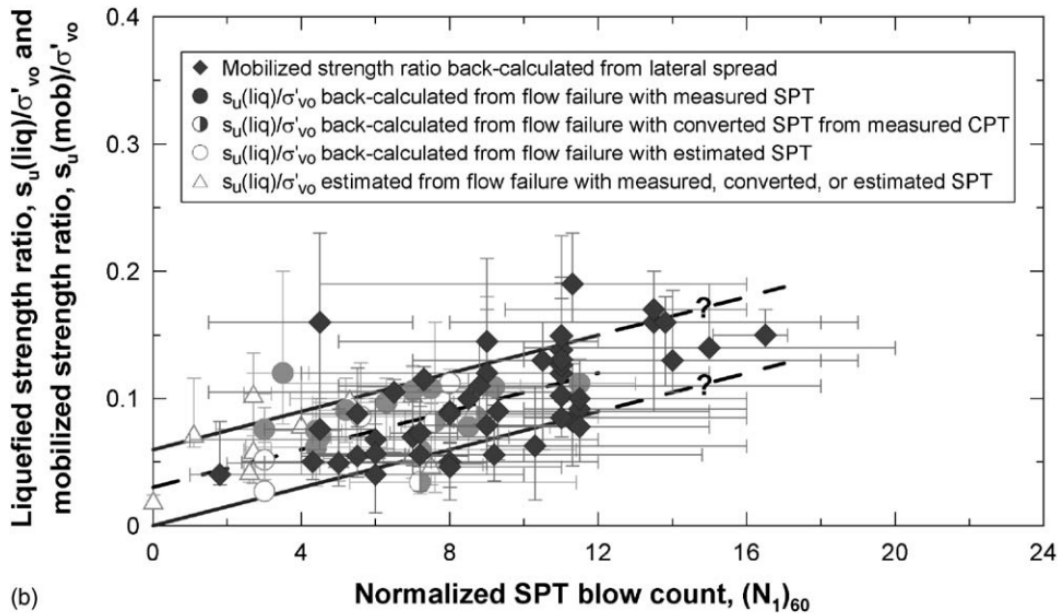
The above procedure for evaluating post liquefaction residual strength is based on back analyses of large deformation flow failures. However, Olson and Johnson (2008) report that they get similar values of post liquefaction shear strength from back analysis of lateral spreading case histories.

### 3.3.2 Flow Failures

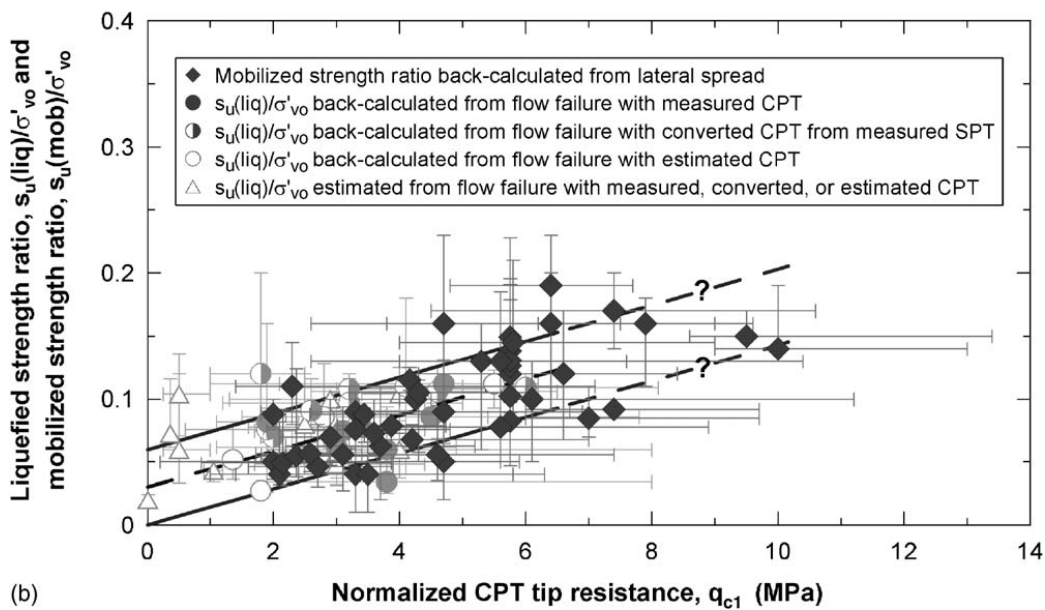
As discussed above, flow failures are the most catastrophic form of ground failure that may be triggered when liquefaction occurs. These large translational or rotational flow failures are produced by existing static stresses when average shearing stresses on potential failure surfaces exceed the average residual strength of the liquefied soil.

To assess the potential for flow failure, the static strength properties of the soil in liquefied layer are replaced with the residual strength ( $S_r$ ) of liquefied soil. A conventional slope stability check is then conducted. No seismic coefficient is used during this evaluation, thus the stability analysis represents the conditions after completion of earthquake shaking. The resulting factor of safety defines the potential for flow failures. If the factor of safety is less than 1.0, a flow failure is predicted.

The estimation of deformation associated with flow sliding cannot be easily made. The deformations can be on the order of tens of feet, depending on the geometry of the flowing ground and the types and layering of soil. In the absence of the reliable methods for predicting deformations, it is usually necessary



(b)



(b)

Figure 3-7 Correlation between the Undrained Residual Strength Ratio,  $S_r/\sigma'_{vo}$  and a) standardized normalized SPT blow count,  $(N_1)_{60}$  and b) normalized CPT tip resistance,  $q_{c1}$  (Olson and Johnson, 2008)

to simply assume that the soil will undergo unlimited lateral deformations. If the loads imposed by these deformations exceed those that can be tolerated by the structure, some type of ground remediation will likely be required. This situation should be brought to the attention of the owner and a strategy for dealing with the flow problem agreed upon.

### 3.3.3 Lateral Spreading Displacement Evaluations

The vulnerability of highway bridges to earthquake-induced ground failures arising from liquefaction has been clearly demonstrated by the extensive damage observed in past earthquakes. Damage has been often associated not only with flow sliding but also with progressive but limited lateral spreading deformations on the order of feet, driven by earthquake ground shaking subsequent to liquefaction but with deformations ceasing at the end of the earthquake. The damage associated with lateral spreading can be more limited than the damage associated with flow sliding and depends upon the magnitude of lateral spreading and the structure characteristics. Damage modes associated with lateral spreading deformations are related to displacement demands on abutments, piers, and piles to foundation damage and/or span collapse. Representative damage in the 1964 Alaska and Niigata earthquakes and the 1991 Costa Rica earthquake has been documented by Youd (1993). Damage of the 1995 Kobe earthquake is described by Tokimatsu and Asaka (1998). Two specific examples of lateral spread pile damage are noted below.

The first example is that of the performance of the Landing Road bridge in the 1987 Edgecumbe earthquake (New Zealand) documented by Berrill et al. (1997). The bridge approach spans at the riverbanks were supported by concrete wall piers founded on battered prestressed concrete piles. Liquefaction induced lateral spreading in the liquefiable sand layer on the order of 6 feet were estimated adjacent to the bridge piers from field observations. Back analyses and observations from excavations adjacent to the bridge piers indicated that the piles successfully resisted the passive pressures mobilized against the piers, albeit cracks in the piles suggested plastic hinges in the piles were on the verge of forming, as shown schematically in Figure 3-8.

In the Kobe earthquake, field investigations using borehole cameras and slope indicators showed that failures of piles in lateral spreading zones concentrated at the interfaces between liquefied and non-liquefied layers, as well as near pile heads. Also lateral pile analyses using  $p$ - $y$  interface springs together with pile deformations induced by estimated ground displacement profiles were consistent with observed pile performance (Tokimatsu and Asaka, 1998), as shown in Figure 3-9.

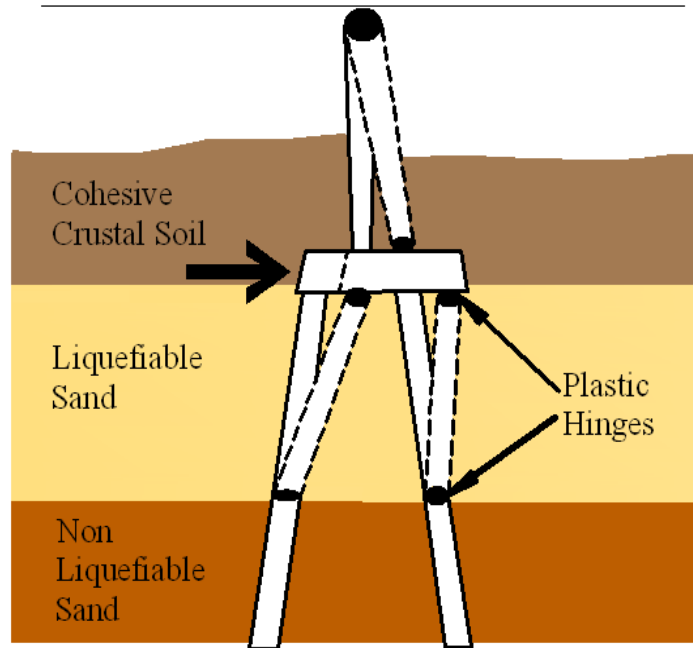


Figure 3-8 Landing Road Bridge Lateral Spread (after Berrill et al., 1997)

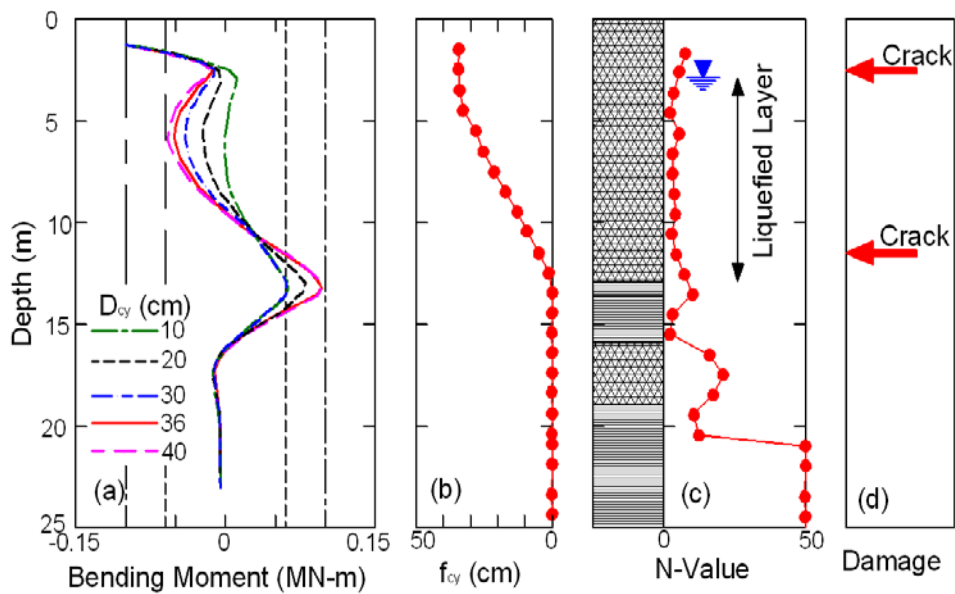


Figure 3-9 Site and Damage Characteristics for a Precast Concrete Pile Subjected to a Lateral Spread in the Kobe Earthquake (after Tokimatsu and Asaka, 1998)

The evaluation of the mode and magnitude of liquefaction induced lateral ground deformations involves considerable uncertainty and is the subject of on-going research. The current state of the practice for evaluating lateral spreading deformations uses the Newmark sliding block approach on an assumed dominant failure plane at the base of the liquefied zone. Hence free field displacements are defined by an estimated lateral displacement on a discrete failure surface, as shown in Figure 3-10.

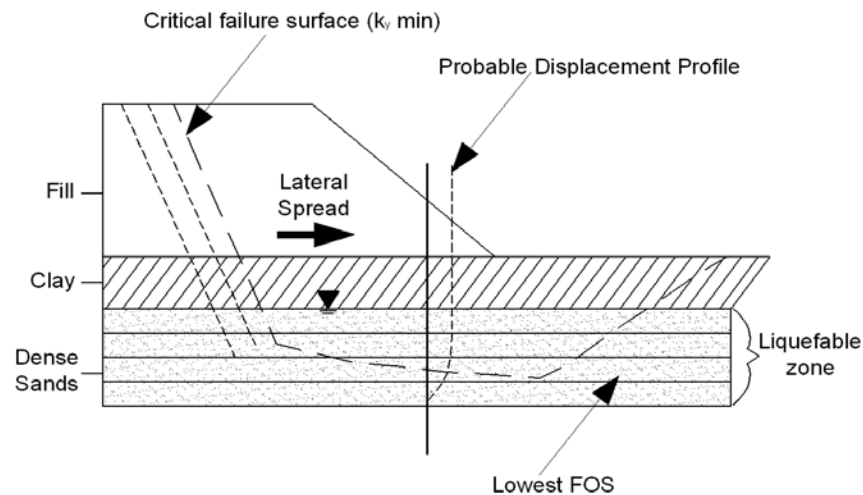


Figure 3-10 Newmark Sliding Block Analysis

Despite the limitations of the Newmark method when applied to evaluation of liquefaction-induced lateral spreading deformations (e.g. assumptions of a constant yield acceleration based on residual strength, a concentrated sliding surface, a rigid sliding block), it provides a consistent and simple framework for analysis. Further, because lateral spreading typically occurs at relatively shallow depths and due to the base isolation effect of low residual strength layers, the dynamic effects within the sliding mass are likely to be minimal and can be neglected. Hence Newmark displacement relationships such as those provided in equations 3-3 and 3-4 below may be used to calculate lateral spread displacement values by setting  $k_{max}$  equal to the PGA and computing the yield acceleration,  $k_y$ , in a limit equilibrium analysis using residual strength values in the critical liquefied layer. This type of analysis implicitly assumes that liquefaction occurs instantaneously at the start of earthquake shaking and thus should provide a somewhat conservative assessment of lateral spreading deformations.

Sliding block displacement analyses were conducted as part of the NCHRP 12-70 Project using an extensive database of earthquake records. The objective of these analyses was to establish updated relationships between displacement ( $d$ ) and the following three terms: the ratio  $k_y/k_{max}$ ,  $k_{max}$ , and the peak ground velocity, PGV, where  $k_y$  is the yield acceleration and  $k_{max}$  is the peak average acceleration of the

sliding mass. Based on regression analyses, the following simplified relationships were established and are recommended for design purposes:

For all sites except CEUS rock sites (Categories A and B), the displacement (in inches) can be estimated by the following equation:

$$\begin{aligned} \log(d) = & -1.51 - 0.74 \cdot \log(k_y / k_{\max}) + \\ & 3.27 \cdot \log(1 - k_y / k_{\max}) - 0.80 \\ & \log(k_{\max}) + 1.59 \cdot \log(PGV) \end{aligned} \quad 3-3$$

For CEUS rock sites (Categories A and B, displacement (in inches) can be estimated by:

$$\begin{aligned} \log(d) = & -1.31 - 0.93 \cdot \log(k_y / k_{\max}) + \\ & 4.52 \cdot \log(1 - k_y / k_{\max}) - 0.46 \\ & \log(k_{\max}) + 1.12 \cdot \log(PGV) \end{aligned} \quad 3-4$$

In the above equations it is necessary to estimate the peak ground velocity (PGV), the yield acceleration ( $k_y$ ), and the peak average acceleration ( $k_{\max}$ ). Values of PGV can be determined using the following correlation between PGV and spectral ordinates at one second ( $S_1$ ) from the seismic hazard analysis.

$$PGV \cdot (in/sec) = 38 \cdot F_v \cdot S_1 \quad 3-5$$

where  $S_1$  is the spectral acceleration at 1 second for Site Class B (reference site conditions) and  $F_v$  is the Site Class adjustment factor. For shallow sliding, e.g. lateral spreading due to liquefaction, the value of  $k_{\max}$  may be taken as the peak ground acceleration (PGA). The value of  $k_y$  is the seismic coefficient that results in a factor of safety of 1.0 in a pseudo-static limit equilibrium analysis for the liquefied condition.

Where highway bridge damage associated with the expected magnitude of flow sliding or lateral spreading is unacceptable, mitigation methods need to be addressed. Apart from relocating the bridge to another less vulnerable site, two basic mitigation options are normally considered.

- 1) Foundation/bridge structural retrofit to accommodate the predicted liquefaction and related ground deformation demands. This requires soil-foundation structure interaction analyses to determine if

the deformation and load capacity of the existing foundation/bridge system is adequate to accommodate the ground deformation demands without collapse or can meet prescribed performance criteria. If not, mitigation methods focused on strengthening the structural foundation system can be evaluated, and costs compared to the ground modification mitigation option noted below.

- 2) The use of site remediation techniques, where stabilizing measures or ground modification and improvement approaches are undertaken to prevent liquefaction and/or minimize ground displacement demands. Such methods include, for example, the use of vibro-stone columns to form an embankment or buttress through the liquefiable zone.

A design approach for evaluating and mitigating the effects of liquefaction induced lateral spreads are documented in the Recommended LFRD Guidelines for the Seismic Design of Highway Bridges (NCHRP 12-49, 2003).

### **3.4 LIQUEFACTION IMPACTS ON DEEP FOUNDATIONS**

#### **3.4.1 Liquefaction Impacts on Vertical and Lateral Resistance**

Liquefaction may result in a reduction of both the vertical and lateral resistance of soil. The reduction in vertical resistance may be taken into account by assigning zero side resistance in all soils above the lowest liquefiable soil layer, even in layers not susceptible to liquefaction. Elimination of the side resistance in the non-liquefiable layers above the liquefiable layer is advised due to the potential for venting of seismically-generated excess pore water pressure by upwards flow of pore water along the sides of the pile, thereby reducing the side resistance. The reduction in lateral resistance is usually accounted for by modifying the p-y relationship for lateral loading. Two approaches have been recommend for modification of the p-y resistance in lateral soil (FHWA, 2011): 1) use of a p-multiplier of 0.1 (i.e. reducing the lateral resistance of the liquefied soil by 90% compared to the non-liquefied state; and 2) use procedures for developing p-y curves in soft cohesive soils in conjunction with the post-liquefaction residual strength of the soil to develop p-y curves for the liquefied soil zones. The methods discussed in the previous section for evaluating the shear strength of liquefied soils in a lateral spreading analysis may be used to evaluate the post-liquefaction residual strength if the second approach is employed. These recommendations are developed primarily on the basis of centrifuge testing of model pile foundations in liquefied soil: there is little field evidence to support either method. However, as the lateral resistance of a deep foundation in liquefied soil is generally governed by the structural stiffness of

the foundation element, these two approaches are likely to produce similar results and either approach is acceptable.

### **3.4.2 Liquefaction Impacts on Vertical and Lateral Loads**

Liquefaction impacts on vertical and lateral loads on piles include vertical loading due to downdrag resulting from liquefaction-induced soil settlement and lateral loading resulting from liquefaction-induced lateral spreading. In both cases, the increased loads are generally decoupled from the seismic inertia loads, i.e. the liquefaction-induced soil settlement and lateral spreading are assumed to occur after the peak inertial loading. Liquefaction-induced downdrag may be accounted for by applying the side resistance of the soils above the lowest liquefiable layer in the soil profile as a negative (downward) load on the pile. Liquefaction-induced lateral spreading loads may be considered by treating the lateral displacement as a kinematic load and applying the calculated lateral displacement in each soil layer as a displacement to the base of the p-y spring representing that layer. The p-y resistance of the soil in the liquefied layers is reduced as described above in such an analysis. Note that the calculated lateral displacement of the pile cap or footing in such an analysis should be applied as a kinematic load to the bridge structure itself, but the displacement is usually assumed to occur after the peak inertial loading and so this analysis is usually decoupled from the analysis for the inertial loads on the bridge.

Field observations and centrifuge model tests clearly demonstrate that the most important case with respect to increased lateral loading on foundations is the case in which liquefaction at depth induces lateral spreading of a non-liquefied overlying soil layer (or “crust”). In such cases, the non-liquefied crust may apply full passive pressure to the foundation element and pile cap or embedded footing. When soil liquefies all the way to the ground surface, the applied lateral loads (and associated lateral displacement) are significantly reduced. However, consideration must be given to the possibility that the deeper liquefiable soil layers may liquefy first and isolate the overlying layers from strong shaking, inhibiting their potential to liquefy. Therefore, the assumption that soil will liquefy above the lowest (deepest) liquefiable layer and thereby reduce the imposed lateral loads on the foundation may not be justified. Furthermore, assuming the soil liquefies all the way to the ground surface will reduce the lateral resistance and may therefore increase the inertial response of the structure. Thus, in some cases the design engineer may find it necessary to consider liquefaction all the way to the ground surface in the inertial response analysis and consider development of a non-liquefiable crust above the deepest liquefiable layer in a post-liquefaction kinematic loading analysis.

## 3.5 SOIL SETTLEMENT HAZARD

### 3.5.1 Hazard Description and Initial Screening

Free-field settlements may accompany liquefaction; these settlements may be associated with both post-earthquake dissipation of pore water pressures induced by liquefaction and resulting soil consolidation and densification and with soil loss due to venting of liquefied soil at the ground surface. If pore water pressures develop during ground shaking, but not to a level sufficient to cause liquefaction, their post-earthquake dissipation may also result in post-earthquake settlement, but the magnitude of such settlement will be less than that occurring due to liquefaction.

Settlements can also occur in dry or partially-saturated soils above the groundwater table. Such settlements are associated with the earthquake shaking and occur during ground shaking but are not associated with pore water pressure development and liquefaction. The mechanism in this case is densification of the soil during ground shaking: the earthquake-induced cyclic shear stresses cause the soil grains to adjust into a denser state of packing. A component of seismic settlement may also be associated with lateral spreading of the ground. Some lateral spreading-related settlement may occur even in the absence of noticeable slope displacement or lateral spreading through weak foundation soils.

Loose natural soils and uncompacted and poorly compacted fills are susceptible to densification and settlement due to earthquake shaking. While the magnitude of such settlement may be smaller than liquefaction-induced settlement, if the densification does not occur uniformly over an area, the resulting differential settlements can be damaging to a bridge.

It can be assumed that a significant hazard due to differential compaction *does not* exist if both of the following screening criteria are satisfied.

- The geologic materials underlying foundations and below the groundwater table do not liquefy.
- The geologic materials underlying foundations and above the groundwater table are either: Pleistocene in geologic age (older than 11,000 years); stiff clays or clayey silts; or cohesionless sands, silts, and gravels with a minimum  $(N_1)_{60}$  of 20 blows/foot or  $q_{1CN}$  greater than 100.

Note that these criteria are not intended to be applied to embankment fills. The potential for settlement of fills is strongly dependent on the degree of compaction of the fill and settlements should be estimated using the procedures described below.

### 3.5.2 Procedure for Settlement Evaluation of Unsaturated Cohesionless Soils

Observations in past earthquakes have indicated that earthquake induced ground shaking can induce significant settlement in dry or unsaturated cohesionless soil deposits. In the 1971 San Fernando earthquake for example, settlements of 4 to 6 inches were reported under a building on spread footings on a 40 ft deep sand fill (Seed and Silver, 1972). Laboratory tests to study the settlement of dry sands under cyclic loading were first initiated by Silver and Seed (1971) and led to the widely used design procedure developed by Tokimatsu and Seed (1987). This procedure has been summarized in a FHWA Geotechnical Engineering Circular (FHWA, 2011) and is reproduced below as a series of steps.

Step 1: From borings and soundings, in situ testing and laboratory index tests, develop a detailed understanding of the project site subsurface conditions, including stratigraphy, layer geometry, material properties and their variability, and the areal extent of potential problem zones. Establish the zones to be analyzed and develop idealized, representative sections amenable to analysis. The subsurface data used to develop the representative sections should include normalized standardized SPT blow counts,  $(N_1)_{60}$  (or results of some other test, e.g., the CPT from which  $(N_1)_{60}$  can be inferred) and the unit weight of the soil.

Step 2: Evaluate the total vertical stress,  $\sigma_v$  and the mean normal effective stress,  $\sigma'_m$  at several layers within the deposit at the time of exploration and for design. The design values should include stresses resulting from highway facility construction. Outside of the highway facility footprint, the exploration and design values are generally the same.

For unsaturated sand,  $\sigma'_m$  for most practical purposes can be estimated using the approximation:

$$\sigma'_m \approx 0.65 \cdot \sigma_v \quad 3-6$$

Step 3: Evaluate the soil flexibility factor,  $r_d$ , using one of the approaches presented in Section 3.2.3.

Step 4: Evaluate  $\gamma_{eff} \left( \frac{G_{eff}}{G_{max}} \right)$  using the Tokimatsu and Seed (1987) equation:

$$\gamma_{eff} \left( \frac{G_{eff}}{G_{max}} \right) = \left( \frac{0.65 \cdot \alpha_{max} \cdot \sigma_v \cdot r_d}{g \cdot G_{max}} \right) \quad 3-7$$

where

- $\gamma_{eff} (G_{eff} / G_{max})$  is a hypothetical effect shear stress factor  
 $\alpha_{max}$  is the peak ground surface acceleration  
 $G$  is the acceleration of gravity  
 $G_{max}$  is the shear modulus of the soil at small strain

Note that  $G_{max} = \rho \cdot V_s^2$ , where  $V_s$  is the shear wave velocity and  $\rho$  is the mass density of the soil (which is equal to the total unit weight divided by the acceleration of gravity). Alternatively,  $G_{max}$  (in psf) can be evaluated from the correlation given below (Seed and Idriss, 1970):

$$G_{max} = 20 \left[ (N_1)_{60} \right]^{1/3} (\sigma'_m)^{1/2} \cdot 10^3 \quad 3-8$$

where

- $(N_1)_{60}$  is the normalized standardized SPT blow count  
 $\sigma'_m$  is the mean normal effective stress in psf.

Step 5: Evaluate  $\gamma_{eff}$  as a function of  $\gamma_{eff} (G_{eff} / G_{max})$  and  $\sigma'_m$  using the chart reproduced in Figure 3-11.

Step 6: Assuming that  $\gamma_{eff} \approx \gamma_c$ , where  $\gamma_c$  is the cyclic shear strain, evaluate the volumetric strain due to compaction,  $\varepsilon_c$  for an earthquake of magnitude 7.5 (15 cycles) using the chart reproduced in Figure 3-12.

Step 7: Correct for earthquake (moment) magnitude other than  $M_w$  7.5 using the correction factors reproduced in Table 3-2.

Step 8: Multiply the volumetric strain due to compaction for each layer by two to correct for the multidirectional shaking effect, as recommended by Tokimatsu and Seed (1987), to get the representative volumetric strain for each layer.

Step 9: Calculate seismic settlements of each layer by multiplying the layer thickness by the representative volumetric strain evaluated in Step 8. Sum up the layer settlements to obtain the total seismic settlement for the analyzed profile.

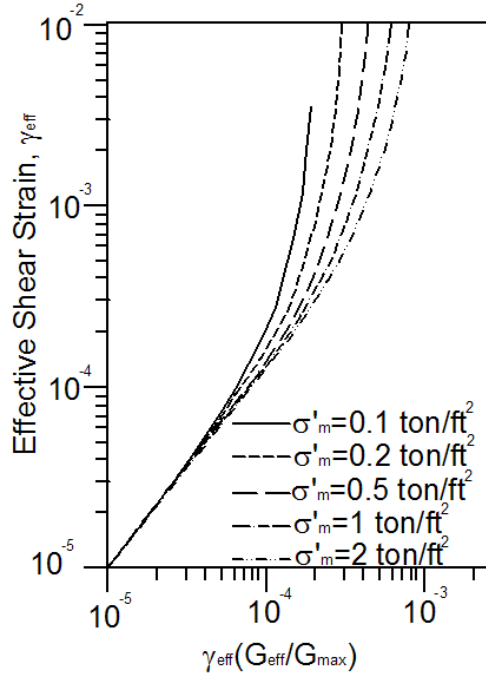


Figure 3-11 Plot for Determination of Earthquake-induced Shear Strain in Sand Deposits (Tokimatsu and Seed, 1987)

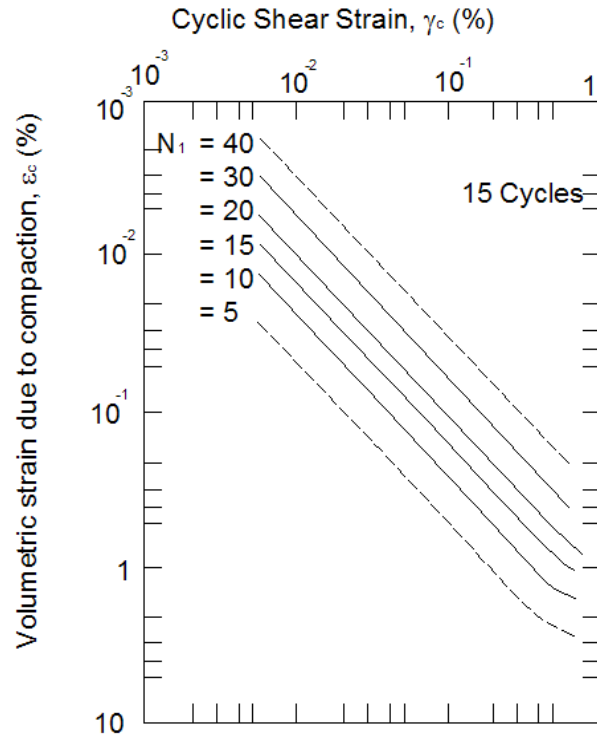


Figure 3-12 Relationship between Volumetric Strain, Cyclic Shear Strain, and Penetration Resistance for Unsaturated Sands (Tokimatsu and Seed, 1987)

**TABLE 3-2 INFLUENCE OF EARTHQUAKE MAGNITUDE ON VOLUMETRIC STRAIN RATIO FOR DRY SANDS (after TOKIMATSU AND SEED, 1987)**

Earthquake Magnitude	Number of Representative Cycles at $0.65 \tau_{\max}$	Volumetric Strain Ratio $\varepsilon_{C,N} / \varepsilon_{C,N} = 15$
8.5	26	1.25
7.5	15	1.0
6.75	10	0.85
6	5	0.6
5.25	2-3	0.4

Seed and Silver (1972) computed the seismic settlement in a 50-ft thick deposit of sand with a relative density of 45% which was subjected to a maximum surface acceleration of 0.45g (see Figure 3-13). They concluded that the computed settlement of 2.5 in. was in fairly good agreement with the observed settlement of the soil deposit during the San Fernando earthquake of 1971. The same soil profile has been evaluated using the simplified method above. The results of the analysis are shown in Table 3-3, and the results are compared with those by Seed and Silver (1972) in Figure 3-13. It may be noted that the strain distribution determined by the approximate method is in good agreement with the values computed by

Seed and Silver and that the settlement estimated by the simplified procedure is in reasonable accordance with that determined previously.

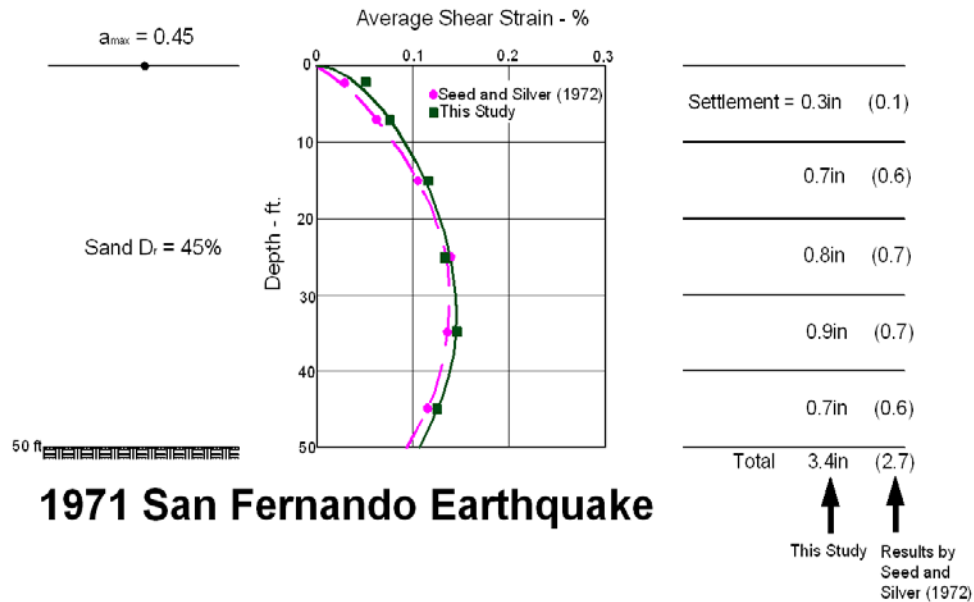


Figure 3-13 Computation of Settlement for 50-ft Deep Sand Layer

**TABLE 3-3 COMPUTATION OF SETTLEMENT FOR DEPOSIT OF DRY SAND**

Layer No.	Thick-ness (ft)	$\sigma_o = \sigma'_o$ (psf)	$D_r$ (%)	$N_I$	$G_{max}^a$ (ksf)	$\gamma_{eff}(G_e/G_{max})$	$\gamma_{eff}$	$\epsilon_{C,M} = 7.5$ (%)	$\epsilon_{C,M} = 6.6^b$ (%)	$2\epsilon_{C,M} = 6.6^c$ (%)	Settle-ment (in)
(1)	(2)	(3)	(4)	(5)	(6)	(7)	(8)	(9)	(10)	(11)	(12)
1	5	240	45	9	520	0.00013	0	0.14	0.11	0.22	0.13
2	5	714	45	9	900	2.3	8	0.23	0.18	0.36	0.22
3	10	1425	45	9	1270	3.2	12	0.35	0.28	0.56	0.67
4	10	2375	45	9	1630	4	14	0.4	0.32	0.64	0.77
5	10	3325	45	9	1930	4.5	15	0.45	0.36	0.72	0.86
6	10	4275	45	9	2190	4.6	13	0.38	0.3	0.6	0.72
Total											3.37
<sup>a</sup> $G_{max} = K_2 * 1000(\sigma'_m)^{1/2} = 20N_I^{1/3} (\sigma'_m)^{1/2} * 1000$											
<sup>b</sup> $\epsilon_{C,M=6.6} / \epsilon_{C,M=7.5} = 0.8$											
<sup>c</sup> Multidirectional effect											

### 3.5.3 Procedure for Post-Earthquake Settlement of Liquefied Soils

As discussed in Section 3.4.1, another consequence of earthquake induced liquefaction is the dissipation of the earthquake-generated excess pore-water pressures, leading to post earthquake settlement. Based on experimental studies, Tokimatsu and Seed (1987) developed a simple chart based procedure for estimating post liquefaction settlement at level ground sites. The Tokimatsu and Seed (1987) chart for a magnitude 7.5 earthquake is shown in Figure 3-14. The volumetric strains corresponding to the blowcount ( $N_1$ )<sub>60</sub> and cyclic stress ratio (CSR) for each liquefied layer should be multiplied by layer thickness to estimate total settlement in each layer. Note that the settlement estimates are valid for level-ground sites that have no potential for lateral spreading and do not account for soil loss due to venting of liquefied soil at the ground surface. For lateral spreading sites and sites where soil loss occurs, settlement will likely to be larger than at level ground sites where there is no soil loss or lateral spreading.

During the 1995 Kobe (Hyooken-Nanbu) earthquake, total settlements in the range of 1.6 ft to 2.3 ft were observed at sites where the soil liquefied. However, in the case of these observations, the differential settlements were small as evidenced from the limited cracks in the paved areas (Bardet et al., 1997). Similar observations made during the 1994 Northridge earthquake suggest that the differential settlements due to pore pressure dissipation may be only a fraction of the total settlement if the ground conditions are relatively uniform. Except for liquefaction with lateral spreading, the observed liquefaction-induced settlements during the Northridge earthquake were less than those observed in Kobe. In various observations in the San Fernando Valley, particularly in the Woodland Hills area, the ground settlements were found to be relatively uniform. This phenomenon may be attributable to the following conditions: (1) presence of deep alluvial sediments; (2) relatively horizontal layering; (3) significant fines content in the soils.

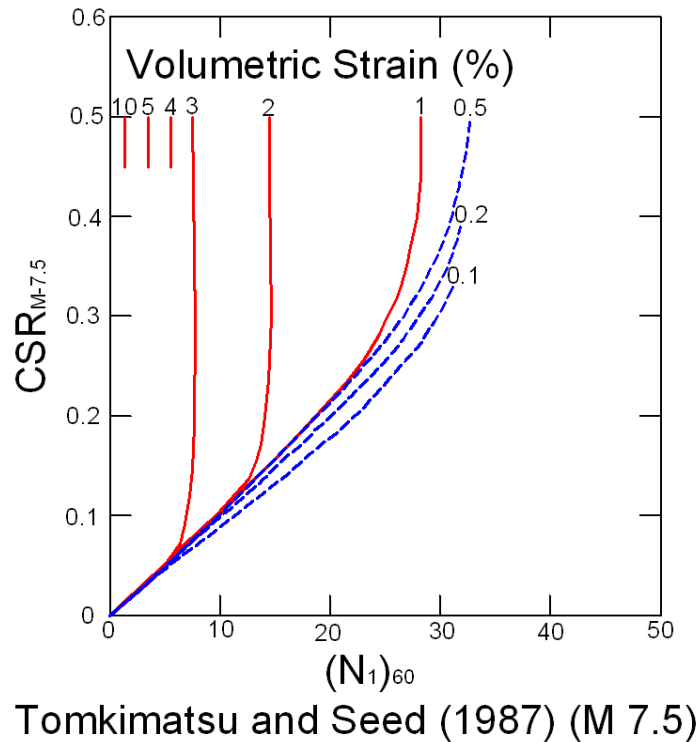


Figure 3-14 Curves for Estimation of Post-liquefaction Volumetric Strain using SPT Data and Cyclic Stress Ratio for  $M_w$  7.5 Earthquakes (Tokimatsu and Seed, 1987)

The above observations suggest that the differential settlements at level-ground sites with uniform soil conditions may be small even if the total settlement is large. However, in the absence of extensive site investigation, it is suggested that a differential settlement on the order of one-half of the total settlement be used in the design. The actual differential settlement value used is dependent upon a variety of factors, including the type and span(s) of the structure, bearing elevation of the foundation, subsurface conditions (relatively uniform versus highly variable laterally), number and spacing of borings and CPT soundings.

### 3.6 SEISMIC SLOPE INSTABILITY HAZARD

Earthquake induced slope stability may damage bridge approach embankments, abutments, foundations or superstructures, block bridge approaches, and rupture pipelines or culverts. Common modes of instability for soil slopes include rotational (circular) failure surfaces and sliding block (planar) failure surfaces. Failure modes for rock slopes also include toppling of rock blocks.

### **3.6.1 Hazard Description and Initial Screening**

In any stability analysis, all possible failure mechanisms must be evaluated to find the critical failure surface, i.e. the failure surface with the lowest seismic capacity to demand (C/D) ratio (i.e. lowest factor of safety) or cumulative seismic displacement. However, an experienced geotechnical specialist can usually identify a limited number of failure mechanisms that need to be evaluated in the seismic stability analysis. In general, circular failure surfaces will govern stability in a homogeneous material while sliding block failure modes also need to be evaluated in soil profiles with thin, weak layers (including liquefiable soil layers) or for relatively thin soil layers underlain by rock or much stronger soil layers and rock toppling failures need to be considered where there are slopes composed of blocky rock.

The first step in screening a site for seismic slope instability is to determine if there is any past history of static or seismic slope instability at the site and at other sites where the same geological formations are present. Geologic formations subject to instability are usually well known by local geotechnical professionals. Relic landslides are often identified in local and regional geologic maps and can also be identified using aerial photographs. Often times, the potential for slope instability can be related to slope inclination and orientation in specific geologic formations. However, grading for a highway can often create steeper slopes than present in the natural environment and thus local experience cannot be relied upon as the sole criterion to establish if slope instability is a concern. Slopes steeper than the natural geologic terrain may need a detailed stability evaluation even if there is no past history of slope instability in the area.

### **3.6.2 Slope Instability and Displacement Estimates**

If initial reconnaissance and the preliminary geotechnical investigation establish that there is a potential for slope instability impacting the bridge, a detailed seismic slope stability assessment is required. An important consideration in seismic slope stability is establishing whether the potentially unstable geologic formations will experience strength loss when sheared. Slopes composed of a material with a significant post-peak strength reduction when sheared should be designed using the post-peak strength in seismic analyses and should be designed for unconditional seismic stability if the static factor of safety using the post-peak strength is less than 1.0.

Seismic slope stability assessments are typically conducted using pseudo-static limit equilibrium analysis. In a pseudo-static limit equilibrium analysis, the effect of the earthquake is modeled by applying a

horizontal force to the centroid of the failure mass (or to the centroid of the slices in a method of slices stability analysis). The horizontal force in a pseudo-static limit equilibrium analysis is described by the seismic coefficient, the percentage of the weight of the potential failure mass that is applied as the horizontal force. When designing for unconditional stability (e.g. when designing a slope in a highly sensitive soil or in a brittle soil or rock),  $k_{max}$ , the average peak ground acceleration (after correcting for local site conditions) of the potential slide mass is employed as the seismic coefficient and a deformation analysis is not conducted. For small failure masses (e.g. slopes less than 20 ft in height),  $k_{max}$  (and thus the seismic coefficient) may be assumed to be equal to the PGA. For larger potential soil masses,  $k_{max}$  is adjusted based upon the size of the mass as described below. In the stability analysis of a soil that is not subject to post-peak strength loss or that is designed using the post-peak strength, the seismic coefficient is determined by adjusting the peak ground acceleration (after correcting it for local site conditions) by two factors: one for spatial and temporal incoherence (to get the value of  $k_{max}$ ) and one for the allowable seismic displacement.

Spatial and temporal incoherence result in an averaging of the earthquake ground motion over the potential soil mass such that the peak average acceleration of the potential failure mass,  $k_{max}$ , is usually less than and never greater than the peak ground acceleration (PGA). The ratio of  $k_{max}$  to the PGA depends upon the dimensions of the potential failure mass and the characteristics of the earthquake ground motion. NCHP Report 611 (NCHRP, 2008) presents the following equations:

$$\alpha = 1 + [0.01 H (0.5 \beta - 1)] \quad 3-9$$

$$\beta = (F_V S_1) / k_{max} \quad 3-10$$

where  $\alpha = k_{max}/PGA$

H = slope height and is limited to a maximum value of 100 ft; and

$(F_V S_1) = S_{D1}$ , the site-corrected value of the spectral acceleration at 1 second spectral period.

NCHRP further recommends that  $\alpha$  can be assumed equal to 1.0 for H less than 20 ft.

To get the seismic coefficient,  $k_{max}$  may be reduced by a ductility factor that depends upon the allowable seismic deformation. Based upon findings in the NCHRP 12-70 project, FHWA (2011) recommends a ductility factor of 0.5 be used for initial analyses of slopes that can accommodate up to 2 inches of seismic displacement based upon observations that soil slopes not subject to post-peak strength loss (or that were analyzed using the post-peak strength) that had a pseudo-static factor of safety (capacity to demand ratio) equal to or greater than 1, i.e. slopes designed using a seismic coefficient equal to  $0.5 k_{max}$ , typically experience negligible deformation (e.g. minor cracking) in an earthquake. However, many

slopes can accommodate significantly more than minor cracking in an earthquake. Therefore, the criterion of a pseudo-static factor of safety of 1 using a seismic coefficient of  $0.5 k_{\max}$ , may be considered a secondary screening level for seismic slope stability.

In cases where the pseudo-static factor of safety using a seismic coefficient equal to  $0.5 k_{\max}$  is less than 1.0 and more than 2 inches of seismic deformation can be accommodated, Equations 3.3 and 3.4 can be used to calculate a seismic displacement for comparison to an acceptable value. Use of Equations 3.3 and 3.4, requires values for  $k_{\max}$ , the yield acceleration ( $k_y$ ), and the Peak Ground Velocity (PGV). The value of  $k_{\max}$  is calculated as described above, the PGV may be calculated in Equation 3.5, and  $k_y$  is calculated from limit equilibrium analyses as the seismic coefficient that yields a factor of safety of 1.0. Once again, in soils with a post-peak decrease in shear strength, the post-peak strength may be employed in the limit equilibrium analysis (for  $k_y$ ).

### **3.7 SURFACE FAULT RUPTURE HAZARD**

#### **3.7.1 Hazard Description and Initial Screening**

Surface fault rupture refers to the shearing displacements that occur along an active fault trace when movement on the fault extends to the ground surface, or the depth of a bridge foundation. Displacements can range from inches to feet. Because surface fault displacements tend to occur abruptly, often across a narrow zone, fault rupture is potentially very damaging to a bridge, particularly if it occurs directly below the structure. It is also difficult and often cost-prohibitive to mitigate. Few active faults have been identified in the central and eastern United States, east of the Rocky Mountains, and the hazard of surface fault rupture is generally low in this area as opposed to some parts of the western United States.

Surface fault ruptures generally are expected to occur along existing traces of active faults. Therefore, it can be assumed that a significant hazard of surface fault rupture does not exist if it can be established that either:

- There is no evidence of a fault trace traversing the bridge site, or
- If a fault trace does cross the bridge site, it has been established that the fault is not an active fault. Faults are generally considered to be active faults with a significant potential for future earthquakes and displacements if they have experienced displacements during the past approximately 11,000 years (Holocene time).

Hazard screening for fault rupture should involve, as a minimum, the following steps:

- 1) Review of geologic maps as well as discussions with geologists in government agencies and at universities who are knowledgeable about the geology of the area, and
- 2) Site reconnaissance and review of aerial photographs, looking for geomorphic expression of faulting. If there is uncertainty in the fault location or its activity, the screening criteria should be applied conservatively.

If a surface fault rupture hazard cannot be screened out, the owner may decide to accept the risk or evaluate the hazard and consequences in detail. If detailed evaluations are carried out, they should be oriented toward:

- 1) Establishing the fault or fault zone location relative to a bridge site if it is not clearly established in the screening stage,
- 2) Establishing the activity of the fault if it traverses a bridge, and
- 3) Evaluating fault rupture characteristics; i.e., amount of fault displacement, width of zone of displacement, and distribution of slip across the zone for horizontal and vertical components of displacement. A probabilistic assessment of the likelihood of different magnitudes of fault displacement during the life of the bridge may also be useful in decision-making.

The distribution of ground displacements associated with fault rupture will depend upon the type of faulting (as shown on Figure 3-15, the amount of slip, the distribution into strike-slip and dip-slip components, and the width of the zone of ground deformation.

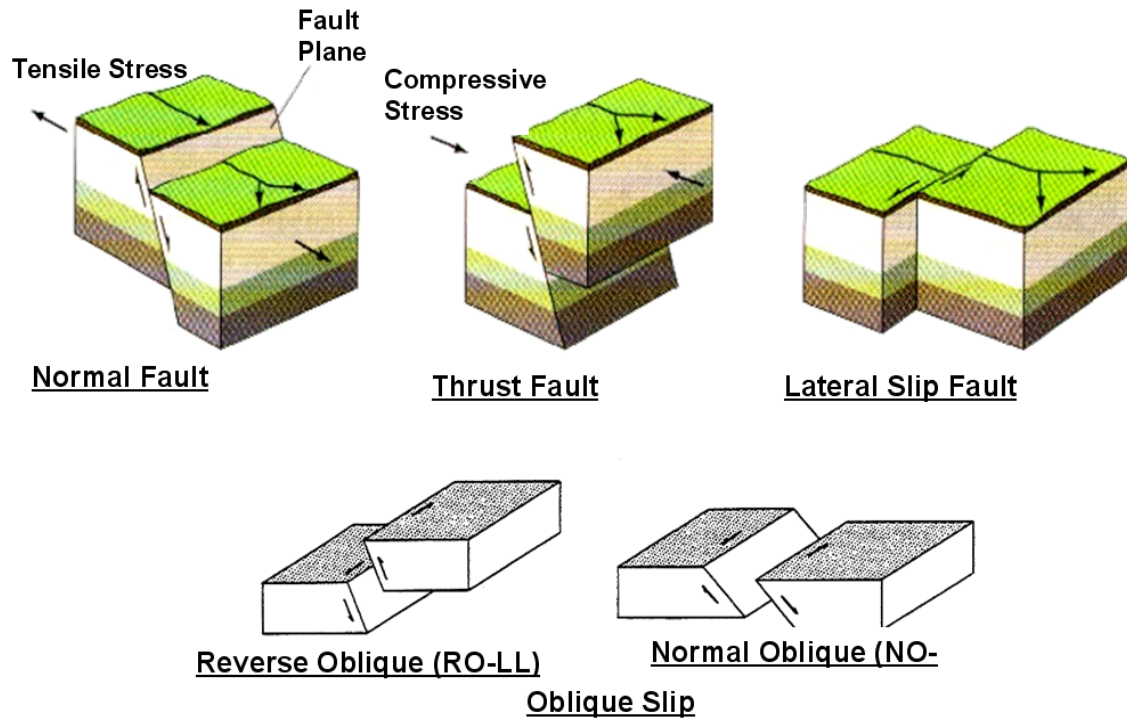


Figure 3-15 Types of Earthquake Faults

There are several steps that can be taken to confirm and define the location of faults. Further assessments are not required if it can be shown, on the basis of the procedures outlined below, that there are no faults passing beneath the site.

1) Interpretation of Aerial Photographs

Aerial photographs can be an excellent supplementary resource to geologic and topographic maps of the site and vicinity for identifying faults. Older photographs are particularly useful if they depict the site and /or its environs prior to development activities that would have altered or destroyed landforms that indicate the presence of faults. For many parts of the country, stereo photographic coverage is available as far back as the 1920s or 1930s. Aerial photographs are usually available from several sources including private companies and from various governmental agencies including the U.S. Geological Survey (USGS), U.S. Department of Agriculture (Soil Conservation Service), Bureau of Land Management, and the Forest Service. The USGS maintains the repository for federal photographic resources at its EROS Data Center, Sioux Falls, South Dakota 57198.

## 2) Contacting Knowledgeable Geologists

Geologists and other earth scientists familiar with geologic and tectonic conditions in the site vicinity may be willing to share their knowledge. These geologists might work for governmental agencies (federal, state, and local), teach and conduct research at nearby colleges and universities, or practice as consultants.

## 3) Ground Reconnaissance of Site and Vicinity

A walk-down of the site and its vicinity should be conducted to observe unusual topographic conditions and evaluate any geologic relationships visible in cuts, channels, or other exposures. Features requiring a field assessment might have been previously identified during the geologic and topographic map review, aerial photography interpretation, and/or during conversations with geologists.

## 4) Surface Exploration

Faults obscured by overburden soils, site grading, and/or structures can potentially be located by one or more techniques. Geophysical techniques such as seismic refraction surveying provide a remote means of identifying the location of steps in a buried bedrock surface and the juxtaposition of earth materials with different elastic properties. Geophysical surveys require specialized equipment and expertise, and their results may sometimes be difficult to interpret. Trenching investigations are commonly used to expose subsurface conditions to a depth of 15 to 20 ft. While expensive, trenches have the potential to locate faults precisely and provide exposures for assessing their slip geometry and slip history. Borings can also be used to assess the nature of subsurface materials and to identify discontinuities in material type or elevation that might indicate the presence of faults.

If it is determined that faults pass beneath the site, it is essential to assess their activity by determining the timing of the most recent slip(s) as discussed below. If it is determined, based on the procedures outlined below, that the faults are not active faults, further assessments are not required.

## 5) Assess Fault Relationship to Young Deposits/Surfaces

The most definitive assessment of the recent history of fault slip can be made in natural or artificial exposures of the fault where it is in contact with earth materials and/or surfaces of Quaternary age (last 1.8 million years). Quaternary deposits might include residual soils, glacial sediments like till, loess,

alluvium, colluvium, beach and dune sands, and other poorly consolidated surficial materials. Surfaces with visible expressions of fault displacements might include marine, lake, and stream terraces, and other erosional and depositional surface. A variety of age-dating techniques, including radiocarbon analysis and soil profile development, can be used to estimate the timing of the most recent fault slip.

#### 6) Evaluate Local Seismicity

If stratigraphic data are not available for assessment of fault activity, historical seismicity patterns might provide useful information. Maps and up-to-date plots depicting historical seismicity surrounding the site and vicinity can be obtained from the USGS at its National Earthquake Information Center in Golden, Colorado. Additional seismicity information may be obtained from state geologic agencies and from colleges and universities that maintain a network of seismographs (e.g. California Institute of Technology, University of California, Berkeley, University of Nevada, Reno, University of Washington, and the Multidisciplinary Center for Earthquake Engineering Research, buffalo, New York). If the fault(s) that pass beneath the site are spatially associated with historical seismicity, and particularly if the seismicity and fault trends are coincident, the faults should probably be considered active.

#### 7) Evaluate Structural Relationships

In the absence of both stratigraphic and seismological data, an assessment of the geometric/structural relationships between faults at the site and faults of known activity in the region could be useful. Although less definitive than the two prior criteria, the probability that the site fault is active increases if it is structurally associated with another active fault, and if it is favorably oriented relative to stresses in the current tectonic environment.

### **3.7.2 Fault Rupture Characteristics and Displacement Estimates**

If the site evaluation indicates one or more active faults are present beneath the site, the characteristics of future slip on the faults should be estimated. Several methods can be used to estimate the size of future displacements. These include:

- 1) Observations of the amount of displacement during past surface-faulting earthquakes.
- 2) Empirical relations that relate displacement to earthquake magnitude or to fault rupture length.
- 3) Calculated values based on the cumulative fault displacement or fault slip rate.

The most reliable fault displacement assessments are based on past events. Observations of historical surface ruptures and geologic evidence of paleoseismic events provide the most useful indication of the location, nature, and size of the future events. Where the geologic conditions do not permit a direct assessment of the size of past fault ruptures, the amount of displacement must be estimated using indirect methods. Empirical relations between displacement and earthquake magnitude based on historical surface-faulting earthquakes (e.g. Wells and Coppersmith, 1994) provide a convenient means for assessing the amount of fault displacement. An example of such a relationship is shown in Figure 3-16.

In the plots in Figure 3-16, maximum displacement along the length of a fault rupture is correlated with earthquake magnitude. Maximum displacement typically occurs along a very limited section of the fault rupture length. Relationships are also available for the average displacement along the rupture length (e.g. in Wells and Coppersmith, 1994). The average size of past displacements may also be calculated by dividing the cumulative displacement along the fault by the number of events that produced the displacement or by multiplying the geologic slip rate of the fault by the recurrence interval for major earthquakes on the fault. Data from well-documented historical earthquakes indicate that the ratio of the average displacement to the maximum displacement ranges between 0.2 and 0.8 and averages 0.5 (Wells and Coppersmith, 1994). Exactly where along the fault the maximum displacement may occur is unknown and therefore the maximum displacement is recommended for use in design.

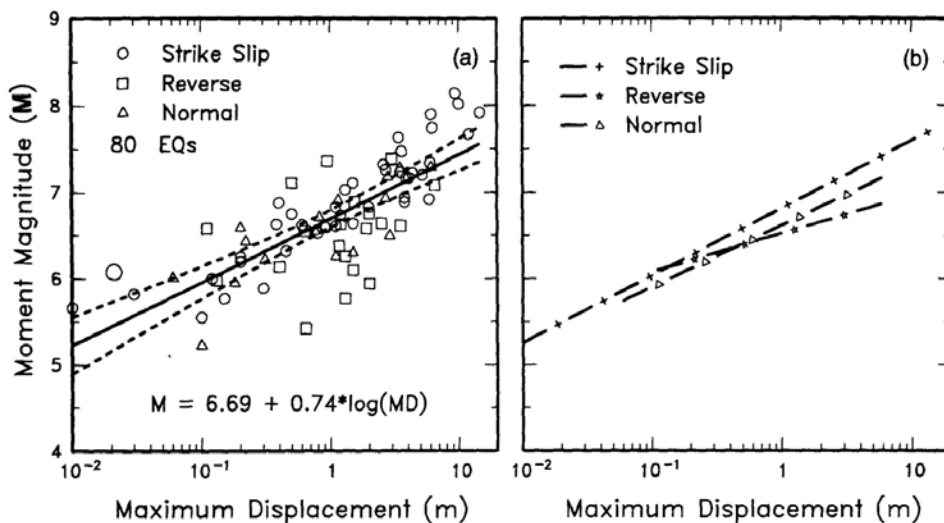


Figure 3-16 Relationship between Maximum Surface Fault Displacement and Earthquake Moment Magnitude (Wells and Coppersmith, 1994)

Predicting the width of the zone and the distribution of slip across the zone of surface deformation associated with a surface faulting event is more difficult than predicting the total displacement. The best

means for assessing the width of faulting is site-specific trenching that crosses the entire zone. Historical records indicate that the width of the zone of deformation is highly variable along the length of a fault. No empirical relationships having general applicability have been developed that relate the size of the earthquake or the amount of displacement on the primary fault trace to the width of the zone or to the amount of secondary deformation. The historical record indicates, and fault modeling shows that the width of the zone of deformation and the amount of secondary deformation tend to vary as a function of the dip of the fault and the sense of slip. Steeply dipping faults, such as vertical strike-slip faults, tend to have narrower zones of surface deformation than shallow-dipping faults. For dipping faults, the zone of deformation is generally much wider on the hanging wall side than on the foot wall side. Low-angle reverse faults (thrust faults) tend to have the widest zones of deformation.

Probabilistic methods for assessing the hazard of fault rupture have been developed that are similar to the probabilistic seismic hazard analysis (PSHA) methods used to assess earthquake ground motions. A PSHA for fault rupture defines the likelihood that various amounts of displacement will be exceeded at a site during a specified time period. For critical bridges, such analyses could be considered to assess whether the likelihood of surface fault rupture is high enough to warrant design for hazard and to aid in quantifying design values of displacement.

### **3.8 SUMMARY**

This chapter presents an overview of geotechnical seismic hazards related to liquefaction, seismic settlement, fault rupture, and slope instability. Liquefaction induced ground deformations are a significant source of damage in earthquakes. Liquefaction hazard (the potential for seismically generated pore pressure leading to reduced soil shear strength, slope failures and associated ground deformations) is discussed in detail. Laboratory and site investigation methods to determine the liquefaction strength of site soils (including SPT and CPT methods) are discussed leading to empirical evaluation procedures commonly used to determine the potential for triggering liquefaction. Screening approaches to assess the need for such evaluations in regions of low seismicity are also described. The various methods for the determination of post liquefaction residual undrained strength are reviewed. The impact of liquefaction on the vertical and lateral capacity of deep foundations is discussed.

The potential for post liquefaction flow failure under static loads is addressed along with a discussion of earthquake induced lateral spreading displacement. Both empirical and numerical methods for

determining lateral spreading displacement potential are reviewed with particular emphasis on Newmark approaches. The soil settlement hazard includes both the post-liquefaction settlement of saturated cohesionless soil and the settlement of unsaturated cohesionless soil subject to seismic loading. Emphasis is placed on the commonly used Tokimatsu and Seed analysis approach for evaluating these settlements. The loads applied by liquefaction-induced lateral displacement and settlement on bridge foundations are discussed. Slope instability can damage and/or displace foundations, bridge abutments, and approach embankments and block access to the bridge. Methods for assessing seismic slope stability and seismically-induced slope displacements are presented. Reviews of fault types and field identification approaches for fault rupture hazard are provided, together with rupture characteristics and procedure for estimating fault displacement.

The discussion on hazards presented in Chapter 3 provides background source material for subsequent Chapters. In particular the liquefaction hazard discussion related to lateral spread deformations and post liquefaction settlement will also be utilized in the evaluation of bridge-foundation and bridge-abutment systems as well as in the design and development of corresponding mitigation measures.

## CHAPTER 4

### PRINCIPLES OF SEISMIC DESIGN

#### 4.1 GENERAL

Modern seismic design for bridges in the U.S. accepts the fact that a bridge will be damaged and responds inelastically during the design earthquake, an event with a return period of about 1,000 years. Such response is unlike that expected for most other load combinations, because earthquake loads are so large that to design for them elastically would be prohibitively expensive, except for the most critical of long-span bridges. Damage is therefore explicitly permitted and is expected under the design earthquake loading. But not all damage is acceptable. Only ductile yielding is permitted and then only in members specifically designed and detailed for such behavior. Brittle failure is not permitted at any time. Ensuring that a bridge can sustain the magnitude and reversal of earthquake loading without collapse requires design principles and detailing that are different from those required for most other load types.

Overall, the expected seismic performance for non-essential and non-critical bridges is that they could withstand smaller, more frequent earthquakes without significant damage and they would be able to withstand larger earthquakes without posing a threat to life safety and without collapse. These objectives form the basis of the limits established in the design standards and the return period selected for the design event, which is 1000 years. In general, only the upper level earthquake is checked during design, based on the expectation that bridges so designed would resist smaller earthquakes without damage by default. This approach is taken, in part, to simplify the seismic design effort. For essential or critical bridges, an approach that permits less damage is taken. However, the focus of this chapter is on the more common non-essential and non-critical bridges where the design approach often does permit significant damage.

The approach to design for earthquake loading requires a somewhat different way of thinking on the part of the designer than design for other load cases. Typically, providing additional strength or capacity is thought of as advantageous from a safety perspective, although such practice might make the design less cost effective. However, for seismic design there is a need to estimate the maximum forces that can be developed in the structure and design for those forces, so that appropriate displacement capacity is provided. This means that simply adding more strength in one element, without regard to its impact on other parts of the structural system, is not an appropriate practice for seismic design.

In some geographic locations the seismicity of the area may be low enough that elastic response is all that is expected and required. In such locations, seismic design is relatively simple. However, in many locations the ability of a bridge to deform inelastically and in a ductile manner is a necessity. The use of inelastic response has both economic and technical bases. Economically, it is prudent to permit some damage to avoid spending undue resources on an extreme event with low likelihood of occurrence. Technically, it is prudent to design structures using fusing action that limits internal forces. This makes the structure less vulnerable to earthquake events that are larger than the design event. This chapter explains the principles that underpin modern seismic design and that have evolved to ensure such fusing action, which is known in earthquake engineering as ductile response. Note also that this chapter discusses only the general principles and concepts behind modern seismic design and is not intended to provide exhaustive treatment of the entire topic.

Capacity design principles were introduced in Chapter 1 to frame the approach taken in modern seismic design. This approach can be summarized in three steps:

- 1) Choose structural elements of the structure that will deform inelastically, form a plastic mechanism, and sustain damage under the action of lateral earthquake loading – identification of the yielding links and assignment of their capacities.
- 2) Design and detail those elements to continue to resist applied loading with little or no degradation under continued deformation and under reversal of loading – detailing for ductility.
- 3) Develop a complete load path in the structure whereby other elements of the structure will not fail before the yielding links reach their maximum resistances or capacities, and configure the system to provide sufficient deformability so that yielding can occur – capacity-protected design (or simply “capacity protection”).

The capacity design concept can be illustrated using an analogy to a chain, as described by Paulay and Priestley (1992) and as shown in Figure 4-1. If one link of the chain is ductile and that link’s tensile strength is less than the strength of the other links, which may even be brittle, then the chain will exhibit ductile behavior based on the behavior of the one ductile link. However, if any of the brittle links have strengths lower than that of the ductile link, then the chain will exhibit brittle behavior. In the case of a bridge, the entire structural system is analogous to the chain, and individual elements, such as columns, foundations, abutments, and superstructure comprise the links in the chain.

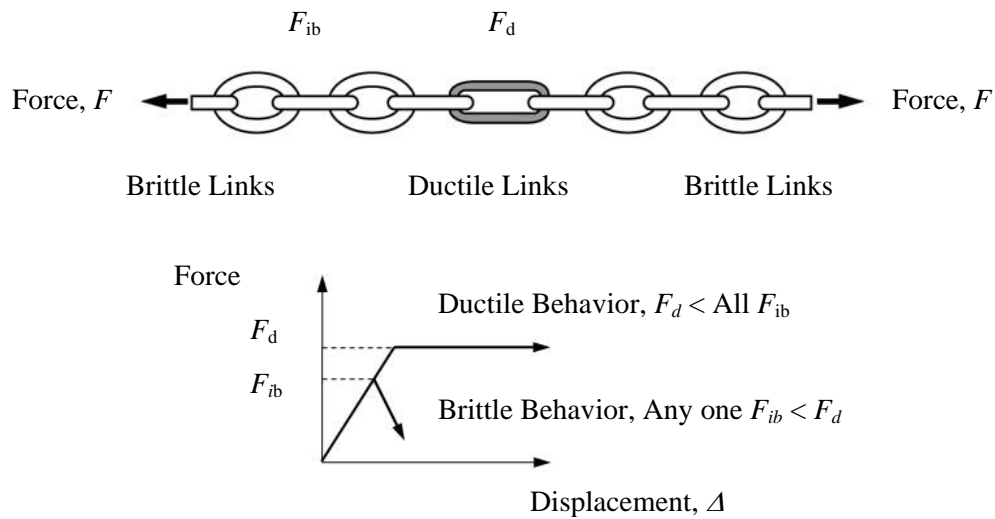


Figure 4-1 Chain Analogy for Capacity Design (after Paulay and Priestley, 1992)

The focus of this chapter is on Steps 1 and 3 of the capacity design approach as applied in the conceptual seismic design of a bridge’s lateral-force-resisting system, also known as the Earthquake Resisting System (ERS), which is discussed in more detail at the end of this chapter. In practice, application of the capacity design approach often conflicts with other constraints of design. Therefore, this chapter will explain preferred seismic design features. It will also explore cases where those features may not always be attainable and explain how the seismic design may be improved for those cases.

As mentioned above, the seismic ‘demand’ is not the same throughout the country. Therefore, the philosophy of seismic design that is used for bridge design in the U.S.<sup>1</sup> increases the rigor of the seismic design requirements as the seismicity increases. Consequently, the concepts that are explained in this chapter vary in importance as the seismic demand increases. The exact nature of this variance is discussed in subsequent chapters where specific practices for the two methods of seismic design, force-based and displacement-based, are presented.

<sup>1</sup> AASHTO LRFD *Bridge Design Specifications* 2013) and AASHTO *Guide Specifications for LRFD Seismic Bridge Design* (2014)

## 4.2 STRUCTURAL FORM

A bridge's behavior under seismic loading is determined by its structural form, which is simply a way to describe the composition of bridge geometry, structural type, member strengths, and member interconnections/articulations. These three attributes combine to define how lateral loads will be induced in a bridge by an earthquake and how such loads will be resisted by the bridge.

When earlier bridge designs, for instance those that evolved solely to optimize the resistance of gravity loading, are viewed from the perspective of seismic loading, many potential flaws emerge. One of these flaws is continuity of structural elements. For example, elements that might sit atop one another and work well for resisting vertical gravity loads may not be adequate when subject to lateral loading. This is because the integrity of the entire system may be lost if individual pieces become dislodged (e.g. beams falling off their supports). Bridge behavior in past earthquakes has clearly illustrated this vulnerability. For example, providing adequate support length is a primary requirement in modern seismic design.

Additionally, construction techniques that may provide adequate safety under the monotonic elastic-range gravity loading may not work adequately when subjected to inelastic cyclic loading (e.g. columns whose reinforcing steel is spliced at potential high moment sites under lateral loading). Therefore, providing proper detailing of structural members is another primary requirement.

Unlike design to resist well-defined gravity loads with no structural damage, the expected performance under earthquake loading is to permit potentially significant damage, but prevent the structure from collapsing or otherwise posing a life-safety hazard. This 'expected-damage' approach, by its nature, takes structures near the limit of survival. The structural concept and its form are then central to ensuring success in earthquake resistant design.

### 4.2.1 Basic Requirements

The notion of permitting damage for normal bridges (i.e. non-essential and non-critical bridges), using ductile response, is rooted in three sets of observations related to Figure 4-2.

- 1) If elastic response was chosen as a design performance objective, then different earthquakes – either with different magnitudes or different distances from the bridge site – would produce

different internal force effects. These internal effects would depend on how far along the load-displacement curve an earthquake ‘pushed’ the bridge. Greater intensity shaking would produce larger forces and displacements. Such response would lay along the straight, sloping line, A, representing elastic response. The forces so induced in many cases would be so large as to render the structure uneconomical to build.

- 2) If on the other hand, ductile response was chosen, then the internal forces are limited by the yielding elements forming a plastic mechanism and are thus somewhat invariant to the earthquake shaking amplitude. Such response is reflected by line B. However, larger earthquakes will produce larger deformations, thus the system must be capable of withstanding those displacements. This can be achieved by proper detailing of the yielding elements, and the associated damage permits economically designed structures to withstand the design earthquake.
- 3) Thirdly, the maximum displacement of an inelastic system can be estimated by analysis of a similar system responding elastically, using appropriate approximation methods developed from studies of yielding systems. Thus, commonly used elastic analysis techniques can be used to assist the seismic design process for normal bridges. For more specialized structures not covered by the AASHTO seismic design procedures, more direct dynamic analysis procedures that account explicitly for inelastic dynamic response are required.

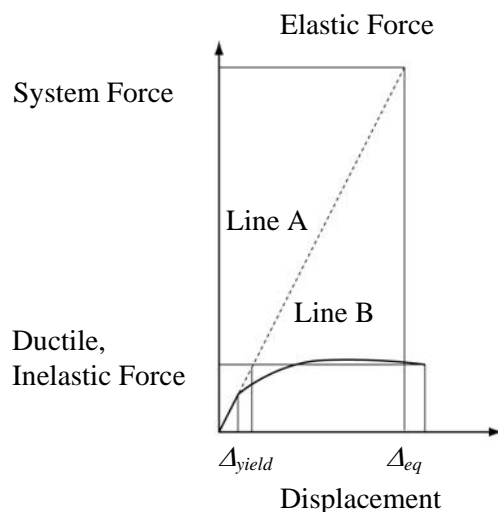


Figure 4-2 Force-Displacement Relationships for Elastic and Ductile Systems

Evident from the first two items in the list above, the structure or system load versus displacement response is useful in determining and understanding the expected response. This concept has emerged in recent years as a central tool for the designer to address seismic loading. The load-displacement curves shown in Figure 4-2 are intended to be representative of system response, although element and subsystem response (e.g. individual bents) will also have similar response. For a bridge, this means the response is inclusive of the entire structure, including the intermediate bents, superstructure, foundations and abutments. From a mechanics perspective, the overall force-displacement relationship for a bridge is the combination of all contributing lateral resisting elements. This would include the contribution from all intermediate substructure elements along with the superstructure and abutments. Thus, the basic requirement for seismic design is for the entire system to be considered and for ductile behavior to be included in the system design to the extent possible. This remains true even though the design focus is often conducted on a bent-by-bent basis. The consideration of system response and behavior will often require consideration of a hierarchy of preferred failure modes and load paths. These are discussed below.

#### **4.2.2 Load Paths**

Consideration of earthquake loading on structures must start with mechanics. It is clear that the ground deforms during an earthquake, thus inducing lateral loading effects on a bridge or structure. Recently, many discussions of seismic design methods are in the context of either "force-based" or "displacement-based" methods, and this may leave the listener with the impression that only forces or only displacements are important. In fact, both methods require consideration of both forces and displacements. However, the displacement-based method is founded on a more complete and more direct consideration of the inelastic response of a structure, whereas the force-based method uses simplifications that often conceal the expected inelastic response. Thus, the trend in earthquake engineering is for displacement-based methods to replace force-based methods. However, the structure does not know how it was designed and will respond singularly in a manner that the design engineer must understand and control, in order to produce effective seismic designs.

### 4.2.2.1 Dynamic Equilibrium

Structural dynamics as it applies to bridges is discussed in Chapter 5. However, the principle of dynamic equilibrium is useful in understanding the topics considered in this chapter, and so dynamic equilibrium is discussed below. Most civil and structural engineers are comfortable with static equilibrium, but when considering dynamic response the comfort level often drops. Yet the concept of equilibrium still holds, albeit in the form of dynamic forces, which can be represented with quasi-static loading to simplify the design effort. This is the approach used for normal bridge seismic design.

The basic notion of dynamic equilibrium is contained in the following material. Even though the equations of equilibrium are differential equations that must be solved appropriately, the algebraic relationship of the forces is the primary subject in this chapter. Two powerful ideas are developed in this section:

- 1) Earthquake “loading” can be represented using appropriately amplified static forces that are applied to the mass of the structure.
- 2) The designer can control the internal forces developed during an earthquake by proportioning the structure to form a plastic mechanism.

Those readers who are comfortable with these concepts or wish to skip over the derivation of these concepts may continue reading with the next section, 4.2.2.2.

Considering a simple structure as shown in Figure 4-3, the internal earthquake-induced forces acting on the mass are shown. Equilibrium of these forces is given by Equation 4-1, where the inertial force of the mass is represented by the mass times its acceleration. This effect is known as d’Alembert’s principle, which expresses Newton’s second law of motion in terms of an “inertial force” (Clough and Penzien, 1993). The spring and damping forces are often considered as a single force, or damping may in some cases be neglected. Both are shown here as combined forces in the columns. When the structure is founded on a base that does not move, the spring, damping and inertial forces are all functions only of the relative displacement, velocity and acceleration between the mass of the SDOF structure and its base and any applied loads. In this case the acceleration of the ground is, by definition, zero.

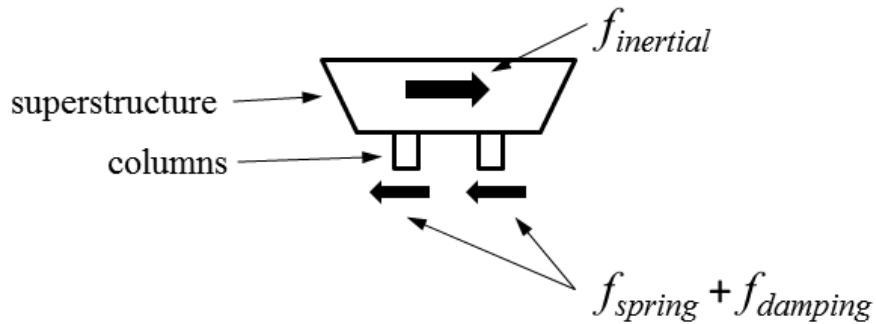


Figure 4-3 Equilibrium of Forces on Single-Degree-of-Freedom (SDOF) Structure

$$f_{inertial} + f_{damping} + f_{spring} = 0 \quad 4-1$$

where,

$f_{inertial}$  = inertial force associated with the mass

$f_{damping}$  = damping force

$f_{spring}$  = spring or restoring force.

When the base of the structure can move, as in the case of an earthquake, then there is another displacement included, that of the ground. See Figure 4-4. The second derivative of this displacement, or acceleration of the ground, affects only the inertial force, because the spring and damping forces are functions only of the relative displacement or relative velocity between the SDOF mass and its foundation. Thus, the inertial force is a function of the total acceleration (i.e. the sum of the ground and relative accelerations). Equilibrium for the case where the ground moves is provided by Equation 4-2 and the total acceleration is given by Equation 4-3. Only the total acceleration affects the mass and induces its inertial effect, which is a combination of ground and relative accelerations.

$$m\ddot{u}_{total} + c\dot{u} + ku = 0 \quad 4-2$$

where

$m$  = mass of the SDOF system

$c$  = damping constant of the system

$k$  = lateral stiffness of the system

$\ddot{u}_{total}$  = total acceleration of the mass

$\dot{u}$  = velocity of the mass relative to the foundation

$u$  = displacement of the mass relative to the foundation

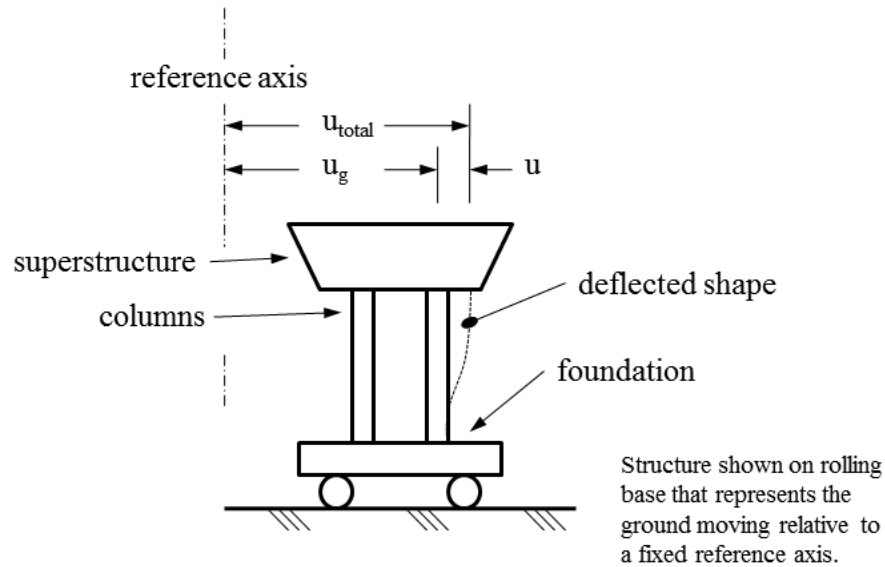


Figure 4-4 Influence of Ground Excitation

$$\ddot{u}_{total} = \ddot{u}_g + \ddot{u} \quad 4-3$$

where  $\ddot{u}$  = acceleration of the mass relative to the foundation

and  $\ddot{u}_g$  = acceleration of the ground

Because both the acceleration of the ground and the mass are known, the inertial effect due to the ground movement can be moved to the right-hand-side of Equation 4-4, yielding the “equation of motion” for the system.

$$m\ddot{u} + c\dot{u} + ku = -m\ddot{u}_g \quad 4-4$$

Once this is done, the equation of motion can be solved for the response of the SDOF system. When the maximum responses are calculated and presented as a function of the system vibration period or frequency the resulting plots are known as response spectra. These were discussed in Chapter 2. Spectra for relative displacement, relative velocity, and total acceleration (often referred to as absolute acceleration) are typically attained. Response spectra provide the solutions for the equation of motion, thereby relieving the designer from having to develop the dynamic response.

The inertial force of the SDOF system is proportional to the response spectrum acceleration, and it includes both the ground acceleration effect and the relative acceleration effect. When these accelerations are combined the inertial force can be amplified above that due to the ground acceleration alone.

It is important to understand the difference between the total and ground accelerations. The total acceleration contains any dynamic amplification of the structure mass added to the effect of the ground acceleration, alone. Prior to the recent adoption of the 1000-year return period earthquake for bridge design, the seismic accelerations that were mapped throughout the country were based on the ground acceleration. New with the 1000-year approach is the representation of the ground motion in spectral acceleration terms. Spectral acceleration is the total acceleration for a SDOF system. In the range of periods for many bridges, say 0.5 to about 1.5 seconds, the spectral acceleration is generally greater than the ground acceleration. In the longer period ranges, the spectral acceleration is typically less than the ground acceleration.

One additional equilibrium consideration, inelastic response, requires looking back to Figure 4-2 and Equation 4-1. The use of ductile systems, where the maximum element forces developed in the system are somewhat less than those calculated for an equivalent fully elastic system, affects the maximum inertial forces that are developed in the system. In the case of a yielding system, the spring force,  $f_{spring} = ku$ , becomes a function of displacement that is not linear elastic. The precise function is not important here. Equation 4-1 shows that the inertial force is algebraically equal to the damping force and spring restoring force. If damping is primarily introduced by deformations of the columns, we can consider the sum of the damping and spring force as the resistance of the columns for an individual bent-type structure (See Figure 4-3.).

When yielding of the columns occur thereby producing the nonlinear force-limited response as seen in Figure 4-2, the inertial force of the system is limited. This is the result of maintaining equilibrium at all times. Considering Equation 4-3, this force limitation means that the relative acceleration is induced in exact proportion to balance the inelastic force developed in the columns and the earthquake-induced ground acceleration portion of the inertial force,  $m\ddot{u}_g$ . Thus, the designer can control the maximum inertial force that will be developed in the structure, by controlling the maximum lateral force that the structural system can deliver. And importantly, he/she can control that force without having to solve an inelastic time history dynamic analysis, which is formally necessary to precisely calculate the complete dynamic response. Because the emphasis of the design approach is on the peak dynamic response rather than on the full time history of response, consideration of equilibrium at the moment of maximum response is all that is required of the designer. This direct control of internal forces in the hands of the designer is an extremely powerful result from the application of equilibrium concepts.

Equilibrium and the equivalence between ground movement and mass-applied loading (Equation 4-4) permits the application of a dynamically amplified, but inelastically limited lateral load to the mass of a structure when calculating loading effects. Basically, static loading effects can be considered to design the load path. The displacements of the structure also follow from this same application of equilibrium.

#### **4.2.2.2 Lateral Load Paths in Bridges**

Using the equilibrium concepts from the previous section, load paths developed in typical bridges can be considered. Lateral load paths are the conceptual route that loads follow from the point of application to the points of resistance by the foundation. In the case of seismic loading, the point of application is taken as the mass points where the inertial effects are generated, and the points of resistance are the foundations' reactions against the soil for such loading. This may appear reversed from the observation that the ground moves beneath the structure and thereby induces forces and displacements in the structure, but the equivalent loading represented by Figure 4-3 effectively turns the load path around for discussions related to equilibrium. It is most useful to consider the load path from the top, down when considering lateral loading effects.

One of the simplest types of bridges for seismic lateral loading in the transverse direction is a long viaduct with a uniform stiffness substructure where all bents move laterally the same amount. In this case, the inertial load developed is from the mass that is also tributary or adjacent to each bent. Such a lateral system is similar to that discussed using Figure 4-3. The lateral load path under transverse loading is traced through the superstructure to the nearest bent, through the cap beam of the bent into the columns, from the columns into the foundations, and finally into the soil.

Using the concepts of capacity design, the yielding forces in the columns would be assigned as in Figure 4-5, where the plastic moment capacities are established at the top and bottom of the columns. Because the configuration of the columns and frame, along with the assigned yield moments, produces a unique plastic mechanism and plastic lateral resistance, the forces developed in the system above and below the yielding column portion can be determined once the full plastic mechanism has formed. To be conservative and to prevent the weak or yielding links – normally plastic hinges - from forming elsewhere, overstrength factors are applied to the plastic moments to account for higher than expected

sectional forces. With these forces, the design of the superstructure, cap beam, columns, and foundation elements may be completed.

It is important to recognize that plastic hinges are not true hinges where zero moments are transferred. Instead plastic moments are transferred, as shown by the moment diagram of Figure 4-5, at the locations corresponding to the plastic hinges. Thus the bent still has significant lateral resistance and can still support dead loads and resulting  $P-\Delta$  effects.

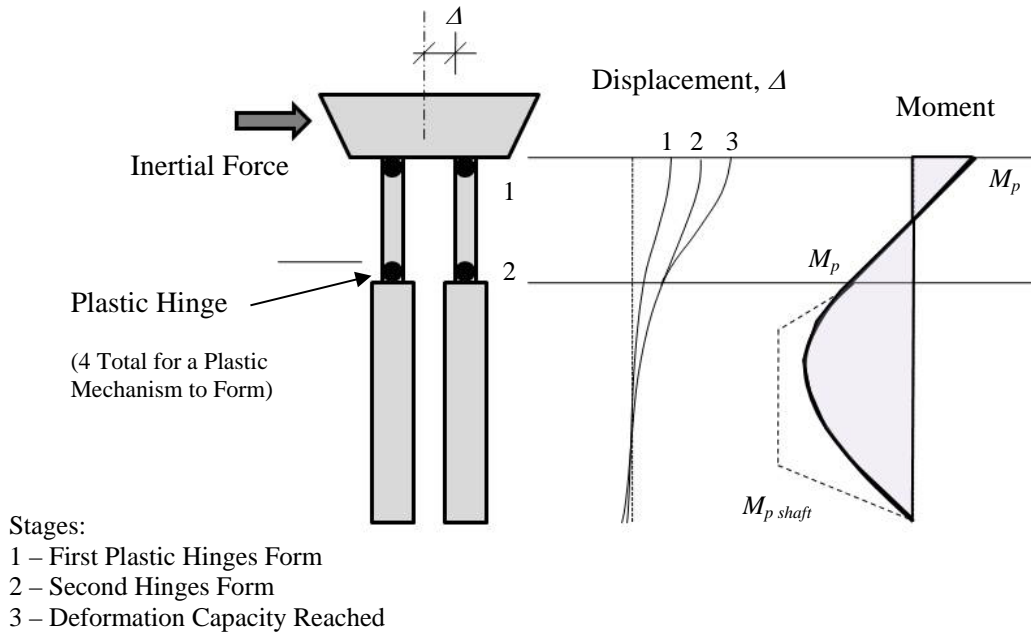


Figure 4-5 Lateral Moments Induced in a Two-Column Bent

A more common type of structure than the long viaduct considered above is the two-span overcrossing. For this type of structure loaded in the transverse direction, the superstructure forms a diaphragm that spans between abutments and therefore acts in parallel with the lateral resistance of the center bent. Such a case is shown schematically in Figure 4-6. This structure is considered to have a continuous superstructure over the center bent and is thus able to span between the abutments to resist lateral loading. Depending on the in-plan aspect ratio of the superstructure, and depending on the superstructure framing, the diaphragm load path may be much stiffer and stronger than the load path through the center bent to its foundation. For instance, if the superstructure is a concrete box girder, which is 70-feet wide, and the spans are 100 feet each, then the diaphragm would have an aspect ratio of 1-to-3. The superstructure lateral stiffness, in such a case, would clearly be much larger than the lateral resistance of the center bent.

The diaphragm bending effect and a qualitative depiction of the relative lateral resistance contributions from the bent and the superstructure spanning between the abutments are shown in Figure 4-7.

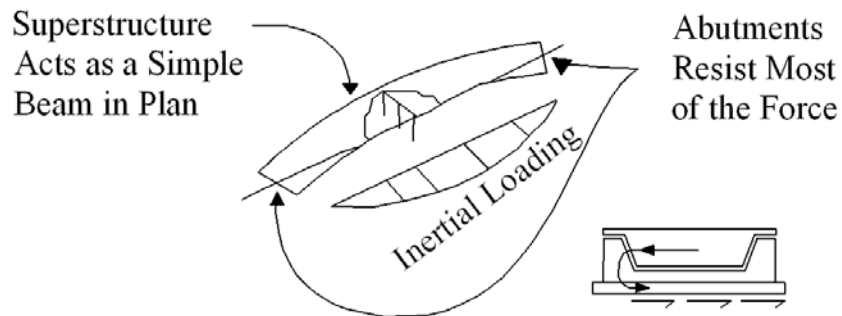


Figure 4-6 Lateral Load Path of a Two-Span Bridge Under Transverse Seismic Loading

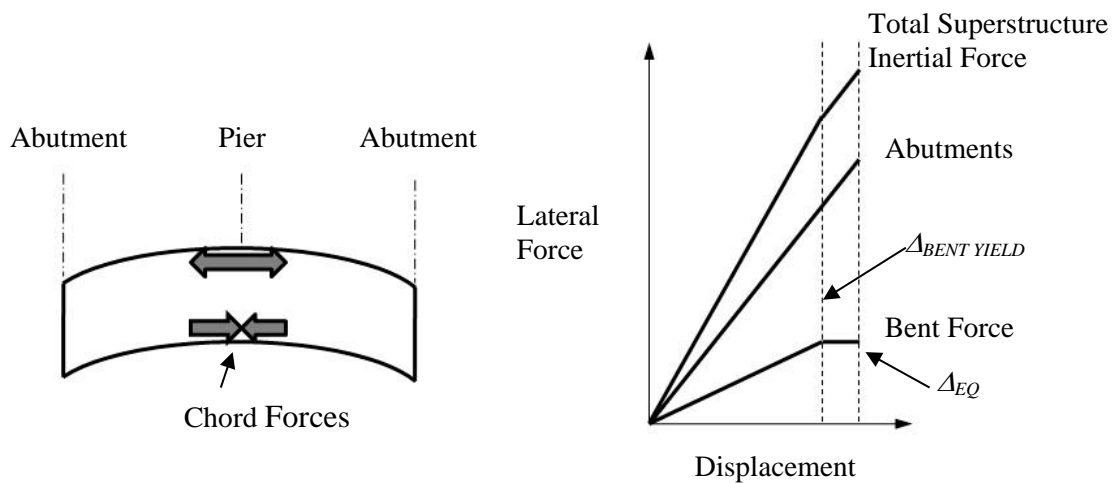


Figure 4-7 Superstructure Bending and Relative Lateral Load Distribution in Two-Span Continuous Bridge

Reflecting back to the ductile system lateral response plot of Figure 4-2, it is easy to see that system ductile response would be difficult to achieve without either yielding the superstructure or the abutments. This is true regardless of how weak the center bent is made. Thus considering the abutment shown in Figure 4-6 and considering that permitting yielding in the superstructure is not preferred due to challenges of preserving the integrity of the vertical gravity support system; there are only two logical choices: resist the transverse inertial forces elastically or introduce yielding into the abutment. Yielding in the abutment could be included by permitting sliding on the soil or by permitting yielding of piles beneath the

abutment, depending on the foundation type. Alternately, fusible shear keys might be considered, although sustained ductile response after first yield of the keys would be difficult to justify. Thus, one can see from this example of system lateral load resistance that system-level ductile response can be challenging to achieve for even the simplest, most common bridge configurations.

However, the response described above is not necessarily indicative of poor design or structural form because enough resistance is provided to sustain the design earthquake by elastic response, and significant redundancy exists in the system; so collapse would be unlikely if unwanted damage to the superstructure occurred. When such response is chosen, it is good practice to design the system to have a preferred hierarchy of failure modes. For instance, if the superstructure was designed to behave elastically in the design earthquake, it would still be desirable to have the abutment transverse shear keys fuse before the superstructure incurred damage that might jeopardize its dead load supporting capability. Controlling the hierarchy of such failure modes is the designer's prime responsibility in seismic design, and capacity design provides the framework with which to achieve this control.

If the superstructure for the example two-span bridge shown in Figure 4-6 is changed to prestressed concrete girders with a cast-in-place deck and full integral diaphragm over the center bent, then importance of capacity protection can be conceptually illustrated. As the inertial forces develop in the superstructure, the maximum superstructure moment about the vertical axis will occur near the center bent, as shown in Figure 4-7. Because the superstructure is effectively spliced together at that point and because the girders are optimized primarily around vertical load carrying capacity, careful attention must be paid to the reinforcement used to tie the two spans together. This is particularly important if the girders are not supported on sufficiently long supports, whose lengths along the girders are at least the minimum prescriptive lengths. Typically, such integral construction does not meet the minimum support lengths. Thus the designer must ensure that the superstructure can sustain the forces that will be induced, even if these are elastic-based design earthquake forces, rather than plastic mechanism forces. When elastic forces are used factors of safety in the range of 1.2 to 2.0 are used to increase the elastic demands for added conservatism.

A third example illustrates similar behavior considerations for a steel superstructure with a composite concrete deck. Consider first a continuous steel superstructure comprised of steel I-girders, using the same 1-to-3 aspect ratio in plan. The behavior under transverse loading would be similar to that shown in Figure 4-6. In this case, the deck and girders will still be required to resist the induced moments about a vertical axis without failure. If the center pier is fairly flexible in the transverse direction, as in the case of

a multi-column pier, substantial moments will be induced in the superstructure above the pier due to the diaphragm action of the superstructure spanning between abutments. The forces that the abutment cross frames or end diaphragms will have to transmit between the deck and the abutment may be substantial. On the other hand, if the center pier is relatively stiff, as in the case of a wall pier, then the pier may become a significant lateral force resisting element and largely prevent the abutments from being the predominant transverse lateral-load-resisting elements.

If this configuration were changed to two simple, single spans, instead of a continuous two-span bridge, then the center pier would take its proportional share of the transverse inertial forces without the associated large moments being induced in the deck. In such a case, the potential for unseating of the spans and impact of the two spans against one another as they deflect laterally, as shown in Figure 4-8, would need to be considered.

This series of examples of lateral, transverse load path illustrates the importance of articulation of a bridge. The manner in which the superstructure in particular is articulated has a large impact on where and how forces are resisted within the structure.

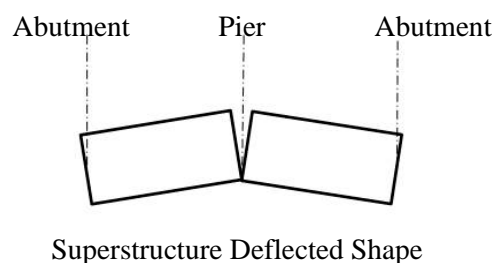


Figure 4-8 Transverse Deformation of Superstructure for Two-Span Non-Continuous Bridge

Loading in the longitudinal direction must also be considered in earthquake design. Consider the same two-span bridge as above with seat-type abutments that permits longitudinal movement of the superstructure relative to the abutment. Seismic loading will act along the entire length of this structure in a relatively uniform fashion owing to the relatively uniform distribution of mass along the superstructure. The lateral load path is shown in Figure 4-9. In this case, the articulation provided by the seat-type abutments means that little longitudinal load will be resisted by the abutments provided that the superstructure does not close the gap between it and the abutment backwall. Such unrestrained movement at the abutment places the bulk of the inertial forces on the intermediate bent. This will likely require that

the pier be sized stiffer and stronger in the longitudinal direction than if the abutments participate in the seismic resistance. The choice of how much lateral load to place on each substructure unit is one that must be worked through in the early phases of design, because the lateral resisting elements must be sized accordingly. Choosing one lateral load path (e.g. pier columns only) versus an alternate load path (pier columns and abutment and soil), as shown in Figure 4-10, will have a significant effect on the seismic design of a bridge.

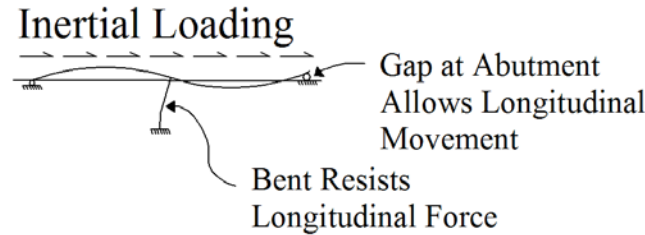


Figure 4-9 Lateral Load Path of a Two-Span Bridge Under Longitudinal Seismic Loading

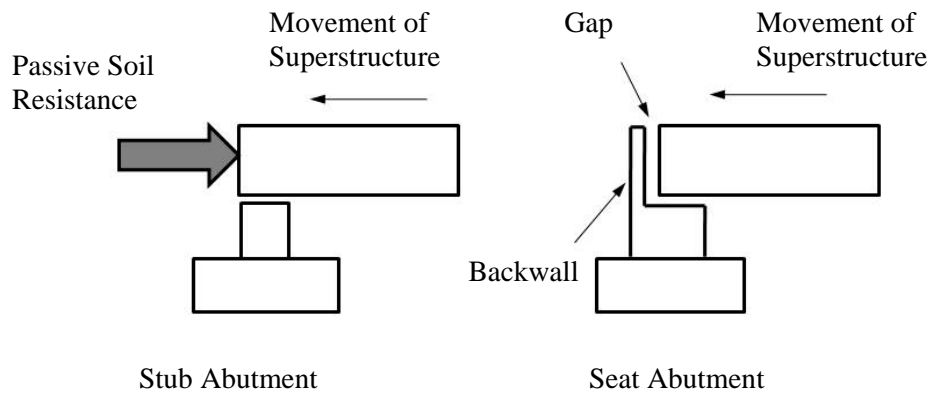


Figure 4-10 Different Longitudinal Behavior for Stub and Seat Abutments

The previous examples illustrate the constraints that real structures place on the ideal objective of capacity design. It is not always easy or possible to configure a bridge to truly be capacity designed. The remainder of this chapter will focus on issues related to the conceptual selection and development of various earthquake resisting systems. These systems have always been a part of seismic design, and although they are not addressed directly in the *LRFD Bridge Design Specifications*, or Division I-A of the *Standard Specifications* (AASHTO, 2002), they are described in the 1986 FHWA Manual on Seismic

Design and Retrofit of Bridges (Buckle et.al., 1986). They are also explicitly called out in the *Guide Specifications* where the term Earthquake Resisting System (ERS) is formally defined. To that end, the discussion in the sections below utilizes the same terminology and concepts as the *Guide Specifications* even though the concepts are also applicable to designs performed using the *LRFD Specifications*.

### **4.2.3 Simplicity, Integrity, and Symmetry**

The examples discussed in the preceding section partially illuminate the concept of incorporating simplicity, integrity and symmetry into the ERS. Simplicity infers that the ERS is clear, justifiable, and designable. Integrity infers that appropriate elements of a structure are adequately connected to resist an earthquake, and symmetry infers that balanced stiffness, mass, and strength are incorporated into the design to the extent possible. In some cases, these concepts will conflict with other non-seismic constraints, for example alignment where high skews are often the norm. So the seismic designer must weigh the advantages and disadvantages of various configurations to develop a reasonable approach.

In section 4.2.1, one of the essential observations about modern seismic design is that response predicted using elastic analysis can be used to design bridges that are intended to respond inelastically. This observation is based on bridges being regular enough to respond in modes that can be predicted with elastic analysis. Thus the more complex a bridge becomes, the less reliable elastic techniques are to accurately predict the response. In recognition of this, most bridge seismic design specifications place limits on features that complicate the response, such as relative stiffness between bents, span length variation, skew, and horizontal curvature. As these features become less favorable to response and response prediction, more advanced analysis and design requirements are invoked. The specifics of these procedures and the associated limits are discussed in Chapters 5 and 8.

#### **4.2.3.1 Balanced Stiffness and Frame Geometry**

Caltrans (2013) and the AASHTO *Guide Specifications* both strongly encourage certain regular features of bridges. One is balanced stiffness and the other is balanced frame geometry.

With reference to Figure 4-11, Caltrans' balanced stiffness provision strongly encourages that any two piers within a frame or between any two columns in a pier have a difference in stiffness of no more than

50 percent. Additionally, the variation in stiffness between adjacent piers within a frame or between adjacent columns within a pier should not differ by more than 25 percent.

Caltrans' balanced frame geometry provision strongly encourages that adjacent frames (i.e. structural units on either side of an articulation joint, such as an in-span hinge) have fundamental vibration periods that are within 30 percent of one another (i.e. the ratio of their periods is 0.70 or greater, if the shorter period is in the numerator). See Figure 4-11. These provisions encourage designers to configure bridges in a fashion favorable to earthquake resistance. Such constraints may not be simple to achieve. For example when the heights of adjacent substructure elements, either piers along a bridge or columns along a pier, vary significantly, balanced stiffness, as defined above, is difficult to achieve and alternative structural forms or modifications to common details are usually considered.

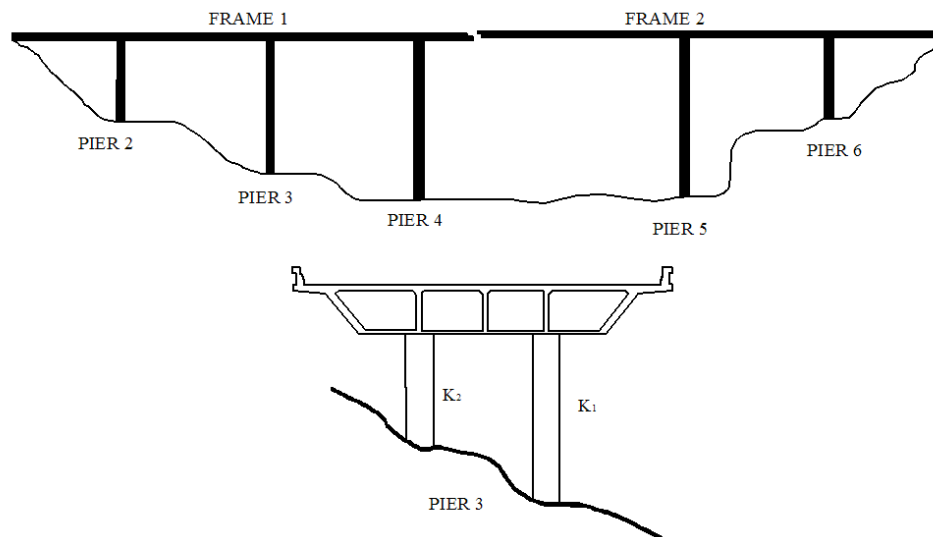


Figure 4-11 Balanced Frame Stiffness and Geometry (adapted from Caltrans, 2013)

Thus, one technique used to help achieve balance in bridge lateral performance is the 'isolation casing' as shown in Figure 4-12. These are useful with column-to-drilled shaft type foundations where a permanent casing that has a larger diameter than the column is extended up from the shaft. The top of the shaft is held below the normal ground grade level, thus producing an annular space or 'well' around the column. This space provides room for the column to deflect laterally without engaging the soil. This configuration effectively makes the column longer and less stiff. By controlling the depth of the well, adjacent columns or bents can be built with similar stiffnesses. When using such a concept, engineers must develop details to prevent access to the space, to prevent the space from filling with unwanted material, and to provide

inspection access. Additionally, if water can enter the space and freeze, that condition must be considered, either by appropriate design calculations or by preventing water from intruding into the space.

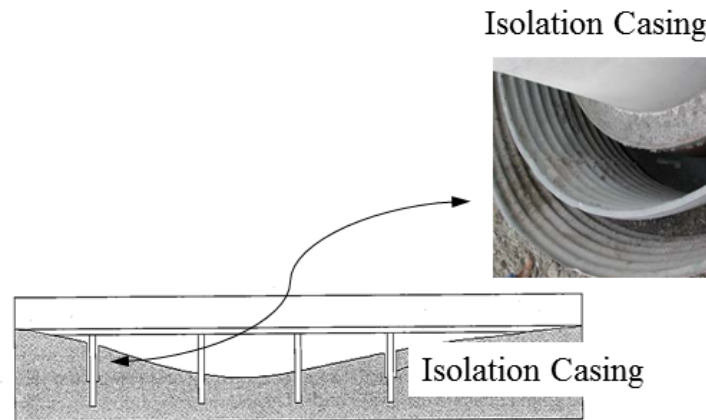


Figure 4-12 Isolation Casings (Keever, 2008, Yashinsky and Karshenas, 2003)

The isolation casing concept is not the only one that can be used to attempt to balance the stiffness and dynamic characteristics of a bridge. An alternate approach would be to place a sliding or isolation-type bearing at the top of the column to prevent large shear forces from being attracted to the short column. Other concepts include the following: (Caltrans, 2013):

- 1) Adjusting the effective column height by lowering footings,
- 2) Using oversized drilled shafts,
- 3) Modified end fixities/restraints (as with the alternate approach described above),
- 4) Varying the column cross section and longitudinal reinforcement,
- 5) Adding or relocating columns or bents,
- 6) Modifying hinge/expansion joint articulation,
- 7) Reducing or redistributing the superstructure mass.
- 8) Incorporating seismic isolators or dampers.

#### 4.2.3.2 Skew and Curvature

Skew and curvature, particularly horizontal curves, are features that can make bridge dynamic response more complex and make design more difficult. Bridge seismic design specifications typically require

additional support lengths for higher skews and require more advanced (e.g. multimode dynamic, Chapter 5) analysis for higher curvatures. Additionally, skews and curvature complicate the dynamic analysis in terms of required boundary conditions and the effectiveness of soil resistance and compliance. Both skew and curvature tend to couple lateral response in the transverse and longitudinal directions. These issues are discussed further in Chapter 5. However, the strategy for keeping bridge response and behavior more predictable and regular is to minimize skew and curvature to the extent possible. Skews should be kept consistent from bent-to-bent and should be minimized overall, to less than 30 degrees, if possible, (Yashinsky and Karshenas, 2003). Curvature should be minimized to the extent possible. These strategies typically will conflict with layout of roadway alignment, earthworks, and span length, because skew and curvature are typically a function of roadway alignment not simply the bridge structure, alone. So the incentive to minimize these features becomes a trade-off between seismic performance and cost.

#### **4.2.3.3 Articulation, Restrainers, and Support Length**

The articulation or release of certain internal forces for thermal movement, construction ease, seismic force considerations, or other reasons has a significant effect on the response of bridges. The in-span hinge shown between Bents 4 and 5 in Figure 4-12 is an example of such releases, as would be sliding or pin bearings at abutments or over bent caps, as shown for the two spans in Figure 4-8 and for abutments in Figure 4-10. When continuity of the structure is reduced by such articulation, there is potential for unfavorable seismic response that can lead to unseating of spans, for example. The strategy to avoid such problems in order of preference is:

- 1) Use continuous or integral construction.
- 2) Provide generous support lengths.
- 3) Provide restrainers or shock transmission units to interconnect adjacent frames.

Restrainers are the least preferable because past experience in California has shown that the forces in restrainers under the design earthquake are quite difficult to predict and may be difficult to design as capacity-protected elements (FHWA, 2006). Therefore, for new construction they are not the preferred solution for preventing unseating.

The use of internal releases, such as moment release, is often a viable strategy for controlling earthquake response and induced forces, as well as, capacity protecting adjacent ERS elements. For example, the

choice to provide an integral bent cap (fixed conditions) or a cap with a moment release (pinned conditions) permits the control of relative bent stiffness and permits control of the amount of moment that must be resisted by the superstructure. The use of a pinned-top bent for a relatively short column can balance the stiffness and resistance from taller columns that develop plastic hinges at their tops and bottoms (i.e. fixed-fixed construction). This is often a strategy used to achieve the balance suggested in Section 4.2.3.1, above. The use of a pinned condition at the top of a column or bent cap also eliminates the need to carry large moments into the superstructure for capacity protection. This force transfer can be an important issue for certain superstructure types; for example, precast I-girders are often difficult to capacity protect, particularly for moments that produce tension on the bottom flange of the girder near supports.

#### **4.2.3.4 Summary**

In summary, it is clear that choices made early in selecting bridge type, articulation, and configuration can have a significant effect on the seismic design and ultimately on seismic response. It is thus important that the designer think through the desired seismic response, load path, and the details of how a bridge's components will be interconnected.

#### **4.2.4 Acceptable and Unacceptable Structural Form**

As described earlier, the behavior of a bridge under seismic loading is determined by its structural form – that is its geometry, structural type, member strengths, and member interconnections/articulations. Certain features of structural form related to the plastic hinging elements for example, can be classified with respect to their suitability for effective seismic design. These earthquake resisting elements can be thought of as individual building blocks that are used to determine the overall seismic structural form. A collection of these elements then define the Earthquake Resisting System (ERS), which in turn can be generally classified in terms of a global design strategy, as discussed in Section 4.3.

For the purpose of encouraging good practice in seismic design, Earthquake Resisting Elements (ERE) are formally defined in the *Guide Specifications for LRFD Seismic Bridge Design*, and listings of EREs are categorized as either “Permissible”, “Permissible that Require Owner’s Approval”, or “Not Recommended for New Bridges”. Whereas such listings are new features to seismic design specifications

and do not appear in the LRFD *Specifications*, or Division I-A of the *Standard Specifications* (AASHTO, 2002), they have their roots in the 1986 FHWA Manual on Seismic Design and Retrofit (Buckle et. al., 1986) and are applicable to any bridge regardless of the Specifications used for its design. The concept is also a very useful tool for designers during preliminary design or at the Type, Size and Location (TS&L) stage of design.

Example listings of the three ERE categories are provided in Tables 4-1 through Table 4-3, which are taken from the *Guide Specifications*.

One guiding principle that distinguishes elements in the three categories is the desire to keep potential damage in locations that can be inspected. Thus, plastic hinges should form above ground, and such hinges fall into the “permissible” category. Alternately, plastic hinges that form below the ground line (i.e. in-ground plastic hinges) are not preferred and thus fall within the “permissible with owner’s approval” category. Unlike previous versions of the seismic design specifications, such hinge locations are not prohibited, but instead simply discouraged. This recognizes the fact that in-ground plastic hinging may not be avoidable in all cases. For example Case 6 of Table 4-2 – plastic hinging in piles below a wall pier, Case 7 – plastic hinging in piles supporting an integral abutment, and Case 8 – plastic hinging in piles with the same strength as the extension above ground. When such behavior is expected, it may be utilized with the approval of the owner. This is important for two reasons: in-ground damage may be difficult or impossible to detect, and repair of damage related to in-ground hinging will likely not be repairable. The owner needs to understand this, both from post-earthquake inspection and potential repair perspectives.

Note that plastic hinges that form just below the ground line and are accessible by reasonable excavation are permissible, as shown for Cases 2 and 7 of Table 4-1, respectively. Likewise Case 7 of Table 4-2 for integral abutments on piles is a special case that some authorities may elect to permit without restriction, because inspection of such piles is possible. However, this case is included in the “with Owner’s Approval” category so that an owner has control over the use of such systems. The system shown in Case 7 is actually a rugged system seismically, because it engages the soil behind the abutment to a great degree. This limits the deformations that other parts of the bridge would experience in an earthquake.

Other features that require owners approval are rocking beyond the partial uplift traditionally permitted in seismic design of bridges by the AASHTO specifications, passive soil resistance without reduction to 70 percent of the full passive value, sliding of spread footings, plunging or pullout of more than the outer

rows of piles in group foundations, batter pile systems designed to mobilize the full soil resistance before structural capacity of the pile is reached. These cases represent conditions that are less conservative than traditional design methods, although if done correctly by taking into account actual resistance values and actual behavior, these systems should perform well and meet the life-safety objective of no collapse. In some cases, design limits may need to be developed in order to take advantage of the behaviors listed. However, in other cases, such as in-ground plastic hinging, the Guide Specifications include appropriate limits already.

**TABLE 4-1 PERMISSIBLE EARTHQUAKE RESISTING ELEMENTS**

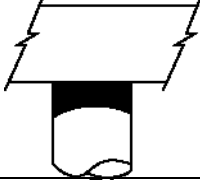
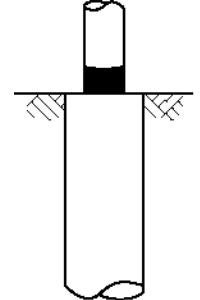
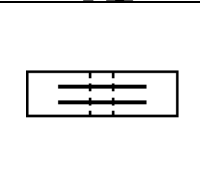
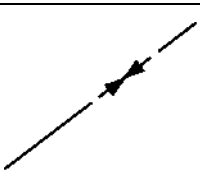
Case	Earthquake Resisting Elements	Description
1		Plastic hinges below cap beams including pile bents.
2		Above ground/ near ground plastic hinges.
3		Seismic isolation bearings or bearings designed to accommodate expected seismic displacements with no damage.
4		Tensile yielding and inelastic compression buckling of ductile concentrically braced frames.

Table 4-1 Continued Next Page

**TABLE 4-1 CONTINUED PERMISSIBLE EARTHQUAKE RESISTING ELEMENTS**

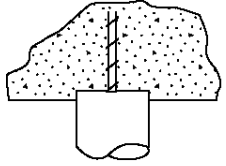
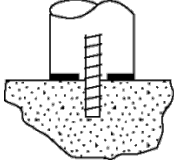
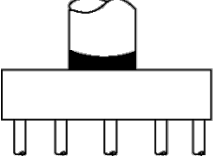
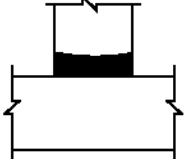
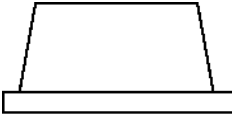
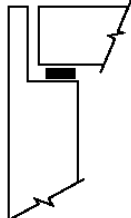
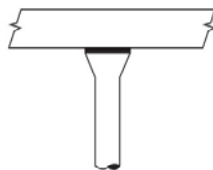
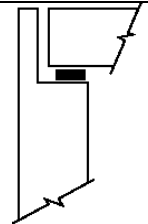
Case	Earthquake Resisting Elements	Description
5		Piles with “pinned-head” conditions.
6		Columns with moment reducing or pinned hinge details.
7		Capacity-protected pile caps, including caps with battered piles, which behave elastically.
8		Plastic hinges at base of wall piers in weak direction.
9		Pier walls with or without piles.
10		Spread footings that satisfy limited overturning criteria.
11		Passive abutment resistance required as part of ERS, but a limited passive resistance has been counted on for design.
12		Seat abutments whose backwall is designed to fuse or break away after impact by the superstructure. The superstructure is configured to sustain the impact forces.

Table 4-1 Continued Next Page

**TABLE 4-1 CONTINUED PERMISSIBLE EARTHQUAKE RESISTING ELEMENTS**

Case	Earthquake Resisting Elements	Description
13		Columns with architectural flares.
14		Seat abutments whose backwall is designed to resist the expected impact force in an essentially elastic manner.

**TABLE 4-2 PERMISSIBLE EARTHQUAKE RESISTING ELEMENTS THAT REQUIRE OWNER'S APPROVAL**

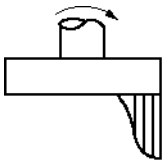
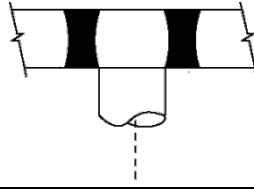
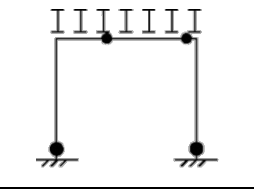
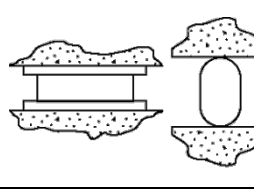
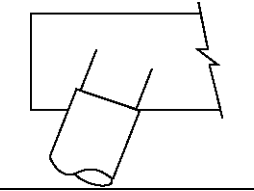
Case	Earthquake Resisting Elements	Description
1		Passive abutment resistance required as part of ERS, and the passive strength corresponds to the maximum strength that is expected to be mobilized (i.e. no conservative limiting of passive resistance has been assumed).
2		Sliding of spread footing abutment allowed in order to limit force transferred. Limit movement to adjacent bent displacement capacity.
3		Ductile cross frames at the supports in the superstructure
4		Foundations permitted to rock where potential uplift exceeds traditional partial uplift limits or where rocking dynamics is considered when developing the demand displacements.

Table 4-2 Continued Next Page

**TABLE 4-2 CONTINUED PERMISSIBLE EARTHQUAKE RESISTING ELEMENTS THAT REQUIRE OWNER'S APPROVAL**

Case	Earthquake Resisting Elements	Description
5		<p>More than the outer line of piles in group systems allowed to plunge or uplift under seismic loadings.</p>
6		<p>Wall piers on pile foundations that are not strong enough to force plastic hinging into the wall, and are not designed for the design earthquake elastic forces.</p>
7		<p>Plumb piles that are not capacity-protected (e.g., integral abutment piles or pile-supported seat abutments that are not fused transversely).</p>
8		<p>In-ground hinging in shafts or piles where the plastic hinging occurs deep enough that post-earthquake inspection or repair is not possible.</p>
9		<p>Batter pile systems in which the geotechnical capacities and/or in-ground hinging define the plastic mechanisms.</p>

**TABLE 4-3 EARTHQUAKE RESISTING ELEMENTS NOT RECOMMENDED FOR NEW BRIDGES**

Case	Earthquake Resisting Elements	Description
1		Plastic hinges in superstructure.
2		Cap beam plastic hinging (particularly hinging that leads to vertical girder movement) also includes eccentric braced frames with girders supported by cap beams.
3		Bearing systems that do not provide for the expected displacements and/or forces (e.g. rocker bearings)
4		Battered-pile systems that are not designed to fuse geotechnically or structurally by elements with adequate ductility capacity.

The final category for EREs is “Not Recommended for New Bridges”. This category contains four examples of EREs that have performed poorly in past earthquakes and are strongly discouraged.

Cases 1 and 2 of Table 4-3 depict plastic hinging in either the superstructure or in the cap beams of a pier. These are not recommended due to the difficulty in assuring that robust and sustained deformation capacity can be achieved. The interaction of gravity loading can also complicate such mechanisms; thus these locations of plastic hinging are discouraged. Note that this is opposite of the intended plastic mechanisms for buildings, where hinging is restricted to beams. Such practice is used to assure that the more heavily loaded columns do not hinge and jeopardize the performance of the system with potentially poor inelastic behavior. This is not the case with bridges where the axial load levels in columns and piers tend to be relatively low and where the horizontal framing system of the superstructure is optimized around the gravity loading to increase span lengths.

Case 3 of Table 4-3 illustrates bearings that may topple or otherwise be damaged under earthquake loading. The reason for limiting the use of such hardware is that potential movements of the

superstructure after failure of such elements may produce unseating and collapse or high impact from dropping spans.

Case 4 of Table 4-3 illustrates battered piles that are not strong enough to prevent structural tension failure in the piles. Such failure is not ductile under cyclic loading and can occur at relatively small loading levels because battered piles attract high axial forces due to their orientation. This is an example of where stiffness preferred to control other types of lateral loading makes battered pile systems appear desirable, but for seismic loading these systems are vulnerable because they attract large forces and cannot deform in a sustained ductile manner. Trade-offs between such constraints will have to be made. If battered piles are chosen as a lateral ERE, then they should be designed to develop the upper-bound geotechnical pull-out capacity, in which case they are in the ‘Require Owner’s Approval’ category.

In general, the theme of the three categories is that ductile, predictable response that limits the overall forces in the system while providing displacement capacity is desirable. Elements that limit the ability of a structure to perform in this manner are generally less desirable. While not explicitly mentioned in the three categories, another condition is generally unacceptable. Elements that are capable of resisting the design earthquake elastically are not acceptable if there is a possibility they will fail in a brittle, non-ductile manner at loadings slightly higher than the design earthquake. Such behavior does not meet the general desire to design a bridge to withstand slightly higher loadings without abrupt failure, because earthquake loadings are unpredictable. Some reserve displacement capacity is always desirable.

## **4.3 EARTHQUAKE RESISTING SYSTEMS AND GLOBAL DESIGN STRATEGIES**

### **4.3.1 Earthquake Resisting Systems**

The logical extension of earthquake resisting elements (EREs) is to the system or bridge level. The response of the entire bridge is what is important, and the EREs are but individual contributors. At the system level the lateral resisting system known as the Earthquake Resisting System (ERS) must be identified and rationally designed. Examples of preferred or permissible ERSs are provided in Table 4-4. Several approaches are shown for both the longitudinal and transverse directions. Conventional plastic hinging as described for the ERE is permitted for the intermediate substructure locations. Isolation bearings are also permitted, although they are not permitted in tandem with plastic hinging at a given pier location. They are permitted in tandem with plastic hinges at other pier locations, as seen in Case 4.

Generally, the permissible ERS are a combination of permissible ERE. This can be seen by comparing the referenced features in Table 4-4 with those permissible elements in Table 4-1.

### 4.3.2 Global Design Strategies

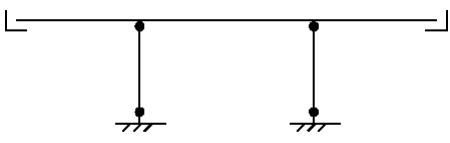
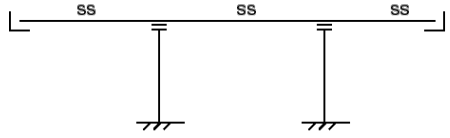
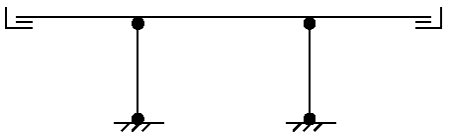
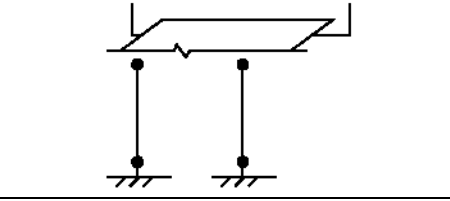
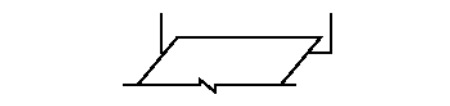
To further classify the intended response of bridges and to assist the designer in choosing an overall system that will achieve the performance goals for seismic design, the concept of a global design strategy is introduced in the *Guide Specifications* but is not limited to bridges designed using these specifications. The approach is applicable to any bridge, regardless of the specification used for its design. In the *Guide Specifications* three Global Design Strategies are explicitly listed as follows:

- 1) Type 1 - Ductile Substructure with Essentially Elastic Superstructure
- 2) Type 2 - Essentially Elastic Substructure with Ductile Superstructure
- 3) Type 3 - Elastic Superstructure and Elastic Substructure with Fusing Interface

Additionally, a fourth strategy is the elastic approach where the structure is designed to remain elastic in the design earthquake. Owing to its simplicity, this strategy is discussed first in this section.

As a general rule, the global design strategies are not mixed. For example, a ductile superstructure generally would not be used in tandem with a ductile substructure, particularly at a given bent. Combining strategies in that fashion results in relatively complex response that cannot be estimated using the linear elastic and non-linear static techniques that are most commonly used in bridge seismic design. However, under the correct conditions, for example limited curvature, the global strategies can be combined for transverse and longitudinal response, where one strategy is used in one direction and one in the other. The global strategies primarily relate to the response of individual bents. Thus, the strategies should be considered in the context of the overall ERS, and in particular permissible systems, as described in Section 4.3.1.

**TABLE 4-4 PERMISSIBLE EARTHQUAKE RESISTING SYSTEMS**

Case	Earthquake Resisting Systems	Description of ERS
1		<p>Longitudinal Response:</p> <ul style="list-style-type: none"> <li>• Plastic hinges in inspectable locations or elastic design of columns.</li> <li>• Abutment resistance not required as part of ERS.</li> <li>• Knock-off backwalls of abutments permissible.</li> </ul>
2		<p>Longitudinal Response:</p> <ul style="list-style-type: none"> <li>• Isolation bearings accommodate full displacement.</li> <li>• Abutment resistance not required as part of ERS.</li> </ul>
3		<p>Longitudinal Response:</p> <ul style="list-style-type: none"> <li>• Multiple simply supported spans with adequate support lengths.</li> <li>• Plastic hinges in inspectable locations or elastic design of columns.</li> </ul>
4		<p>Longitudinal or Transverse Response:</p> <ul style="list-style-type: none"> <li>• Plastic hinges in inspectable locations or elastic design of columns.</li> <li>• Isolation bearings with or without energy dissipaters to limit overall displacements.</li> </ul>
5		<p>Transverse Response:</p> <ul style="list-style-type: none"> <li>• Plastic hinges in inspectable locations or elastic design of columns.</li> <li>• Abutment not required in ERS, breakaway shear keys permissible.</li> </ul>
6		<p>Transverse or Longitudinal Response:</p> <ul style="list-style-type: none"> <li>• Abutment required to resist design earthquake elastically.</li> <li>• Longitudinal passive pressure less than 70 percent of maximum that can be mobilized.</li> </ul>

### 4.3.3 Essentially Elastic Substructure with Elastic Superstructure

For the low seismic areas of the country, resisting seismic loads elastically, without explicitly building into the structure features to enhance its ductility, is a valid design approach. As the seismic design loadings increase, this strategy is less attractive. If the approach is used, the designer and the owner should understand that poor performance may result in earthquakes that are larger than the design earthquake. For example, shear failure, foundation damage, or other undesirable failure modes could

occur in such cases, although the chances of such behavior should typically be quite small. When the essentially elastic approach is used in the higher seismic areas of the country, the designer should consider increasing the design forces above the elastic force level for added assurance of good performance.

Another instance where this design strategy is appropriate is for Critical or Essential bridges where disruption of service should be prevented for the design earthquake. In such cases, the design of the structure should ensure that the ERE and ERS remain ‘essentially elastic’ so that damage that might cause the structure to be closed will be prevented. In this context, essentially elastic means that some elements may be loaded slightly past their yield points, even approaching their nominal capacity. However, strain levels should be kept low enough that spalling of concrete does not occur, shear failures do not occur, and residual displacement of the structure is either prevented or small enough that the service level of the structure is not altered.

#### **4.3.4 Ductile Substructure with Essentially Elastic Superstructure**

The conventional design approach has been to configure the bridge, and in particular the intermediate substructure, to respond in a ductile manner to the design earthquake and prevent damage from occurring in the superstructure. This generally means keeping the superstructure elastic, and this strategy is the focus of the capacity design method contained in both the existing LRFD *Bridge Design Specifications* and the new *Guide Specifications*. This type of response is characterized by the behavior and plastic mechanism shown in

Figure 4-13, where yielding is confined to the substructure. The bulk of the design procedures in the LRFD and Guide Specification documents focus on this strategy. Additionally, this strategy includes both permissible ERE and those that require Owner’s approval (e.g. in-ground hinging and pile loading in excess of the geotechnical capacity – pile plunging or pullout).

#### **4.3.5 Essentially Elastic Substructure with Ductile Superstructure**

The use of a ductile superstructure is a relatively new strategy for design of bridges, and it was developed first as a retrofit strategy for existing bridges (FHWA, 2006). The idea behind this strategy, which is

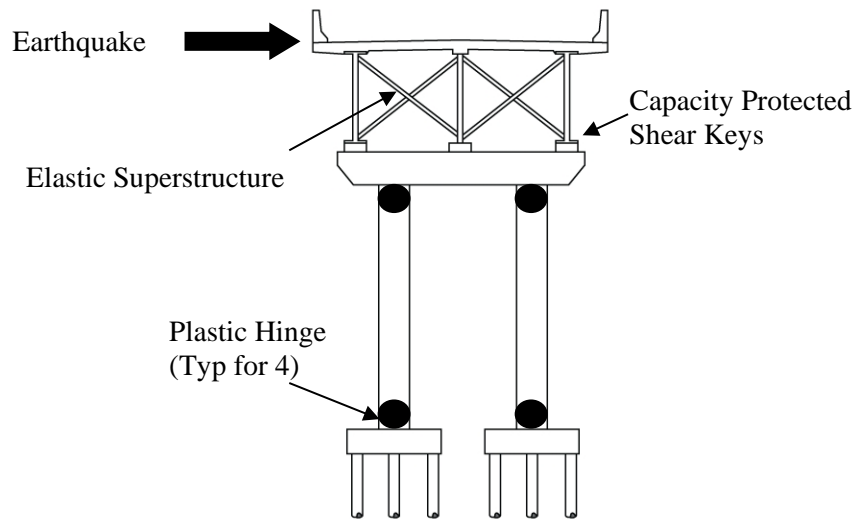


Figure 4-13 Type 1 - Ductile Substructure and Elastic Superstructure

effective only in the transverse direction and for steel I-girder superstructures, is that cross bracing between the girders can be detailed to be sufficiently ductile to dissipate earthquake-induced kinetic energy. With such a strategy only the cross frames at the piers and abutments are considered as yielding elements. Cross frames in the span do not experience significant inelastic action in these systems. The concept is shown schematically in Figure 4-14, where essentially all the energy dissipation occurs in the steel cross frames, which have been detailed to provide ductile response. In this strategy, capacity design applies to the cross frame primary members, and capacity protection is applied to the cross frame connections, deck, girders, bearings, and substructure. Because this strategy is only effective in the transverse direction, a conventional yielding substructure or and isolation (fusing interface) strategy will be necessary in the longitudinal direction.

Because this type of global strategy is essentially an emerging technology, the design requirements for such systems are not yet fully developed, and therefore are not as detailed as those for the Type 1 strategy. For example, there is currently no mention of ductile superstructures in the LRFD *Bridge Design Specifications* seismic design procedures, and the coverage in the new Guide Specification is not exhaustive, and appropriate design methodologies are still under development. Consequently, the designer may have to bring other reference materials to bear in designing such systems (FHWA, 2006, Carden, et. al. 2007 and Carden, et. al. 2006). Also, there are currently no displacement-based design

procedures that have been developed; so design of new structures using a Type 2 global strategy must use force-based design with R factors, as described in Chapter 7.

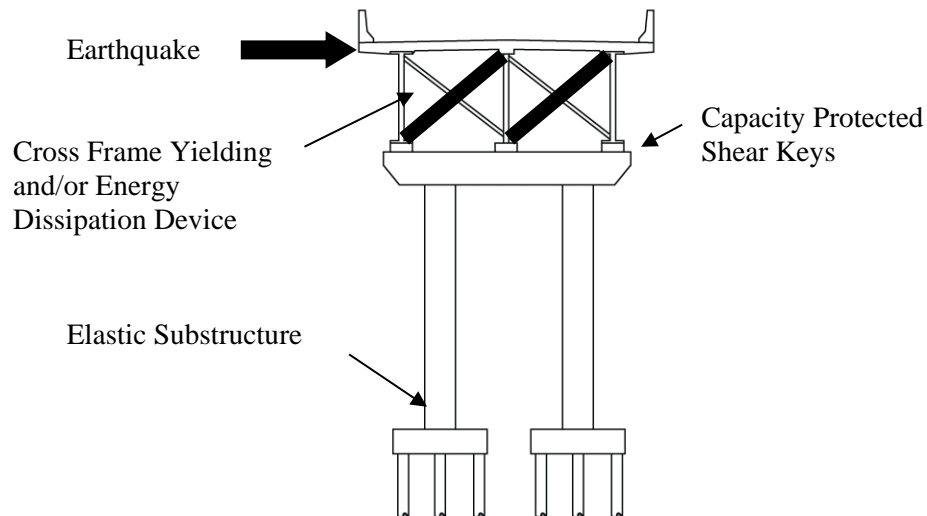


Figure 4-14 Type 2 - Elastic Substructure with Ductile Superstructure

#### 4.3.6 Elastic Superstructure and Elastic Substructure with Fusing Interface

The approach of placing a fusing interface between the substructure and superstructure accommodates a number of different concepts where the seismic displacement capacity of a bridge is provided at this interface, as shown in Figure 4-15. The most common and most mature technology for such elements is seismic isolation, whereby a bearing that increases bridge lateral flexibility and provides some additional damping is placed between the superstructure and substructure. Other devices that provide additional damping or energy dissipation, whether passive or active, have also been proposed in a number of forms and some have been used (FHWA, 2006). Typically, the methods of design required for such elements are beyond the scope of the AASHTO LRFD *Bridge Design Specifications* or the *Guide Specifications*. For example, the AASHTO *Guide Specification for Seismic Isolation Design* would be used for design of seismically isolated bridges.

Alternately, a simple form of fusing can be provided by shear keys that are designed to break away when loaded with large lateral forces. In such cases, support lengths need to be increased to accommodate the

expected relative displacements following the failure of the shear keys. Because the actual resistance and failure point of CIP shear keys or blocks is highly variable and likely non-ductile, conservative practice is

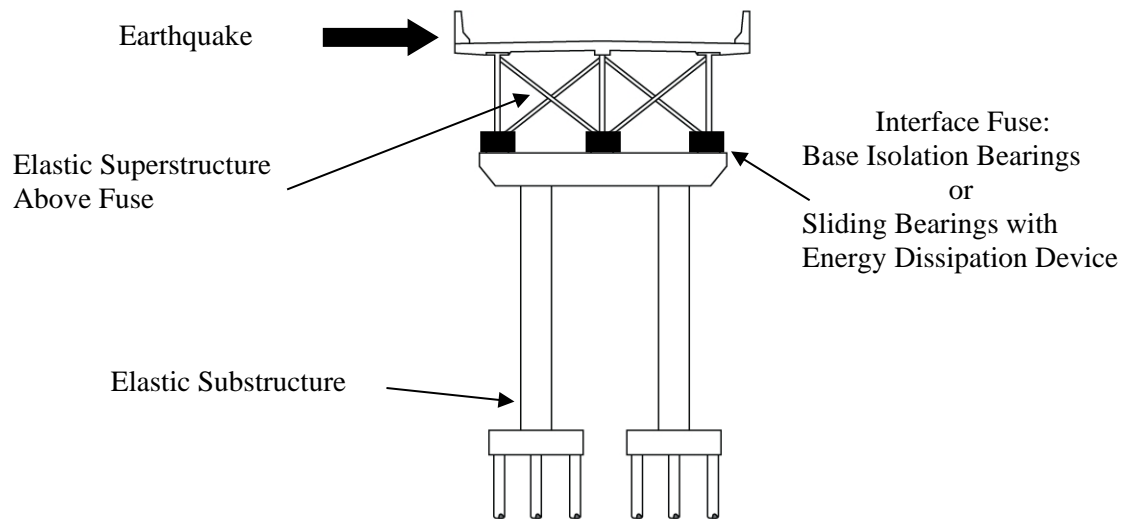


Figure 4-15 Type 3 - Elastic Substructure and Superstructure with a Fusing Interface

warranted with respect to providing support length, and the general prescriptive methods of the AASHTO *LRFD Bridge Design Specifications* or the *Guide Specifications* should be followed.

#### 4.4 SUMMARY

In summary, the principles of seismic design that are used for the design of bridges are simple in concept, but sometimes challenging to apply in practice. This chapter has described principles that can be used to design bridges to resist the effects of large, potentially damaging earthquakes.

- The principle of capacity design - yielding of selected elements accompanied by protecting all the other elements in the bridge against damage - underpins the design approach included in the design specifications used throughout the country.
- The notion that the designer can control the seismic behavior by permitting force-limiting yielding and ductile response is an effective tool for addressing the unpredictable nature of earthquake

loading in a rational way. However, designers must be aware of the various structural elements that participate in seismic resistance and must control the nature of the loads to those elements in order to prevent premature or unexpected failure of the bridge system. This is accomplished using capacity design principles.

- The concept of lateral load path is an effective tool for identifying the elements involved and in designing those elements to handle earthquake loading effects.
- Some types and locations of inelastic response are preferable for ease of access for inspection and repair. However, in cases where inelastic response cannot be confined to certain locations, the Owner should then be involved in decisions related to assignment of yielding/damage incurring elements.
- Finally, four global design strategies of seismic design are available to the designer as tools to organize the hierarchy of where yielding or damage may occur between the substructure and superstructure.

Good design practice is to work through the general concepts presented in this chapter early in the design, such that the simplest, most effective, seismic lateral force resisting system is identified and utilized.

The concepts presented in this chapter will underpin the more detailed application concepts presented in subsequent chapters. For example, Chapter 5 will present methods that are used to determine the seismic demands, whether forces or displacements, which earthquakes can induce. Chapter 6 explains how design demands are formulated and how the plastic mechanism is established, thereby providing the internal force limitation as described in Section 4.2.2.1 above. Then Chapter 7 explains how the parts of the structure that are chosen to yield are designed to withstand the expected plastic deformations. This chapter also explains how the parts of the structure that should not experience yielding are designed to preclude such response. Chapter 8 outlines the seismic provisions of both the AASHTO *LRFD Specifications* and the *Guide Specifications* to explain in detail how capacity design is implemented and guided by the AASHTO design provisions. Chapter 9 provides an introduction to seismic isolation design, which corresponds to Global Strategy Type 3. Finally, Chapter 10 gives an introduction to seismic retrofitting of bridges. This topic is based on the logical extension of the principles of capacity design for new bridges to existing bridges, while recognizing that one cannot always fully apply the principles to existing structures. Overall, each subsequent chapter fills in a piece of the seismic design puzzle to complete the overall goal of understanding modern seismic design principles and how they fit together.



## **CHAPTER 5**

### **DEMAND ANALYSIS**

#### **5.1 GENERAL**

Various analytical methods are presented in this chapter for the purpose of estimating the force and displacement demands on a bridge during an earthquake. These methods range from approximate to rigorous, and from simple to complex. Most assume that a bridge remains elastic (or essentially elastic) during an earthquake, but as noted in Section 4.1, this is frequently not the case. It is uneconomic to design a bridge to perform elastically during moderate-to-large earthquakes and the results of elastic analyses must be modified during design to account for the expected nonlinearity (inelasticity), as discussed in the Chapter 6. In recent years explicit nonlinear methods have become available that give consistently reliable results and these are also presented below. Both approximate and rigorous methods are included. One is an equivalent static method and the other a nonlinear dynamic (time history) method. In addition to explaining response spectrum and time history methods for uniform ground motion, a method for handling spatially varying ground motion (multiple support excitation) is summarized. Limitations on the applicability of all methods are discussed.

All but the simplest of the methods explained in this chapter, require computer software for their implementation. It follows that, in practice, a designer need not be intimately familiar with the details of each method since these have been coded into commercially available software. Instead a designer needs to know the relative merits of each method and when they should (and should not) be used. Furthermore, the designer is responsible for developing the physical model of the bridge to be analyzed, and this should be done with great care. For this reason advice on modeling is also given in this chapter. Topics covered include the distribution of mass and stiffness, the modeling of structural members, connections, foundations, abutments, in-span hinges and expansion joints, and the representation of damping. Bridges with skew, curvature, partially submerged piers, and imposed support displacements are also discussed.

For reasons of limited space, and the fact that analytical software is readily available, the material in this chapter focuses on the principles of each method and not the details. These may be found in many text books on structural dynamics, such as Clough and Penzien (1993), and Chopra (2012). Additional detail on modeling can be found in Priestley, Seible and Calvi (1996). It is also noted that the FHWA Seismic Retrofitting Manual has relevant information on analytical methods and bridge modeling (FHWA, 2006).

### 5.1.1 Bridge Structural Dynamics

Although highway bridges are complex structural systems, their analysis for service loads has become routine with the availability of sophisticated computer software for static analysis. But when the loads are dynamic, as in an earthquake, the situation is not as straightforward and particularly if the bridge exceeds its elastic limit and becomes nonlinear. Extensive numerical computation may be required and interpreting the results must be done with care. Numerical models should be used that capture all of the important effects, and modeling errors should be minimized to an acceptable level.

To develop an understanding of bridge structural dynamics it is helpful to begin with simple bridges that behave essentially as single spring-mass systems, i.e. as a single degree-of-freedom system, and then move on to more complicated bridges that have multiple degrees-of-freedom. Both are described in this section.

#### 5.1.1.1 Single-Degree-of-Freedom Behavior

When the mass of a bridge may be assumed to be concentrated at a single point, and a single displacement describes the motion of that point, the bridge may be modeled as a single degree-of-freedom system (SDOF). For example, the dynamic behavior in the span-wise direction of the 2-span bridge shown in Figure 5-1a may be represented by the single displacement,  $u$ , of the superstructure. This is possible because the superstructure is effectively rigid in this direction and all points along its length have the same displacement,  $u$ , including the center of mass.

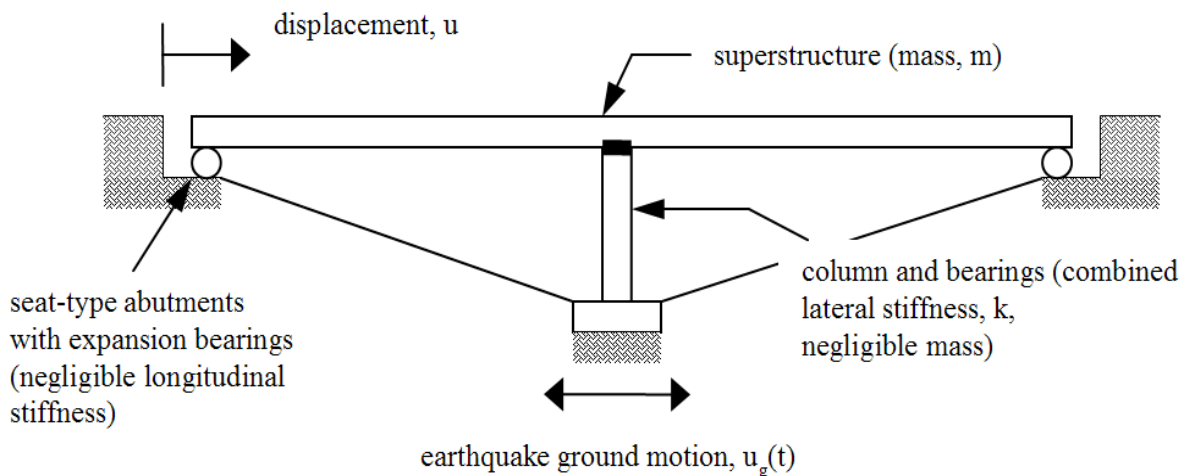


Figure 5-1a Two-Span Bridge Subject to Longitudinal Earthquake Ground Motion

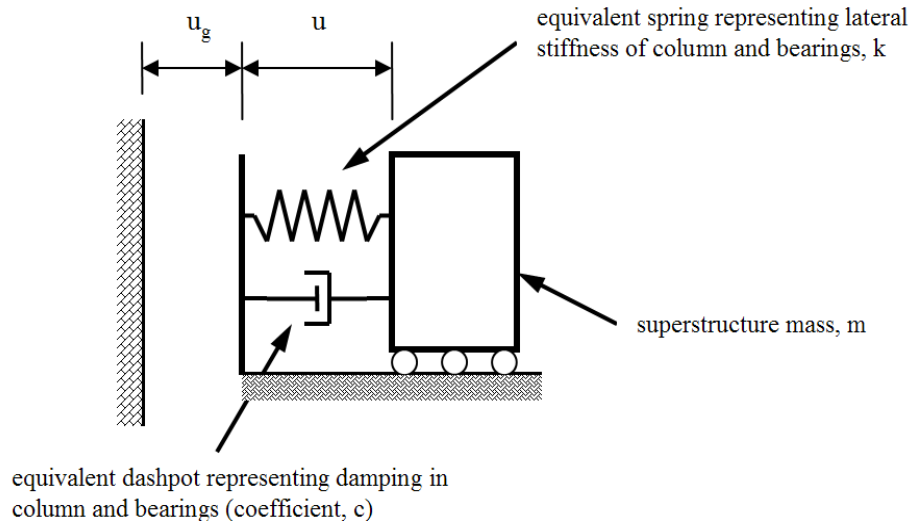


Figure 5-1b Single-Degree-of-Freedom Spring-Mass Model for Bridge in Longitudinal Direction

Single-degree-of-freedom systems may be represented by simple spring-mass models (with or without dashpots to represent damping) as shown in Figure 5-1b. The inertial, spring, and damping forces that act on the mass must be in equilibrium at all times and, as explained in Section 4.2.2.1, this leads to the following equation of equilibrium for a bridge that acts as a SDOF:

$$m\ddot{u} + c\dot{u} + ku = -m\ddot{u}_g \quad 5-1$$

- where
- $m$  = total mass of bridge concentrated at a single point
  - $k$  = combined lateral stiffness of bearings, piers, and foundations supporting mass
  - $c$  = damping constant, assuming bridge is viscously damped
  - $\ddot{u}_g$  = time history of earthquake ground acceleration
  - $\ddot{u}$  = acceleration of the mass relative to the ground
  - $\dot{u}$  = velocity of the mass relative to the ground, and
  - $u$  = displacement of the mass relative to the ground.

Closed form solutions to this equation are available in many text books on structural dynamics, provided the bridge remains elastic and the ground motion is either harmonic, periodic, a single pulse, or a step or ramp function. Since earthquake ground motions are none of these, but arbitrary in nature, a solution to Equation 5-1 is obtained using one or more numerical integration techniques that step through time.

As a first step towards solving Equation 5-1, it is useful to begin with the case of free vibration of an undamped bridge. In this case the equation of equilibrium (also called the equation of motion) is given by

$$m\ddot{u} + ku = 0 \quad 5-2$$

This equation has a closed-form solution since the right-hand side is now zero, and is given by:

$$u = u_0 \cos \omega t + \left( \frac{\dot{u}_0}{\omega} \right) \sin \omega t \quad 5-3$$

where  $u_0$  = initial displacement

$\dot{u}_0$  = initial velocity, and

$\omega$  = natural frequency of vibration (rads/sec).

Substitution into Equation 5-2 and subsequent simplification gives:

$$\omega^2 = \frac{k}{m} \quad 5-4$$

from which

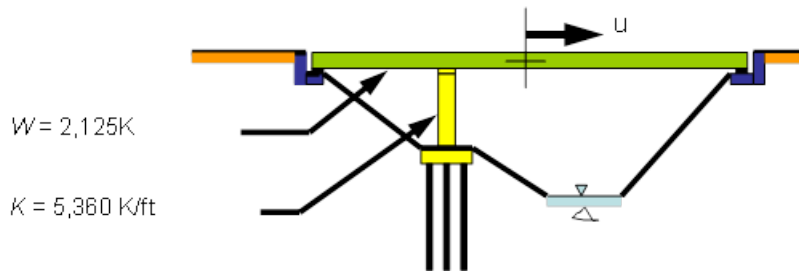
$$T = \frac{2\pi}{\omega} = 2\pi \sqrt{\left( \frac{m}{k} \right)} \quad 5-5$$

where  $T$  = period of undamped bridge (sec).

Example 5-1 illustrates the calculation of the period of a bridge using Equation 5-5. Equation 5-1 may also be used to study free vibration in damped systems, again by setting the right hand side to zero. Example 5-2 gives the solution for this situation and typical results for various amounts of damping.

## EXAMPLE 5-1 - PERIOD OF VIBRATION

The superstructure of a 2-span bridge weighs 2,125K. The longitudinal stiffness of the single column pier is 5,360 K/ft. Calculate the period of the bridge in the longitudinal direction.



$$T = 2\pi \sqrt{\frac{m}{k}} = 2\pi \sqrt{\frac{W}{gk}} = 2\pi \sqrt{\frac{2,125}{32.2(5,360)}} = \underline{0.70 \text{ sec}}$$

Note that the mass of the superstructure is calculated from its weight; i.e.  $m = W/g$ , and that, in this example, the stiffness of the bearings at the seat-type abutments are assumed to be negligible compared to that of the pier.

Returning to the solution of Equation 5-1, several time-stepping methods have been developed for the numerical integration of this second order differential equation that has an arbitrary load function ( $\ddot{u}_g$ ) on the right hand side of the equation. These include the superposition method and the finite difference method, but the one that is most commonly used in seismic applications is Newmark's Method. The only assumption made in this method is the way the relative acceleration ( $\ddot{u}_g$ ) varies within a time step,  $\Delta t$ . It can be applied to both linear and nonlinear systems, and is particularly useful when a time history of response is required, and not just the maximum value. It is described further in Sections 5.2.5 and 5.3.2.

### 5.1.1.2 Multi-Degree-of-Freedom Behavior

In most bridges the largest concentration of mass is in the superstructure, but even then it is distributed along the length of the bridge and not lumped at say the mid-span point. In the SDOF model described above, all of the mass is assumed to be concentrated at one point. Clearly a better representation of the

## EXAMPLE 5-2 - DAMPED FREE VIBRATION

For damped free vibration  $\ddot{u}_g = 0$  and  $c \neq 0$

Equation of motion 5-1 becomes

$$m\ddot{u} + c\dot{u} + ku = 0$$

Solution is:

$$u = Ae^{-h\omega t} \cos(\omega_D t - \phi)$$

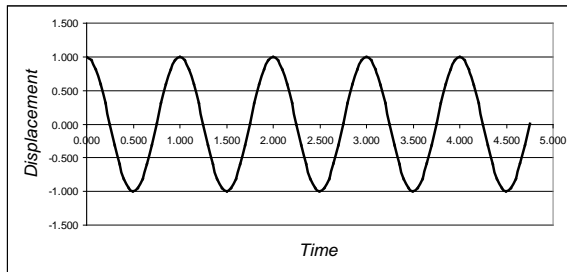
where

$$A = \frac{u_0}{\sqrt{1-h^2}} \quad h = \frac{c}{2\sqrt{km}} \quad \sin \phi = h$$

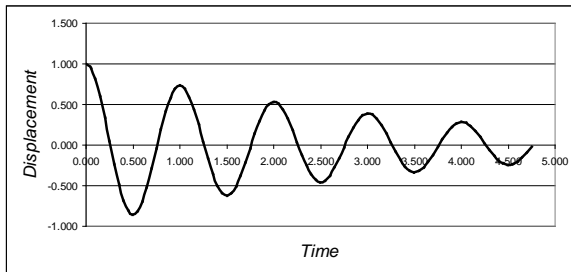
and damped angular frequency =

$$\omega_D = \omega\sqrt{1-h^2}$$

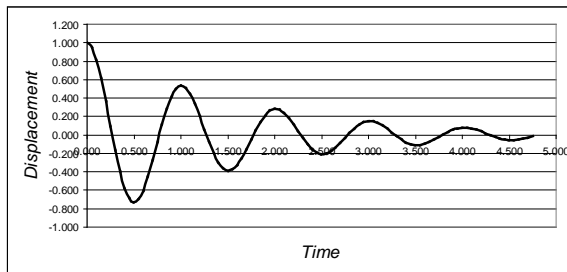
Time histories of displacement ( $u$ ) are shown below for a single degree-of-freedom system with undamped natural period ( $T$ ) = 1.00 sec, released from an initial displacement ( $u_0$ ) = 1.0 inch, for various damping ratios ( $h$ ). Observe that a small amount of damping can make a significant reduction in displacement from cycle-to-cycle. For example, when  $h = 0.10$  (10%), each successive cycle is about one-half of the previous cycle. Also note that when  $h = 1.0$  (100%), the system no longer oscillates but returns to zero displacement without vibration. Such a system is said to be *critically damped*.



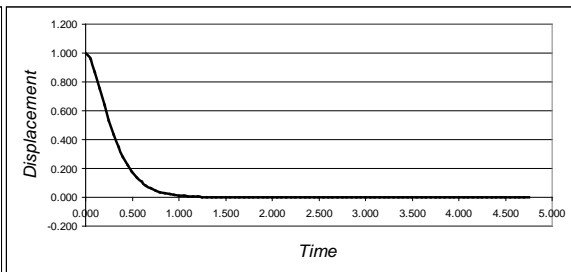
Damping ratio  $h = 0.0$



Damping ratio  $h = 0.05$



Damping ratio  $h = 0.10$



Damping ratio  $h = 1.0$

mass would be obtained if it were distributed to a number of points along the length, say to the quarter points of each span, as shown in Figure 5-2. Each point is assigned a displacement degree of freedom and this model is therefore a multiple degree-of-freedom system (MDOF). For each degree of freedom, an equation of equilibrium can be developed like that in Equation 5-1, and these can be assembled into a single matrix equation as follows:

$$M\ddot{u} + C\dot{u} + Ku = -M1\ddot{u}_g \quad 5-6$$

- where  $M$  = mass matrix of bridge  
 $C$  = damping matrix of bridge  
 $K$  = stiffness matrix of bridge  
 $1$  = influence vector which relates the displacement degrees-of-freedom in  $u$  to those in the ground motion,  $u_g$ , and in simple bridge models is a unit vector and  $= \langle 1.0 \ 1.0 \ 1.0 \ \dots \ 1.0 \rangle^T$   
 $\ddot{u}_g$  = time history of ground acceleration (time varying scalar)  
 $\ddot{u}$  = acceleration of the mass relative to the ground (time varying vector)  
 $\dot{u}$  = velocity of the mass relative to the ground (time varying vector), and  
 $u$  = displacement of the mass relative to the ground (time varying vector).

If there are  $N$  degrees of freedom, all of the matrices in Equations 5-6 are  $N \times N$  in size and the vectors are  $N \times 1$ .

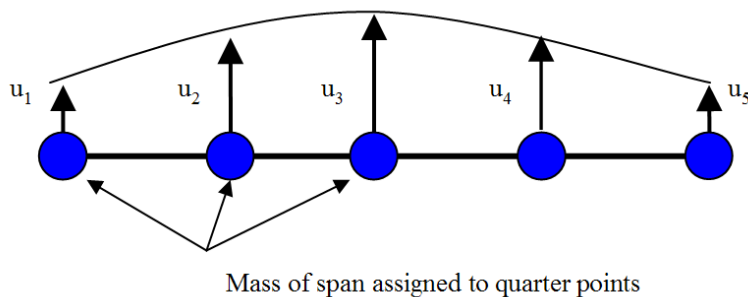


Figure 5-2 Plan View of a Span with Mass Assigned to Quarter Points and Corresponding Transverse Displacement Degrees-of-Freedom

Closed form solutions to this equation are available in many text books on structural dynamics, provided the system remains elastic and the ground motion is either harmonic, periodic, a single pulse, or a step or ramp function. Since earthquake ground motions are none of these, but arbitrary in nature, a solution to Equation 5-6 must be obtained using numerical integration techniques that step through time.

As a first step towards solving Equation 5-6, it is useful to begin with the case of free vibration of an undamped bridge. In this case, the equation of equilibrium (also called the equation of motion) is given by

$$M\ddot{u} + Ku = 0 \quad 5-7$$

This equation has a closed-form solution since the right hand side is now a vector of zeroes, and is given by:

$$u = u_0 \cos \omega t + \left( \frac{\dot{u}_0}{\omega} \right) \sin \omega t \quad 5-8$$

where  $u_0$  = vector of initial displacements

$\dot{u}_0$  = vector of initial velocities, and

$\omega$  = natural frequency of vibration (rads/sec).

Substitution into Equation 5-7 and subsequent simplification gives:

$$[K - \omega^2 M]u = 0 \quad 5-9$$

Equation 5-9 represents a classical eigenvalue problem, where there are more unknowns ( $N+1$ ) than equations to solve for them ( $N$ ). A solution is only possible if one of the unknowns (either  $\omega$  or one of the displacement degrees of freedom,  $u_i$ ) is given a value, e.g., let  $u_1 = 1.0$ . Then the solution can proceed for the remaining degrees of freedom. As a result there will be  $N$  values for  $\omega^2$ , at which equilibrium can be satisfied, and  $N$  corresponding sets of displacements,  $u$ . Each solution is called a mode of vibration with a distinct frequency  $\omega_i$  ( $i = 1, N$ ).

Since one of the displacement degrees of freedom has been given a predetermined value (in this case  $u_1 = 1.0$ ), the values of the other displacement degrees of freedoms are relative to this value, and it is said the mode has been 'normalized' (to  $u_1$  in this case). Furthermore, the symbol  $\phi$  is used instead of  $u$  to

recognize the fact that the solution for displacement is only a relative one. If  $\omega^2$  is replaced by  $\lambda$ , the equations of equilibrium for mode  $i$  can be written as:

$$[K - \lambda_i M] \phi_i = 0 \quad 5-10$$

Several numerical methods are available to solve this equation and calculate the eigenvalue ( $\lambda_i$ ) and eigenvector ( $\phi_i$ ). Once all of the  $\phi_i$  have been found they may be assembled into a single matrix, called the modal array ( $\Phi$ ), as follows:

$$\Phi = [\phi_1 \ \phi_2 \ \phi_3 \ \dots \ \phi_i \ \dots \ \phi_N] \quad 5-11$$

It follows that the modal periods ( $T_i$ ) are given by:

$$T_i = \frac{2\pi}{\omega_i} = \frac{2\pi}{\sqrt{\lambda_i}} \quad 5-12$$

Example 5-3 illustrates the calculation of the transverse modal frequencies and mode shapes for a bridge with 2 degrees-of-freedom using Equation 5-10 and 5-12.

Returning to the solution of Equation 5-6, several time-stepping methods are available for the numerical integration of this second order differential equation. But since this equation represents  $N$  coupled equations that need to be satisfied simultaneously at all points in time, these methods are computationally intensive. This effort is usually only warranted for the linear analysis of bridges with non-classical damping, or the nonlinear analysis of bridges that are of critical importance as described in Section 5.3.2. The preferred approach to solving Equation 5-6 is to transform the coordinate system for these equations, to a system where the equations are uncoupled from each other and can be solved independently of each other. The procedure is as follows:

## EXAMPLE 5-3 - MODES OF VIBRATION

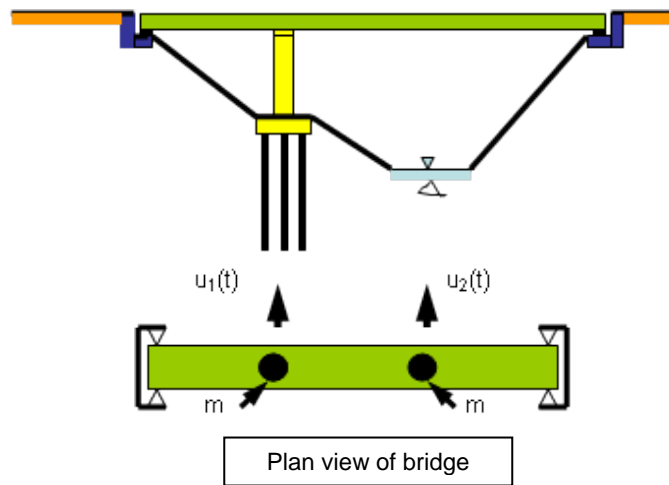
The superstructure of a 2-span bridge weighs 2,125 K. Assuming one third of this weight is located at each of the third-points along the span, calculate the periods and shapes of the transverse modes of vibration.

For this 2-dof model the lateral stiffness and mass matrices have been determined to be

$$\mathbf{K} = \begin{bmatrix} 13,560 & -4,100 \\ -4,100 & 8,200 \end{bmatrix} \quad \text{K/ft}$$

$$\mathbf{M} = \begin{bmatrix} 22.0 & 0 \\ 0 & 22.0 \end{bmatrix} \quad \text{Ksec}^2/\text{ft},$$

since 
$$m = \frac{W/g}{3} = \frac{2125/32.2}{3} = 22.0$$



Solution of  
gives

$$[\mathbf{K} - \lambda\mathbf{M}]\boldsymbol{\phi} = \mathbf{0}$$

$$\lambda = \begin{Bmatrix} \lambda_1 \\ \lambda_2 \end{Bmatrix} = \begin{Bmatrix} 272.05 \\ 717.60 \end{Bmatrix}$$

and therefore

$$\omega_1 = \sqrt{\lambda_1} = \sqrt{272.05} = 16.49 \quad \text{radians/sec}$$

$$\omega_2 = \sqrt{\lambda_2} = \sqrt{717.60} = 26.79$$

from which

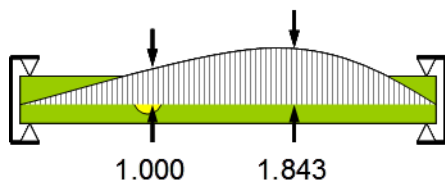
$$T_1 = \frac{2\pi}{\omega_1} = \frac{2\pi}{16.49} = 0.38 \quad \text{Period first mode (sec)}$$

$$T_2 = \frac{2\pi}{\omega_2} = \frac{2\pi}{26.79} = 0.23 \quad \text{Period second mode (sec)}$$

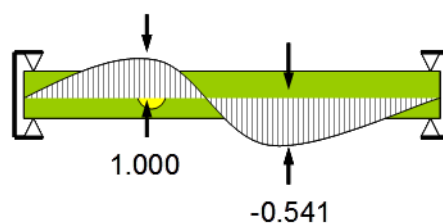
Solution also gives  
mode shapes

$$\boldsymbol{\Phi} = [\boldsymbol{\phi}_1 \quad \boldsymbol{\phi}_2] = \begin{bmatrix} 1.000 & 1.000 \\ 1.843 & -0.541 \end{bmatrix}$$

First Mode,  $T_1 = 0.38$  sec



Second Mode,  $T_2 = 0.23$  sec



Let

$$u = \phi_1 q_1 + \phi_2 q_2 + \phi_3 q_3 \dots + \phi_i q_i \dots + \phi_N q_N = \Phi q \quad 5-13$$

where  $q = \langle q_1 \ q_2 \ q_3 \ \dots \ q_i \ \dots \ q_N \rangle^T$ , and

$q_i$  is defined as a modal coordinate that varies with time and has units of displacement.

Equation 5-13 implies that any displaced shape  $u$  of a MDOF system can be represented by a linear combination of its mode shapes, provided each mode is scaled by a factor called a modal coordinate ( $q_i$ ).

Example 5-4 illustrates this process for a 2-span bridge displaced to a given transverse shape.

Substitute for  $u$  in Equation 5-6 and pre-multiply both sides of equation by  $\Phi^T$  to obtain the following:

$$\Phi^T M \Phi \ddot{q} + \Phi^T C \Phi \dot{q} + \Phi^T K \Phi q = -\Phi^T M 1 \ddot{u}_g \quad 5-14$$

Equation 5-14 can be written as:

$$\underline{M} \ddot{q} + \underline{C} \dot{q} + \underline{K} q = -\underline{L} \ddot{u}_g \quad 5-15$$

where  $\underline{M} = \Phi^T M \Phi$ ,  $\underline{C} = \Phi^T C \Phi$ ,  $\underline{K} = \Phi^T K \Phi$ , and  $\underline{L} = \Phi^T M 1$ .

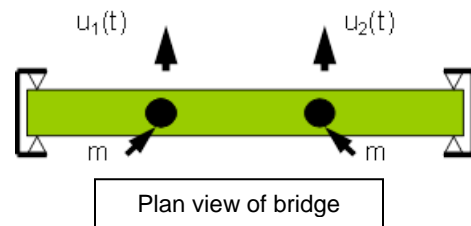
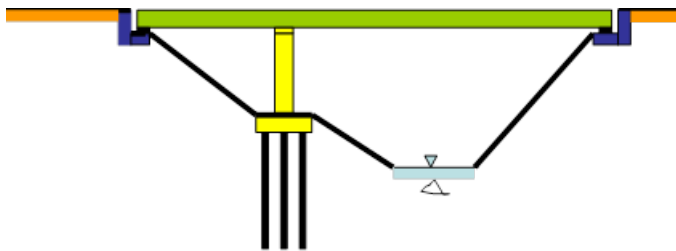
Due to the mass and stiffness orthogonality conditions (Chopra 2012) of the mode shapes  $\phi_i$ ,  $\underline{M}$  and  $\underline{K}$  are diagonal matrices. If the damping in the bridge can be represented by Rayleigh damping, i.e. if it is classically damped,  $\underline{C}$  is also a diagonal matrix. Therefore Equation 5-15 represents a set of  $N$  uncoupled equations that can be solved independently of each other. The  $i^{\text{th}}$  equation in this set is as follows:

$$\underline{M}_{ii} \ddot{q}_i + \underline{C}_{ii} \dot{q}_i + \underline{K}_{ii} q_i = -\underline{L}_i \ddot{u}_g \quad 5-16$$

where  $\underline{M}_{ii} = \phi_i^T M \phi_i$ ,  $\underline{C}_{ii} = \phi_i^T C \phi_i$ ,  $\underline{K}_{ii} = \phi_i^T K \phi_i$ , and  $\underline{L}_i = \phi_i^T M 1$ .

## EXAMPLE 5-4 - MODAL COORDINATES

The superstructure of the 2-span bridge in Example 5-3 is displaced into the shape shown in the plan view below. Decompose this shape into its modal contributions, i.e., find the modal coordinates corresponding to this shape.



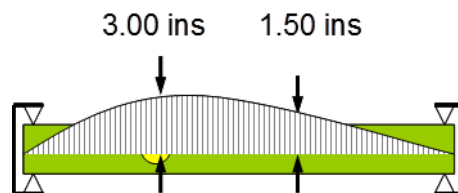
Imposed shape is  $u = \begin{Bmatrix} 3.00 \\ 1.50 \end{Bmatrix}$  as shown at right:

Solve Equation 5-13 for modal coordinates,  $q$

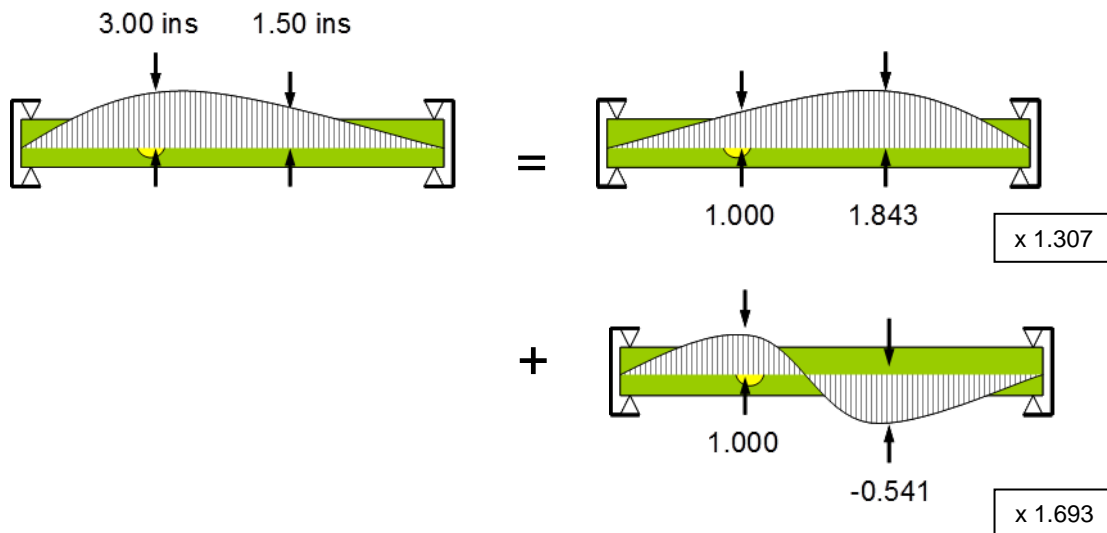
i.e., solve  $u = \Phi q$

where  $u$  is as above and  $\Phi = [\phi_1 \quad \phi_2] = \begin{bmatrix} 1.000 & 1.000 \\ 1.843 & -0.541 \end{bmatrix}$

to give  $q = \begin{Bmatrix} 1.307 \\ 1.693 \end{Bmatrix}$ , modal coordinates for given shape



In summary the given shape is equal to 1.307 x (mode shape No.1) + 1.693 x (mode shape no. 2), as below:



Since the damping ratio,  $h_i$ , for mode  $i = \underline{C}_{ii} / 2\sqrt{(\underline{K}_{ii} \underline{M}_{ii})}$ , and  $\omega_i^2 = \underline{K}_{ii} / \underline{M}_{ii}$ , Equation 5-16 can be written as:

$$\ddot{q}_i + 2h_i\omega_i\dot{q}_i + \omega_i^2q_i = -\left(\frac{L_i}{\underline{M}_{ii}}\right)\ddot{u}_g = -\Gamma_i\ddot{u}_g \quad 5-17$$

where  $\Gamma_i$  is a scalar and called the modal participation factor for mode  $i$  and is given by:

$$\Gamma_i = \frac{L_i}{\underline{M}_{ii}} = \frac{\phi_i^T M \mathbf{1}}{\phi_i^T M \phi_i} \quad 5-18$$

Equation 5-17 is solved for  $q_i(t)$  using one of the time stepping numerical integration procedures noted above for single degree of freedom systems. The solution for  $u(t)$  is then obtained using Equation 5-13.

### 5.1.2 Elastic and Nonlinear Behavior

Under service loads, bridge members are designed to stay within their elastic range, but this is not always economically feasible during extreme loads such as a medium-to-large earthquake. As discussed in Chapter 4, yielding is expected during a large earthquake with consequential damage. But this damage is considered acceptable provided it does not cause collapse of a span and is readily accessible (i.e. above ground). Column yield is preferred to yielding in the superstructure and columns are therefore detailed to sustain large plastic deformations without rupture or buckling of the reinforcing steel. Yield followed by plastic deformation in a so-called plastic hinge, is the main source of nonlinear behavior in a bridge during an earthquake. Other sources of nonlinearity include inelastic soil properties and large displacements that occur just prior to, and during, collapse.

For many years the most common way to analyze a nonlinear bridge was to solve an equivalent linear problem using equivalent linearized properties. In this way, elastic methods of analysis could still be used to estimate nonlinear response, but the degree of conservatism, or lack of conservatism, in the results was not known. However with the development of explicit nonlinear static and dynamic methods (pushover and time history methods respectively) more rigorous methods are now available and should be used wherever possible, particularly in high seismic areas.

With some of the software tools available today, analysis for large displacement effects is feasible but not done routinely. It is only necessary in very special circumstances, and should only be carried out by those with expertise in modeling and interpretation of results.

### **5.1.3 Summary and Limitations of Analysis Methods**

Six methods of analysis are described in this chapter. These methods are summarized in Table 5-1 along with their applications and limitations.

## **5.2 ELASTIC ANALYSIS METHODS**

### **5.2.1 General**

Four methods of analysis are briefly described in this section. Each assumes that the structure remains elastic under load and the displacements are small. These four methods are:

- Uniform Load Method (also known as Equivalent Static Analysis)
- Single Mode Spectral Method (also known as Equivalent Static Analysis)
- Multi-Mode Spectral Method (also known as Elastic Dynamic Analysis)
- Time History Method

The uniform load and single mode methods are essentially equivalent static methods of analysis that use a uniform lateral load to approximate the effect of seismic loads but to different levels of rigor. These methods are suitable for regular bridges that respond principally in their fundamental mode of vibration, which are generally those satisfying the requirements of Table 5-2. For structures not satisfying these requirements, the multi-mode method of analysis should be used, or alternatively an elastic time history method.

### **5.2.2 Uniform Load Method**

The uniform load method (AASHTO 2002, 2013, 2014) is based on the fundamental mode of vibration in the longitudinal (or transverse) direction, using a single spring-mass oscillator to represent the dynamic properties of the bridge in this direction. The stiffness of this equivalent spring is calculated using the maximum displacement that occurs when an arbitrary uniform lateral load is applied to the bridge.

**TABLE 5-1 METHODS OF ANALYSIS**

Method	Single/ Multiple Mode	Elastic/ Nonlinear	Remarks	Applications / limitations
Uniform Load Method	Single	Elastic	Equivalent static method of analysis; modal period derived from stiffness of bridge under uniform lateral load; uses response spectrum to define earthquake loads; maximum forces and displacements determined for use in design.	Applicable to regular conventional bridges dominated by first mode (see Table 5-2); method known to overestimate abutment reactions; good back-of-the-envelope check on more rigorous methods; elastic response.
Single Mode Spectral Analysis Method	Single	Elastic	Equivalent static method of analysis; modal period derived from energy principles; uses response spectrum to define earthquake loads; maximum forces and displacements determined for use in design; also known as the $\alpha \beta \gamma$ method.	Applicable to regular conventional bridges that respond primarily in a single mode (see Table 5-2); quick check on more rigorous MDOF methods; elastic response.
Multi Mode Spectral Analysis Method	Multiple (selected modes)	Elastic	Multiple mode shapes and frequencies calculated; maximum modal response to ground motion obtained for a selected number of modes using response spectrum to define earthquake loads; combination of modal responses by CQC or SRSS methods to obtain design displacements and forces.	Applicable to irregular conventional bridges; does not need ground motion time history; number of selected modes should capture at least 90% of total mass of bridge; major limitation is elastic response but gives good results for bridges that remain 'essentially' elastic such as those in low-to- moderate seismic zones.
Elastic Time History	Multiple (selected modes)	Elastic	Most rigorous of elastic methods; uses time history to define earthquake loads; displacement and force time histories determined for use in design.	Applicable to irregular and un-conventional bridges responding essentially elastically; time histories need to be defined and may need scaling; major limitation is elastic response.
Nonlinear Static Procedure	Single Degree-of-Freedom	Nonlinear materials	Explicitly includes nonlinear behavior in determination of bridge capacity (pushover analysis); uses response spectrum to define earthquake loads and elastic methods to obtain displacement demand. Variations include (1) direct pushover method , and (2) iterative capacity / demand spectrum method.	Applicable to regular conventional bridges that respond primarily in a single mode (see Table 5-2). Method does not account for changes in dynamic response as structure softens. Effects of higher modes are excluded.
Nonlinear Dynamic Procedure	Multiple Degrees-of-Freedom	Nonlinear materials	Most rigorous of the nonlinear methods; uses a time history to define earthquake loads; displacement and force time histories are determined for use in design. Automatically accounts for higher mode effects and shifts in inertial load patterns as structural softening occurs.	Applicable to a wide range of bridges including irregular and un-conventional bridges; time histories need to be defined and may need scaling; solution is iterative and may be time consuming for large bridges. More efficient solution techniques are available for bridges with few nonlinear members. Results can be highly sensitive to small changes in load and material properties. Third party peer review is often required.

**TABLE 5-2 RESTRICTIONS ON THE APPLICATION OF THE UNIFORM LOAD AND SINGLE MODE SPECTRAL METHODS (AASHTO, 2013, AASHTO 2014)**

Parameter	Value				
Number of spans	2	3	4	5	6
Maximum subtended angle for a curved bridge (Note that this limit is 30 degrees in the <i>Guide Specifications for LRFD Seismic Bridge Design.</i> )	90°	90°	90°	90°	90°
Maximum span length ratio from span-to-span	3	2	2	1.5	1.5
Maximum pier stiffness ratio from span-to-span, excluding abutments	—	4	4	3	2

The spectral acceleration, at the modal period  $T$ , is found from a site-specific acceleration response spectrum (Section 2.6) or from the spectrum in Figure 2-9 (Section 2.5). It is then used to calculate an equivalent uniform load from which design forces are determined. This method may be applied in either the longitudinal or transverse direction.

While all displacements and most member forces are calculated with satisfactory accuracy, the method is known to overestimate the transverse shears at the abutments by up to 100 percent. If such conservatism is undesirable, but a single mode representation is appropriate, then the single mode spectral analysis method (Section 5.2.3) is recommended.

The steps in the uniform load method are as below. An example of the method is given in Example 5-5.

Step 1: Calculate the static displacements  $V_s(x)$  due to an assumed uniform load,  $p_0$ . The uniform loading  $p_0$  is applied over the length of the bridge; it has the dimensions of force/unit length, and usually set equal to 1.0. The static displacement  $V_s(x)$  has the dimension of length.

Step 2: Calculate the lateral stiffness of the bridge,  $K$ , and total weight,  $W$ , from the following expressions:

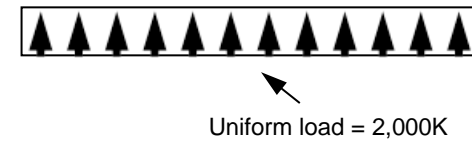
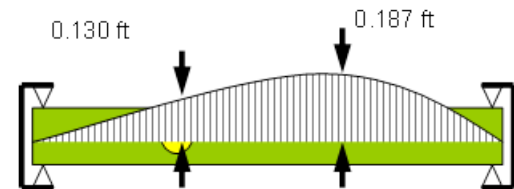
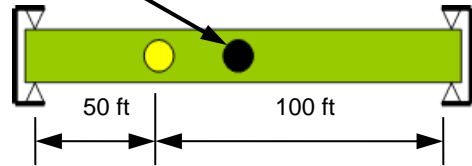
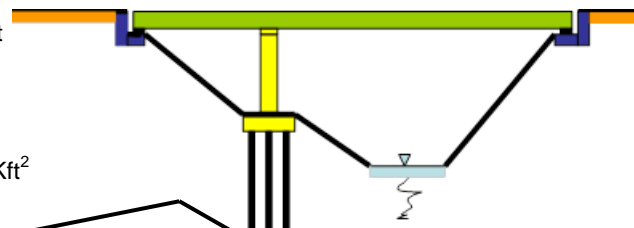
$$K = \frac{p_0 L}{V_{s, \max}} \quad 5-19$$

## EXAMPLE 5-5 - UNIFORM LOAD METHOD

Use the Uniform Load Method to determine the maximum shear in the column of the bridge at the right if subjected to the El Centro Earthquake (1940) in the transverse direction. Assume 2% damping.

Total bridge weight = 2,125 K  
 In-plane flexural rigidity of superstructure =  $126 \times 10^6$  Kft<sup>2</sup>  
 Lateral stiffness of column = 8,077 K/ft

Total mass of bridge, assumed lumped at midpoint =  $2125 / g$   
 $= 2125 / 32.2$   
 $= 66 \text{ K sec}^2/\text{ft}$



**Step 1.** Apply arbitrary uniform transverse load to bridge,  $P_0 = 2,000 \text{ K}$  and use statics to calculate the deflected shape and column shear as follows: maximum deflection,  $V_s(x)_{\max} = 0.187 \text{ ft}$ , and column shear =  $8,077 \times 0.130 = 1,050 \text{ K}$ .

Note  $p_0 = P_0/L = 2,000/150 = 13.33 \text{ K/ft}$  in this case.

**Step 2.** Calculate transverse stiffness of bridge,  $K_T$  from Equation 5-19:

$$K_T = \frac{P_0}{V_s(x)_{\max}} = \frac{2000}{0.187} = 10,695 \text{ K / ft}$$

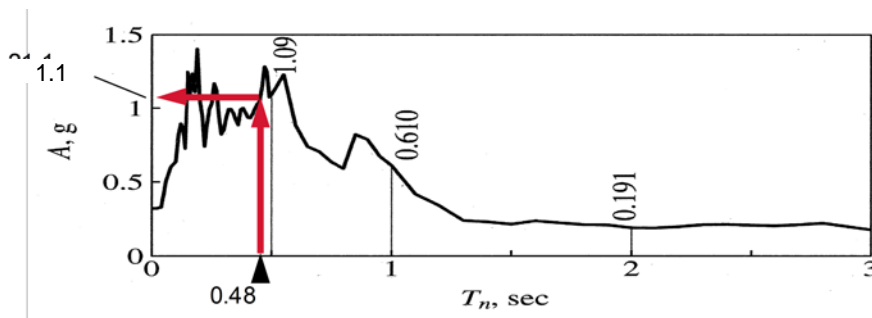
**Step 3.** Calculate transverse period,  $T_T$ , from Equation 5-21:

$$T_T = 2\pi \sqrt{\frac{W}{gK_T}} = 2\pi \sqrt{\frac{2,125}{32.2(10,695)}} = 0.48 \text{ s}$$

**Step 4.** Calculate equivalent static load,  $p_e$  from Equation 5-22:

$$p_e = \frac{C_s W}{L} = \frac{1.1(2,125)}{150} = 15.58 \text{ K / ft}$$

where  $C_s = A/g = 1.1$  from 2%-damped El Centro Spectrum at period,  $T = 0.48 \text{ s}$



**Step 5.** Scale results of static analysis (Step 1) by  $p_e/p_0 = 15.58/13.33 = 1.168$ , and obtain:

Maximum displacement =  $1.168 \times 0.187 = 0.218 \text{ ft}$   
 Maximum column shear =  $1.168 \times 1,050 = 1,226 \text{ K}$ , and  
 Total base shear =  $1.168 \times 2,000 = 2,336 \text{ K}$

$$W = \int_0^L w(x)dx \quad 5-20$$

where  $L$  = total length of the bridge,  
 $V_{s, max}$  = maximum value of  $V_s(x)$ , and  
 $w(x)$  = unfactored dead load of the bridge superstructure and tributary substructure.

The weight should also take into account the participating mass of structural elements such as columns, pier caps, and abutments. Note that live load should not be included in the calculation of period, but should be considered in the gravity load analyses that are combined with the earthquake analyses in the Extreme Event I Load Combination (Table 8-4). The live load to be considered ( $\gamma_{EQ}$  in Table 8-4) is usually taken as 50% of the design live load, reflecting the unlikely occurrence of the bridge being fully loaded at the time of the design earthquake.

Step 3: Calculate the period of the bridge,  $T_m$ , using the expression:

$$T_m = 2\pi \sqrt{\frac{W}{gK}} \quad 5-21$$

where  $g$  = acceleration due to gravity.

Step 4: Calculate the equivalent static earthquake loading,  $p_e$ , from the expression:

$$p_e = \frac{C_s W}{L} \quad 5-22$$

where  $C_s = S_a / g$   
 $S_a$  = spectral acceleration at period  $T$ , from a site-specific response spectrum, and  
 $p_e$  = equivalent uniform static seismic loading per unit length of bridge applied to represent the primary mode of vibration.

If a site-specific spectrum is not available,  $C_s$  may be obtained from Figure 2-9.

Step 5: Calculate the displacements and member forces for use in evaluation either by applying  $p_e$  to the structure and performing a second static analysis, or by scaling the results of Step 1 by the ratio  $p_e / p_o$ .

### 5.2.3 Single-Mode Spectral Analysis Method

The single-mode method of spectral analysis (AASHTO, 2002, 2013, 2014) is based on the fundamental mode of vibration in either the longitudinal or transverse direction. This mode shape is found by applying a uniform horizontal load to the structure and calculating the corresponding deformed shape. The modal period is then calculated by equating the maximum potential and kinetic energies associated with this approximate mode shape. The amplitude of the displaced shape is found from a static analysis of the bridge for equivalent loads calculated from a site-specific acceleration response spectrum, or the elastic seismic response coefficient,  $C_{sm}$ , given in Figure 2-9. This amplitude is then used to determine force effects.

The single-mode method, as described in the following steps, may be used either in the longitudinal or transverse direction. An example of this method is given in Example 5-6. Other examples are to be found in ATC (1981) and AASHTO (1983).

Step 1: Calculate the static displacements  $v_s(x)$  due to a uniform loading  $p_o$ , as shown in Figure 5-3.

Step 2: Calculate factors  $\alpha$ ,  $\beta$ , and  $\gamma$  as follows:

$$\alpha = \int v_s(x) dx \quad 5-23$$

$$\beta = \int w(x) v_s(x) dx \quad 5-24$$

$$\gamma = \int w(x) v_s^2(x) dx \quad 5-25$$

where  $v_s(x)$  = displacements corresponding to  $p_o$

$p_o$  = arbitrary uniform load, usually taken to be 1.0 K/ft, and

$w(x)$  = dead load of the bridge superstructure and tributary substructure

## EXAMPLE 5-6 - SINGLE MODE METHOD

Repeat Example 5-5 using the Single Mode Spectral Analysis Method to determine the maximum shear in the column of the bridge at the right if subjected to the El Centro Earthquake (1940) in the transverse direction. Assume 2% damping.

From Example 5-5:

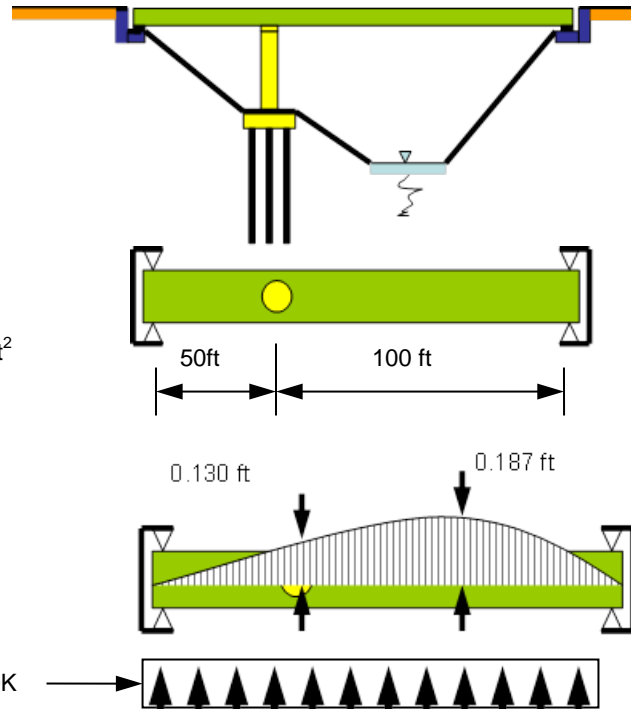
Total weight of bridge = 2,125 K

Total length of bridge = 150 ft

Weight/unit length ( $w$ ) = 2,125/150 = 14.167 K/ft

In-plane flexural rigidity of superstructure =  $126 \times 10^6$  Kft<sup>2</sup>

Lateral stiffness of single column pier,  $k_{pier} = 8,077$  K/ft



**Step 1.** Apply uniform transverse load to bridge,  $P_0 = 2,000$  K and using statics calculate the deflected shape,  $V_s(x)$ . Enter deflections in Column 2 of table below.

Calculate  $p_0 = 2,000/150 = 13.333$  K/ft

Uniform load = 2,000K

**Step 2.** Calculate  $\alpha$ ,  $\beta$ , and  $\gamma$  from Equations 5-23, 5-24, 5-25.

Use trapezoidal rule to evaluate integrals as shown below. Note interval between ordinates is constant at 25 ft.

1	2	3	
Distance along bridge, $x$ (ft)	Deflected shape, $V_s(x)$ from Step 1 (ft)	(Deflections) <sup>2</sup> $V_s(x)^2$ (ft <sup>2</sup> )	
0	0	0	
25	0.0696	0.00484	
50	0.1300	0.01690	
75	0.1830	0.03349	
100	0.1870	0.03497	
125	0.1200	0.01440	
150	0	0	

Trapezoidal Rule gives:

$$\int V_s(x) dx = (0.5 \times 0 + 0.0696 + 0.1300 + 0.1830 + 0.1870 + 0.1200 + 0.5 \times 0) \times 25 = 0.6896 \times 25 = 17.24 \text{ ft}^2$$

$$\int V_s(x)^2 dx = (0.5 \times 0 + 0.00484 + 0.01690 + 0.03349 + 0.03497 + 0.01440 + 0.5 \times 0) \times 25 = 0.1046 \times 25 = 2.615 \text{ ft}^3$$

$$\text{Hence } \alpha = \int V_s(x) dx = 17.24 \text{ ft}^2$$

$$\beta = \int w(x) V_s(x) dx = w \int V_s(x) dx = 14.167 \times 17.24 = 244.24 \text{ Kft}$$

$$\text{and } \gamma = \int w(x) V_s(x)^2 dx = w \int V_s(x)^2 dx = 14.167 \times 2.615 = 37.05 \text{ Kft}^2$$

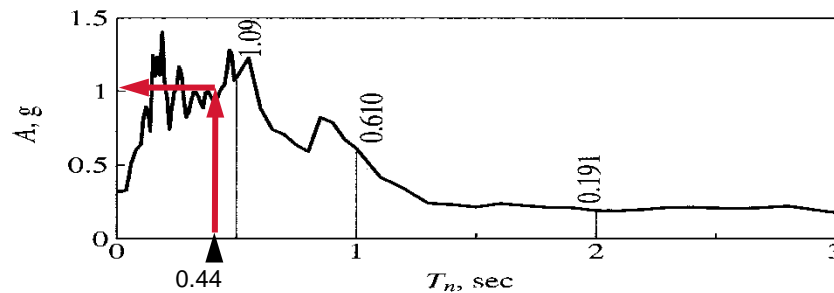
**Step 3.** Calculate Period ,  $T$ , from Equation 5-26:

$$T = 2\pi \sqrt{\frac{\gamma}{p_0 g \alpha}} = 2\pi \sqrt{\frac{37.05}{13.33g17.24}} = 0.444 \text{ sec}$$

**Step 4.** Calculate equivalent static earthquake loading  $p_e(x)$  from Equation 5-27:

$$p_e(x) = \frac{\beta C_{sm}}{\gamma} w(x) v_s(x) = \frac{244.24(1.0)}{37.05} (14.167) v_s(x) = 93.39 v_s(x)$$

where  $C_{sm} = A/g = 1.0$  from the 2%-damped Acceleration Spectrum for the El Centro Earthquake at period  $T = 0.44$  s.



Values for  $p_e(x)$  are given in Column 4 in table below.

1	2	3	4	5
Distance along bridge, x (ft)	Deflected shape, $V_s(x)$ from Step 1 (ft)	(Deflections) <sup>2</sup> $V_s(x)^2$ (ft <sup>2</sup> )	Equivalent static earthquake loading, $p_e(x)$ (K/ft)	Displacements due to equivalent earthquake loading (ft)
0	0	0	0	0
25	0.0696	0.00484	6.50	0.067
50	0.1300	0.01690	12.14	0.133
75	0.1830	0.03349	17.09	0.198
100	0.1870	0.03497	17.46	0.206
125	0.1200	0.01440	11.21	0.131
150	0	0	0	0

Total earthquake load =  $\int p_e(x) dx = 1,610 \text{ K} = \text{Total Base Shear}$

**Step 5.** Calculate displacements and forces in bridge using static analysis for equivalent earthquake loading  $p_e(x)$

- Superstructure displacements are given in Column 5 in above table.
- Maximum column shear =  $k_{\text{pier}} V_s(50) = 8,077 \times 0.133 = 1,074 \text{ K}$

Results are compared against those from Uniform Load Method in table below.

	Uniform Load Method Ex 5-5	Single Mode Method Ex 5-6
Period - Transverse (sec)	0.48	0.44
Maximum Displacement (ft)	0.218	0.206
Maximum Column Shear (K)	1,226	1,074
Total Base Shear (K)	2,336	1,610

The computed factors,  $\alpha$ ,  $\beta$ , and  $\gamma$  have dimensions of  $L^2$ , FL and  $FL^2$ , respectively.

Step 3: Calculate the period of the bridge as follows:

$$T_m = 2\pi \sqrt{\frac{\gamma}{p_o g \alpha}} \quad 5-26$$

where  $g$  = acceleration of gravity.

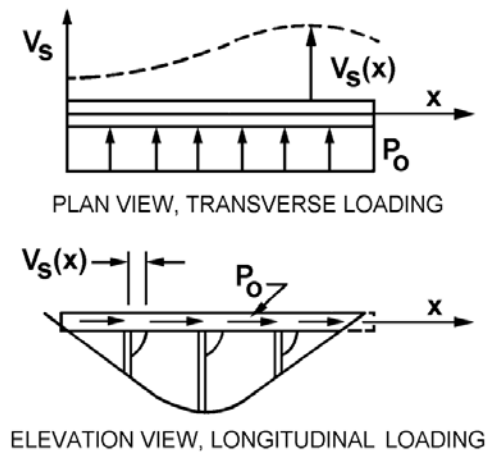


Figure 5-3 Transverse and Longitudinal Loading,  $p_o$ , and Displacement,  $v_s(x)$

Step 4: Calculate the equivalent static earthquake loading  $p_e(x)$  as follows:

$$p_e(x) = \frac{\beta C_{sm}}{\gamma} w(x) v_s(x) \quad 5-27$$

where  $C_{sm} = S_a/g$

$S_a$  = spectral acceleration at period  $T_m$ , from a site-specific response spectrum, and

$p_e(x)$  = intensity of the equivalent static seismic loading applied to represent the primary mode of vibration.

If a site-specific spectrum is not available,  $C_{sm}$  may be obtained from Figure 2-9.

Step 5: Apply loading  $p_e(x)$  to the structure, and determine the resulting member force effects and displacements by static analysis.

#### 5.2.4 Multi-Mode Spectral Analysis Method

The elastic multi-mode spectral analysis method (AASHTO, 2002, 2013, 2014) should be used for bridges in which other modes, in addition to the fundamental mode, participate significantly in the response of the bridge. These modes may be in the same coordinate direction as the fundamental mode, or in one of the other two orthogonal directions, or have coupled response in two or three directions. Measures to determine the number of ‘significant’ modes are discussed in Step 2 below. A three-dimensional model should be used to represent the bridge.

The method has seven basic steps as described below.

Step 1: Calculate the mode shape  $\phi_i$  and natural frequency  $\omega_i$  for  $i^{\text{th}}$  mode of vibration of the bridge using Equation 5-10. Repeat this step for as many modes ( $n$ ) as considered necessary to adequately represent the dynamic response of the bridge. The maximum value for  $n$  will be the total number of degrees of freedom in the structural model used to analyze the bridge ( $N$ ), and ideally  $n = N$ . But this may lead to excessive, and often unnecessary, computational effort. Instead, a lower number is frequently used to reduce the effort but still maintain accuracy. As a guide,  $n$  may be taken as 3 times the number of spans, which means the minimum value for  $n$  is 3. But this number should be checked against the relative size of the modal participation factors as explained in Step 2.

Assemble the modal array ( $\Phi$ ) as defined in Equation 5-11.

Step 2: Calculate the modal participation factor for each mode ( $\Gamma_i$ ) using Equation 5-18. In general, modal participation factors become smaller with increasing mode number and can decrease to the point where the corresponding modes have no significant effect on the response. In such a case the number of modes included in an analysis ( $n$ ) may be reduced without seriously affecting accuracy, as noted in Step 1. But selecting ‘ $n$ ’ based on the magnitude of  $\Gamma_n$  alone is not as simple as taking a value where  $\Gamma_n < 0.01$  say, because there is no guarantee that a higher mode will not have a  $\Gamma_i > 0.01$ . Also, the size of  $\Gamma_n$  depends on the way the mode shapes have been normalized and it is therefore not possible to set a generic cut-off value above which all modal contributions may be ignored. A better way to determine ‘ $n$ ’ is to use the

‘effective modal mass participation factor’ for mode  $i$  to determine the cutoff point. This factor is defined as:

$$R_i = \frac{M_i^*}{M_T} \quad 5-28$$

where  $M_i^*$  = effective modal mass in mode  $i = \Gamma_i^2 [\phi_i^T M \phi_i] = \Gamma_i^2 \underline{M}_{ii}$ , and  
 $M_T$  = total mass of bridge.

It can be shown (Chopra, 2012) that the modal mass  $M_i^*$  is a measure of the contribution of the  $i^{\text{th}}$  mode to the total base shear in the bridge summed over the piers and abutments. It can also be shown that  $M_i^*$  is independent of the way the mode shapes are normalized and the sum of these masses is equal to the total mass of the bridge, i.e.

$$M_1^* + M_2^* + M_3^* \dots + M_i^* \dots + M_N^* = M_T \quad 5-29$$

It follows that the mass participation factors ( $R_i$ ) are also independent of the way the mode shapes are normalized and that they sum to unity. In this case it is now possible to base the number of modes to be used in an analysis ( $n$ ) on the participation of a minimum percentage of the total mass of the bridge in the response, say 90%. That is, choose ‘ $n$ ’ such that:

$$M_1^* + M_2^* + M_3^* \dots + M_n^* > 0.9M_T \quad 5-30$$

This percentage is based on past experience with the analysis of conventional bridges. For non-conventional bridges, or large multi-segment bridges, it may be necessary to raise this figure to 95% to ensure accurate results in all of the critical members and components which tend to be governed by higher mode effects.

Step 3: For each mode, solve for the maximum value of its modal coordinate ( $q_i$ ) using Equation 5-17. As noted in Section 5.1.1.2, this equation may be solved using a numerical integration procedure to obtain a time history for  $q_i(t)$ , and hence  $u(t)$ . But if only the maximum value of  $u$  is required for design purposes, a time history solution is not necessary, and a displacement response spectrum could be used to find  $q_{imax}$

and hence  $u_{max}$ . As noted in Section 2.4.1, displacement response spectra may be found from acceleration spectra using the relationship:

$$S_d = \frac{S_a}{\omega^2} = \frac{T^2 S_a}{4\pi^2} \quad 5-31$$

where  $S_d$  = maximum displacement of a SDOF system with period  $T$  and damping,  $h$  subject to  $\ddot{u}_g(t)$  and

$S_a$  = maximum acceleration of same system subject to  $\ddot{u}_g(t)$

It follows that:

$$q_{i\max} = \Gamma_i S_{di} = \frac{\Gamma_i S_{ai}}{\omega_i^2} = \frac{\Gamma_i T_i^2 S_{ai}}{4\pi^2} \quad 5-32$$

where  $S_{di}$  = maximum displacement of a system with damping  $h_i$  and period  $T_i$  subject to  $\ddot{u}_g(t)$ , and

$S_{ai}$  = maximum acceleration of a system with damping  $h_i$  and period  $T_i$  subject to  $\ddot{u}_g(t)$ .

If the ground motion  $\ddot{u}_g(t)$  and its spectrum  $S_a$  are not available, the design spectrum given in Figure 2-9 may be used. This spectrum is for a 5% damped system and needs to be scaled when the damping ratio  $h_i$  is greater than (or less than) 0.05. This may be done by dividing the spectral ordinates by  $(20h_i)^{0.3}$  for periods greater than  $T_s$ , and by  $(20h_i)^{0.5}$  for periods less than or equal to  $T_s$ , where  $T_s$  is defined in Figure 2-9. This method should not be used to scale the spectrum when the damping ratio exceeds 30%. If a bridge is to be seismically isolated, scaling of the spectrum should only be done for periods greater than 80% of the effective isolated period.

**Step 4:** For each mode, calculate the maximum displacements in the bridge using the definition of a modal coordinate, i.e.:

$$u_{i\max} = \phi_i q_{i\max} \quad 5-33$$

Step 5: For each mode calculate the equivalent set of static external loads ( $f_{si}$ ) necessary to hold the bridge in the shape given by  $u_{imax}$ , using the bridge stiffness matrix,  $K$ , as follows:

$$f_{si} = Ku_{imax} \quad 5-34$$

Calculate the total base shear ( $F_{basei}$ ) for each mode as follows:

$$F_{basei} = 1^T f_{si} = 1^T Ku_{imax} \quad 5-35$$

Step 6: For each mode calculate the internal member forces  $S_i$  (bending moments, shear forces, axial forces) that correspond to the shape given by  $u_{imax}$ , using the member stiffness matrix,  $k$ , and displacement transformation matrix,  $a$ , as follows:

$$S_i = kau_{imax} \quad 5-36$$

Step 7: Calculate design displacements and member forces by combining the modal values obtained in Steps 4, 5 and 6 above. The Complete Quadratic Combination method (Chopra, 2012) is recommended for this purpose especially if there is only one component to be considered in the ground motion. Alternative methods include the square-root-of-the-sum-of-the-squares method (SRSS) which gives good results when the modal periods are well-separated. Design member forces,  $S_{design}$ , by the SRSS method, are as follows:

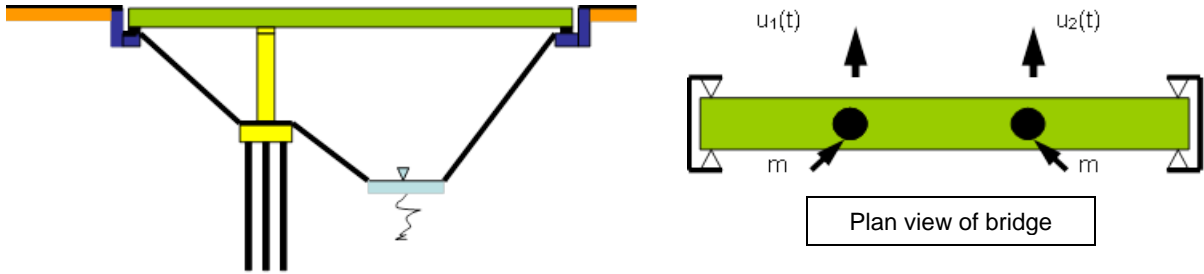
$$S_{design} = \sqrt{(S_1^2 + S_2^2 + S_3^2 + \dots + S_i^2 + \dots + S_N^2)} \quad 5-37$$

Member forces and displacements due to two or three simultaneous components of ground motion should be estimated by the SRSS method. This method assumes these components are independent of each other (i.e., they are uncorrelated), which is an adequate assumption when evaluating a bridge because the spectrum in Figure 2-9 is intended to represent the principal directions of ground motion. This assumption may not be valid for near-fault ground motions, which can exhibit strong correlation between the horizontal components.

An example of the Multimode Spectral Analysis Method is given in Example 5-7.

## EXAMPLE 5-7 -MULTIMODE SPECTRAL ANALYSIS METHOD

Calculate the design displacements of the 2 masses in the superstructure of the 2-span bridge in Example 5-3 and shown below subject to the El Centro Earthquake. i.e., calculate  $u_{1max}$  and  $u_{2max}$ . Assume 2% damping. Combine the modal maxima using the SRSS rule (Equation 5-37)



Summary of Modal and Design Displacements				
	Mode 1	Mode 2	Design Displacements	
Period, $T_i$ (sec)	0.38	0.23	<p style="text-align: center;">Acceleration Spectrum for El Centro Earthquake, 2% damping</p>	
Mode shape, $\phi_i$	1.000 1.834	1.000 -0.541		
Participation Factor, $\Gamma_i$	0.645	0.355		
Effective Modal Mass Ratio, $R_i$	0.918	0.082		
Spectral Acceleration, A	0.9g	1.2g		
Spectral Displ., $D_i = AT_i^2 / 4\pi^2$ (in)	1.27	0.62		
$q_{imax} = \Gamma_i D_i$ (in)	0.82	0.22		
$U_{imax} = \phi_i q_{imax}$ (in)	0.82 1.50	0.22 -0.12		$= \sqrt{[0.82^2 + 0.22^2]} = 0.85$ in $= \sqrt{[1.50^2 + (-0.12)^2]} = 1.51$ in

**Answer:** Design value for  $u_1 = 0.85$  ins and design value for  $u_2 = 1.51$  ins for this earthquake and 2% damping.

**Note:** As seen in these results for displacement, the second mode is not significant, This is consistent with the fact that  $R_1 = 0.918 > 0.90$  which implies only one mode need be considered in the analysis.

### 5.2.5 Time History Method

Elastic time history methods provide displacements and member actions as a function of time, assuming all members remain elastic and no displacement limit is exceeded. These methods are more rigorous than the uniform load and multi-mode spectral methods described above, and may be used for irregular bridges with complex geometries and/or on poor foundations. They do, however, require the development of at least three sets of acceleration time histories for the bridge site and a minimum of three analyses is therefore performed, one for each set. Each set includes three components of the ground motion (two horizontal and one vertical). The maximum response for any single quantity (such as the transverse bending moment at the top of a particular column) from these three analyses, should be used for design. If more than seven sets of ground motions are used, the mean of the responses may be taken for evaluating the demand on the bridge.

In the absence of site-specific ground motions, time histories may be synthetically generated using the response spectrum for the site (Figure 2-9). Procedures for developing these so-called 'spectrum-compatible' time histories are discussed in Section 2.8.

#### 5.2.5.1 Newmark's Procedure for Time History Solutions of Linear Single Degree-of-Freedom Systems

Both Equations 5-1 and 5-17 can be solved using any numerical integration procedure for uncoupled second-order differential equations. But as noted in Section 5.1.1.1, the method most commonly used in seismic applications is Newmark's Method since it is applicable to both linear and nonlinear systems. As in all time-stepping methods, the duration of the input motion is divided into a finite number of small time steps,  $\Delta t$ , and assumptions are made about how the load varies, or the system behaves, or both, during  $\Delta t$ . In Newmark's method, the relative acceleration ( $\ddot{u}(t)$ ) during a time step is assumed to be either:

- (a) constant and equal to the average of the beginning and ending values, or
- (b) a linear variation between the beginning and ending values.

The constant acceleration procedure for linear SDOF bridges is summarized in Table 5-3 (in which the relative acceleration  $\ddot{u}(t)$  is denoted by  $u''$  and velocity  $\dot{u}(t)$  by  $u'$ ). It is noted that this procedure is unconditionally stable and the accuracy of the solution is solely dependent on a suitable choice for  $\Delta t$  in order to adequately represent the input excitation. Generally  $\Delta t \leq 0.01$  sec for earthquake input ground motions.

### 5.2.5.2 Newmark's Procedure for Time History Solutions of Linear Multi-Degree-of-Freedom Systems

Equation 5-6 can be solved using any numerical integration procedure for coupled second-order differential equations. But as noted in Section 5.1.1.1, the method most commonly used in seismic applications is Newmark's Method since it is applicable to both linear and nonlinear systems. As in all time-stepping methods, the duration of the input motion is divided into a finite number of small time steps,  $\Delta t$ , and assumptions made about how the load varies, or the system behaves, or both, during  $\Delta t$ . In Newmark's method, the relative acceleration ( $\ddot{u}(t)$ ) during a time step is assumed to be either:

- (a) constant and equal to the average of the beginning and ending values, or
- (b) a linear variation between the beginning and ending values.

The constant acceleration procedure for linear MDOF bridges is summarized in Table 5-4. (In this table the relative acceleration  $\ddot{u}(t)$  is denoted by  $u''$  and velocity  $\dot{u}(t)$  by  $u'$ .) As noted in the previous section, this procedure is unconditionally stable and the accuracy of the solution is solely dependent on the size of the time step,  $\Delta t$ .

**TABLE 5-3 - NUMERICAL INTEGRATION PROCEDURE FOR LINEAR SDOF BRIDGES**

Newmark's Constant Acceleration Method for Linear SDOF Bridges	
Solve: $mu'' + cu' + ku = -mu_g''(t)$ given time history of ground motion, $u_g''(t)$ , and initial conditions, $u_0$ and $u_0'$	
<b>Step 1. Setup and Initial Conditions</b>	
1.1	Select $\Delta t$ and number of time steps, $N_{\text{steps}}$
1.2	Calculate $k^* = k + 2c/\Delta t + 4m/\Delta t^2$
1.3	Calculate $a = 4m/\Delta t + 2c$ , and $b = 2m$
1.4	Calculate initial acceleration $u_0'' = (-mu_{g0}'' - cu_0' - ku_0) / m$
<b>Step 2. Step-by-Step Integration</b>	
2.1	Set $i = 0$
2.2	Calculate $\Delta p_i = -m(u_{gi+1}'' - u_{gi}'')$
2.3	Calculate $\Delta p_i^* = \Delta p_i + a u_i' + b u_i''$
2.4	Calculate $\Delta u_i = \Delta p_i^* / k^*$
2.5	Calculate $\Delta u_i' = (2/\Delta t) \Delta u_i - 2 u_i'$
2.6	Calculate $\Delta u_i'' = (4/\Delta t^2) \Delta u_i - (4/\Delta t) u_i' - 2 u_i''$
2.7	Calculate $u_{i+1} = (u_i + \Delta u_i)$ ; $u_{i+1}' = (u_i' + \Delta u_i')$ ; and $u_{i+1}'' = (u_i'' + \Delta u_i'')$
2.8	Set $i = i+1$
2.9	If $i \leq (N_{\text{steps}} - 1)$ go to Step 2.2
2.10	End

**TABLE 5-4 - NUMERICAL INTEGRATION PROCEDURE FOR LINEAR MDOF BRIDGES**

<b>Newmark's Constant Acceleration Method for Linear MDOF Systems</b>	
Solve: $\mathbf{M}\mathbf{u}'' + \mathbf{C}\mathbf{u}' + \mathbf{K}\mathbf{u} = -\mathbf{M}\mathbf{1}u_g''(t)$ given time history of ground motion, $u_g''(t)$ , and initial conditions, $\mathbf{u}_0$ and $\mathbf{u}_0'$	
<b>Step 1. Setup and Initial Conditions</b>	
1.1	Select $\Delta t$ and number of steps, $N_{\text{steps}}$
1.2	Calculate $\mathbf{K}^* = \mathbf{K} + (2/\Delta t)\mathbf{C} + (4/\Delta t^2)\mathbf{M}$
1.3	Calculate $\mathbf{a} = (4/\Delta t)\mathbf{M} + 2\mathbf{C}$ ; and $\mathbf{b} = 2\mathbf{M}$
1.4	Solve $\mathbf{M}\mathbf{u}_0'' = -\mathbf{M}\mathbf{u}_{g0}'' - \mathbf{C}\mathbf{u}_0' - \mathbf{K}\mathbf{u}_0$ - for vector of initial accelerations, $\mathbf{u}_0''$
<b>Step 2. Step-by-Step Integration</b>	
2.1	Set $i = 0$
2.2	Calculate $\Delta\mathbf{p}_i = -\mathbf{M}(\mathbf{u}_{gi+1}'' - \mathbf{u}_{gi}'')$
2.3	Calculate $\Delta\mathbf{p}_i^* = \Delta\mathbf{p}_i + \mathbf{a}\mathbf{u}_i' + \mathbf{b}\mathbf{u}_i''$
2.4	Solve $\mathbf{K}^*\Delta\mathbf{u}_i = \Delta\mathbf{p}_i^*$ - for vector of incremental displacements, $\Delta\mathbf{u}_i$
2.5	Calculate $\Delta\mathbf{u}_i' = (2/\Delta t)\Delta\mathbf{u}_i - 2\mathbf{u}_i'$
2.6	Calculate $\Delta\mathbf{u}_i'' = (4/\Delta t^2)\Delta\mathbf{u}_i - (4/\Delta t)\mathbf{u}_i' - 2\mathbf{u}_i''$
2.7	Calculate $\mathbf{u}_{i+1} = (\mathbf{u}_i + \Delta\mathbf{u}_i)$ ; $\mathbf{u}_{i+1}' = (\mathbf{u}_i' + \Delta\mathbf{u}_i')$ ; and $\mathbf{u}_{i+1}'' = (\mathbf{u}_i'' + \Delta\mathbf{u}_i'')$
2.8	Set $i = i+1$
2.9	If $i \leq (N_{\text{steps}} - 1)$ go to Step 2.2
2.10	End

## 5.3 NONLINEAR ANALYSIS METHODS

### 5.3.1 Nonlinear Static Methods

Two nonlinear static methods of analysis are described in this section. These are:

- Structure Capacity/Demand Method (also known as the Pushover Method), and
- Capacity Spectrum Method

Both methods use elastic methods of analysis to determine the demand on a bridge and explicit nonlinear techniques to assess the capacity of the bridge to resist these demands.

### **5.3.1.1 Structure Capacity/Demand (Pushover) Method**

#### **5.3.1.1.1 Approach**

This method is a two-step approach. First, it requires a displacement capacity evaluation using a pushover analysis, also known as the nonlinear static procedure. Such an analysis considers each relevant limit state and level of functionality, including  $P-\Delta$  effects. Second, it requires an elastic response spectrum (or time history) analysis to assess the displacement demands on the bridge.

#### **5.3.1.1.2 Displacement Capacity Evaluation**

The objective of a displacement capacity evaluation is to determine the displacement at which the earthquake resisting members of a bridge (usually the piers) reach their inelastic deformation capacity. Damage states are typically defined by local deformation limits, such as plastic hinge rotation. But other damage states include footing settlement and uplift, abutment displacement and backwall damage. Displacements may be limited by a loss of capacity such as the degradation of strength under large inelastic deformations, or  $P-\Delta$  effects.

This evaluation should be applied to individual piers to determine their lateral load-displacement behavior. It should be performed independently in both the longitudinal and transverse directions, and should identify those components of a pier which are first to reach their inelastic capacities. The displacement at which the first component reaches its capacity defines the displacement capacity for the pier. The model used for this analysis should include all of the components providing resistance, and use realistic force-deformation relationships for these components, including abutments and foundations.

For piers with simple geometries (e.g., a single-column pier), the maximum displacement capacity can usually be found by hand calculation, using an assumed plastic hinge mechanism and a maximum allowable deformation capacity for the plastic hinges and foundations. If the interaction between axial force and moment is significant, iteration will be necessary to determine the capacity of the collapse mechanism.

For more complicated piers or foundations, displacement capacity can be evaluated by a nonlinear static analysis, commonly referred to as a pushover analysis.

As noted above, evaluation of the displacement capacity is conducted on individual piers. Although forces may be redistributed from pier-to-pier as the displacement increases and yielding begins to occur (particularly so for bridges with piers of different stiffness and strength), the objective of this evaluation is to determine the maximum displacement capacity of each pier. This capacity is then compared with the results from an elastic demand analysis, which does consider the behavior of the bridge as a whole, and includes the effect of piers with different stiffnesses.

The structural model used for the evaluation should be based on the expected capacities of the inelastic components. The model for footings and abutments should include the nonlinear force–deformation behavior, including uplift, gap opening and closing. Stiffness and strength degradation of inelastic components, and the effects of loads acting through the lateral displacement ( $P$ - $\Delta$ ), should be considered. The maximum displacement of a pier is achieved when a component reaches its maximum permissible deformation. Maximum plastic hinge rotations for structural components are given in Chapter 7. The maximum deformation for foundations and abutments are limited by geometric constraints on the structure.

Although this evaluation is based on monotonically increasing displacement, the effects of cyclic loading must be considered when selecting an appropriate model and establishing a maximum inelastic deformation. This includes strength and stiffness degradation and low-cycle fatigue.

#### **5.3.1.1.3 Demands**

The uniform load or single mode method may be used for structures satisfying the ‘regularity’ requirements of Table 5-2. For structures not satisfying these requirements, the multi-mode spectral analysis method of dynamic analysis should be used, or alternatively an elastic time history method. These methods are described in Section 5.2.

#### **5.3.1.1.4 Procedure**

This procedure has five steps as below:

Step 1: Determine the strength and deformation capacity for each pier of the bridge.

Step 2: For each pier, carry out a nonlinear static pushover analysis and determine the superstructure displacement,  $\Delta_{ci}$ , at each of the following limit states (i):

1. First yield
2. Slight damage with cracking
3. Moderate damage that is repairable
4. Irreparable damage at the limit of life safety, and
5. Structural collapse.

Step 3: Determine the sum of the non-seismic displacement demands  $\Sigma\Delta_{NSdi}$  for each of the load combinations given, for example, in AASHTO (2002, 2013).

Step 4: Determine the response spectrum parameters,  $S_s$  and  $S_l$  and site factors,  $F_a$  and  $F_v$  (Figure 2-9 and Tables 2-4 and 2-5). Perform an elastic dynamic analysis to determine the seismic displacement demands,  $\Delta_{EQdi}$ , on each pier of the bridge. These elastic displacements may need to be increased in short-period bridges in accordance with the amplification factors given in AASHTO (2013, 2014). Additionally, directional combinations of earthquake contribution will normally need to be considered. The analysis should reflect the anticipated condition of the structure and the foundation during this earthquake. Generally this means that the stiffness used to calculate the modal period for use in Figure 2-9 should reflect the anticipated condition of the bridge. But since this is not known at the beginning of an analysis, it is usual to base the stiffness on an assumed level of cracking and plasticity as recommended in Table 5-7.

Step 5: Determine the capacity/demand ratio ( $r_{LSi}$ ) for each limit state ( $i$ ) from the following:

$$r_{LSi} = \frac{(\Delta_{ci} - \Sigma\Delta_{NSdi})}{\Delta_{EQdi}} \quad 5-38$$

If  $r_{LSi} \geq 1.5$ , limit state  $i$  is not likely to be reached

If  $r_{LSi} < 1.5$ , limit state  $i$  may be reached, and if less than 1.0 it will be reached. A decision needs to be made whether the occurrence of this limit state is acceptable. Factors influencing this decision include the nature of the limit state (first cracking vs span collapse) and the likelihood of occurrence of the earthquake (return period). If the situation is unacceptable (span collapse in a frequent earthquake, say), the capacity of the bridge needs to be increased and the analysis repeated.

### 5.3.1.1.5 Restrictions

This method is a general approach and has few restrictions. However, the capacity analysis is limited to a pier-by-pier evaluation which does not necessarily capture the capacity of the bridge as a whole. Furthermore, the equal displacement assumption (Figure 1-9) is used to find the demand, and the system damping is assumed to be 5%. On the other hand, comparison of results with those from nonlinear time history analyses, show these limitations are not significant for regular highway bridges. However, it would be wise to check the performance of a complex bridge with the potential for substantial inelastic behavior, or of a bridge of major importance, using a time history method and explicit modeling of nonlinear bridge capacity, such as that described in the Section 5.3.2.

### 5.3.1.2 Capacity / Demand Spectrum Method

This method is similar to that given in the previous section in that a pushover curve is used to represent the capacity of the bridge, but the assumptions of equal displacements and 5% damping are no longer necessary. Instead the demand is derived from the intersection of the pushover curve and the design acceleration response spectrum after scaling for the actual damping in the yielding structure.

#### 5.3.1.2.1 Modified Acceleration Response Spectrum

As noted previously, the earthquake demand on a bridge may be represented by a response spectrum. Both acceleration and displacement spectra are used, but by far the most common is the acceleration spectrum. These spectra, when scaled by seismic mass, give the seismic forces acting through the center of mass of the bridge. Figure 2-9 shows the acceleration spectrum recommended by AASHTO for the seismic design of highway bridges, and by FHWA for the retrofit of existing bridges. This spectrum assumes 5% viscous damping in the bridge and should be modified for other damping values. A value of 5% is appropriate for essentially elastic behavior but once yielding occurs, and other forms of damage begin to occur and the damping level increases. Two damping factors are introduced for this purpose,  $B_S$  and  $B_L$ , for use in the short and long period ranges of the spectrum respectively. A procedure for calculating  $B_S$  and  $B_L$  is given in Table 5-5, which shows that both factors depend on the displacement ductility factor  $\mu$ , defined as follows:

$$\mu = \frac{\Delta}{\Delta_y} \quad 5-39$$

where  $\Delta$  is the displacement at which ductility is being calculated, and  $\Delta_y$  is the yield displacement.

A seismic demand coefficient,  $C_d$ , is defined as follows:

$$C_d = \frac{S_a}{g} \quad 5-40$$

where:  $S_a$  = spectral acceleration defined in Figure 2-9,

$$\text{i.e. } S_a = g \left[ \frac{F_v S_1}{B_L T} \right] \quad \text{for long-period bridges, } (T > T_s) \quad 5-41a$$

$$\text{and } S_a = g \left[ \frac{F_a S_s}{B_s} \right] \quad \text{for short-period bridges, } (T < T_s) \quad 5-41b$$

This is the traditional form of a demand spectrum ( $S_a$  vs period  $T$ ), but it is also convenient to express  $C_d$  in terms of  $S_d$  (spectral displacement) rather than period. To do so,  $S_d$  is first written as follows:

$$S_d = \frac{S_a}{\omega^2} = S_a \left[ \frac{T^2}{4\pi^2} \right] = \left[ \frac{F_v S_1}{B_L} \right] \frac{Tg}{4\pi^2} \quad \text{for } T > T_s \quad 5-42$$

where  $\omega$  is the angular frequency and equals  $2\pi/T$  (rads/sec).

**TABLE 5-5 - EFFECTIVE VISCOUS DAMPING RATIOS AND DAMPING FACTORS,  $B_s$  AND  $B_L$**

Substructure Type	Effective Viscous Damping Ratio, $h_{eff}$	Damping Factor, $B_s$	Damping Factor, $B_L$
Nonductile, conventionally-designed columns	$0.05 + 0.16(1-1/\mu)^1$	$[h_{eff}/0.05]^{0.5}$	$[h_{eff}/0.05]^{0.3}$
Ductile, sesimically-designed columns	$0.05 + 0.24(1-1/\mu)^1$		
<b>Note:</b> 1. $\mu$ = displacement ductility factor (Equation 5-39)			

Combining Equations 5-40, 5-41a and 5-42, to eliminate the period  $T$ , gives  $C_d$  for long period bridges as:

$$C_d = \left[ \frac{g}{S_d} \right] \left[ \frac{F_v S_1}{2\pi B_L} \right]^2 \text{ for } T \geq T_s \quad 5-43a$$

Figure 5-4 shows  $C_d$  plotted against  $S_d$  for a particular value of damping factor  $B_L$ . This spectrum is seen to have a shape similar to that of the traditional, period-based spectrum and that  $C_d$  decreases as  $S_d$  increases.

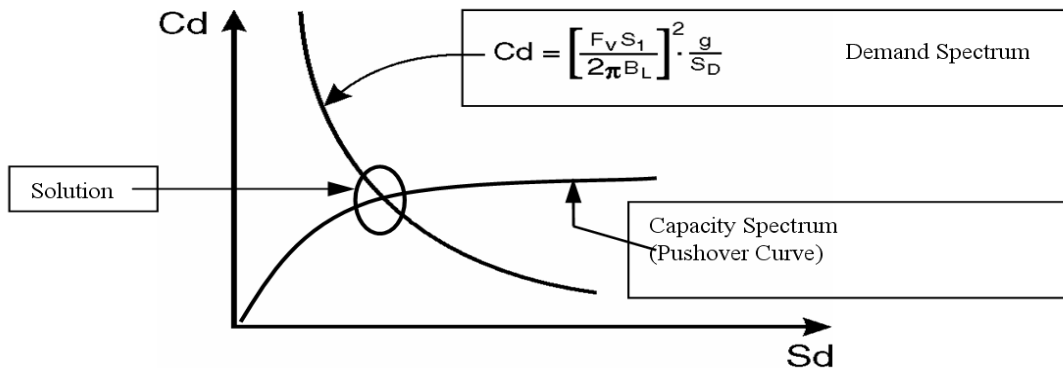


Figure 5-4 Capacity / Demand Spectrum

Further, by combining Equations 5-40 and 5-41b,  $C_d$  for short period bridges can be shown to be given by:

$$C_d = \frac{F_a S_s}{B_s} \text{ for } T < T_s \quad 5-43b$$

### 5.3.1.2.2 Capacity / Demand Spectrum

It is possible to combine the pushover capacity curve and the demand spectrum in a single plot, Figure 5-4. The result is known as a capacity / demand spectrum. There are many possible uses for such a plot, one of which provides capacity/demand ratios for a complete bridge subject to a given earthquake, and the other calculates bridge response ( $F$ ,  $\Delta$ ) to a given earthquake. A step-by-step procedure for calculating bridge response is given in the following section.

### 5.3.1.2.3 Calculation of Bridge Response

Capacity / demand spectra may be used to determine the response of a bridge with a known capacity spectrum ( $C_c$  vs  $\Delta$ ) during a given earthquake with a known demand spectrum ( $C_d$  vs  $S_d$ ). The difficulty, however, is that the final displacement is unknown and both the capacity coefficient ( $C_c$ ) and the damping factor ( $B_L$ ) cannot be calculated in advance. Iteration is therefore used, starting with an initial estimate for displacement and iterating until the assumed value and the calculated value are in agreement. Basic steps in the method are listed below.

Step 1: Determine if the bridge has a long period of vibration by comparing the elastic period  $T$  with  $T_S$  (Figure 2-9). If not, go to Step 8 (procedure for short period bridges).

*Procedure for long period bridges:*

Step 2: Start iteration by setting  $\Delta$  equal to the displacement of the bridge assuming elastic behavior, and calculate ductility factor  $\mu$  (Equation 5-39).

Step 3: Calculate the damping factor  $B_L$  using Table 5-5.

Step 4: Calculate the capacity coefficient  $C_c = F / W$ , where  $F$  is the capacity of the bridge at displacement  $\Delta$ .

Step 5: Set  $C_d = C_c$  and solve for  $S_d$  in Equation 5-43a, i.e.,

$$S_d = \left[ \frac{g}{C_c} \right] \left[ \frac{F_v S_1}{2\pi B_L} \right]^2 \quad 5-44a$$

Step 6: Compare  $S_d$  with value for  $\Delta$  (see Step 2 or previous Step 6) and if in agreement, go to Step 7. Otherwise set  $\Delta = S_d$ , recalculate  $\mu$ , and go to Step 3.

Step 7: Calculate forces in individual piers, bearings and foundations using  $\Delta$ , and compare sum with total lateral force on bridge (base shear)  $V$ , using  $V = C_c W$ .

*Procedure for short period bridges:*

Step 8: Start iteration by setting  $\Delta$  equal to the displacement of the bridge assuming elastic behavior, and calculate ductility factor  $\mu$  (Equation 5-39).

Step 9: Calculate the damping factor  $B_S$  using Table 5-5.

Step 10: Calculate the capacity coefficient  $C_c = F / W$ , where  $F$  is the capacity of the bridge at displacement  $\Delta$ .

Step 11: Calculate effective stiffness from  $K_{eff} = C_c W / \Delta$ .

Step 12: From equation 5-43b, calculate  $C_d = F_a S_S / B_S$ .

Step 13: Calculate  $S_d$  from  $S_d = C_d W / K_{eff}$  and by substituting results from Steps 11 and 12 obtain:

$$S_d = \left[ \frac{\Delta}{C_c} \right] \left[ \frac{F_a S_S}{B_S} \right] \quad 5-44b$$

Step 14: Compare  $S_d$  with value for  $\Delta$  (see Step 8 or value from previous Step 14) and if in agreement go to Step 15, otherwise set  $\Delta = S_d$ , recalculate  $\mu$ , and go to Step 9.

Step 15: Calculate forces in individual piers, bearings and foundations using  $\Delta$ , and compare sum with total lateral force on bridge (base shear)  $V$ , using  $V = C_c W$ .

### 5.3.2 Nonlinear Dynamic Methods

Nonlinear dynamic methods are time history methods that calculate the demand on a bridge while explicitly including the nonlinear properties of the members. Usually the source of the nonlinearity is yielding in the plastic hinges in the columns in which case the structure stiffness matrix  $K$  needs to be updated as the column softens and degrades during the passage of an earthquake. To reflect this situation the equation of equilibrium for a multi-degree of freedom system (Equation 5-6) is rewritten as

$$M\ddot{u} + C\dot{u} + K(u)u = -M1\ddot{u}_g \quad 5-45$$

where  $K(u)$  = nonlinear structure stiffness matrix that varies with displacement  $u$ .

Solutions to Equation 5-45 involve step-by-step integration of the coupled equations (sometimes called direct integration). In addition to the basic Newmark approach, fast nonlinear analysis procedures have been developed that are computationally more efficient to implement for the majority of nonlinear structures.

### 5.3.2.1 Basic Step-by-Step Numerical Integration Procedure (Newmark's Procedure)

As noted in Section 5.2.5, there are several methods for solving Equation 5-6 that use step-by-step numerical integration techniques. The one most favored in seismic analysis is Newmark's Method for which there are two versions: one that assumes constant acceleration and one that assumes a linear variation of acceleration within each time step. Both can be adapted to solve nonlinear problems. Table 5-6 summarizes the steps involved when using the constant acceleration method for a nonlinear system. (In this table the relative acceleration  $\ddot{u}(t)$  is denoted by  $u''$ , and velocity  $\dot{u}(t)$  by  $u'$ .)

The procedure in Table 5-6 can be very time consuming for at least two reasons. First, the size of the time step  $\Delta t$  must be kept small so as to accurately track the transition from elastic to post-yield stiffness and from the loading to the unloading branches of the nonlinear hysteretic curve for each member. A small time step means a large number of steps ( $N_{steps}$ ) for the same total duration of earthquake. The second reason is that two steps in Table 5-6 are complex and can be very time consuming. These are the calculation of the tangent stiffness matrix in Step 2.4 and the iterative solution of the equations in Step 2.6 using, say, the Newton-Raphson procedure. Since both steps are repeated for every time step, a single nonlinear analysis of a typical bridge, with several hundred degrees-of-freedom, can take several hours using a basic time-stepping procedure.

### 5.3.2.2 Fast Nonlinear Analysis Procedure (Wilson's Approach)

One of the reasons the basic method in Table 5-6 is time consuming is that for every time step, every member is checked for possible nonlinearity and its stiffness matrix reformulated, when in fact only a limited number of members in a typical bridge do in fact become nonlinear during an earthquake.

Significant savings in execution time can be achieved if those members likely to yield are predetermined ahead of time. These members are then represented by nonlinear elements in the structural model of the bridge and the remainder of the bridge is represented by linear elements.

**TABLE 5-6 - BASIC NUMERICAL INTEGRATION PROCEDURE FOR NONLINEAR MDOF BRIDGES**

Newmark's Constant Acceleration Method for Nonlinear MDOF Systems	
Solve: $\mathbf{M} \mathbf{u}'' + \mathbf{C} \mathbf{u}' + \mathbf{K}(\mathbf{u}) \mathbf{u} = -\mathbf{M} \mathbf{1} u_g''(t)$ given time history of ground motion, $u_g''(t)$ , and initial conditions, $\mathbf{u}_0$ and $\mathbf{u}_0'$ .	
<b>Step 1. Setup and Initial Conditions</b>	
1.1 1.2 1.3	Select $\Delta t$ and number of steps, $N_{\text{steps}}$ Calculate $\mathbf{a} = (4/\Delta t) \mathbf{M} + 2\mathbf{C}$ ; and $\mathbf{b} = 2\mathbf{M}$ Solve $\mathbf{M} \mathbf{u}_0'' = -\mathbf{M} \mathbf{u}_{g0}'' - \mathbf{C} \mathbf{u}_0' - \mathbf{f}_s(\mathbf{u}_0)$ - for vector of initial accelerations, $\mathbf{u}_0''$
<b>Step 2. Step-by-Step Integration</b>	
2.1 2.2 2.3 2.4 2.5 2.6 2.7 2.8 2.9 2.10 2.11 2.12	Set $i = 0$ Calculate $\Delta \mathbf{p}_i = -\mathbf{M} (\mathbf{u}_{gi+1}'' - \mathbf{u}_{gi}'')$ Calculate $\Delta \mathbf{p}_i^* = \Delta \mathbf{p}_i + \mathbf{a} \mathbf{u}_i' + \mathbf{b} \mathbf{u}_i''$ Determine tangent stiffness matrix, $\mathbf{K}_i$ Calculate $\mathbf{K}_i^* = \mathbf{K}_i + (2/\Delta t) \mathbf{C} + (4/\Delta t^2) \mathbf{M}$ Solve $\mathbf{K}_i^* \Delta \mathbf{u}_i = \Delta \mathbf{p}_i^*$ - for vector of incremental displacements, $\Delta \mathbf{u}_i$ , using iterative procedure Calculate $\Delta \mathbf{u}_i' = (2/\Delta t) \Delta \mathbf{u}_i - 2\mathbf{u}_i'$ Calculate $\Delta \mathbf{u}_i'' = (4/\Delta t^2) \Delta \mathbf{u}_i - (4/\Delta t) \mathbf{u}_i' - 2\mathbf{u}_i''$ Calculate $\mathbf{u}_{i+1} = (\mathbf{u}_i + \Delta \mathbf{u}_i)$ ; $\mathbf{u}_{i+1}' = (\mathbf{u}_i' + \Delta \mathbf{u}_i')$ ; and $\mathbf{u}_{i+1}'' = (\mathbf{u}_i'' + \Delta \mathbf{u}_i'')$ Set $i = i + 1$ If $i \leq (N_{\text{steps}} - 1)$ go to Step 2.2 End

This technique is implemented in the computer program SAP2000 for the three dimensional static and dynamic analysis of structures (CSI, 1998). For this purpose Equation 5-45 is replaced by:

$$M\ddot{u} + C\dot{u} + K_L u + r_N = -M\ddot{u}_g \quad 5-46$$

where  $K_L$  = stiffness matrix for linear elastic elements in bridge, and

$r_N$  = vector of forces associated with the nonlinear elements (called Nlinks in SAP).

If a linear effective stiffness is used to represent the properties of each nonlinear element, a stiffness matrix for the nonlinear elements in the bridge,  $K_N$ , can be assembled, and the structure stiffness,  $K$ , can be found as follows:

$$K = K_L + K_N \quad 5-47$$

Substitution for  $K_L$  in Equation 5-46, followed by rearrangement of terms, gives:

$$M\ddot{u} + C\dot{u} + Ku = -M\ddot{u}_g - [r_N - K_N u] \quad 5-48$$

These coupled equations may be solved using any step-by-step numerical integration procedure, such as Newmark's method (Section 5.3.2.1), and whereas iteration is still required, only  $r_N$  and  $K_N$  need to be found at each step (and each time step) giving rise to a very efficient numerical process.

## 5.4 ANALYSIS METHODS FOR IMPOSED SUPPORT DISPLACEMENTS

### 5.4.1 Elastic Method for Multiple Support Excitation

The analysis of a bridge with multiple support excitation begins with the explicit inclusion of the support degrees of freedom in the equations of motion. There will  $N$  of these equations where  $N$  is the sum of the structure displacement degrees of freedom ( $N_s$ ) and the support displacement degrees of freedom ( $N_g$ ). Furthermore, these equations are written in terms of absolute displacement as shown in Equation 5-49 for the case of no damping.

$$M\ddot{u}^t + Ku^t = p(t) \quad 5-49$$

where  $M$  = mass matrix ( $N \times N$ )

$K$  = structure stiffness matrix ( $N \times N$ )

$u^t$  =  $\langle u_s^t \ u_g \rangle^T$  ( $N \times 1$  vector)

$u_s^t$  = vector of absolute structure displacements ( $N_s \times 1$ )

$u_g$  = vector of absolute support displacements due to ground motion ( $N_g \times 1$ )

$p(t)$  =  $\langle 0 \ p_g(t) \rangle^T$  ( $N \times 1$  vector)

$0$  = externally applied loads to structure = null vector in this case ( $N_s \times 1$ ), and  
 $p_g(t)$  = support reactions ( $N_g \times 1$  vector)

As noted above, for the purpose of this derivation, damping has been omitted from Equation 5-49, but may be included without difficulty. The mass and stiffness matrices can be partitioned into submatrices according to the structure and support degrees of freedom respectively, in which case Equation 5-49 can be written as:

$$\begin{bmatrix} M_{ss} & 0 \\ 0 & M_{gg} \end{bmatrix} \begin{Bmatrix} \ddot{u}_s^t \\ \ddot{u}_g \end{Bmatrix} + \begin{bmatrix} K_{ss} & K_{sg} \\ K_{gs} & K_{gg} \end{bmatrix} \begin{Bmatrix} u_s^t \\ u_g \end{Bmatrix} = \begin{Bmatrix} 0 \\ p_g(t) \end{Bmatrix} \quad 5-50$$

The multiple support excitation problem can therefore be seen as one where it is required to find the time history of absolute structure displacements,  $u_s^t$ , given the time history of support displacements,  $u_g$ , which may vary from support to support. Relative structure displacements, and hence member forces, can then be found by taking the difference between these two time histories.

It is helpful to recognize that  $u_s^t$  is composed of two parts. The first is due to the quasi-static effect of applying non-uniform support displacements and occurs independently of the rate of loading. The second is due to the dynamic effect of applying time-varying support displacements and is very dependent on the rate of loading. The quasi-static effect is zero if the support motions are identical or if the structure is statically determinate. The dynamic effect is zero if support displacements do not vary with time. It follows that  $u^t$  may be written as:

$$u^t = \begin{Bmatrix} u_s^t \\ u_g \end{Bmatrix} = \begin{Bmatrix} u_s^s \\ u_g \end{Bmatrix} + \begin{Bmatrix} u \\ o \end{Bmatrix} \quad 5-51$$

where  $u_s^s$  = vector of absolute structure displacements due to quasi-static application of support motions ( $N_s \times 1$ ), and

$u$  = vector of absolute structure displacements due to dynamic application of support motions ( $N_s \times 1$ ).

Substituting Equation 5-51 into Equation 5-50 and partitioning the result gives:

$$u_s^s = -K_{ss}^{-1} K_{sg} u_g = i u_g \quad 5-52$$

where  $i$  is an influence matrix ( $N_s \times N_g$ ) describing the effect of the support displacements on the structure displacements, and is given by:

$$i = -K_{ss}^{-1} K_{sg} \quad 5-53$$

Substituting Equations 5-53 and 5-51 into Equation 5-50 and partitioning the result gives:

$$M_{ss} \ddot{u} + K_{ss} u = -M_{ss} i \ddot{u}_g(t) \quad 5-54$$

Equation 5-54 may be solved for  $u$  either by transforming into modal coordinates and using Newmark's Method (Section 5.2.5.1), or by direct integration (Section 5.3.2.1). It follows that:

$$u_s^t = u_s^s + u = i u_g + u \quad 5-55$$

Member forces (bending moment, shear force, and axial force) are found from relative displacements, such as the drift in a column which is given by:

$$\delta = u_j^t - u_{gk} \quad 5-56$$

where  $\delta$  = relative displacement in the column, and

$j, k$  = column joint numbers in superstructure and foundation respectively.

It can be noted from Equations 5-54 and 5-55, that the analysis of multiple support excitation requires the time history of ground displacement,  $u_g(t)$ , and that for the ground acceleration,  $\ddot{u}_g(t)$ , to be known (for the same earthquake). This is in contrast to the time history solution for uniform excitation where only the acceleration record is required.

## 5.4.2 Elastic Method for Statically Imposed Support Displacements

The analysis of a bridge with statically imposed support displacements is very similar to that for multiple support excitation except that the dynamic effect is zero (Section 5.4.1). Again the support degrees-of-freedom ( $N_g$ ) are explicitly included in the equations of equilibrium which are written in terms of absolute displacement, as shown in Equation 5-57.

$$K u^t = p \quad 5-57$$

where  $u^t = \langle u_s^t \ u_g \rangle^T$  ( $N \times 1$  vector)  
 $u_s^t$  = vector of absolute structure displacements ( $N_s \times 1$ )  
 $u_g$  = vector of absolute imposed support displacements ( $N_g \times 1$ )  
 $p = \langle 0 \ p_g \rangle^T$  ( $N \times 1$  vector)  
 $0$  = externally applied loads to structure = null vector in this case ( $N_s \times 1$ ), and  
 $p_g$  = support reactions ( $N_g \times 1$  vector)

As with multiple support excitation, Equation 5-57 may be partitioned according the superstructure and substructure degrees of freedom as follows:

$$\begin{bmatrix} K_{ss} & K_{sg} \\ K_{gs} & K_{gg} \end{bmatrix} \begin{Bmatrix} u_s^t \\ u_g \end{Bmatrix} = \begin{Bmatrix} 0 \\ p_g \end{Bmatrix} \quad 5-58$$

In Section 5.4.1 (multiple support excitation),  $u_s^t$  was the sum of the quasi-static displacements,  $u_s^s$ , and the dynamic displacements,  $u$ . But as noted above,  $u = 0$  in this case and thus  $u_s^t$  is identical to  $u_s^s$ . It follows that:

$$u_s^t = i u_g \quad 5-59$$

where  $i = -K_{ss}^{-1} K_{sg}$

Member forces (bending moment, shear force, and axial force) are found from relative displacements, such as the drift in a column:

$$\delta = u_j^t - u_{gk}$$

5-60

where  $\delta$  = relative displacement in the column, and

$j, k$  = column joint numbers in superstructure and foundation respectively.

## 5.5 ANALYSIS METHODS FOR SOIL-FOUNDATION-STRUCTURE INTERACTION

### 5.5.1 General

The behavior of a bridge during an earthquake is strongly dependent on the stiffness and strength of its foundation system, which includes the abutments and piers, footings, and piles. Dynamic response is determined by these two parameters, which in turn influence the earthquake demands on the bridge and the distribution of these loads to the structural and foundation components.

The rigorous analysis of the dynamic response of a soil-foundation-bridge system where the footings, abutments, piles (if any) and soils are explicitly included in the bridge model, is complex and difficult (Pecker and Pender, 2000). If the soil is idealized as an elastic continuum, then a substructuring approach may be used. In this case, the problem is separated into three steps:

Step 1: Analyze the influence of the stiffness and geometry of a massless foundation system on the free-field ground motion, leading to modified structural input motions at the foundation level (i.e., kinematic interaction).

Step 2: Analyze the frequency-dependent impedance characteristics of the foundation system under cyclic loading, in the form of a foundation stiffness matrix.

Step 3: Analyze the inertial response of the structure to the foundation input motions (from step 1), using the pile cap stiffness matrix to account for foundation compliance (i.e., inertial interaction).

Except for cases involving deep, and relatively stiff, foundations in soft soils and for large rigid shallow foundations, the effect of kinematic interaction is normally neglected in practice, and the foundation-input

motions are assumed to be the same as the free-field motions. As a result, the inertial interaction of a bridge with its foundation is the major focus of the material presented in this section.

### **5.5.2 Shallow Footings**

Procedures for evaluating soil-footing-bridge interaction have evolved over time from the theory of continuum mechanics. Frequency-dependent stiffness and damping parameters for low amplitude, machine-foundation vibration problems have been adapted to earthquake soil-foundation-structure interaction (SFSI) problems<sup>1</sup>. But for practical modeling purposes, the frequency dependence of the stiffness parameters may be ignored, and static or slow cyclic values for stiffness may be used instead. This is a reasonable assumption considering the range of frequencies in earthquake ground motions. Similarly, frequency-dependent radiation-damping due to wave propagation away from a footing is not considered. For most footing sizes, radiation damping values are small and difficult to quantify in a nonlinear soil.

In addition to developing secant stiffness parameters, the mobilization of the moment capacity of the footing is of concern in many design and retrofit applications and is addressed in Chapter 7. For practical modeling purposes, soil capacity may be evaluated assuming pseudo-static inertial loading on a footing from the bridge above. This is a reasonable assumption, considering normal factors of safety under static loading, the stiff or dense soils associated with spread footings, and the difficulties in determining phase relations between soil and foundation motions in a coupled problem<sup>2</sup>.

Transient uplift of shallow foundations (i.e. foundation rocking) during an earthquake is an acceptable mechanism for reducing seismic forces in bridge substructures. In a first order analysis, a common simplification is to assume the footing is supported on a rigid-perfectly-plastic soil with an assumed uniform compressive capacity<sup>3</sup>.

### **5.5.3 Piles**

Two distinct approaches to soil-pile-structure interaction under dynamic loading have been developed. One approach evolved from slow cyclic (long period) lateral loading tests on piles conducted in the 1970's, which were motivated originally by the need to develop pile design criteria for offshore structures

---

<sup>1</sup> Mylonakis et al. (2002); Pecker and Pender (2000)

<sup>2</sup> *ibid*

<sup>3</sup> Appendix A, AASHTO LRFD Guide Specifications for Seismic Design (2014)

subjected to wave loading. These studies led to analytical methods based on the use of nonlinear Winkler springs to model soil-pile interaction under cyclic lateral and axial loading. The second approach evolved from other studies conducted in the 1970's, originally motivated by machine foundation vibration problems, where the problem was driven by the need to develop frequency dependent stiffness and damping (i.e., impedance functions), to determine resonant frequency and amplitude characteristics of supporting pile foundations. In this approach, the model used was that of a vibrating mass supported by pile foundations in an elastic continuum.

Elastic impedance functions for piles and pile groups have been studied by numerous researchers and a large number of closed form analytical solutions are available<sup>4</sup>. Early research on this subject was stimulated by the need to establish analysis methods for vibrating machine foundations, where the higher frequencies of loading lead to radiation damping, and foundation stiffness is strongly frequency dependent. In addition, amplitudes of vibration are generally small, and the assumption of an elastic soil is reasonable.

However, soil-pile interaction under larger earthquake-induced inertial loading can lead to strongly nonlinear soil behavior, particularly in the vicinity of the pile interface, and the use of the elastic approach becomes impractical for routine structural design under seismic loading. Fortunately, given the relatively low frequency range of earthquake inertial loading and the nature of representative pile foundation systems for bridges and buildings, stiffness functions are essentially frequency independent and static loading stiffness values are a reasonable approximation. In addition, the radiation damping component of energy loss arising from wave propagation away from the foundation is considerably reduced at lower frequencies, particularly in the presence of nonlinear soil behavior. Whereas fully coupled nonlinear solutions to the seismic loading problem, using finite element methods, are theoretically possible and have been used to a limited extent, the analytical complexity is daunting and impractical for routine design.

Given the complexity of nonlinear coupled models, the Winkler model, as represented by a series of independent or uncoupled lateral and axial springs (linear or nonlinear) simulating soil-pile interaction in the lateral and axial directions, provides the most convenient means of analyzing the response of pile foundation systems to earthquake loading. The pile is modeled by beam-column elements, supported by linear or nonlinear spring elements, and both kinematic and inertial interaction effects may be included (Matlock et al., 1978, 1981). Free-field earthquake ground motions determined from one-dimensional site

---

<sup>4</sup> Novak (1991); Pender (1993); Gazetas and Mylonakis (1998); Pecker and Pender (2000)

response analyses may be used as displacement input motions for the spring elements. The analysis method is embodied in the computer program SPASM (Single Pile Analysis with Support Motion), as described by Matlock et al. (1978), and applications to bridges have been developed<sup>5</sup> using this modeling concept.

Whereas the effects of the kinematic interaction can be significant for some pile-soil configurations (for example, larger diameter piles in soft soils or for sudden changes in soil stiffness with depth), piles may be assumed to deform in a compatible manner within the free-field. For such cases, free-field displacements are generally much less than those induced by inertial interaction. Hence, it can be assumed that inertial interaction dominates pile foundation response and that stiffness functions may be represented by values under static or slow cyclic conditions with foundation input motions assumed to be near surface free-field motions. This approach has had widespread application in the analysis of soil-pile-structure interaction analyses (Martin and Lam, 1995) and forms the basis for the stiffness and capacity modeling approaches described in Chapter 7.

## 5.6 MODELING RECOMMENDATIONS FOR BRIDGE STRUCTURES

### 5.6.1 General

Mathematical models used for dynamic analysis should include the strength, stiffness, mass, and energy dissipation characteristics of the structural members and components of the bridge.

Depending on the method of dynamic analysis, different approximations may be used for modeling these quantities. One-dimensional, beam-column members are sufficient for the earthquake analysis of most regular bridges (Table 5-2), and grid or finite element models are usually not necessary. Joint size should be included in these models. The advantage of these simple models (sometimes referred to as *spine* models or *stick* models) is that they permit rapid interpretation of results and a quick check on load path and equilibrium.

Irregular bridges (Table 5-2) include those with skew and horizontal curvature, and three-dimensional finite element or hybrid stick models should be used in these cases to more carefully represent the load

---

<sup>5</sup> Lam and Law (2000); Gazetas and Mylonakis (1998)

path, particularly at piers and abutments. See Figure 5-5 for range of bridge models commonly used in bridge analysis.

Short columns or piers may be modeled as a single element, but tall columns should have two or more elements. This is particularly true if the piers have significant mass as in the case of a concrete bridge, or are framed systems as in the case of a steel tower.

It is not necessary to model bridges with multiple segments as one complete bridge. Each segment (also called a *longitudinal frame* or simply a *frame*) should have sufficient capacity to resist the inertial loads generated within that segment and may be analyzed as a freebody or stand-alone structure. However when the segments have large differences in their modal periods, out-of-phase motion may occur and the frames may adversely interact with each other, causing impact and/or unseating at the hinges.

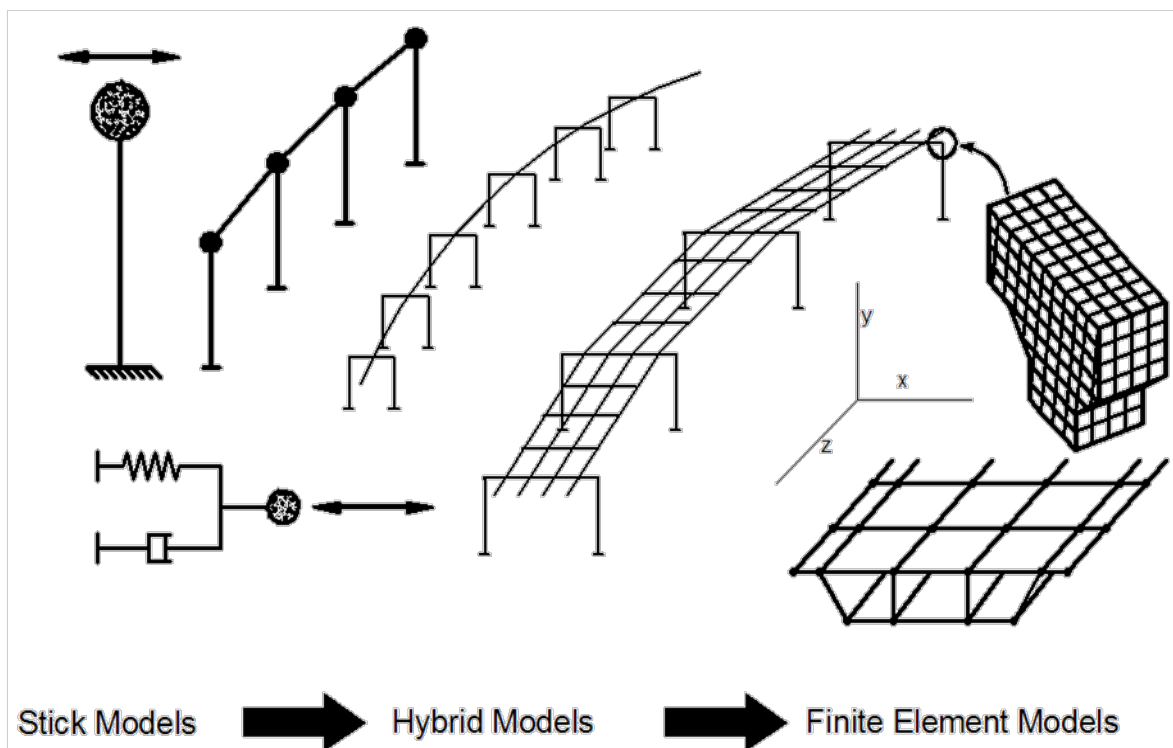


Figure 5-5 Range of Common Bridge Models from Simple Stick Linear Models to Finite Element Three-Dimensional Models

To account for these effects, the number of segments that should be included in a model depends on the ratio of the fundamental periods. For bridges in which the period ratio of adjacent segments is less than

0.70 (shorter period divided by longer period), it is recommended that the model be limited to five segments. The first and fifth segments in the model are considered to be boundary segments, representing the interaction with the remainder of the structure. The response of the three interior segments can then be used for evaluation. For bridges with segments that have period ratios between 0.70 and 1.0, less than five segments may be used in the model if desired. For a bridge with more than five segments, several different models are required to be analyzed.

Response of a bridge in two orthogonal horizontal directions should be determined in the seismic analysis and the results combined to determine demand forces and deformations.

If the bridge is located within 6 miles of a known active fault, the response in the vertical direction should also be determined and combined with the horizontal response. These bridges should also be subjected to a site-specific study to determine both the horizontal and vertical ground motions for use in the above analyses. Explicit analysis for vertical motions need not be carried out for regular bridges located more than 6 miles from an active fault. For irregular bridges, such as those with long flexible spans, C-shaped piers, or with other large eccentricities in the load path for vertical loads, an analysis in the vertical direction should be included.

### **5.6.2 Distribution of Mass**

Modeling the mass of a bridge should consider the degree of discretization and the expected motion during an earthquake. The number and location of the displacement degrees of freedom in a bridge model determine the way mass is represented and distributed throughout the structure. As most of the mass of a bridge is in the superstructure, four to five elements per span are generally sufficient to represent the superstructure. For *spine* models of superstructures, the beam elements have the same neutral axis as the superstructure and rigid links are then used to locate the mass centroid relative to the neutral axis of these elements.

For single column piers, C-shaped piers, or other unusual configurations, the rotational mass moment of inertia of the superstructure about the longitudinal axis should be included. The mass of the pier caps should also be included.

Live load mass is not usually included in the seismic analysis of a bridge. See explanatory note in Step 2 of the Uniform Load Method in Section 5.2.2.

### 5.6.3 Distribution of Stiffness and Modeling of Structural Members and Connections

The mathematical model should represent the stiffness of individual structural elements considering material properties and section dimensions. When an elastic analysis is used to determine the response of an inelastic structure, several assumptions are necessary, of which the most important is that stiffness may be based on an equivalent linearized value. For inelastic columns, common practice is to use cracked section properties for concrete members and full section properties for steel members as explained in Section 5.6.4. This value for stiffness is sometimes called a tangential stiffness. However, for seismic isolators, abutments, and foundation soils, stiffness is calculated from the maximum expected deformation. This value is then known as a secant stiffness. The distribution of forces from an elastic analysis should be carefully reviewed to verify that the results are consistent with the expected nonlinear behavior of the earthquake resisting elements.

In the Structure Capacity/Demand Method (Pushover Method) described in Section 5.3.1.1, the mathematical model should use strength values that are based on expected material properties. For nonlinear dynamic analysis, the model should use the actual stiffness and strength values of the hysteretic elements under seismic loads.

### 5.6.4 Distribution of Stiffness and Modeling of Substructures and Abutments

The stiffness of structural steel members should be based on elastic properties. For reinforced concrete piers, stiffness should be based on cracked section properties, as explained in this section.

Analytical methods for seismic demand generally use stiffness values that are representative of deformations close to the deformations at yield. At these levels of deformation, even prior to yield, reinforced concrete elements crack. The effect of cracking on stiffness depends on the cross-section, longitudinal reinforcement ratio, axial load, and amount of bond slip. The cracked flexural stiffness of a reinforced concrete member can be obtained by moment–curvature analysis of the cross-section, with modifications for bond-slip. In many cases, it is impractical to compute the effective stiffness in this manner, and instead, effective stiffness quantities are assumed based on component rigidity values such as those shown in Table 5-7.

From Table 5-7 it is noted that for flexurally-dominated regions, where plastic hinging is expected to occur at the ends of the member, the effective flexural rigidity,  $E_c I_{eff}$ , may be determined from the ‘theoretical’ yield curvature given by:

$$\phi_y = \frac{2\varepsilon_y}{D'} = \frac{M_n}{E_c I_{eff}} \quad 5-61$$

where:  $\varepsilon_y$  = yield strain =  $f_y / E_s$

$f_y$  = yield stress (theoretical value, i.e., specified value)

$E_s$  = elastic modulus of steel

$D'$  = center-to-center distance between the outer layers of longitudinal reinforcement in a rectangular section normal to axis of bending, or pitch circle diameter of the longitudinal reinforcement in a circular section, generally assumed to be 80 percent of overall beam depth or overall column diameter, and

$M_n$  = nominal yield moment (theoretical yield strength) of the member.

**TABLE 5-7 - COMPONENT RIGIDITIES**

Component	Flexural Rigidity	Shear Rigidity	Axial Rigidity
Reinforced concrete columns, beams and caps where cracking (but not hinging) is expected	$0.5 E_c I_g$	$0.4 E_c A_w$	$E_c A_g$
Prestressed concrete beams, caps and piles where cracking is not expected	$E_c I_g$	$0.4 E_c A_w$	$E_c A_g$
Concrete columns, piles and walls where plastic hinging is expected	$M_n D' / 2\varepsilon_y$	$0.2 E_c A_g$	$0.5 E_c A_g$
<p><b>Note:</b> <math>E_c</math> = elastic modulus of concrete  <math>I_g</math> = moment of inertia using gross dimensions  <math>A_w</math> = shear area of column or beam  <math>A_g</math> = cross-sectional area of column or beam using gross dimensions  <math>M_n</math> = nominal moment capacity of column or beam  <math>D'</math> = distance between outer layers of longitudinal reinforcement, and  <math>\varepsilon_y</math> = yield strain of steel reinforcement.</p>			

Thus the effective flexural rigidity of a severely cracked structural concrete column is:

$$E_c I_{eff} = \frac{M_n D'}{2\varepsilon_y} \quad 5-62$$

This rigidity will generally be somewhat less than  $0.5 E_c I_g$  ( $I_g$  is the moment of inertia of the gross, uncracked section), which is a commonly assumed value for reinforced concrete members, when only a moderate amount of cracking and no plastic hinging is expected.

Table 5-7 also lists effective values for the shear and axial rigidity of cracked and uncracked reinforced concrete beams and columns with and without plastic hinges. In addition, the torsional stiffness of a cracked reinforced concrete column may be taken as 20 percent of the uncracked value.

For a displacement capacity assessment (pushover method), the strength of structural steel components in the model should be based on their expected plastic capacity. The flexural strength of reinforced and prestressed elements should be based on the expected material properties of the steel and concrete. The objective here is to determine the displacement at which the inelastic components reach their deformation capacity. The deformation capacity is usually expressed in terms of a maximum plastic rotation of hinge zones. The maximum deformation capacity is the sum of the deformation at yield and the plastic deformation.

The stiffness of other elements that are not subjected to inelastic response and damage should be based on elastic properties, including the effects of concrete cracking. The stiffness of pier caps should be included in the model. Pile caps and joints in reinforced concrete substructures may be assumed to be rigid.

### **5.6.5 Modeling of In-span hinges and Expansion Joints**

Modelling expansion joints and in-span hinges is a 2-step process. First, a compression model is used that assumes the joint at the bearing or hinge is closed and can transfer longitudinal forces. Then, a tension model is used that assumes the joint or hinge is open and cannot transfer longitudinal forces. The stiffness of restraining devices, such as cable restrainers or shock transmission units, is included in the tension model. Two separate analyses are run, one for each model, and the larger value for a particular force or deformation is used in design.

The use of compression and tension models is expected to provide a reasonable bound on forces (compression model) and displacements (tension model). A compression model need not be considered for expansion bearings if calculations show that longitudinal forces cannot be transferred through the superstructures at the bearing.

### **5.6.6 Modeling of Bridge Superstructures, Skew and Curved Geometry**

The stiffness of the superstructure should be consistent with the load path (Section 4.2.2.2) including consideration of composite behavior between girders and decks, and the effective width of the superstructure components that are monolithic with the piers.

For a stick model of the superstructure, the stiffness can be represented by equivalent section properties for axial deformation, flexure about two axes, torsion, and possibly shear deformation in two directions. The calculation of the section stiffness should represent reasonable assumptions about the three-dimensional flow of forces in the superstructure, including composite behavior.

For small skew angles the effect of skew can be neglected in the model of the superstructure. However, for larger angles, the geometry of the connection between superstructure and piers must be explicitly included.

For reinforced concrete box girders, the effective stiffness may be based on 75 percent of the gross stiffness to account for cracking. For prestressed concrete box girders, the full gross stiffness should be used. The torsional stiffness may be based on a rational shear flow without reduction due to cracking. The flexural stiffness of the superstructure taken about a transverse axis should be reduced near piers when there is a moment transfer between the superstructure and pier because of shear lag effects. The reduced stiffness should be used in modeling the superstructure.

### **5.6.7 Modeling of Bridges with Imposed Support Displacements**

In general, the effect of gross soil movement and liquefaction should be included in the analysis. However, the need for sophisticated modeling of foundations and abutments depends on the sensitivity of the structure to foundation movements and the degree of conservatism that can be tolerated in the calculated forces. When gross soil movement or liquefaction is possible, and an analysis is required, the model should represent the change in support conditions and additional loads imposed on the substructure due to soil movement.

When the results of a seismic analysis are expected to be sensitive to foundation properties, these properties should be bounded between upper and lower limits of strength and stiffness and multiple analyses carried out. Strength and stiffness values should, however, be consistent with the expected

deformations of the soil and the goals of the analysis. The sensitivity of results to the assumptions made about these properties may then be used to direct site investigations for the bridge under consideration.

### **5.6.8 Modeling of Bridges with Partially Submerged Members**

The seismic response of a bridge with piers in deep water is affected by the hydrodynamic mass of a volume of water that is forced to move with the piers. A reasonable estimate of the hydrodynamic added mass is the mass of a cylinder of water of diameter equal to the column width perpendicular to the direction of motion and length equal to the immersed depth. This mass should be added to the mass of the pier when modeling the mass of a bridge (Section 5.6.2). For circular columns this effect is sufficiently small to be neglected. Since the immersed depth may vary with time, upper and lower bounds on the effective pier mass should be considered in the analysis.

### **5.6.9 Representation of Damping**

Energy dissipation in a bridge, including that developed by the footings and abutments, may be represented with sufficient accuracy by viscous damping. The selection of an effective viscous damping ratio depends on the type of dynamic analysis and the configuration of the bridge. In an elastic response spectrum analysis, this ratio is based on the energy dissipation due to small-to-moderate deformations of the members and soil.

Damping may be neglected in the calculation of natural frequencies and associated mode shapes. The effects of damping should be considered when the dynamic response for seismic loads is considered. This is usually done by scaling the earthquake response spectrum for the correct amount of damping. In time history solutions, Rayleigh damping is typically used to permit different levels of damping in different modes. (Rayleigh damping is a combination of mass and stiffness proportional damping. See Chopra 2012.)

Suitable damping values may be obtained from field measurements of induced free vibrations or from forced vibration tests. In lieu of measurements, the following values may be used for the equivalent viscous damping ratio:

- Concrete bridges: 5%
- Welded and bolted steel bridges: 2%, and
- Timber bridges: 5%.

For a single-span or two-span bridge with abutments that are expected to develop significant passive pressure in the longitudinal direction, a damping ratio of up to 10% may be used for the longitudinal vibration modes.

Equivalent viscous damping may be used to represent the energy dissipated in the cyclic loading of members beyond yield, but only when a secant stiffness model is used for the entire bridge. For single-degree-of-freedom models, the equivalence can be established within a satisfactory degree of accuracy.

## **5.7 SUMMARY**

Various analytical methods have been presented in this chapter for the purpose of estimating the force and displacement demands on a bridge during an earthquake. These methods range from approximate to rigorous, and from simple to complex. Most assume that a bridge remains elastic (or essentially elastic) during an earthquake, but as noted in Section 4.1, this is frequently not the case. It is uneconomic to design a bridge to perform elastically during moderate-to-large earthquakes and the results of elastic analyses must be modified during design to account for the expected nonlinearity (inelasticity), as discussed in the Chapter 6. In recent years explicit nonlinear methods have become available that give consistently reliable results and these have also been presented. Both approximate and rigorous methods have been summarized. One is an equivalent static method and the other a nonlinear dynamic (time history) method. In addition to explaining response spectrum and time history methods for uniform ground motion, a method for handling spatially varying ground motion (multiple support excitation) has also been summarized. Limitations on the applicability of all methods have been discussed.

All but the simplest of the methods explained in this chapter, require computer software for their implementation. It follows that, in practice, a designer need not be intimately familiar with the details of each method since these have been coded into commercially available software. Instead a designer needs to know the relative merits of each method and when they should (and should not) be used. Furthermore, the designer is responsible for developing the physical model of the bridge to be analyzed, and this should be done with great care. For this reason advice on modeling has been given in this chapter. Topics covered included the distribution of mass and stiffness, the modeling of structural members, connections, foundations, abutments, in-span hinges and expansion joints, and the representation of damping. Bridges with skew, curvature, partially submerged piers, and imposed support displacements have also been discussed.

For reasons of limited space, and the fact that analytical software is readily available, the material in this chapter has focused on the principles of each method, and not the details. These may be found in textbooks on structural dynamics and bridge design.



## CHAPTER 6

### BEHAVIOR OF INELASTIC BRIDGES

#### 6.1 GENERAL

The purpose of this chapter is to provide background information and calculation methods to support the design of bridge structures that are intended to respond inelastically to large earthquakes. As outlined in Chapter 4, inelastic ductile action has the advantages of limiting the inertial forces that must be accommodated, but with the penalty that some damage is incurred. This approach is acceptable if, and only if, we can reliably design bridges to deliver ductile inelastic response. The details of how such action is obtained and how we quantitatively predict such action is the focus of this chapter. Chapter 4 discussed the response of bridges as a whole, including load paths and preferred modes of behavior. Chapter 5 discussed methodology for estimating the demands that earthquakes can induce in bridges, and this chapter illustrates how the capacity of inelastic structures is provided and estimated.

The first section of this chapter presents measured laboratory response of bridge substructure elements, including reinforced concrete columns and walls, subject to inelastic lateral loading similar to the loading an earthquake would induce. Various details are included to illustrate preferred performance and to illustrate performance that should be avoided or suppressed. The second section deals with methods for estimating the inelastic response demands that a given structural element will need to endure during a large earthquake. These methods involve empirical procedures for modifying elastic response results, which are relatively simple to develop, in order to estimate the response of the same structure when it responds inelastically. The third section of this chapter provides an overview of the procedure for calculating inelastic force vs. displacement relationships for yielding substructure elements such that a displacement capacity may be estimated. Finally, the last section provides an overview of relationships, developed from databases of test and analytical results, which provide estimates of inelastic displacement capacities for different limits states. Such relationships are used in the Guide Specifications to simplify the determination of displacement capacity.

The material covered in this chapter is applicable to both the LRFD *Bridge Design Specifications (LRFD Specifications)* and the AASHTO *Guide Specifications for LRFD Seismic Bridge Design (Guide Specifications)*. The applicability to the *LRFD Specifications* is largely as background explaining the

necessity for the prescriptive detailing and other prescriptive controls that are imposed. For the *Guide Specifications*, the material in this chapter serves as background and a primer on how to apply the displacement calculation methods that form the basis of the *Guide Specifications* approach. The actual application of the two design methods is contained in Chapters 7 and 8. If we recall the three capacity design principles outlined in Chapters 1 and 4, the material in this chapter largely revolves around the second step, designing and detailing the elements, which have been chosen to be the inelastic elements, to be adequately ductile and able to accommodate the deformations that an earthquake will place on them.

## **6.2 MEASURED BEHAVIOR OF INELASTIC RESPONSE**

### **6.2.1 General**

Lessons learned from past earthquakes and research performed during the last three decades has added considerable knowledge about the behavior of individual components that are included in the system and are often expected to deform inelastically. This knowledge has led to the advancement of our design specifications, culminating in the two design specifications discussed in this manual. This section describes the fundamental characteristics of selected key components that are most commonly used in bridge construction for enhanced seismic resistance, and it reviews selected laboratory data to illustrate physically what performance is desired or is intended to be suppressed. The components discussed in this section do not represent an exhaustive list of elements requiring adequate inelastic cyclic capacities to resist seismic loading. Today research reports covering the seismic testing of specific structural elements or systems are available from a number of different agencies, both federal and state. Many of these are available for download and can be used to assist engineers in development of specific designs. For this manual, the selected components for discussion are:

- Circular and rectangular columns
- Columns reinforced with interlocking hoops or spirals
- Columns with integral or non-integral flares
- Pier walls
- Shear keys

Identifying, controlling and quantifying the elastic and post-elastic (inelastic) behavior of these components is essential for our seismic design approaches, which are predicated on repeatable and reliable inelastic response. Beginning in earnest in the 1950s, experimentation to support the development of strength design began to adequately characterize the post-elastic response of structural elements. The notion of ductility as a desirable inherent property of structural elements gained widespread acceptance. Then the 1971 San Fernando earthquake damaged a number of bridges, some of which were relatively new and designed to the latest specifications. This experience initiated a flurry of experimental work to improve the seismic performance of bridges, and this work has continued to this day, sustained by the continued learning process that each significant earthquake seems to reinvigorate. Today, bridge design practice is supported by ever more in-depth research and work to verify the expected response of bridge components and the overall earthquake systems, as discussed in Chapter 4.

### **6.2.2 Circular and Rectangular Tied Reinforced Concrete Columns**

Experience and research has shown that transverse reinforcement in the zones of yielding is critical to the successful performance of reinforced concrete columns during earthquakes. Transverse reinforcement serves to confine the main longitudinal reinforcement and the concrete within the core of the column, thus preventing buckling of the main longitudinal reinforcement and the severe loss of compression strength in the concrete. Additionally, transverse reinforcement is effective as shear reinforcement and increases the shear capacity, which is critically needed for capacity protection of reinforced concrete columns.

Modern bridge design standards such as the LRFD *Bridge Design Specifications* require minimum transverse confinement reinforcement and sufficient shear reinforcement to resist the shear forces developed by the formation of plastic hinges. Special attention is also always given to the reinforcement details to ensure that transverse reinforcement remains effective during the cyclic loading that occurs during large earthquakes.

Unfortunately, prior to 1971 the transverse reinforcement placed in most bridge columns was totally inadequate by today's knowledge and current design provisions. For example, a typical pre-1971 AASHTO detail consisted of transverse hoops of ½ inch diameter steel bars (No. 4 bar) spaced at 12 inches on center. Hoops were lap spliced and crossties were not required to support rectangular hoops at intermediate points away from the member corners. The column damage suffered during the San Fernando earthquake demonstrated the inadequacy of this type of detailing as shown in Figure 6-1.



Figure 6-1 Poorly Confined Column in 1971 San Fernando Earthquake

In addition to poorly detailed transverse reinforcement, pre-1971 columns often contained a longitudinal bar lap splice just above the footing or foundation level. This location will often experience high flexural demands and potentially inelastic demands (rotation). Damage to lap splice locations was observed and subsequent testing of poorly confined columns with lap-spliced reinforcement at the base of the column showed a reliable displacement ductility capacity of only 1.5 (i.e. displacement capacity equal to 1.5 times the yield displacement) before degradation began to take place. Once the degradation (loss of cover in the splice zone) began, the deterioration of lateral resistance was rapid, and converges on the lateral capacity of the concrete alone. This is not acceptable performance.

The poor hysteric behavior of such a column is shown in Figure 6-2. In this figure, the degradation of strength is evident by the reduction in maximum lateral resisting force as the displacement or drift demand is increased. Additionally, the pinched shape of the load-displacement “hysteresis” loops is undesirable and indicative of the poor energy dissipation capacity of columns with lap splices. Effectively, the “unconfined” cover concrete spalls away and leaves the longitudinal bars unable to transfer tensile forces through the splice. For a single column, cantilever pier such deterioration could lead to stability problems and potential collapse. For multi-column piers serious problems could also arise, even though there is more redundancy than for single-column piers.

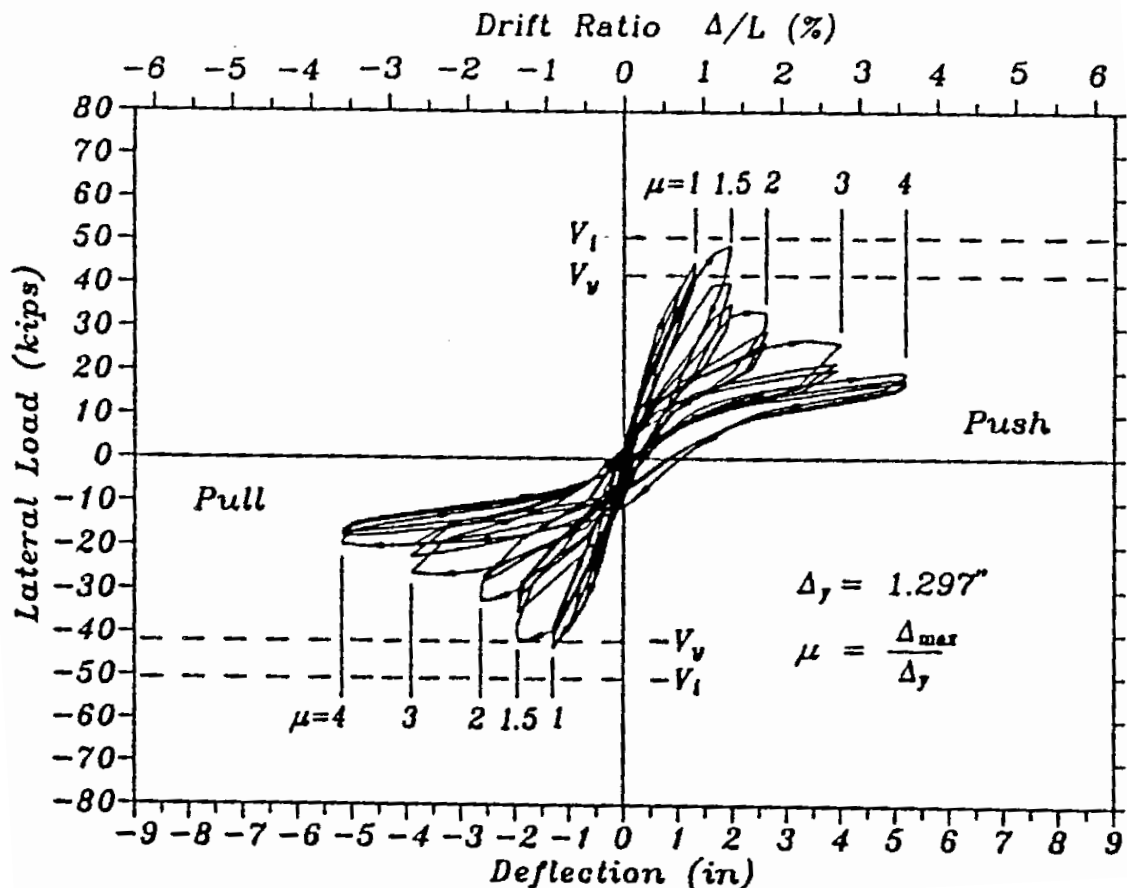


Figure 6-2 Poorly Confined Column with Lap Spliced Longitudinal Reinforcement at the base (Priestley, Seible and Chai, 1992)

The performance of the concrete, itself, is highly dependent on the amount of confinement reinforcement present. Confinement reinforcement affects the stress-strain curve for concrete, enhancing both the strength and the deformability (ductility) of the material as shown qualitatively in Figure 6-3. In earthquake engineering, the large increase in deformation capacity is extremely important. If concrete strains are limited to 0.003 or 0.004, as they are for non-seismic design, adequate ductility capacities in high seismic areas cannot be achieved. Instead, the increase in ductility capacity provided by confinement is exploited. In reinforced concrete structures, confinement is supplied passively by closely spaced spiral, hoop or tie reinforcement. When the concrete section is under compression, Poisson's effect will produce lateral expansion as shown in Figure 6-4. The stiffer confining reinforcement restrains this expansion, thereby exerting a confining pressure, which then enhances the concrete's strength and deformation capacity.

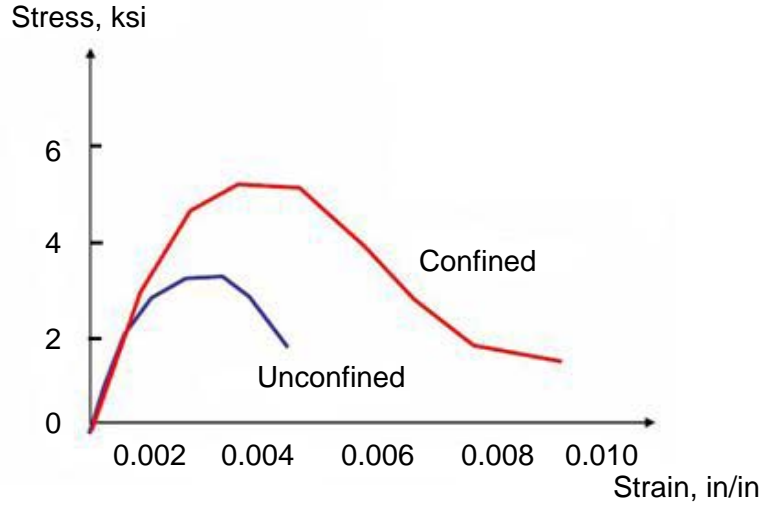


Figure 6-3 Stress vs. Strain Curve for Unconfined and Confined Concrete

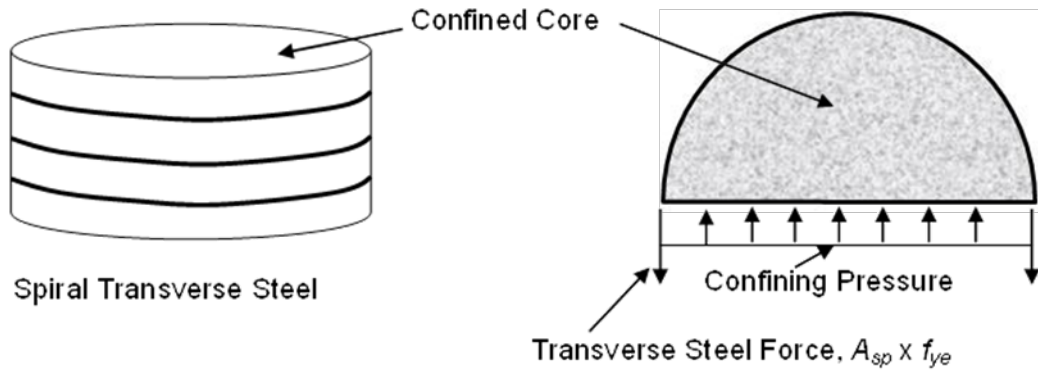


Figure 6-4 Poisson's Effect on Confined Concrete Columns in Compression

Consequently, both the *LRFD Specifications* and *Guide Specifications* have detailing requirements for the arrangement of the transverse reinforcement to ensure adequate confinement for seismic resistance as illustrated in Figure 6-5. The most efficient type of confining reinforcement is circular hoops or spiral reinforcement as shown schematically in Figure 6-5. The confinement provided by these arrangements not only enhances the concrete properties, but it also ensures that the longitudinal steel will act compositely with the concrete, even after loss of the exterior concrete. The cover concrete tends to spall off the section under high strain demands, because it is not confined. Once this shell of concrete is gone

or damaged, the main bars must be prevented from buckling and they must still act in concert with the core concrete, which is confined. Also, the transverse steel must be adequately developed by anchoring the tails of the bars back into the core concrete or welding the bars together. The close spacing of transverse steel elements with their confining effect is required not only across the section as shown in the figures, but also along the length of the section (along the length of the member). Attention to the details of the configuration of the transverse steel is one of the most important elements of a successful seismic design.

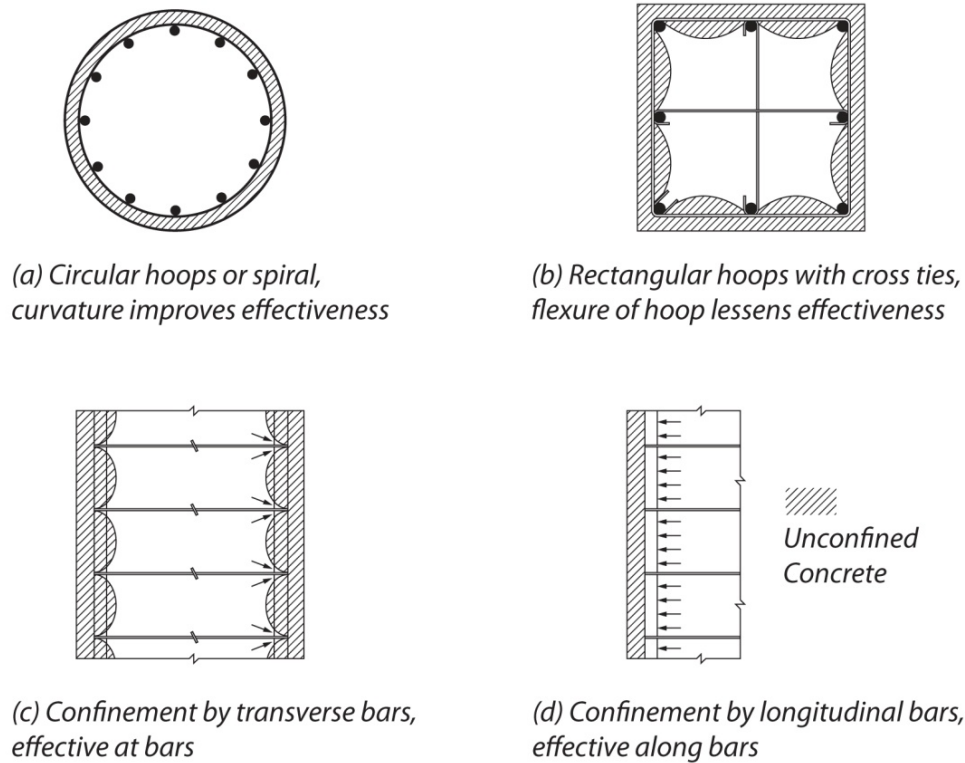


Figure 6-5 Examples of Effective Confinement (after Paulay and Priestley, 1992)

Laboratory tests have shown that closely spaced rectangular ties enhance the strength and ductility of concrete, although not as effectively as circular spirals. Tests by Chan (1955) suggested that when considering strength enhancement, the efficiency of square ties may be 50% of that of the same volume of circular spirals. This is because rectangular ties apply only a confining pressure near the corners of the ties, since lateral pressure from the concrete will cause lateral bowing of the tie sides, whereas circular spirals and hoops, because of their shape are capable of applying a uniform confining pressure all around

the circumference. With the addition of cross-ties, the efficiency of the ties is improved, although it never reaches that of the spiral or circular hoop.

However, testing has verified that a significant improvement in the ductility of the concrete resulted from the use of closely spaced rectangular ties. In high seismic regions, the use of circular columns or rectangular column with interlocking spirals or hoops is most reliable as discussed further in Section 6.2.3.

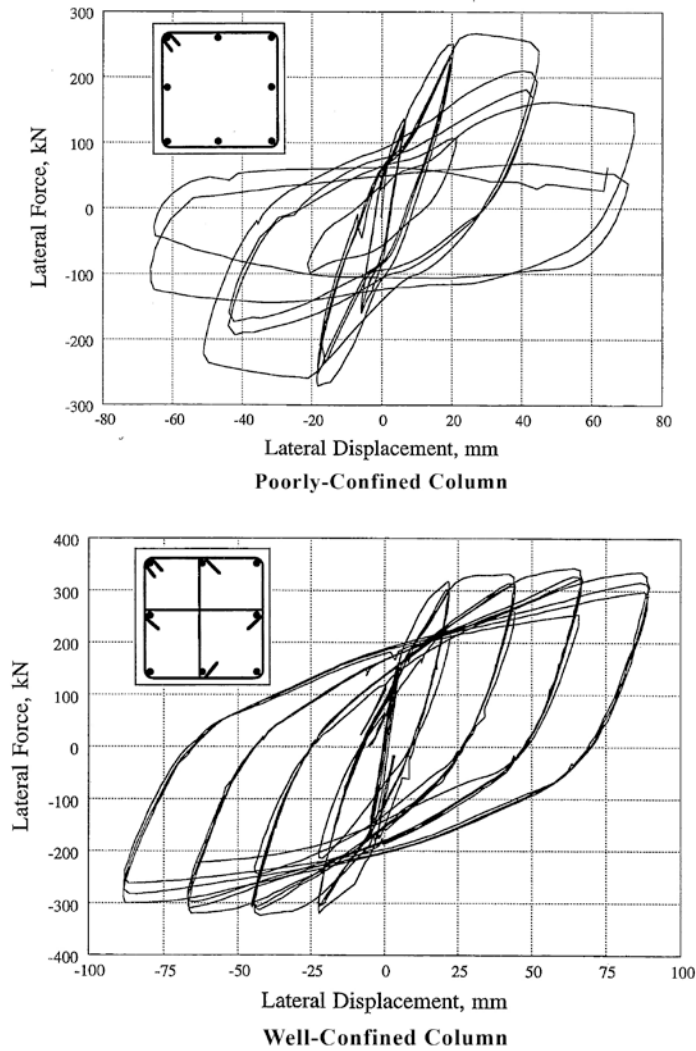


Figure 6-6 Hysteretic Behavior of Poorly and Well Confined Square Reinforced Concrete Columns

The above descriptions and figures largely are for axial compressive loading. However, the same improvements from confinement extend to flexural loading, because the compression portion of a

flexurally loaded element experience the same deterioration effects if confinement is not present. For example, Figure 6-6 illustrates the behavior of two identical column cross-sections. The sections are for cantilever columns loaded laterally. The total area of transverse reinforcement is the same for both columns; however, one column has no crossties. For the section where no crossties are provided, there is significant loss of stiffness and strength under cyclic loading as shown in Figure 6-6, where the maximum force attained for each loading cycle is less than the previous cycle. The addition of crossties, one in each direction, provides a tremendous benefit in maintaining the strength of the section as shown in Figure 6-6 owing to the confinement effects described above. In the second figure each loop nearly overlays the previous one, which indicates preservation of strength and energy dissipation capacity.

In order to ensure that the response of a concrete column under lateral loading is adequately robust and ductile, special reinforcement detailing is required. The amount of specialized detailing required depends on the expected seismic deformation demands. Therefore, in lower seismic regions the detailing can be less rigorous. This is particularly true for confinement effects, but less so for shear. Transverse steel required to provide adequate shear resistance must always be provided. Shear failure in a column can lead to abrupt loss of gravity load carrying capacity (collapse) as shown in Figure 6-7.



Figure 6-7 Shear Failure of a Column in the 1971 San Fernando Earthquake

Figure 6-8 and Figure 6-9 show typical transverse steel arrangements for a single column bent and a multi-column bent, respectively. The increased density of transverse reinforcement to provide confinement in the locations where inelastic action is expected is shown at the top and bottoms of the columns. These areas are known as plastic hinging zones and the length over which these zones extend are typically taken as the maximum of:

- a prescribed multiple of the cross sectional dimension in the direction of bending
- the length of column over which the moment demand exceeds some fraction of the maximum plastic moment, sometimes expressed as a fraction of the length of the column, or
- the analytically calculated plastic hinge length discussed later in this chapter

The use of several different dimensions is meant to ensure that no unforeseen combinations of moment gradient along the member or member sizing result in inadequate coverage of the confinement zones for inelastic action.

Splicing of column vertical reinforcement is another important detailing issue in the higher seismic regions. Splicing should be avoided if possible, or at a minimum, splice locations should be kept well away from member regions expected to experience inelastic action. In general, splices should be in locations where the flexural or tension demands never approach yield under seismic loading. As with other loading types, staggering of spliced bars is better than splicing all at one location, but this can often be problematic with the sharp moment gradients that occur with lateral loading. Typically, column cages with height less than 60 feet can be constructed with no splicing of longitudinal reinforcement. For column cage reinforcement greater than 60 feet, allowable splice regions depend on the column configurations, such as multi-column bents, moment-reducing (pin) detailing, or fixity to the foundation (See Figure 6-8 and Figure 6-9). In general, the longitudinal steel would be spliced in the middle regions of the column, although with a pin detail at the base, splicing could occur closer to the bottom.

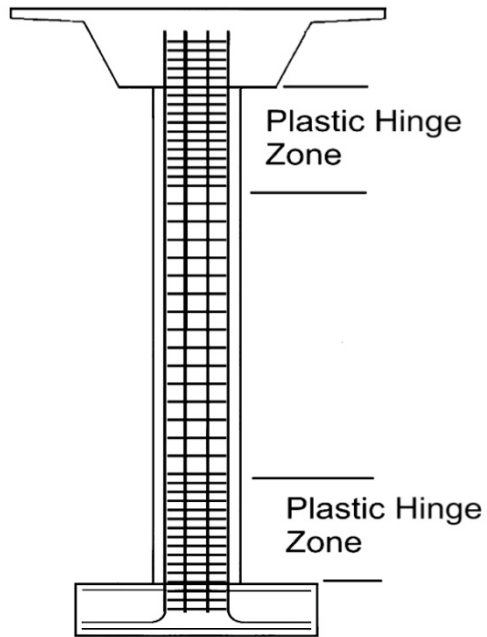


Figure 6-8 Single Column Lateral Reinforcement in Plastic Hinge Zone Region

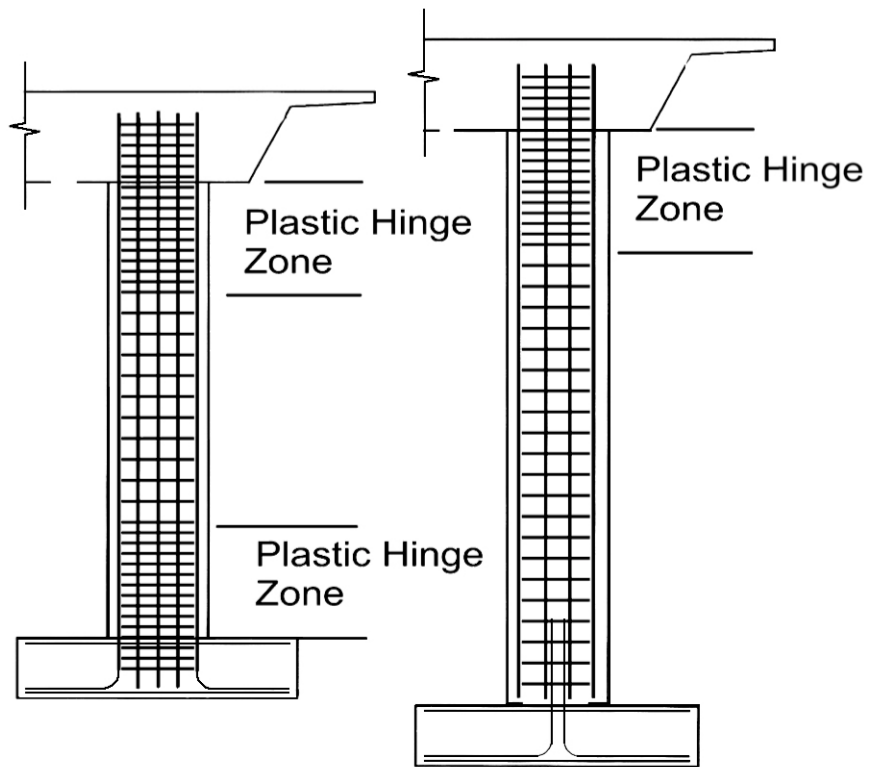


Figure 6-9 Multi-Column Lateral Reinforcement in Plastic Hinge Region

### 6.2.3 Columns with Interlocking Hoops or Spirals

As mentioned in the previous section, spiral or circular hoop reinforcement can be more effective than rectangular ties. Thus for square or rectangular columns, the improved performance from a spiral or circular configuration can be largely achieved by the use of so-called interlocking spirals (or hoops) (Sanchez et. al., 1997). Therefore, double or triple interlocking spirals are being used as transverse reinforcement in bridge columns especially in large rectangular cross sections not only because they provide more effective confinement than rectangular hoops but also because interlocking spirals make the column fabrication process easier as shown in Figure 6-10 and Figure 6-11.

The most critical design parameters of reinforced concrete columns with interlocking spirals are the level of average shear stress, and the horizontal distance center-to-center of the spirals. The average shear stress is defined as the ratio of the plastic shear demand over the effective shear area. The effective shear area is taken as the gross area multiplied by 0.8. In addition, effect of horizontal crossties connecting the spirals is deemed important in certain specific cases as mentioned below.

Figure 6-10 and Figure 6-11 show two types of columns with interlocking transverse spirals or hoops. The main vertical reinforcement is typically along the perimeter, although some vertical reinforcement is required in the interlocking portion to tie the overlapping spirals together. The vertical reinforcement, in the interlocking portion, is sized with respect to the size of bars used outside the interlocking portion. The vertical bars, in the interlocking portion, are not typically developed in the footing or the superstructure. The *Guide Specifications* addresses minimum requirements for detailing column with interlocking hoops or spirals, although the *LRFD Specifications* does not.

The lateral-load behavior of columns with interlocking spirals is shown in Figure 6-12 and Figure 6-13 (McLean and Buckingham, 1994). These two test specimens had spirals separated by  $1.2R$ , where  $R$  is the radius of one spiral. The first figure illustrates behavior when the section is flexurally controlled (i.e. the shear strength exceeds the lateral shear required to yield the section). The performance of this test specimen is seen to be adequate by the repeated ability to attain large inelastic displacements without significant loss of strength. However, the test results in the second figure illustrate the tendency of columns to lose their lateral strength at low ductility demands, if the shear strength is not adequate. In this second case, the shear resistance gradually degraded as inelastic deformations accrued, and this behavior is to be avoided because it could lead to failures as illustrated in Figure 6-7.

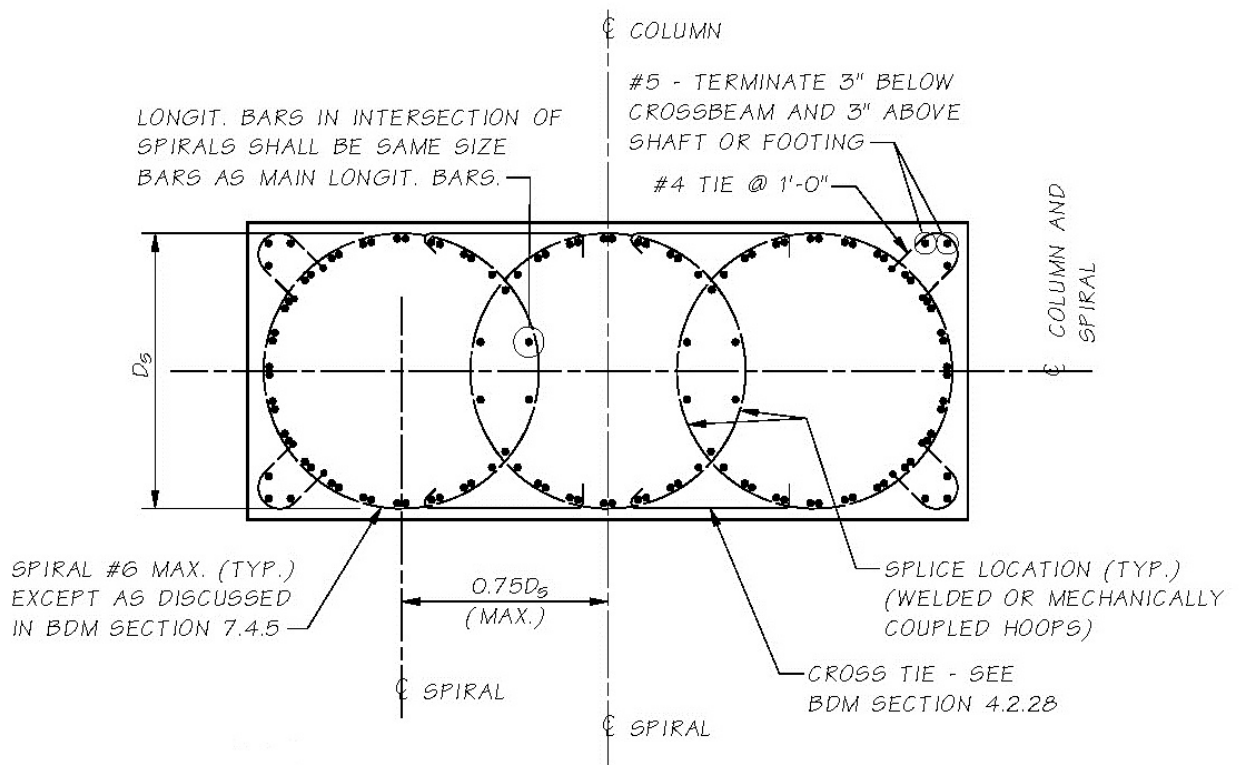


Figure 6-10 Interlocking Spirals Column Section (WSDOT, 2014)

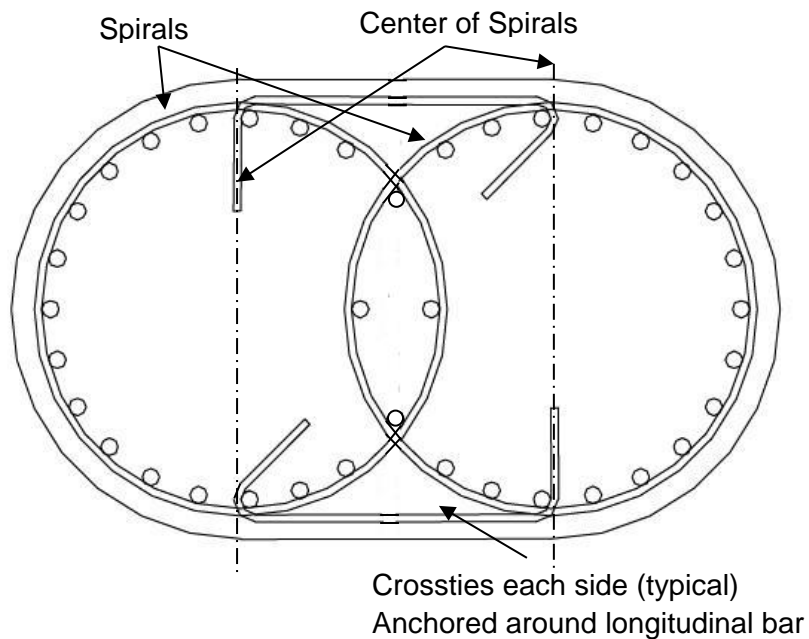


Figure 6-11 Interlocking Spirals with Crossties (Correal, Saiidi, and Sanders, 2004)

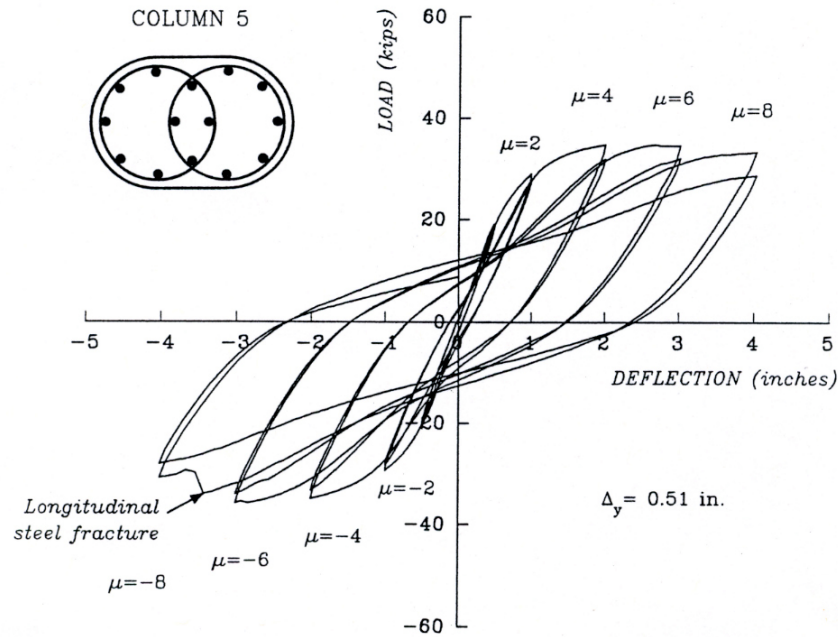


Figure 6-12 Flexurally Controlled Interlocking Spiral Test Results (McLean and Buckingham, 1994)

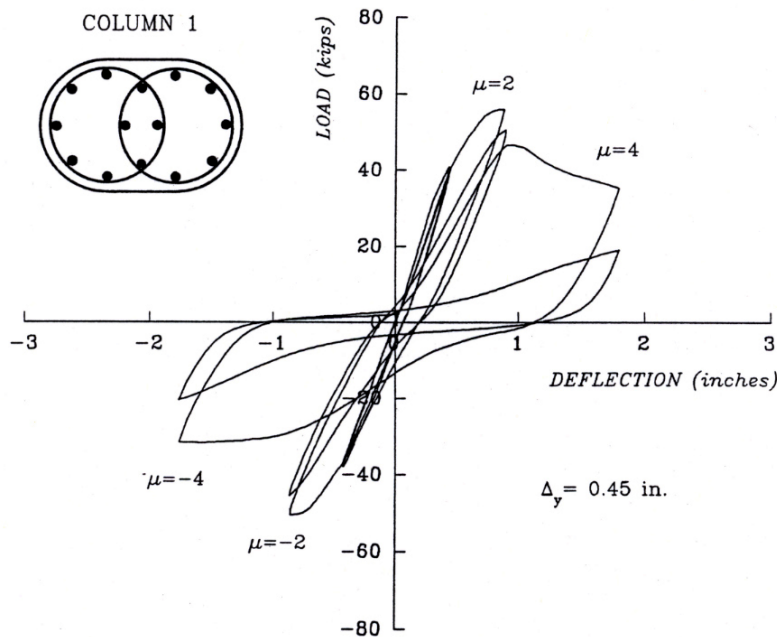


Figure 6-13 Shear Controlled Interlocking Spiral Test Results (McLean and Buckingham, 1994)

Columns subjected to high shear stress and center-to-center distance of  $1.5R$  are typically less ductile than columns with lower shear stresses and smaller center-to-center spacing. In columns with high shear

stresses – average shear demand on the effective cross section exceeds  $3\sqrt{f'_c}$ , crossties added along the sides are recommended regardless of center-to-center distance (Correal et. al. 2004). Horizontal cross-ties similar to the cross-ties shown in Figure 6-11 should be used. The spacing of the additional crossties can be taken as twice the spacing of the spirals. The maximum spacing of crossties should not exceed 2 times the spacing of the spirals. The crossties connecting the hoops reduce vertical cracks in the interlocking region in columns subjected to high average shear stress with center-to-center distance of  $1.5R$ .

Testing at the University of Nevada, Reno (Correal et. al. 2004) has shown that typical analytical models, based only on flexural deformation, underestimate the yield and ultimate displacements. This finding is important to consider for non-slender columns where this effect is most pronounced. The addition of bond-slip and shear deformation improved the correlation with the test results. Thus, the analytical displacement capacity of these types of columns developed solely based on flexural deformation tends to be overly conservative.

#### **6.2.4 Flared Columns**

The Northridge earthquake of 1994 revealed seismic performance problems with flared bridge columns. As seen in Figure 6-14, the SR 118 Mission-Gothic undercrossing suffered catastrophic damage due to problems inherent in its flared columns. Flared columns suffered severe damage during past earthquakes due to inadequate design assumptions and procedures. The erroneous assumption that flares, even nominally reinforced flares, will break away and thus will have no significant structural influence on the seismic behavior of a bridge, leads to designs that do not satisfy the seismic performance objectives. Some of the potential seismic issues with flared bridge columns are discussed below.

The increased size of the column's cross section in the flare region increases the column's flexural capacity. Even lightly reinforced flares contribute to a significant increase in the column's flexural capacity, because a concrete compression zone will occur outside of the column's confined core thus increasing the section's lever arm, and hence the moment capacity. This flexural capacity may return to that of the unflared column's, but only after the flare concrete has completely spalled off from the column. This was thought when the column has seen large rotations, and the flared cross section has seen large compression strains sufficient for concrete crushing. However, this spalling may not happen due to inelastic action occurring elsewhere, as discussed below.



Figure 6-14 Damage to Integral Flared Columns in the 1994 Northridge Earthquake (Nada, Sanders, and Saiidi, 2003)

Because of the increase in the column's flexural capacity in the flare region, a flexural hinge does not form at the level of shear calculated for the non-flared column. The additional shear and moment are transferred into the cap-beam. In many cases the cap beam will not have sufficient reserve strength to handle this increase in shear and moment demand. Therefore one of the possible seismic hazards of flared columns is damage to the adjacent members.

The increased shear demand due to the reduction of the column effective length must also be resisted by the column. The potential shear failure may occur at a reduced level of displacement ductility, after a flexural hinge has formed within the column, or in severe cases it may occur before a flexural hinge develops. This brittle shear failure with no ductility, dissipates little energy, and leaves the column unable to carry its required dead load. This undesirable mode of failure must be avoided.

In cases where the column initially has sufficient shear capacity to resist the increased shear demand, a plastic hinge may form away from its intended location near the soffit. In theory, the column's plastic hinge will form where the moment demand first exceeds the moment capacity. In flared columns this is away from the soffit near the bottom of the flare. If a plastic hinge forms away from the soffit, near the

bottom of the flare, the effective length of the column is reduced. This has two important implications. The first is that the effective column length is reduced, which increases the shear demands on the column. The second implication is that the reduction of the effective column length also reduces the bridge structure's displacement capacity.

New flared columns may be designed in either of two ways. The column flare may be designed integrally or monolithically with the cap beam, or the flare may be isolated from the cap beam. If the flares are designed integral with the cap beam, the flare geometry should be kept as slender as possible. If this solution is chosen, it must be realized that the moment necessary to induce plastic hinging will be greater than that of an equivalent non-flared column. Hence, the adjacent members must be designed with sufficient capacity to withstand the increased input forces and still remain elastic. Another consideration with this approach is that there may be non-structural damage to the lightly reinforced flares. Such damage will require repair after an earthquake, and the visible damage may result in a negative public perception of the safety of the structure. Accordingly, it is desirable to limit, or if possible avoid, unnecessary damage.

An important design consideration of columns with flares that are not isolated from the cap beam is that large inclined compression struts develop to transfer the compression resultants in the activated flare region around the gap in the soffit to the column/cap beam interface. Large tension forces develop in the flares to balance the inclined compression struts. This problem is solved by providing an increased level of transverse flare reinforcement to take these large tension forces. A volumetric reinforcement close to 0.5% is found to result in an acceptable level damage of the flare that would prevent failure of the flare. Due to the larger forces and detailing difficulties with monolithic flared columns, that form of flare is not the preferred design approach for new flared columns, especially in high seismic regions.

The preferred design solution is to isolate the flares from the cap beam using a gap at the top of the flare. Columns with isolated flares exhibit seismic performance that is similar to that of equivalent columns without flares. Figure 6-15 shows the progression of damage to isolated flared column in laboratory testing. Figure 6-16 shows flare configurations and the reinforcement detailing in the isolated flare. The flares are designed to terminate short of the cap beam. A gap of sufficient thickness is left between the flares and the soffit. The thickness of the soffit gap is determined by calculating the rotational demand on the plastic hinge, and ensuring that the gap does not close under the predicted maximum rotation of the hinge.

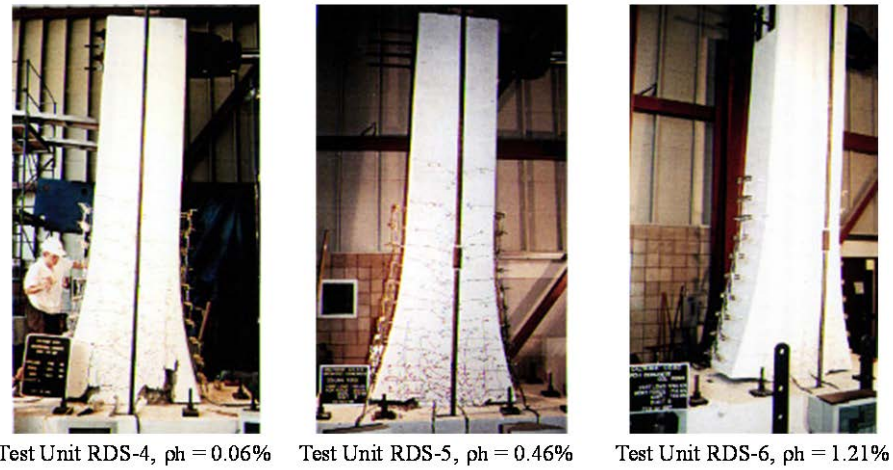


Figure 6-15    Damage to Isolated Flared Columns with 2 inch Soffit Gaps (Sanchez, Seible, and Priestley, 1997)

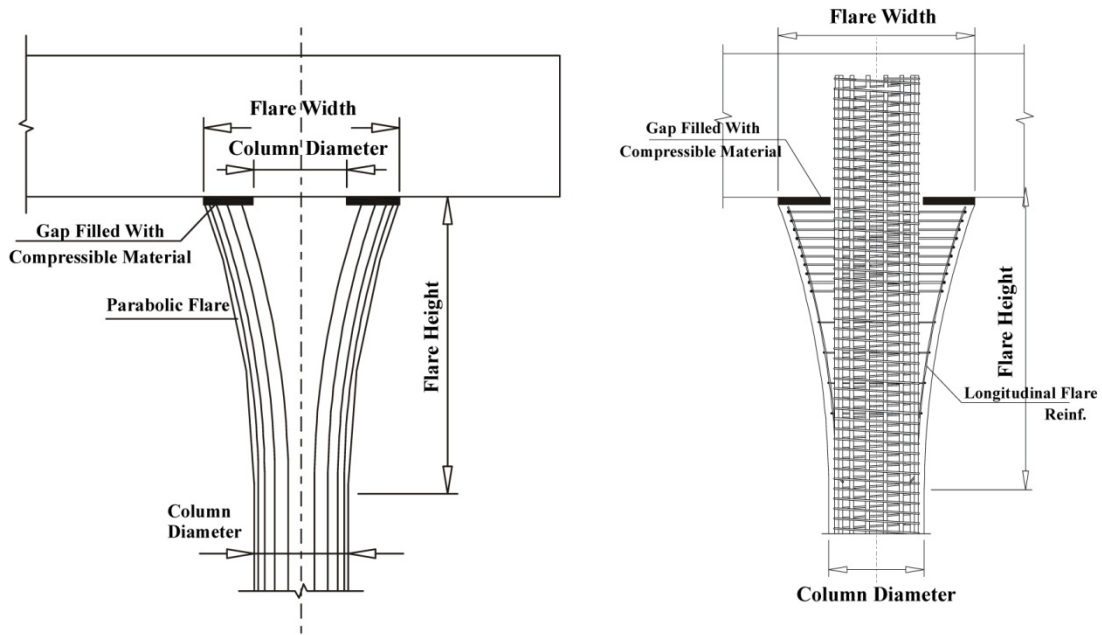


Figure 6-16    Detail of Reinforcement in Isolated Flared Column (Nada, Sanders, and Saiidi, 2003)

## 6.2.5 Pier Walls

Records of structural damage to bridges in past earthquakes have shown limited damage to pier walls. This is attributed to the relatively low axial load ratio (applied load/capacity of the cross-section) carried by pier walls in comparison with columns, the larger ductility of the pier wall than that exhibited by columns, and lastly, because bridges supported on pier walls are generally less common than those supported by columns, certainly in the western U.S. where the larger earthquakes have occurred in this country. Damage to masonry pier walls has been seen in other parts of the world following large damaging earthquakes, and masonry construction in higher seismic zones should be avoided. The discussion of this section concerns modern reinforced concrete wall performance.

Testing of pier walls conducted at University of California at Irvine (Haroun et. al., 1993) has shown great resistance to transverse as well as longitudinal loading. As pier walls structures are stiffer in the transverse direction, longitudinal response influenced by wall weak-axis flexural behavior will dominate the behavior of the structure even with skewed piers. In many cases, the response of a foundation with piles or shafts or a non-monolithic joint to the superstructure may also dominate the behavior, again producing response mainly in the longitudinal direction. In the strong direction, pier walls are proportioned for average shear stresses not exceeding  $8\sqrt{f'_c}$ . The ultimate shear demand in the wall is taken as the lesser of:

- the unreduced elastic force demand derived from analysis
- the ultimate strength in the foundation that can in turn transmit the forces back into the wall
- the ultimate strength of a connection between the wall and the superstructure

Testing of walls in the strong direction has shown an effective stiffness that is less than the stiffness calculated theoretically based on gross area and elastic shear modulus. The findings are illustrated in Figure 6-17 and translate into an effective shear stiffness that can be computed by reducing the elastic shear stiffness by the ratio of effective-to-gross flexural stiffness ( $EI_{eff}/EI_g$ ).

The current design requirements for bridge pier walls have improved the seismic performance of pier walls, specifically in the weak direction. These improvements include: increasing the steel ratios of the vertical and the horizontal reinforcement, placing the horizontal bars on the outside of the vertical bars, and extending the vertical bars into the foundation, thereby eliminating the need for lap splices. In

addition, crossties are now uniformly distributed along the wall height to improve their flexural strength and ductility in the weak direction.

Testing of walls in the weak direction has led to the following findings (Haroun et. al., 1994):

- A minimum displacement ductility factor of 4.0 was observed for all walls regardless of the density of the transverse ties. As shown in Figure 6-18 the walls with lower percentage of vertical reinforcement (“L” Walls, with 1.3 percent steel) exhibited higher ductility due to the ability of transverse ties to delay buckling of the vertical wall reinforcement.
- All walls with the higher reinforcement ratio (“H” Walls, with 2.3 percent steel) failed at nearly the same ductility level regardless of the distribution of the crossties. This is attributed to the observation that crossties in this case could not provide sufficient confinement to the pier wall section.
- Large lateral forces associated with bar lateral deformation were generated and transmitted to the crossties in the walls with the higher reinforcement ratio. These forces exceeded the ties’ capacity to prevent bar buckling. It is therefore recommended not to use the larger size bars for the vertical reinforcement.
- Failure of the crossties occurred by the opening of their ends. It is recommended that crossties with improved end details and a longer hook length be used in high seismic regions.

In summary, pier walls have shown ductile behavior in the laboratory and behaved well during past earthquakes. Current practice in high seismic regions still shows conservatism drawn from the assumption that weak axis behavior of walls is similar to column behavior; therefore, a higher transverse reinforcement ratio is used in potential plastic hinge zones as shown in Figure 6-19. This practice is relatively conservative in light of experimental data, however is considered an inexpensive insurance for attaining a reliable ductile behavior given the uncertainty of earthquake loading (Haroun et. al., 1994).

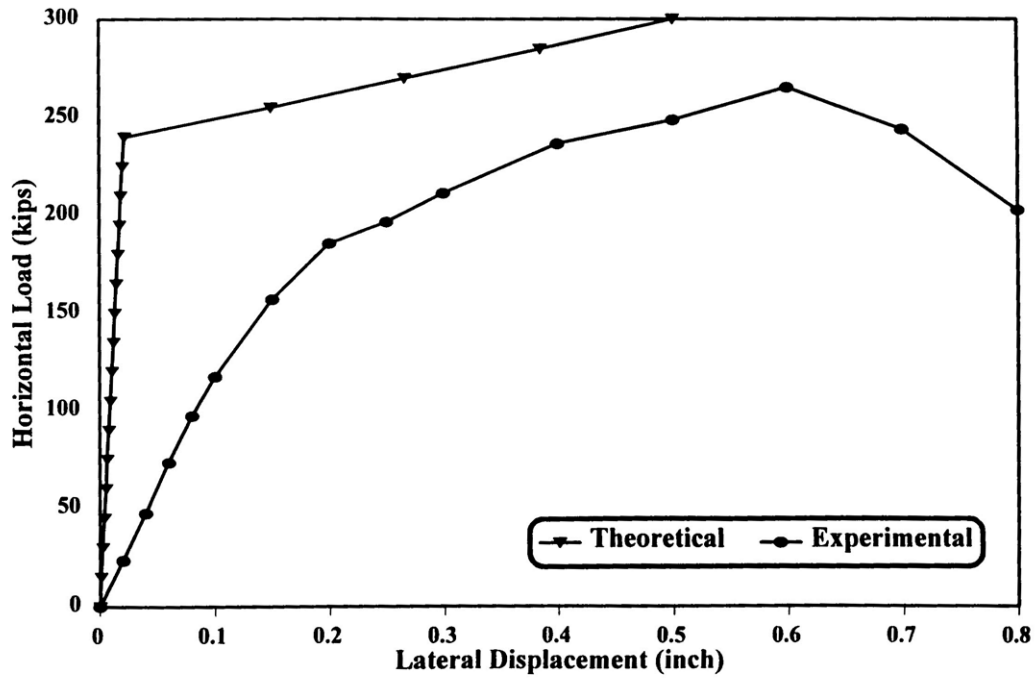


Figure 6-17 Load Versus Top Displacement of Strong Axis Pier Wall (Haroun et.al., 1993)

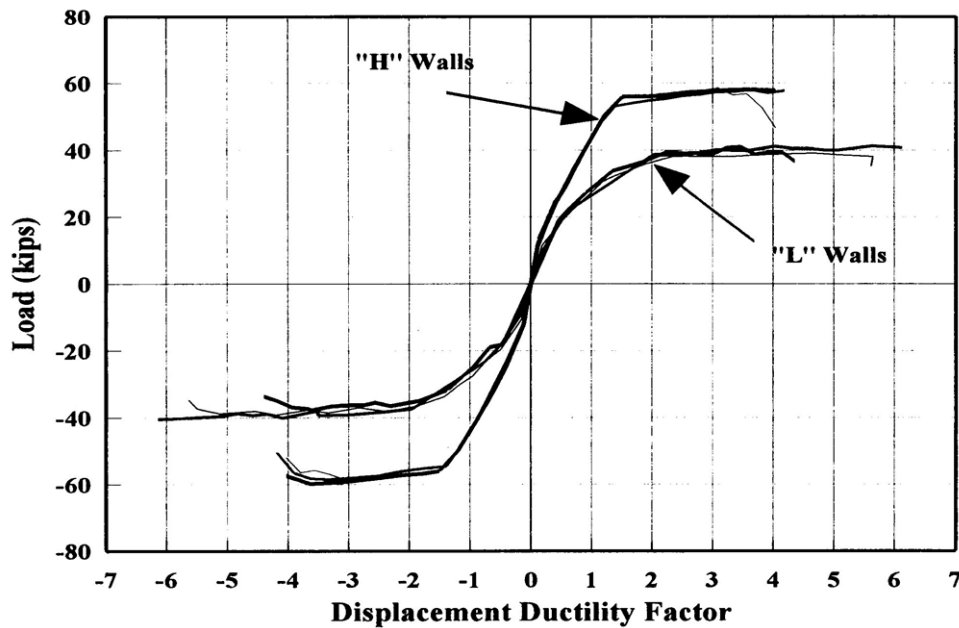


Figure 6-18 Force Displacement Envelope of Pier Wall Hysteresis Loops (Haroun et.al., 1994)

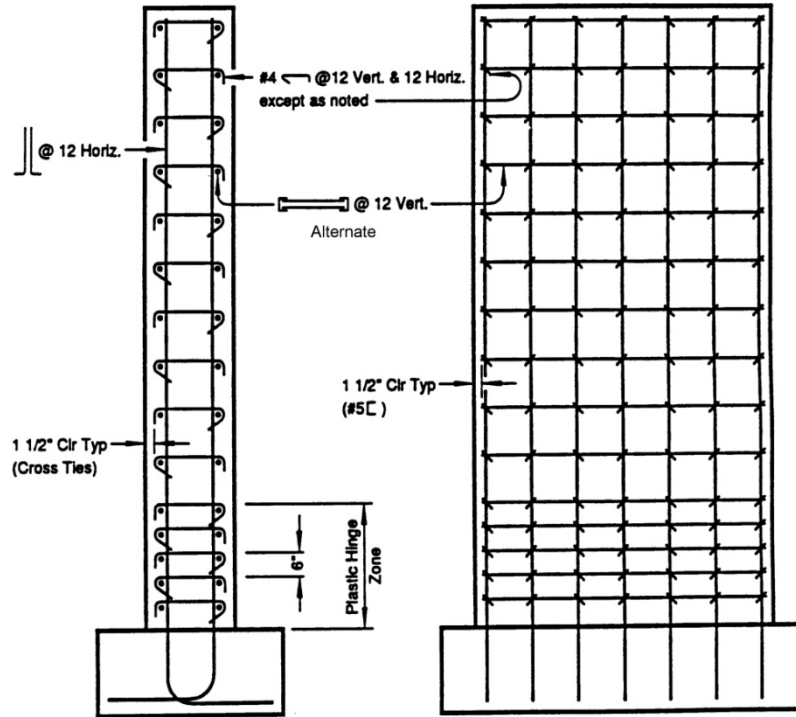


Figure 6-19 Lateral Pier Wall Reinforcement within the Plastic Region (Caltrans, 1999)

### 6.2.6 Shear Keys

Shear keys are commonly used at the abutments of small to medium span bridges to provide transverse connectivity for the bridge superstructure under lateral loads. They may also be used to transmit lateral loads at intermediate piers in structures that do not have an integral connection between the substructure and superstructure. Shear keys do not carry gravity loads, but in the event of an earthquake are required to transfer the lateral load from the superstructure to the abutment, to a pier or across movement joints of in-span hinges. It is also assumed in practice that once their capacity has been exceeded shear keys provide no further restraint (i.e. fuse) for the superstructure. Damage to shear keys under a major seismic event is permissible provided such damage will not result in collapse of the bridge or unseating of the superstructure.

Two types of shear keys may be used. Interior shear keys may be constructed within the width of the superstructure, and exterior shear keys may be provided at either side of the superstructure. Both types of shear keys have been tested by University of California, San Diego (UCSD) (Bozorgzadeh et. al., 2007 and Megally et. al., 2002). Generally, large exterior shear keys are only used at abutments. Interior keys,

which act in either direction transversely, are used within the width of the superstructure and because interior keys are not as accessible as exterior keys, it is recommended that such keys be avoided where access for repair may not be available, as is the case with box girders. Generally, interior shear keys that are used with I-girder type (open soffit) bridges are accessible for inspection and repair. Interior keys are also used to restrain girders supported on intermediate piers and thus are an important link to the load path carried from the superstructure to the foundation.

The mechanism used to carry shear across an interface between members connected with reinforcing bars is known as sliding shear friction. Extensive tests have been performed on pre-cracked or non-cracked sections to determine the performance of reinforced concrete sections using this mechanism. The aggregate interlock along the interface provides friction, with a passive normal force provided by the reinforcing steel that crosses the shear interface. For slip along the interface to occur with a rough surface, there is a tendency for the key to lift off the interface, which activates the shear friction reinforcement. A coefficient of friction is assigned based on the interface roughness, and this coefficient multiplied by the normal compressive force on the interface determines the shear resistance. For monolithic construction using normal weight concrete this coefficient is often taken as 1.4, reflecting the benefit of the rough surface.

Based on UCSD Testing (Megally et. al., 2002), the response of interior sacrificial shear keys can be characterized by several behavioral regions as lateral load to the key is increased. The first region has no load or stiffness, during which the response is controlled by the properties of any joint filler, such as expanded polystyrene, used to fill the gap between the shear key and the bridge superstructure. The next region is dominated by a strut-and-tie mechanism, which transfers the applied load to the abutment. High strength and stiffness characterizes this region, with the shear key remaining essentially rigid. This response is maintained under cyclic loading until the load reached its peak value. This value is most accurately calculated based on the cracking strength of the concrete. After the horizontal crack has propagated completely through the shear key, the response switches to a sliding shear friction mechanism. The vertical reinforcing bars of the shear key provide clamping forces between the shear key and the abutment stem wall or the pier cap. A high coefficient of friction is provided by aggregate interlock (Bozorgzadeh et. al., 2007).

As the loading cycles increase, the strength and stiffness degrade rapidly. Degradation of aggregate interlock reduces the coefficient of friction. Concrete spalling on the sides of the shear key exposes the outer reinforcing bars, thus reducing the clamping force available. The clamping force is further reduced

as fracture of the shear key reinforcement occurs. Although the contribution of each of these sources varies, the total degradation is found to decrease approximately linearly from the peak resistance.

Figure 6-20 shows a typical hysteretic response of shear keys. Results of tests show that the aspect ratio and reinforcement ratio have little effect on response of interior shear keys. All tests show the similar characteristics and magnitudes of response. The aspect ratio does, however, affect the degradation of the shear key resistance and observed damage levels, as the behavior transitions from shear dominant to flexurally dominant. Less degradation of the friction load under cyclic loading was observed for larger height-to-depth aspect ratios. Figure 6-21 shows four damage levels corresponding to yielding (Level II), initiation of local sliding mechanism (Level III), full development of mechanism (Level IV) and strength degradation (Level V). It is clear that the response of these shear keys is not particularly ductile, although there is significant resistance even at relatively large displacements. The levels of damage range from possible repair, minor repair, complete repair and full replacement. For capacity calculation related to load path in a shear key, it is important to consider an appropriate overstrength factor of a shear key as it affects the response of adjacent components. A value of 1.5 times the nominal interface shear strength of the shear key is used in the *Guide Specifications*. It should be recognized that yielding and damage accrual in shear keys is not intended to be a desired ductile energy absorbing behavior. Instead, such response is used to provide a fuse to protect adjacent elements. Once such fusing occurs, adequate support width will also be required to prevent unseating of the superstructure.

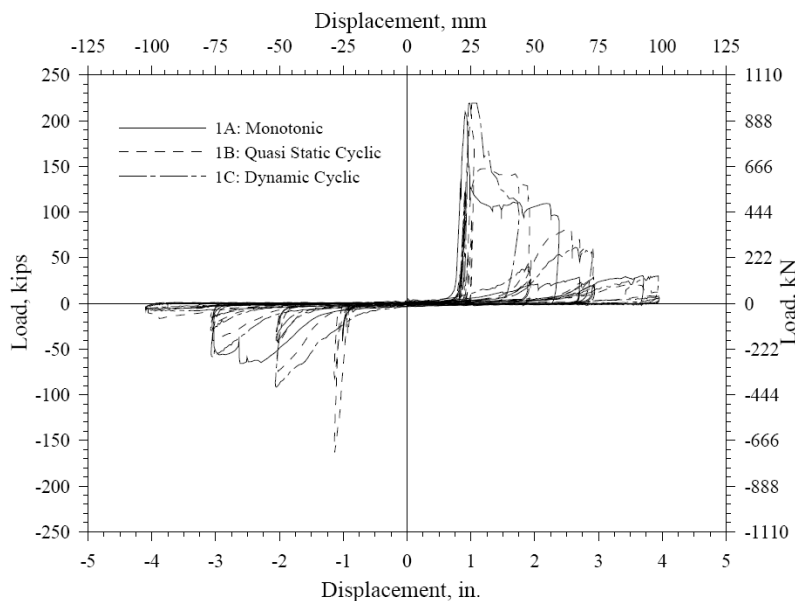


Figure 6-20 Load Displacement Curve for an Interior Shear Key (Megally et. al., 2002)

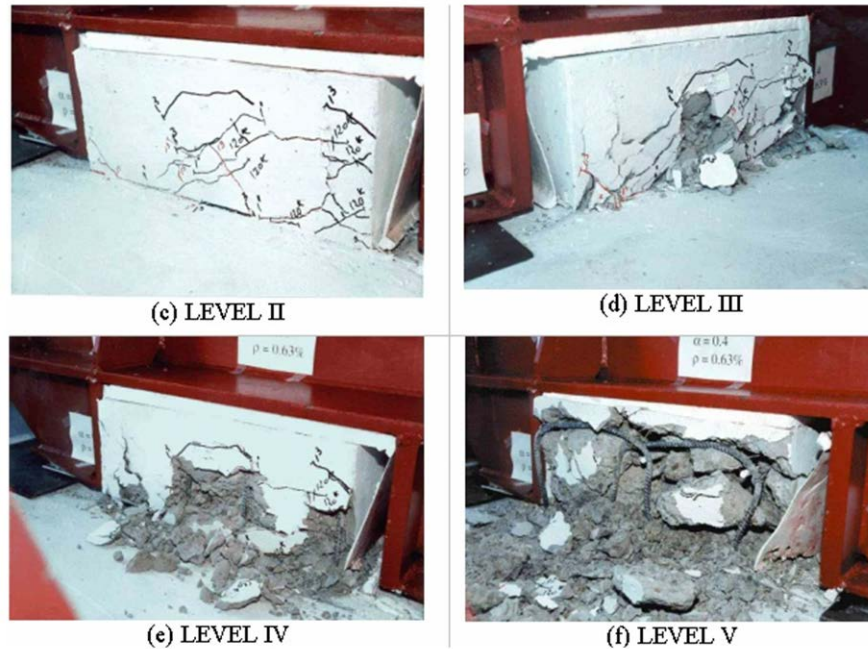


Figure 6-21 Shear Key Damage Levels (Megally et. al., 2002)

### 6.3 METHODS OF ESTIMATING BRIDGE RESPONSE USING ELASTIC ANALYSIS

#### 6.3.1 Estimating Inelastic Response Using Elastic Analysis

In this manual a recurring theme of modern seismic design of bridges is use of a yielding or inelastic structure to limit forces in the bridge, although these limited forces are accompanied by some damage. The analysis methods we often utilize are based on linear elastic (no damage) response that most bridge engineers are familiar and comfortable with. However, a structure that responds inelastically should ideally be analyzed using inelastic techniques, unless there are procedures available to estimate the inelastic response using elastic techniques. This is exactly what is done, except for more important critical/essential bridges that may be analyzed directly using inelastic time history techniques.

There are two primary methods for estimating the inelastic response of a structure using linear elastic analysis methods. One is an empirical method, often referred to as the Equal Displacement Method or Principle, although this is somewhat of a misnomer. The development of this method, which is the basis of bridge seismic design in accordance with the AASHTO specifications, will be described below in

detail. The other method, called the Capacity Spectrum Method, is often used with base isolation and other seismic design approaches where elements that add quantifiable damping to the system are used, although this is not a restraint to the use of the method. The capacity spectrum method is discussed in Chapter 5 and in Chapter 9.

In summary, the equal displacement method seeks to estimate the maximum displacement that a yielding or inelastic single degree of freedom (SDOF) system will experience, using an elastic analysis of the identical system without yielding. For this method to work best, the response should generally be in a primary or single mode of vibration. Likewise, the capacity spectrum method assumes a SDOF response and determines the inelastic response by using secant stiffnesses for the primary yielding members and additional viscous damping to represent the energy dissipation corresponding to yielding hysteresis. The two methods are independent of one another and should not be combined.

Early studies on seismic response focused on relatively simple systems. The determination of the elastic response of single-degree-of-freedom systems to earthquake records was discussed as early as 1941 (Housner). The idea that structures could be designed for forces less than those corresponding to elastic response was presented by Housner in 1956. Subsequently, Veletsos and Newmark (1960) emphasized using displacement demands in conjunction with target ductility factors to arrive at system strength. In 1960, Muto observed that the maximum inelastic displacements of single-degree-of-freedom systems were not significantly different from those of elastic systems having the same initial period and damping. In the same year, Veletsos and Newmark (1960) made a similar observation. These observations, made for a small number of inelastic SDOF systems, came to be known later as the “equal displacement rule.” Veletsos and Newmark also observed that for short period structures the equal displacement rule transitioned to an “equal energy rule”, whereby the equality was that at the maximum displacement the energy stored plus that dissipated was equivalent to that stored in the elastic system. This was the first recognition of an adjustment to the equal displacement rule. Notwithstanding, Muto concluded that the tendency for nearly equal displacements could suggest the use of a structural design method based on the maximum displacement.

Shimazaki and Sozen (1984) later determined conditions for which the equal displacement rule is applicable. They found that the equal displacement rule held for structures with vibration period greater than a characteristic period,  $T_g$ . For structures with initial period less than  $T_g$ , peak inelastic displacements were approximately equal to the peak displacements of elastic systems if the yield strength was sufficiently large. For weaker structures, the peak inelastic displacements were significantly larger

than those computed for elastic systems. Furthermore, the basis for the coefficient method was extended based on Miranda and Bertero's 1996 work, as described in ATC-49 (2003). The AASHTO specifications, both *LRFD Specifications* and *Guide Specifications*, contain provisions for adjusting or "magnifying" elastic displacement demand for short period structures where the "Equal Displacement" principle does not apply.

The Equal Displacement method is founded on the premise that the displacement of an inelastic system, with mass  $M$ , stiffness  $K$ , and strength  $F_y$ , subjected to a particular ground motion, is approximately equal to the displacement of the same system responding elastically. Thus, the displacement of a system is independent of the yield strength of the system. Figure 6-22 shows the results of a series of inelastic time history analyses wherein all parameters were kept the same as in the original model except for the yield strength, which was systematically increased in 500 kip increments to a maximum of 3,500 kips. The maximum displacement attained by each model is shown denoted as "actual behavior". The structure with 3,500 kip strength remains elastic during the earthquake. Note that the displacement appears to be somewhat independent of yield strength, but the ductility demand is much higher for relatively lower strengths. The assumption of equal displacements is shown on the right. The basic assumption is that the displacement demand is relatively insensitive to system yield strength unless a large reduction factor is used to obtain the design strength.

The conclusions based on this simple comparison must be tempered by the fact that these results are for a single period structure for a single ground motion. The studies done in the early 1960s focused on a small number of periods, yield strengths and ground motions. However, by the 1980s and 1990s significant computational power permitted many variables to be considered and permitted statistical methods to be appropriately applied. The result is that the equal displacement rule holds up well for longer period structures, but does not predict inelastic displacements as well for short period structures. The methods included in the AASHTO *LRFD Specifications* and *Guide Specifications* are based on the more rigorous analyses and are basically the same as the method described in ATC-32 (1996). Thus, while equal displacement still is appropriate, the transition to zero period now is based on statistical results and not the equal energy approach postulated in the 1960s. An example of the transition is shown in Figure 6-23. In the figure, the amount of force reduction below the full elastic force that can be permitted and still meeting target displacement ductility is shown. The reduction factors,  $R_{\mu}$ , are shown as a function of period of vibration of the SDOF structure. What is apparent is that as the period of the structure approaches zero (i.e. the structure becomes very stiff), the amount of force reduction for a given target ductility drops, until at zero period, the full elastic force must be used with no reduction. However, in the

longer period range the force reduction and the ductility are approximately equal, and this is the range where the “equal displacement” rule applies.

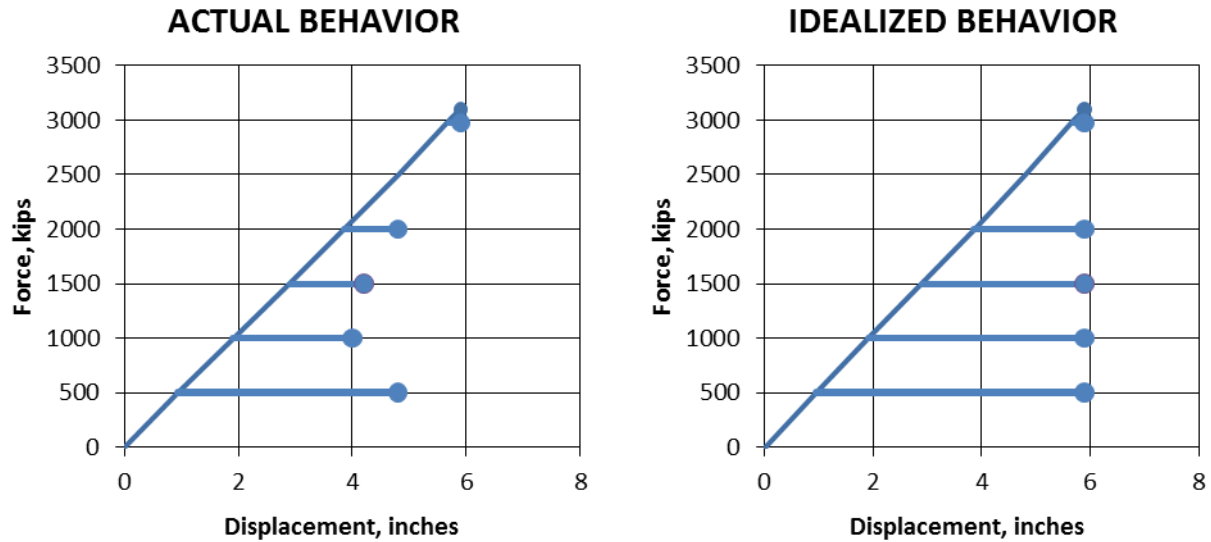


Figure 6-22 Comparison of Response for Linear Elastic and Inelastic Bilinear Systems

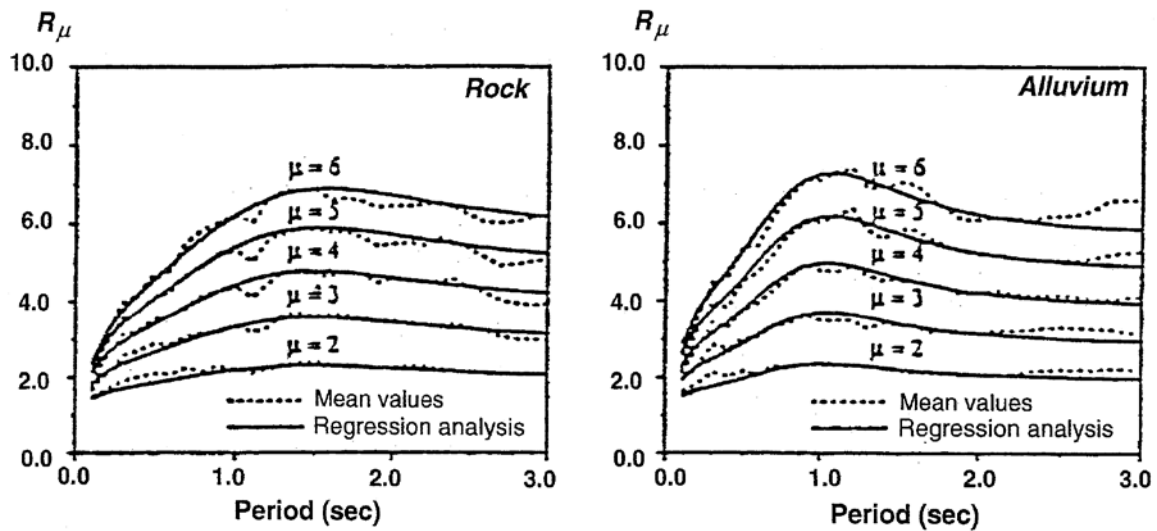


Figure 6-23 Adjustment for Estimating Inelastic Displacements (ATC-49, 2003)

### 6.3.2 Estimation of Response Between Adjacent Frames

The relative hinge displacement,  $\Delta_{eq}$ , adopted in the LRFD *Guide Specifications* is determined following guidelines by Desroches & Fenves (1997) cited the FHWA *Seismic Retrofitting Manual for Highway Structures*, 2006.

$$\Delta_{eq} = \sqrt{(D_{min}^2 + D_{max}^2 - 2\rho_{12}D_{min}D_{max})} \quad 6-1$$

where:

$D_{min}$  = Displacement of the short period frame

$D_{max}$  = Displacement of the long period frame.

The correlation coefficient  $\rho_{12}$  is calculated as:

$$\rho_{12} = \frac{8\varepsilon^2(1+\beta)(\beta)^{3/2}}{(1-\beta^2)^2 + 4\varepsilon^2(1+\beta)^2(\beta)} \quad 6-2$$

where:

$$\beta = \frac{T_2}{T_1}$$

$T_2$  and  $T_1$  being the first and second modes of the structure system.

The damping ratio  $\varepsilon$  is calculated as:

$$\varepsilon = 5\% + \frac{1}{\pi} \left( 1 - 0.95/\sqrt{\mu} - 0.05\sqrt{\mu} \right) \quad 6-3$$

where  $\mu$  is the ductility factor

Considering the displacement ratio  $\alpha$ :

$$\alpha = \frac{D_{min}}{D_{max}} \quad 6-4$$

$$\Delta_{eq} = \sqrt{(\alpha^2 D_{max}^2 + D_{max}^2 - 2\rho_{12}\alpha D_{max}^2)} \quad 6-5$$

$$= \sqrt{(\alpha^2 + 1 - 2\alpha\rho_{12})} \quad 6-6$$

In the long period range,  $\alpha$  is also equal to the ratio of the short period frame over the long period frame.

$$\alpha = \frac{T_{short}}{T_{long}} \quad 6-7$$

Figure 6-24 shows  $D_{max}$  vs. the ratio  $\alpha$  for the following:

- a.  $D_{eq}$  for a target ductility of 2 shown as Curve 1
- b.  $D_{eq}$  for a target ductility of 4 shown as Curve 2
- c. Caltrans SDC shown as Curve 3
- d. Relative hinge displacement based on (Trochalakis et. al. 1997) shown as Curve 4

Considering the potential variations in actual bridge designs, a multiplier on the relative displacement,  $\Delta_{eq}$ , was set equal to 1.1  $D_{max}$  the peak value of Curves 1, plus a safety factor of 1.5 was further applied amounting to  $\Delta_{eq}$  being equal to 1.65  $D_{max}$ . This factor was subsequently used in the *Guide Specifications* as described in Chapter 8. The refinement to use the calculated displacement, rather than the previously used prescriptive support widths for the highest seismic regions, is based on the more detailed modeling that is used for these regions.

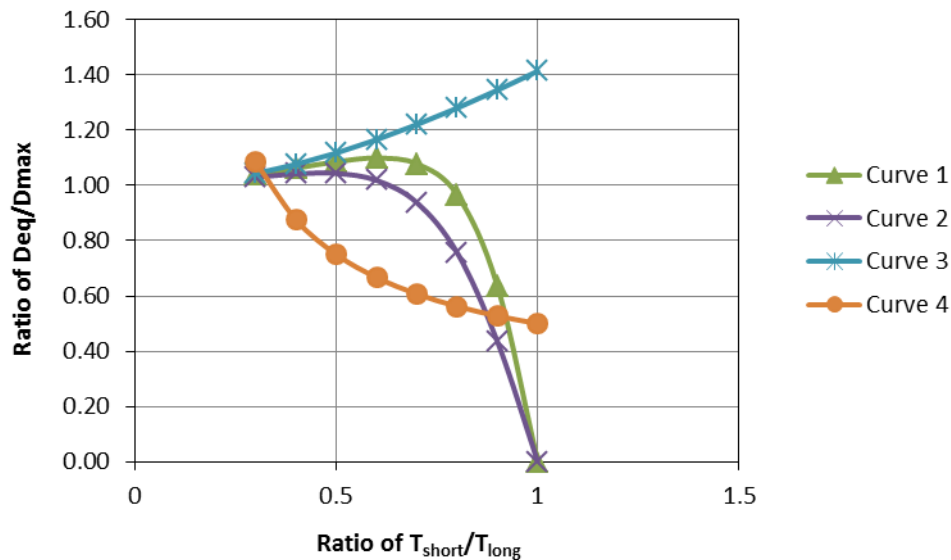


Figure 6-24 Relative Seismic Displacement vs. Period Ratio

## 6.4 CALCULATION OF INELASTIC RESPONSE

### 6.4.1 General

Fundamental to the successful design of any structure designed to sustain inelastic deformations to resist extreme events, such as earthquakes, is the ability to accurately calculate the deformation capacity and corresponding resistance of the structure. Such calculations may be used in the calibration of a prescriptive design procedure or they may be used during the design of each structure. This section provides an introduction to the procedures for making such calculations.

### 6.4.2 Nominal and Expected Strength

Traditionally with the *LRFD Specifications*, nominal material strengths have been used because it was generally accepted that a lower bound on resistance was desirable. This follows from the design approach for gravity and non-seismic loads where adequate margin against a failure due to insufficient strength is required. Nominal strengths are typically based on values for which at least 90 percent of the material

will have greater strength values, particularly for material properties such as those for steel (Mirza and MacGregor, 1979) as illustrated by distribution of yield strength for 273 tests in Figure 6-25. For concrete more variability is normal due to conservative mix designs and strength gain with age. Thus usually if additional strength is provided, that is just extra margin and thus conservative. Consequently, the nominal material strengths are used for the establishment of member strengths.

However when nominal strengths are used for design, the maximum strength that can be developed (i.e. overstrength condition) may be much larger than the strength calculated using nominal properties. This difference is illustrated in Figure 6-26, which shows the relationship between the maximum (overstrength) flexural strength at maximum ductility to the nominal strength based on the traditional ACI method for circular cross sections (Priestley, Seible and Calvi, 1996). The curves shown are for different longitudinal reinforcing steel ratios,  $\rho_l$ . The difference in the two moments can be quite large ranging from about 1.3 to 1.8. The normal value that has historically been used in bridge design is 1.3, which is on the low end of the range.

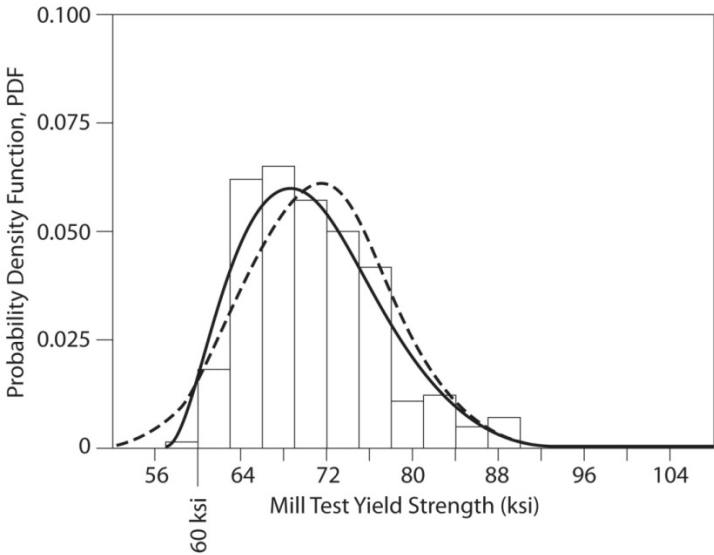


Figure 6-25 Sample Distribution of A615 Grade 60 Steel Yield Strength (after Mirza and MacGregor, 1979)

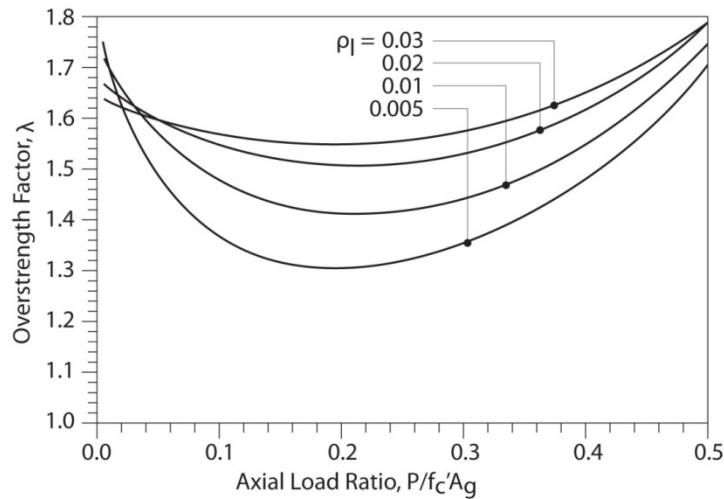


Figure 6-26 Ratio of Maximum Flexural Strength to the Nominal Strength for Circular Cross Sections (after Priestley, Seible and Calvi, 1996)

As Priestley et. al. (1996) state, “It follows that for seismic design, the consequences of overprediction of the design flexural strength of a plastic hinge are less significant than those of underpredicting the overstrength capacity.” To prevent unconservatism in design more recent approaches have been to use strengths approximately equal to the average strength for the calculation of the baseline resistance of the structural elements. Caltrans (2013), for example, uses an expected steel strength of 68 ksi for ASTM A706 Grade 60 reinforcement based on data they have collected. Likewise, the concrete compressive strength is also increased to reflect its more likely average strength. Finally, to more accurately predict the actual strengths more accurate stress-strain relationships are used to capture such effects as strain hardening and confinement. These are discussed in more detail in the sections that follow.

In moving to a displacement-based design method as used in the *Guide Specifications*, more realistic forces are desired because the focus is on predicting actual behavior; so expected strengths are used, and these are calculated using average material strengths rather than nominal material strengths.

### 6.4.3 Overstrength

Overstrength factors are used to establish upper bounds on member strength to account for a number of causes that a member might be stronger than expected. These include: actual material strengths that are higher than the nominal or the expected values, strain hardening of longitudinal steel, confinement effects that increase member strength at relatively high inelastic displacements, and uncertainties in assessment methods that may lead to under prediction of internal forces. Such evaluation of overstrength is most often handled with the application of simple increase factors, such as those shown in Figure 6-26. Overstrength factors are not meant to account for addition of reinforcing above that which is shown in the design.

When performing capacity design, it is appropriate to use concurrently acting forces that are unfactored (i.e., at their nominal values), because these are the best estimate of the forces that will actually be acting on the structure at the time an earthquake occurs. The importance of this with respect to overstrength, as discussed above, is that flexural resistance of concrete columns in typical bridges increases with axial compression on the column. Thus, if the gravity loads were factored upward, the flexural resistance of the columns would be overestimated, resulting in unrealistically high forces for use in capacity design.

Once the member strengths are obtained, a static analysis of the pier is conducted to determine the lateral forces present when a full plastic mechanism has formed in the pier. This process for the *LRFD Specifications* method is essentially an abbreviated pushover analysis that is used only to determine the internal and resisting forces of the pier. The entire pier is analyzed in order to capture potential framing effects where column axial forces change as lateral (inertial) load is applied. For the *Guide Specifications* method this calculation is done as part of the pushover used to assess displacement capacity. When the assessment of the plastic mechanism forces is made, the potential for the yielding elements to have greater-than-expected strengths must also be taken into account. This is normally handled by using overstrength factors that are applied to the member strengths calculated using nominal or expected material values.

The *LRFD Specifications*, and before that Division I-A, use a 1.3 overstrength factor applied to nominal strengths. As seen in Figure 6-26, this value is a bit low. However, this is partially offset in the LRFD method by a low estimate of the concrete contribution to shear strength, which is the primary action the overstrength factor is meant to protect in the LRFD method. In the *Guide Specifications*, factors of 1.2 and 1.4 for A706 Grade 60 and A615 Grade 60 steels are used in conjunction with expected values.

While these factors appear low relative to those in Figure 6-26, they are not due to the use of expected strength values for material strengths and the required use of moment-curvature analysis, which will directly account for strain hardening. For structural steel sections a 1.2 overstrength factor is recommended.

Note that such pushover analyses to establish the maximum overstrength forces in a pier would be a separate calculation from the pushover analysis used to check the deformation capacity of the pier. The deformation capacity should be checked using the best estimate of the member resistances and the development of forces for assessing capacity-protected members should be use overstrength forces, instead.

#### 6.4.4 Cross-Sectional Analysis

The traditional cross-sectional analysis that engineers are used to performing is the development of an axial-moment strength interaction relationship for either steel or reinforced concrete sections. Most often software, whether commercial or developed for use in-house, is utilized for developing interaction curves. These are typically developed for a cross section only, but may be extended to include member buckling effects due to slenderness, if desired. For bridge seismic design where the columns are the yielding elements, the axial-moment interaction relationship for a column will be focus in establishing the strength of the yielding element and subsequently the column and pier as a whole. Normally, the approach for calculating such strength has been to use a simplified approach based on an equivalent rectangular stress block. The resulting strength corresponds to a single point of cross-sectional deformation or curvature. Traditionally, this strength corresponds to the attainment of an extreme compression fiber strain in the concrete of 0.003. This is because the rectangular stress block was originally derived for this unique condition. In most cases, this is all that is required for a force-based design method is used as with the traditional design method of the *LRFD Specifications*. The force-based design method (FBM) is discussed in Chapter 7.

For seismic design and assessment where calculations of yielding effects and deformations are desired, as with a displacement-based method or where precise calculations of capacity are needed with assessment and retrofit, moment-curvature analysis is used to establish the flexural moment vs. cross-sectional deformation (curvature) relationship for the section. The curvatures can then be summed or integrated along the member to determine rotation and subsequently displacement. Thus, where only the moment

capacity (flexural strength) may be of interest in a force-based method, the deformation relationships are essential for calculated structure displacements in the displacement-based method, especially where inelastic deformations are accounted for, as with the *Guide Specifications*. The displacement-based design method (DBM) is discussed in Chapter 7.

The primary locations where inelastic deformations are permitted, other than in the soil, are the plastic hinges. Thus, development of moment-curvature relationships for the plastic hinging region is essential for calculation of structure deformations.

Moment-curvature analysis is typically conducted for individual axial force levels (e.g., set the axial force and calculate the full monotonic moment versus curvature relationship up the failure point.) A qualitative moment-curvature relationship is shown in Figure 6-27 for a circular section such as that in Figure 6-28.

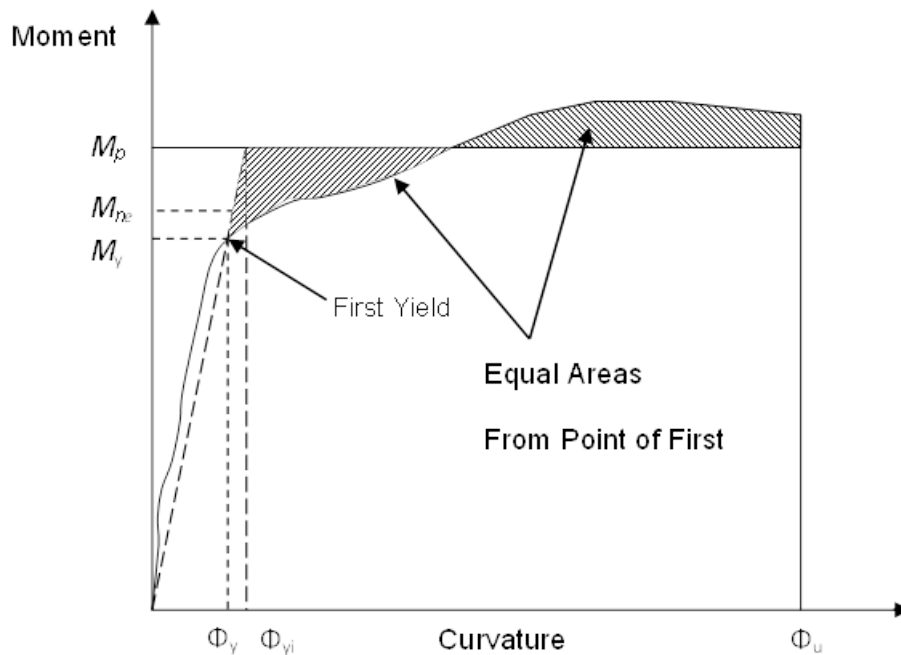


Figure 6-27 Moment-Curvature Relationship (Caltrans, 2013)

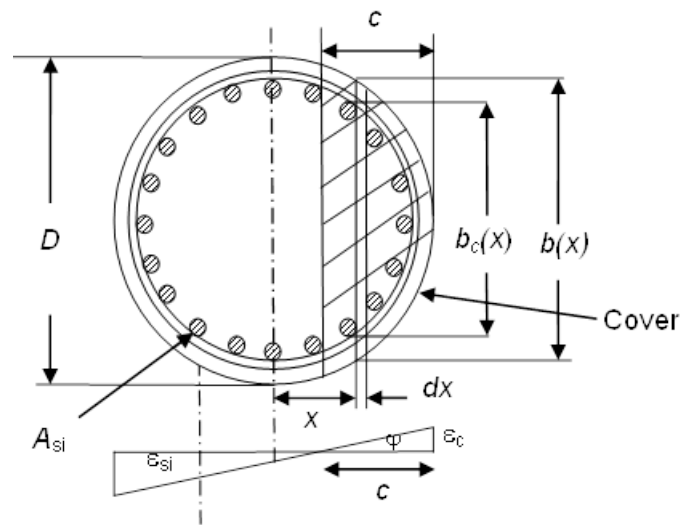


Figure 6-28 Moment-Curvature Sectional Analysis

- In the figures:
- $M_y$  - Moment when extreme tension bar reaches yield
  - $M_p$  - Calculated plastic moment based on equivalent bilinear representation
  - $\phi_y$  - Curvature when first bar reaches yield
  - $\phi_{yi}$  - Effective or “idealized” yield curvature at  $M_p$
  - $\phi_u$  - Ultimate curvature
  - $\epsilon_c$  - Extreme compression fiber strain
  - $\epsilon_{si}$  - strain in bar  $i$
  - $b_x$  - width of section at slice  $x$
  - $b_{cx}$  - width of confined concrete at slice  $x$
  - $c$  - neutral axis depth
  - $x$  - depth of slice under consideration
  - $\phi$  - curvature ( $\epsilon_c / c$ )

Moment-curvature analysis is conducted by the procedure listed in Table 6-1. The values are calculated up to the limiting value for either the concrete or the steel. These limits are either maximum compressive strain the section can endure or the maximum tensile strain that the steel can endure, and typical limits are provided in Section 6.4.5.

**TABLE 6-1 PROCEDURE FOR CALCULATING MOMENT-CURVATURE**

Steps in Moment-Curvature Analysis
1. Model section with geometric and stress-strain relations for concrete, confined concrete, and steel.
2. Set extreme compression fiber strain, $\epsilon_c$ .
3. Guess a neutral axis depth, $c$ .
4. Calculate strains at various depths of section, $\epsilon_x$ .
5. Calculate stress in bars and in slices of concrete based on constitutive models, $f_{sx}$ and $f_{cx}$ .
6. Sum forces and compare to applied axial load, $P = P_{applied}$ ?
7. If axial load matches that applied, go to step 8 otherwise go back to 3 and guess a new depth.
8. Sum moments about center of gravity of section to get $M$ .
9. Calculate curvature as quotient of extreme compression fiber strain and neutral axis depth, $\phi$ .
10. Repeat steps 2 through 9 until limiting concrete or steel strain is attained.

The plot of the moment-curvature relationship usually appears like that shown in Figure 6-27, and the post-yield portion of the curve often continues to rise after yield. For simplicity, the moment-curvature relationship is often represented as a bilinear, elastic-perfectly plastic curve as shown by the dashed line in the figure. The initial elastic portion of the curve represents the effective flexural stiffness,  $E_c I_{eff}$ , that is used in modeling reinforced concrete sections, as described in Chapter 5. The constant moment portion of the curve,  $M_p$ , is often calculated by extending a linear elastic portion of the curve through the first yield point ( $M_y, \phi_y$ ) then solving for  $M_p$  that balances the shaded areas above and below the line. This introduces some slight error into the calculations, but the error is not significant relative to other approximations that are used in the process of calculating inelastic displacements. The overstrength factors are likewise derived to include the less conservative maximum  $M_p$  that occurs with the approximation.

Typically, moment-curvature relationships are developed assuming strain compatibility between the concrete and steel at any given level in the cross section. When such compatibility is known to be

incorrect and bar slip occurs, this is usually taken into account by adjusting the plastic hinge length used to calculate rotations and deflections from curvatures. The use of a simplified elastic, perfectly plastic moment-curvature relation with a constant plastic moment requires that a plastic hinge length be used in order to calculate deflections. Other approaches are acceptable, but they can be quite complex. The simplified method outlined in the AASHTO *Guide Specifications*, and outlined here, is calibrated with laboratory tests, thus making the method semi-empirical, but reasonably accurate.

The moment-curvature relations should include, strain hardening of the reinforcing steel, confinement effects of the concrete, spalling effects of unconfined concrete, and expected yield and ultimate stress values for the materials used. Descriptions of the material stress strain properties are provided in the next section.

Moment-curvature relationships only need to be developed for plastic hinging regions, because other parts of the structure should remain essentially elastic.

## **6.4.5 Material Requirements and Properties**

This section provides a summary of typical properties that are used for seismic design of bridges. The properties are the same that are used in both the Caltrans *Seismic Design Criteria* and the AASHTO *Guide Specifications*. The properties are presented for use in monotonic loading calculations, such as those used for pushover analysis. Properties appropriate for cyclic load-displacement calculations, such as those that might be used in time history analysis are beyond the scope of this manual.

### **6.4.5.1 Reinforcing Steel**

Reinforcing steel is normally in the form of deformed bars of ASTM A615 or A706 Grade 60 materials. Deformed or smooth wire is also used in some cases for spiral reinforcement. High strength alloy bars are typically not used for reinforcement where plastic hinging can occur because the high strength and limited ductility normally do not work appropriately when inelastic action is expected. Typically, steel design yield strength is restricted to 75 ksi, even if the actual yield is higher. However, work is currently being done investigating use of unbounded high-strength bars that would provide displacement capacity

for a pier system, although they would not behave by yielding as is presumed in the current design procedures.

A706 low-alloy steel is preferred in areas where significant ductility is likely to be required because this type of steel has a tight limit on the range of yield stress (60 to 78 ksi). A706 is both more ductile and more weldable than A615 steel due to its controlled carbon content. Accordingly, A706 is recommended for use in plastic hinging zones for all but the lowest of seismic areas. Only steels with yield strengths up to 60 ksi are recommended for plastic hinging applications.

Higher strength reinforcing steel is now available in A706 with yield strengths up to 80 ksi. A706 Grade 80 is permissible in capacity protected members due to its inherent strength control and elongation characteristics. The use of A615 steels with nominal yield strengths greater than 60 ksi is not recommended for capacity protected members due to lack of stress-strain data and seismic test results.

With the use of displacement-based design and quantitative approaches to deformability, full monotonic stress strain properties of reinforcement are required.

Properties of reinforcing steel are often related to a typical curve as shown in Figure 6-29.

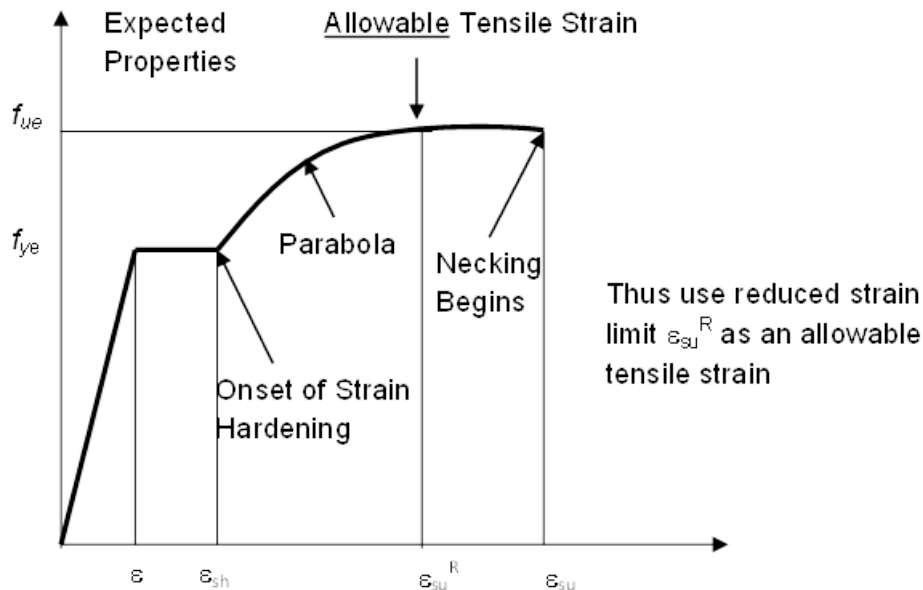


Figure 6-29 Stress-Strain Curve for Mild Reinforcing Steel (Caltrans, 2013)

In the figure,

- $f_{ye}$  - expected yield stress
- $f_{ue}$  - expected ultimate tensile stress
- $\epsilon_{ye}$  - expected yield strain
- $\epsilon_{sh}$  - onset of strain hardening
- $\epsilon_{su}^R$  - permissible tensile strain limit
- $\epsilon_{su}$  - ultimate tensile strain limit when necking begins

Note that the strain hardening portion of the curve can be modeled mathematically as a parabola with its vertex (i.e., its zero slope point) centered at the ultimate stress point. This portion of the curve can be modeled in terms of  $f_s$  and  $\epsilon_s$  using,

$$f_s = f_{ue} - (f_{ue} - f_{ye}) \left( \frac{e_{su} - e_s}{e_{su} - e_{sh}} \right)^2 \quad 6-8$$

Values commonly ascribed to these properties are given in Table 6-2.

Additionally, Young's modulus,  $E_s$ , may be taken as 29,000 ksi. The reduced ultimate tensile strain limit is used to reduce the probability of early bar rupture and to account for the cyclic nature of the loading. Thus, this limit would normally be applied as the limiting steel strain in a moment-curvature analysis. Of course the analysis could be run further than this limiting value, but the sectional capacity would be based on this if the reinforcing steel controlled (i.e., reached its limit before the confined concrete reached its limit.).

#### 6.4.5.2 Prestressing Steel

Prestressing steel that may warrant modeling in cross sectional analyses of potential plastic hinge regions, such as those in prestressed concrete pile bents will normally be 7-wire low relaxation strand of either 250 or 270 ksi strength. The strand may be modeled as linearly elastic up to a strain of 0.0076 for 250 ksi strand and up to 0.0086 for 270 ksi strand. Beyond the elastic limit the strand is modeled with a modified hyperbola as defined below.

**TABLE 6-2 PROPERTIES OF REINFORCING STEEL**

Property	Notation	Bar Size	ASTM 706 (Gr 60)	ASTM 615 (Gr 60)
Specified Minimum Yield Stress (ksi)	$f_{ye}$	#3-#18	60	60
Expected Yield Stress (ksi)	$f_{ye}$	#3-#18	68	68
Expected Tensile Strength (ksi)	$f_{ue}$	#3-#18	95	95
Expected Yield Strain	$\epsilon_{ye}$	#3-#18	0.0023	0.0023
Onset of Strain Hardening	$\epsilon_{sh}$	#3-#8	0.015	0.015
		#9	0.0125	0.0125
		#10 & #11	0.0115	0.0115
		#14	0.0075	0.0075
		#18	0.0050	0.0050
Reduced Ultimate Strain	$\epsilon_{su}^R$	#4 - #10	0.090	0.060
		#11 - #18	0.060	0.040
Ultimate Tensile Strain	$\epsilon_{su}$	#4 - #10	0.120	0.090
		#11 - #18	0.090	0.060

Thus for 250 ksi strand:

$$\epsilon_{ps} \leq 0.0076, \text{ then } f_{ps} = 28,500 (\epsilon_{ps}) \text{ (ksi)} \quad 6-9$$

and

$$\epsilon_{ps} > 0.0076, \text{ then } f_{ps} = 250 - 0.25 / \epsilon_{ps} \text{ (ksi)} \quad 6-10$$

Thus for 270 ksi strand:

$$\epsilon_{ps} \leq 0.0086, \text{ then } f_{ps} = 28,500 (\epsilon_{ps}) \quad (\text{ksi}) \quad 6-11$$

and

$$\epsilon_{ps} > 0.0086, \text{ then } f_{ps} = 270 - 0.04/(\epsilon_{ps} - 0.007) \quad (\text{ksi}) \quad 6-12$$

For prestressing steel the reduced ultimate prestress steel strain that should be used is often taken as 0.03.

### 6.4.5.3 Concrete

Concrete is typically provided using conservative mix designs that produce the required 28-day strength without undue problems or rejections in the field. Additionally concrete may be batched using any of a number of admixtures, additives, or types that usually provide some benefit during construction or some increased environmental resistance. Consequently, not only will the concrete continue to gain strength with age, but the strength gain rate may also be a function of mix design features for construction. For seismic loading, it is the in-situ strength when the earthquake strikes that is of interest. Thus, expected, rather than nominal, strengths are now being used with displacement-based methods to design and assess structures. A typical increase factor for new design is 1.3, where the expected strength is 1.3 times the nominal (Caltrans, 2013 and AASHTO, 2014). For retrofit and assessment where concrete has been in place for many years, 1.5 had been used.

For modeling concrete under seismic loading, the nature of confinement of the concrete section is important, as discussed in Section 6.2.2. This applies to modeling the concrete in potential plastic hinge zones. Otherwise, normal concrete design software, which does not differentiate base on confinement, is acceptable. Normally, concrete cover that is outside of the transverse steel is considered unconfined, because it can spall off of the section under large compressive strains. The concrete inside the transverse steel is considered confined, provided such steel is spaced sufficiently close, provides sufficient confining pressure and is adequately anchored. The prescriptive detailing used for configuring the transverse steel is intended to ensure that the concrete is adequately confined.

A common constitutive model for concrete is that proposed by Mander et.al. (1988). The form of the model is shown in Figure 6-30 for both confined and unconfined concrete. It can be see qualitatively that substantial increase in both the stress and strain can be achieved with confining effects. The model

provides procedures for both rectangular and circular sections. The basic premise is that energy stored in the transverse steel (elastic or inelastic) as the concrete attempts to strain outward against the steel is available to balance the energy stored in the compressed concrete and longitudinal bars. Obviously, once the confining effect is lost by fracture of the transverse bars, then the concrete stress and strain capacity is likewise lost. The amount of enhancement of both concrete strength and strain capacity is a function of transverse steel content, arrangement, and strength. Therefore, the effect of the transverse steel layout on deformation capacity of a column can be assessed via this relationship. For DBM, this becomes one of the prime tools that a designer has to improve deformation capacity of a pier. Such was is not the case with the FBM method where a prescriptive quantity of transverse steel is required and no calculation of its effect is made. Thus there is a direct tie in the DBM method between section detailing and structural deformation capacity.

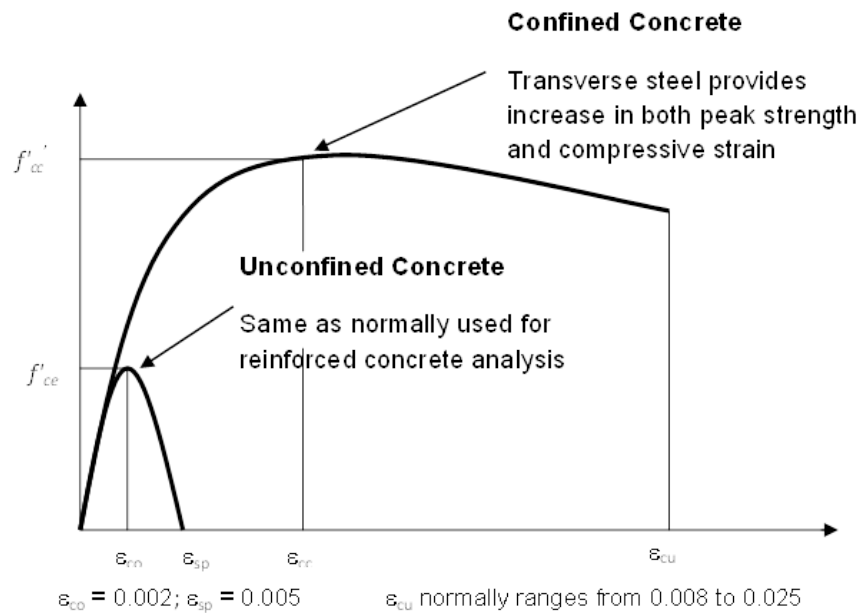


Figure 6-30 Stress-Strain Model for Monotonic Loading of Confined and Unconfined Concrete (Mander et. al., 1988)

The mathematical expressions used to calculate the confining effect of the transverse steel are relatively complex. The expressions are not detailed because the complete description can be found in Mander et.al. (1988). Also, this model is already programmed into software available for generating moment-curvature relations. However, as always, it is the user’s responsibility to ensure that the appropriate material limits are used in the calculations performed by software.

The maximum confined concrete compressive strain limit, corresponding to hoop fracture, typically used by programs employing the Mander model is given by (Priestley et. al., 1996)

$$\varepsilon_{cu} = 0.004 + \frac{1.4\rho_s f_{yh} \varepsilon_{su}}{f'_{cc}} \geq 0.005 \quad 6-13$$

where,

- $f_{yh}$  = the hoop or spiral yield stress
- $f'_{cc}$  = the confined concrete strength
- $\varepsilon_{su}$  = the transverse steel strain at the maximum stress
- $\rho_s$  = volumetric ratio of the confining steel.

Typical values for the confined concrete compressive strain range from 0.008 to 0.025. Where inspection and repair of damage is difficult or impossible, for example with in-ground plastic hinges, it is recommended that the maximum compressive strain be limited to 0.020 or less.

The transverse steel content,  $\rho_s = 4A_{sp}/D's$  for circular sections, and  $\rho_s = \rho_x + \rho_y$  for rectangular sections. For rectangular sections,  $\rho_x$  and  $\rho_y$  can be defined considering the section shown in Figure 6-31.

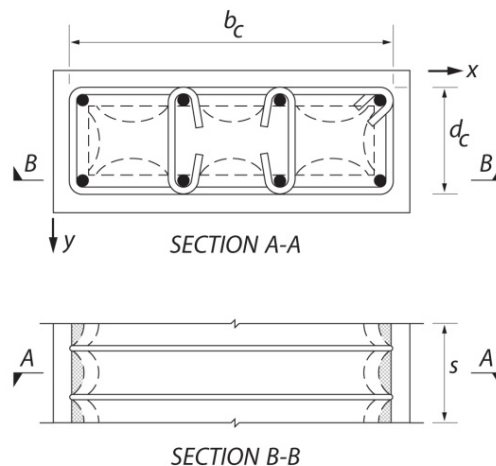


Figure 6-31 Definition of Parameters for Rectangular Sections (after Mander et al., 1988)

Using the figure axes and definitions,  $\rho_x = A_{sx}/sd_c$  and  $\rho_y = A_{sy}/sb_c$ . The spacing of the hoops or spiral is “s”. The area of steel effective in the x direction is the total area of transverse steel acting parallel to the long face, because this steel acts to produce a confining pressure along the  $d_c$  dimension or short face. Similarly, the area of steel effective in the y direction is the total area of transverse steel acting parallel to the short face.

For the unconfined cover concrete, the maximum stress is assumed to occur at a strain,  $\epsilon_{co} = 0.002$ , which is a commonly accepted value, and the maximum strain achieved at complete loss of the unconfined concrete capacity is,  $\epsilon_{sp} = 0.005$ .

#### 6.4.5.4 Structural Steel

Structural steel requirements for portions of the structure that will remain essentially elastic (i.e., capacity-protected elements) are governed by the AASHTO LRFD *Bridge Design Specifications*. For ductile elements that are part of the bridge’s EREs, additional requirements are necessary. Currently, the only design provisions in AASHTO for ductile steel elements that are EREs are force-based. This includes steel columns, pile bents, and ductile diaphragms. Consequently, the requirements for steel are primarily prescriptive for material types, material strengths, and detailing requirements.

When steel elements are part of a ductile system that is expected to experience relatively large inelastic demands, as would be the case in the higher seismic zones or categories, material types are limited. Materials that are recommended for such ductile elements are: ASTM A709, Grades 50 and 50W; ASTM A992; ASTM A500 Grade B, and ASTM A501. When lower demands are expected, as in the lower seismic zones, then ASTM A709 Grade 36 may be used. Additionally, pipe used in ductile systems, for example pipe piles, must meet ASTM A53 Grade B or API 5L X52.

Expected yield values as a multiple of the nominal yield stress for these various grades of steel from the *Guide Specifications* are given in Table 6-3.

**TABLE 6-3 EXPECTED YIELD STRESS VERSUS NOMINAL YIELD STRESS FOR STEEL  
(AASHTO, 2009)**

Steel Type and Grade	<i>F<sub>ye</sub> / F<sub>y</sub></i>
ASTM A709 Grade 50, Grade 50W, and A992	1.1
ASTM A500 Grade B and A 501	1.4
ASTM A 709 Grade 36 and A53 Grade B	1.5
API 5L X52	1.2

#### **6.4.5.5 Welding Requirements for Structural Steel**

Welding of structural steel is governed by AASHTO/AWS D1.5 (2010). For elements that are part of an ERE and are expected to experience inelastic deformations, under-matched welds are not permitted, and both the base metal and weld filler materials should have adequate notch toughness. This is achieved by meeting the ASTM A709/A709M, Paragraph 10, Fracture Critical (F) Tension Members, Zone 3 requirements for the base metal. The weld filler should meet the Zone III requirements for AWS D1.5.

#### **6.4.6 System Strength and Deformation**

##### **6.4.6.1 Determination of System Strength**

As a structure is loaded to the point of forming a plastic mechanism, the forces developed are not proportional to those predicted from elastic analysis. To address this, traditional force-based seismic design (FBM) has used a partial pushover analysis to establish the maximum forces present within a pier at the development of a plastic mechanism. However, rather than track the forces and displacements from zero lateral load to the mechanism load, a simple determination of lateral force only is made at the mechanism level. This uses the lower bound theorem of plasticity (Hodge, 1981), whereby a complete plastic mechanism is postulated, which renders the system internally determinate, and then the corresponding lateral load to cause the mechanism is calculated. The lower bound name of this technique derives from the fact that the lateral load so determined will be less than or equal to the true lateral load. Thus, if an incorrect mechanism is guessed, the lateral load will be underestimated.

The problem of guessing correct mechanisms in bridge design is essentially avoided by the first and third steps of capacity design. That is, after the desired mechanism is established (first step), all other potential plastic mechanisms are suppressed by making the structure sufficiently strong at the locations of other potential plastic hinges (third step). Thus, where traditional plastic design requires guessing mechanisms, with capacity-protected design the designer retains control of where and how yielding will occur.

For multi-column piers, the calculation of the maximum lateral load and associated column forces should consider the change in axial load in individual columns due to frame action, as the lateral load is increased. For reinforced concrete columns the increase in axial load on one side will typically lead to increased yield moment capacity, while the opposite is true on the side of the pier where the columns experience reduced compression. Some software programs take this effect into account directly. For instance, programs that perform pushover analysis track internal force changes as loading is applied and therefore directly account for the changes in yield moment capacity. However, when performing this calculation by hand or spreadsheet, an iterative approach is often required.

Another factor that contributes to a structural element being stronger than nominal is potential overstrength of the materials and the potential for strain hardening. As shown earlier in this chapter, such overstrength can lead to the plastic hinging portion of a column being somewhat stronger than the nominal material strengths would produce. This overstrength must be accounted for in capacity-protection because failure to do so could lead to premature yielding in an undesirable, potentially non-ductile, location, leading in turn to the premature failure of the yielding element. The establishment of overstrength forces in the system requires that the pushover analysis, whether used to determine only forces (as in FBM) or both displacements and forces (as in DBM), must be accomplished using the overstrength factors. This means that pushover solely to assess displacement capacity would not use the overstrength factors, while the analysis to determine the maximum forces for capacity protection would use such factors.

Once the system forces under the overstrength condition are determined, the capacity protection design of elements that are not part of the yielding EREs can be designed. Generally, for the seismic case these elements are designed to remain essentially elastic and undamaged. With appropriate overstrength factors essentially elastic behavior will be ensured by using resistance factors,  $\phi = 1.0$ , with the nominal material properties of the capacity-protected elements. In some cases, for example with shear where additional conservatism is warranted lower resistance factors are used. It is certainly conservative to use the normal resistance factors for the capacity protection design.

#### **6.4.6.2 Determination and Assessment of System Deformation Capacity**

When using the DBM, actual calculation of the deformation capacity of a bridge is required. The demands caused the design earthquake are compared against the displacement capacities, and acceptability of the design is judged. This may be assessed on a pier-by-pier basis with pushover analysis of individual piers to calculate capacity, which is compared to displacement demands from elastic analysis of the entire bridge. Alternately, displacement acceptability could be assessed using full time history analysis where the ‘capacity’ in terms of hysteretic response is built into the analytical model. Discussion of nonlinear time history analysis is beyond the scope of this chapter.

Typically, moment-curvature relations for the plastic hinging section of the columns are used to build the overall system displacement capacity. The moment-curvature relation is used to calculate a maximum permissible plastic curvature, which is integrated over (multiplied by) a prescribed plastic hinge length to calculate plastic rotation capacity of the plastic hinge site. This rotation is then used to calculate a plastic deformation of the column. If plastic moments can occur at both ends of the column, then both top and bottom capacities are considered in calculating the column’s plastic displacement capacity. More than likely, the plastic hinge at one or the other end will control (limit) the column’s plastic deformation capacity, because it is unlikely that both will reach their limiting curvatures at the same displacement. To determine the pier or system capacity this assessment must be done for all the pier’s columns and the effects of overturning on axial force, moment and curvature capacity must be considered. To the plastic displacement capacity is added the column elastic deformation and the foundation and cap beam deformations, if the flexibility of the foundations and cap beams have been used in the demand model. It is most important, for instance, that foundation and cap beam compliance are consistently included in both the demand and capacity analyses. If such compliance is not consistently included, the possibility for unconservative results exists, for example where demand does not include foundation compliance and the displacement capacity calculation does.

#### **6.4.6.3 Deformation Capacity of Reinforced Concrete Members**

A displacement capacity evaluation of a bridge or portion of a bridge, for example a pier or frame is accomplished using a pushover analysis as described in Chapter 5. This analysis is typically done to track the nonlinear relationship between applied load and deformation for the structure as a lateral load is monotonically increased from an initial elastic condition to failure. This provides an estimate of the

capacity of each critical structural member, from first yield to collapse. The results are member performance in terms of force versus deformation, moment versus rotation, or shear force versus distortion.

Cap beams, columns, footings and piles may be modeled as line elements with concentrated plastic hinges occurring at their ends. Other models, such as those with distributed plasticity, distributed flexibility, or general-purpose nonlinear finite element analysis may also be used, provided it can be demonstrated that their theoretical response agrees reasonably well with experimental results for members similar to those being modeled.

Guidelines for determining the deformation capacity of bridge components are given in this section. In particular, procedures are given for calculating the plastic curvatures, rotations, and drift angle for the deformation-based limit states.

Consider for example the calculation of the load vs. displacement relationship as a cantilever column is loaded from zero lateral load to the attainment of the ultimate displacement,  $\Delta_u$ , with a monotonically applied lateral (shear) load,  $F$ , at the superstructure level is illustrated in Figure 6-32. Ultimate, in this case, corresponds to the attainment of a capacity limit state, which could be rupture of the tension steel, crushing of concrete, or other local failure modes. The range of possible limit states is discussed later in this section. Figure 6-32 illustrates four stages of loading. The first stage corresponds to the undeformed structure. The second stage is the elastic range prior to yield of the idealized section. The third stage illustrates plastic deformation prior to attainment of the maximum permissible plastic rotation that corresponds to reaching the first limit state of ultimate displacement. The fourth and final stage corresponds to the beginning of the loss of lateral strength of the column. For example, as longitudinal bars buckle and fracture and as the concrete crushes, the lateral strength of the column diminishes. A schematic lateral load vs. displacement plot for this column is shown in Figure 6-33.

Each stage is described as follows.

Between Stage 0 and 1 the column is elastic and the elastic component of deflection,  $\Delta_e$  is:

$$\Delta_e = \frac{FL^3}{3E_c I_{eff}} \quad 6-14$$

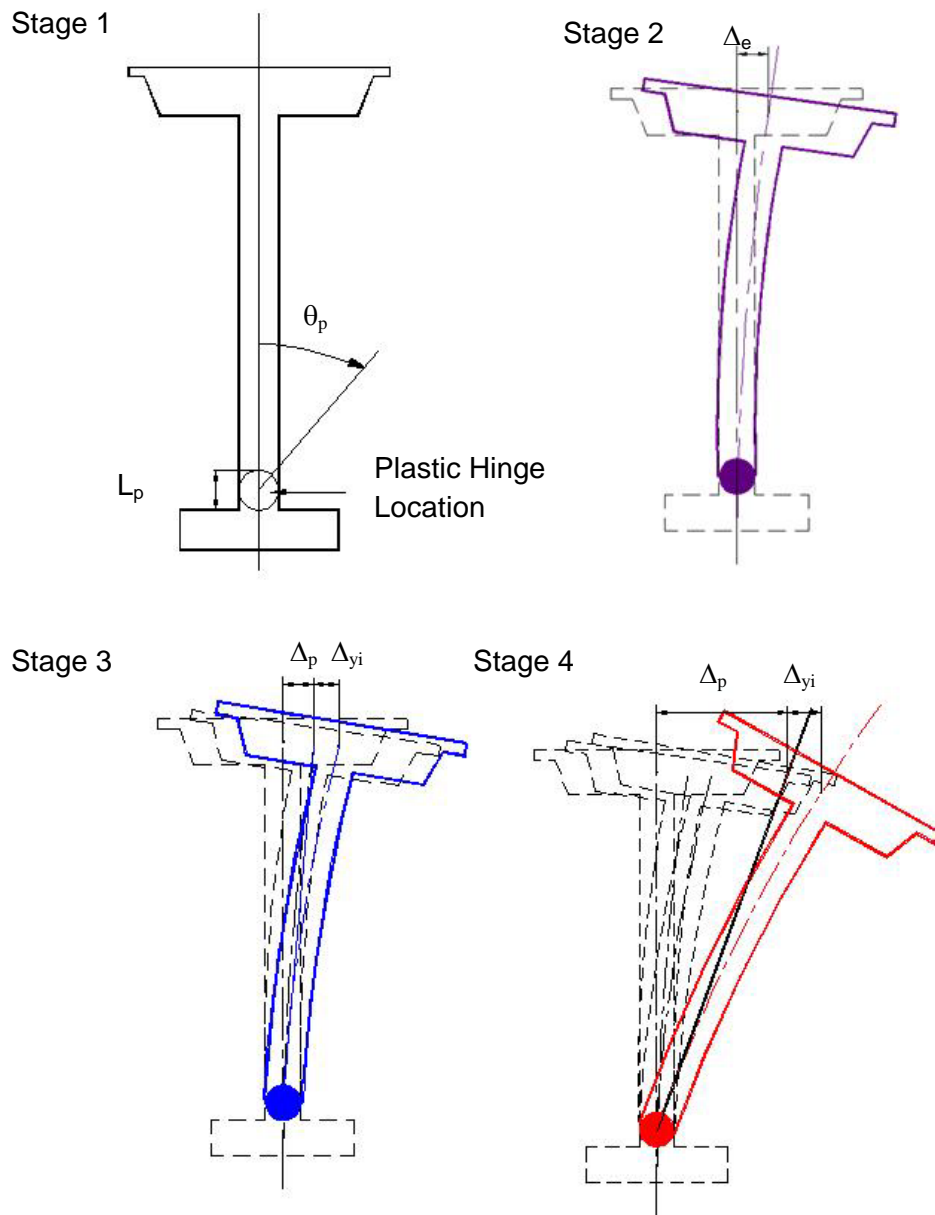


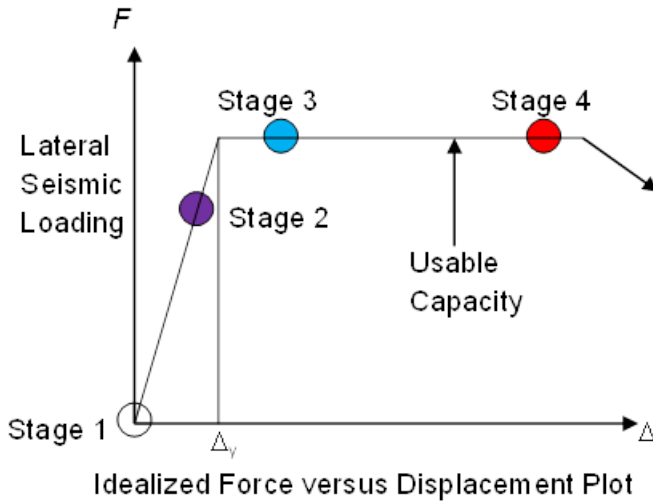
Figure 6-32 Plastic Hinging Mechanism for a Cantilever Column

where:

$L$  = the length from the fixed end to the free tip (or the inflection point of a fixed-fixed beam-column element)

$E_c I_{eff}$  = the effective flexural stiffness of the member, including cracking effects

When the plastic strength of the member ( $F_p, M_p$ ) is reached and  $\Delta_e = \Delta_{yi}$ , the idealized yield displacement is given by:



Stages	Description
1	Zero lateral load
2	Just prior to yielding
3	Just following formation of the plastic hinge

Figure 6-33 Plastic Hinge Stages

$$\Delta_{yi} = \frac{F_p L^3}{3E_c I_{eff}} = \frac{M_p L^2}{3EI_{eff}} = \frac{1}{3} \phi_{yi} L^2 \quad 6-15$$

where:

- $M_p$  = the plastic moment capacity
- $\phi_{yi}$  = the idealized yield curvature.

For the plastic displacement component,  $\Delta_p$ :

$$\Delta_p = \phi_p L_p (L - 0.5L_p) \quad 6-16$$

where:

- $L_p$  = the equivalent plastic hinge length
- $\phi_p$  = the plastic curvature as defined below.

The total displacement;  $\Delta_u$ , is given by:

$$\Delta_u = \Delta_{yi} + \Delta_p \quad 6-17$$

where:

- $\Delta_{yi}$  = the elastic component of displacement corresponding to the idealized yield

$\Delta_p$  = the plastic component of displacement

The analytical plastic hinge length for columns,  $L_p$ , may be taken as the equivalent length of column over which the plastic curvature is assumed constant for estimating the plastic rotation. The plastic displacement of an equivalent cantilever member from the point of maximum moment to the point of contra-flexure may be determined using the plastic rotation and the equivalent cantilever length.

The plastic hinging length varies depending on the configuration of the column. A few examples are given below.

For reinforced concrete columns framing into a footing, an integral bent cap, an oversized shaft, cased shaft, or top of pile in a pile bent, the plastic hinge length,  $L_p$  in inches, may be determined as:

$$L_p = 0.08L + 0.15f_{ye}d_{bl} \geq 0.3f_{ye}d_{bl} \quad 6-18$$

where:

$L$  = length of column from point of maximum moment to the point of moment contraflexure (in.)

$f_{ye}$  = expected yield strength of longitudinal column  
reinforcing steel bars (ksi)

$d_{bl}$  = nominal diameter of longitudinal column  
reinforcing steel bars (in.)

The first term in Equation 6-18 quantifies the spread of plasticity along the member (i.e. 8 percent of the cantilever length). The second term quantifies the length of plastic strain penetration into the adjacent element (e.g., footing, cap beam, etc.).

For non-cased prismatic drilled shafts, reinforced concrete piles, and prestressed concrete piles, the soil contact tends to distribute the curvatures along the member, and the analytical plastic hinge length, below ground  $L_p$  (in.), may be determined as:

$$L_p = 0.1H' + D^* \leq 1.5D^* \quad 6-19$$

where:

$D^*$  = diameter of circular shafts or cross section dimension in direction under  
consideration for oblong shafts (in.)

$H'$  = length of shaft from the ground surface to point of contraflexure above ground (in.)

For members where significant confinement is present in the plastic hinging region, as with columns with steel jackets or for horizontally isolated flared reinforced concrete columns, the plastic hinge length,  $L_p$  in in., may be determined as:

$$L_p = G_f + 0.3f_{ye}d_{bl} \quad 6-20$$

where:

$G_f$  = gap between the isolated flare or top of jacket and the soffit of the bent cap (in.)  
 $f_{ye}$  = expected yield strength of longitudinal column reinforcing steel bars (ksi)  
 $d_{bl}$  = nominal diameter of longitudinal column reinforcing steel bars (in.)

The elastic component of the total drift is related to the member slenderness and the plastic drift is given by the plastic hinge rotation, which in turn is related to the plastic curvature within the plastic hinge zone.

The plastic rotational capacity of a member should be based on the governing limit state for that member. The governing limit state is the state that has the least plastic rotational (or plastic curvature) capacity. Values of  $\phi_p$  for several deformation-based limit states are given in Table 6-4. Ideally, plastic curvatures and plastic rotations for the following limit states may be considered:

- 1) Compression failure of unconfined concrete (i.e., spalling of the concrete cover)
- 2) Compression failure of confined concrete
- 3) Longitudinal tensile fracture of reinforcing bars
- 4) Compression failure due to buckling of the longitudinal reinforcement
- 5) Low cycle fatigue of the longitudinal reinforcement
- 6) Failure of the lap-splice zone
- 7) Shear failure of the member that limits ductile behavior
- 8) Failure of an adjacent joint

Modern detailing is intended to delay limit states 4 through 8 to ensure that these limit states typically occur after attainment of the “Compression Failure of Confined Concrete” limit state. The limit state of “longitudinal fracture of reinforcing” may control in sections with very low reinforcement while

“Compression Failure of Unconfined Concrete” is typically not a concern since a confined core is provided and a Life Safety/No Collapse criterion is all that is considered; thus spalling damage is permitted. This limit state can control for existing construction where no confined concrete is present.

In addition, capacity protection of column shear is a fundamental requirement in low, moderate and high seismic regions and is covered in detail in Chapter 7 of this manual. Capacity protection of column joints is also typically required in moderate and high seismic zones. Lap splicing is not permitted in the plastic hinge region in moderate and high seismic zones. Therefore, only “Compression Failure of Confined Concrete” and “longitudinal fracture of reinforcing” are normally considered in deriving the plastic and curvature of a member plastic hinge zone. Other limit states are inhibited or delayed to a displacement larger than the two limit states mentioned above.

**TABLE 6-4 VALUES OF PLASTIC CURVATURE CORRESPONDING TO VARIOUS LIMIT STATES IN REINFORCED CONCRETE COLUMNS AND BEAMS, FHWA (2006)**

Column or Beam Limit State	Plastic Curvature, $\phi_p$
Compression failure, unconfined Concrete	$\phi_p = \frac{\epsilon_{cu}}{c} - \phi_y$
Compression failure, confined concrete	$\phi_p = \frac{\epsilon_{cu}}{(c - d'')} - \phi_y$
Fracture of longitudinal reinforcement	$\phi_p = \frac{\epsilon_{smax}}{(d - c)} - \phi_y$
Buckling of longitudinal bars	$\phi_p = \frac{\epsilon_b}{(c - d')} - \phi_y$
Low-cycle fatigue of longitudinal reinforcement	$\phi_p = \frac{2\epsilon_{ap}}{(d - d')} = \frac{2\epsilon_{ap}}{D'}$

The limits listed in the table, which are expressed in terms of plastic curvature, are covered in more detail below:

1) Compression Failure of Unconfined Concrete

The plastic curvature corresponding to compression failure in unconfined concrete is given by:

$$\phi_p = \frac{\epsilon_{cu}}{c} - \phi_y \quad 6-21$$

where:

$\epsilon_{cu}$  = the ultimate concrete compression strain for concrete, which should be limited to 0.005 for unconfined concrete, and  $c$  is the depth from the extreme compression fiber to the neutral axis. This limit state represents a transformation stage to a section with spalled concrete cover.

## 2) Compression Failure of Confined Concrete

For concrete confined by transverse hoops, cross-ties, or spirals, the compression strain is limited by first fracture within the confining steel. While this type of failure depends on the cyclic load history, a conservative estimate of the plastic curvature can be obtained from:

$$\phi_p = \frac{\epsilon_{cu}}{(c - d'')} - \phi_y \quad 6-22$$

where:

- $c$  = depth from the extreme compression fiber of the cover concrete (which is expected to spall) to the neutral axis,
- $d''$  = distance from the extreme compression fiber of the cover concrete to the centerline of the perimeter hoop (thus,  $c - d''$  is the depth of confined concrete under compression), and
- $\epsilon_{cu}$  = ultimate compression strain of the confined core concrete, as given by:

$$\epsilon_{cu} = 0.005 + \frac{1.4 \rho_s f_{yh} \epsilon_{su}}{f'_{cc}} \quad 6-23$$

- $\epsilon_{su}$  = strain at the maximum stress of the transverse reinforcement,
- $f_{yh}$  = yield stress of the transverse steel,
- $\rho_s$  = volumetric ratio of transverse steel, and
- $f'_{cc}$  = confined concrete strength.

For bridge columns that have confined concrete details, the displacement capacity is typically governed by this limit state unless a maximum allowable ductility capacity is imposed. In this latter case, the displacement capacity is limited to the product of the idealized yield displacement  $\Delta_{yi}$  times the maximum allowable ductility. Note that the base strain level of 0.005 as indicated in the equation above is different in the *Guide Specifications*, which by reference is 0.004.

### 3) Fracture of the Longitudinal Reinforcement

fracture occurs when the tensile strain reaches a critical level, as given by  $\epsilon_{s,max}$ . This failure mode is only likely under near-field impulse-type ground motions where there is essentially a monotonic (pushover) response. The plastic curvature in this case is given by:

$$\phi_p = \frac{\epsilon_{s,max}}{(d-c)} - \phi_y \quad 6-24$$

where:

$d$  = is the depth to the outer layer of tension steel from the extreme compression fiber, and  $c$  is the depth to the neutral axis. The tensile strain  $\epsilon_{s,max}$  is a function of the material and grade of the rebar used for longitudinal reinforcement.

### 4) Buckling of Longitudinal Bars

If a compression member has inadequate transverse reinforcement and the spacing of the spirals, hoops, or cross-ties in potential plastic hinge zones exceeds six longitudinal bar diameters (i.e.,  $s > 6d_b$ ), then local buckling at high compressive strains in the longitudinal reinforcement is likely. The plastic curvature of this failure mode can be determined from:

$$\phi_p = \frac{\epsilon_b}{(c-d')} - \phi_y \quad 6-25$$

where:

$d'$  = is the distance from the extreme compression fiber to the center of the nearest compression reinforcing bars, and  $\varepsilon_b$  is the buckling strain in the longitudinal reinforcing steel. If  $6d_b < s < 30d_b$ , the buckling strain may be taken as twice the yield strain of the longitudinal steel as expressed in the formula below:

$$\varepsilon_b = \frac{2f_y}{E_s} \quad 6-26$$

Following the AASHTO detailing provisions, this limit state is inhibited.

#### 5) Low Cycle Fatigue of Longitudinal Reinforcement

Since earthquakes induce cyclic loads in bridges, low cycle fatigue failure of the longitudinal reinforcement is possible. This is especially so if the column is well confined and other types of failure, as described above, are prevented. The plastic curvature that leads to a low cycle fatigue failure is given by:

$$\phi_p = \frac{2\varepsilon_{ap}}{(d - d')} = \frac{2\varepsilon_{ap}}{D'} \quad 6-27$$

where:

$D'$  = distance between the outer layers of longitudinal steel in a rectangular section ( $d - d'$ ), or the pitch circle diameter of the longitudinal reinforcement in a circular section,

$\varepsilon_{ap}$  = plastic strain amplitude, as given by:

$$\varepsilon_{ap} = 0.08(2N_f)^{-0.5} \quad 6-28$$

$N_f$  = effective number of equal-amplitude cycles of loading that lead to fracture, which can be approximated by:

$$N_f = 3.5(T_n)^{-1/3} \quad 6-29$$

provided that:  $2 \leq N_f \leq 10$ , and

$T_n$  = natural period of vibration of the bridge.

A different approach for inhibiting this limit state is to limit the longitudinal reinforcement maximum strain  $\mathcal{E}_{s,max}$  to 6.

#### 6) Failure in the Lap-splice Zone

For ease of construction, it may be practical to have a lap-splice zone at the base of a column where the starter bars from the footing or pile cap are lapped with the flexural reinforcement of the column. This is generally also the location of the plastic hinge zone. The presence of the lap-splice within the plastic hinge may lead to two different behavior modes related to slippage and yielding of the reinforcement depending on the length of the lap-splice that is provided. It is possible that, if the bond between the reinforcing steel and column concrete is satisfactory, the effective plastic hinge is reduced in length and behavior is then more difficult to predict and estimate.

Lap splicing must be avoided in the plastic hinging zones where potentially high ductility demands are expected. The LRFD *Bridge Design Specifications* and the *Guide Specifications* handle this in slightly different manners. In the lower seismic zones, the *Guide Specifications* specifically limit the inelastic behavior permitted. Thus, designs by that method do permit lap splices in the lower zones. No such limit is provided by the LRFD *Bridge Design Specifications*, thus lap splicing is prohibited, except in the lowest zone.

Limit states 7 “Shear Failure” and 8 “Joint Failure” are typically inhibited according to capacity design principles and are covered in Chapter 7 of this Manual.

## 6.5 SYSTEM DEFORMATION CAPACITY OF STEEL SUBSTRUCTURES

### 6.5.1 General

When structural steel is used in substructure where inelastic action is expected, detailing that ensures adequate ductility must be used. In general, five types of expected performance and levels of damage can be defined for steel bridges as shown on the plot included in Figure 6-34, and these include:

- a) Elastic behavior with almost no damage
- b) Local yielding, very minor local buckling, some slippage at the connections and minor damage
- c) Inelastic behavior with yielding, noticeable local buckling, repeated slippage, overall buckling and a level of damage that can be easily detected and repaired without closing the bridge for extended period of time
- d) Significant yielding, local and overall buckling with significant damage to super-structure but no collapse.
- e) Major fractures and widespread damage resulting in partial or full collapse.

In steel structures, inelasticity is usually concentrated in areas of high strain or high curvature demands. In most cases, the inelastic areas include the location of plastic hinges for bending elements and yielding or buckling for axially loaded elements. The global ductility of a structural system directly depends on ductility of inelastic zones of its components. By conducting pushover analysis, an approximate relationship between local and global ductility of the system can be established. Although, pushover techniques and associated material limits for steel have not been included in the *Guide Specifications*, ultimately these are expected to be included. However, it is still appropriate to discuss steel behavior in similar terms to those used for reinforced concrete in earlier sections.

In order to establish ductility capacity of a structure, first the ductility of the material used in the structure is established. Then, in order of progression, the ductility of cross sections is established, then that of the components (members and connections), subassemblies and finally displacement ductility of the entire structure is established. As an example, Figure 6-35 shows potential forms of ductile inelastic deformations that can develop in a typical steel bent, and these are:

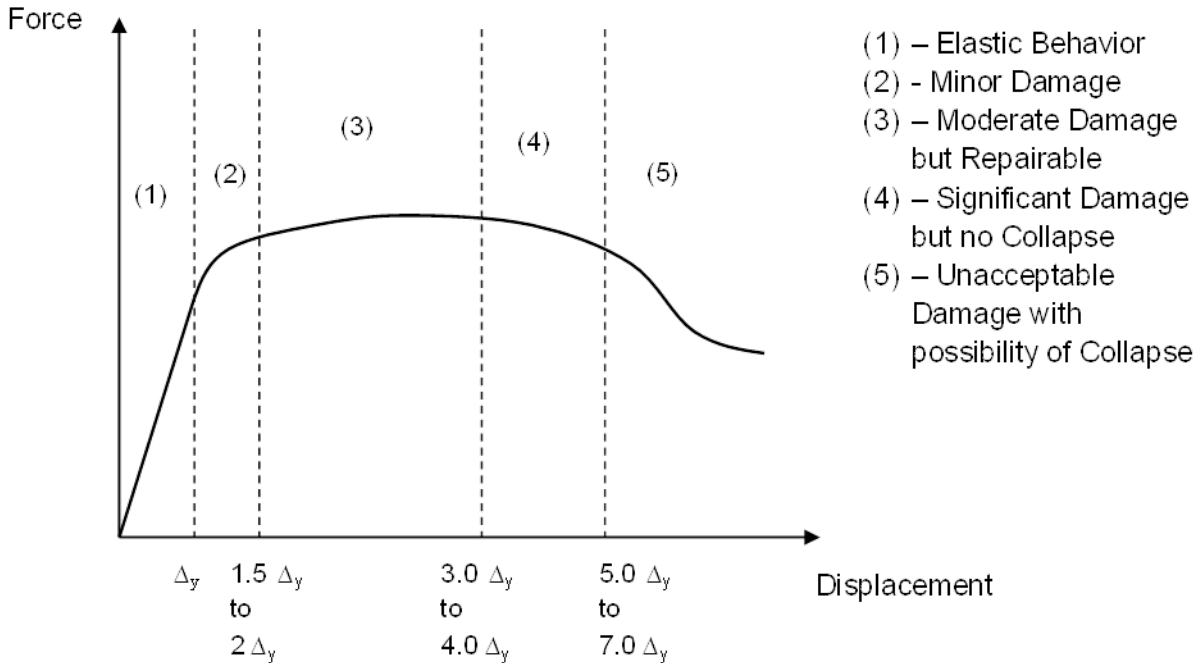


Figure 6-34 Five Regions of Expected Performance and Damage for Steel

- Ductile deformations occur at the base as well as top of the piers including limited and desirable slippage at the connections and limited and desirable rocking and slippage at the base
- Ductile deformation due to the plastic hinge formation in the main members
- Ductile deformations of superstructure bearings
- Ductile deformation in the cross bracing of the superstructure

To achieve ductile behavior, steel elements used as part of the ERS must meet slenderness limits that apply to members as a whole (slenderness ratios) and localized parts of members (width-to-thickness ratios). These are intended to control member buckling and local buckling, respectively, in order to ensure adequate seismic performance without premature loss of resistance and deformation capacity. The limiting ratios are more restrictive than those that apply to members that remain elastic, because inelastic action tends to reduce the effective stiffness of the elements, thus permitting buckling at lower loads. The requirements are listed in detail in the *AASHTO Guide Specifications* and are given in Figure 6-5.

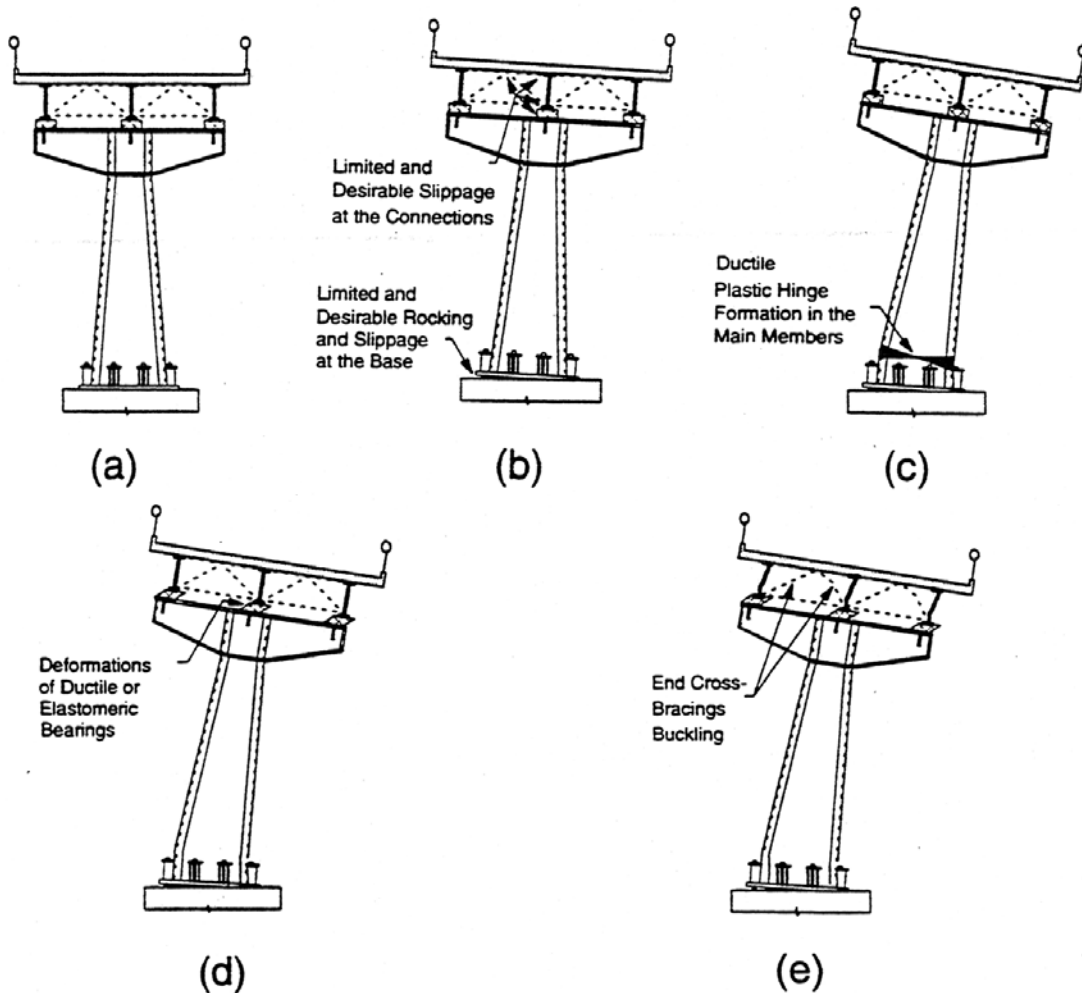


Figure 6-35 Areas of Potential Inelastic Deformations in Steel Substructure

### 6.5.2 Local Buckling

Limited information on the relationship between the  $b/t$  (width to thickness) ratio and the cyclic ductility and cyclic fracture of the locally buckled areas of steel members is available. Tests results of steel sections under monotonic bending have indicated that if  $b/t$  is less than  $\lambda_p$ , then the rotational ductility of the plastic hinge can be as high as 10 to 12. In addition, it is established that when the  $b/t$  ratio is less than  $\lambda_p$ , the formation of the local buckling is delayed until axial strains reach strain hardening of the steel which is on the order of about 0.015 in/in.

**TABLE 6-5 LIMITING WIDTH-THICKNESS RATIOS**

Description of Elements	Width-Thickness Ratios	Essentially Elastic Components $\lambda_r$	Ductile Members $\lambda_p$
<b>UNSTIFFENED ELEMENTS</b>			
Flexure and uniform compression in flanges of rolled or built-up I-shaped sections.	$\frac{b}{t}$	$0.56\sqrt{\frac{E}{F_y}}$	$0.30\sqrt{\frac{E}{F_y}}$
Uniform compression in flanges of H-pile sections.	$\frac{b}{t}$	$0.56\sqrt{\frac{E}{F_y}}$	$0.45\sqrt{\frac{E}{F_y}}$
Uniform compression in legs of single angles, legs of double angle members with separators, or flanges of tees.	$\frac{b}{t}$	$0.45\sqrt{\frac{E}{F_y}}$	$0.30\sqrt{\frac{E}{F_y}}$
Uniform compression in stems of rolled tees.	$\frac{d}{t}$	$0.75\sqrt{\frac{E}{F_y}}$	$0.30\sqrt{\frac{E}{F_y}}$
<b>STIFFENED ELEMENTS</b>			
Rectangular HSS in axial compression and/or flexural compression	$\frac{b}{t}$ $\frac{h}{t_w}$	$1.40\sqrt{\frac{E}{F_y}}$	$0.64\sqrt{\frac{E}{F_y}}$ (tubes)
Unsupported width of perforated cover plates.	$\frac{b}{t}$	$1.86\sqrt{\frac{E}{F_y}}$	$0.88\sqrt{\frac{E}{F_y}}$
All other uniformly compressed stiffened elements that are supported along 2 edges.	$\frac{b}{t}$ $\frac{h}{t_w}$	$1.49\sqrt{\frac{E}{F_y}}$	$0.64\sqrt{\frac{E}{F_y}}$ (laced) $0.88\sqrt{\frac{E}{F_y}}$ (others)

Table 6-5 Continued Next Page

**TABLE 6-5 CONTINUED      LIMITING WIDTH-THICKNESS RATIOS**

Description of Elements	Width-Thickness Ratios	Essentially Elastic Components $\lambda_r$	Ductile Members $\lambda_p$
Webs in flexural compression or combined flexural and axial compression.	$\frac{h}{t_w}$	$5.70 \sqrt{\frac{E}{F_y} \left( 1 - \frac{0.74 P_u}{\phi_b P_y} \right)}$	<p>If <math>P_u \leq 0.125 \phi_b P_y</math>, then:</p> $3.14 \sqrt{\frac{E}{F_y} \left( 1 - \frac{1.54 P_u}{\phi_b P_y} \right)}$ <p>If <math>P_u &gt; 0.125 \phi_b P_y</math>, then:</p> $1.12 \sqrt{\frac{E}{F_y} \left( 2.33 - \frac{P_u}{\phi_b P_y} \right)} \geq 1.49 \sqrt{\frac{E}{F_y}}$
Longitudinally stiffened plates in compression.	$\frac{b}{t}$	$0.66 \sqrt{\frac{kE}{F_y}}$	$0.44 \sqrt{\frac{kE}{F_y}}$
Round HSS in axial compression or flexure	$\frac{D}{t}$	$\frac{0.09E}{F_y}$	$\frac{0.044E}{F_y}$

Limited results of the cyclic tests of axially loaded members also indicate that if the  $b/t$  ratio is less than  $\lambda_p$ , cyclic behavior of the locally buckled area will be quite ductile and premature fracture of the locally buckled area is not expected. Therefore, based on the available test results (Astaneh-Asl, 1996), it can be concluded that if  $b/t$  is less than  $\lambda_p$ , the locally buckled area will have a cyclic bending ductility of at least 6. The ductility of 6 for compact members is consistent current practices requiring a rotational ductility of 6 to 8 for plastically designed members.

If the  $b/t$  ratio is greater than  $\lambda_p$ , then ductility of the locally buckled area is expected to be somewhat less than 6. Studies of the local buckling under monotonic loading have indicated that if  $b/t$  is greater than  $\lambda_r$ , local buckling will start as soon as or before the yield strain is reached. In addition, in members with high  $b/t$  ratio, when local buckling occurs, the strength and stiffness significantly drops indicating essentially brittle behavior. Therefore, in a conservative manner, ductility of the members with  $b/t$  ratio equal to  $\lambda_r$  is assumed to be 1.0. For  $b/t$  values between  $\lambda_p$  and  $\lambda_r$ , a linear interpolation may be used. The  $\lambda_p$  and

$\lambda_r$  are the limiting values of  $b/t$  for plastic behavior without buckling or inelastic local buckling. Values of  $\lambda_p$  and  $\lambda_r$  can be expressed as:

$$\lambda_p = k_p \sqrt{\frac{E}{F_y}} \quad 6-30$$

$$\lambda_r = k \sqrt{\frac{E}{F_y}} \quad 6-31$$

The *Guide Specifications* provide limiting values of  $\lambda_r$  and  $\lambda_p$ , as shown in Equation 6-30 and Equation 6-31.

### 6.5.3 Over-all Member Buckling

When a member buckles, the compressive capacity drops. The rate of decrease of the compressive strength is an indicator of the post buckling ductility of the member. Studies of the post buckling behavior of axially loaded members are limited; however, they indicate that post-buckling ductility is directly related to the slenderness of the member  $\lambda$  given as

$$\lambda = \left( \frac{kL}{\pi r} \right)^2 \left( \frac{F}{E} \right) \quad 6-32$$

For slenderness parameter,  $\lambda$ , less than 1.0, a post-buckling ductility of 4 is reasonable. For  $\lambda$  values of 2.25 or greater, where buckling is elastic, a ductility of 1.0 can be assumed. For cyclic post buckling ductility, the above limit of 4 is further reduced for essential members and a ductility of 3 is assigned for  $\lambda$  of 1.0 or less for essential members of steel bridges. For  $\lambda$  between 1.0 and 2.25, a linear interpolation may be used.

### 6.5.4 Connections

Several failure mechanisms or limit states related to connections of elements are described below. These mechanisms impact the various component ductilities that comprise the overall system ductility of a typical steel structure:

a) Effects of Weld Fracture on Component Ductility

Weld fracture usually results in sudden brittle failure with a decrease of strength and stiffness. Due to the complex, inelastic cyclic behavior of weldments and the uncertainties involved, cyclic testing of realistic weld specimens is currently the most reliable way to establish the ductility of a welded connection or member. The main factors that affect ductility of a welded component in a steel structure are design, workmanship, quality control, inspection, geometry of the weld, presence of notches, tri-axial state of stress, temperature, type of weld and the base metal used. Due to the above parameters, shop welded and field bolted connections are most desirable and common.

b) Bolt Fracture

A bolt fracture is not usually as brittle as a weld fracture. In a welded component, if a crack develops in the weld and propagates, it can propagate throughout the entire weld line and result in total fracture, due to continuity of the weld line. However, in a bolted or riveted connection when a number of bolts and rivets fail, the load is shed to the remaining connectors.

c) Fracture of Net Area

When the net section of a bolted or a riveted member fractures, the strength, stiffness and ductility are reduced to zero. In built-up members, it is possible that only part of the section fractures and the remaining section could still carry some load. However, due to uncertainties with regard to the cyclic fracture of the net areas, even a partial fracture of the net area should be considered the end of the ductile cyclic behavior.

When a steel member with a hole is subjected to tension, one of the two failure modes can occur: (a) yielding of the gross area or (b) fracture of the net area. Limited available cyclic test data (Astaneh-Asl, 1996) indicate that if the connection is proportioned such that fracture on the net area does not control over yield on the gross area, then the member will demonstrate ductile cyclic behavior by yielding the gross area.

## 6.6 ESTIMATION OF INELASTIC RESPONSE

### 6.6.1 Damage of Bridge Columns

Past earthquakes have provided valuable lessons on the behavior of yielding components and most importantly bridge columns. Although most bridge columns within the area of heavy damage in the San Fernando earthquake of 1971 had inadequate transverse reinforcement details, there was a vast difference in the way they performed. For many of the heavily damaged columns, it appeared that shear was the primary mode of failure whether it was due to inadequacy of the initial shear capacity, or the degradation of shear capacity resulting from confinement failure.

Based on the San Fernando post-earthquake investigations, a method of screening existing bridges with poor column confinement details for column vulnerability was derived for purpose of seismic rating. The following relationship for the Column Vulnerability Rating (*CVR*) was established and is used in the FHWA *Seismic Retrofit Manual for Highway Structures: Part -1 Bridges* (2006) to provide a simple assessment of column vulnerability:

$$CVR = 13 - 6 \frac{L_c}{P_s F b_{max}} \quad 6-33$$

where

$L_c$	=	The effective height of the column
$P_s$	=	Percent main reinforcing steel
$b_{max}$	=	Maximum transverse column dimension
$F$	=	2.0 For multicolumn bents – both ends fixed
$F$	=	1.0 For multicolumn bents – one end fixed
$F$	=	1.5 For single column bents – both ends fixed – box girder superstructure
$F$	=	1.25 For single column bents – both ends fixed – non-box girder flexible superstructure

This method provides a simple means for assessing, in an approximate but meaningful fashion, the vulnerability of columns to seismic loading and the likelihood of poor performance. The higher the *CVR* rating indicates the more vulnerable the column. Some observations should be made about the Column Vulnerability Rating expression. First it is noted that columns with higher longitudinal reinforcement

ratios are considered more vulnerable than similar columns with lower reinforcement ratios. This is only the case for columns which experience approximately equal ductility demands. It is noted that all the bridges considered in the original formulation were in the short-to-medium period range. It is expected that for bridges having longer periods, the proposed parameters as indicators of individual column damage become less significant since both the maximum and cumulative curvature ductility demands will be less. In general, the primary mode of column failure is flexural, not shear, in long-period structures.

The intensity and duration of the earthquake ground motion will also affect the performance of a column. Greater maximum and cumulative ductility demands will cause a more rapid degradation of column strength. Based on the *CVR* formulation mentioned above, it is clear that the column aspect ratio (depth over equivalent column length) is a prominent parameter in predicting damage intensity. Consequently, an approximate measure, such as the *CVR*, may be used as an indicator for low to moderate seismic regions where column reinforcement ratio may not be as high as in those locales where seismic loading governs column design.

### **6.6.2 Performance of Bridge Columns**

Research over the last two decades has amassed considerable data with which to correlate column performance criteria to simple variables. Three different schematic curves shown in Figure 6-36 illustrates the “backbone” (envelope of cyclic response) curve for brittle, strength degrading, and ductile behavior. Examples of corresponding damage are shown in Figure 6-37 and Figure 6-38. More detail relating damage to deformation levels for various bridge elements can be found in Caltrans *Visual Inspection & Capacity Assessment of Earthquake Damaged Reinforced Concrete Bridge Elements* (2008), which is available online. The capacity design approach used in the AASHTO seismic design provisions, both *LRFD Specifications* and *Guide Specifications*, seek to ensure that significant ductility capacity is provided in the moderate to high seismic regions of the country. For the lower seismic regions, the required ductility capacity is not expected to be as high because the seismic demands are expected to be lower.

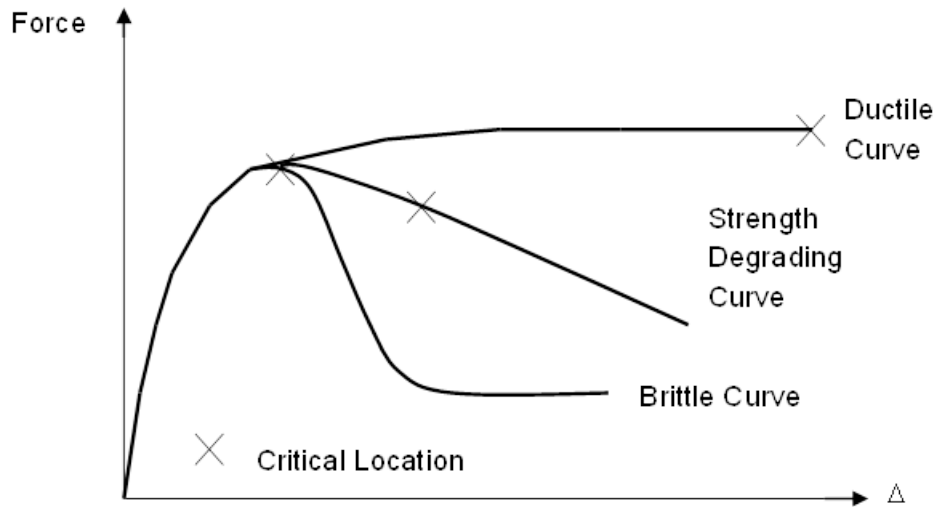


Figure 6-36 Column Performance Identification Curves

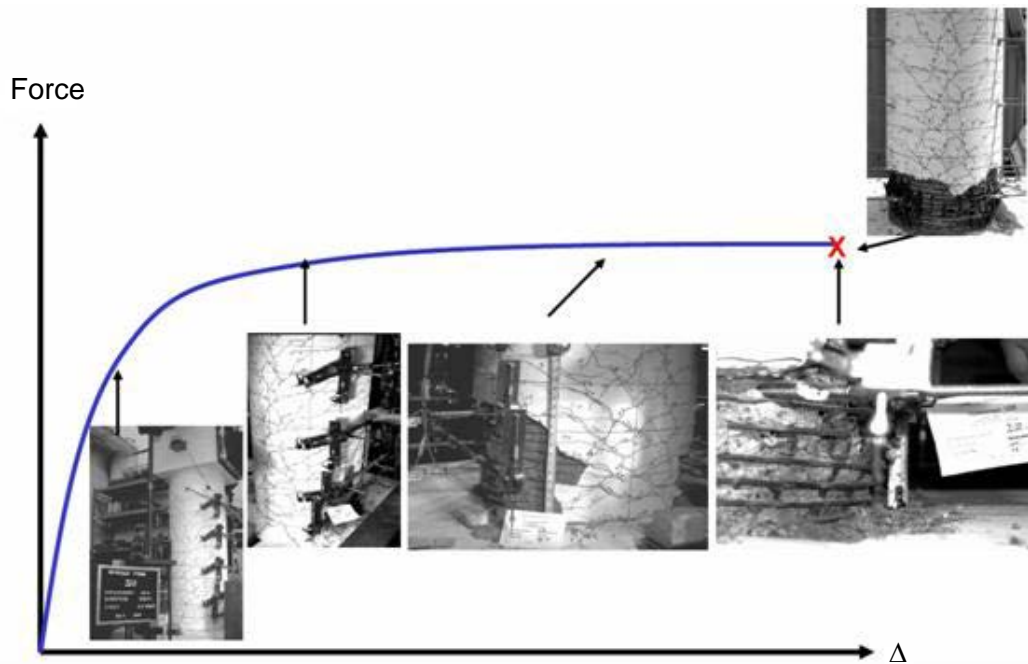


Figure 6-37 Ductile Performance Damage Levels

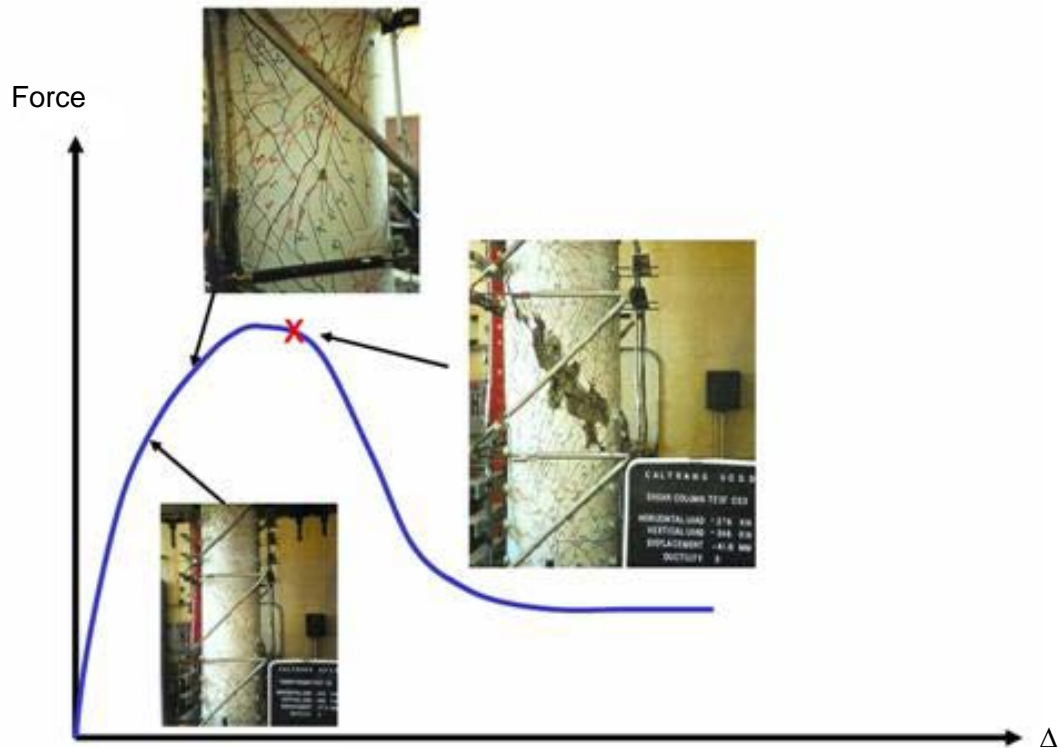


Figure 6-38 Brittle Performance Damage Level

It is therefore possible to develop “implicit” displacement capacity equations to provide a simple method of estimating the displacement capacity of reinforced concrete columns. Such simple expressions could be used to estimate capacities in any region of the country, but the method would be particularly useful in the low to moderate seismic regions. The method could be used to eliminate the need to perform a more refined capacity analysis using the pushover analysis technique, as outlined in Section 6.4. If the method were sufficiently conservative, then the simplification of neglecting many parameters in the check could be safely justified. This approach was developed by Imbsen (2006) for inclusion in the *Guide Specifications*, and although they are only included in the *Guide Specifications*, the capacities provided are applicable to columns designed using the *LRFD Specifications*, although the results may be somewhat conservative due to the differences in detailing requirements between the two specifications. However, except for these differences, the equations are independent of design procedure and provide useful reasonableness checks regardless of design procedure. The development of the method is outlined below.

The development of the equations, as they appear in the *Guide Specifications*, uses the research conducted by Berry and Eberhard (2003) to develop a procedure to estimate flexural damage in reinforced concrete

columns. Their research focused on developing fragility curves for two flexural damage states, concrete cover spalling and buckling of the longitudinal reinforcing steel bars. The database used in the development of the fragility curves included physical test results on 274 rectangular reinforced columns and 160 spiral reinforced columns.

As an example of the relationships produced, the curve designated as “Experimental C1” in Figure 6-39 shows the “Drift Capacity” using Berry and Eberhard’s equation for spalling using an assumed maximum axial load for bridge columns of  $0.1 f'c A_g$ . The drift capacity is plotted as a function of  $D/H$  where  $D$  is the diameter or depth of the column in the direction of loading and  $H$  is the column height, taken as length from inflection point to the point of maximum moment. In this instance, the drift capacity corresponds to the average onset of spalling.

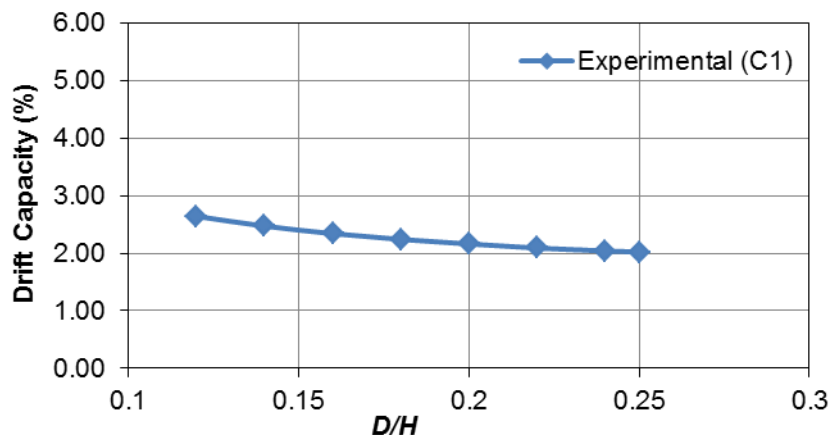


Figure 6-39 Drift Capacity for Reinforced Concrete Spalling from Berry and Eberhard (Imbsen, 2006)

To augment the test results and the expression for spalling, developed by Berry and Eberhard, into a more general capacity equation, a second database, as shown in Table 6-6, was generated.

The columns of the second database were then evaluated numerically considering three design limit states; yield, spalling, and attainment of a ductility of four. The calculation method outlined in Section 6.4 was used for these calculations. The displacement corresponding to yielding of the reinforcing steel, as shown in Figure 6-40 for the curve designated as Yield (C2), was determined. Then, onset of concrete spalling was then evaluated for a concrete compressive strain of 0.005 and plotted as Spalling (C3) in the figure. Additionally, the columns were evaluated at a ductility,  $\mu$ , equal to 4, which is designated as Ductility 4 (C4).

**TABLE 6-6 ANALYTICAL DATA BASE COLUMN PARAMETERS**

Column diameter $D$ (ft)	Rein. Steel (%)	Column Height $H$ (ft)	Aspect Ratio, $D/H$
3	1, 2, 3, 4	20	0.15
4	1, 2, 3, 4	20, 30	0.2, 0.1333
5	1, 2, 3, 4	20, 30, 40	0.25, 0.167, 0.125
6	1, 2, 3, 4	30, 40, 50	0.2, 0.15, 0.12
7	1, 2, 3, 4	30, 40, 50	0.23, 0.175, 0.14

The columns of the second database were then evaluated numerically considering three design limit states; yield, spalling, and attainment of a ductility of four. The calculation method outlined in Section 6.4 was used for these calculations. The displacement corresponding to yielding of the reinforcing steel, as shown in Figure 6-40 for the curve designated as Yield (C2), was determined. Then, onset of concrete spalling was then evaluated for a concrete compressive strain of 0.005 and plotted as Spalling (C3) in the figure. Additionally, the columns were evaluated at a ductility,  $\mu$ , equal to 4, which is designated as Ductility 4 (C4).

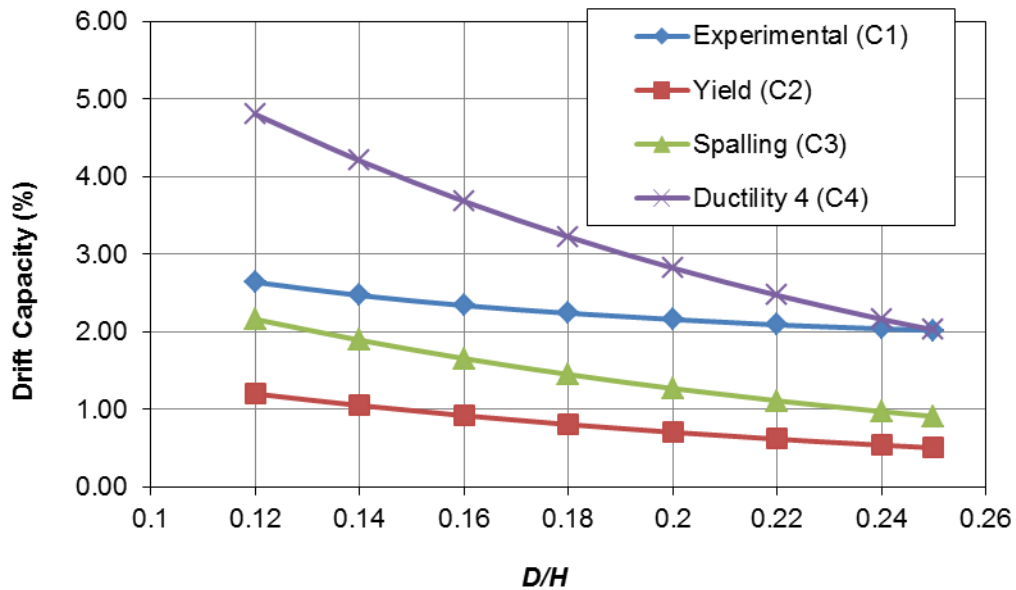


Figure 6-40 Plots Showing the Calculated Drift Capacity vs.  $D/H$  for the Columns of Table 6-6 (Imbsen, 2006)

Columns for bridges in lower seismic areas are targeted for a drift capacity corresponding to minor damage, because full ductile detailing is not required in these areas. Concrete spalling is considered as the limit state for this case. Figure 6-41 contains curves of both experimentally determined limit state attainment and the calculated threshold of that same limit state. For instance, there are two curves for the spalling limit state, Curve 1 is for the onset of spalling as determined experimentally and Curve 3 is spalling as determined analytically.

It can be seen that the analytical results are more conservative than those determined experimentally, since the threshold of spalling by calculation occurs at a lower drift. Thus, an average of these two results may be taken as a conservative predictor of attaining this limit state. This is shown by the following equation:

$$\text{Drift Capacity Low Seismic} = \frac{\text{Curve3} + \text{Curve1}}{2} \quad 6-34$$

The average designated as Low Seismic (C5) in Figure 6-41, is thus the modified conservative predictor of the onset of spalling.

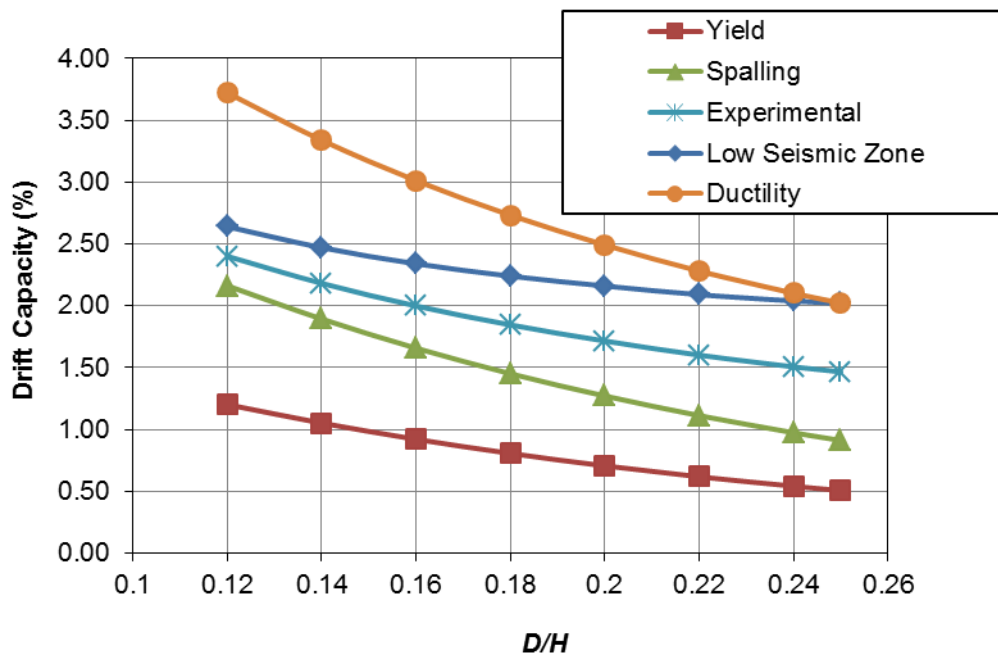


Figure 6-41 Plot Showing the Determination of the Drift Capacity for a Low Seismic Zone (Imbsen, 2006)

For moderate seismic regions, the drift capacity is targeted to a maximum drift corresponding to moderate damage. The approach in this case, is to take an average of the experimental spalling results (i.e. Curve 1) and the calculated ductility,  $\mu$ , equal to 4 (i.e. Curve 4) obtained by taking an average as:

$$\text{Drift Capacity Moderate Seismic} = \frac{\text{Curve4} + \text{Curve1}}{2} \quad 6-35$$

The average is designated as moderate seismic (C6) in Figure 6-42, is thus the conservative predictor of damage somewhere beyond spalling but less than achieving a ductility of four.

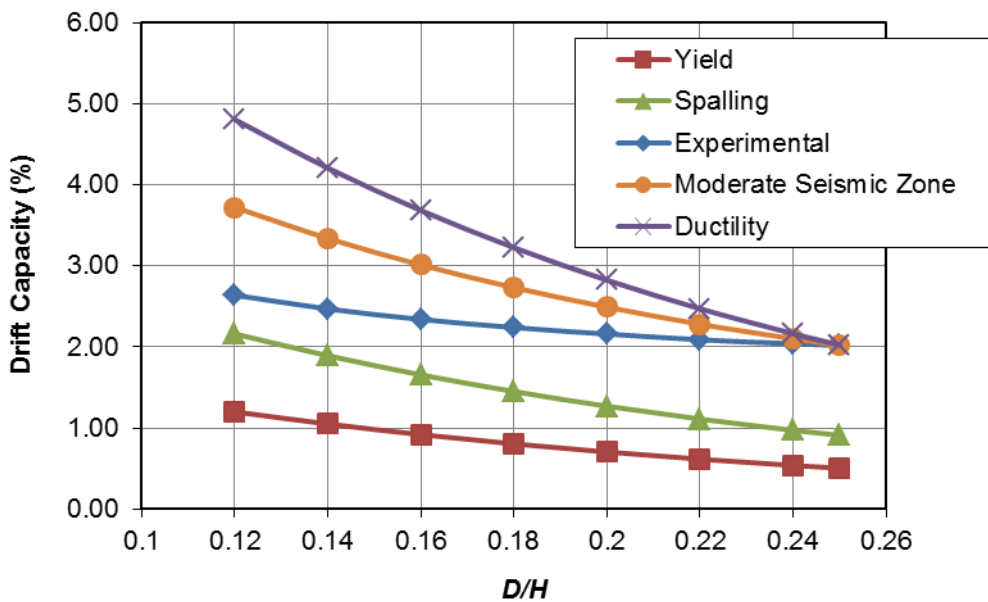


Figure 6-42 Plot Showing the Determination of the Drift Capacity for a Moderate Seismic Zone (Imbsen, 2006)

The damage levels for the ‘low’ and ‘moderate’ seismic zones would range between the minimal to moderate (middle of the plot) range as shown in Figure 6-37. Spalling would be expected to occur just after the curves rolls over and a ductility of four would be occur on the plateau, but prior to the attainment of the ultimate limit state. In general, the limits in the implicit approach were selected to be conservative for flexurally dominated response, and the ductility of four is conservatively described as three in the *Guide Specifications*. This conservatism holds provided that unwanted brittle modes of failure, such as shear failure, as illustrated in Figure 6-38, are prevented. Thus even in the lower seismic regions brittle

failure modes that jeopardize the vertical load carrying capacity must be prevented. This is evident from the rapid drop in lateral resistance as shown in the figure.

The two implicit displacement capacity curves that have been established for low and moderate seismic regions will be seen in subsequent chapters of this manual when the specific design methods are described.

## **6.7 SUMMARY**

The purpose of this chapter is to provide background material that supports relying on inelastic response in order for bridges to withstand large earthquakes. As outlined in Chapter 4, reliance on such response is only appropriate if the inelastic elements of the structure can indeed endure the expected post-yield deformations induced by ground shaking. The first sections of this chapter provided background from large-scale laboratory testing of bridge elements that quantified their inelastic response and capacities. Key to successful seismic performance is appropriate “detailing” of structural elements, which includes configuration and geometry of reinforcement for concrete members and sizing of plate thickness for steel members. Material properties have also been presented, along with the methodology for calculating inelastic displacements for reinforced concrete members, which comprise the most commonly used structural inelastic member types for bridges. Descriptions of local failure mechanisms for both reinforced concrete members and steel members have been provided to help designers understand the various modes of failure possible so that prevention of such failures can be prevented. Finally, an “implicit” method for determining displacement capacity of reinforced concrete columns has been presented. The various forms of that method conservatively predict displacements that correspond to different damage states. The material presented in the chapter serves as a basis for understanding the AASHTO design methodologies and the prescriptive requirements applicable to seismic design.



## CHAPTER 7

### SEISMIC DESIGN METHODS

#### 7.1 GENERAL

This Chapter describes the two methods of seismic design currently available to the bridge designer. The parameters used and the methods of computation for both methods are described in this chapter. Both are viewed in tandem with the selection of the earthquake hazard level chosen for the Life Safety-Collapse Prevention criteria. The first method as included in the *LRFD Specifications* is known as a Force-Based Method (FBM). This method has been used for many years and enjoys a wide range of acceptance and understanding by practicing bridge engineers. The second method is known as the Displacement-Based Method (DBM), which is the basis of the recently adopted *AASHTO Guide Specifications for Seismic Bridge Design (Guide Specifications)*.

The basic underlying philosophy used in both methods is to design a bridge that has, in its entirety, both ductility and deformability with some reserve to resist an earthquake even greater than anticipated in the design. The traditional approach in seismic bridge design has been to select key components that provide the ductility (e.g. columns) - and deformability (e.g. adequate capacity in movement joints) to resist the design level earthquake ground motions. Once these key components are selected, the remaining components are designed to provide a load path and displacements to accommodate the forces and deformations imposed on the selected key components without the remaining components losing their strength. This is known as capacity design approach, and this likewise has been part of the AASHTO seismic design approach for many years. The basic steps of the design process are outlined in Table 7-1.

As observed from damage caused by a number of earthquakes that have struck areas with bridges designed using older methodologies, columns did not have the strength or deformation capacity required to keep bridges from collapsing. Additionally, support and hinge widths could not accommodate the earthquake imposed displacements and eventually led to collapse. The basic geometry of a typical bridge, designed to support multiple lanes of vehicular traffic, yields a superstructure that is significantly stiffer than the substructure. Although substructures could have been designed to carry the fully elastic lateral loads imposed by the superstructure during an earthquake, it was deemed impractical to design this way from a cost point of view. Bridge engineers did, however, recognize that design forces could be reduced provided that ductility was designed into the structure. Thus, with the benefit of lower design forces

came the requirement to provide ductility or inelastic deformation capacity. Through the recent decades a great deal of test data on reinforced concrete columns loaded under simulated earthquake conditions have provided keen insight into the reasonableness of a ductile design approach with the columns selected as the component for the yielding element. This decision has been substantiated more recently with large-scale and shake table laboratory tests conducted on reinforced concrete columns.

**TABLE 7-1 GENERAL STEPS FOR SEISMIC DESIGN**

Step	Design Activity
1.	Determine seismic input.
2.	Establish design procedures.
3.	Identify the earthquake resisting system – desired plastic mechanism.
4.	Perform demand analysis.
5.	Design and check the earthquake resisting elements (ductile or other elements).
6.	Capacity protect the remaining elements.

This chapter describes both the FBM and the DBM seismic design of bridges. Additionally, the chapter covers capacity protection of elements that are not part of the primary energy dissipation mechanism. Fundamentally, both methods seek the same end – a capacity designed structure where certain elements are meant to yield, are designed to be ductile, and all the rest are designed to remain essentially elastic. This strategy is, of course, the three principles of capacity design, as discussed in earlier chapters. As stated, both the FBM and DBM are focused on the same result; it is only the method of achieving the end that differs. In this chapter, the concept of using prescribed ductility, "R", factors to reduce elastic forces to design level forces is described for the FBM. The DBM on-the-other hand considers inelastic deformation capacity determined by conducting section analysis to obtain moment versus curvature relationships on columns designed for service load conditions.

Both methods require the determination of the seismic demand analysis. This process, which is similar for either method, includes generating a global analytical model, conducting a response analysis and selecting the forces and displacements from the analytical results for use in design of individual bridge components. The complexity of the analytical process is based on both the seismic hazard and the geometry of the bridge. Varying seismic hazard is recognized in both methods, but the specifics are not

germane to this chapter. In general, increasing hazard will be reflected in increasingly rigorous requirements for the seismic design. In addition, an increase in hazard results in yielding of ductile components through the formation of plastic hinges and increased ductility demands for the higher hazards locations. In the end, the bridge's demand must be compared and successfully reconciled against its capacity. This is accomplished for both methods, but in a different fashion for each.

Although much attention to date has focused on reinforced concrete columns in the substructure, structural steel, concrete filled steel pipes, and reinforced concrete wall piers are often used as yielding components in the substructure. Additionally, yielding components may be selected in the superstructure such as, steel end diaphragms placed between steel girders, as discussed with Type 2 structures in Chapter 4. Additionally, Seismic Response Modification Devices (SMRD) may be used as a key component at the interface between the superstructure and substructure to provide isolation and/or energy dissipation.

### **7.1.1 Methods of Linearization for Design**

As mentioned in previous chapters, modern seismic design often depends on the estimation of inelastic results using linear elastic analysis procedures. This is more of a convenience than a recognition of reality. We might prefer to analyze inelastic response of our yielding bridges using inelastic response history techniques, but those are not always economical to use for design. They often are cost effective for large important bridges, but are not usually cost effective for the normal two, three or four span overcrossing or undercrossing.

To address this problem, techniques have been developed to estimate inelastic response from elastic response, and these were briefly described in Chapter 6. For longer period structures, the displacement of a yielding structure is taken equal to the displacement of an elastic structure with the same period and mass. For shorter periods, there is a transition zone that rationally and conservatively interpolates the response all the way down to zero period. This will be described in more detail in Chapter 8.

Other key contributors to the response must be addressed and potentially linearized to facilitate linear elastic analysis procedures. An example is foundations where the soil response is markedly nonlinear. For these cases, we often analyze the foundation statically under lateral loading and determine the expected response, inclusive of nonlinear action. Then an equivalent stiffness is generated from this

analysis and the structure reanalyzed. The process is iterated until a reasonable convergence of response is obtained. In this fashion, nonlinear effects, such as  $P$ - $y$  curves and pile foundations can be included in the demand analysis in a reasonable fashion.

It is also essential to recall that a statistically based method is available and used (i.e., a part of the specifications) for adjusting the elastic analysis results for estimating displacements for the expected inelastic response. This adjustment was discussed in Chapter 6. In general the adjustment for estimating inelastic response from elastic analysis results is based on an assumption that the inelastic system response is that of a single-degree-of-freedom (SDOF) system and does not fully or explicitly account for multi-degree-of-freedom (MDOF) system response. Fortunately, many bridges do respond essentially as a SDOF system.

An example includes the analysis of a complex multi-degree of freedom curved ramp which considers the application of an equivalent SDOF system to a MDOF system. This application is illustrated in Figure 7-2 and Figure 7-3. Figure 7-1 shows a schematic of a bridge with seismic forces applied in the transverse direction. The bridge has three frames with a typical frame shown in Figure 7-2. Given the slenderness of Bent 1, 2, and 3, the force-displacement capacity for all three bents is shown in Figure 7-3. More details are provided in Chapter 7 on the development of a force deflection curve for an individual bent. The total force deformation response for the frame as a whole is found by adding the bent forces for given displacements, as shown in Figure 7-3, and the resulting frame mechanism strength  $V_f$ , and yield displacement  $\Delta_y$  are calculated from intersection of the initial slope and final slope of the response. The superposition of the force displacement curves for all three bents show that loss of strength for the total frame is governed by the displacement capacity of Bent 3 being the bent with the least displacement capacity. The application demand of adjustment or magnification approach to convert elastic results to inelastic results is generally conservative – as described in Chapter 6 and recalling that the adjustment method requires the bridge to be approximated as a SDOF system with bilinear inelastic response. That said, the designer should be alert to cases where economical and reasonable design cannot be achieved and a more refined design can be achieved with more advanced techniques.

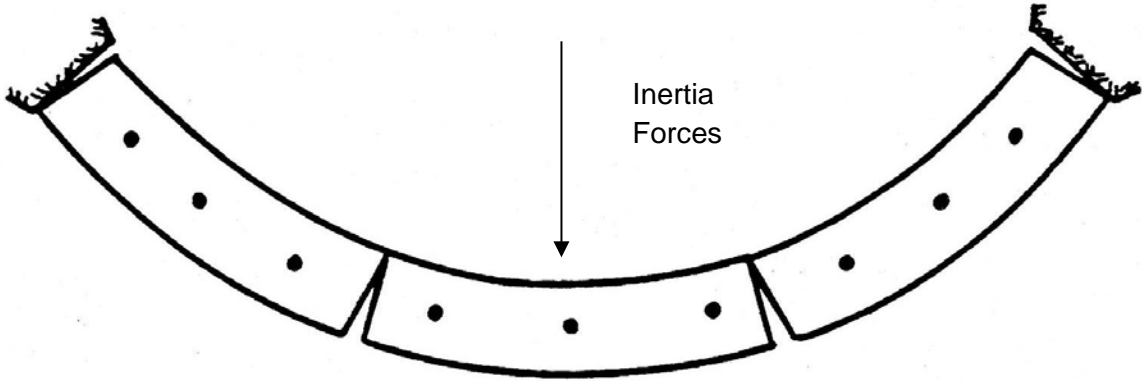


Figure 7-1 Transverse Seismic Forces

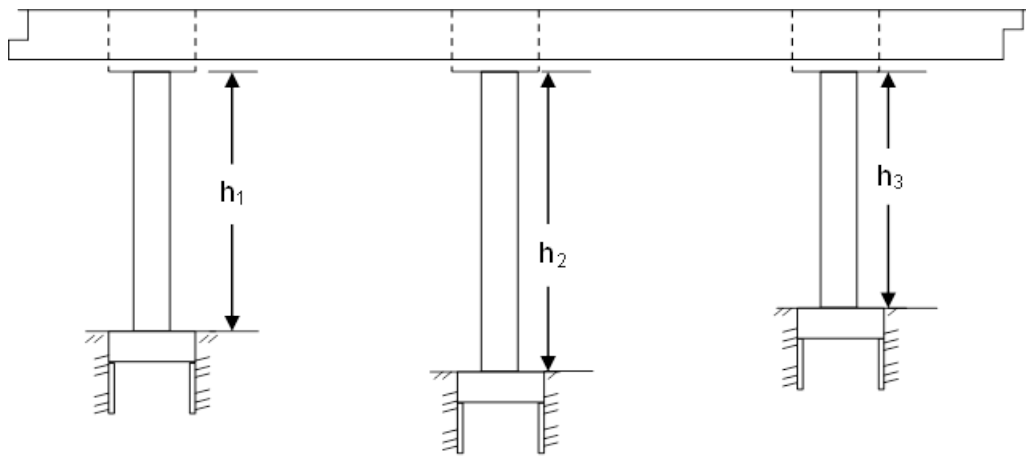


Figure 7-2 Frame Elevation

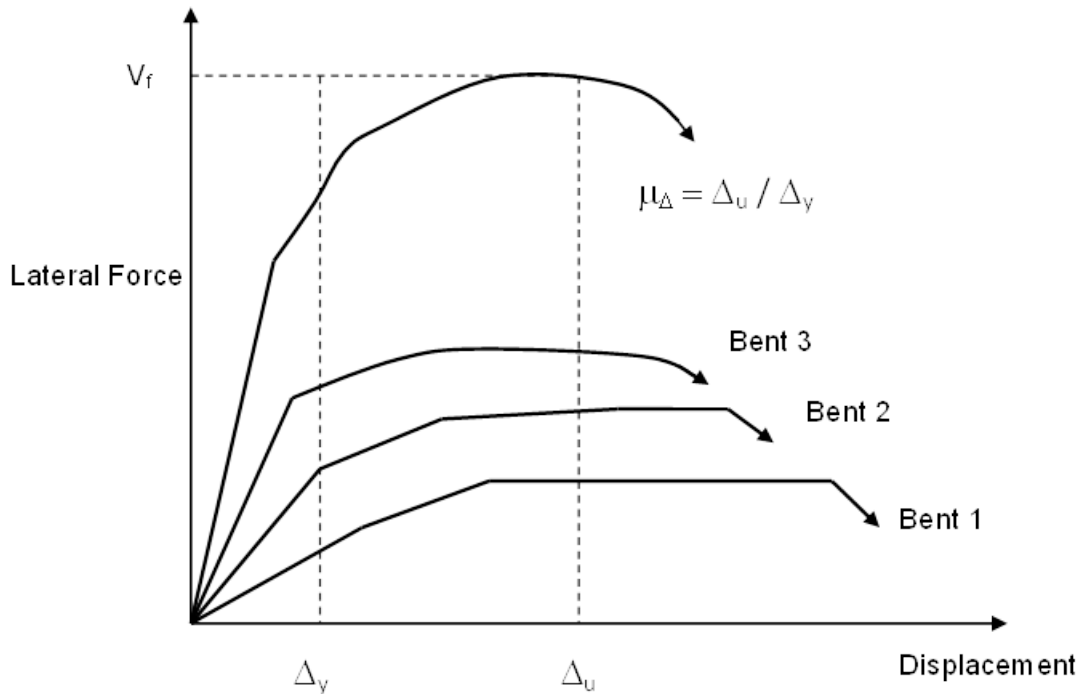


Figure 7-3 Composite Force-Displacement Curves

### 7.1.2 Seismic Load Combinations

The detailed seismic design of a bridge is often accomplished following the design for all the service load conditions, unless the seismic loading is expected to control. Earthquake loading is considered an extreme limit state having a unique occurrence with a return period of 1000 years that is significantly greater than the design life of 75 years for a new bridge.

This extreme condition limit state should include permanent loads that are likely to be present when an earthquake occurs. Such load include permanent loads, internal force sustained loads, water loads. Usually, unless specific site conditions dictate otherwise, local pier scour and contraction scour depths are not be included in the design. However, the effects due to degradation of the channel should be considered.

Live load coincident with an earthquake is considered on a project specific basis. Live load is typically considered only for critical and essential bridges. In the past editions of the Standard Specifications, live load was not considered at all. The possibility of some partial live load, acting with earthquakes should

be considered. According to the *LRFD Specifications*, application of Turkstra's Rule for combining uncorrelated loads indicates that  $\gamma_{EQ} = 0.50$  is reasonable for a wide range of values of average daily truck traffic (ADTT), and this value is recommended by both AASHTO seismic specifications when live load is to be considered concurrently with seismic loading. The selection of the value normally requires consensus of the Owner. In some cases, including half the live load may be unreasonably large given the expected traffic conditions, especially the density of trucks, or the geometric arrangement of actual lanes on the bridge. For Critical or Essential structures a more precise value of the live load factor may be warranted on a project-specific basis. When live load is considered, it is not included in the seismic mass. Only the gravity effects are included, because the vehicle suspension systems are thought to de-couple the bridge and vehicle dynamic responses.

It should be noted that differences between the force-based procedure and the displacement-based procedure, as included in the AASHTO specifications, exist. In particular, there are differences in how permanent loads are included in the design checks. Such differences are not philosophically a part of the seismic design method, but instead derive from perceived difficulties of including permanent loads with the two methodologies. For example, in the FBM, a set of permanent load factors is included in the load combination. Typically, the seismic demand analysis is run for a single value of permanent load, which is the nominal dead load and earth loads. The design forces are then calculated by adjusting the permanent load gravity effect whose value may take on values greater than one or less than one. The factors less than one have the effect of increasing the design forces if the static permanent load helps resist the earthquake effects. Likewise, the factors that are greater than one increase the design forces if the permanent load acts as a concurrent load with the seismic effects. Load combinations with these factors are simply compiled in the FBM and an enveloping resistance is selected for the member. This is a fairly simple process. However, in the DBM procedure, such variations in the permanent loads by multiple load factors require multiple assessments to be run and the demand versus capacity evaluated for each. This requires significant additional effort. This exclusion is reasonable because the predominant permanent load is typically the dead load. Variations in the dead load would also affect the seismic inertial loading, which would affect the seismic demand analysis. With the significant approximations made between the elastic demand analysis and the actual inelastic response, the additional refinement of varying the permanent loads by a small amount in the seismic displacement demand model is not warranted.

## 7.2 FORCE-BASED DESIGN METHOD

The Force-Based Design Method (FBM) is the method traditionally used by the AASHTO *LRFD Specifications*. The method develops seismic design forces for the yielding elements by dividing the elastic seismic forces obtained from the demand analysis by the appropriate Response Modification Factor ( $R$ ).

Response modification factors ( $R$ ) were introduced with the objective of achieving seismic performance of bridges in accordance with the following principles (AASHTO, 2013):

- Small to moderate earthquakes should be resisted within the elastic range of the structural components without significant damage.
- Realistic seismic ground motion intensities are used to determine elastic demand forces that are subsequently reduced by the factor  $R$  to be used in the design procedures.
- Exposure to shaking from large earthquakes should not cause collapse of all or part of the bridge. Where possible, damage that does occur should be readily detectable and accessible for inspection and subsequent repair if necessary.

The  $R$  factors are used to obtain the design forces for each component using the results of the demand analysis of the bridge when subject to the seismic loads defined by elastic design spectra. Inherent in the  $R$  value is the assumption that the columns will yield when subjected to the elastic demand forces induced by the design ground motions. Graphically, the concept of the  $R$ -factor approach is illustrated in Figure 7-4. In the figure the force,  $F$ , and displacement,  $\Delta$ , are global measures of the bridge response, for instance total base shear and maximum displacement of the bridge. The elastic response line represents the response of the bridge if no damage and no yielding occur. An elastic analysis is based on such conditions. The maximum force obtained during shaking from an earthquake corresponds to the peak of the elastic curve and would likely be a large force to design to resist. An alternate approach that permits yielding is shown by the lower bilinear plot, where the peak elastic force has been reduced. This reduction is produced by the  $R$  factor. If the bridge actually forms its plastic mechanism all at once at the point of departure from the linear elastic response curve and the period of vibration is such that the equal displacement rule applies, then the  $R$  factor also corresponds to the ductility factor. Thus, the  $R$  factor is often synonymously thought of as the ductility demand. This may not always be the case. Nonetheless, the figure illustrates the basis of the  $R$  factor method (FBM).

The procedure for applying the FBM is provided in **TABLE 7-2**. As noted in the table, other concurrently acting loads are considered with the seismic forces. The effect of the other loads cannot be reduced by  $R$ . Only the effects of yielding elements may be reduced by  $R$ , and these typically are the moments in the yielding columns. Other internal force effects, such as axial force and shear should not be reduced by  $R$  and assignment of appropriate design values for column axial and shear becomes part of the capacity protection process.

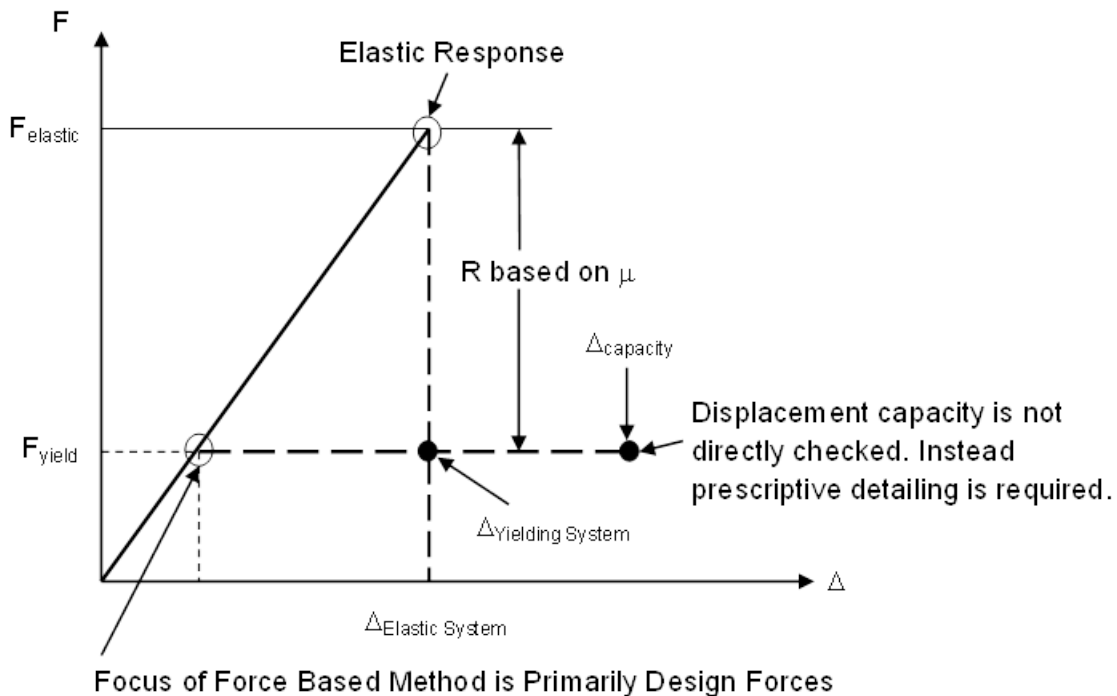


Figure 7-4 Force-Based Method for Lateral System Force vs. Displacement

The rationale used in the development of the  $R$  values for columns, piers and pile bents is based on considerations of ductility and redundancy provided by the various support systems. The wall type pier loaded in its strong direction, for example, is assumed to have minimal ductility capacity and redundancy, while a multiple column bent with well-detailed ductile columns, is assumed to have good ductility capacity and redundancy and is therefore assigned the highest value of  $R$ . For these two example cases,  $R$  is assigned by the *LRFD Specifications* as 2 and 5, respectively. Although the capacity of a column in a single column bent is similar to that of a column in a multiple column bent, there is no lateral load redundancy, and therefore a lower  $R$  value of 3 is assigned to single column bents. Other examples are pile bents and batter pile piles. At the time the  $R$  values were compiled there was little or no information available on the performance of substructures composed of extended pile bents. Thus conservatively low

**TABLE 7-2 FORCE-BASED METHOD – GENERAL APPROACH**

Step	FBM Design Activity
1.	Analyze demand model for elastic forces.
2.	Combine orthogonal responses.
3.	Reduce seismic moments by R factor (yielding elements only).
4.	Combine with other concurrent loads.
5.	Calculate the required strength of the yielding elements.
6.	Choose the reinforcement in yielding elements.
7.	Detail yielding elements <u>prescriptively</u> for ductility.
8.	Capacity protect non-yielding elements.

factors were assigned based on the judgment of potential pile bent performance in comparison to that of the other three types of substructure. It was believed that there should be a reduction in the ductility capacity of pile bents with batter piles and therefore lower more conservative  $R$  was assigned to these systems. From this discussion it is apparent that the use of lower  $R$  values, in general, should be more conservative, meaning that the more lateral strength is supplied to the bridge, the lower will be the inelastic demands.

The last case of the batter pile bent illustrates a fundamental issue. Batter piles that predominantly respond as axial force members have no definitive plastic mechanism, unless the piles are designed to mobilize the geotechnical capacities. Thus, realistically batter pile bents should be designed with careful attention to expected performance, and an  $R$  of 1.0 (i.e., no inelastic reduction for ductility) should be considered.

An extension of the  $R$  factor method is used in the *LRFD Specifications*. Instead of solely designing the yielding elements using  $R$ , factor of 1.0 or less are assigned to connections. Such components are designed for the elastic forces or for greater than the elastic forces, the components include abutments and expansion joints within the superstructure. This approach is adopted in part to accommodate the redistribution of forces to the abutment that occur when a bridge responds inelastically in the columns and to maintain the overall integrity of the bridge structure at these important non-ductile joints. Thus, the use

of small  $R$  factors for these elements is a simplified method for capacity protecting elements that should not be damaged in the design earthquake. This practice is simple, easy to apply, but may not in all cases achieve its goal of preventing damage at the particular locations. Again the designer is encouraged to consider the results of such designs carefully to ensure the end goal is achieved.

However, it should be noted that for bridges in higher seismic regions, the recommended design forces for column connections are the forces that can be developed by plastic hinging of the columns. This means that internal forces corresponding to the attainment of a plastic mechanism must be calculated, not simply the design forces using the  $R$  factor. This process means that if the yielding elements are stronger than required for whatever reason, that accurate internal forces are calculated for the seismic loading case. These plastic mechanism forces are generally smaller than the elastic values.

Once the yielding elements are designed, then the remainder of the bridge can be designed using capacity protection principles. The general approach for capacity protection is to amplify the basic plastic mechanism internal forces by a factor to account for potential overstrength of the yielding elements. These factors were discussed in Chapter 6 and are intended to generate an upper bound to the forces that the yielding elements can transmit to those elements, such as foundations, which should not experience damage in the design earthquake.

It is important to note that no direct check of the displacement capacity is made with the FBM. Forces are derived using the  $R$  factor, then the yielding members are designed to provide the requisite strength. The member and bridge displacement capacity is presumed to be provided by prescriptive detailing. The detailing requirements have their basis in laboratory tests that show that the details will provide at least the ductility implied by the  $R$  factors used. Thus the detailing provisions and the  $R$  factor magnitudes are interlinked to ensure adequate ductility in the bridge. Example details that must be addressed are transverse reinforcing steel, anchorage and development of reinforcement, extent of appropriate confinement steel for reinforced concrete. For structural steel in the yielding substructure, details would include appropriate element slenderness ratios, limitations on net sections relative to gross section, welding details and filler metal. Additionally, such items as support lengths for articulation and movement joints are conservatively proportioned to prevent unseating or dropped spans from seismically induced movements of the bridge.

### 7.3 DISPLACEMENT-BASED DESIGN METHOD

The Displacement-Based Method (DBM) is the method used in the *Guide Specifications*. Fundamentally, it has the same objective as the FBD, but the means are different. The DBM, unlike the FBM, does not provide a path to a unique design force for the yielding elements. Instead, provided that a minimum lateral strength threshold is provided for each pier, the designer is free to proportion the yielding system as necessary to ensure that the displacement demand is less than the displacement capacity at each pier. That is, of course, provided all the non-seismic load cases are also satisfied. Thus, the designer simply proposes a lateral system and corresponding element strengths then checks to ensure that the displacement capacity is adequate. The capacity is based on the ductility of the yielding column elements, and their displacement capacities may be controlled by both the longitudinal and transverse reinforcement provided in the columns and the configuration of the substructure (e.g., height-to-width aspect ratios of columns, end continuity, etc.). In the end, a direct check of the displacement capacity relative to the demand is made. The process used in the DBM is outlined in Table 7-3.

**TABLE 7-3 DISPLACEMENT-BASED METHOD – GENERAL APPROACH**

Step	DBM Design Activity
1.	Design for non-seismic cases / minimum strength.
2.	Develop the demand model.
3.	Analyze model for elastic <u>displacements</u> and perform directional combinations.
4.	Develop displacement assessment model.
5.	Determine maximum permissible displacement.
6.	Compare with demand displacements.
7.	<u>Adjust</u> detailing so capacity exceeds demand.
8.	Capacity protects non-yielding elements.

Like the FBM, a demand model is used. However, the demand is simply the displacement, and this includes the effect of multiple modes of vibration, directional combination, and foundation flexibility just as the demand model for the FBM does. Thus, the output of the demand model may be viewed as target

displacements that each pier or substructure unit of the bridge must be able to resist without damage that leads to premature loss of strength. These target displacement demands are adjusted to appropriately estimate the inelastic displacements from the elastic analysis, just as with the FBM.

The DBM capacity evaluation involves conducting a sectional analysis to obtain the component moment vs. curvature relationship, and analysis to calculate the load-displacement characteristics of the bridge (displacement assessment model) and a subsequent determination of the displacement capacity (permissible displacement) of the substructure. The displacement capacity is then compared to the seismic demand to evaluate the ability of the component to resist the earthquake event. If the displacement capacity is inadequate, then additional confinement steel can be added to improve the sectional ductility, which is reflected in the moment-curvature relationship. The displacement check is then recalculated and the process repeated until adequate displacement capacity is obtained. Alternately, the configuration of the bridge including column fixity, clear height, etc can be changed to improve the displacement capacity. Strategies for this type of refinement are discussed in Chapter 4.

The displacement capacities for lower seismic regions may be obtained using implicit formulas to simplify the capacity determination for the bridge designer. These implicit methods were discussed in Chapter 6. Or alternatively the designer can directly assess the displacement capacity vs. demand by pushover analysis. The pushover method is preferred in the higher seismic hazard regions, because it give more accurate results for the particular bridge, inclusive of foundation and superstructure flexibility. The implicit formulas were derived using combination of the results of physical tests conducted on reinforced concrete columns and the results of parametric studies conducted on a group of columns using the section moment versus curvature relationship and pushover analyses as described in Section 6.3. The Implicit Equations were developed for reinforced concrete columns because they are predominately used for bridge substructures as described in Section 6.1. The methodology as used may be extended to structural steel or concrete filled steel pipe columns.

For seismic design purposes, a bridge may be typically categorized according to its intended structural seismic response in terms of an acceptable damage level (i.e., ductility demand). These categories are a tool to differentiate between those bridges that are expected to provide significant deformability and ductility in the design earthquake and those that are not required to be so ductile. Generally, in the higher seismic hazard regions, a bridge will need to provide significant ductility and this response is categorized as Conventional Ductile Response (i.e. Full-Ductility Structures). In these cases, a full plastic mechanism is intended to develop several times during horizontal seismic loading, and the plastic mechanism should

be defined clearly as part of the design strategy. Structural details and member proportions should ensure large ductility capacity,  $\mu_c$ , under load reversals without significant strength degradation with ductility demands in the range of  $4.0 \leq \mu_D \leq 6.0$ . This response is anticipated for a bridge in higher seismic regions designed for a life safety/no collapse criteria.

In the lower seismic hazard regions, significant ductility may not be required and these structures are categorized as Limited-Ductility Response. In these cases, a plastic mechanism as described above for Full-Ductility Structures is intended to develop during horizontal loading, but ductility demands are reduced ( $\mu_D \leq 4.0$ ). Detailing and proportioning requirements in these cases are less than those required for the Full-Ductility Structures. This level of response can be permitted because the direct assessment of displacement capacity permits the designer to more accurately provide detailing that is commensurate with the expected seismic demand.

In addition to assessing the displacement demand against the displacement capacity, a direct check of local member ductility demands may be required to minimize the risk of stretching the limits of ductility demands and deformability of columns beyond what had been proven by experimental testing. Local demands are found by isolating a portion of a column into an equivalent cantilever element, then calculating the ductility demand on the isolated element at the design earthquake level. The local member ductility demand,  $\mu_D$ , should generally satisfy the following, where the single column bents are more restricted due to their lack of lateral load redundancy and where added conservatism is warranted for cases where inspection and repair is difficult or impossible:

- $\mu_D \leq 5$  For single column bents
- $\mu_D \leq 6$  For multiple column bents
- $\mu_D \leq 4$  When in-ground plastic hinging is anticipated

As with the FBM, example details that must be addressed to ensure adequate displacement capacity are transverse reinforcing steel, anchorage and development of reinforcement, extent of appropriate confinement steel for reinforced concrete. For structural steel in the yielding substructure, details would include appropriate element slenderness ratios, limitations on net sections relative to gross section, welding details and filler metal.

As with the FBM, once the yielding elements are designed, then the remainder of the bridge can be designed using capacity protection principles. The general approach for capacity protection is to amplify the basic plastic mechanism internal forces by a factor to account for potential overstrength of the yielding elements. These factors were discussed in Chapter 6 and are intended to generate an upper bound to the forces that the yielding elements can transmit to those elements, such as foundations, which should not experience damage in the design earthquake. Note that the magnitudes of the overstrength factors are different between the LFRD Specifications and the *Guide Specifications*. This is covered in more detail in Chapter 8.

Additionally, such items as support lengths for articulation and movement joints are conservatively proportioned to prevent unseating or dropped spans from seismically induced movements of the bridge.

#### **7.4 COMPARISON OF THE TWO DESIGN METHODS**

With the FBM,  $R$  values are prescribed in the design provisions and generally used to size yielding elements (e.g., columns) in a bridge. No verification of the actual displacement or ductility demands on the individual columns is made, and prescriptive detailing is used to ensure that adequate ductility is included in the yielding elements.

With the DBM, the displacement capacity of each column is evaluated and compared with the displacement demand on the individual columns. The plastic deformation capacity is determined using individual member moment versus curvature relationships derived from material strain capacities. A local member ductility demand is also calculated and compared with maximum allowable ductility demands. With either the displacement or ductility checks, detailing can be customized to improve deformability, as necessary.

Both methods use capacity protection principles to protect those elements that are not part of the yielding system.

## 7.5 CAPACITY DESIGN OF PIERS

### 7.5.1 Member Actions for Single- and Multi-Column Piers Using Capacity Design Principles

The principles of capacity design require that the members that are not part of the primary energy-dissipating system have strengths equal to or greater than the overstrength capacity of the primary energy-dissipating members (e.g. columns with plastic hinges at their ends). Therefore, one of the first things that must be done is to determine the magnitudes and distributions of the internal forces that accompany the overstrength forces. This requires either a pushover analysis or a “partial pushover” of the bridge or piers to establish the forces present when a plastic mechanism has formed and the full overstrength capacities of the yielding elements has developed, as shown in Figure 7-5. This process was described in Section 6.4.4 in the previous chapter.

These plastic mechanism forces should not be calculated using elastic analysis, because redistribution of the internal forces may occur as a full plastic form. This is particularly the case when more than one plastic hinge must form and where overturning changes the axial forces on the columns, which then change the yield moments according to the  $P$ - $M$  interaction relationship. Both the *LRFD Specifications* and *Guide Specifications* contain detailed procedures for accomplishing this determination of the full plastic mechanism condition.

A detail to consider is the location of the plastic hinge when assessing this plastic mechanism. With the FBM an actual length of the plastic hinge is never calculated for the purposes of analyzing the structure. However, in the DBM a plastic hinge length is calculated as described in Chapter 6. When performing the partial pushover analysis described above, the designer must select the location of the overstrength moments in the columns. With the FBM this has traditionally been taken at the top of foundation or soffit of the cap beam. The corresponding plastic shears then are calculated with the sum of these two moments divided by the distance between them, the clear height of the column. The *Guide Specifications*, using a figure similar to Figure 7-5, show the length as the clear height minus half the plastic hinge length on each end. This is conservative since the length is shorter than the clear height, producing a larger plastic shear. However, recall that the components of the plastic hinge length, as described in Chapter 6, include a length of plasticity (bar yielding) that spreads along the member and a strain penetration length that extends back into the adjacent member. These lengths often are similar to one another; thus realistically the location of the center of the plastic hinge is very near the end of the member. Therefore, the use of the

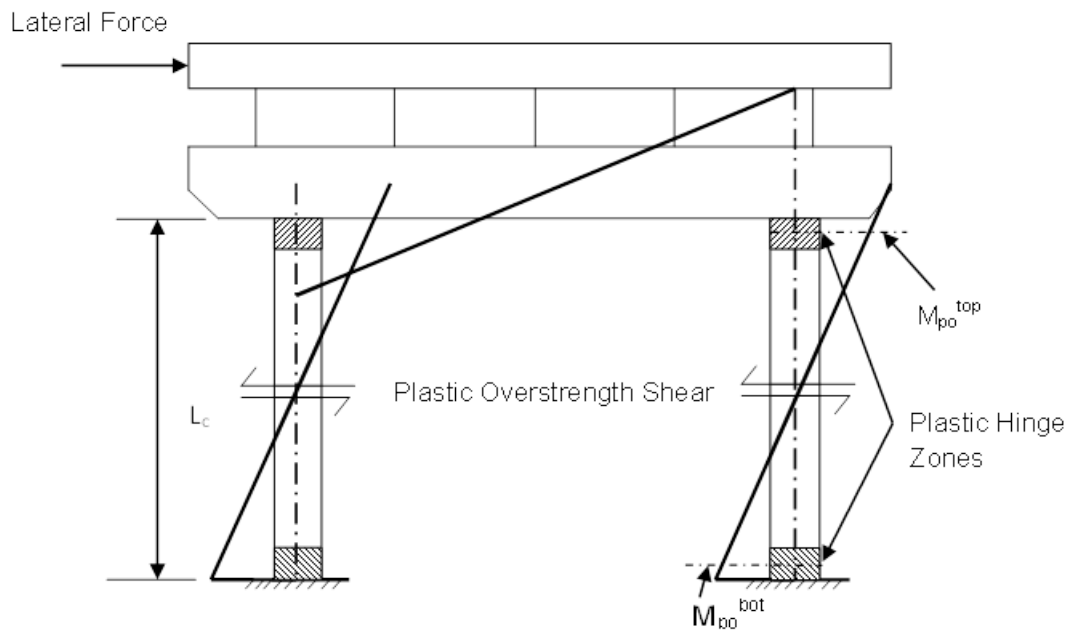
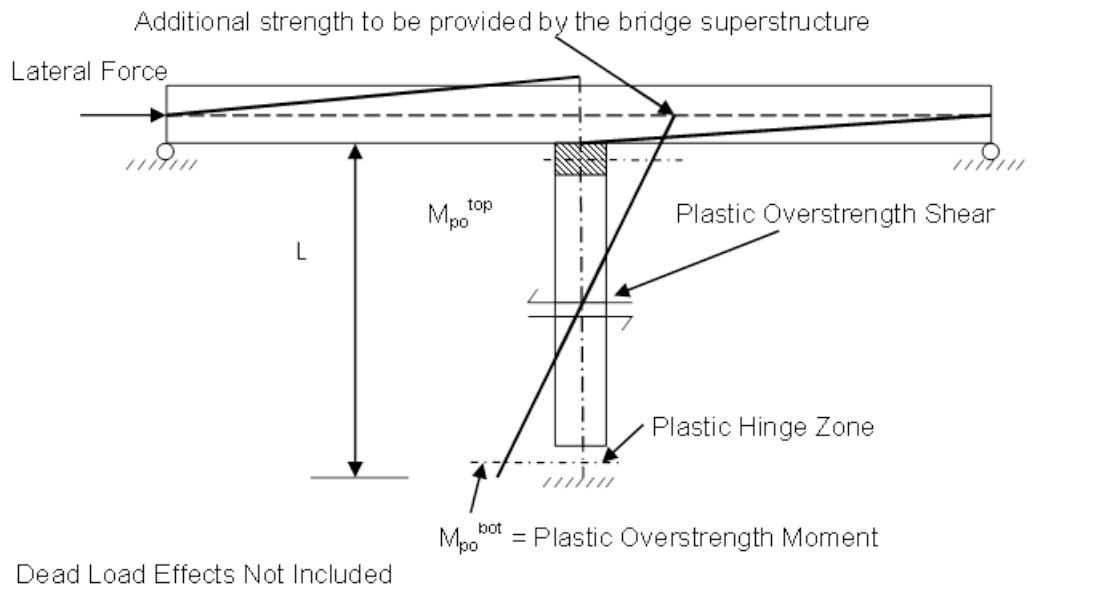


Figure 7-5 Capacity Design of Bridges Using Overstrength  
 Top: Longitudinal Response for Integral Bent With Non-integral Abutments, and  
 Bottom: Transverse Response for Dual Column Pier

member clear height is reasonable for this partial pushover calculation. The plastic hinge length is an approximation developed from laboratory tests and the formulas are somewhat crude.

The designer should keep in mind that the purpose of this partial pushover is to estimate the maximum internal forces in the pier, and thus the forces calculated (DBM) or estimated (FBM) from the  $R$  factor will not be the same. This is because an overstrength factor is applied, but also because the pier may not form a full plastic mechanism under the design earthquake loading.

It should be kept in mind that the locations of plastic hinging may not be clearly defined; thus a conservative estimate of the hinging locations should be used in order to calculate conservative forces for the capacity design process. For example, drilled shafts are designed to resist the plastic shear with hinging at the top of the shaft, even if in-ground hinging is expected under lower bound soil resistances. Similarly, pile bents, where hinging must occur in ground before a complete plastic mechanism forms, are designed for a conservative estimate of plastic hinging locations.

### 7.5.2 Capacity Protection of Reinforced Concrete Columns

This section covers capacity protection of columns, and although the columns are normally the selected yielding elements, certain aspects of column design falls into the capacity protection category. According to the capacity design philosophy undesirable failure mechanisms, such as shear, be inhibited, and undesirable failure mechanisms, such as longitudinal bar splice failure, should not occur.

The primary concern and need to capacity protect columns is to prevent shear failure, and because of the importance of adequate shear design in prevention of collapse or partial collapse, the topic is discussed in detail in this section. Reinforced concrete columns are designed with adequate transverse reinforcement to prevent a possible shear failure. As with non-seismic design, the nominal shear capacity  $V_n$  needs to be greater than the shear demand  $V_u$  with due allowance for a resistance factor  $\phi_s$ , which is typically equal to 0.9.

The nominal shear strength,  $V_n$ , of columns may be computed in the most general sense based on three components:

$$V_n = V_c + V_p + V_s \quad 7-1$$

where  $V_c$ ,  $V_s$  and  $V_p$  are the contributions from concrete, transverse reinforcement and axial load shear resisting mechanisms, respectively. The axial load term is often included in some fashion with the concrete contribution term.

Modern reinforced concrete shear models reflect the fact that the concrete contribution to shear resistance in a plastic hinge zone diminishes as inelastic flexural demands increase.

Figure 7-6 shows the model used by the *Guide Specifications* and also by Caltrans (2013) for the concrete contribution to shear strength in the plastic hinge zone. The strength of the column concrete shear resisting mechanism shown in the figure is based on the following equation:

$$V_c = kA_e \sqrt{f'_c} \tag{7-2}$$

where:

$A_e$  = effective area of the cross section for shear resistance typically equal to  $0.8A_g$

$f'_c$  = compressive strength of concrete (ksi)

and  $k$  depends on the displacement ductility demand ratio indicative of damage in the confined concrete within the plastic hinge zone.

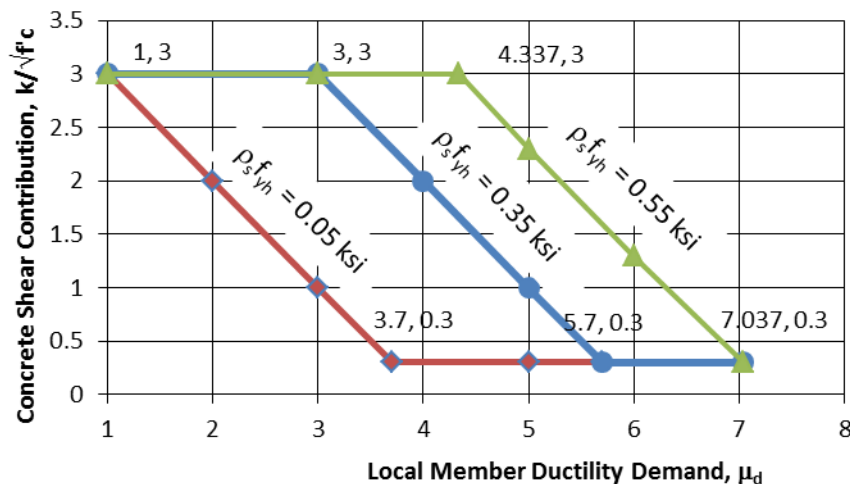


Figure 7-6 Concrete Column Shear Degradation Models (Net of Axial Effects)

The model presented here and used in the *Guide Specifications* is approximately a median predictor of behavior ( $k = 3$  maximum), rather than a lower bound method as used in the *LFRD Specifications* ( $k = 2$ ). The median behavioral model is included in this discussion because it more accurately reflects the shear contribution as deformations accrue. As can be seen in the figure, the contribution of the concrete drops as member ductility demand goes up; however, the transverse steel (represented by the product,  $\rho_s f_{yh}$ , in the figure) tends to confine concrete and preserve its contribution, increasing the ductility where the concrete contribution diminishes.

Axial load contribution to the shear resisting mechanism is shown in Figure 7-7, where an inclined strut develops and the horizontal component is the shear contribution. The *Guide Specifications* recognize the axial contribution with an additional multiplier applied to  $k$ . If the axial force is tensile, then the concrete contribution is zero. This is logical. The *LFRD Specifications* take a similar approach, with a value of zero contribution at zero axial load but only transition to the full non-seismic concrete shear resistance at  $0.10f'_c A_g$ ; thus the axial effect is simply one of keeping the concrete confined and effect in resisting some shear. This is a conservative approach.

The contribution from the reinforcing steel is similar to that use for non-seismic cases. For members that are reinforced with circular hoops, spirals or interlocking hoops or spirals, as shown in Figure 7-8 and Figure 7-9, the nominal shear reinforcement strength,  $V_s$ , is taken as:

$$V_s = \frac{\pi}{2} \left( \frac{n A_{sp} f_{yh} D'}{s} \right) \quad 7-3$$

where:

- $n$  = number of individual interlocking spiral or hoop core sections
- $A_{sp}$  = area of spiral or hoop reinforcement (in.<sup>2</sup>)
- $f_{yh}$  = yield stress of spiral or hoop reinforcement (ksi)
- $D'$  = core diameter of column measured from center of spiral or hoop (in.)
- $s$  = spacing of spiral or hoop reinforcement (in.)

Spirals represent an effective and economical solution. Where more than one spiral cage is used to confine an oblong column core, the spirals are interlocked with longitudinal bars as shown in Figure 7-9. Circular welded hoops are becoming popular, and they provide an advantage over spirals in that failure of one hoop does not result in the loss of others.

For members that are reinforced with rectangular ties or stirrups, as shown in Figure 7-10 and Figure 7-11, including pier walls in the weak direction, the nominal shear reinforcement strength,  $V_s$ , shall be taken as:

$$V_s = \left( \frac{A_v f_{yh} d}{s} \right) \quad 7-4$$

where:

$A_v$  = cross sectional area of shear reinforcement in the direction of loading ( $\text{in}^2$ )

$d$  = depth of section in direction of loading (in)

$f_{yh}$  = yield stress of tie reinforcement (ksi)

$s$  = spacing of tie reinforcement (in)

The required total area of transverse reinforcement should be determined for both principal axes of a rectangular or oblong column, and the greater value should be used.

In addition, the shear reinforcement is limited to both minimum values and maximum values. The minimum is used to ensure a minimum ductility level and may be thought of as providing some control over crack width to preserve the concrete aggregate interlock mechanism. These minimums vary with seismic hazard level, with higher minimums in the higher seismic regions. The maximum reinforcement value is meant to prevent concrete crushing and the avoid having the reinforcing steel contribute too much to the strength. If splices in locations where plastic hinges cannot be avoided then mechanical couplers that are capable of developing the tensile strength of the bars should be used.

Finally, the longitudinal steel should only be spliced in a yielding member away from areas where yielding occurs. Older construction permitted splicing of foundation dowels with column bars at the top of the foundation. This is a poor location for a splice when a column is expected to develop a plastic hinge in this location. Instead, it is best to not splice bars at all or to splice them in the middle of a column, provided such conditions as flares do not move plastic hinging in toward the middle region.

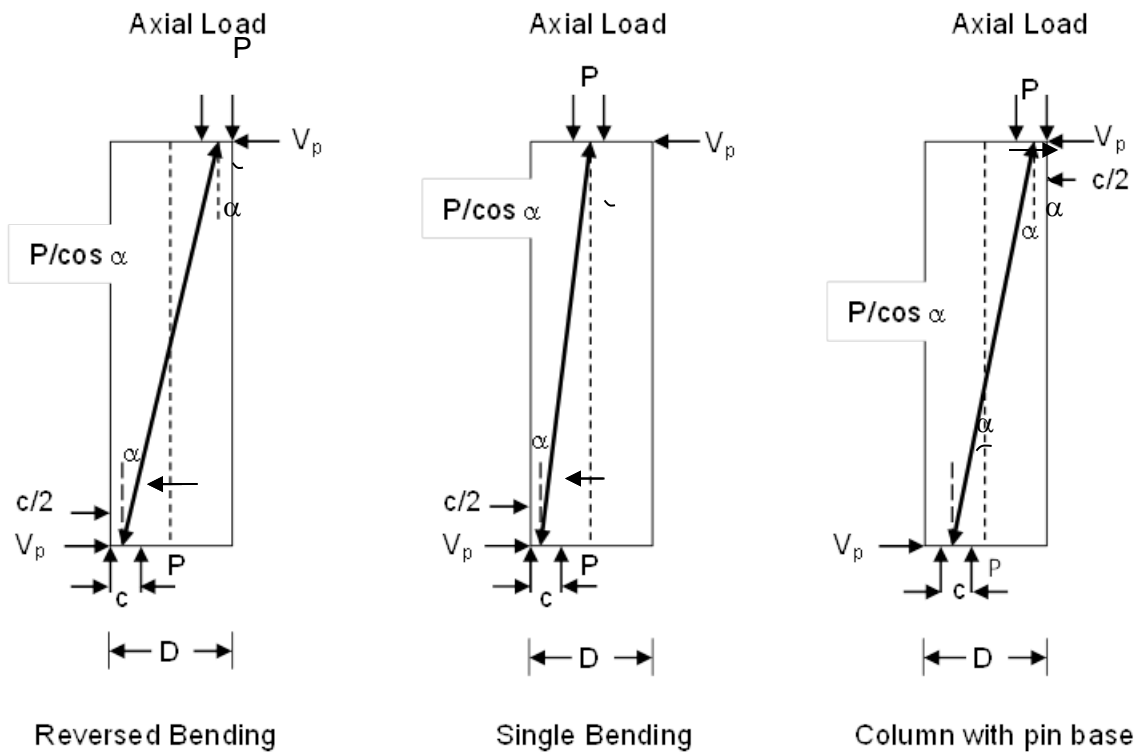


Figure 7-7 Contribution of Column and/or Cap Beam Axial Force to Shear Strength (after Priestley et. al., 1996)

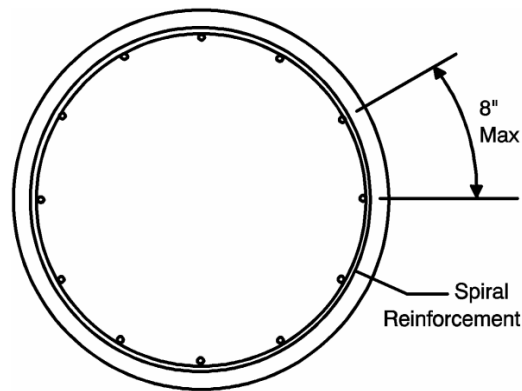


Figure 7-8 Single Spiral Transverse Reinforcement (AASHTO, 2014)

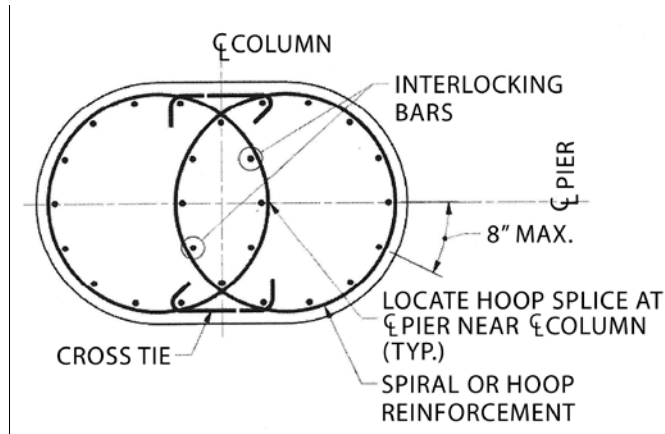


Figure 7-9 Column Interlocking Spiral Details (AASHTO, 2014)

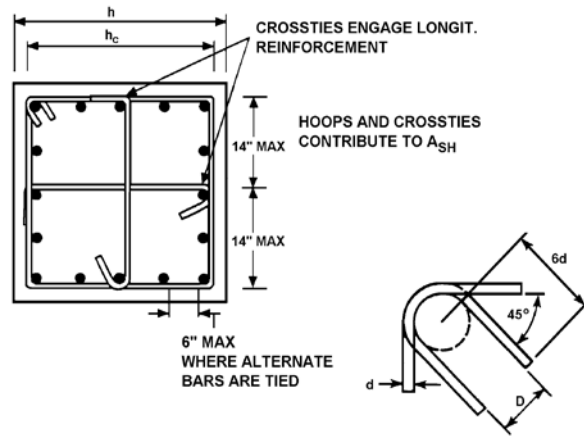


Figure 7-10 Column Tie Details (AASHTO, 2009)

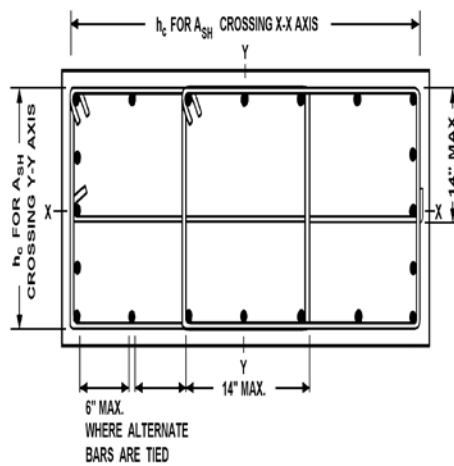


Figure 7-11 Column Tie Details (AASHTO, 2009)

### 7.5.3 Capacity Protection of Steel Columns and Moment-Resisting Steel Frames

Reports of damage to steel bridges during past earthquakes (the 1994 Northridge (EERI, 1995a) and the 1995 Hyogo-Ken Nanbu Japan (EERI, 1995b) earthquakes) revealed that, in almost all reported cases of damage, the steel superstructures carrying bridge gravity loads can survive earthquake loading. In many cases in these earthquakes, damage to primary members was minor while in most cases damage to secondary members was relatively localized and easily repairable. The exceptions to this desirable damage pattern were dropped spans, due to inadequate support lengths or crushing of bearings due to lack of sufficient strength and ductility, and several steel columns in Japan where local buckling or connection failure occurred.

Although uncommon, substructures composed of structural steel may also be used in compliance with a ductile system for a seismic design strategy. Such structures could be ductile moment-resisting frames, constructed with steel I-shape beams and columns connected with their webs in a common plane. For moderate to high seismic regions, the columns are designed as ductile structural elements using a limited force reduction factor,  $R$ . (Currently, the *Guide Specifications* do not include a displacement-base approach for the design of steel substructures.) The cap beams, panel zones at column-beam intersections and the connections are designed as essentially elastic capacity protected elements.

Properly detailed, fully welded, column-to-beam or beam-to-column connections in the moment-resisting frames that would typically be used in bridges can exhibit sufficient ductile behavior and perform adequately during earthquakes. Strategies to move plastic hinges away from the joints are not required by the AASHTO specifications. However, the designer may still elect to provide measures (such as haunches at the end of yielding members) to locate plastic hinges some distance away from the welded beam-to-column or column-to-beam joint (FEMA, 2000a, 2000b). However, this type of system has seldom been used in bridges.

Although beams, columns and panel zones can all be designed, detailed and braced to undergo severe inelastic straining and absorb energy, it is common in bridges to favor systems proportioned so that plastic hinges form in the columns. This is consistent with the philosophy adopted for concrete bridges. At plastic hinge locations, members absorb energy by undergoing inelastic cyclic bending while maintaining their resistance. Therefore, plastic design rules apply, namely, limitations on width-to-thickness ratios, web-to-flange weld capacity, web shear resistance, and lateral support. Full penetration

flange and web welds are required at column-to-beam (or beam-to-column) connections. These are essential details to ensure that unwanted weak links do not form in the columns.

Even though some bridges could be configured and designed to develop stable plastic hinging in beams without loss of structural integrity, the large gravity loads that are supported by those beams also make plastic hinging in the span likely as part of the plastic collapse mechanism. The resulting deformations can damage the superstructure (for example, the diaphragms or deck). Therefore, the consensus is that a design strategy based on plastic hinging in the beam should not be included in seismic design of highway bridges.

Axial load in columns is also restricted to avoid early deterioration of beam-column flexural strengths and ductility when subject to high axial loads. Tests by Popov et al. (1975) showed that W-shaped columns subjected to inelastic cyclic loading suffered sudden failure due to excessive local buckling and strength degradation when the maximum axial compressive load exceeded  $0.50A_gF_y$ . Tests by Schneider et al. (1992) showed that moment-resisting steel frames with hinging columns suffer rapid strength and stiffness deterioration when the columns are subjected to compressive load equal to approximately  $0.25A_gF_y$ .

#### **7.5.4 Capacity Protection of Cap Beams**

The design of the cap beam is performed using the column overstrength forces to ensure that the cap beam remains essentially elastic and inelastic deformations are concentrated in the column plastic hinges under the combined gravity and seismic loads. Design moments and shear forces based on column plastic mechanism combined with dead load analysis must be used to derive required top and bottom steel as well as the transverse reinforcement layout.

Capacity protection of the beam entails designing against shear demand similarly to shear design of column, and flexural demands, although the shear capacity calculation does not need to consider degradation of the concrete resistance due to inelastic action. The cap beam flexural capacity is calculated based on nominal properties and a maximum concrete strain of 0.003 to 0.005 representing crushing of unconfined concrete limit state. This approach is used because no inelastic action is permitted in the cap beams.

The width of the cap beam is chosen typically based on the column width and an additional one foot on both faces of the cap is normal in higher seismic regions. The additional width is used to accommodate joint reinforcement required in moderate and high seismic zones.

The cap beam depth is dimensioned to ensure that the column longitudinal bars have sufficient development length into the joint region and extend to the level of the beam top steel. For adequate capacity protection in high seismic regions, the anchorage length should not be reduced by means of adding hooks or mechanical anchorage devices. However, headed reinforcement may be used provided that adequate joint shear stresses are maintained as described in 7.5.6. In the case of cap beams built integrally with the superstructure and where the steel in the top slab or deck is used to transmit seismic forces, positive anchorage of the top steel with the column bars using J-bars, hairpins, or headed bars should be considered. This helps provide a complete load path for the resisting lateral seismic forces.

#### **7.5.5 Flexural Design and Capacity Protection of Reinforced Concrete Wall Piers**

Reinforced concrete wall piers (or pier walls as they are also called) are typically defined as columns whose height-to-width ratio is less than 2.5. Typically, substructure elements have a squat aspect ratio such as this in one direction, but in the orthogonal direction the element may be relatively thin. For such elements, the lateral behavior in the strong direction is shear dominant, but in the weak (thin) direction they are flexurally controlled. The behavior in the stiff direction can be highly influenced by foundations, which may be more flexible than the wall, or the connections to the superstructure, which also may be weak or soft links. In the weak direction, the response is clearly more flexible than the strong; thus the overall behavior of the bridge may be influenced significantly by bending along this weak axis. Normally, such differences in behavior will be reflected in the demand analysis.

The current practice for design is to require minimum horizontal and vertical reinforcement ratios, as has long been the case for reinforced concrete walls, with the vertical always being larger than the horizontal. The spacing of the reinforcement both horizontally and vertically usually is limited to 18 in. The reinforcement required for shear in the strong direction should be continuous, should be distributed uniformly, and only the horizontal steel contributes, although the concrete also contributes. Horizontal and vertical layers of reinforcement should be provided on each face of a pier. Splices in horizontal pier reinforcement are typically staggered to avoid weakened sections.

The shear capacity for pier walls in the weak direction is calculated as for tied columns. The reinforcement in the form of ties that cross the wall should be anchored as best as possible, in order to develop the shear truss mechanism of resistance. These cross ties should be anchored on both ends if possible, but alternating 90 and 135-degree hooks are often required for constructability. The cross ties also provide confinement of the plastic hinging region in the weak direction.

Capacity protection of walls will require the identification of the strengths of the connecting or bearing elements on top of the wall and the strengths of the foundation elements beneath the wall. With the exception of forming a plastic hinge in the weak direction, which should be accomplished if at all possible, the adjacent connecting elements may be the weak links in the system, particularly in the strong direction. This may require permitting and detailing for plastic hinging in the foundations (e.g. in pile foundations) or it may require consideration of bearing failure above the wall, in which case adequate support lengths should be provided to prevent unseating. Wall piers require the designer to apply engineering beyond simply applying prescriptive code provisions; the designer must identify and account for weak links that may not be “normal”. Thus wall piers force a designer to truly apply the principles of capacity design.

### **7.5.6 Capacity Protection of Beam-Column Joints**

Since the 1989 Loma Prieta earthquake, there has been greater awareness of joint shear performance in the seismic design of bridges. While damage associated with joint shear will not necessarily create a sudden collapse mechanism, degradation of several adjacent joints can result in a loss of moment carrying capacity that could lead to instability of the structure with potential collapse. As a joint is cycled during a seismic event, its stiffness may degrade and eventually lose its ability to carry adequate moment.

The shear strength of beam-column joints can be assessed in a manner similar to the column elements. A principal stress approach is usually adopted, as this is the major determinant in joint performance. A beam-column joint will remain essentially elastic and uncracked, providing that the principal tensile stress in the joint is less than  $3.5\sqrt{f'_{ce}}$  psi (*Guide Specifications*, Caltrans (2013), and Priestley, et.al. (2007)) provide detailed methodologies for calculating the principal stresses in a joint.) When the principal tensile stress exceeds this level, diagonal cracking of the joint can be expected. The joint strength as limited by concrete alone will be limited to a maximum principal stress of  $5.0\sqrt{f'_{ce}}$  psi, at which point,

full diagonal cracking of the joint will have developed. If the joint shear demand arising from the flexural overstrength capacity exceeds this limit, then the joint is said to be shear-critical and the structural performance will be governed by the reduced joint strength, unless additional reinforcing steel is provided. Additional reinforcing is provided in the form of transverse steel primarily around the column longitudinal bars. These are normally supplied in direct proportion to the column steel content, but also in inverse proportion to the column bar development length, both of which increase the joint shear stress. The *Guide Specifications* contain detailed prescriptive details for joint reinforcement. The *LFRD Specifications* do not. However, there is no reason not to apply the joint shear provisions in the *Guide Specifications* to designs performed to *LFRD*. The prescriptive requirements are largely keyed to the steel contents of either the column or the cap beam. The joint principal stresses are calculated using the overstrength forces from the column developed as described throughout this chapter.

From a behavioral perspective, the lateral deformation for a system susceptible to a joint shear mechanism is established based on the two components listed below:

- a) Lateral displacement induced by the effects of a local joint shear mechanism related to the shearing and normal forces within the joint and acting on the concrete (Figure 7-12)
- b) Lateral displacement induced by the effects of local elongation and slip of column longitudinal reinforcement related to the transfer of force from the steel to the joint concrete (Figure 7-13)

These two components are therefore highly interrelated. The combined effect is considered and referred to as joint shear response. Based on available experimental data, two main characteristics of joint shear response are highlighted:

- 1) The relationship between the rate of softening and the strength of the joint. A weaker joint tends to soften at a faster rate prior to reaching its maximum joint shear capacity.
- 2) The relationship between the strength of the joint and the length of the plastic deformation plateau.

As seen from the plot included in Figure 7-14, weak and moderate strength joints have limited ductility capacities that are satisfactory for demands in low seismic regions. In light of this inherent capacity, which has been confirmed by experimental data, the capacity protection of beam-column joints is only required in moderate to high seismic regions. The capacity protection of a strong joint is typically characterized by better development of the column longitudinal bars and better confinement of the joint

region. The provisions of the *Guide Specifications* for joints seek to produce strong joints with good ductility capacity.

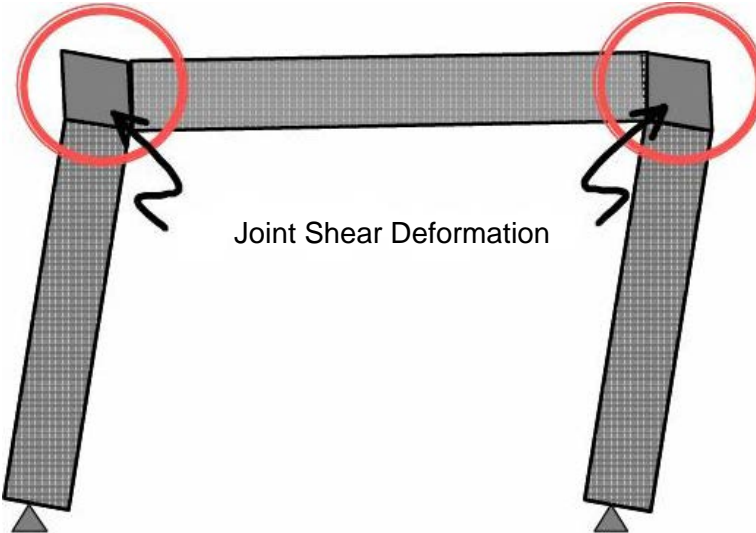


Figure 7-12 Joint Shear Deformation in a Two Column Bent

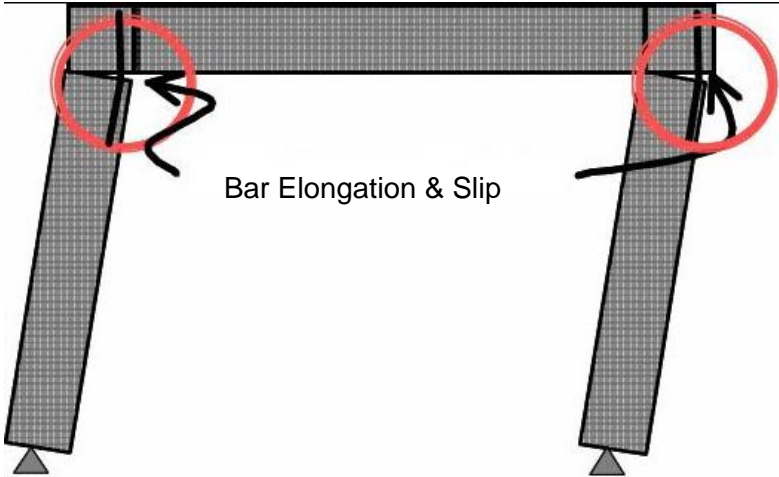


Figure 7-13 Reinforcement Elongation and Slip Deformation in a Two-Column Bent

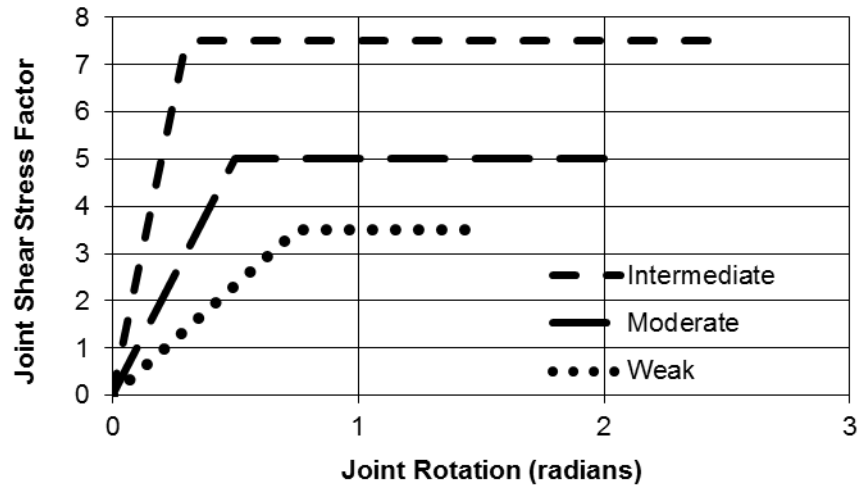


Figure 7-14 Joint Classification for Rotational Capacity

## 7.6 CAPACITY DESIGN OF FOUNDATIONS AND ABUTMENTS

In the preceding sections, capacity design principles have been discussed for the design of the part of the substructure above the foundations. It has been shown that the major steps in capacity design are as follows:

1. Choose the structural elements in a bridge that may deform inelastically if required in a moderate-to-large earthquake.
2. Detail these elements to sustain inelastic cyclic actions without fracture or collapse, and
3. Prevent the rest of the bridge from suffering damage by making these remaining elements and components sufficiently strong.

This section focuses on the third step in the list above, as this step includes the foundations and abutments. The section outlines how the applied forces and member actions are determined for design purposes using the principles of the capacity-protected design. Then the steps required to design such elements are discussed. Cases where the preferred capacity-protection approach does not apply are explained, and finally the relationship between capacity-protection of the foundations and abutments and liquefied soil conditions is explored. Beyond the information provided in this section, additional discussion of design and detailing of bridge foundations can be found in Priestley et. al. (1996).

## 7.6.1 Member Actions in Foundations and Abutments Using Capacity Design Principles

The concept of capacity-protection of foundations stems from the practical desire to prevent damage to elements where it cannot be detected or where it cannot be repaired. For most foundations both of these are true. Additionally, damage that could contribute to structural instability or a collapse hazard must be avoided if the life-safety performance requirement is to be met. Not all, but certain failure modes, of a foundation could contribute to potential collapse, and such modes must be avoided. For example, shear failure near the ground surface in drilled shafts could lead to a collapse hazard, and should be avoided.

The typical approach for designing foundations and abutments using capacity protection is provided in Table 7-4. The goal is to ensure that the foundations and abutments of a bridge can safely sustain the maximum forces that the structure could impose during a moderate-to large earthquake.

**TABLE 7-4 APPROACH FOR CAPACITY DESIGN OF FOUNDATIONS**

Step	General Approach
1.	Define the desired plastic mechanism in the substructure (pier) above the foundation.
2.	Perform a limit analysis to determine the associated overstrength forces in each pier.
3.	Apply overstrength forces in piers to the foundation.
4.	Develop a free-body diagram with the applied forces and soil resistances in equilibrium with one another.
5.	Design/check the foundation to assure that it can accommodate the overstrength forces both from a geotechnical and a structural point of view.

### 7.6.1.1 Overstrength Plastic Mechanism Forces

The forces that physically can be applied by the substructure on the foundation are those corresponding to the formation of a full plastic mechanism in the pier above the foundation. As was discussed earlier in this chapter, materials often are stronger than their nominal strengths, particularly when loaded into strain ranges where strain hardening is present. Therefore all factors that could contribute to the structure being stronger than anticipated using nominal or expected material properties, alone, need to be considered. Therefore overstrength factors, as discussed earlier, are used to calculate the maximum internal forces.

### 7.6.1.2 Elastic Analysis and Load Combinations

In modern seismic design, the focus is on capacity design and capacity-protection of elements such as foundations where damage is undesirable. However for reasons of simplicity, design specifications typically permit designers to use the full elastic forces that would be experienced if no yielding took place during the design earthquake. This practice is normally permitted as an alternate to full capacity design. Typically, using such forces would lead to much larger and stronger sections than designs based on development of a plastic mechanism. In some locations, though, the seismic forces may be small enough that the columns, as sized for non-earthquake load cases, could actually resist the design earthquake without yielding. Thus, a structure could resist the seismic forces with no extra design effort or costs. This practice is not generally desirable because there may be little or no margin left to resist earthquakes that are larger than the design earthquake. The reliance on elastic design makes the selection of the design earthquake much more important. On the other hand, because the philosophy of capacity design is the desire to have a fusing, plastic mechanism identified to limit the internal forces induced during an earthquake, the potential for larger-than-design earthquakes is not a significant issue.

Therefore, in general, the design loads used for seismic design of foundations and abutments should be those corresponding to the development of a plastic mechanism within the structure. These forces typically will be smaller than the unreduced elastic forces calculated assuming no yield or damage occurs. The design loads are therefore based on plasticity in the substructure (pier), full overstrength in the yielding elements, (e.g., the columns), and some level of gravity load present in the structure.

Logically, the gravity load effect present with the application of earthquake lateral loading should be the dead load of the structure, plus any portion of the live load assumed to be present during an earthquake. (Noting that live load is not included in the seismic mass, as discussed earlier.) Additionally, some design methods, for example that in the *LRFD Specifications*, require variable dead loads to be considered for the seismic case. The loading is varied by using load factors for dead load that are greater or less than one. This produces a bounding effect whereby dead load that helps resist lateral loading is conservatively undercounted. Then dead load that produces a driving effect, which produces internal forces in the same sense as those due to earthquake loading, is conservatively increased to provide an additional margin of safety. This is a rational approach, but requires a number of loading cases and several lateral plastic mechanisms to be investigated. The bookkeeping effort required for this step can be significant.

By contrast, the *Guide Specifications* require only the nominal dead and live load (if present) to be considered. In other words, no additional load factors are used. This approach is also rational from the perspective that the inertial effects are the result of the gravity loads. Thus if the driving load does not change, the resistance from that same load should likewise remain unchanged.

### **7.6.1.3 Effect of Structural Form and Earthquake Resisting Elements (EREs) on the Desired Behavior**

The choice of lateral resisting system can have a dramatic effect on the actual forces that may be developed and delivered to the foundation and abutment system. For shorter bridges where the abutments often play a key role in resisting inertial loading, the amount of loading transferred to the foundations will be strongly correlated to the presence of the abutment resisting systems. For example, if the abutments are counted upon to resist seismic forces in the longitudinal direction, the forces that the intermediate substructure foundations must resist will be smaller than if the abutments are not considered part of the lateral force resisting system. However the intermediate substructure foundations still should be designed using capacity-protection principles.

Certain EREs, as defined in Chapter 4, will affect the ability of the system and individual piers to form plastic mechanisms. In some cases, the formation of a plastic mechanism will necessitate yielding below the ground surface, i.e., in the foundation itself. Under such conditions, it will be impossible to capacity-protect the foundation, defined herein as the portion of the pier that is below ground. In such cases an exception will need to be made to the capacity-protection of the foundation. Examples of such conditions and approaches for the design of such elements are included in Section 7.6.4.

### **7.6.1.4 Fusing Elements**

Fusing elements may be included in the load path to the foundation system, and these can be viewed as analogous to the fusing action provided by conventional plastic hinging in columns. An example of a fusing element is the fusible shear key, which is sometimes used at an abutment to limit the forces transmitted to the abutment foundation, thus preventing damage to the foundation. Such elements are somewhat difficult to design because accurate failure modes and failure forces are necessary. It must be remembered that much of our design methodology is based on lower bound estimates of resistance, which

are ordinarily conservative. Fusible elements require the opposite. For such elements one must be able to clearly and accurately predict the maximum force that the element can deliver. This ideally requires laboratory testing to support the design methods used. For example, Caltrans (Bozorgzadeh et. al., 2007) has developed an external shear key detail that has a well-defined failure mode and reliable rupture strength.

However, there are many other cases where designers will have to make their own informed estimates of fusing element capacities. For example, attempting to define the yield or breakaway failure loads of wingwalls and backwalls may require such calculations. As a general rule, predictions of flexurally dominated yielding are more reliable than those for shearing failure. Thus, calculations for the lateral forces associated with the yielding of wingwalls are typically more reliable than those for the breakaway forces of abutment backwalls. This is particularly true if more than one line of failure is required for backwall failure, such as when three sides of a backwall must be designed and detailed to breakaway at the same time.

### **7.6.2 Capacity Protection of Foundations**

As discussed above, forces from the yielding plastic mechanism above the ground are calculated as the seismic “design” forces for the foundations. These forces are then applied to a free body diagram, FBM, of the foundation, the various components of the foundation are checked for possible failure modes, and then checked for acceptable behavior consistent with the demand model used for the structure. This process is described in the sections below.

It is important to recognize that foundations must be adequate from both the structural and geotechnical perspective. The structural aspects of adequacy are related to provision of adequate strength and stiffness, although typically most attention is paid to the strength. This is often the case because conventional sizes and shape of foundations provide adequate stiffness, almost by default. In those cases where flexibility is suspected of playing a key role, then such flexibility will normally be included in the structural demand model.

Geotechnically, the reverse is often true for seismic loading, and stiffness is a key parameter. Soil is inherently non-linear in its response to loading, and therefore, one of the most important measures of adequate geotechnical behavior is whether the structure can tolerate the displacements induced by the

geotechnical deformations of the foundation-soil system. Whether such behavior is adequate requires careful coordination between the geotechnical and structural engineers. Thus, while some static load cases may be considered (using the conventional approach of the geotechnical engineer reporting strengths early in the design process and the structural engineer using these at a later date), seismic design typically requires a more iterative approach.

### 7.6.2.1 Resistance Components

Each type of foundation resists lateral forces in a unique manner related to how loads are transferred to the surrounding soil. In general, foundations may be split into two categories, shallow and deep. Shallow foundations for bridges are generally spread footings. Deep foundations use piles, drilled shafts or caissons extending to a depth where adequate vertical capacity (at a minimum) is reached. However, much of the lateral resistance provided by deep foundations is often developed at relatively shallow depths, unless loss of soil strength occurs due to liquefaction. Deep foundations can be built of individual piles or groups of piles connected together by a pile cap. Examples are shown in Figure 7-15.

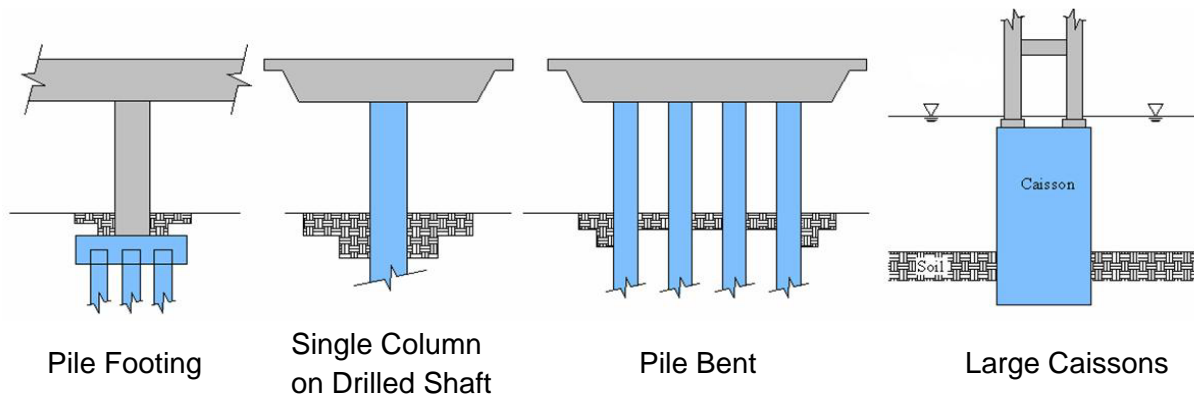


Figure 7-15 Types of Deep Foundations Used for Bridges

Spread footings provide resistance to lateral loading through friction beneath the base, friction along the sides and passive soil resistance against the edge of the footing being pushed into the soil. Often not all of these mechanisms will be included in the estimation of resistance, because a more reliable and conservative single mechanism may be used to size the footing. For instance, friction along the base may be the only mechanism used in the calculation. That does not mean that the other mechanisms are not

present, and they should at least be considered by the designer to ensure that they could not precipitate an undesirable failure mode.

Deep foundations provide lateral resistance as the pile or shaft moves toward the soil. Typically this movement is greater at the ground surface and therefore the resistance can be greater there. However, this resistance depends on the stiffness of the surrounding soil, which may vary along the depth of the pile. Under lateral displacement, such variations in stiffness lead to induced lateral forces against the pile that vary with depth. Generally, the lateral stiffness of the soil increases with depth.

### **7.6.2.2 Developing Foundation Free-Body Diagrams (FBDs)**

The development of FBDs for foundations must be done with care to capture the appropriate loading conditions. Much time is often spent with analytical demand models that are linear elastic and these models are analyzed with the full demand response spectrum as input. Therefore the forces that are reported from such models are not always the forces the designer should use for the capacity-protected design of the footings. Instead, the forces corresponding to the development of a plastic hinging mechanism in the columns or structure above the footing should typically be used.

Under the action of plastic hinging forces the distribution of forces in the soil beneath the footing or adjacent to the piles or shafts may not be the same as the distribution predicted from an elastic model. Typically, the designer will have calculated plastic hinging forces from the mechanism analysis for the pier when designing the pier. The worst combination of these forces is then considered when sizing the foundations.

*Spread Footings:* The limit states for spread footing design for earthquake loading permits some uplift of the footing from the soil. This is reasonable because the loading is transient and because there is still an appropriate margin between limited uplift and the overturning instability of the pier. Often there is insufficient axial load on a bridge footing to resist the full plastic moment without any uplift, and additional weight would need to be added to the foundation if uplift were to be completely prevented. This would make the foundation much more expensive. However partial uplift means that the full axial load will be borne on only part of the footing, and therefore the potential for localized failure of the foundation must be considered. These failure modes are discussed in the next section.

Development of the FBD requires using the plastic hinging forces as the ‘driving’ loads for the foundation, and then calculating appropriate resistance forces in the soil that are in equilibrium with the applied loads. Commonly for spread footings, the footing is assumed to be rigid relative to the soil. This assumption is based on the footing being sufficiently thick that it is very stiff relative to the soil modulus. Most spread footings will meet this requirement. Thus with plastic hinging forces as input and the rigid assumption for the footing, common methods for the mechanics of materials can be utilized to develop the soil forces acting on the base of the footing. Typical methods have been established for soils with linear elastic behavior for cases of full soil contact and for cases with partial uplift. Formulae and their derivation can be found in common foundation texts, such as Bowles (1982).

*LFRD* gravity design relies on ultimate soil resistance when calculating stresses on footings. Reliance on the same approach for seismic design is acceptable for calculating a bound on resistance, but this approach will not yield correct results when assessing a given size of footing with applied plastic moment, because the soil stresses may be less than ultimate when equilibrium is reached. This must be considered when developing the forces that are in equilibrium on the foundation.

Often the seismic load case will govern the sizing of spread footings when the design is based on capacity protection. This can be the case particularly when the soil has a high bearing capacity. In such cases, limits states prescribed by the design specifications, that restrict the eccentricity of the axial load are used to establish the size of the footing. In some cases, the size of the foundation can become large enough that the use of a deep foundation to provide uplift resistance may be necessary. Particularly when foundations are to be installed around existing facilities and utilities, the potential size of shallow foundations may become a problem. Thus, it is advisable to develop preliminary sizes of the foundations early in the design process.

Resistance forces that the designer may wish to conservatively neglect may be omitted from the check of foundations. For instance, it is common practice to ignore the passive and frictional side resistance against spread footings if the depth of cover is two feet or less. In such cases, the lateral resistance is provided entirely by friction acting on the base of the footing.

*Piles and Drilled Shafts* For deep foundations the development of FBDs for design depends on the foundation modeling technique used. Two common techniques are the equivalent depth-to-fixity method and the other is the “Winkler” method. In the first technique, an equivalent length of column is extended below the base of the column to approximate the foundation effects, typically stiffness. In the second, the

pile or shaft is modeled as a structural element and independent uniaxial springs, nonlinear if necessary, are connected to the structural element (pile or shaft) and the system analyzed for response. This second approach is used by the commonly used programs that model piles using P-y behavior.

Thus, if a pile foundation is being designed using the depth-to-fixity method, the foundation FBD is obtained from the basic model. This is simple in concept, but somewhat cumbersome in practice. The depth-to-fixity method was developed simply to provide an equivalent stiffness and equivalent maximum moment for an applied lateral load. The two depths are not the same, with the equivalent depth for maximum moment being slightly shorter than the depth for stiffness. Often designers use the maximum moment from the stiffness model to give a simple, conservative, result. However, the distribution of forces along the pile, to use for the design and detailing of the pile or shaft, is not available from this method. These forces can be bounded for simple soil layering and properties, but may not be sufficiently accurate for more complex deposits. Close coordination with the geotechnical engineer is required.

For the Winkler method, software is typically used to develop the forces, displacements and equivalent stiffness for inclusion in the model for the demand analysis. This same software can be used to determine the internal forces in the piles for design and detailing, and most programs will provide output of internal moments, shears and distribution of applied load from the soil. However, the global analysis and capacity-protection design may use different forces and these will require different analyses of the foundation system. This is discussed in more detail in 7.6.2.4.

### **7.6.2.3 Failure Modes / Structural**

Foundations may fail in a number of different ways, some of these geotechnical in nature and some are structural.

Spread Footings and Pile Caps Structural failure modes for spread footings and pile caps are:

1. One-way shear failure (beam shear failure)
2. Flexural yielding of reinforcement, either on top or on the bottom of the footing or cap
3. Joint shear failure
4. Anchorage pull-out, either of the column or of piles
5. Failure of the adjacent piles, either in compression, tension, flexure or shear.

These failure modes are also illustrated schematically in Figure 7-16. The 1971 San Fernando earthquake clearly demonstrated the need for adequate anchorage and confinement (NBS, 1971). The 1989 Loma Prieta earthquake demonstrated the need for adequate joint shear force transfer mechanisms (EERI, 1990), and this has been reinforced with results from laboratory testing (Priestley et.al., 1992). Other potential foundation failure mechanisms that have not necessarily been seen in earthquakes, but should nonetheless be considered are: top of footing flexure, particularly in pile caps, shear failure and the need for adequate anchorage of piles and columns. Finally, the piles themselves must be able to sustain the forces that may be imposed, and therefore similar failure modes in the piles must also be considered.

In capacity-protected design, all of these failure modes must be suppressed. Failure to identify and prevent any of these modes of failure could lead to a collapse hazard under seismic loading.

Some of these failure modes are obvious and well known, while others are not. The need for bottom reinforcing steel in spread footings follows directly from gravity design, which is well known. However, for earthquake design the amount of bottom steel may vary from that required for gravity design. This is due to the permissible partial uplift conditions discussed in 7.6.2.2 where the distribution of loading could be drastically different from the gravity load case. In cases where full rocking is used, the footing must be able to develop and transmit the forces associated with mobilization of the ultimate soil compressive strength at the outer edge of the foundation. Care to develop the steel adequately and to provide adequate shear capacity must be taken. The common case of partial uplift also requires the designer to consider these effects, but not to the same degree.

One feature of the joint shear force transfer mechanism that should be considered in any new design is the need to turn column bars inward, not outward, in the footing joint area. The use of outwardly splayed bars has a long history and is rooted in constructability, not structural mechanics. Structural failure with outward facing bars will be in the form of inadequate joint capacity and inability to develop the full strength of the attached column. However, it is impossible to turn all the end hooks of a typical sized circular column in toward the center of the column. However, to achieve a reasonably rugged joint design, as many bars as possible should be turned inward. This then achieves a compromise of sorts between constructability and seismic performance.

Preventing failure from occurring in the foundation is one of the precepts of capacity design. Therefore the designer must understand the ramifications of using certain design methods that are “end runs” on true capacity design. For instance, using the elastic unreduced forces instead of the plastic mechanism forces

can lead to potential foundation failure modes, either geotechnically (rocking) or structurally: flexure or shear, if a larger-than-design earthquake occurs. This can occur because using elastic forces for design does not focus clearly on a preferred hierarchy of failure modes for seismic loading.

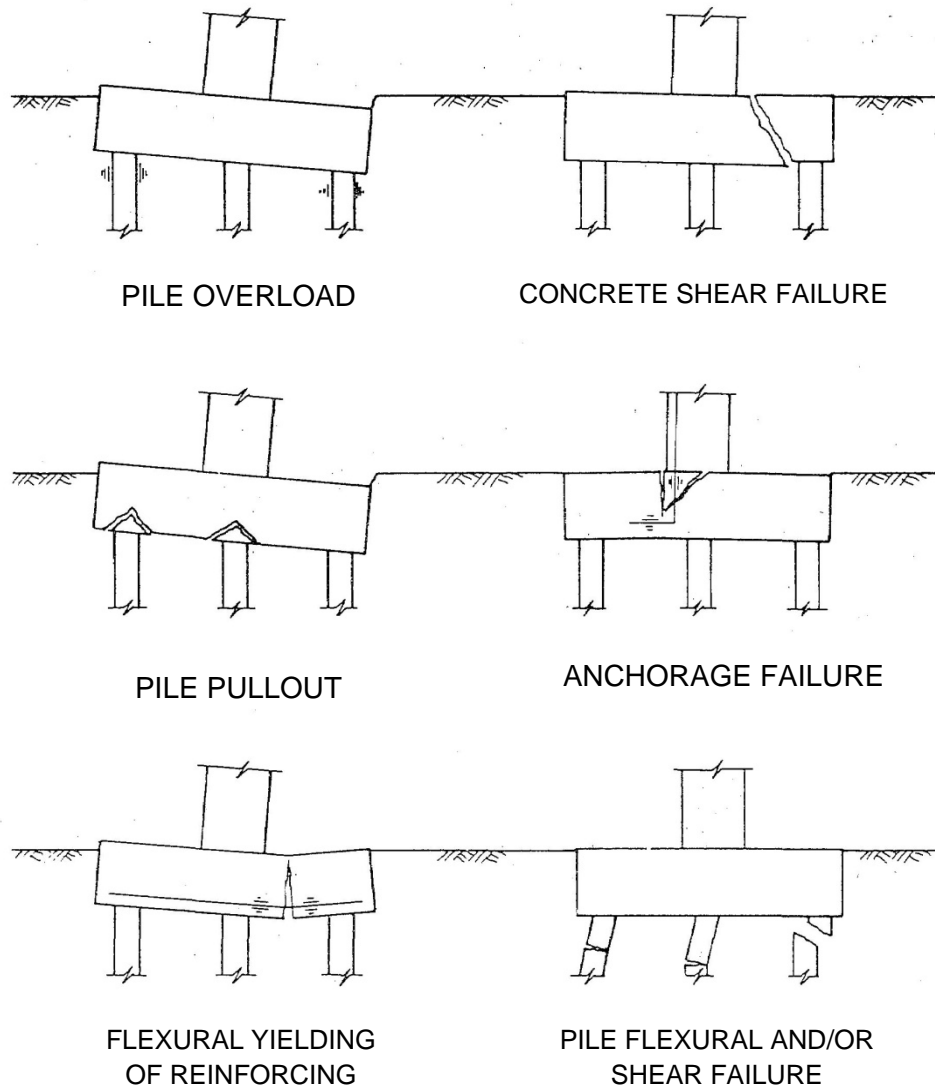


Figure 7-16 Spread Footing and Pile Cap Failure Modes (FHWA, 1995)

An example where this practice may be tempting to the designer is the use of architecturally oversized columns, where the capacity-protection of the foundations could lead to very large and expensive foundations. Thus, if the designer chooses not to capacity-protect the foundation, and there are cases where this may be expedient, then criteria should be developed for the project whereby a preferred failure

mode is established and undesirable failure modes are suppressed. For example, consider a large wall pier that has been sized for ice loading and founded on rock in the middle of a stream. Designing a foundation using capacity-protection principles, where the force-limiting plastic mechanism for weak-axis bending is flexural yielding of the wall, may lead to large foundations that have difficulty satisfying environmental requirements, and are difficult to construct. Alternately, rocking of the pier might be a chosen failure mode, along with passive soil resistance of the abutment backwalls in order to provide an adequate overall Earthquake Resisting Systems (ERS) for the bridge (AASHTO, 2014). In such a case, flexural, shear, and other structural failure modes of the wall's footings would need to be assessed and suppressed, while permitting the smaller foundation to rock onto its edge.

Likewise, when using force-based design with R-factors, foundation failure modes may not be suppressed when, instead of true capacity design, reduced R-factors (e.g.  $R/2$ ) are used to calculate the design forces for the foundations. This practice has been permitted in lower seismic areas by design specifications, but the ramifications of using such an approach should be clearly understood by the designer and owner.

*Deep Foundations:* Structural failure modes of deep foundations include:

1. Flexural yielding
2. Tension yielding
3. Shear failure
4. Anchorage/connection failure (pile-to-cap or shaft-to-column)

The capacity-protection design process for deep foundations is rooted in determining the appropriate plastic hinging mechanism force and designing the pile or shaft to resist the corresponding forces.

If the foundation element is a pile that is connected to a pile cap, then typically the plastic hinging forces are applied to the pile cap and the individual piles need only resist the transferred forces without experiencing inelastic action, themselves.

If the foundation element is a drilled shaft, then ideally the shaft would be designed to resist the plastic hinging forces applied to the shaft from the base of the column. In some cases, particularly with deep soft soil deposits or with shafts of the same size as the attached columns, it may be physically impossible to develop a plastic hinge in the column above the shaft. In those cases, plastic hinging may develop in the shaft instead. A similar condition occurs with plumb piles in pile bents where the pile has the same size and strength above and below ground. With pile bents it is typically impossible to design the piles to remain undamaged below the ground surface. This is not the preferred lateral force ERE configuration,

but this type of construction is often used for smaller bridges, and is popular in many states. Discussion of the cases where inelastic action occurs below ground is included in 7.6.4.

In the case of an oversized drilled shaft where the shaft is larger and stronger than the column, conventional capacity-protection principles dictate designing for the maximum forces that can be delivered. These are obtained by calculating the plastic hinging mechanism forces that can be delivered at the top of the shaft. These forces are then be applied to the drilled shaft, the internal force distribution determined and the design completed based on these forces. This approach should suppress any undesirable failure mechanisms.

#### 7.6.2.4 Soil Deformations and Reconciliation with Modeling

When the analytical model of the structure is assembled and analyzed, the designer usually does not know how large the plastic mechanism forces will be. Thus, the design process can be iterative, and the process as it relates to the analytical modeling is outlined in Table 7-5.

**TABLE 7-5 APPROACH FOR DESIGNING FOUNDATIONS FOR SEISMIC LOADING**

Step	Design Activity
1.	Choose the type and initial size of the foundation.
2.	Judge whether stiffness effects should be considered in the analytical demand model (i.e., will the response be sensitive to the foundation stiffness).
3.	Develop stiffness relations to include in the analytical demand model.
4.	Estimate preliminary required design strengths of the yielding elements of the chosen plastic mechanism.
5.	Develop foundation FBDs using the plastic mechanism forces and appropriate soil resistances.
6.	Calculate internal foundation forces relative to capacity (e.g., moment, axial, shear) and evaluate reinforcement detailing geometry (e.g., development lengths).
7.	Evaluate geotechnical limit states (e.g., bearing pressure, frictional resistance, passive resistance, potential settlement, and downdrag).
8.	Evaluate overall pier or structure stability (e.g., uplift/location of resultant axial force).
9.	Revise design and analysis as required.

The ideal goal is to have the stiffness of the soil-foundation system that is used in the demand model correspond to the development of the chosen plastic hinging mechanism. However, this goal is often not met due to the iteration required. In these cases, the soil springs that are used correspond to the elastic demand analysis and are not necessarily consistent with plastic hinging. In many cases, this practice may be acceptable, provided it is recognized as a bounding method. If the plastic hinging forces are smaller than the elastic unreduced forces, then the founding soil will be over softened. This typically will lead to larger displacements and therefore is conservative with respect to deformations. If a more accurate representation of foundation forces is desired, the forces applied to the foundation to determine stiffness need not exceed the plastic hinging forces with overstrength considered.

#### **7.6.2.5 Other Load Interaction Effects**

Liquefaction. Liquefaction can reduce both the soil stiffness and strength around a foundation. Most foundations in areas susceptible to liquefaction are deep foundations. The effect of liquefaction on the capacity-protection of the foundations can be significant, to the point where capacity-protection can no longer restrict the damage to above-ground, inspectable locations. In cases where liquefaction occurs, the design must first be developed without consideration of liquefaction, and this corresponds to the response of the bridge before liquefaction develops. Then a separate and second check is made using the liquefied properties of the soil. In this case, alternate criteria that permit damage below ground may be necessary, or the foundation is designed for the elastic unreduced forces occurring from liquefaction. If this is done, the designer should still ensure that a plastic mechanism can safely form, even if it occurs in a larger-than-design earthquake, and brittle failure modes such as shear in the foundation should be considered and suppressed.

Scour. Scour often is handled as a secondary case where the extremes of lateral support around a foundation are considered relative to the earthquake loading effects. Since the worst case scour is itself an extreme event and is not likely to occur simultaneously with the design earthquake, the maximum scour condition is not usually combined with earthquake effects.

Foundation types that are susceptible to scour are usually deep foundations. Thus one of the primary considerations is the identification of the soil resistances that are likely to be lost due to scour. These can include passive resistance around pile caps and resistance over the upper lengths of piles where soil may have been removed. Also where soil is alternately being removed and later re-deposited around the

foundation, the designer should consider using reduced stiffness and strength parameters since this soil will not be compacted around the foundation. Such soil will have a lower lateral resistance than present immediately after the foundation was driven or placed.

### **7.6.3 Capacity Protection of Abutments**

Capacity-protection of abutments typically attempts to prevent damage to the abutment foundations. Otherwise abutments are often permitted to incur some damage, and they can sustain certain types of damage without posing a life-safety hazard. One type of damage that is not permitted, however, is the unseating of the adjacent superstructure. This type of damage is prevented by providing adequate support lengths. This aspect of abutment design is not typically thought of as capacity-protected design, although a bridge must possess sufficient displacement capacity and articulation to prevent unwanted failures, such as a dropped span.

Another factor that complicates the capacity-protection of abutments is the fact that the adjacent superstructure typically cannot tolerate large overload forces and remain undamaged. Thus, the choices for the design of abutments are often limited to:

1. providing some type of fusing mechanism (Caltrans, 2013), such as sacrificial shear keys, yielding walls, ductile diaphragms, or specific hardware such as seismic isolators, or
2. resisting the full unreduced earthquake forces without damage

The accurate prediction of soil-based passive forces or the breakaway forces of fusing elements is not truly possible today. Therefore bounding analyses and designs, whereby several bounding models provide the expected extremes of behavior, are typically required.

#### **7.6.3.1 Use of Abutments in Analytical Demand Model**

The use of abutments in the analytical model, and more specifically in the ERS, is an evaluation that the designer must make. Abutments may significantly influence the response of a bridge, and some abutment types may lend themselves to being included in the ERS more than others. Abutments are often built to

engage significant amounts of adjacent soil under lateral loading. Thus they can play a significant role in limiting or reducing the relative displacements that a bridge would be expected to experience.

Transverse and longitudinal responses are often quite different. In the transverse direction, the abutments may have shear keys that either resist all forces expected or they may fuse to capacity-protect the foundation of the abutments below the keys. In the longitudinal direction, significant resistance can be mobilized from the passive soil resistance of the abutment backfill. Examples of these types of behaviors are shown in Chapter 4.

*Longitudinal Response:* Some designers and some agencies prefer to ignore the abutment contribution to earthquake resistance in the interest of conservatism or in the interest of simplicity. However, some types of abutments such as integral abutments, where the abutment foundations are permanently attached to the superstructure, can provide rugged seismic performance and should be included in the analytical demand model. For other abutment types, such as seat abutments, where articulation is included between the superstructure and the abutment, the choice is less clear. In cases, where longitudinal movements occur freely before the abutment backfill is mobilized, some designers prefer to size the intermediate substructure to resist all the seismic loading. Then if the gap between the superstructure and backwall is closed, any additional resistance simply provides additional safety.

If the abutments are included in the demand model, their contribution to resistance is typically included using a secant stiffness model, as described in Chapter 5. The secant stiffness formulation implies that if the maximum abutment resistance is exceeded, then the abutment stiffness is reduced to represent, in an approximately linear manner, the nonlinear behavior of the soil. Additionally, one of the primary sources of abutment nonlinearity is the compression-only behavior of the soil, since the abutment backfill soil works primarily in compression. Inclusion of this effect in the analytical demand model is often accomplished by dividing a single abutment's resistance and stiffness by one half and distributing half to either end of a bridge. Obviously, this requires that the bridge be continuous between the abutments, and it requires that there be little or no skew. If significant skew is present, the lines of action of the abutment forces are not collinear, and thus this simplification is not valid because the unbalanced moment effect of the two skewed abutments is not appropriately captured.

When significant skew is present and abutment longitudinal compression-only response is included, then linear elastic dynamic models are not appropriate for developing demands. Instead, bounding analyses where only one abutment is effective at a time are more realistic. However, to develop an understanding

of the expected behavior, static models using pushover analysis should be used. Time history modeling is also acceptable, but such analysis is typically only economical on important or very large bridges.

When the secant stiffness method is used, iterative estimates of the stiffness are often required if the displacements of the structure mobilize the full passive resistance. The secant stiffness approach is a powerful one because significant nonlinearities, such as those due to the gap between superstructure and backwall, can be included directly in the demand model.

*Transverse Response.* Transverse abutment response is often coupled with the superstructure through shear keys. Such keys may be proportioned to either carry the full unreduced elastic loads that may be expected, or they may be designed to fuse at a prescribed force level to limit the forces transferred. In addition to shear keys, wing or curtain walls may be configured to provide lateral resistance, and these walls may also be designed to fuse or develop plastic hinges before they break completely away from the bridge.

### **7.6.3.2 Developing Abutment Free Body Diagrams**

Establishing FBDs of abutments requires the determination of the forces that the structure will deliver to the abutments. This requires the identification of any fusing elements and estimates of potential elastic forces that will be developed if fusing does not occur. There are several fusing mechanisms that may be utilized, and these include breakaway shear keys, mobilization of full passive resistance behind the end diaphragm, yielding wingwalls, and spread footings that slide beneath the abutments. In addition, isolation bearings, sliding bearings, or yielding diaphragms may be used to limit or prevent forces from being attracted to the abutments. Similar to the development of FBDs for foundations, the development of abutment FBDs for capacity-protected design begins with estimates of the maximum forces that can be delivered to the abutments. Unlike the intermediate substructure, where the piers can develop plastic hinging mechanisms, only fusing elements will be effective at the abutments in limiting the forces to be resisted by these elements. Once the maximum forces are established, the resisting mechanism forces can be calculated and the internal force distribution in the abutment determined.

As noted above, when the passive resistance of the abutment backfill is used to limit longitudinal forces, which are active only in compression, the soil stiffness is often divided in half and distributed to each end of the bridge. This facilitates linear elastic dynamic analyses and will typically produce reasonable

displacements for the bridge. However, when the abutments are designed, the designer must account for the actual forces that are expected to act against the abutment. This then would require the analytical model forces to be doubled to estimate the actual forces. This requires coordination between the analyst and the designer, if they are different people.

### 7.6.3.3 Failure Modes / Structural

Structural failure modes of abutments include desirable failure modes, such as shear key fusing or backwalls that breakaway to limit the structural response, and undesirable modes of failure, such as damage to the supporting piles, yielding of internal elements in the abutment, and shear types of failure in the walls comprising the abutments.

Some modes of failure affect the magnitude and distribution of the soil forces acting against the abutment. For example, the passive resistance values developed and used by Caltrans for backfill soil is based on the abutment wall moving into the soil in a translational mode, not a rotational one. Therefore, the soil forces acting against the backwall will be best estimated if the abutment is configured to displace in a translational mode. An overhanging stub abutment wall, such as that shown in Figure 7-17, will most closely match this behavior. An integral abutment will likewise produce a close approximation of translational motion, because the stiff superstructure will resist rotation of the backwall. On the other hand, seat-type abutments supported by single rows of piles or seat-type abutments that are relatively tall will tend to rotate into the soil rather than translate. The rotation will reduce the effectiveness of the backfill soil and will tend to reduce the overall stiffness.

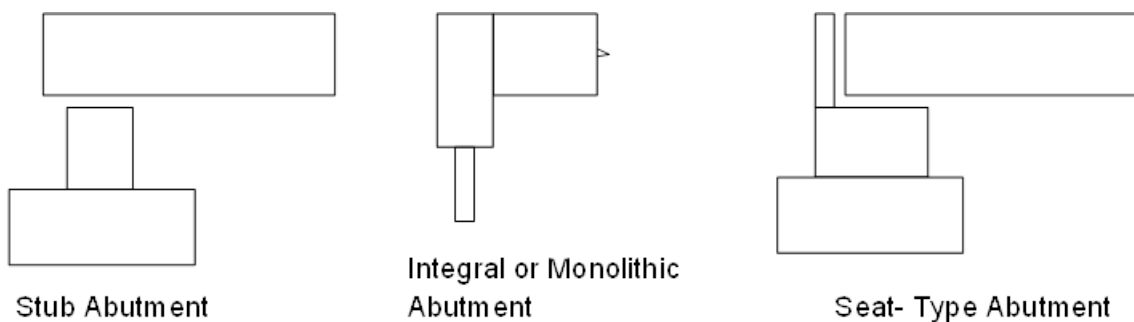


Figure 7-17 Types of Abutments

Integral abutments will tend to induce inelastic effects in the supporting piles. This tendency is often offset by detailing the pile-to-end diaphragm connection to be approximately a pinned connection, which can be effective, both for seismic and thermal loading. Nonetheless, deformation of the abutment may produce yielding in the piles whether at the abutment connection or in the ground. When designing an integral abutment it is necessary to estimate the resistance of the piles at their plastic mechanism level and design the connection and abutment using capacity-protection principles to suppress damage in the end diaphragm.

In general, abutments should be designed to mobilize the likely soil forces that can occur. This is true regardless of whether the abutment is considered part of the ERS. For abutments in contact with backfill soil, the back wall or end diaphragm should be designed to resist the passive forces that the soil can induce. Likewise, seat-type abutments where the superstructure could ultimately impact the backwall should have the expected load path evaluated. Steel superstructures, for example, could require local strengthening at such contact points to avoid the potential for localized yielding.

#### **7.6.3.4 Soil Deformations and Reconciliation with Modeling**

Typically when abutment resistance is included as part of the ERS, then, as the analysis proceeds, checks of this resistance must be made to ensure the appropriate stiffness is included in the model. Therefore, as the model is analyzed the designer should check whether any gaps at the abutment have closed and whether the full available passive resistance has been reached. Depending on these checks the abutment stiffnesses in the model are adjusted accordingly using the secant approach described in Chapter 5. Then once the analysis and any required iterations are complete, the soil deformations and forces will be consistent with the demand modeling.

#### **7.6.4 Exceptions to Capacity-Protected Design of Foundations and Abutments**

As indicated in several of the sections above, there are cases where capacity-protection of the foundations or abutments is not possible, or for some reason not preferable. In the *Guide Specifications* such cases are recognized and permitted with the Owner's approval. This recognizes that exceptions do occur. The *LRFD Specifications* do not address such a situation, other than design for full elastic forces. However, it is reasonable to develop project-specific criteria to deal with cases where capacity protection is not possible or economical.

#### **7.6.4.1 Definition of Exceptions**

Cases where capacity-protected design of the foundations is impossible are usually related to either:

1. An element above the foundation is too large and strong to economically capacity-protect the foundation from its plastic forces, or
2. The foundation, itself, is too flexible to be able to develop the necessary resistance to force plastic hinging to occur above the foundation.

The desired behavior is to restrict plastic response to above-ground locations and to design the below ground “foundations” to remain undamaged.

The first case can be illustrated with architectural columns that are larger than they need to be for seismic resistance, alone. This condition can occur in higher seismic zones where larger than necessary columns are desired for non-structural reasons. The condition can also occur in lower seismic areas where the seismic forces are not sufficiently high to control, and non-seismic loads or minimum steel content govern the design.

The second case can occur when deep loose soils surround the piles or drilled shafts. In this case the upper soil layers may not offer significant lateral resistance and the location of the maximum moments in the piles will occur well below the ground surface. Poor soils alone may cause this condition, or liquefaction may produce this condition after liquefaction-induced loss of soil strength occurs.

The second case also occurs for pile bents where the piles have the same properties and strength below ground as they have above ground. In this case, plastic hinging typically cannot be forced to occur above ground.

#### **7.6.4.2 Developing Design Forces and Design Criteria**

Performance criteria for cases where plastic hinging occurs in the ground, or not at all, should consider potential acceptable alternate behaviors. Such behavior may include defining a location or zone of the foundation in the ground where plastic action is likely and then designing the zone to be ductile. Or such

behavior could include accommodation of the design ground motion with elastic response, thereby incurring no damage.

In the case of a drilled shaft or pile, where in-ground hinging cannot be suppressed, the shaft could be designed with appropriate confining reinforcement and designed with adequate allowance for shear force. In this case the shaft will effectively be capacity-protected below the expected plastic hinge location. When such behavior is permitted, the possibility of stiffer soils in the upper layers forcing the plastic hinging to occur at shallower depths must be considered. Often it is simple enough to provide adequate shear strength such that shear failure would never be expected even if the plastic hinging occurred above ground. It is the designer's responsibility to bound the possible response behaviors and allow for them in design.

In the case of large and strong elements above the foundation such as wall piers, that preclude capacity-protection of the foundation, the designer should identify and design for an acceptable ultimate resistance condition. For example, a large wall pier may warrant a footing that will rock. However, other failure modes, that might occur prior to development of the full rocking resistance, must be suppressed.

#### **7.6.5 Liquefaction Design Requirements with Softened/Weakened Ground**

The presence of liquefaction during ground shaking can lead to altered site soil properties that complicate capacity-protection of the foundations. When liquefaction is possible at a given site or near a foundation, deep foundations will be required. Due to the potential for loss of all, or a significant portion, of the vertical load carrying capability of the soil, a spread footing should not be founded above liquefiable layers.

Because liquefaction takes finite time to develop, and liquefaction may even occur after the peak vibration response has occurred, the designer must bound the possible responses and foundation conditions. Therefore, on one hand a column-shaft system might be designed for plastic hinging above ground should the peak vibration response precede liquefaction. Then, on the other hand, the same system might also be designed to accommodate plastic moments at some depth below the ground surface after liquefaction develops. This two-step approach to designing for liquefaction has been included in both AASHTO seismic design specifications. In many cases, the structure can endure the expected displacements associated with liquefied site response without developing a plastic hinge in the ground in

the design earthquake. However, if a larger earthquake occurred, plastic hinging might be expected in the ground, thus providing a capacity-protected design for this greater-than-the-design earthquake condition would be reasonable and prudent. Often this condition can be addressed more cost effectively than can the condition where plastic hinging forces are simply applied to the top of the shaft with the liquefied soil properties. In such a case, significant amounts of reinforcement may be required in the shaft to accommodate a condition that physically is not likely to occur.

An approach to the design of foundations subject to liquefaction where no lateral movement (flow or spreading) is expected is outlined in Table 7-6.

**TABLE 7-6 APPROACH FOR DESIGNING FOUNDATIONS SUBJECT TO LIQUEFACTION - NO LATERAL MOVEMENT EXPECTED**

Step	Design Activity
1.	Design foundations for non-liquefied conditions (i.e., design for earthquake loading assuming no liquefaction occurs).
2.	Capacity-protect the foundations for the no-liquefaction case.
3.	Reanalyze the structure with liquefied soil properties and appropriate input earthquake loading.
4.	Re-evaluate the pier plastic mechanism that is likely to occur.
5.	Evaluate whether the foundation can be capacity-protected reasonably and economically with above-ground inelastic action.
6.	If the answer to Step 5 is no, then evaluate the in-ground plastic mechanism and determine likely internal pier/foundation forces. (The designer may choose to establish foundation flexural strength to resist forces under liquefied conditions at the limit of elastic behavior.)
7.	To the extent possible, detail the foundations to provide ductile behavior for earthquake loading larger than the design earthquake (i.e., make the piles or shafts ductile elements to handle loadings that may be larger than expected).
8.	Evaluate specific liquefaction-induced loadings, such as downdrag.

### 7.6.5.1 Soil Resistance Becomes the Load

When soil shear strength is lost during liquefaction and there is a gradient of elevation that will permit the soil to move laterally (down slope), there is the potential for lateral kinematic loading of the soil against

the foundations of a bridge. In general, if the soil liquefies and requires no additional lateral acceleration to induce lateral movement, lateral flow occurs. This condition is unstable because movement occurs solely under the action of gravity. Thus, soil displacements may be unbounded. Alternately, if the soil liquefies but additional lateral acceleration is required to produce lateral movement, then lateral spreading occurs. Lateral spreading is manifested by incremental lurches of the soil and, at the end of earthquake shaking, movement stops. Either condition may produce forces against a bridge's foundations that are not related to the vibration-based, acceleration-induced response of a bridge that is the typical focus of seismic design.

Lateral loading may be exacerbated by the presence of non-liquefied material – often referred to as a crust – that may ride on top of the liquefied layers. As material moves toward and around a bridge foundation, liquefied material may pass around the foundations, especially if they offer a reduced resistance, such as individual piles do. However, non-liquefied material will retain some or all of its shear strength and can induce very large forces against a foundation. The distributed forces that such laterally moving material may induce may be determined by the peak passive resistance that the liquefied soil and non-liquefied crust can produce (i.e., the peak of the p-y resistance curve appropriate for the depth under consideration). It can be discerned that under conditions where a non-liquefied crust or a partially liquefied soil moves toward a foundation system the foundation may be forced to move with the soil. The actual movement is defined by the combined compatibility of the structural system and soil mass movement. Calculating such displacements and forces is beyond the scope of this chapter. However, the concept of capacity protection can be extended to outline a structural design approach for such lateral flow or spreading conditions.

Capacity design principles can be used to assist the designer to produce a rational design for foundations subject to liquefaction-induced lateral flow or spread (ATC, 2003). Fundamental to successfully accommodating soil movements around or against foundations is the acceptance of inelastic action in the foundations, themselves. Only relatively modest soil movements can be resisted by foundations that remain fully elastic. Fortunately lateral loading of this type is monotonic, in that the soil only moves in one direction. Thus, the loading is less severe than the cyclic inelastic loading that the substructure above the foundations is subjected to during vibration-based seismic loading.

Often estimates of the maximum expected lateral movement of soil are given as ranges of displacement, and these ranges may be large - on the order of feet. Therefore, the strategy for resisting such loads is to use a combination of inelastic displacement in the foundations and reduced ground displacements provided by site remediation techniques, such as stone columns. Such a combined approach can often

produce an acceptable lateral soil displacement that the foundations can tolerate, although the foundations may be damaged to the point that they require replacement following a large earthquake. Design for such a case involves the steps outlined in Table 7-7. This section is only intended to provide an introductory description to loading due lateral movements of soil. For more detailed discussion of this phenomenon, the reader is referred to Chapter 2 and the MCEER/ATC 49-1 document.

**TABLE 7-7 APPROACH FOR DESIGNING FOUNDATIONS SUBJECT TO LIQUEFACTION - LATERAL FLOW OR SPREADING KINEMATIC LOADING CASE**

Step	Design Activity
1.	Determine the likely lateral movement of the soil, including failure planes and increased resistance of any ground improvements – piles, stone columns, etc.
2.	Determine whether flow or spreading conditions are likely to occur.
3.	Determine whether soil will flow around foundations or move the foundations in a compatible fashion. Bounding analyses may be useful for this step.
4.	Establish a likely plastic mechanism for the foundations, but include the effects of the bridge superstructure and abutments, as appropriate. Include determination of displacement capacity.
5.	Re-evaluate Step 1, as appropriate.
6.	Evaluate lateral displacements relative to the ability of the structure to deform.
7.	Add ground improvement elements, as required, to bring estimated soil and foundation displacement into parity with foundation displacement capacity.
8.	Detail foundations for ductile action, particularly around locations of likely plastic hinges, but extend detailing over generous lengths of the foundations to accommodate uncertainties in response.

## 7.7 CAPACITY DESIGN OF SUPERSTRUCTURES AND CONNECTIONS

The primary mass of a bridge is the superstructure. The primary mass of a bridge that responds and contributes to inelastic action in an earthquake is the superstructure. This is because the superstructure mass, being the highest off the supporting ground, experiences the most dynamic amplification. Thus the designer must consider the load path from the point of inertial load generation to the supporting and lateral-load-resisting substructure. Where the inertial forces concentrate before entering the substructure is often the place where potential earthquake-induced problems will develop. These same locations can

also be the places where various elements of the bridge are connected together, particularly if it is not a monolithic cast-in-place (CIP) structure.

The main capacity design activity related to superstructure is to ensure that moments and forces can be adequately transferred between the substructure and superstructure. Additionally, these same forces and moments must be able to be distributed from the connections throughout the superstructure to the areas where the inertial forces arise.

The actual definition of superstructure and substructure can become clouded relative to seismic design, and they are not related to the traditional pay items used when building a bridge. Examples of three possible superstructure-to-substructure connections are shown in Figure 7-18. In the first figure, a CIP box girder bridge supported on columns will typically be constructed with the cap beam inside the box girder. Thus the top of the pier and the superstructure are one in the same. In the second figure, a steel plate girder bridge will often be constructed with the plate girders supported by bearings on a dropped cap beam that has effectively no moment continuity with the superstructure in the longitudinal direction. A third variant is a prestressed concrete girder bridge where the girders are supported on a first-stage dropped cap beam during construction then integrated into the cap with a second stage diaphragm with moment continuity in the longitudinal direction. The force transfer mechanisms of these three configurations are different and have an impact on how the superstructure is capacity protected in the vicinity of the substructure connections.

Additionally, the manner in which forces are transferred between substructure locations and in particular to abutments affects the internal inertial force distribution and can have an impact on capacity protection of the superstructure. If for example, transverse inertial forces are resisted primarily by abutments in a two-span highway overcrossing bridge, then the primary inertial load path will be through the superstructure as a beam to the abutments. Thus, inertial superstructure forces that would appear to be tributary to the center pier may, in fact, make their way to the abutments instead. These force transfer mechanisms will be discussed in this section.



(a) CIP box



(b) Steel girders on bearings



(c) P/S Girders integral with cap

Figure 7-18 Three Common Superstructure-to-Substructure Configurations

### 7.7.1 Capacity Protection of Superstructures

The same philosophy as described for foundations also applies to superstructures, prevent damage where it would be difficult to repair or difficult to detect during inspection. The manner in which the design forces are obtained is the same for superstructures as for foundations, as described in the Section 7.6.1, including the development of the overstrength forces.

Once the overstrength forces are determined and the participating portion of the superstructure is identified, the design proceeds using the approaches for non-seismic design. Exceptions are where prescriptive detailing requirements may be necessary, such as quantities and placement for joint shear reinforcement. However in general, the detailing requirements are similar to other non-seismic cases.

Capacity protection of the superstructure is not directly addressed in the *LRFD Specifications*. However, it is appropriate to determine the likely forces that the superstructure must resist and check that those forces can be resisted. The *Guide Specifications* do require that the superstructure be capacity protected.

#### 7.7.1.1 Developing Free-Body Diagrams (FBDs) for Forces at Piers

The design forces that would be used for design of the capacity protected elements of cap beams and superstructure adjacent to pier locations would be determined using pushover with appropriate overstrength factors. Using these forces both the cap beam and the superstructure design could be completed. Of course, the development of FBDs of the relevant elements would depend on the type of superstructure-substructure connection and, in particular, whether moment in the longitudinal direction was transferred to the superstructure. All forces should be accounted for, including the axial forces induced in the cap beams due to shear from the columns. These forces can be significant enough to affect the moment capacity of the cap beams under lateral seismic loading. Gravity forces would also be applied when considering the concurrent forces acting on the system. Such forces would include the self-weight of the structure, but also could include a portion of the design live load, if warranted.

Longitudinal Moment Transfer: Consider the case of the cap beam that is integral with and embedded within the superstructure and longitudinal moment is transferred. The width of the superstructure relative to individual columns that support the superstructure and the column spacing can be relatively large.

Hence, not all of the superstructure will be effective in resisting the longitudinal moment the column will transfer. Tributary widths of superstructure are defined based on whether the superstructure is a closed

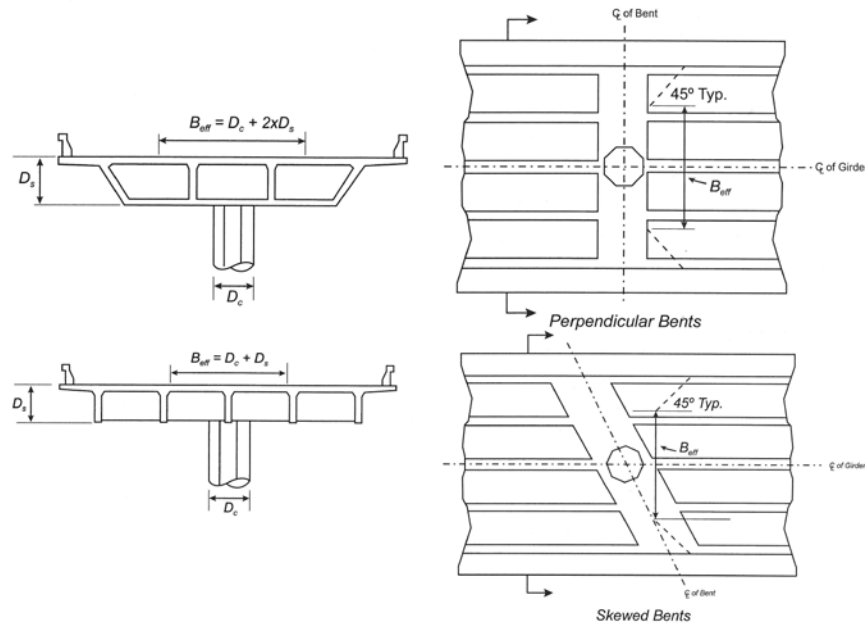


Figure 7-19 Effective Superstructure Width (AASHTO, 2014)

box section or an open soffit section made up of individual girders. These two cases are shown in Figure 7-19 for both tangent bridges and skewed bridges.

These figures show the dimensions of the superstructure that are considered to be effective for resisting the column overstrength forces, inclusive of the change in force due to eccentricity of action from the top of column to the centroid of the superstructure. The non-seismic forces that act concurrently would be distributed according to the stiffness and configuration of the entire superstructure. Column forces would be distributed ahead and back from the cap beam in accordance with the overall bridge stiffness and configuration. For example, if in-span hinges are included in adjacent spans then they will affect the distribution of moment to each side of the cap beam.

Reinforcement should be detailed and developed to resist the forces calculated. Extension of steel from the adjacent girders should be considered as required to resist the forces. Reinforcement will be required for both positive (concave down) and negative (concave up) bending of the superstructure adjacent to the pier, and additional reinforcement to that for all but the seismic load case could be required.

If splicing devices are used in this zone, they should be capable of developing the strength of the capacity protected elements and should thus be capable of achieving roughly a 2 percent tensile strain. These would correspond to “Service Splices” as defined by Caltrans (2001).

If prestressed precast girders are used with integral cap construction, often a dropped first-stage cap is used to support the girders during construction. Then a partial or full-depth and width diaphragm is cast between the girders and integral with the deck. With appropriate steel detailing, joint shear sizing, and size of cap and diaphragm, the column overstrength forces can be transferred and the strength of the upper part of the columns developed for seismic resistance. In such cases, the dimensions shown in Figure 7-19 may be adjusted to account for additional spread of resistance due to the additional depth of cap beam provided that torsional and flexural strength and stiffness exists to resist the induced forces.

Transverse Design of Cap Beam: Where integral cap construction is used with box girder construction, a portion of the box top and bottom slabs will participate with the cap beam itself, and generally the width taken of each is 6 times the thickness of the slab. This can help provide additional reinforcing for the cap at an advantageous lever arm. Under seismic loading with reversals of input moments from the columns, cap-beams will require reinforcement in both the top and the bottom throughout their length, unlike the gravity cases where cutoffs of bars could be entertained.

The widths of cap beams should be wider than the columns that frame into them in order to adequately resist the overstrength forces and to incorporate the required reinforcement, to provide adequate development of longitudinal steel as might be required, and to provide adequate joint shear capacity. The amount of steel that will physically fit through the longitudinal bars projecting upward into the cap beams often is well less than what is required. Thus additional width of the cap beam will normally be required to accommodate these bars.

Detailed discussion of cap beam joint shear design is covered in Section 7.5.6. As covered in that section, there are a number of prescriptive detailing provisions now considered appropriate for modern reinforced concrete joint design. The sizing of the cap beam and joint area will often be controlled by or at least require consideration of joint shear design.

### 7.7.1.2 Developing Free-Body Diagrams (FBDs) for Forces in Superstructure as a Whole

Seismic design is often focused primarily on the ductile or yielding elements of the structure with much attention going into the sizing, selection and detailing of those elements. However, the inertial forces originate largely in the superstructure and may be distributed between substructure locations in accordance with global or system stiffnesses that are much different than those of individual piers, particularly for loading in the transverse direction.

In Chapter 4 the case of a stiff superstructure in the plan dimensions spanning between abutments over a single ductile interior pier was considered. In that example, the bulk of the transverse inertial forces were transferred directly to the abutments and the stiffness, either fully elastic or inclusive of yielding, of the center pier was not significant. The implication of this is that the superstructure can experience large inertial forces even though ductile design is used for the piers.

While damage to bridge superstructures is not common, design consideration of the entire load path, including the superstructure is reasonable. The simplest way to check that the superstructure can globally transmit the expected forces is to extract the forces from the elastic demand analysis and check the superstructure for those forces. In reality, yielding of intermediate piers will alter the internal force distribution in the superstructure, and may induce higher internal forces than predicted using the elastic forces. However, to the extent that the displacements of the elastic system match those of the yielding bridge system the internal forces in the superstructure from the elastic model may not be unrealistic.

However, if the internal forces inclusive of yielding are desired they can be estimated by first estimating the plastic shear capacity of each pier location, then solving for a distribution of inertial load that would satisfy the abutment boundary conditions and be in equilibrium with the pier plastic shears. This may be a bounding exercise with some trial and error required, depending on how accurate an estimate is desired and the degree to which the abutments interact with the intermediate piers. If the superstructure is considered a rigid body and the abutments are assigned transverse stiffnesses, inclusive of the shear keys to the soil, an approximate analysis can be carried out. The objective is to obtain a reasonable estimate of the internal forces at the overstrength level and check the superstructure for adequate strength. Example calculations of this type are shown by Priestley et.al. (1996).

Conditions where this may be of more concern are girder bridges where an individual girder line could be pulled apart by the tensile action of flexure in the superstructure. Normally enough reinforcement is

present in the deck that little if any additional steel is required. However, in some cases, for example prestressed spliced girder bridges the gravity shear capacity of the girder lines could be adversely affected by seismically induced tension in the superstructure. Thus, either additional reinforcement could be added or fusible shear keys designed.

### **7.7.2 Design of Ductile End Diaphragms**

Ductile end diaphragms are a relatively new design concept for steel plate girder bridges loaded in the transverse direction whereby yielding of the cross frames at the pier locations provides energy dissipation and internal force limitation, rather than the substructure. The concept was first postulated for retrofit of steel bridges with wall piers that had little displacement accommodation capability. Fundamentally, the use of ductile elements in the superstructure, itself, is a departure from traditional seismic design. The concept is given its own “Global Design Strategy” designation of Type 2 in the *Guide Specifications*, and the first design provisions for such systems have been included in the *Guide Specifications*.

The concept for this type of ERS is that the diagonal braces used for cross frames at the pier locations could be made sufficiently ductile to dissipate earthquake induced energy demands. The use of braced frame systems, either concentric or eccentric, has a long history of successful use in the building industry. It has been substantiated by testing of braced frames in that industry that with proper attention to the yielding elements within the frame, capacity protection of frame elements that should not be damaged, and use of appropriate detailing that adequate performance of the braced frame could be achieved. For use in bridges the compatibility of the deformable brace system with that of the gravity-load-bearing girder system must be considered such that instability of the girder system is prevented.

The design procedure currently available for this type of ERS is force-based. DBM provisions have not yet been developed for the system. However, since this is a new system cyclic testing is necessary to substantiate that a given configuration of ductile diaphragm works as expected. Thus, deformation based criteria could be developed on a site-specific and system-specific basis.

### 7.7.3 Capacity Protection of Bearings, Restrainers and Shear Keys

Shear Keys: Shear keys range from small concrete ‘girder stops’ to large shear resisting walls for box girder superstructures. Generally, shear keys are designed for the forces indicated by the elastic demand analysis of the bridge. More accurate forces that reflect yielding at the intermediate piers could be developed using the process described above.

Once the elastic demand forces or the overstrength system yield forces are determined, capacity protection design of shear keys proceeds by considering the keys as corbels that act laterally rather than vertically. The procedure outlined in the *LRFD Specifications* for corbels and brackets or those for strut and tie mechanisms may be used. The design features may be considered in reference to Figure 7-20. The corbel provisions require reinforcement for the direct tension effect of the lateral force on the key acting above the resisting plane. This reinforcement needs to be positively developed and should be located in a position to best resist the induced tensile force using a strut-and-tie analogy (i.e., near the loaded side of the shear key). Then additionally, shear friction steel should be provided to develop the interface shear capacity based on the appropriate roughness resulting from the construction process. This approach would be used for individual girder shear blocks or keys resisting the entire superstructure lateral force, as in the case of a concrete box girder.

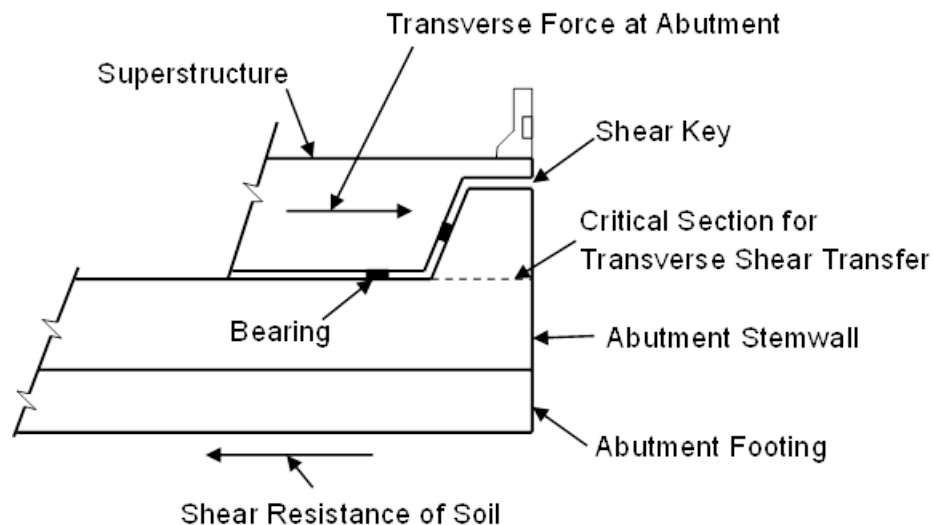


Figure 7-20 External Shear Key for Box Girder Bridge

It should be recognized that shear key forces can become quite large, especially when skews are involved and particularly when wall piers are involved. The overall bridge behavior with skewed piers is such that movement of piers in their longitudinal, skewed direction can induce large forces in abutment shear keys. Then coupled with the skewed geometry, some shear keys may be more heavily loaded than others due to eccentricities caused by the skew. In such cases, a spine demand model alone may not properly calculate the shear key forces, thus requiring elements that extend out to the shear key location from the spine to be included. Additionally, response spectrum analyses will incorrectly provide shear key forces if only one shear key at a time can act. The designer may need to perform static analyses in such case to develop appropriate shear key demand forces.

Fusing of shear keys can be an appropriate strategy to control forces in the superstructure. If fusing shear keys are used, care must be taken to have adequate system stiffness, redundancy and resistance to handle the dynamic effects after the shear keys have failed. Additionally, appropriate overstrength forces must be used to bound the expected response. Fusible shear keys should be reinforced using more predictable materials, such as A706 Grade 60 reinforcement, rather than A615 Grade 60.

Restrainers: Restrainers are often used in retrofit to prevent unseating of superstructure elements when insufficient support lengths are available. Restrainers can be used in new design, but generally they should not be used in lieu of adequate support length. Prediction of forces in restrainers has proven to be a difficult challenge and currently no satisfactory simple method of prediction of restrainer forces exists.

Bearings: The design of bearings, like shear keys may either use the system elastic forces or plastic overstrength forces determined from consideration of pier plasticity and superstructure diaphragm action between abutments.

## **7.8 DISPLACEMENT CAPACITY OF BRIDGE STRUCTURES**

The ability to tolerate displacements is the fundamental objective of modern seismic design of bridges. While some design procedures focus on inertial and internal forces, the end result of a good seismic design is displacement capacity. This capacity is instilled in a bridge by the process of capacity design as outlined throughout this manual where appropriate member design and detailing provide a structure that can tolerate displacements well into the inelastic range. The specific displacement checks that are part of

the DBM method as outlined in Chapter 6 ensure that the substructure units that are the main elements of the lateral force resisting system (ERS) will behave as intended.

The displacement demands that could occur in a large earthquake may be due to the inertial vibration response of the bridge, itself, or they may be the result of ground movements as outlined in Section 7.6.5, or both. The displacement assessment must identify the possibility of each and ensure that both types of displacements are addressed when necessary.

### **7.8.1 Minimum Support Lengths**

In addition to the ability of individual piers to tolerate the displacements that may occur, portions of the bridge that are articulated with seat-type joints must also tolerate the expected displacements. Joints and the seats that accompany them are included in bridges for a number of reasons, most of which are not seismic. Regardless of the reason for including such disruptions in the load path, adequate support lengths must be included at such joints to prevent unseating and the potential for dropped spans. Dropped spans have been one of the more dramatic failures that have occurred in actual earthquakes, although it is generally considered that prevention of dropped spans is one of the easiest parts of earthquake design. This is usually achieved by the use of generous support lengths in the seat arrangement.

Support lengths, when included in new design, are relatively simple to make large enough to prevent unseating of adjacent spans. In retrofit practice, the improvement of available support length is often one of the best uses of resources.

Traditionally, prescriptive formulae have been used to specify minimum support lengths. These formulae usually account for geometric features of a bridge, such as span length, height of columns and skew angles. The relationships are normally set up to be conservative and simple to calculate and to intrinsically include movement of the ground and foundation, as well. The relationships then provide an empirical basis for a minimum support length, which is then checked against the calculated displacements of the bridge and the larger of the two used to size the actual support lengths.

The term ‘support length’ is now used to differentiate between the older term, seat width, which is literally the actual width of the surface. Support length is used to denote the actual overlap of support surface and supported element.

Both the FBM and DBM methods rely on prescriptive support lengths. These lengths are normally much larger than the calculated displacements because they account for things that the analysis may or may not include, such as foundation movement with the passage of surface waves and movements at the outer edges of a bridge. The latter condition has been demonstrated repeatedly in earthquakes in bridges that have large skews, where the outer girders or web lines may be unseated due by rotation effects about a vertical axis. To provide adequate safety under expected earthquake conditions, the prescriptive support lengths typically increase with seismic hazard (i.e., by seismic zone or category).

Where support lengths are inadequate, as in the case of existing construction, either increased length can be added or restrainers used to prevent unseating. In new construction, the support length should always be made adequate, and reliance on restrainers as the primary means of preventing unseating should be avoided.

### **7.8.2 P- $\Delta$ Effects**

The action of lateral forces that produce lateral displacements the gravity load of a pier will also produce additional moment in the pier, the moment being the product of the load,  $P$ , and the deflection,  $\Delta$ , as shown in Figure 7-21. Because this moment must be resisted by the pier, along with the moment due to the lateral load itself, the ability of the pier to resist lateral load is diminished. This reduction increases with lateral displacement, and in the extreme, the effect can render the system unstable laterally. Under such an extreme condition, the pier and its supported gravity load would displacement laterally without any additional externally applied lateral load. If the lateral resistance of the pier is plotted against its lateral displacement, the reduction in lateral resistance can be subtracted from the resistance considered without  $P-\Delta$  to find the actual resistance available as a function of displacement. An example of this is shown in the figure. It is clear that due to the negative (downward sloping) stiffness in the curve that includes  $P-\Delta$ , instability could occur for a given lateral load. Instability would indicate that force acting in the opposite direction would be required to resist further lateral displacement.

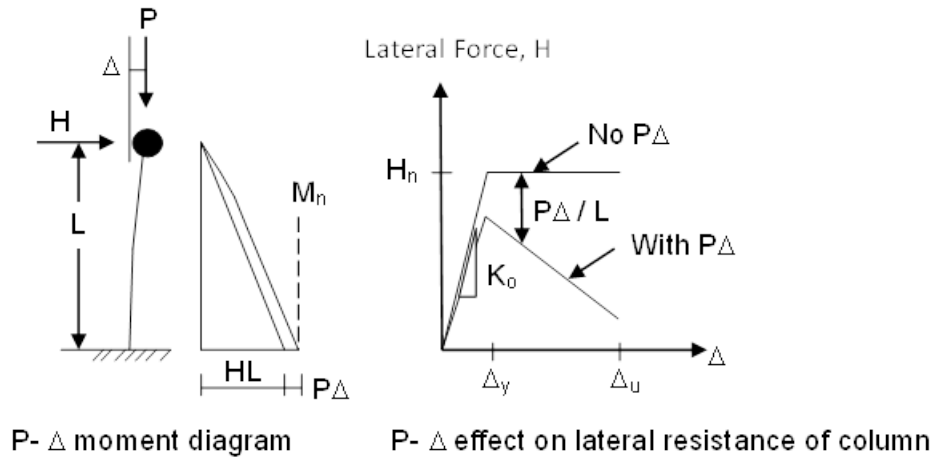


Figure 7-21 Effect of  $P-\Delta$  on a Single-Column Pier (after Priestley et. al., 1996)

Because seismic loading is transient, in that the lateral load is applied only momentarily before it reverses, the  $P-\Delta$  reduction can cause a structure to gradually de-center itself as each progressive cycle of loading occurs, even though the individual load cycles are insufficient to cause instability by themselves. This is shown in Figure 7-22 for two different hysteretic behaviors, elastic-perfectly plastic and degrading stiffness. It can be seen in figure (a) that a pulse of loading results in a residual displacement of magnitude B. Then further inelastic loading causes the residual displacement to increase, in part because the strength of the structure is progressively weaker in the direction of first yielding. However, with degrading stiffness behavior that is more representative of reinforced concrete construction this effect is not as severe. This is because the unloading stiffness and in particular stiffness of loading in the opposite direction (BC) is softer than the original stiffness. Consequently the residual displacements (D & E) tend not to be as big and tend to diminish as further cyclic loading occurs. Additionally if the structure has any hardening after the first yield point, the  $P-\Delta$  effect is further diminished. However,  $P-\Delta$  must still be considered with degrading stiffness types of structures, such as reinforced concrete piers.

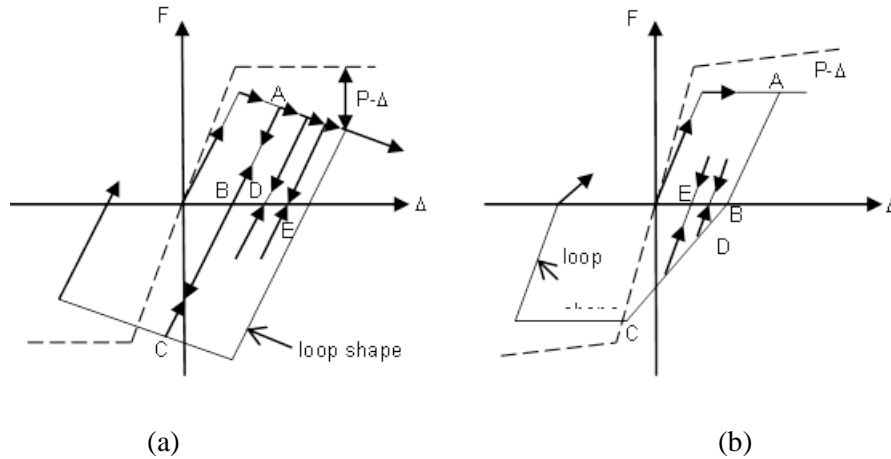


Figure 7-22 P- $\Delta$  Effect on Cyclic Response (after Priestley et. al., 1996)  
 (a) Elastic-Perfectly Plastic Hysteresis, and (b) Degrading Stiffness Hysteresis

The strategy that has long been used to control  $P-\Delta$  effects under seismic loading is to ensure that sufficient post-yield base shear capacity is present in the system to reduce the tendency of the structure to become unstable under seismic loading. This can be accomplished with a stability index,  $\theta$ , which is the ratio of the  $P-\Delta$  moment to the base moment that produces the base shear resistance of the structure. Thus, the current approach for bridges is to ensure that the  $P-\Delta$  moment does not exceed 25% of the plastic resisting moment. If this limit is observed then instability or other problems related to  $P-\Delta$  effects should not occur. This limit is supported by analytical work done by MacRae, Priestley, and Tao (1993) that investigated the influence of hysteresis shape, post-yield stiffness, and ductility demands.

It should be noted that end fixity affects the relationship between destabilizing  $P-\Delta$  moment and resisting moment. Thus, individual  $P-\Delta$  moments are compared to local resisting moments in the pier and should be calculated as the moment of an equivalent cantilever (i.e., the  $P-\Delta$  moment considering the end of the member relative to the point of contraflexure). Additionally, for multi-column pier loading in the plane of the columns, the  $P-\Delta$  effect can be considered based on the system, not individual column, resistances, since it is the system that can experience instability, not individual columns. In such a case the  $P-\Delta$  moment divided by the effective pier height would be compared to the base shear capacity of the pier, and the  $P-\Delta$  effect so calculated should not exceed 25 percent of that base shear. However, if the pier does not fully form a plastic mechanism, then the lateral resistance present at the design displacement should be

used to make the check. This distinction is not typically made in the design specifications. It is incumbent on the designer to ensure that the resistance and demand are consistent with one another.

Also it should be noted when  $P-\Delta$  is considered for the seismic load case, which includes system yielding, the normal *LRFD* moment magnification procedure is not also applied at the same time. The moment magnification approach is derived and valid for elements and systems that response essentially elastically. Thus, the stability coefficient method described above, which was derived from analytical time history studies of yielding systems, takes the place of the moment magnification process.

## 7.9 SUMMARY

This chapter covers the two basic design methodologies used by the AASHTO seismic design specifications. These are the force-based method (FBM), which is used in the *LRFD Specifications*, and the displacement-based method (DBM), which is used in the *Guide Specifications*. The focus of the chapter is to provide the fundamentals of the two methods, rather than the specific requirements of the AASHTO specifications. Specific requirements from AASHTO were presented to illustrate the two methods, where relevant. Design activities were outlined for each method to help the reader understand the common elements of each method. Coupled with each design method is the assurance that the bridge will have adequate lateral displacement capacity, which of course is directly checked in DBM, but which also must be considered when using the FBM. The provision of adequate support lengths where superstructure rests on substructure is part of this overall check, as is the consideration of  $P-\Delta$  effects.

Capacity design of the piers was presented with a particular focus on the prevention of shear failure of columns. The *Guide Specification* method of shear design was presented in detail. This method adjusts downward the concrete contribution to shear strength as flexural plastic hinging damage is incurred in the column yield zones. Capacity protection of cap beams, steel frames, wall piers and beam-column joints was also covered.

Capacity design procedures for foundations and abutments were covered, including development of the forces that act on the foundation elements when plastic hinging of the substructure above the foundation occurs. The capacity design of foundations and abutments depends on identifying potential modes of failure and suppressing them. Potential modes of failure were presented.

Additionally, loadings that may produce inelastic action in the foundations were discussed, and such loading typically arises from liquefaction-induced ground movements, such as lateral spreading. Conceptual methods for mitigating such hazards were presented.

Finally, capacity protection methods for superstructures and bearings, restrainers and shear keys were presented.

## CHAPTER 8

### AASHTO SEISMIC DESIGN SPECIFICATIONS

#### 8.1 GENERAL

The two design specifications currently available to the practicing bridge engineer in the United States are described in this chapter, and they are based on the FBM and DBM covered in Chapter 7. This chapter should not be used in lieu of the actual specifications, themselves. Designers should always work directly from the specifications that are required for a particular project.

As a preamble to the following discussions, it is helpful to review the history of the development of seismic design criteria since the occurrence of the San Fernando earthquake that occurred on February 11, 1971. Modern seismic design of bridges began as a result of this earthquake. Extensive damage to bridges due to the strong motion ground vibration effects was coupled with large structure displacements, which were the primary cause of failures in the earthquake. Prior earthquake damage to bridges was primarily caused by foundation failures resulting from excessive ground deformation, loss of stability and bearing capacity of soils. As a direct result of such failures, substructures have often tilted, settled, slid or overturned; thus severe cracking or complete failure has often been experienced.

Prior to the San Fernando earthquake, bridges were designed using a simple static coefficient method similar to that being used for buildings. After the San Fernando earthquake it became apparent that the seismic design requirements were inadequate and that the design methodology should be critically examined. Recognizing the urgent need for new design provisions, Caltrans began to develop new criteria and participated jointly with the U.S. Department of Transportation to fund critically needed research related to the seismic effects on bridge systems. Caltrans released their first modern day seismic design criteria for use in production design in 1973. These criteria included the following components:

- 1) The relationship of the bridge site to active faults (seismic hazard),
- 2) Seismic response of the soils at the site (site class),
- 3) Dynamic response characteristics of the bridge system subjected to ground shaking,
- 4) Reductions in the elastic seismic forces by the R-factor to account for ductility.

Their design criteria were adopted by AASHTO in 1975 with the addition of the seismic hazard for the United States and remained in effect until 1990.

A subsequent effort, ATC-6 (1981), funded by the FHWA was adopted by AASHTO in 1983 as Guide Specifications for Seismic Design of Bridges. The premise of these guidelines was that they were applicable to all parts of the United States. The seismic risk varied throughout the country. Unlike the previously adopted Caltrans criteria, which essentially had only one seismic design category, the new Guide Specifications (ATC-6) introduced four Seismic Performance Categories (SPC). The categories were established on the basis of a ground Acceleration Coefficient (A) taken from a USGS map and the newly introduced Importance Classification (IC) of the bridge. Different degrees of complexity and sophistication of the seismic analysis and design were specified for each of the four Seismic Performance Categories. Local soil site effects were accounted for using three different site coefficients.

Ductility reductions were specified on a component basis using Response Modification Factors (R) to account for energy dissipation and redundancy. The reductions are applied to the forces obtained from elastic dynamic response analysis. These reductions were based on research findings and the observations of damaged suffered to bridges in past earthquakes. ATC-6 also introduced the concept of minimum support lengths to account for the uncertainty from variable support motion due to the effects of traveling waves. The rigid body support motion typically used in the dynamic response analysis did not account for differential ground motions. This criterion uses a Force-Based Approach (FBM) with prescribed R factors applied to the elastic forces to obtain in the final design forces. The ATC-6 Guide Specification was adopted by AASHTO as Division I-A in 1990 and replaced the 1975 AASHTO Criteria.

The AASHTO LRFD *Bridge Design Specifications*, adopted in 1994, essentially incorporated Division I-A into the *LRFD Specifications* and format. There have been minor updates, but the specifications did not undergo any significant changes until 2007, at which time the hazard was revised from a 500-year to a 1000-year return period (i.e. 10% probability of exceedence in 50 years was changed to a 7% probability of exceedence in 75 years). It is important to mention that the increase in the design earthquake return period did not result in a uniform increase in seismic demands for all geographic locations. In addition, the NEHRP site classifications, as described in Chapter 2, were adopted to ensure a consistent set of seismic demands to the LRFD *Guide Specifications*.

The LRFD and *Guide Specifications* seismic provisions are recognized as equal methods for performing the seismic design of a bridge. The LRFD *Bridge Design Specifications* specifically permits either method to be used, and thus both methods are legally permitted and are acceptable by the *LRFD Specifications*. This chapter includes a discussion of each of the two specifications and along with the common features and their differences. To provide some structure to the discussions it is helpful to list the seismic design steps for a bridge as shown in Table 8-1. In Chapter 7 this listing was introduced, and in this chapter additional detail is added to the list to clarify the components of each step and how those steps are reflected in the AASHTO seismic design provisions.

**TABLE 8-1 GENERAL STEPS FOR SEISMIC DESIGN**

Step	Design Activity
1.	<b>Determine Seismic Input</b> <ul style="list-style-type: none"> <li>a) Seismic hazard</li> <li>b) Site classification</li> <li>c) Response spectra or other input</li> </ul>
2.	<b>Establish Design Procedures</b> <ul style="list-style-type: none"> <li>a) Seismic Zone or Design Category</li> <li>b) Importance</li> <li>c) Analysis procedures</li> <li>d) Foundation modeling</li> </ul>
3.	<b>Identify the Earthquake Resisting System and Global Design Strategy</b> <ul style="list-style-type: none"> <li>a) Where damage or yielding will be accepted</li> <li>b) What system of deformation tolerance/articulation will be used</li> <li>c) Participation of abutments</li> <li>d) Use of non-preferred EREs</li> </ul>
4.	<b>Perform Demand Analysis</b> <ul style="list-style-type: none"> <li>a) Linear elastic, pseudo static loading</li> <li>b) Multimode elastic method</li> <li>c) Time history method</li> <li>d) Directional combination</li> </ul>
5.	<b>Design and Check Earthquake Resisting Elements (Ductile or Other)</b> <ul style="list-style-type: none"> <li>a) Force-based – Use of R, Extreme Event load factors</li> <li>b) Displacement-based - Non-seismic loads or minimum strengths, displacement assessment, P-Δ Effects</li> <li>c) Detailing of ductile EREs</li> </ul>
6.	<b>Capacity Protect the Remaining Elements</b> <ul style="list-style-type: none"> <li>a) Shear in ductile EREs</li> <li>b) Cap beams</li> <li>c) Foundations and abutments</li> <li>d) Superstructure, connections, bearings, support lengths</li> </ul>

Figure 8-1 and Figure 8-2 provide a summary comparison of the FBM and DBM as they are applied in the AASHTO seismic design provisions, and the discussion here is meant to provide a brief and simple overview of the design provisions. The figures are based on four different zones or categories, which control the rigor of the seismic design provisions. The lower zones have fewer and simpler requirements, and the higher zones have more detailed requirements. “Partitioning” of the country into zones is described in a subsequent section. In the first figure, the demand that a bridge can tolerate is shown qualitatively, and may be thought of as the lateral displacement capacity. This capacity defines the limit of the seismic demands that can be safely resisted by the bridge, and the capacity is controlled by the detailing of the reinforcement used in the structure, including both transverse and longitudinal bars.

The level of rigor for detailing the reinforcement is shown in the second figure. As can be seen, for the lowest zone, very little detailing is required. As the zones increase, the FBM has a “one-size-fits-all” approach to transverse steel that begins with the second zone and remains the same through the highest zone. In contrast, the DBM has progressively increasing rigor proportional to the zone. The result of these two detailing approaches is that the FBM should produce a bridge with a higher displacement capacity in the lower zones than the DBM would produce. In fact, the capacity should be nearly constant with the FBM. The DBM requires less transverse steel and so provides only limited ductility capacity in the lower zones. This inherent difference between the two methods does mean that for structures designed using the DBM in the lower zones there may be less displacement capacity available for resisting earthquakes larger than the design earthquake. This is simply the result of how the prescriptive detailing provisions were set up for the two methods.

In the highest, zone, the DBM transverse steel is variable such that the capacity may be improved by increasing the confinement steel. These two plots illustrate, qualitatively, that the displacement capacity and the steel detailing are inextricably linked, notwithstanding the fact that displacement capacity is not directly checked in the DBM of the *Guide Specifications*. Nonetheless, the DBM prescriptive detailing provides a safety factor of sorts to cover the fact that no direct check of displacement capacity is made.

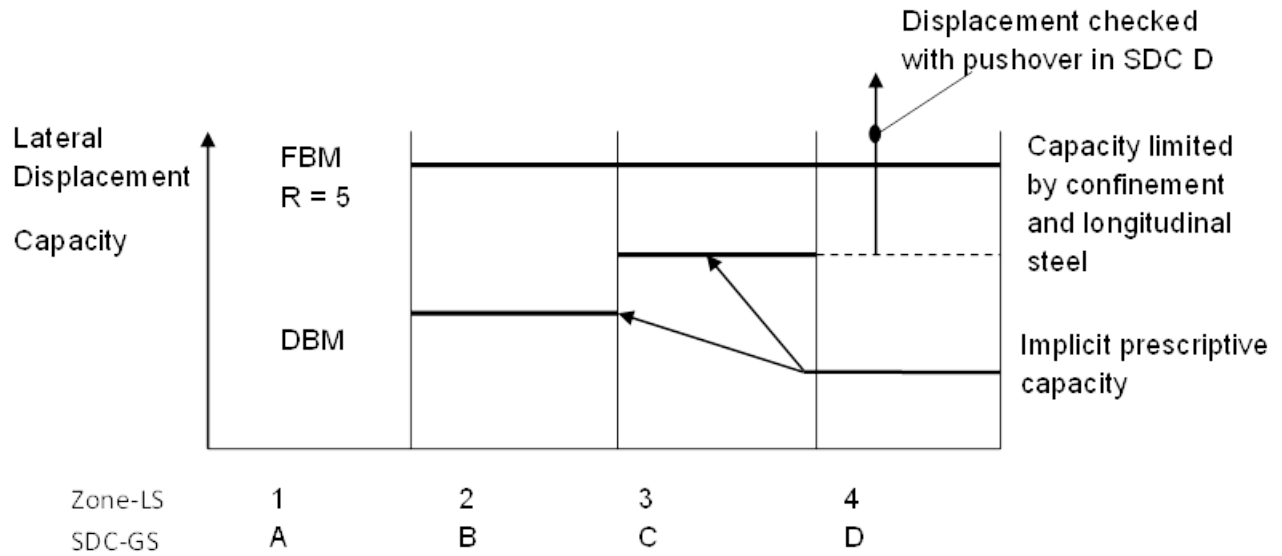


Figure 8-1 Seismic Capacity using *LFRD Specifications (LS)* and *Guide Specifications (GS)*

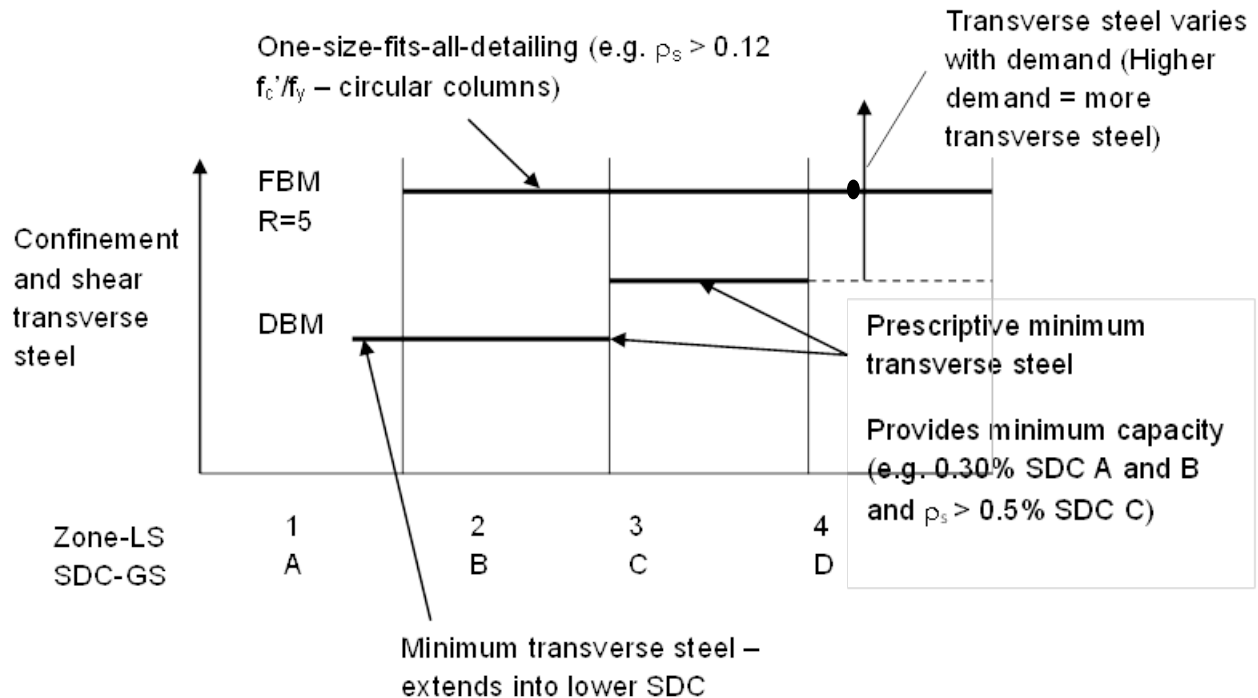


Figure 8-2 Confinement Requirements using *LFRD Specifications (LS)* and *Guide Specifications (GS)*

## 8.2 COMMON FEATURES OF AASHTO LRFD AND GUIDE SPECIFICATIONS

Many features between the LRFD and *Guide Specifications* are identical or “near common”. For example, the seismic hazard, site coefficients, partitioning, liquefaction assessment requirements, support lengths,  $P-\Delta$  provisions and lower seismic region support length requirements are essentially the same. Other features, such as modeling, reinforced concrete detailing and foundation design requirements are very similar. This section describes these common features between the two design procedures.

### 8.2.1 Determine Seismic Input

As mentioned earlier, a significant change occurred when the AASHTO *LRFD Bridge Design Specifications* changed from a 500-year to a 1000-year return period seismic hazard. This change was made in conjunction with incorporation of the NEHRP Site Classification. These changes were made prior to the adoption of the *Guide Specifications*, and it was recognized that both design specifications must have the same input seismic motion, or an unacceptable inconsistency would exist. Therefore, the seismic hazard and site classification were changed in the LRFD simultaneously with the adoption of the *Guide Specifications* as an alternate design procedure.

Similarly, the FHWA *Seismic Retrofitting Manual for Highway Structures: Part I-Bridges* (2006) also uses the same seismic hazard. The NCHRP Project 12-70, Report 611 (2008) “Seismic Analysis and Design of Retaining Walls, Buried Structures, Slopes, and Embankments” likewise include the 1000-year hazard.

The seismic ground motion shaking hazard and the site effects are described in Chapter 2 for both the *LRFD Specifications* and the *Guide Specifications*. Ground motions and design response spectra for use with both AASHTO Specifications are determined using either a General Procedure or a Site-Specific Procedure, both of which are described in Chapter 2.

## 8.2.2 Establish Design Procedures

Establishing design procedures includes such activities as determining the seismic zone or category, which then requires the selection of demand analysis techniques, modeling approaches, rigor of detailing, and capacity protection specifics. While many procedures are identical or nearly so, some are not quite so close. One procedure or consideration that falls into this category is “Operational Classification,” which is used to be referred to as Importance. This consideration is important to discuss in the “Common Features” section, because this issue is germane to every bridge design, in that it is always considered at some level in the early stages of design. In the *LRFD Specifications*, Operational Classification covers:

- Critical Bridges, which should remain open to all traffic after the design earthquake and be usable by emergency vehicles and for security/defense purposes immediately after a large earthquake (e.g. a 2500-year event).
- Essential Bridges, which are those bridges that should be open to emergency vehicles and for security/defense purposes immediately after a design earthquake (i.e., a 1000-year event).
- Other Bridges, which are bridges that are not Critical or Essential.

The *LRFD Specifications* has limited provisions, such as selection of more conservative R-factors for Critical and Essential Bridges, but that is essentially the limit of the provisions addressing these two higher performance objectives. The *Guide Specifications* essentially cover only the third category of “Other Bridges”. In a practical application of the design of one of the two higher categories, a site-specific and bridge-specific design criteria should be developed to ensure that the performance desired by the Owner is likely to be achieved. To that end, the majority of the *LRFD Specifications* and the entirety of the *Guide Specifications* are dedicated to the Other Bridge category. Likewise the Caltrans SDC (2013), from which the framework of the *Guide Specifications* was adopted, covers the “Ordinary Standard” or Other Bridge category.

The establishment of the design procedures also includes selection of the type of analysis that will be undertaken and the degree of sophistication used to model such items as the foundations. In general, the lower seismic regions of the country will have less restrictive requirements, and in the higher seismic regions more rigor is required in the analytical model to accurately capture the expected seismic response. Modeling is discussed in more detail in the following sections.

### 8.2.2.1 Performance (Seismic Zones and Seismic Design Categories)

The two specifications both use a system of partitioning of the country into seismic regions, ranging from low to high, to control the amount of effort or rigor required to design a bridge for seismic effects. The idea is that in the lowest hazard regions, very little actually need be done to account for the possibility of a damaging earthquake during the life of the bridge. In contrast, the largest hazard regions should require significant design attention to earthquake resistance, including detailed analysis, detailing, and consideration of structural form, as described in Chapter 4. The separation of the country into different zones is accomplished using the design spectral acceleration coefficient at 1.0-second,  $S_{DI}$ . In the LRFD Specification, these are called Seismic Zones, and in the *Guide Specifications*, these are called Seismic Design Categories. The zones range from 1, the lowest, to 4, the highest. Likewise, the SDCs, as they are abbreviated, range from SDC A to D. The spectral acceleration boundaries are the same for the two specifications, and these are listed in Table 8-2.

**TABLE 8-2 SEISMIC PARTITIONS FOR BOTH SPECIFICATIONS**

Acceleration Coefficient, $S_{DI}$	Seismic Zone – LRFD Specifications	Seismic Design Category (SDC) – Guide Specifications
$S_{DI} \leq 0.15$	1	A
$0.15 \leq S_{DI} < 0.30$	2	B
$0.30 \leq S_{DI} < 0.50$	3	C
$0.50 \leq S_{DI}$	4	D

It should be noted and recalled that the Acceleration Coefficient is the design spectral acceleration coefficient at 1.0-second,  $S_{DI}$ , which includes both the local seismic hazard and the local site effects. Thus, unlike previous editions of seismic provisions, these new provisions are a function of both regional acceleration and site amplification effects. Therefore, a site on poor soil may have a higher zone or category, while a nearby site with firm soil, might be a lower zone or category. Thus, it is now impossible to map the zones and categories without consideration of the site soil conditions.

### **8.2.3 Identify the Earthquake Resisting System and Global Design Strategy**

The identification of Earthquake Resisting Systems was first introduced in ATC-49 (2003) and subsequently included in the *Guide Specifications*. Global Design Strategies were first introduced in the *Guide Specifications*. Both of these concepts were included in *Guide Specifications*, they are discussed in Chapter 4 where it is noted that the concepts are valid for both design specifications and should be considered by designers to assist them in determining how their designs should work and how to approach the design.

### **8.2.4 Demand Analysis**

A demand analysis is conducted to determine the seismic response of a bridge to a given earthquake hazard. The model used to conduct the response analysis is dependent on many factors which include:

1. Seismic hazard at the bridge site.
2. Complexity of the bridge and its foundation.
3. Selected seismic design strategy
4. Desired performance during the earthquake.

The range of analytical techniques and modeling extends from simple static analysis using spline line elements to nonlinear time history analysis using a detailed model. The analysis technique and model selected should be refined enough to adequately determine the seismic response analysis. Figure 5-5 in Chapter 5 shows the progression of models ranging from the simple model to the more complex finite element model. There are several computer programs available that offer a wide range of dynamic response analyses and models. Some of the programs have model generating capabilities specifically for bridges. Other more general purpose programs require additional user input. Table 8-3 shows typical features that the user may consider in evaluating the advantages of one software package versus another.

There are several analytical methods that may be used for the demand analysis which are described in detail in Chapter 5 which include:

- Equivalent Static Analysis
- Elastic Dynamic Analysis
- Nonlinear Time History

Although these methods have been introduced in Chapter 5, this chapter is more focused on the application of these methods and in turn how the results are used for design.

**TABLE 8-3 FEATURES TO CONSIDER FOR SOFTWARE**

Item	Programs
Analysis Options	Static, Multi-Mode Spectral, Pushover, Capacity Spectrum, Time History, Nonlinear Analysis
Material Nonlinear	Multi-linear, Yield Surface, Concrete Model
Geometric Nonlinear	Large Deflection, P- $\Delta$ Analysis, Stability Analysis
Structural Damping	Viscous Damper, Base Isolator, Energy Devices
Boundary Element	Gap Element, Hook Element, Friction Element
Dynamic Analysis	Modal Analysis, Linear and Nonlinear Dynamic Analysis, Multi-Support Excitation
Hardware Mechanics	PC, Mainframe, Mac
Structural Design	Steel Structure, Concrete Structure, Composite Structure
Input Data	Text File, User Interface, CAD File
Output Results	Real Time Display, Automatic Interactive, Tabular Presentation

#### 8.2.4.1 Loading

The detailed seismic design of a bridge is performed following the design for all the service loads. Earthquake loading is considered an Extreme Event limit state having a unique occurrence with a return period that is significantly greater than the design life of a bridge.

According to *LRFD Specifications* Article 1.3.2.5, the extreme event limit state is taken to ensure the structural survival of a bridge during a major earthquake or flood, or when collided by a vessel, vehicle, or ice flow, possibly under scoured conditions. The load combination Extreme Event I, related to earthquake loading, used in the *LRFD Specifications* and corresponding load factors are shown in Table 8-4.

**TABLE 8-4 LOAD COMBINATIONS AND LOAD FACTORS  
(LRFD SPECIFICATIONS TABLE 3.4.1-1)**

Load Combination Limit State	Load Type (See LRFD Specifications for Definitions)									Extreme Events (Use one at a time)			
	DC DD DW EH EV ES EL	LL IM CE BR PL LS	WA	WS	WL	FR	TU CR SH	TG	SE	Earthquake Load	Ice Load	Vehicular Collisions Force	Vessel Collision Force
STRENGTH I (unless noted)	$\gamma_p$	1.75	1.00	-	-	1.00	0.50/1.20	$\gamma_{TG}$	$\gamma_{SE}$	-	-	-	-
STRENGTH II	$\gamma_p$	1.35	1.00	-	-	1.00	0.50/1.20	$\gamma_{TG}$	$\gamma_{SE}$	-	-	-	-
STRENGTH III	$\gamma_p$	-	1.00	1.40	-	1.00	0.50/1.20	$\gamma_{TG}$	$\gamma_{SE}$	-	-	-	-
STRENGTH IV	$\gamma_p$	-	1.00	-	-	1.00	0.50/1.20	-	-	-	-	-	-
STRENGTH V	$\gamma_p$	1.35	1.00	0.40	1.00	1.00	0.50/1.20	$\gamma_{TG}$	$\gamma_{SE}$	-	-	-	-
EXTREME EVENT I	$\gamma_p$	$\gamma_{EQ}$	1.00	-	-	1.00	-	-	-	1.00	-	-	-
EXTREME EVENT II	$\gamma_p$	0.50	1.00	-	-	1.00	-	-	-	-	1.00	1.00	1.00
SERVICE I	1.00	1.00	1.00	0.30	1.00	1.00	1.00/1.20	$\gamma_{TG}$	$\gamma_{SE}$	-	-	-	-
SERVICE II	1.00	1.30	1.00	-	-	1.00	1.00/1.20	-	-	-	-	-	-
SERVICE III	1.00	0.80	1.00	-	-	1.00	1.00/1.20	$\gamma_{TG}$	$\gamma_{SE}$	-	-	-	-
SERVICE IV	1.00	-	1.00	0.70	-	1.00	1.00/1.20	-	1.00	-	-	-	-
FATIGUE – LL, IM & CE ONLY	-	0.75	-	-	-	-	-	-	-	-	-	-	-

Following the *LRFD Specifications* the design forces are determined using the Response Modification Factors,  $R$ , of *LRFD Specifications* Article 3.10.7. The Response Modification Factor is described in more detail in Chapter 7. The seismic design in the *LRFD Specifications* is performed according to a force loading combination as covered in depth in Chapter 7. In contrast, the seismic design in the *Guide*

*Specifications* is performed as a displacement demand to capacity check to a structure that is designed for all other loading combinations. The articulations of the structure are further fine-tuned or modified if needed in moderate to high seismic regions as established in Seismic Design Categories C and D of the *Guide Specifications*. These two approaches are covered more in depth in Chapter 7 of this Manual.

#### **8.2.4.2 Directional Combinations**

As presented in Chapter 2, the earthquake ground motion at a bridge site is characterized by design spectra for representing two horizontal components and potentially one vertical component for the site. Generally, vertical motions are less than horizontal motions and the time of occurrence of the maximum vertical movement does not necessarily coincide with that of the maximum horizontal movement. For these two reasons vertical earthquake consideration is generally ignored except for bridges having unusual framing or geometrical configurations. Bridges having components sloped in the vertical direction, column outriggers and “C” bents will be affected by vertical ground motions.

The intent of the seismic design is to apply the earthquake loading in the direction that results in the structure’s “most critical” seismic load condition. Finding the most critical direction is an iterative procedure that is time consuming. To simplify for the seismic design of bridges, the 30% rule is used to account for the directional uncertainty of the earthquake ground motion and account for the most critical condition at the component level.

According to the both the LRFD and *Guide Specifications*, the elastic seismic force effects along each of the principal axes of each component resulting from analyses in the two perpendicular global directions is combined to form two load cases in accordance with the 30% rule as follows:

- 100 percent of the absolute value of the force effects in one of the two perpendicular directions combined with 30 percent of the absolute value of the force effects in the second perpendicular direction, and
- 100 percent of the absolute value of the force effects in the second perpendicular direction combined with 30 percent of the absolute value of the force effects in the first perpendicular direction.

However, where foundation and/or column connection forces are determined from plastic hinging of the columns specified in *LRFD Specifications* Article 3.10.9.4.3, the resulting force effects on other components may be determined without consideration of combined load cases specified in Table 6.1-1. For the purpose of this provision, “column connection forces” are taken as the shear and moment, computed on the basis of the column plastic hinging. The axial load is taken as that resulting from the appropriate load combination with the axial load, if any, associated with plastic hinging taken as the earthquake load, *EQ*. If a pier is designed as a column as specified in *LRFD Specifications* Article 3.10.7.2, this exception is taken to apply for the weak direction of the pier where force effects resulting from plastic hinging are used. The combination load cases specified must be used for the strong direction of the pier. The exception to these load combinations indicated at the end of this section should also apply to bridges in Zone 2 where foundation forces are determined from plastic hinging of the columns.

Similarly, the *Guide Specifications* considers a combination of orthogonal seismic displacement demands to account for the directional uncertainty of earthquake motions and the simultaneous occurrences of earthquake forces in two perpendicular horizontal directions.

In the application of the *Guide Specifications*, there are some component design procedures that require the development of elastic seismic forces using orthogonal combination. The procedure for developing such forces is the same as that for displacements and is similar to the *LRFD Specifications*.

### **8.2.4.3 Analytical Model Appropriate for the Selected Design Strategy**

A complete bridge system may be composed of a single frame or a series of frames separated by expansion joints and/or articulated construction joints. A bridge is composed of a superstructure and a supporting substructure. Individual frame sections are supported on their respective substructures. Substructures consist of piers, single column or multiple column bents that are supported on their respective foundations.

The determination of the seismic response of a bridge includes the development of an analytical model followed by the response analysis of the analytical model to predict the resulting dynamic response for component design. Both the development of the analytical model and the selected analysis procedure are dependent on the seismic hazard, selected seismic design strategy and the complexity of the bridge.

There are various levels or degrees of refinement in the analytical model and analytical procedures that are available to the designer.

Following *LRFD Specifications* Article 3.10.7.2 seismic loads are assumed to act in any lateral direction. Usually the orthogonal axes are the longitudinal and transverse axes of the bridge. In the case of a curved bridge, the longitudinal axis may be the chord joining the two abutments.

In straight and large radius (i.e., 3000 feet and greater) bridges, the selection of the longitudinal axis as the chord joining the two abutments is considered an appropriate approach.

In curved bridges, the longitudinal and transverse modes are strongly coupled (i.e., periods of vibration are close). Curved and radial bridges' abutment boundary conditions are not the same as those in straight bridges. Several runs should be performed to bound the coupled behavior.

#### **8.2.4.4 Demand Analysis**

The entire bridge Earthquake Resistant System (ERS) for analysis purposes is referred to as the “global” model, whereas an individual bent or column is referred to as a “local” model. The term “global response” describes the overall behavior of the bridge system including the effects of adjacent components, subsystems, or boundary conditions. The term “local response” refers to the behavior of an individual component or subsystem being analyzed to determine, for example, its forces and deformations.

The designer should consider the stage of design in selecting the analysis method to be used. Often an equivalent static analysis may suffice for a preliminary design followed by a more detailed elastic dynamic analysis (i.e., modal response spectrum analysis) or even in special cases nonlinear time history analysis in the final stages of design.

##### **8.2.4.4.1 Equivalent Static Analysis**

The Equivalent Static Analysis (ESA) assumes the seismic response of a bridge can be obtained in a single mode of vibration in the transverse direction and a single mode in the longitudinal direction. As

mentioned in Chapter 5, there are two equivalent static methods: 1) the Uniform Load Method (see Section 5.2.2) and 2) the Single-Mode Spectral Analysis Method (see Section 5.2.3). This assumption holds for simple bridges that are on tangent alignments, uniform span lengths and column heights with no unusual constraints. Although these methods are not generally used in design they are helpful for preliminary design and checking.

#### **8.2.4.4.2 Elastic Dynamic Analysis**

This method requires the use of a computer program and in general does not have constraints other than being restricted to linear elastic behavior. There are several available computer programs from which to choose to conduct this type of analysis. The analysis method used by the program is a multi-modal analysis, which is based on the superposition of modal response as described in Chapter 5.

### **8.2.5 Design and Check the Earthquake Resisting Elements**

Typically, the columns and piers are the key components that are designed for potential inelastic flexural action (i.e., the formation of plastic hinging) to occur. This seismic design strategy is usually identified in the preliminary design stage. Reinforcement is required to provide both confinement and strength when flexural yielding occurs. The confinement is provided by transverse reinforcement, which may be either spirals or hoops in circular sections and ties in rectangular sections. Transverse reinforcement also contributes to the necessary member shear strength. The flexural strength is provided for by the longitudinal steel. The flexural ductility capacity is controlled by the size and spacing of the confinement steel and the plastic hinge moment capacity is controlled by the amount of longitudinal steel. The confinement steel enables high compression strains to develop within the concrete core after spalling of the concrete cover. The transverse reinforcement also restrains the longitudinal reinforcement against buckling. The transverse steel must be well anchored to resist the high compressive inelastic strains imposed on the concrete core.

The design and check of the earthquake resisting elements are unique to each of the two AASHTO specifications with the exception of support lengths. Thus, support lengths are discussed in this common features section.

### 8.2.5.1 Support Lengths

The support length requirements were purposely kept the same between the two specifications with one minor difference, and thus support lengths are described in this section on common features. The remaining design tasks are different and deferred to Section 8.3.5 for the *LRFD Specifications* and 8.4.5 for the *Guide Specifications*. It has been observed in past earthquakes that bridges often collapse because they do not have adequate support lengths to accommodate the structure movements and the relative ground displacements between the supports. The lengths of the supports must accommodate the displacements resulting from the overall inelastic response at the system, possible independent movement of the various components of the substructure and the out-of-phase displacements and rotations resulting from the traveling surface wave motions that occur in the ground during an earthquake.

A multimode response spectrum analysis may be used to obtain an estimate of the relative displacements at adjacent segments of a bridge if the foundation flexibility is included. A more detailed nonlinear time history analysis, which includes the effects of traveling waves, yielding components within the structural system, friction at the supports due to relative movements, impact of adjacent segments and resistance of the soil embankments behind the abutments will provide a better estimate of the relative movements. However, with the uncertainty associated with such detailed analysis, the effort required is often not practical for design.

A more practical approach is to calculate minimum support lengths using simple empirical formulae based on bridge segment lengths between expansion joints and average column heights within the bridge segment between the adjacent expansion joints. The intent of these formulae is to provide generous support lengths to account for uncertainties in modeling, methodology, and site response. It should be noted that the cost for such generous support lengths is relatively small and easily justified based on the addition assurance against collapse.

Support lengths at expansion bearings without restrainers, shock transmission units (STUs), or dampers should be at least the length calculated using the method below, otherwise, longitudinal restrainers are to be provided. Note that the support length calculated for,  $N$ , as shown in Figure 8-3 is modified by the percentage given in Table 8-5 shown below, and note that the coefficient,  $A_s$ , is defined in Figure 2-9.

As shown in Table 8-5, 75% of the basic support length is required for the lowest seismic zone, 100% is required for the higher end of Zone 1, and 150% of the equation value is required for the higher three zones.

Figure 8-3 shows the basic definition of “support length”. Note that this term is new relative to the old “seat width” term. The distinction is that seat width implies the full width of the supporting face, whereas support length only applies to the length of the seat available to support the span.

**TABLE 8-5 PERCENTAGE N BY ZONE AND ACCELERATION COEFFICIENT  $A_s$ , LRFD SPECIFICATIONS**

Zone	Acceleration Coefficient, $A_s$	Percent, $N$
1	$<0.05$	$\geq 75$
1	$\geq 0.05$ and $\leq 0.15$	100
2	All Applicable	150
3	All Applicable	150
4	All Applicable	150

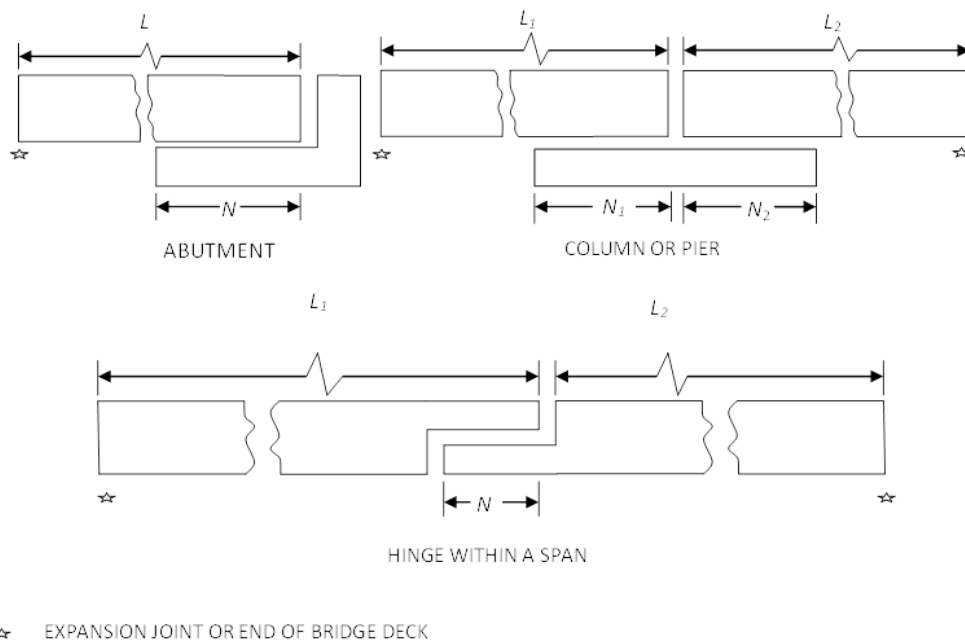


Figure 8-3 Support Length,  $N$

The empirical support length is taken as:

$$N = (8 + 0.02L + 0.08H)(1 + 0.000125S^2) \quad 8-1$$

where:

- $N$  = minimum support length measured normal to the centerline of bearing (in.)
- $L$  = length of the bridge deck to the adjacent expansion joint, or the end of the bridge deck; for hinges within a span,  $L$  is the sum of the distances to either side of the hinge; for single-span bridges,  $L$  equals the length of the bridge deck (ft.)
- $H$  = for abutments, average height of columns supporting the bridge deck from the abutment to the next expansion joint (ft.) for columns and/or piers, column, or pier height (ft.) for hinges within a span, average height of the adjacent two columns or piers (ft.) 0.0 for single-span bridges (ft.)
- $S$  = skew of support measured from line normal to span ( $^{\circ}$ )

Support lengths are equal to the length of the overlap between the superstructure and the support as shown in Figure 8-3. To satisfy the minimum values for  $N$  in this Article, the overall support length will be larger than  $N$  by an amount equal to movements due to prestress shortening, creep, shrinkage, and thermal expansion/contraction. The formulation of the value for  $N$  includes an allowance for cover concrete at the end of the girder and face of the seat in order to ensure bearing against the unreinforced concrete section of the seat.

Table 8-6 shows the percentages of support length required for the *Guide Specifications*, and the requirements are identical for the lower three SDCs, but for the SDC D an alternative form is provided.

**TABLE 8-6 PERCENTAGE N BY ZONE AND ACCELERATION COEFFICIENT  $A_s$ , GUIDE SPECIFICATIONS**

SDC	Acceleration Coefficient, $A_s$	Percent, $N$
A	<0.05	$\geq 75$
A	$\geq 0.05$ and $\leq 0.15$	100
B	All Applicable	150
C	All Applicable	150
D	$N = (4 + 1.65\Delta_{eq})(1 + 0.00025S^2) \geq 24$	

The 1.65 multiplier applied to the relative hinge displacement,  $\Delta_{eq}$ , adopted in the *Guide Specifications* was determined following work done by Desroches & Fenves as described in Chapter 6.

### 8.2.5.2 Minimum Force and Displacement Design for Single-Span

Requirements for single-span bridges are not as rigorous as for multi-span bridges because of their generally favorable response to seismic loads in past earthquakes. As a result, single-span bridges need not be analyzed for seismic loads regardless of the Zone or SDC, and design requirements are limited to minimum support lengths and connection forces. Adequate support lengths are required in both the transverse and longitudinal directions, if not restrained. Connection forces are based on the premise that the bridge is stiff and that the fundamental period of response will be short; thus the bridge is assumed to move in-phase with the ground with little or no dynamic amplification. The reduced requirements are also based on the assumption that there are no vulnerable substructures (i.e., no columns) and that a rigid (or near-rigid) superstructure is in place to distribute the in-plane loads to the abutments.

Single-span bridges are treated alike regardless of their Zone/SDC and are treated alike in both specifications. For single-span bridges a minimum design connection force in the restrained directions between the superstructure and the substructure should be at least as large as the product of the Site Factor,  $F_{pga}$ , the acceleration coefficient,  $A_s$ , the peak ground acceleration coefficient for Site Class B and the tributary permanent load. As an example, consider the bridge shown in Figure 8-4. In this example, the two ends of the bridge are restrained transversely, and the tributary seismic load would be the permanent vertical reactions at each end. In the longitudinal direction a fixed bearing is assumed in this example at the left end with a sliding bearing at the right end. Under this condition the tributary seismic load at the left end would be the entire bridge permanent load. At the right end, the seismic design force would be zero. The design of the connections for the specified forces should be carried through the structure sufficiently to ensure adequate load path. Furthermore, if a single-span bridge is indeed a frame, as in the case of tall integral abutments, the seismic analysis may be foregone, but the design of the walls for the appropriate forces must still be completed.

Minimum support lengths,  $N$ , as given in the specifications should be used. Support lengths at expansion bearings of multi-span bridges must comply with the minimum support lengths unless STUs, SRMDs or dampers are provided in order to control the superstructure movements and reduce the seat requirements.

Because a demand analysis is not required, for SDC D the support length should be calculated as 150 percent of the empirical support length.

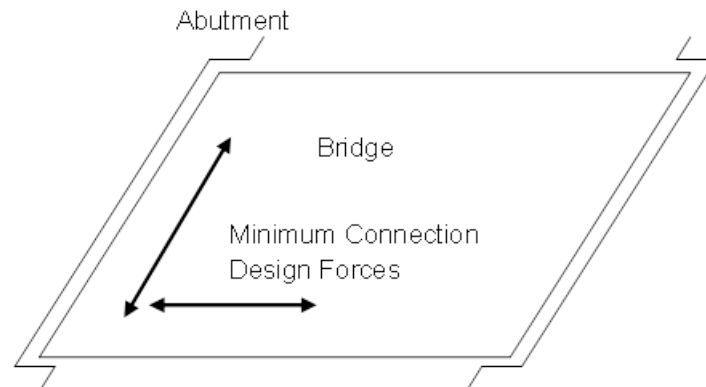


Figure 8-4 Single-Span Bridge – Minimum Design Forces

### 8.2.5.3 Bridges in Seismic Zone 1 and SDC A

Bridges in Seismic Zone 1 and SDC A each have acceleration coefficients,  $S_{D1} \leq 0.15$ . For bridges on sites in Zones/SDC where the acceleration coefficient is less than 0.05, the horizontal design connection force in the restrained directions must be at least 0.15 times the vertical reaction due to the tributary permanent load and the tributary live loads assumed to be present during an earthquake as shown in Figure 8-5.

For all other sites in Zone 1 or SDC A, the horizontal design connection force in the restrained directions must be at least 0.25 times the vertical reaction due to the tributary permanent load and the tributary live loads assumed to exist during an earthquake, as shown in Figure 8-6.

The provisions of Seismic Zone 1 are used as minimum requirements in lieu of more rigorous analysis. The division of Zone 1 at an acceleration coefficient 0.05 for sites with favorable soil condition is an arbitrary expedience intended to provide some relief to parts of the country with very low seismicity. The magnitude of live load assumed to exist at the time of the earthquake,  $\gamma_{eq}$ , should be consistent with the value of  $\gamma_{eq}$  used in conjunction with Table 8-4.

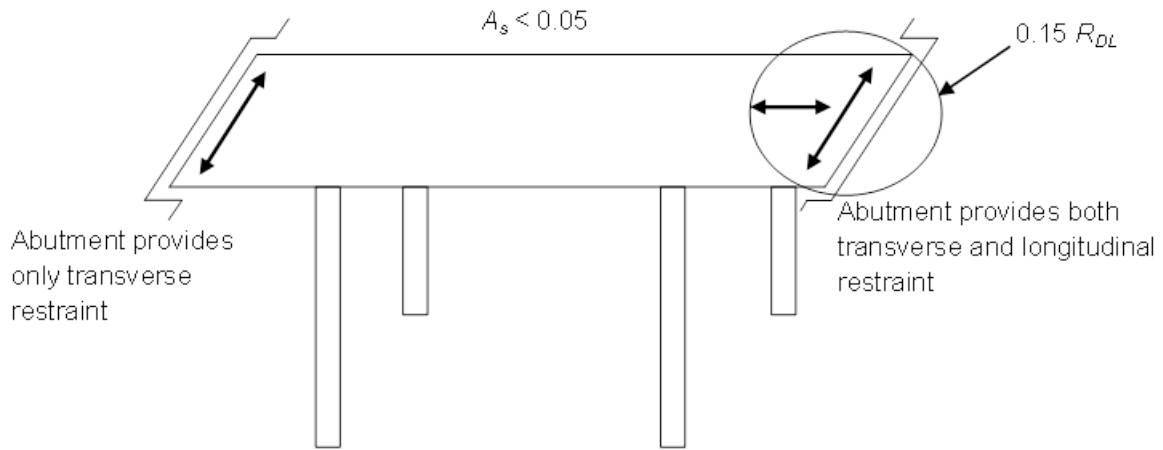


Figure 8-5 Zone 1 and SDC A – Design Forces for Acceleration Coefficient  $A_s < 0.05$

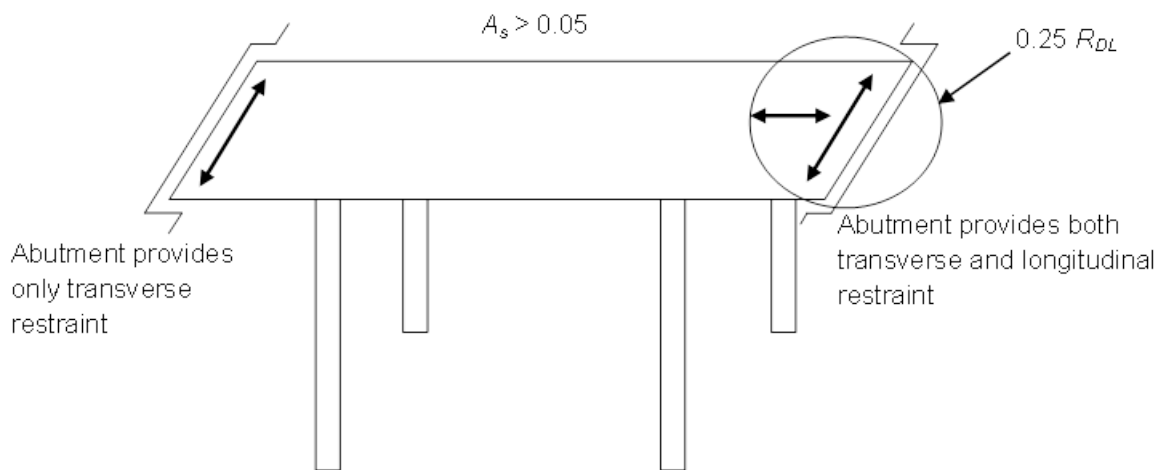


Figure 8-6 Zone 1 and SDC A – Design Forces for Acceleration Coefficient  $A_s \geq 0.05$

Each bearing and its connection to the masonry and sole plates are designed to resist the same horizontal seismic design forces transmitted through the bearing as those calculated above.

For each uninterrupted segment of a superstructure, the tributary permanent load at the line of fixed bearings, used to determine the longitudinal connection design force, is the total permanent load of the segment. If each bearing supporting an uninterrupted segment or simply supported span is restrained in the transverse direction, the tributary permanent load used to determine the connection design force is the permanent load reaction at that bearing. Elastomeric bearings supporting a continuous segment or simply supported span do not provide any significant restraint due to the flexibility of the bearings.

### **8.2.6 Liquefaction**

The requirements for liquefaction assessment and preliminary guidance for mitigation of liquefaction effects is common to both specifications. More detail on this topic is included in earlier chapters of this document and in the companion course, 130094 “LRFD Seismic Analysis and Design of Transportation Structures, Features and Foundations”.

### **8.2.7 Capacity Protection**

Capacity protection begins with the selection of those components that will provide either yielding (plastic hinging) or some other form of energy dissipation. The methodology used in performing the design on the ductile elements (i.e. columns) has significant consequence on the capacity protected elements. The methodologies are somewhat different in the *LRFD Specifications* and the *Guide Specifications*, one being a FBM and the other a DBM, and are covered in detail in Article 8.3.6 for the *LRFD Specifications* and Article 8.4.6 for the *Guide Specifications*.

#### **8.2.7.1 Overstrength Forces**

There are two simplified procedures used to determine the overstrength forces associated with the plastic hinging. One method is applicable to a single column pier, a pier wall in the longitudinal direction or an applicable multi-column bent in the longitudinal direction. A second method is used for a multi-column bent in the transverse direction where overturning axial forces can significantly alter the flexural yielding behavior. These methods are covered in Chapter 6 of this Manual. While both specifications recognize

the use of overstrength forces, they differ in the parameters and factors used in determining the section flexural capacity of the ductile member, which is typically a column.

Following the *LRFD Specifications* the column overstrength factor for reinforced concrete columns is 1.3 and 1.25 for structural steel columns. The use of the factors 1.3 and 1.25 is associated with nominal flexural resistance (strength) established based on procedures outlined in the Specifications. All loads acting on the capacity protected member should be considered when determining the factored nominal capacity of the member. For example, the axial demands (including tension in columns or uplift in piles) imparted on a bent cap beam or footing due to the lateral overturning demands should be considered when calculating a cap beam's or footing's nominal capacity. Typically, the design forces in the capacity protected member resulting from the overstrength plastic hinge capacity and other demands are taken at the face of the column.

Following the *Guide Specifications* an overstrength magnifier,  $\lambda_{mo}$ , is applied to the plastic moment capacity of the inelastic member such that:

$$M_{po} = \lambda_{mo} M_p \quad 8-2$$

where:

- $M_p$  = idealized plastic moment capacity of reinforced concrete member based on expected material properties (kip-ft) (See Chapter 6 for expected property definitions.)
- $M_{po}$  = overstrength plastic moment capacity (kip-ft)
- $\lambda_{mo}$  = overstrength magnifier
  - = 1.2 for ASTM A 706 Grade 60 reinforcement
  - = 1.4 for ASTM A 615 Grade 60 reinforcement

The overstrength magnifier,  $\lambda_{mo}$ , accounts for:

- Material strength variations between the column and adjacent members (e.g., superstructure, bent cap, footings, oversized pile shafts), and
- Column moment capacities greater than the idealized plastic moment capacity.

Capacity protected members such as footings, bent caps, oversized pile shafts, joints, and integral superstructure elements that are adjacent to the plastic hinge locations are designed to remain essentially elastic when the plastic hinge reaches its overstrength moment capacity,  $M_{po}$ . The expected nominal capacity,  $M_{ne}$ , is used in establishing the required capacity of members remaining “essentially elastic” (behavior limit state of members that must resist the overstrength effects of the inelastic members), and such capacity should be determined based on a strain compatibility analysis using a  $M-\phi$  diagram as illustrated in Chapter 6. The expected nominal moment capacity,  $M_{ne}$ , for essentially elastic response is based on the expected concrete and reinforcing steel strengths when the concrete strain reaches a magnitude of 0.003.

### 8.2.8 Capacity Protected Elements

Based on the bridge damage caused by earthquakes and the deficiencies in the design that have been correlated to the damage, current design and detailing requirements have been established to prevent catastrophic damage in future earthquakes. This section focuses on explaining the *LRFD Specifications* and *Guide Specifications* design of the key components that are part of the load path and must be capacity protected to carry the superstructure loads to the foundation. The components that are included in the seismic load path include:

1. Columns and wall piers
2. Superstructures
3. Footings and Piles

The components listed above may be separated into two groups: 1) the columns are normally thought of as ductile yielding components and 2) superstructures and foundations are normally thought of as capacity protected components. Certain features, shear for example, of columns and wall piers must be thought of as capacity protected elements, even though the columns (or walls) are also part of the yielding system. Except for the lower seismic zones, each of these components require special detailing to function either as a yielding element or a capacity protected member participating in the load path.

### 8.2.8.1 Columns and Piers

To ensure that the ductile inelastic flexural response is achieved, it is essential that non-ductile failure modes are inhibited. For example, if the demand shear force associated with the plastic hinging (and particularly overstrength plastic hinging) is not adequately resisted, then a sudden brittle failure of the column is likely. This type of failure is unacceptable. The requirements of each of the two specifications are discussed in their respective sections, but with regard to this issue they are similar.

Transverse reinforcement requirements are specified separately inside the plastic hinge region and outside the plastic hinge (i.e., elastic) region of a column or pier that are designed for plastic hinging in the end regions. The spacing is either prescribed as maximum dimensions or calculated based on the shear demand, the concrete contribution to the shear capacity, and the steel contribution to the shear capacity. The reasons for more stringent requirements for reinforcement near the ends of members is the potential loss of shear capacity due to inelastic action, as described in Chapter 7, and the need to confine the flexural plastic hinging zone.

### 8.2.8.2 Superstructures

Following the *LRFD Specifications* or *Guide Specifications*, the superstructure is intended to be capacity protected, due to its relatively higher stiffness and the fact that post-earthquake repair may be extensive, expensive, and difficult. Typically, the procedures to ensure capacity protection in the *Guide Specifications* are structure-specific as they relate to various types of superstructures. Because inelastic action is to be prevented in the superstructure, its design does not require consideration of inelastic cyclic behavior. This is significant because it is typically challenging to instill inelastic cyclic ductility capacity in most common superstructures. This is a major advantage of the capacity design concept.

Following the *LRFD Specifications* or *Guide Specifications*, the design of non-integral cap beams in the transverse direction is similar between the two documents with the exception of the magnitude of forces impacted by different over-strength factors in both specifications. For capacity protection in the longitudinal direction, the superstructure design is treated separately in the *Guide Specifications* for integral and non-integral bent caps.

### 8.2.8.3 Foundations

Following the *LRFD Specifications* or *Guide Specifications*, footings are designed as capacity protected members based on the overstrength loading induced by the column. Using the *LRFD Specifications* loading of the footing is considered along a diagonal plan direction, in addition to the main orthogonal directions of the footing. According to the *Guide Specifications* the only loading directions considered are the principal directions in the plane of the pier and normal to the plane of the pier. Additionally, the load path from the column to the piles under seismic loading must be considered and is treated based on the size of the piles and the type of soil.

Typically when smaller driven piles (18-in. or less) are used in soil, they are treated as axial-only components regardless of the type of connection to the pile cap. In such a case, the moment generated at top of the pile is ignored and the pile cap is designed as a member subject to a linear distribution of axial forces from the pile group. This simplification also requires a minimum depth of cap relative to the cap's length from the face of column. For footings situated in softer soil, a smaller pile subject to lateral displacement may not have sufficient lateral strength or displacement capacity. In this case, larger piles would be used to address the strength and displacement demands. For a pile cap connecting larger piles, designs should be based on capacity protection principles and would account for the larger moments induced at the tops of the piles.

When pile foundations are subject to liquefaction or lateral spreading ground movements, plastic hinging is permitted in the piles according to the *Guide Specifications*, but only if a displacement capacity check is performed following procedures similar to those used to check columns. Furthermore, column to pile-cap monolithic connection joint shear is explicitly evaluated according to the *Guide Specifications* taking into account the rigidity effect of the cap and the moment transfer distribution in the orthogonal directions of the column cross section.

## 8.3 AASHTO LRFD SPECIFICATIONS

The AASHTO *LRFD Specifications* uses the Force-Based Method, as previously discussed. This approach has become a well-accepted procedure which enjoys a wide range of acceptance by the engineering community for the seismic design of bridges. Using this approach, the strength is first determined using calculated elastic seismic forces which are subsequently reduced by force-reduction

factors for design. These reduction factors coupled with prescriptive confinement detailing to ensure adequate ductility are the basis for this procedure. This section includes a description of this procedure and details on its application. The description includes the same outline as that used in Section 8.2 covering the common features of the two specifications.

### **8.3.1 Determine Seismic Input**

The determination of the seismic input is covered in Chapter 2.

### **8.3.2 Establish Design Procedures**

The establishment of design procedures in many respects is the same for both specifications with the exception of performance levels covered in the *LRFD Specifications*. The differences, which are minor, are covered in Section 8.2.2 which describes the common features of the two specifications.

### **8.3.3 Identify the Earthquake Resisting System and Global Design Strategy**

These concepts are included in the *Guide Specifications* and are presented in more detail in Chapter 4.

### **8.3.4 Demand Analysis**

The use of a demand analysis is common to both of the specifications and is covered in more detail in Section 8.2.4. The common features include: 1) Loading, 2) Directional combinations, and 3) Modeling for a selected design strategy. There is however one difference in how the *LRFD Specifications* address live loads and this is described in more detail below.

Live load coincident with an earthquake,  $\gamma_{EQ}$ , is considered on a project specific basis. Live load is typically considered only for critical and essential bridges. However, some agencies have implemented a conservative approach of requiring partial live load concurrent with earthquake loading, where traffic congestion is common.

Although the earthquake limit state includes water loads, *WA*, the effects due to *WA* are considerably less significant than the effects on the structure stability due to degradation. Therefore, unless specific site conditions dictate otherwise, local pier scour and contraction scour depths should not be included in the seismic design. However, the effects due to degradation of the channel should be considered.

### **8.3.5 Design and Check the Earthquake Resisting Elements**

The design of the Earthquake Resisting Elements (ERE) includes selection of a sufficiently strong and ductile member, typically a column, which can safely endure the displacements estimated to be imposed by the design earthquake. The *LFRD Specifications* rely on *R* factors to ensure this minimum strength, and the Guide Specifications directly provide a minimum lateral resistance. Additionally, the ERE must be detailed such that the system has adequate ductility. Both specifications provide significant provisions regarding detailing of substructure elements to ensure adequate ductility. The provisions are not identical, but they do provide consistent results within the design methodology employed for the given specification (e.g. FBM or DBM).

### **8.3.6 Design Procedures Using Response Modification Factors**

In general, the *LFRD Specifications* use Response Modification Factors, *R* factors, to determine the design forces for establishing the requisite forces for selecting reinforcement or checking section adequacy for earthquake loading.

### **8.3.7 Bridges in Seismic Zone 2**

Bridges in this zone have acceleration coefficients, in the range  $0.15 < S_{DI} \leq 0.30$ . In Zone 2, a seismic demand analysis is required. The applicable analysis procedures are described in Section 5 of this Reference Manual. Except for foundations, seismic design forces for all components, including pile bents and retaining walls, are determined by dividing the elastic seismic forces after the directional combination, by the appropriate response modification factor, *R*, specified in Table 8-7.

The directional combination will typically result in two load cases, where each direction is dominant in one load case. These forces are combined with the permanent loads and any live load required to be

considered, and from this combination, the strength of the component is determined. A resistance factor is included to determine the required strength.

Seismic design forces for foundations, other than pile bents and retaining walls, are determined by dividing elastic seismic forces, by half of the response modification factor, R, from Table 8-8 and applied as shown in Figure 8-7, for the substructure component to which it is attached. This reduction in the R factor for the foundations is intended to provide added strength to the foundation thereby forcing the plastic hinging to occur in the ductile column. The value of R/2 should not be taken as less than 1.0.

**TABLE 8-7 RESPONSE MODIFICATION FACTORS – SUBSTRUCTURES  
(LRFD SPECIFICATIONS TABLE 3.10.7.1-1)**

Substructure	Importance Category		
	Critical	Essential	Other
Wall-type piers - large dimension	1.5	1.5	2.0
Reinforced concrete pile bents			
• Vertical piles only	1.5	2.0	3.0
• With batter piles	1.5	1.5	2.0
Single Columns	1.5	2.0	3.0
Steel or composite steel and concrete pile bents			
• Vertical piles only	1.5	3.5	5.0
• With batter piles	1.5	2.0	3.0
Multiple column bents	1.5	3.5	5.0

**TABLE 8-8 RESPONSE MODIFICATION FACTORS – CONNECTIONS  
(LRFD SPECIFICATIONS TABLE 3.10.7.1-2)**

Connection	All Importance Categories
Superstructure to abutment	0.8
Expansion joints within a span of the superstructure	0.8
Columns, piers, or pile bents to cap beam or superstructure	1.0
Columns or piers to foundations	1.0

As described in the *LRFD Specifications* for Seismic Zone 2, the design forces for foundations, which include the footings, pile caps and piles, are as depicted in Figure 8-7. The design forces are essentially twice the seismic design forces of the columns. This is generally conservative and was adopted to simplify the design procedure for bridges in Zone 2. However, if seismic forces do not govern the design of columns and piers, there is a possibility that during an earthquake the foundations will be subjected to forces larger than the design forces. For example, this may occur due to unintended column overstrength that may exceed the capacity of the foundations. An estimate of this effect may be found by using a resistance factor,  $\phi$ , of 1.3 for reinforced concrete columns and 1.25 for structural steel columns. It is also possible that even in cases when seismic loads govern the column design, that columns may have insufficient shear strength to enable a ductile flexural mechanism to develop, but instead allow a brittle shear failure to occur. Again, this situation is due to potential overstrength in the flexural capacity of columns and can sometimes be prevented by arbitrarily increasing the column design shear by the overstrength factor cited above.

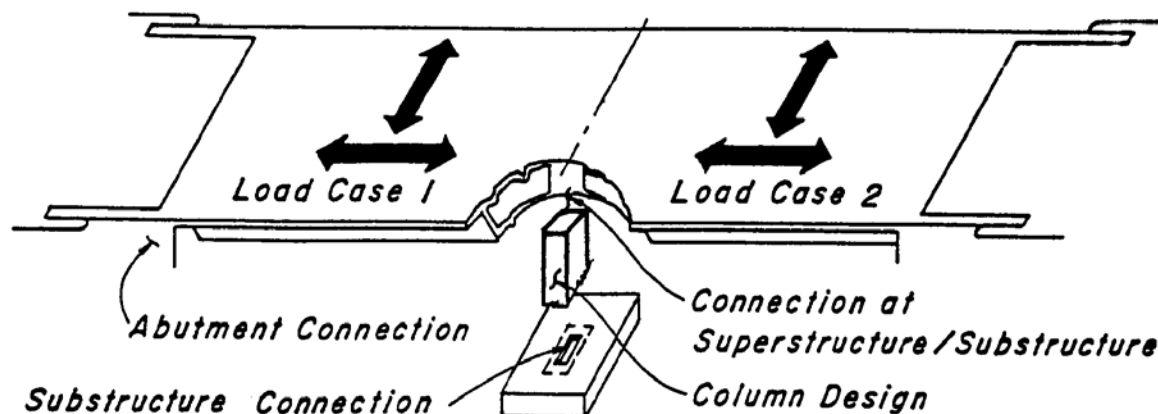


Figure 8-7 Zone 2 – Seismic Design Forces

The seismic design forces at the abutment connections as shown in Figure 8-7 are designed using a “R” Factor of 0.8. The connection at the superstructure/substructure interface is designed using a “R” Factor of 1.0.

Conservatism in the design, and in some cases under-design, of foundations and columns in Zone 2 based on the simplified procedure of this article has been widely debated. In light of the above discussion, it is recommended that for critical or essential bridges in Zone 2 consideration should be given to the use of

the forces as described above in this section applicable to foundations in Zone 3 and Zone 4. Ultimate soil and pile strengths are to be used with the specified foundation seismic design forces.

#### **8.3.7.1 Bridges in Seismic Zones 3 and 4**

Structures in Seismic Zone 3 having an acceleration coefficient  $0.30 < S_{DI} \leq 0.50$  and Seismic Zone 4 having an acceleration coefficient  $0.50 < S_{DI}$  are analyzed according to the minimum requirements as described in Chapter 5 of this Manual.

The design forces, called Modified Design Forces, in a column, pile bent, or wall in weak direction are obtained using  $R$ , Response Modification Factors, from Table 8-7, which are the same factors used for Zone 2. In general, the column seismic moments are developed for the directional combination (100/30 rule), and then they are divided by the  $R$  factor before being combined with the non-seismic permanent loads or any live load effects. These internal forces will be less than the full unreduced elastic forces, thus implying that yielding to some degree will occur in the column under the action of the design earthquake. The column flexural strength is then selected based on these Modified Design Forces.

The design axial forces which control both the flexural design of the column and the shear design requirements are either the maximum or minimum of the unreduced design forces or the values corresponding to plastic hinging of the columns. In most cases, the values of axial load and shear corresponding to plastic hinging of the columns will be lower than the unreduced design forces. The design shear forces are specified so that the possibility of a shear failure in the column is minimized.

From the actual strength selected for the columns, Inelastic Hinging Forces are then calculated. The inelastic forces are intended to be the internal column forces resulting from the development of the overstrength plastic hinging moments in the columns AND the formation of a full plastic mechanism. The assessment of this condition comprises a partial pushover analysis where only the maximum lateral forces are determined, but no displacement information is generated. The *LRFD Specifications* include detailed procedures for the conduct of this partial pushover analysis in Articles 3.10.9.4.3 for both single and multiple-column bents. Accordingly, the procedure is not repeated here.

In some cases, the inelastic plastic hinging forces may exceed the unreduced elastic forces determined from the demand analysis. In such cases, the elastic forces may be used for the capacity protection

design, but generally this is not recommended because the maximum forces in the system have not been identified. For example, in the cases of architecturally oversized columns, columns controlled by non-seismic loadings, such as wind, or columns that are stronger than necessary for whatever reason the forces from an inelastic hinging analysis may exceed the elastic forces. While the *LRFD Specifications* permit the use of the elastic forces in lieu of the inelastic hinging forces, the designer should undertake such a choice only after considering the ramifications of the choice. If an earthquake of larger magnitude occurs, the column, bent or pier may not be ductile; thus failure in an undesired mode could occur.

To demonstrate in more detail the difference between the applications of the “Modified Design Forces” and the “Inelastic Hinging Forces” consider the two column bent shown in Figure 8-8, Figure 8-9, and Figure 8-10. As shown in Figure 8-8, the left column designated Modified Design Forces will be designed using the forces as indicated at the bottom of the column and the column on the right designated Inelastic Hinging Forces will also be designed using the forces at the bottom of the column. As shown on the left column, the elastic moments,  $M_E$ , are reduced by  $R$  for the flexural design. The elastic shear forces,  $V_E$ , are however used for the shear design (i.e., no reduction for the inelastic hinging of the column). The shear forces on the right column,  $V_{PH}$ , correspond to the inelastic hinging force  $M_E/R$  with an overstrength factor of 1.3 applied to the inelastic hinging capacity to prevent a shear failure from occurring. Note that the left column must be designed for the elastic shear and the right column is designed for the plastic shear which is typically much smaller than the elastic shear.

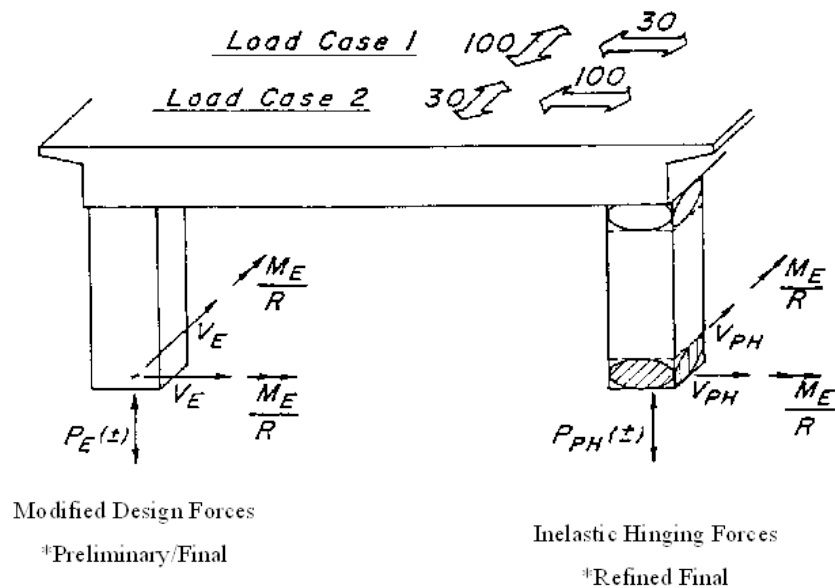


Figure 8-8 Zone 3 and 4 – Column Design Forces for the Application of the Modified Design Forces and the Inelastic Hinging Forces

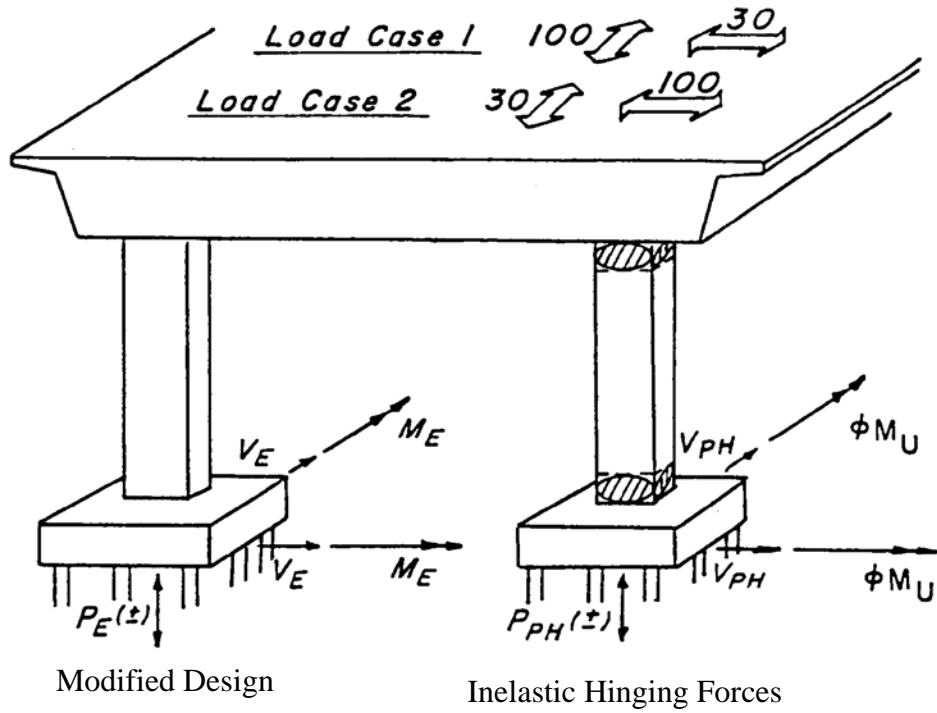


Figure 8-9 Zone 3 and 4 – Footing Design Forces for the Application of the Modified Design Forces and the Inelastic Hinging Forces

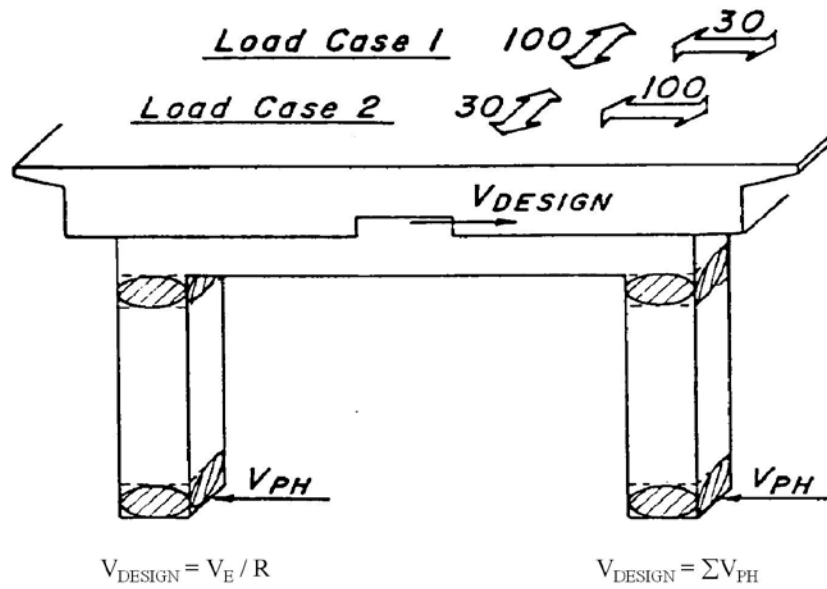


Figure 8-10 Zone 3 and 4 – Design Forces for Connections

### 8.3.7.2 Show Forces and Displacements of Overall System Acceptable

With the *LRFD Specifications* FBM, the design forces are determined from the Modified Design Forces utilizing the *R* factor. A resistance factor for flexure of 0.9 is also applied. Forces are shown to be adequate when sufficient reinforcing steel or sectional strength has been provided.

With the completion of the check for adequate flexural and axial loads the column design for confinement can be made. This check ensures that sufficient confinement exists to supply adequate ductility (post-yield deformability) so that the columns or weak axis wall can survive the inelastic deformations implied with the use of the *R*-factor. Recall the relationship between *R*-factor, displacement capacity and confinement detailing requirements described at the beginning of this chapter. In the plastic hinge regions, at the top and bottom of the column as defined in Article 5.10.114.1d “Transverse Reinforcement for Confinement at Plastic Hinges,” must satisfy either the following equations for circular equations.

$$\rho_s \geq 0.12 \frac{f'_c}{f_y} \quad 8-3$$

where:

$f'_c$  = specified compressive strength of concrete at 28 days, unless another age is specified (ksi)

$f_y$  = yield strength of reinforcing bars (ksi)

or the similar equation for rectangular sections.

$$\rho_s \geq 0.45 \left( \frac{A_g}{A_c} - 1 \right) \frac{f'_c}{f_{yh}} \quad 8-4$$

Within the plastic hinge zones, there are specific requirements for detailing of cross ties, restriction of longitudinal splice locations, bar spacing, and other prescriptive limits that have been shown in the laboratory to provide adequate ductility. Splices in reinforcement must be made by full-welded splices of weldable reinforcing or by full-mechanical connections capable of developing the full tensile strength of the bars. In general, splices in the plastic hinge zone should be avoided. The transverse reinforcement serves as a means to ensure that the axial load carried by the column after spalling of the concrete cover

will be at least equal to the load before spalling and to ensure that buckling of the longitudinal reinforcement is prevented.

The appropriate  $R$  is used for both orthogonal axes of the substructure component. Accordingly, the multi-column bent  $R$  factor is used in both directions. A wall-type concrete pier may be analyzed as a single column in the weak direction if all the provisions for columns, as specified in Section 5 of the *LFRD Specifications*, are satisfied. Wall-type piers may be treated as wide columns in the strong direction provided the appropriate  $R$  factor in this direction is used.

In addition to providing deformability by providing adequate confinement, bridges subject to earthquake ground motion may be susceptible to instability due to  $P-\Delta$  effects. Inadequate strength can result in accumulation of structural displacements in one direction causing excessive ductility demand on plastic hinges in the columns, large residual lateral deformations, and possibly collapse. The lateral resistance of a column is therefore limited to control the additional displacements that  $P-\Delta$  effects can impose, so that such effects will not significantly affect the response of the bridge during an earthquake.

$P-\Delta$  effects lead to a loss of stiffness and loss in strength once yielding occurs in the columns of a bridge. In severe cases, this can result in the force-displacement relationship having a negative slope once a plastic mechanism is fully developed. The value for  $\Delta$  given by Equation 8-5 is such that this reduction in strength is limited to 25 percent of the yield strength of the pier or bent.

An explicit  $P-\Delta$  check was not required in the previous edition of these Specifications but has been introduced herein because two conservative provisions have been relaxed in this revised edition. These are:

- The shape of the response spectrum (Figure 3.10.4.1-1) has been changed from being proportional to  $1/T^{2/3}$  to  $1/T$ . The reason for the  $1/T^{2/3}$  provision in the previous edition was to give conservative estimates of force and displacement in bridges with longer periods ( $>1.0$  secs) which, in an indirect way, provided for such effects as  $P-\Delta$ . With the change of the spectrum to being proportional to  $1/T$ , an explicit check for  $P-\Delta$  is now required.
- The flexural resistance factor,  $\phi$ , for seismic design of columns with high axial loads has been increased from a minimum value of 0.5 to 0.9 (Article 5.10.11.4.1b). Use of a low resistance factor led to additional strength being provided in heavily loaded columns that could be used to offset

reductions due to  $P-\Delta$ , in the previous edition. The increased value for  $\phi$  now permitted in Section 5 is a second reason for requiring an explicit check for  $P-\Delta$ .

The displacement of any column or pier in the longitudinal or transverse direction must satisfy:

$$\Delta P_u < 0.25\phi M_n \quad 8-5$$

in which:

$$\Delta = R_d \Delta_e \quad 8-6$$

If  $T < 1.25T_s$ , then:

$$R_d = \left(1 - \frac{1}{R}\right) \frac{1.25T_s}{T} + \frac{1}{R} \quad 8-7$$

If  $T \geq 1.25T_s$ , then:

$$R_d = 1 \quad 8-8$$

where:

$\Delta$  = displacement of the point of contraflexure in the column or pier relative to the point of fixity for the foundation (in.)

$\Delta_e$  = displacement calculated from elastic seismic analysis (in.)

$T$  = period of fundamental mode of vibration (sec.)

$T_s$  = reference period specified in Article 3.10.4.2 (sec.)

$R$  =  $R$ -factor specified in Article 3.10.7

$P_u$  = axial load on column or pier (kip)

$\phi$  = flexural resistance factor for column specified in Article 5.10.11.4.1b

$M_n$  = nominal flexural strength of column or pier calculated at the axial load on the column or pier (kip-ft.)

It should be noted that if a full plastic mechanism does not form in the design earthquake, then the resistance used for the  $P-\Delta$  check must be correspondingly reduced. The formula given above assumes that full plasticity in the columns has developed. The displacement used in the check, and the resistance used should be consistent with one another. Also, the adjustment, which is reflected in the  $R_d$  factor, is the adjustment to convert an elastic displacement to an inelastic displacement, as described in Chapter 6.

### 8.3.8 Capacity Protection of the Remaining Elements

#### 8.3.8.1 Strength

The required strength to ensure that inelastic deformations occur only in the designated plastic hinges is based on the potential overstrength resistance of the materials in the plastic hinge region. To account for this it is necessary to determine the maximum feasible moment capacity of the plastic hinge and design the remaining portions for the actions due to those included in the Load Combination for the Extreme Event I. Generally overstrength resistance depends on the following factors.

- The actual size of the column and the actual amount of reinforcing steel.
- The effect of an increased steel strength over the specified  $f_y$  and for strain hardening effects.
- The effect of an increased concrete strength over the specified  $f'_c$  and confinement provided by the transverse steel. Also, with time, concrete will gradually increase in strength.
- The effect of an actual concrete ultimate compressive strain above 0.003.

Column size and actual amount of reinforcing steel may be controlled by design requirements other than the Extreme Event I used for the seismic design. The designer will generally select the minimum column size and steel reinforcement ratio to satisfy the controlling load case. Having designed the column the designer must next consider the over strength properties of the materials within the column.

According to the *LRFD Specifications*, columns are required to be designed biaxially and to be investigated for both the minimum and maximum axial forces. The previous edition of these Specifications reduced the flexural resistance factor from 0.9 to 0.5 as the axial load increased from 0 to  $0.20 f'_c A_g$ , because of the trend toward a reduction in ductility capacity as the axial load increases. This

requirement has been removed in this edition of the *LRFD Specifications*, but a *P-Δ* requirement has been added (Article 4.7.4.5) to limit the demand on ductility capacity due to excessive deflection. Also, the *R*-factors have been maintained at their previous levels (Article 3.10.7) even though the return period of the design earthquake has been increased from 500 to 1,000 years. In both the ATC-49 and NCHRP Task 20-7 (193) provisions, the recommended flexural resistance factor is 1.0. However, since the current Specifications are force-based and do not explicitly calculate the ductility demand, limiting the resistance factor to 0.9 was considered justified in lieu of a more rigorous analysis.

The factored shear force  $V_u$  on each principal axis of each column and pile bent is specified in Article 3.10.9.4. The shear design of end regions (potential plastic hinging zones) of columns and pile bents subjected to ductility demand is performed differently than conventional design outside plastic hinge zones. The main difference following the *LRFD Specifications* or the *Guide Specifications* is the evaluation of the concrete shear contribution  $V_c$  and its applicability within a plastic hinge zone.

Following the *LRFD Specifications*,  $V_c$  is taken based on the Sectional Design Model of Article 5.8.3, provided that the minimum factored axial compression force exceeds  $0.10 f_c' A_g$ . For compression forces less than  $0.10 f_c' A_g$ ,  $V_c$  is taken to decrease linearly from the value given in Article 5.8.3 to zero at zero compression force.

As shown above, the *LRFD Specifications* recognizes a special treatment for shear design of end regions with no account of ductility demands as formulated in the *Guide Specifications*. The shear degradation model with respect to ductility demands used in the *Guide Specifications* is covered in Chapter 7. The model used with the *LRFD Specifications* is much simpler and based solely on the axial load present, and this axial load must consider the effects of overturning.

The end regions defined in the *LRFD Specifications* are assumed to extend from the soffit of girders or cap beams at the top of columns or from the top of foundations at the bottom of columns, a distance taken as the greater of:

- The maximum cross-sectional dimension of the column,
- One-sixth of the clear height of the column, or
- 18.0 in.

The end region at the top of the piles in a pile bent is taken as that specified for columns. At the bottom of the pile bent, the end region is considered to extend from three pile diameters below the calculated point of maximum moment to one pile diameter, but should not extend less than 18.0 in. above the mud line.

### 8.3.8.2 Overstrength Forces

The *LRFD Specifications* use member overstrength factors of 1.3 for reinforced concrete. This accounts of the reinforcing steel generally having yield strengths higher than the minimums specified in the design. Additionally, strain hardening will add to the effect of higher yield strength. When combining these two effects it is reasonable to increase steel strength to  $1.25 f_y$ , in computing the column overstrength. Likewise, the concrete strength used in design is based on the 28-day compressive strength, which is generally lower than that expected in the completed structure. Additionally, concrete will gain strength with age, and the strength may be as high as  $1.5 f'_c$ . The compressive strengths are also increased with better confinement provided by the transverse steel. Strain rate effects that are attributed to the rapid loading during an earthquake also contribute to the added concrete strength. Thus it is reasonable to assume an increase of  $1.5 f'_c$  in the calculation of the column overstrength.

Compressive strains of the confined concrete are higher than the 0.003 used for unconfined concrete. Research has shown that the compressive strains may be as high as 0.01 and higher for confined concrete. Thus a reasonable value to assume for ultimate design is 0.01.

The basic 1.3 factor may be used; but in cases where more precise strength value are desired, increases in member properties as shown in Table 8-9 may be used for increased values in the material properties. Or alternately the methods used in the *Guide Specifications* may be used.

**TABLE 8-9 RECOMMENDED OVERSTRENGTH VALUES FOR MATERIALS PROPERTIES  
(APPENDIX B3, AASHTO, 2007)**

Material Property	Overstrength Material Factor
Increased $f_y$ (minimum)	$1.25 f_y$
Increased $f'_c$	$1.5 f'_c$
Increased $\epsilon_c$	0.01

Establishing the overstrength  $P$ - $M$  relations for a column may be accomplished by either running column interaction calculations using the increased material strengths, increasing both the axial force and moment ordinates by an overstrength factor, or simply increasing the moments by the overstrength factor. In general, the first two approaches are more accurate, but the third approach is generally conservative in the lower axial force ranges (i.e., below the balance point).

Having the column design the next step will be to determine the design forces for the connecting footing as shown in Figure 8-9. Examining the footing for the Modified Design Forces, left column, it is observed that the elastic demand forces are to be used for the design. The Inelastic Hinging Forces shown for the right correspond to the column plastic hinging forces with the shear force being equal to the column design shear  $V_{PH}$  and the moment equal to the column inelastic hinging moment multiplied by the overstrength factor,  $\phi$ . Note that in this case both the shear and moment associated with the inelastic hinging will be substantially less than the elastic demand forces obtained for the left column using the Modified Design Forces, in Figure 8-10.

A third application is shown to illustrate the difference in the shear key and bearing design forces. For the Modified Design Method the elastic demand forces are used and for the inelastic hinging the shear forces  $V_{PH}$  for the columns are used, which again will likely be substantially less than the elastic shear forces.

Summarizing, where inelastic hinging is invoked as a basis for seismic design, the force effects resulting from plastic hinging at the top and/or bottom of the column are calculated after the preliminary design of the columns has been completed utilizing the modified design forces specified as the seismic loads. The forces resulting from plastic hinging are then used for determining design forces for most components as identified herein. The procedures for calculating these forces for single-column and pier supports and bents with two or more columns are taken as specified in the following paragraphs.

Inelastic hinges are designed to form before any other failure due to overstress or instability in the structure and/or in the foundation. Inelastic hinges are typically only permitted at locations in columns where they can be readily inspected and/or repaired.

Superstructure and substructure components and their connections to columns are also designed to resist a lateral shear force from the column determined from the factored inelastic flexural resistance of the column using the resistance factors specified herein. These consequential shear forces, calculated on the

basis of inelastic hinging, may be taken as the extreme seismic forces that the bridge is capable of developing.

### **8.3.8.3 Wall Pier Design Forces**

A wall pier, or pier wall as they are also called, is defined as a column with an aspect ratio of less than 2.5 in its strong direction. This means that the height is less than 2.5 times the width. The design forces are those determined for Extreme Event Limit State Load Combination I, except where the wall pier is designed as a column in its weak direction. If the pier is designed as a column, the design forces in the weak direction are all the design requirements for columns. When the forces due to plastic hinging are used in the weak direction, the combination of forces, are applied to determine the elastic moment which is then reduced by the appropriate  $R$ .

The design forces for piers are based on the assumption that a pier has low ductility capacity and no redundancy. As a result, a low  $R$  value of 2 is used in determining the reduced design forces, and only a small amount of inelastic deformation should occur in the pier when subjected to the forces of the design earthquake. If a pier is designed as a column in its weak direction, then both the design forces and, more importantly, the design requirements for columns are applicable.

### **8.3.8.4 Foundation Design Forces**

The design forces for foundations including footings, pile caps and piles may be taken as either those forces determined for the Extreme Event Load Combination I or the forces at the bottom of the columns corresponding to column plastic hinging as described earlier.

When the columns of a bent have a common footing, the final force distribution at the base of the columns after determining the plastic overstrength forces may be used for the design of the footing in the plane of the bent. This force distribution produces lower shear forces and moments on the footing because one exterior column may be in tension and the other in compression due to the seismic overturning moment. This effectively increases the ultimate moments and shear forces on one column and reduces them on the other.

The foundation design forces specified are consistent with the design philosophy of minimizing damage that would not be readily detectable. The recommended design forces are the maximum forces that can be transmitted to the footing by plastic hinging of the column. The alternate design forces are the elastic design forces. It should be noted that these may be somewhat greater than the recommended design forces, although where architectural considerations govern the design of a column, the alternate elastic design forces may be less than the forces resulting from column plastic hinging.

In general, foundation design will use the methods outlined in Chapter 7. The distribution of forces in the foundations is often highly dependent on the surrounding soil conditions. Therefore, variability in the resisting soil conditions should be considered, and bounding analyses are often prudent to ensure the design is realistic and conservative.

#### **8.4 AASHTO LRFD GUIDE SPECIFICATIONS**

Although somewhat transparent to the bridge designer, the AASHTO *Guide Specifications* are a significant departure from the previous provisions. The 1000-year return period was developed as part of this effort, and as mentioned above it, was also adopted for the AASHTO *LRFD Specifications*. The primary change, as shown above, in the seismic design provision is the change from a Force-Based Methodology to a Displacement-Based Methodology. This change is basically the fourth component in seismic design which deals with designing a bridge that is sufficiently ductile that it can withstand large earthquakes with limited and controlled damage, but without collapse or threat to life safety.

In both methods, elastic demands are determined for a bridge that has already been designed for normal service load conditions (i.e. dead load, live load, temperature etc.). Having designed a structure that is adequate for service load conditions, the bridge must be designed to (or at least checked for its ability to resist) an extreme loading condition, based on earthquake loading.

In the DBM, the “*R*” Response Modification Factor, for the ductile concrete column components, has been replaced by an evaluation of the displacement capacity using the combined behavior of strain capacities of the steel and concrete materials, as outlined in Chapter 6 and 7. This initially involves conducting a sectional analysis to obtain the component moment - curvature relationship and a subsequent pushover analysis to obtain the displacement capacity. The displacement capacity is compared to the seismic demand to evaluate the ability of the component to resist the earthquake event. The displacement

capacities for Seismic Design Categories (SDC) B and C may be obtained using implicit formulas to simplify the capacity determination. The implicit formulas were derived using a combination of physical laboratory tests of reinforced concrete columns and parametric studies performed for a group of columns using the sectional and pushover analysis, as described above.

The *Guide Specifications* provide guidance in selecting an overall seismic design strategy, system and elements that are conventionally used and accepted by owners to produce a bridge that will transmit the inertial loads to the foundation without undue damage. Included also in the *Guide Specifications* are:

1. Recommendations on improved modeling soil-structure interactions at abutments and foundations
2. Recommendations on modeling the superstructure and substructure components
3. Recommendations on abutment and foundation design
4. Liquefaction design requirements
5. Design requirements for structural steel components
6. Design requirements for concrete components

As illustrated in

Figure 8-1 and Figure 8-2, the FBM has a one-size-fits-all approach to setting the permissible demand level. Thus for detailing, a similar worst-case one-size-fits-all approach to providing transverse steel is also required. In the *Guide Specifications* with the lower permissible demand levels in the lower SDCs, more liberal transverse steel and detailing requirements are used. In the highest SDC D, a direct quantitative link is provided between transverse steel and permissible demand displacements. Thus, higher demands can be permitted, but only at the added expense of more transverse steel.

#### **8.4.1 Determine Seismic Input**

The determination of the seismic input is common to both specifications, as described earlier.

The design spectra obtained using these procedures are for a uniform hazard as described in Chapter 2. The design response spectrum is for single-degree-of-freedom systems with 5 percent damping.

If additional damping is justified, and this is permitted in the *Guide Specifications*, the damping percent,  $\xi$ , may be increased using the expression for,  $R_D$ , as given in the *Guide Specifications*. This approach is

similar to that used with the Capacity Spectrum Method, and in particular, with seismic isolation, which is covered in a later chapter.

The permitted use of higher damping is contingent upon the use of the soil behind the abutments acting to dissipate energy and limit the overall displacement response of the bridge. Accordingly, the following characteristics must be present in order to justify the use of higher damping, if specific structural damping elements are not used:

- Total bridge length must be less than 300 ft,
- Abutments are designed for sustained soil mobilization,
- Supports are normal or slight skew (less than 20°), and
- The superstructure is continuous without hinges or expansion joints or a reliable load path to the abutments is demonstrated.

#### **8.4.2 Establish Design Procedures**

The establishment of design procedures in many respects is the same for both specifications with the exception of performance levels covered in the *LRFD Specifications*. The differences are covered in Section 8.2.2 and discussed in that section.

#### **8.4.3 Identify the Earthquake Resisting System and Global Design Strategy**

The identification and purpose of the ERS, ERE, and Global Design Strategy are covered in Chapter 4.

##### **8.4.3.1 Seismic Design Categories**

Seismic Design Categories (SDC) were established to reflect the variation in seismic risk across the United States. Recognizing the level of effort required to design for the most severe earthquake regions should not be the same as that in the lower regions, four SDC have been defined. The categories permit variations in the methods of analysis for demand and capacity, minimum support lengths, structural detailing requirements, defining a loading path and earthquake resisting system, foundation and abutment

design requirements, consideration for liquefaction effects, and capacity protection in accordance with seismic risk for the bridge site. A summary checklist of the design requirements for each SDC is provided in Table 8-10.

**TABLE 8-10 REQUIREMENTS BY SEISMIC DESIGN CATEGORY**

Requirements	A	B	C	D
Global Strategy	-----	Recommended	Required	Required
Identification ERS	-----	Recommended	Required	Required
Support Connections	Required	Required	Required	Required
Support Length	Required	Required	Required	Required
Demand Analysis	-----	Required	Required	Required
Implicit Capacity	-----	Required	Required	-----
Push Over Capacity	-----	-----	-----	Required
Detailing – Ductility	-----	SDC B	SDC C	SDC D
Capacity Protection	-----	Recommended	Required	Required
P-Δ Effect	-----	-----	Required	Required
Minimum Lateral Strength	-----	Required	Required	Required
Liquefaction	-----	Recommended	Required	Required

#### **8.4.3.1.1 Partitioning**

The design spectral value  $S_{D1}$  was selected for the partitioning in accordance with the values shown in Table 8.4-1. The design spectral value includes the effects of the soils at the site and the effects of the bridge responding to its modes of vibration. Using the modes of vibration for the shorter periods down to the zero period yields high forces not reflective of a bridge responding to an earthquake as observed from the damage in past earthquakes. Partitioning using the spectral design values at one second is also consistent with a displacement-based approach.

#### **8.4.3.2 Earthquake Resisting Elements and Systems**

The Earthquake Resisting Elements (ERE) and Systems (ERS), along with Global Design Strategies are presented in Chapter 4.

#### **8.4.4 Demand Analysis**

A global model that captures the response of the entire bridge system should be developed. A global model for bridge systems with irregular geometry, in particular curved bridges and skew bridges, should have the actual geometry included. Also, multiple transverse expansion joints, massive substructures components, and foundations supported by soft soil can exhibit dynamic response characteristics that should be included in the models because their effects on the global response is not necessarily obvious and may not be captured by a separate subsystem analysis.

Individual bridge components must have displacement capacities that are greater than the displacement demands derived from the “global” analysis. The displacement demands of a bridge system consisting of multiple simple spans may be derived using the equivalent static analysis outlined in Article 5.4.2. Global analysis requirements as specified in Article 5.1.2 need not to be applied in this case.

For long bridges, creating a finite element model for the entire length of long bridges may not be warranted and, in some cases produces questionable results, especially because out-of-phase movement is expected in long bridges. Dynamic multimodal analysis is based on equal input motions at each of the support points. Therefore, it is recommended that the bridge model not exceed five frames in length with the addition of boundary frames and/or an abutment. Each multi-frame analytical model should be overlapped by at least one useable frame from each model as shown in Figure 8-11. This is a recommendation only, and the designer should evaluate each case individually based on the configuration of the particular bridge being analyzed. It is very difficult to develop one-size-fits-all recommendations for analyzing complex structures.

##### **8.4.4.1 Model of Selected Design Strategy**

According to the *Guide Specifications*, the analytical model is a representation of the earthquake resistant system (ERS) required to be identified in SDC C and D. The ERS model contains established Earthquake Resisting Elements (EREs) that have established and accepted response and corresponding design procedures applicable to the *Guide Specifications*.

Linear elastic dynamic analysis must, as a minimum, be used for the global response analysis. There are however, some limitations in a linear elastic analysis approach which should be considered. The

nonlinear response of yielding columns, gapped expansion joints, earthquake restrainers and nonlinear soil properties can only be approximated using a linear elastic approach. Piece-wise linear analysis may be used to approximate nonlinear response. Sensitivity studies using two bounding conditions may be used to approximate the nonlinear effects.

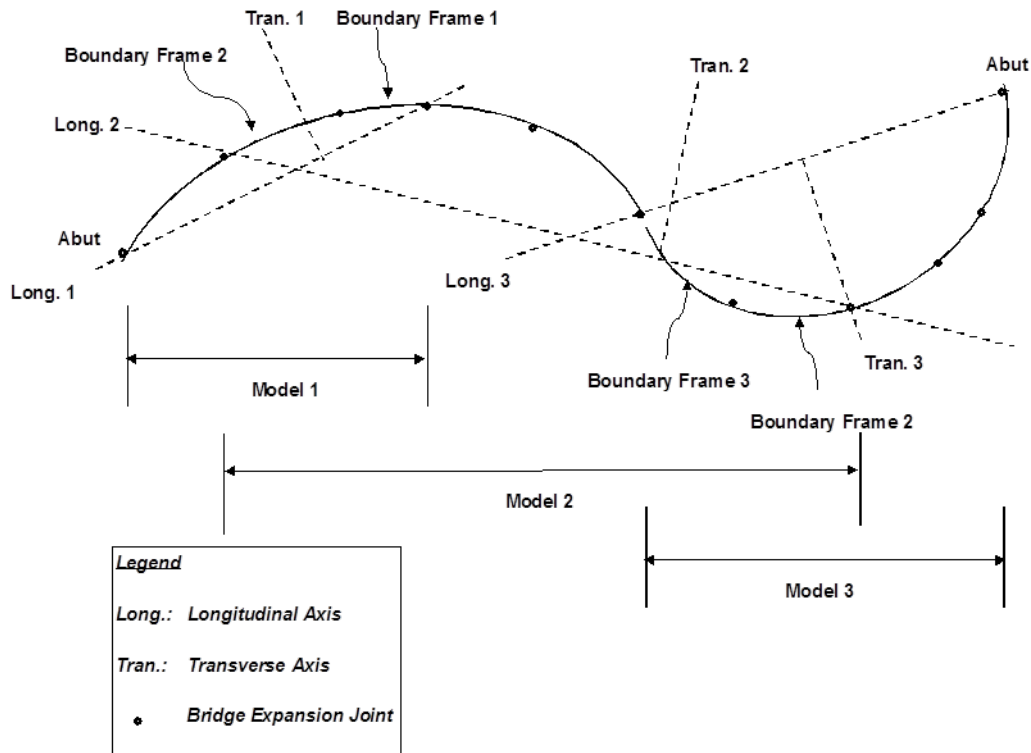


Figure 8-11 Dynamic Analysis Modeling Technique (AASHTO, 2014)

For example, two global dynamic analyses should be developed to approximate the nonlinear response of a bridge with expansion joints because it possesses different characteristics in tension and compression:

- In the tension model, the superstructure joints are permitted to move independently of one another in the longitudinal direction. Appropriate elements connecting the joints may be used to model the effects of earthquake restrainers.
- In the compression model, all of the restrainer elements are inactivated and the superstructure elements are locked longitudinally to capture structural response modes where the joints close up, mobilizing the abutments when applicable.

The determination of whether both a tension model and a compression model are required should be based on consideration of the geometry of the structure. Structures with appreciable superstructure curvature have a bias response to the outside of the curve and may require additional models, which combine the characteristics identified for the tension and compression models.

Long multi-frame bridges may be analyzed with multiple elastic models. A single multi-frame model may not be realistic since it cannot account for out-of-phase movement among the frames. Each multi-frame model may be limited to five frames plus a boundary frame or abutment on each end of the model. Adjacent models must overlap each other by at least one useable frame, as shown in Figure 1. A massless spring should be attached to the dead end of the boundary frames to represent the stiffness of the adjoining structure. The boundary frames provide some continuity between adjacent models but are considered redundant and their analytical results are ignored.

Boundary frames are frames modeled on either side of the bridge multi-frame section from which element forces are of interest. They serve as redundant frames in the sense that analytical results are ignored. The use of at least one boundary frame coupled with massless springs at the “dead” end of the model is recommended. The use of boundary frames is an idealization of the structural system. Engineering judgment should take into consideration the compatibility at the interface between connecting frames of various sets of frames.

#### **8.4.5 Design and Check the Earthquake Resisting Elements**

##### **8.4.5.1 Show Forces and Displacements of Overall System Acceptable**

The *Guide Specifications* identify incremental levels of confinement for different Seismic Design Categories as illustrated in Figure 8-2. The document also emphasizes the effect of slenderness in achieving a certain displacement capacity and recognizes the impact of the type of confinement (spiral and hoops vs. ties) in obtaining a higher displacement capacity. In contrasting the *LRFD Specifications* vs. the *Guide Specifications* as shown in

Figure 8-1, it is observed that the force based approach in the *LRFD Specifications* is set up to permit equally large demands regardless of seismic zone. Whether large demands in lower zones materialize is a

function of other non-seismic loads or constraints controlling. In contrast, the *Guide Specifications* uses several prescriptive levels of capacity that correspond to light damage limit states (e.g. spalling) and the effort to check the structure is low. Thus demands are kept small if the prescriptive values are used. In the highest SDC a full displacement check is done with pushover analysis. With this more detailed check, the permissible demand is increased.

The current state of the practice favors continuous superstructures for the majority of bridges with an objective of minimizing expansion joints to gain functionality, reduce maintenance, and increase life cycle of the bridge. This selection has a favorable impact on the earthquake redundancy of the bridge system. Considering a single performance level of “No Collapse”, the seismic redundancy of the bridge system is enhanced with the increase of the number of plastic hinges that must yield and then fail in order to produce the impending collapse of the structure. This enhanced redundancy translates into a delayed failure (i.e. collapse) provided sufficient support length exists in the bridge system. Therefore two distinctly different aspects of the design process need to be provided:

- a) An appropriate method to design adequate support length(s) considering out of phase motions.
- b) An appropriate method to design the ductile substructure components without undue conservatism.

These two aspects are embedded with different levels of conservatism that need to be calibrated against the single level of hazard considered in the design process.

The first aspect is highly influenced by variation in the periods of the frames on both sides of a joint as well as the damping generated by the ductile behavior of plastic hinges. This aspect is addressed in terms of recommended limits on stiffness or periods of frames on either side of an expansion joint relative to one another.

The second aspect is addressed using a static push-over analysis. As shown in Figure 8-12 the collapse displacement is usually reached at displacements larger than that permitted solely based on material limit states specified in the *Guide Specifications*. Additionally at large displacements, the  $P-\Delta$  line can approach the magnitude of the load-displacement curve of the structure, and under such a condition the structure would become unstable. Thus, limiting the  $P-\Delta$  effect keeps the structure well away from potential instability conditions. It is important to mention that for structures with relatively small gravity loads, a much larger reduction in component strength can be tolerated without reaching structural

collapse. This is especially relevant to bridge columns carrying axial loads typically ranging from  $0.05 f_c A_g$  to  $0.15 f_c A_g$  maximum. In essence, the continuity of the superstructure and low axial loads in columns make a typical bridge more resilient against collapse in a seismic event.

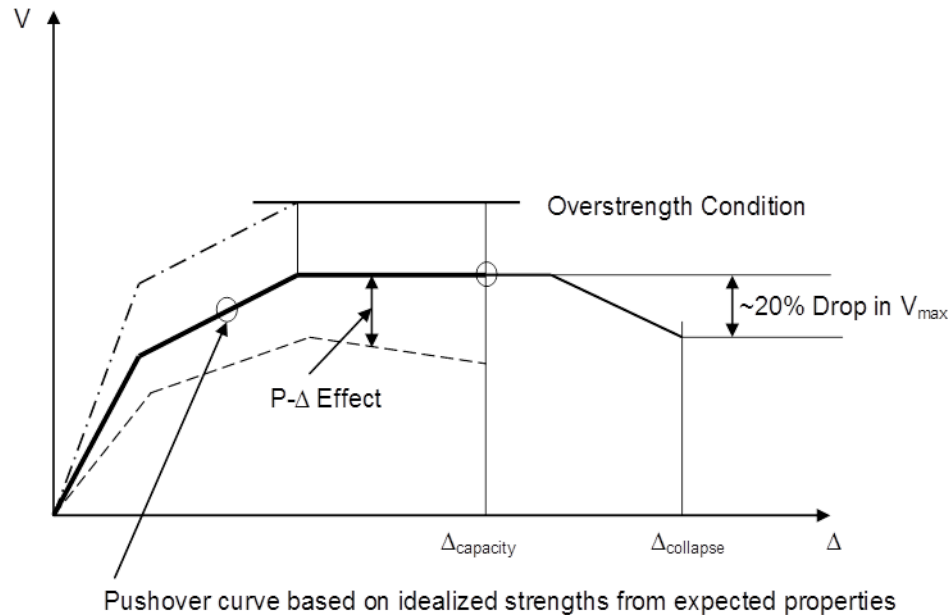


Figure 8-12 Idealized Load – Deflection Curve of a Bridge

Under earthquake ground motions at the supports, the structure or any of its components can fail under a smaller displacement than the displacement  $\Delta_{collapse}$  illustrated in Figure 8-12. This failure is mainly attributed to non-symmetric cumulative plastic displacement that is highly depended on the characteristics of the earthquake ground motions. The “true” displacement capacity is typically associated with the displacement corresponding to a limited decrease in strength of about 20% of the maximum resistance obtained under monotonically increasing deformation. As shown in Figure 8-12 the displacement capacity,  $\Delta_{collapse}$ , can only be established given the descending slope following the region of maximum lateral resistance,  $V_{max}$ . Recognizing the complexity of determining  $\Delta_{collapse}$ , a smaller limit,  $\Delta_{capacity}$ , is used as a conservative and simple measure, based on expected material properties and reduced ultimate tensile steel strains.

### 8.4.5.2 General Design Requirements

For SDC B, C and D, each bridge bent is required to have a displacement capacity that exceeds the displacement demand in each of the local axis of every bent. The local axis of a bent typically coincides with the principal axis of the columns in that bent. This demand displacement will have to be converted to this orientation if the bent is not oriented parallel to the principal axes of the bridge.

The objective of the displacement capacity verification analysis is to determine the displacement at which the earthquake-resisting elements achieve their inelastic deformation capacity. Damage states are defined by local deformation limits, such as plastic hinge rotation, footing settlement or uplift, or abutment displacement. Displacement may be limited by loss of capacity from either degradation of strength under large inelastic deformations or  $P$ - $\Delta$  effects.

For simple piers or bents, the maximum displacement capacity can be evaluated by hand calculations using the defined mechanism and the maximum allowable deformations of the plastic hinges. If interaction between axial force and moment is significant, this iteration is necessary to determine the sequence of plastic hinging.

For more complicated piers or foundations, displacement capacity can be evaluated using a nonlinear static analysis procedure (pushover analysis).

Displacement capacity verification is required for individual piers or bents. Although it is recognized that force redistribution may occur as the displacement increases, particularly for frames with piers of different stiffness and strength, the objective of the capacity verification is to determine the maximum displacement capacity of each pier. The displacement capacity is to be compared with an elastic demand analysis, which considers the effects of different stiffness. Expected material properties are used for the displacement capacity verification, not overstrength properties. The definition of displacement demand permits the inclusion of foundation and superstructure flexibilities for SDC B and C as a matter of analytical convenience so that global analysis results can be used directly in terms of conservative displacement demands on the local substructure axes.

For Type 1 structures comprised of reinforced concrete columns in SDC B and C, the displacement capacity,  $\Delta_c^L$  (in.), of each bent may be determined using an implicit formula based on data that was assembled from column tests. The expressions are simple and easy to use.

The implicit equations for displacement capacity are primarily intended for determining displacement capacities of bridges with single and multiple column reinforced concrete piers for which there is no provision for fusing or isolation between the superstructure and substructure during design event accelerations. The equations are calibrated in terms of the aspect ratio of columns shown to be the main parameter affecting the extent of damage observed in past-earthquake investigations as covered in Chapter 6 of this Manual.

The two implicit equations one for SDC B and the other for SDC were developed by Imbsen (2006) for columns that were either fixed or pinned at their ends. The equations are based on the database results reported by Berry and Eberhard (2003). Therefore the capacities reported by these equations do not include foundation, capbeam or superstructure flexibility effects. Capacities from these equations will normally be conservative relative to demands that include such flexibilities. In such cases, removing the demand displacement component attributable to such flexibilities from the local displacement demand may produce an acceptable result, in lieu of making a higher category check or redesigning the system.

The equation for SDC B corresponds to a limit state of initiation of concrete cover spalling, and the equation for SDC C corresponds to an equivalent column member ductility of 3 or less. These limits are generally conservative in terms of estimating the displacement capacity of reinforced concrete elements detailed in accordance with the applicable provisions for either SDC B or C.

Where in-ground hinging is used as an ERE in SDC C, the designer should consider using the equation for SDC B in order to limit the damage that could occur below grade that would not be easily inspected. Alternately, the method and limits for SDC D could be used.

For SDC D the Nonlinear Static Procedure (NSP), commonly referred to as “pushover” analysis, is used to determine the reliable displacement capacities of a structure or frame as it reaches its limit of deformation. Displacement Capacity determined using the implicit equation for SDC C may be used for SDC D in lieu of pushover analysis. However, the reinforcing details pertinent to SDC D should still be used in this case.

Where foundation and superstructure flexibility can be ignored, the two-dimensional plane frame “pushover” analysis of a bent or a frame can be simplified to a column model (fixed-fixed or fixed-pinned) if it does not cause a significant loss in accuracy in estimating the displacement capacities. The effect of seismic load path on the column axial load and associated member capacities is considered in the simplified pushover model.

This NSP procedure is a key element in the development of the *Guide Specifications*. The pushover method of analysis has seen increasing use throughout the 1990s, especially in California’s and other states’ seismic retrofit programs. This analysis method provides additional information on the expected progressive deformation demands of columns and foundations and as such provides the designer with a greater understanding of the expected performance of the bridge. The pushover method of analysis is used in two ways. First, it encourages designers to be precise in assessing the displacement and ductility capacity. Second, it provides a mechanism to allow use of the ERE’s that require the owner’s approval.

In conducting the “pushover” analysis, the analytical plastic hinge length for columns,  $L_p$ , is taken as the equivalent length of column over which the plastic curvature is assumed constant for estimating the plastic rotation.

Plastic hinge lengths for reinforced concrete columns were determined by conducting prototype tests on columns with various column end conditions. Formulas are provided in the *Guide Specifications* for columns framing into a footing, an integral bent cap, and a shaft. These are discussed in Chapter 6. Also included in the Guidelines are formulas to compute the plastic hinge lengths for non-cased prismatic cast in drilled hole shafts, reinforced concrete piles, prestressed concrete piles, horizontally isolated flared reinforced concrete columns, and concrete filled steel pipe piles.

The relationships for below-ground analytical plastic hinge lengths of concrete filled pipe piles are similar to those of conventional reinforced concrete shafts. The Port of Long Beach Wharf Design Criteria (2007) and research by others suggests that the below-ground analytical plastic hinge length can be taken as  $2D$ .

The member ductility demands for SDC D are limited and are required to be checked. Individual member displacements such as column displacements,  $\Delta_{col}$  are defined as the portion of global displacement attributed to the elastic column idealized displacement  $\Delta_{yi}$  plus the plastic displacement demand  $\Delta_{pd}$  of

an equivalent member from the point of maximum moment to the point of contra-flexure. This means that an equivalent cantilever element must be extracted from the demand model for this calculation. Member section properties are obtained from a Moment-Curvature Analysis and used to calculate  $\Delta_{yi}$  and the plastic displacement capacity  $\Delta_{pc}$ . Requirements as specified in the *Guide Specifications* for maximum allowable individual member ductility demand for SDC D,  $\Delta_D$ , are given for various component types. These values range, for example, from  $\Delta_D \leq 6$  for multiple column bents to  $\Delta_D \leq 1$  for pier walls in the strong direction.

In calculating the yield displacement and plastic displacement demand, any contribution to the displacements from foundation, capbeam, or superstructure should be removed. Inclusion of such flexibilities in the yield displacement may be unconservative, as illustrated in Figure 8-13 where the foundation flexibility changes the apparent yield displacement, but not the plastic increment of displacement.

Where in-ground plastic hinging is part of the plastic mechanism, the effective column length used for yield and plastic deformations is assumed to extend to the in-ground hinge and must be included in the checks. Foundation flexibilities below the expected in-ground hinge should then be removed, as described above.

#### **8.4.5.3 P- $\Delta$ Capacity Requirement for SDC C and D**

Typical highway bridges should be designed so that  $P$ - $\Delta$  effects can be neglected. For columns that do not satisfy Equation 8-5, the designer has the option of considering one or more of the following:

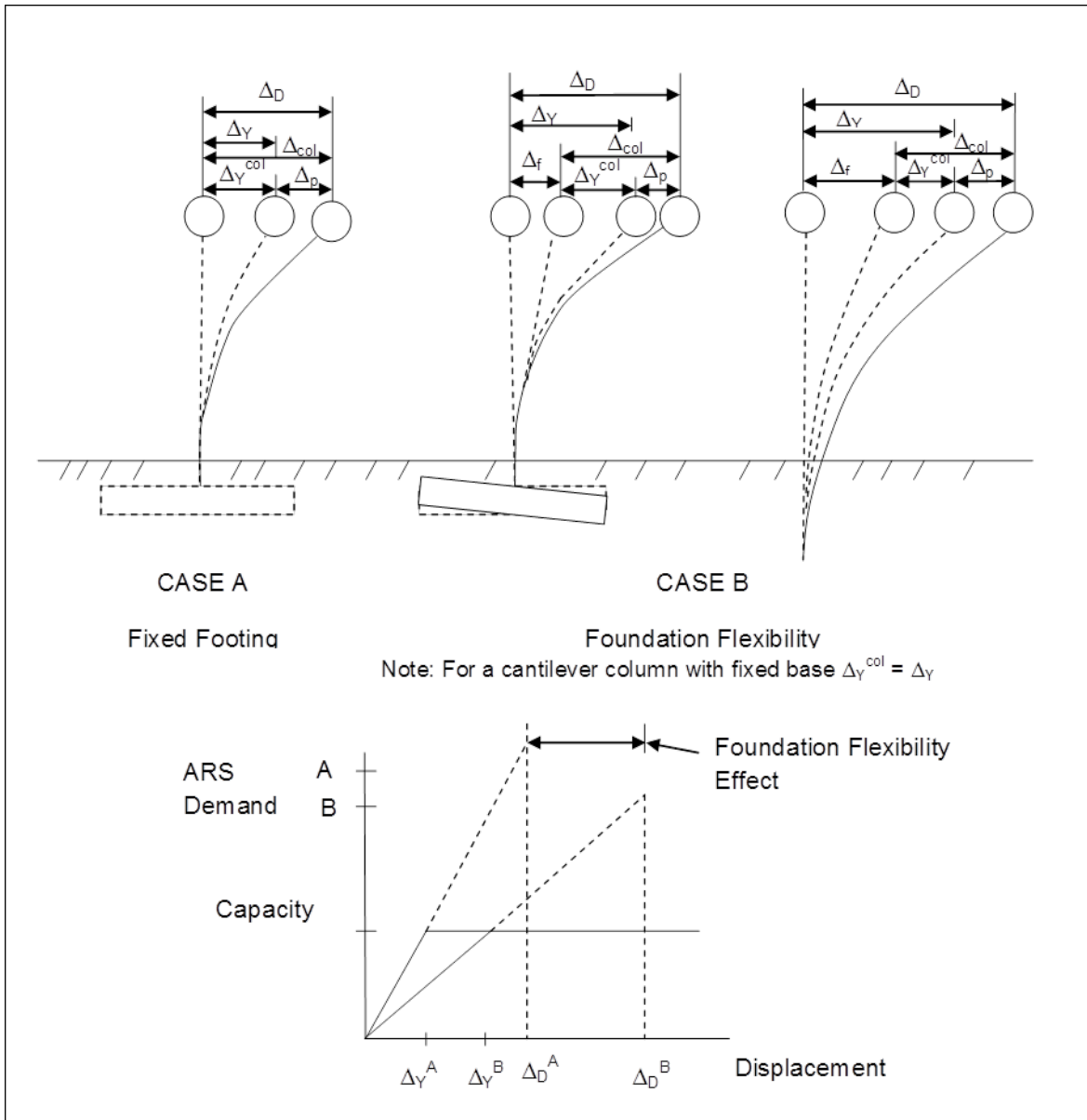


Figure 8-13 Effects of Foundation Flexibility on the Force-Deflection Relation for a Single Column Pier (Caltrans, 2013)

- increasing the column moment capacity by adding longitudinal reinforcement
- adjusting the dynamic characteristics of the bridge as discussed in Article 4.1.3
- reconfiguring the bridge to reduce the dead load demand acting on the column
- using nonlinear time history analysis to explicitly consider  $P-\Delta$  effects

At this time, the only rigorous method for considering  $P-\Delta$  effects in combination with seismic demands is to use a nonlinear time-history analysis. When using nonlinear time-history analysis, post-yield stiffness, stiffness degradation and unloading stiffness models that are capable of capturing the expected structure response due to seismic-induced cyclic loading are required.

The dynamic effects of gravity loads acting through lateral displacements must be included in the design. The magnitude of displacements associated with  $P-\Delta$  effects can only be accurately captured with nonlinear time history analysis. In lieu of such analysis, Equation 8-9 can be used to establish a conservative limit for lateral displacements induced by axial load for columns meeting the displacement demand vs capacity requirements. If Equation 8-9 is satisfied,  $P-\Delta$  effects can typically be ignored.

$$P_{dl} x \Delta_r \leq 0.25 x M_p^{col} \quad 8-9$$

where:

- $\Delta_r$  = The relative lateral offset between the point of contra-flexure and the base of the plastic hinge. For drilled shafts  $\Delta_r = \Delta_D - \Delta_s$
- $\Delta_s$  = The drilled shaft displacement at the point of maximum moment

As described earlier in the chapter, the displacement and resistance used in the  $P-\Delta$  check should be consistent with one another. Thus, if a full mechanism has not formed at the demand displacement, then the resisting moment should be adjusted accordingly to correspond to the resistance available at the estimated seismic displacement.

For steel columns:

$$P_{dl} \Delta_r \leq 0.25 M_n \quad 8-10$$

where:

- $P_{dl}$  = unfactored dead load acting on the column (kip)
- $\Delta_r$  = relative lateral offset between the point of contraflexure and the furthest end of the plastic hinge (in.)
- $M_n$  = idealized plastic moment capacity of reinforced concrete column based upon expected material properties (kip-in.)

$M_n$  = nominal moment capacity of structural steel column based upon nominal material properties (kip-in.)

For a pile cap in Site Classification E, or for cases where a modal analysis shows out-of-phase movement of the bottom of the column relative to the top of the column,  $\Delta_r$  is taken as:

$$\Delta_r = \Delta_D + \Delta_F \quad 8-11$$

where:

$\Delta_D$  = displacement demand as determined in accordance with Article 4.3 (in.)

$\Delta_F$  = pile cap displacement (in.)

When the requirements of these equations are not satisfied,  $P$ - $\Delta$  effects must be considered using a nonlinear time history analysis.

## 8.4.6 Capacity Protection of the Remaining Elements

### 8.4.6.1 Overstrength Forces

For SDC B of the *Guide Specifications*, the expected nominal moment capacity,  $M_{ne}$ , may be used as  $M_p$  in lieu of development of a moment curvature analysis. In essence, the expected nominal moment capacity for the plastic moment capacity is acceptable in SDC B, because inelastic demands are relatively small. This simplification also allows conventional software that can develop the nominal moment capacity as defined in the *AASHTO LRFD Bridge Design Specifications*, albeit with expected material properties, to be used in SDC B.

In contrast, in higher SDC C and D where capacity protection is ensured, the use of a moment curvature analysis is required. Moment-curvature analysis obtains the curvatures associated with a range of moments for a cross-section on the basis of the principles of strain compatibility and equilibrium of forces. A moment-curvature analysis based on strain compatibility and nonlinear stress-strain relations can be used to determine plastic limit states. The results from this rational analysis are used to establish the rotational capacity of plastic hinges as well as the associated plastic deformations. The process of

using the moment-curvature sectional analysis to determine the lateral load-displacement relationship of a frame, column, or pier is an initial step undertaken in conducting a “pushover analysis.”

#### **8.4.6.2 Capacity Protection Force Requirements for SDC B, C and D**

Seismic analysis is required for bridges located in SDC B, C and D. The design force requirement for SDC B is the lesser of the forces resulting from the unreduced elastic seismic forces in columns or pier walls or overstrength plastic hinging moment capacity.

Bridges that are designed in accordance with SDC B are designed and detailed to achieve a displacement ductility,  $\Delta_D$ , of at least 2. Due to the inherently low expected ductility demand, overstrength forces are permitted to be calculated using the nominal moment capacity generated using expected material properties for the yielding elements. This simplifies the designer’s workload in SDC B, and it is reasonable because it is unlikely that deformations will be large enough to create the full overstrength forces in the yielding elements.

The design force requirements for SDC C and D are based on forces resulting from the overstrength plastic hinging moment capacity or the maximum connection capacity following the capacity design principles. These overstrength forces are then applied as demands on the elements to be capacity protected. The capacity protected elements should be capable of resisting these applied overstrength forces while remaining essentially elastic. Expected material properties are permitted to be used when determining the strengths of the capacity protected components.

#### **8.4.6.3 Force Design of Steel Components**

Structural steel components are classified into two categories: Ductile and Essentially Elastic. Based on the characteristics of the bridge system, the designer may utilize one of three options for Global Seismic Design Strategy designated as Type 1, 2, or 3 covered in Chapter 4.

The provisions given in the *Guide Specifications* are used in conjunction with the FBA for seismic design as specialized in the *LRFD Specifications*.

In this section, reference to an “essentially elastic” component is used where the force demand to the nominal capacity ratio of any member in the superstructure is less than 1.5.

For Type 2 structures, the design of the steel superstructure is done using a force-based approach with appropriate reductions for ductility. Those factors are used for the design of all ductile load-carrying members. For SDC B, C, or D a reduction factor,  $R$ , equal to 3 is used for ordinary bracing that is a part of the Earthquake Resistant System (ERS) not having ductile end-diaphragms.

The nominal capacity of a member, connection, or structure is based upon the expected yield strength,  $F_{ye}$ , and the nominal dimensions and details of the final section(s), calculated with all material resistance factors,  $\Delta$ , taken as 1.0. For simply supported spans, with ductile diaphragms, the location of the diaphragms should be placed at the ends of each span as a minimum.

For continuous spans where ductile diaphragms are used, the location of these diaphragms are, as a minimum, placed over each bent and one cross-frame spacing adjacent to the opposite faces of the bent. The use of special diaphragms at opposite faces of an in-span hinge should be carefully assessed to ensure adequate vertical load capacity of the in-span hinge when subjected to deformations in the inelastic range.

For Type 3 structures, the designer must assess the overstrength capacity for the fusing interface including shear keys and bearings, then design for an essentially elastic superstructure and substructure. If isolation devices are used, the superstructure is typically designed as essentially elastic.

#### **8.4.6.4 Ductile Moment Resisting Frames and Single Column Steel Structures for SDC C and D**

Substructures composed of structural steel may typically also be used in compliance with a Type 1 Global Seismic Design Strategy. These structures are ductile moment-resisting frames and bents, constructed with steel I-shape beams and columns connected with their webs in a common plane. For SDC C or D, complying with a Type 1 performance criteria design, the columns may be designed as ductile structural elements using a force reduction factor,  $R$ , not greater than 4. The beams, the panel zone at column-beam intersections and the connections are designed as essentially elastic elements.

#### **8.4.6.5 Concrete Filled Steel Pipe Substructure for SDC C and D**

Concrete filled steel pipes are becoming more popular component for pile extensions due to their ease of construction and favorable ductile behavior. Concrete-filled steel pipes may also be used as columns, piers, or piles expected to develop full plastic hinging of their composite section. Often the performance of such a pipe is controlled by a reinforced concrete section at the top of the pipe section. In such cases, displacement capacity of the reinforced concrete section may be used, particularly if in-ground hinging of the steel pipe is not anticipated in the design earthquake.

For concrete filled steel pipes used in SDC D, the Nonlinear Static Procedure (NSP) is used to determine the reliable displacement capacity of the pipe system. The displacement capacity determined for SDC C may be used in lieu of pushover analysis. The factored moment resistance of a concrete filled steel pipe may be calculated using a strain compatibility approach that utilizes appropriate constitutive material models.

### **8.5 SUMMARY**

This chapter has outlined the AASHTO design procedures for both the *LRFD Specifications* and the *Guide Specifications*. An outline of six design activities has been presented, which conceptually outlines the seismic design process at a level that applies to both design procedures. A number of the specific procedures are common to both specifications, and these are discussed as common features, including seismic input, establishment of design procedures, identification of lateral earthquake resisting system, demand analysis methods, support lengths, minimum connection forces, approach for liquefaction assessment, and general procedures for capacity protection of elements that should not be damaged.

The country is divided into four seismic zones or design categories, depending on which procedure is used. These four categories serve to organize the design procedures in groups of increasing rigor from the lowest seismic areas of the country to the highest. A set of graphics (Figures 8-1 and 8-2) that summarize the results obtained with the two design procedures was discussed. The lateral displacement capacity provided by the two methods may be different, as indicated in the two figures, primarily because the prescriptive detailing requirements are different between the two methods.

The chapter also provided overviews of the unique design procedures for each of the two design procedures. These overviews included topics where the methods differ, for example the force-based method has its own design procedures, including the response modification factors. The displacement-based method of the Guide Specifications has its own unique procedures for determining whether adequate displacement capacity is provided. This procedure has been described conceptually. Other topics, such as P- $\Delta$  requirements and capacity protection requirements have been presented with the features unique to each design method.

Overall the chapter relies on material presented in earlier chapters to provide a complete overview of the AASHTO seismic design procedures, because detailed descriptions of the two methodologies have been discussed in the earlier chapters.



## CHAPTER 9

### SEISMIC ISOLATION

#### 9.1 GENERAL

Seismic isolation is a response modification technique that reduces the demand that earthquakes place on bridges and other structures. Isolation physically uncouples a bridge superstructure from the horizontal components of earthquake ground motion, leading to a substantial reduction in the forces generated by an earthquake. Improved performance is therefore possible for little or no extra cost, and older, seismically deficient bridges may not need strengthening if treated in this manner.

Uncoupling is achieved by interposing mechanical devices with very low horizontal stiffness between the superstructure and substructure as shown in Figure 9-1. These devices are called seismic isolation bearings or simply isolators. Thus, when an isolated bridge is subjected to an earthquake, the deformation occurs in the isolators rather than the substructure elements. This greatly reduces the seismic forces and displacements transmitted from the superstructure to the substructures. More than 200 bridges have been designed or retrofitted in the United States using seismic isolation in the last 20 years, and more than a thousand bridges around world now use this cost-effective technique for seismic protection.

This chapter summarizes the basic principles of seismic isolation, reviews applications to U.S. bridges, presents analysis techniques, and reviews design issues for commonly used isolators such as the lead-rubber isolator, the concave friction isolator and the Eradiquake isolator. The principal source for the material in this chapter is the AASHTO *Guide Specifications for Isolation Design* (AASHTO 2010) and the FHWA/MCEER Special Publication on *Seismic Isolation of Highway Bridges* (Buckle et. al., 2006).

##### 9.1.1 Basic Principles

Seismic isolators in use today possess the following three characteristics:

- Flexibility to lengthen the period of vibration of the bridge to reduce seismic forces in the substructure
- Energy dissipation to limit relative displacements between the superstructure above the isolator and the substructure below, and
- Adequate rigidity for service loads (e.g. wind and vehicle braking) while accommodating environmental effects such as thermal expansion, creep, shrinkage and prestress shortening.

Each of these characteristics is discussed in the sections that follow.

### 9.1.1.1 Flexibility

The low horizontal stiffness of a seismic isolator changes the fundamental period of a bridge and causes it to be much longer than the period without isolation (the so-called ‘fixed-base’ period). This longer period is chosen to be significantly greater than the predominant period of the ground motion and the response of the bridge is reduced as a result. The effect of isolator flexibility on bridge response is illustrated in Figure 9-2. The figure shows a typical normalized acceleration response spectrum (or seismic response coefficient) where the normalized spectral accelerations  $S_S$  and  $S_1$  are 2.5 and 1.5 respectively, the Site Class is B ( $F_v = 1$ ) and the damping is 5%. It is seen that a period shift from 0.5 to 1.5 second, due to the flexibility of the isolation system, results in a 60% reduction in the seismic forces (the normalized spectral acceleration drops from 2.5 to 1.0).

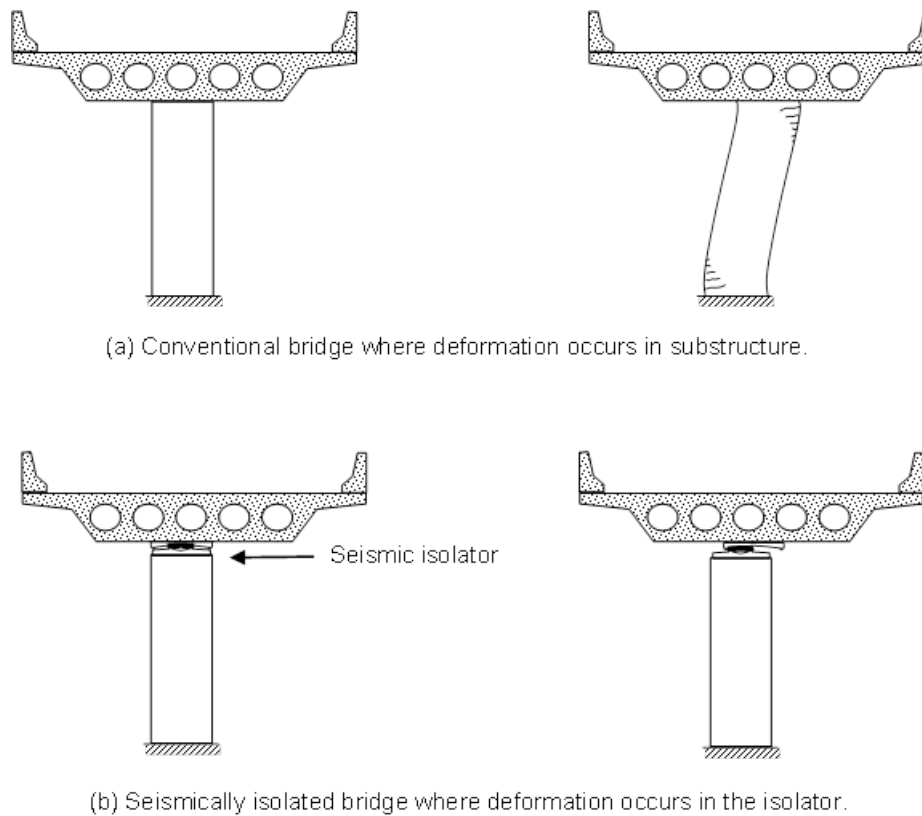


Figure 9-1 Deformations in Conventional and Isolated Bridges During Strong Ground Shaking (Buckle et. al., 2006)

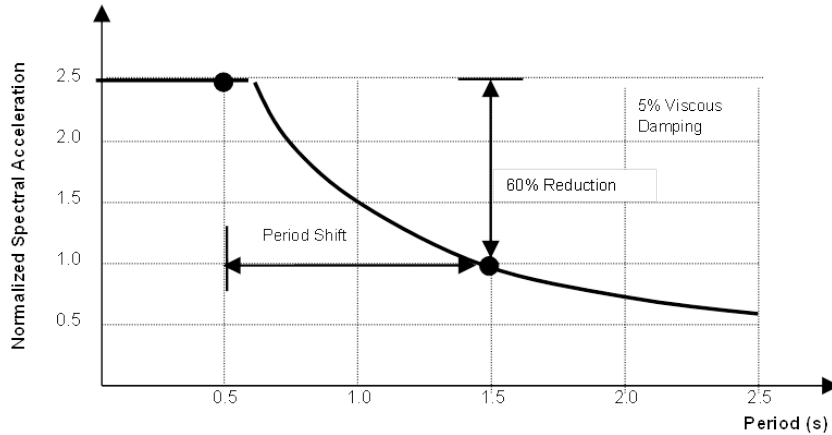
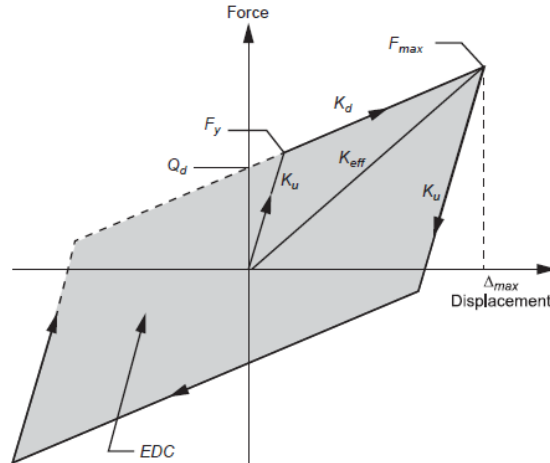


Figure 9-2 Effect of Period Shift Due to Isolator Flexibility on Bridge Response (Buckle et. al., 2006)

### 9.1.1.2 Energy Dissipation

Although the low horizontal stiffness of seismic isolators leads to reduced seismic forces, it may result in larger displacements of the superstructure. Wider expansion joints and increased support lengths may be required to accommodate these displacements. As a consequence, most isolation systems include an energy dissipation mechanism to introduce a significant level of damping into the bridge to limit these displacements to acceptable levels. These mechanisms are frequently hysteretic in nature, which means that there is an offset between the loading and unloading force-displacement curves under reversed (cyclic) loading. Energy, which is not recovered during unloading, is mainly dissipated as heat from the system. For instance, energy may be dissipated by friction in a mechanism that uses sliding plates. Figure 9-3 shows a bilinear force-displacement relationship for a typical seismic isolator that includes an energy dissipator. The shaded area under the curve is the energy dissipated during each cycle of motion of the isolator.

Analytical tools for these nonlinear systems are available using inelastic time-history structural analysis software packages. But these tools can be cumbersome to use and not always suitable for routine design office use. Simplified methods have therefore been developed which use effective elastic properties and an equivalent viscous dashpot to represent the energy dissipation. The effective stiffness ( $K_{eff}$ ) is defined in Figure 9-3 and the equivalent viscous damping ratio ( $h$ ) is calculated as explained below.



- $Q_d$  = Characteristic strength
- $F_y$  = Yield force
- $F_{max}$  = Maximum force
- $K_d$  = Post-elastic stiffness
- $K_u$  = Elastic (unloading) stiffness
- $K_{eff}$  = Effective stiffness
- $\Delta_{max}$  = Maxim bearing displacement
- $EDC$  = Energy dissipated per cycle = Area of hysteresis loop (shaded)

Figure 9-3 Bilinear Representation of Typical Isolator Hysteresis Loop (AASHTO, 2010)

The equivalent viscous damping ratio,  $h$ , is calculated such that the energy dissipated in each cycle of motion of the dashpot is the same as that for the hysteretic device. This is achieved by setting the area under the force-displacement loop of Figure 9-3, which represents the energy dissipated due to hysteretic damping, equal to the work done in one cycle of a viscous device moving through the same peak displacement ( $D_{max}$ ). It can then be shown that:

$$h = \frac{EDC}{2\pi K_{eff} D_{max}^2} \quad 9-1$$

where  $K_{eff}$  and  $D_{max}$  are the effective elastic stiffness and maximum displacement of the isolation system as shown in Figure 9-3, and  $EDC$  is the Energy Dissipated per Cycle of deformation.

Not only are displacements reduced with the increase in damping, but seismic forces are also reduced, compared to say the forces given by a 5%-damped spectrum. Figure 9-4 illustrates this effect. The solid

and dashed curves represent the 5%- and 30%-damped normalized acceleration response spectra respectively, for stiff soil conditions. The increased level of damping, due to the energy dissipated by the isolation system, leads to a further reduction in the seismic forces. It is seen that the 60% reduction at a period of 1.5 sec, due to flexibility, may increase to about 77% when the damping increases from 5% to 30%.

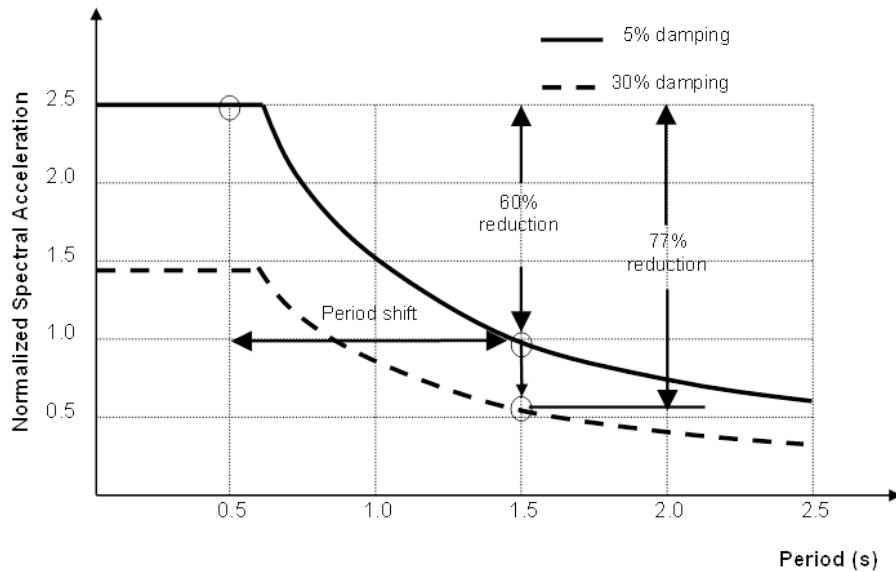


Figure 9-4 Effect of Damping on Bridge Response (Buckle et.al., 2006)

### 9.1.1.3 Rigidity Under Service Loads

The lateral flexibility of a seismic isolator system may cause the superstructure to move unacceptably under service loads, such as wind or vehicle braking forces. Resistance to these forces is important and the dual requirement of rigidity for service loads and flexibility for earthquake loads, is accommodated in a variety of ways. For example, devices that are elastic for wind loads but yield under seismic loads are commonly used. For the same reason, friction devices are popular because the friction coefficient can be adjusted to resist wind load without sliding. It follows that if the wind load is greater than the earthquake load, isolation will not be practical. This is rarely the case in bridge applications but can occur for high-rise buildings.

### 9.1.2 Seismic Isolators

Seismic isolators may generally be classified in one of two categories: those that use elastomeric components and those that use sliding components. The majority of bridge isolators in the United States

are elastomeric-based, with or without a lead core for energy dissipation. These are the so-called lead-rubber bearings (LRB). Sliding isolators are also used and the most common types are the concave friction bearing (CFB) and the Eradiquake bearing (EQS). Both use friction as the energy dissipator. Figure 9-5 shows schematic details of these three isolator types.

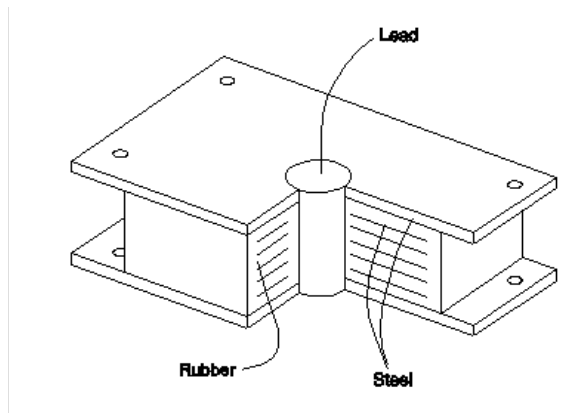
The selection of isolator type is an important decision and should involve careful consideration of a number of factors. These include:

- Axial load to be carried (sliding systems generally have greater capacity than elastomeric devices for axial loads)
- Available clearances (isolators with higher damping ratios, such as lead-rubber bearings, have smaller displacement demands)
- Available space (sliding systems generally have lower profiles than elastomeric devices which may be important in retrofit situations)
- Service loads to be resisted and environmental movements to be accommodated, such as wind, vehicle braking, thermal expansion, creep, and shrinkage.
- Reliability (stability of properties under field conditions over long periods of time)

With regard to the last two bullets, an isolator must be stiff enough to provide resistance to lateral loads due to wind and vehicle braking. In addition to the elasto-plastic and friction devices noted above, lock-up devices and elastomers which are stiff at small shear strain but soften with increasing strain, have been used to resist service loads.

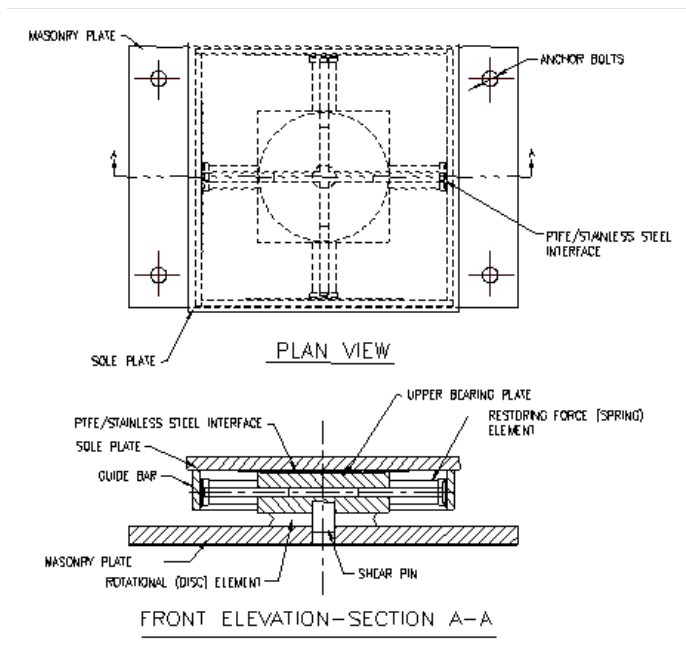
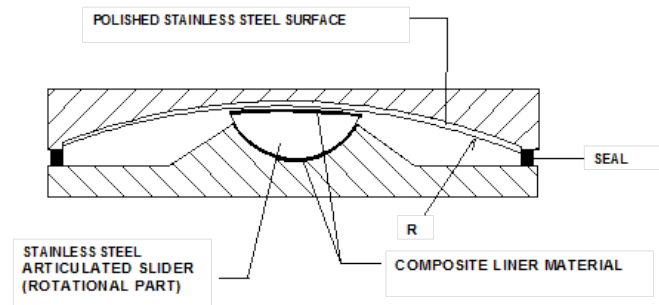
At the same time, the movement of the superstructure due to temperature variation, creep, shrinkage and the like, must be accommodated without over-stressing the substructures. This requires stable properties under field conditions for long periods of time and this fact alone can determine the choice of isolator. The ideal isolator is maintenance free, does not require precise field tolerances to operate successfully, and is constructed from materials that are chemically inert and resistant to atmospheric pollutants, ultra-violet radiation, and de-icing salts.

Assurance that an isolator will perform in an earthquake, as-intended by the designer, is also crucial. It may be many years before the design earthquake occurs, and stable isolator properties are required for this reason as well as the environmental issues noted above. Guidance is available (e.g. AASHTO 2010) to help the designer consider the effects of aging, temperature, wear, contamination, and scragging on isolator performance



(a) Lead-Rubber Isolator

(b) Concave Friction Bearing



(c) Earthquake Isolator

Figure 9-5 Three Types of Seismic Isolator Commonly Used in the United States for Protection of Highway Bridges (Buckle et. al., 2006)

### **9.1.3 Bridge and Site Suitability**

Seismic isolation should be considered whenever improved seismic performance, or reduction of cost, or both, may be achieved. Such benefits can be evaluated on a case-by-case basis using simplified analytical tools such as those described in Section 9.3.1.

Factors affecting bridge and site suitability include superstructure type, site soil conditions and substructure flexibility. These factors are described in the sections below.

#### **9.1.3.1 Superstructure Weight**

Bridges with lightweight superstructures may present difficulties for effective seismic isolation. Such bridges include those with steel girders and concrete deck slabs, and those with precast concrete tee sections. These bridges usually have multiple lines of girders and placement of an isolator under each girder means that the load carried per isolator is low. Consequentially, the ratio of mass-to-isolator stiffness is also low and it may be difficult to obtain a sufficiently large period shift (Figure 9-2) to justify isolation.

Two options might be considered in such circumstances. The first is to use an isolator with a period that is independent of the weight carried (e.g., the concave friction bearing ). The second is to use a cross beam (diaphragm) at the abutments and piers connecting the girder lines at their bearing locations and supported on, say, 2 or 3 isolators at each abutment seat and pier cap. The larger load per isolator improves the mass-to-stiffness ratio and meaningful period shifts become feasible. There are however consequential implications on the distribution of gravity loads to the girders due to the flexibility of the cross beam and the AASHTO live load distribution factors may not apply in such cases. This same flexibility may lead to high-cycle fatigue problems in the connections of the diaphragms to the girders. Both issues can be mitigated by using very stiff cross beams.

#### **9.1.3.2 Soft Soil Sites**

Ground motions at the surface of soft soil sites have significant long-period components. Lengthening the period of a bridge on such a site, by introducing a flexible isolation system, may not be desirable due to the possibility of increased forces, and it may not be practical due to much larger displacements at the abutment seats. Advanced analytical tools and procedures are available when assessing the effectiveness

of isolation in such circumstances, and these should be used in lieu of the approximate methods in Section 9.3.1

Seismic isolation hardware may be used for any purpose that is shown by analysis to provide benefits. For example, engineers in Japan have successfully used seismic isolators for the protection of bridges on soft soil sites by using isolators to redistribute forces (rather than reduce them) among various substructures, and dissipate energy to limit displacements. Called *menshin* design, this approach has been widely used in Japan (Civil Engineering Research Center, 1992; Sugita and Mahin, 1994). This technique is called *partial isolation* in the United States and has been shown to be an effective retrofit tool for existing bridges on stiff sites with inadequate seat widths at abutments and pier caps (Buckle et.al, 1990, 2012). In these situations it is not the period shift that is important but the energy dissipation.

### **9.1.3.3 Flexible Substructures**

It is often stated that flexible structures may not be suitable for seismic isolation, usually in reference to buildings above a certain number of stories in height. The statement implies that, while the use of an isolation system increases the fundamental period, the increase for structures that are already flexible, may not be sufficient to affect the dynamic response in a significant way.

This is also true for bridges, but not to the same extent. The outcome depends on the ratio of the isolator flexibility to the substructure flexibility. If this ratio is greater than unity, favorable response should be found when using isolation. If it is less than unity, the benefit of isolation will be negligible. For typical bridge situations, this ratio is almost always greater than unity.

As shown in Section 9.3.1, a simplified method of analysis may be used to explore this effect in bridges being considered for isolation.

## 9.2 APPLICATIONS

### 9.2.1 Early Applications

#### 9.2.1.1 South Rangitikei River Rail Bridge

One of the earliest applications of ‘modern’ isolation was to the South Rangitikei River Rail Bridge in New Zealand. Constructed in 1974, this 1033-ft long, six span bridge carries a single track of the North Island main trunk rail line across the South Rangitikei River gorge using rocking piers that average 230 ft in height. The superstructure is a continuous prestressed box girder supported monolithically on slender, double stem, reinforced concrete piers (Figure 9-6). The location is in a high seismic zone and the

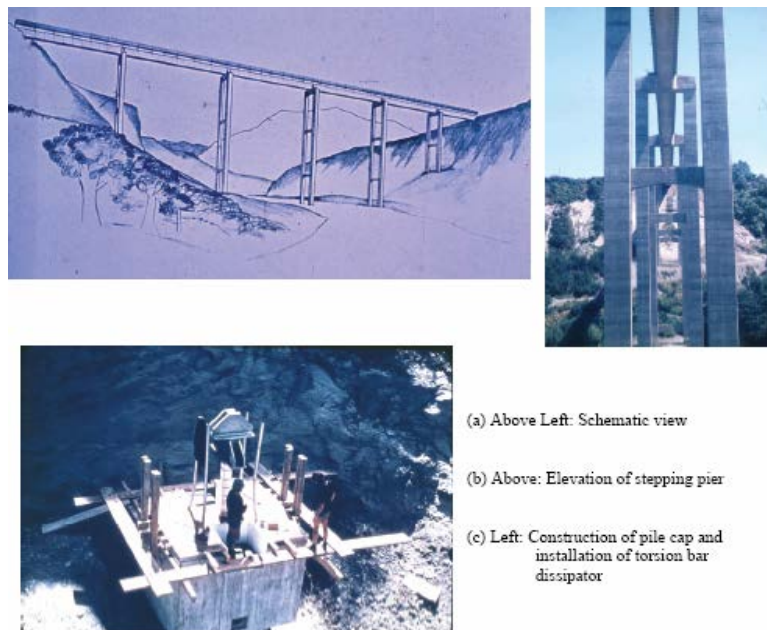


Figure 9-6 South Rangitikei River Rail Bridge, Mangaweka, New Zealand (Buckle et. al., 2006)

designers had difficulty providing adequate capacity for the bending moments and shears at the base of the piers, during a transverse earthquake.

It became apparent that an alternative design strategy was required and the most attractive option was to allow the structure to rock (or step) transversely, thereby reducing the moments and shears to be resisted.

By allowing the piers to step, with each leg lifting vertically off the pile cap, one-at-a-time, the rocking period became considerable longer than the fixed base period, and the induced seismic forces were correspondingly reduced. In this way the piers could remain elastic, reinforcing steel be reduced, and the pier cross sections be smaller, with consequential cost savings.

The arguments in favor of isolating the bridge (by allowing it to rock) were compelling and justified the investigation of the engineering implications of isolating this bridge, the first bridge of its type in New Zealand.

An essential element in the design was to control the transverse movements of the superstructure during rocking to prevent the structure overturning. The solution was to add a pair of mild steel torsion bar dissipators at the base of each pier leg. These devices act to reduce the upward movements of the legs and provide an ultimate stop against excessive vertical travel of the leg. Gravity loads are transferred to the pile cap by pairs of elastomeric pads. It is expected that wind loads may activate the dissipators but only in their elastic range. Their high initial stiffness will keep deflections to acceptable limits under in-service conditions. Twenty torsion bars have been installed, each with a characteristic yield strength of 90 K and a total stroke of 3 inches.

Factors favoring the isolation of this bridge include:

- the isolation mechanism is very simple and judged to be reliable with minimum maintenance requirements, and no mechanical parts that need precise alignment or regular servicing
- the dampers use conventional mild steel, a proven material with well-established yield properties
- several full scale prototype dampers were tested during feasibility design, to study their strain-hardening characteristics and low-cycle fatigue behavior
- extensive analysis of the stepping bridge was carried out using nonlinear numerical simulation tools to gain confidence in the design and understand potential limit states, and
- significant cost savings were possible compared to a conventional capacity design approach.

### **9.2.1.2 Sierra Point Overhead**

The first bridge to be isolated in the United States was the Sierra Point Overhead on US 101 near San Francisco. This highly skewed structure consists of 10 simply supported spans of steel girders with concrete slabs, seated on stand-alone, 3 ft diameter, reinforced concrete columns. The spans range from

26 to 100 ft. This bridge was constructed in the 1950's and had nonductile columns and inadequate seat lengths at the girder supports (Figure 9-7). Isolation was chosen as the preferred retrofit scheme and existing steel bearings were replaced by 15 in-square lead-rubber isolators at the tops of all the columns and on the abutment seats. The reduction in seismic loads, due to the isolation, was sufficiently great that column jacketing and foundation strengthening was not necessary, for the 'design' earthquake ground motions. The bridge was isolated in 1985 and was subject to shaking during the Loma Prieta earthquake in 1989. Although instrumented with four strong motion instruments, records were inconclusive due to high frequency 'noise' in the steel superstructure. The bridge was however undamaged with no visible signs of distress (cracking or residual displacement).

### 9.2.2 Recent Applications

It is believed that the number of isolated bridges in North America is in excess of 200. Since a central registry is not maintained this number is not known with certainty. Aiken and Whittaker compiled a list in 1993 and working from their database and soliciting new entries from the manufacturers of isolation bearings in the United States, an updated list has been compiled and published (Buckle et.al., 2006).



Figure 9-7 Sierra Point Overhead US 101 Near San Francisco (Buckle et. al., 2006)

Based on this information, there are at least 200 isolated bridges in North America (United States, Canada, Mexico, and Puerto Rico). This number includes completed bridges but excludes those under construction or still in design. Twenty-five states have isolated bridges and six of these states have more than 10 such bridges, accounting for about 60% of the population of isolated bridges. Table 9-1 lists these six states and the number of isolated bridges in each. As might be expected, California, with its high seismic risk, leads the list with 13% of the total number of applications. But of interest is the fact that about 40% of the applications are in the four eastern states of New Jersey, New York, Massachusetts and New Hampshire, states with relatively low seismic risk.

About three-quarters of the isolated bridges in the U.S. use lead-rubber isolators, and a little under one-quarter use the EradiQuake isolator. Table 9-2 gives the breakdown of applications by isolator type.

In the last decade there has been a marked increase in the size and capacity of isolators being manufactured and used in bridge design and retrofitting. Most of these applications have been to major structures and some notable examples are summarized in Table 9-3.

**TABLE 9-1 STATES WITH MORE THAN TEN ISOLATED BRIDGES  
(Buckle, et. al., 2006)**

State	Number of isolated bridges <sup>1</sup>	Percentage of total number of isolated bridges in North America <sup>2</sup>
California	28	13%
New Jersey	23	11%
New York	22	11%
Massachusetts	20	10%
New Hampshire	14	7%
Illinois	14	7%
TOTAL	121	59%

**Note** 1. Most recent data April 2003  
2. United States, Canada, Mexico, and Puerto Rico

**TABLE 9-2 BRIDGE APPLICATIONS BY ISOLATOR TYPE**  
(Buckle, et. al., 2006)

Isolator	Applications (% of total number of isolated bridges in North America)
Lead-rubber isolator	75%
Eradiquake isolator	20%
Other: Concave friction bearing, FIP isolator, High damping rubber, Natural rubber bearing	5%

**TABLE 9-3 EXAMPLES OF BRIDGES WITH LARGE ISOLATORS**  
(Buckle et. al., 2006)

Bridge	No. of Isolators and Type <sup>1</sup>	Isolator Dimensions	Axial Load capacity	Remarks
JFK Airport Light Rail Elevated Structure, NY	1300 LRB	18 - 29 in dia	300 – 900 K	600 spans 10 miles total length
Coronado San Diego, CA	54 LRB	41.5 in dia	1,550 K	11 in dia lead core 25 in displ capacity
Benecia-Martinez I-680 Crossing San Francisco Bay, CA	22 CFB	13 ft dia	5,000 K	10 spans Weight 40K / isolator 53 in displ capacity 5 sec isolated period
Memphis I-40 Crossing Mississippi R	18 CFB and LRB		1,000 K	3 miles total length 2, 900ft spans isolated with CFB 24 in displ capacity 4-5 sec isolated period 7 spans isolated with LRB
Boones Bridge, Clackamas Co, OR	32 EQS	37 - 50 in sq	375 - 950 K	5 spans 1137 ft total length
Regional Road 22 / Highway 417 Ontario Canada	6 EQS	36 – 45 in sq	650 -1,500 K	2 spans 240 ft total length
Corinth Canal, Greece	4 flat sliding isolators 12 elastomeric Isolators		13,300 K  1,102 K	Pair curved, 3-span bridges Single large sliding isolator at each pier 3 elastomeric isolators at each abutment

**Note:** 1. LRB = Lead-rubber isolator, CFB = Concave Friction Bearing, EQS = Eradiquake isolator

A decade ago, the largest elastomeric isolator in the U.S. was limited by the fabricator's know-how, to units that were about 24 inches square. Today the upper limit seems to be in the 45-55 inch range with load capacities approaching 2,500 K. Some very long structures have also been isolated with large numbers of moderate-to-large size isolators being used. For example the JFK Airport Light Rail access structure in New York is an isolated viaduct, 10 miles in length with 1300 lead-rubber isolators ranging up to 900 K capacity (Figure 9-8).

Even greater load capacities are possible with sliding isolators. For example a set of 13-foot diameter concave friction bearings have been installed in the Benicia-Martinez bridge in California which have an axial capacity of 5,000 K (Figure 9-9).



Figure 9-8 Lead-Rubber Isolators Being Installed in the JFK Airport Light Rail Viaduct, NY

Another example is the set of isolators provided for a pair of bridges over the Corinth Canal in Greece (Constantinou, 1998). As shown in Figure 9-10, each of these bridges consists of a continuous prestressed concrete box girder supported on abutments by six elastomeric bearings, and at each of two piers by a single sliding bearing. The design was complicated by the fact that the site is in an area of high seismicity, has geological faults in close vicinity and the banks of the canal were of uncertain stability.



Figure 9-9 Concave Friction Bearings Being Installed in the Benicia-Martinez Bridge, CA

A preliminary design called for straight bridges and piers placed as close as possible to the banks so as to reduce the length of the middle span and consequentially the depth of the girder section. By placing the piers at a distance of 360 ft apart, designing a deep foundation and utilizing an isolation system, a satisfactory design was achieved. This early design used a lead-rubber isolation system with four such bearings at each pier location. During the final design, it was decided to use two rather than four bearings at each pier due, primarily, to uncertainties in the distribution of axial load on the bearings. With further refinement in the analysis, it became apparent that the combination of transverse seismic loading and vertical earthquake could cause uplift to one of the two pier bearings and significant overloading of the other bearing. Accordingly, a decision was made to use a single bearing at each pier, provide the bridge with curvature and utilize counterweights in order to completely eliminate bearing uplift problems at the abutment bearings under all possible loading combinations. The maximum design load was 13,300 K for the sliding bearings and 1,012 K for the elastomeric bearings.

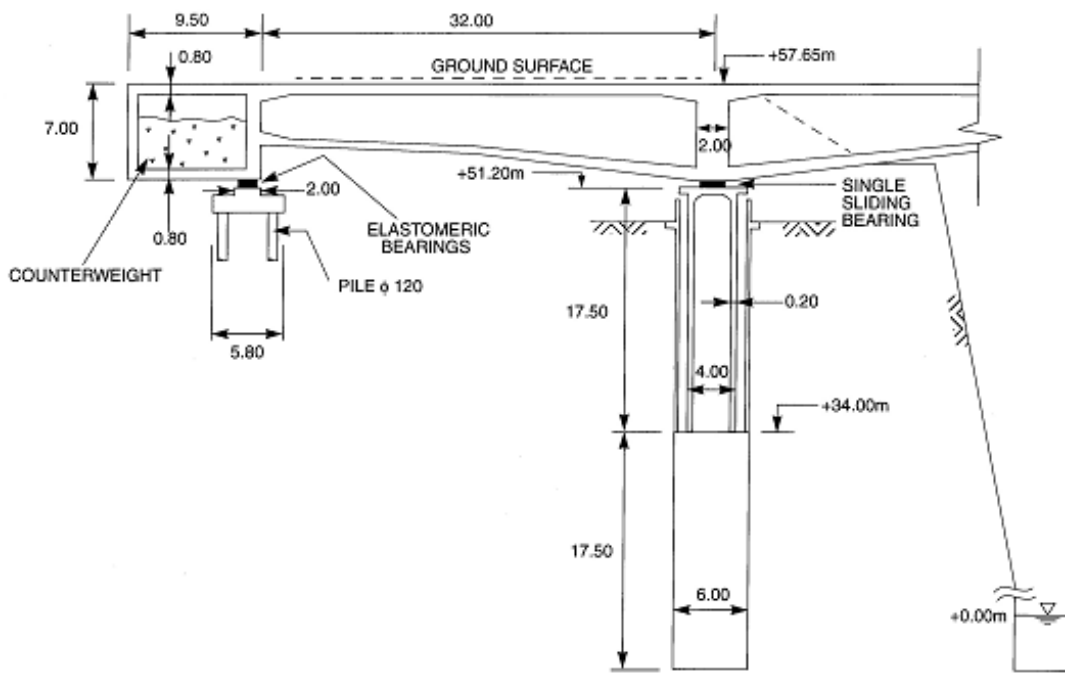
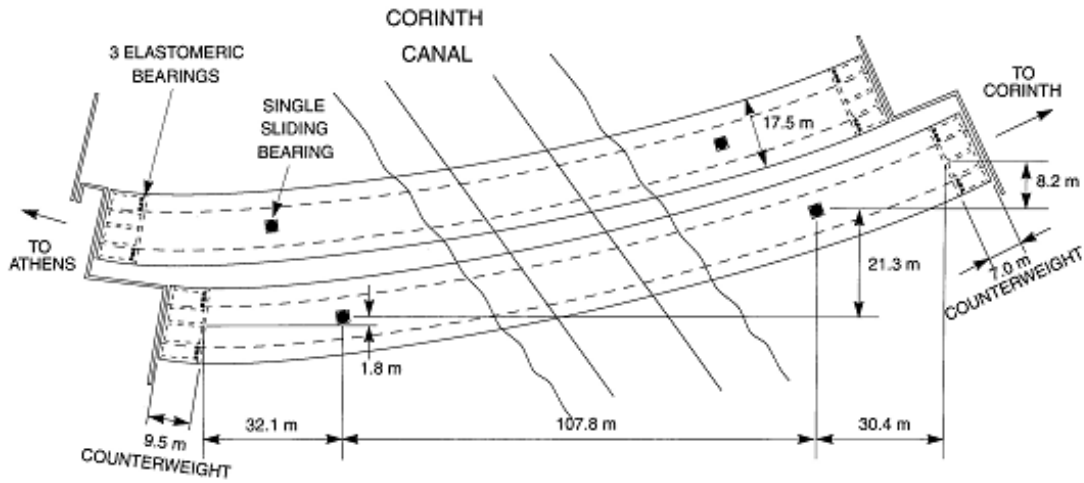


Figure 9-10 Plan and Elevation of Corinth Canal Highway Bridges (Buckle et. al., 2006)

### 9.2.3 Performance of Isolated Bridges in Recent Earthquakes

There is a general lack of field data quantifying the performance of full-scale isolated structures (buildings and bridges) during strong earthquakes. The evidence available to date is generally for low-to-moderate shaking and performance has either been as expected, or the results have been inconclusive. (See, for example, Section 9.2.1 for a note on the performance of the Sierra Point Overhead during the Loma Prieta Earthquake near San Francisco in 1989.) An exception to this general observation is the performance of the Bolu Viaduct in Turkey, which was originally isolated with flat plate sliders and steel energy dissipators. During the 1999 Duzce Earthquake, the causative fault passed under one of the spans imposing lateral offsets on the adjacent spans and destroying the isolators supporting these spans. However no spans collapsed and the isolators have since been replaced with large-capacity concave friction bearings.

## 9.3 ANALYSIS

Since most isolation systems are nonlinear, it might appear at first sight that only nonlinear methods of analysis can be used in their design (such as a nonlinear time history method). However, if the nonlinear properties can be linearized, equivalent linear (elastic) methods may be used, in which case many methods are suitable for isolated bridges. These methods include:

- Simplified Method
- Single Mode Spectral Method
- Multimode Spectral Method
- Time-History Method

The first three methods are elastic methods. The time history method may be either elastic or inelastic. It is used for complex structures or where explicit modeling of energy dissipation is required to better represent isolation systems with high levels of hysteretic damping (equivalent viscous damping > 30%).

All of the above methods are described in AASHTO (2010). Special care is required when modeling the isolators for use in these methods.

The Simplified Method is a variant of the displacement-based method of analysis. It is particularly useful for performing initial designs and checking the feasibility of isolation for a particular bridge. It may be

used as a starting point in design, followed by more rigorous methods as the design progresses. This method is briefly described in Section 9.3.1 and two examples are given of its use.

### **9.3.1 Simplified Method**

#### **9.3.1.1 Assumptions**

- The bridge superstructure acts as a diaphragm that is rigid in-plane and flexible-out-of-plane. Compared to the flexibility of the isolators, bridge superstructures are relatively rigid and this assumption is applicable to a wide range of superstructure types (e.g., box-girders, plate girders with cross-frames, slab and girders with diaphragms and the like).
- The bridge may be modeled as a single-degree-of-freedom system. The uniform load and single mode spectral analysis methods in conventional seismic design make this same assumption, and is subject to the same limitations on applicability.
- The displacement response spectrum for the bridge site is linearly proportional to period within the period range of the isolated bridge (i.e. the spectral velocity is constant and the spectral acceleration is inversely proportional to the period in this range).
- The lateral force-displacement properties of the seismic isolators may be represented by bilinear hysteretic loops.
- Hysteretic energy dissipation can be represented by equivalent viscous damping.
- The design response spectrum may be scaled for different viscous damping ratios by damping factors which are independent of period.

### 9.3.1.2 Basic Equations for Bridges with Stiff Substructures

If all the isolators supporting the superstructure experience the same displacement  $D$ , the properties of individual isolators may be lumped into a single, equivalent, 'system' isolator. This will be true when a single mode of vibration dominates response (Assumption 1 above) and for bridges with stiff substructures. Stiff substructures are assumed in this section and the properties of individual isolators are lumped into a single system isolator. The theory for bridges with flexible substructures is presented in Section 9.3.1.3.

#### 9.3.1.2.1 Effective Stiffness

From Figure 9-3, the effective stiffness  $K_{eff}$ , of a bilinear isolator at displacement  $D$ , is given by:

$$K_{eff} = \frac{F}{D} = \frac{(Q_d + K_d D)}{D} = \frac{Q_d}{D} + K_d \quad 9-2$$

where  $F$  = total lateral force in the isolator at displacement  $D$

$Q_d$  = characteristic strength of the isolator (force in isolator at zero displacement), and

$K_d$  = post yield stiffness of the isolator.

#### 9.3.1.2.2 Effective Period

The effective period  $T_{eff}$ , of single-degree-of-freedom system of mass  $W/g$ , and stiffness  $K_{eff}$  at displacement  $D$ , is given by:

$$T_{eff} = 2\pi \sqrt{\frac{W}{gK_{eff}}} \quad 9-3$$

where  $W$  = weight of bridge superstructure.

#### 9.3.1.2.3 Equivalent Viscous Damping Ratio

The hysteretic energy dissipated in a single cycle of a bilinear isolator is given by the area of the hysteresis loop as follows:

$$Area = 4Q_d(D - D_y) \quad 9-4$$

where  $D_y$  = yield displacement of the isolator.

Substituting this area into Equation 9-1, gives the equivalent viscous damping ratio,  $h$ , as follows:

$$h = \frac{2Q_d(D - D_y)}{\pi K_{eff} D^2} = \frac{2Q_d}{\pi F} \left(1 - \frac{D_y}{D}\right) \quad 9-5$$

#### 9.3.1.2.4 Superstructure Displacement

The displacement  $D$ , of single-degree-of-freedom system with period  $T_{eff}$  and viscous damping ratio  $h$ , is given by AASHTO (2010):

$$D = 10S_{D1} \frac{T_{eff}}{B_L} \text{ (inches)} \quad 9-6$$

$$D = 250S_{D1} \frac{T_{eff}}{B_L} \text{ (mm)} \quad 9-7$$

where  $S_{D1} = F_v S_I$

$F_v$  = site factor for bridge site class (Table 2-5)

$S_I$  = spectral acceleration at 1 sec (Figure 2-9)

$T_{eff}$  = effective period at displacement  $D$  (Equation 9-3), and

$B_L$  = damping factor in long-period range of design spectrum ( $T_{eff} > T_s$ , Figure 2-9); i.e., a displacement reduction factor based on the viscous damping ratio,  $h$ <sup>1</sup>

$$B_L = \left(\frac{h}{0.05}\right)^{0.3} \quad 9-8$$

<sup>1</sup> The use of  $B_L$ -factors to scale response spectra is unreliable for hysteretically-damped systems with viscous damping ratios in excess of 30%. In these cases, a nonlinear time-history analysis is recommended using the actual hysteresis loop(s) rather than damping ratios and  $B_L$ -factors. Alternatively the value of  $B_L$  should be capped at 1.7. If however the dampers are truly viscous, then  $B_L$ -factors greater than 1.7 may be used.

Derivations of Equations 9-6 and 9-7 are given in AASHTO (2010).

#### 9.3.1.2.5 Total Base Shear and individual Isolator Forces

The total lateral force in the system isolator at displacement  $D$  is given by:

$$F = K_{eff} D \quad 9-9$$

This force is the total base shear for the bridge. Individual isolator forces may be found by dividing the base shear by the number of isolators (if all isolators have identical properties), or in proportion to their individual stiffnesses.

Some isolation systems have viscous dampers in place of, or in addition to, the hysteretic dampers, and in such cases the forces in the dampers will be out of phase with those in the bearings (elastomeric or sliding). To find the governing design force, seismic forces should be calculated for three cases and the maximum chosen for design. These cases are:

- a. at maximum bearing displacement (i.e. zero velocity and therefore zero damper force)
- b. at maximum bearing velocity (i.e. zero displacement), and
- c. at maximum superstructure acceleration.

#### 9.3.1.3 Procedure for Bridges with Stiff Substructures

The methodology described here is an iterative one since many of the key parameters describing the properties of the bridge ( $K_{eff}$ ,  $T_{eff}$ , and  $h$ ) depend on the displacement of the bridge, which is not known at the beginning of the analysis. The method therefore begins by assuming a bridge displacement and iterating until convergence is achieved, usually within a few cycles. The steps are as follows:

Step 1: Assume a value for the superstructure displacement  $D$ .

Step 2: Calculate effective stiffness  $K_{eff}$ , from Equation 9-2.

Step 3: Calculate effective period  $T_{eff}$ , from Equation 9-3.

Step 4: Calculate equivalent viscous damping ratio  $h$ , from Equation 9-5.

Step 5: Check  $T_{eff} > T_s$  and obtain damping factor  $B_L$ , from Equation 9-8.

Step 6: Calculate displacement  $D$ , from Equation 9-6 and 9-7.

Step 7: Compare calculated value for displacement  $D$ , with that assumed in Step 1. If in close agreement go to Step 8; if not, repeat from Step 2 using the value for displacement  $D$ , found in Step 6.

Step 8: Calculate the total force in the isolator  $F$ , from Equation 9-9. This force will be the total base shear in the bridge and may be divided by the number of isolators to find individual isolator forces (assuming the isolators have identical properties; otherwise distribute this force in proportion to the stiffnesses of the individual isolators).

Example 9-1 in Section 9.7 illustrates the application of this procedure to a bridge with stiff substructures.

#### **9.3.1.4 Basic Equations for Bridges with Flexible Substructures**

When a bridge has flexible substructures, all the isolators do not experience the same displacements, except in the unlikely event that all the substructures have the same flexibility. To apply the simplified displacement-based method, the effective stiffness of the bridge, used in Step 2 above, must be modified to include the substructure flexibility. Once this has been done the method follows the same steps, and uses the same basic equations, as for the case with stiff substructures.

##### **9.3.1.4.1 Effective Stiffness of Bridge with Flexible Substructures**

The effective stiffness of an isolated superstructure on flexible substructures is obtained by summing the effective stiffnesses of the individual substructures. Figure 9-11 shows an idealized substructure comprising an isolator supported on a flexible column. The isolator is assumed to have bilinear properties and the column is assumed to be elastic.

The effective stiffness of the substructure  $j$  ( $K_{eff,j}$ ) is calculated as follows:

$$K_{eff\ j} = \frac{\alpha K_{sub}}{(1 + \alpha)} \quad 9-10$$

where

$$\alpha = \frac{K_{isol}}{K_{sub}} = \frac{(K_d D + Q_d)}{(K_{sub} D - Q_d)} \quad 9-11$$

$K_{isol}$  = effective stiffness of the isolators supported on substructure at displacement  $D_{isol}$

$$= Q_d / D_{isol} + K_d$$

$K_{sub}$  = stiffness of substructure in direction under consideration (e.g.  $3EI/h^3$  for a single cantilever column of height  $h$  and flexural rigidity  $EI$ )

$D_{isol}$  = isolator displacement

$$D_{isol} = \frac{D}{(1 + \alpha)} \quad 9-12$$

and  $D$  = assumed displacement of superstructure (Step 1).

It follows that the effective stiffness  $K_{eff}$  for the complete bridge with  $N$  substructures is given by:

$$K_{eff} = \sum_{j=1}^N K_{eff\ j} \quad 9-13$$

#### 9.3.1.4.2 Substructure and Isolator Forces

The force in any substructure is given by:

$$F_{sub} = K_{sub} D_{sub} \quad 9-14$$

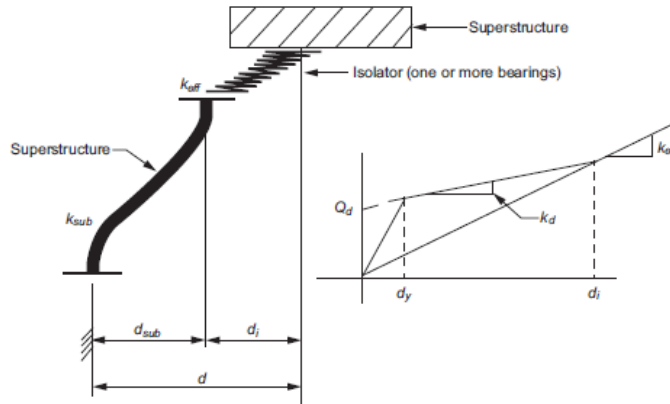
where  $D_{sub}$  = substructure displacement

$$D_{sub} = D - D_{isol} \quad 9-15$$

The force in the isolators supported by the substructure is given by:

$$F_{isol} = K_{isol} D_{isol}$$

It is noted that these two forces ( $F_{sub}$  and  $F_{isol}$ ) should be the same since both the isolator and substructure ‘see’ the same shear force due to the serial nature of the load path.



$$\beta = \frac{\text{Energy Dissipated}}{2\pi K_{eff} d^2} = \frac{\text{Total Energy Dissipated}}{2\pi \sum_j (K_{eff,j} d^2)}$$

$$\beta = \frac{2Q_d (d_i - d_y)}{\pi (d_i + d_{sub})^2 K_{eff}} = \frac{2 \sum_j [Q_d (d_i - d_y)]}{\pi \sum_j [K_{eff,j} (d_i + d_{sub})^2]}$$

**Note:** These equations exclude damping from the substructure.

Figure 9-11 Idealized Deformations in an Isolated Bridge with Flexible Substructures (AASHTO, 2010)

### 9.3.1.5 Procedure for Bridges with Flexible Substructures

The method described here is essentially the same as for stiff substructures but is repeated here in its entirety for completeness. As above, it is an iterative method since many of the key parameters describing the properties of the bridge ( $K_{eff}$ ,  $T_{eff}$ , and  $h$ ) depend on the displacement of the bridge  $D$ , which is not known at the beginning of the analysis. The method therefore begins by assuming a displacement for the bridge superstructure ( $D$ ) and iterating until convergence is achieved, usually within a few cycles. The steps are as follows:

Step 1: Assume a value for the superstructure displacement  $D$ .

- Step 2: Calculate effective stiffness of the bridge  $K_{eff}$ , from Equation 9-13.
- Step 3: Calculate effective period  $T_{eff}$ , from Equation 9-3.
- Step 4: Calculate equivalent viscous damping ratio  $h$ , from Equation 9-5.
- Step 5: Check  $T_{eff} > T_S$  and obtain damping factor  $B_L$ , from Equation 9-8.
- Step 6: Calculate displacement  $D$ , from Equation 9-6 or 9-7.
- Step 7: Compare calculated value for displacement  $D$ , with that assumed in Step 1. If in close agreement go to Step 8; otherwise repeat from Step 2 using the value for displacement  $D$ , found in Step 6.
- Step 8: Calculate the total base shear  $F$ , from Equation 9-9, or by summing individual substructure forces given by Equation 9-14. Isolator forces are equal to the substructure forces or may be found from Equation 9-16. Isolator and substructure displacements are given by Equations 9-12 and 9-15 respectively.

Example 9-2 in Section 9.7 illustrates the application of this procedure to a bridge with flexible substructures.

### 9.3.2 Single and Multimode Spectral Analysis Methods

These methods have been previously described in Chapter 5 (Sections 5.2.3 and 5.2.4), but modifications are required when applied to the analysis of an isolated bridge. First, to find the equivalent linear properties of the isolators for inclusion in a structural model of the bridge, an estimate of the design displacement must be made, followed by iteration if the estimate is significantly in error. Second, the 5 percent damped response spectrum is modified to recognize higher levels of damping in the ‘isolated’ modes, i.e., those modes that involve deflections in the isolators. This is done by scaling the spectrum by the damping coefficient  $B_L$ , for periods greater than  $0.8 T_{eff}$ . The 5 percent damped spectrum is used for all other modes in the multimode method.

Care must be taken when combining the modal results in the multimodal method since the assumption of equal damping in all modes made in the CQC method (Section 5.2.4, Step 7), is not valid in an isolated bridge where the isolated modes may have 3 - 5 times the damping of the structural modes. If the CQC Method cannot be modified to accept different damping in different modes, then the SRSS Method is recommended (Equation 5-37).

As for conventional bridges, the analysis is performed in two orthogonal directions and the results combined according to Article 3.10.8 of AASHTO (2013). These two directions are usually taken as the longitudinal (span-wise) and transverse directions. For a curved bridge, the longitudinal direction may be taken as the chord joining the two abutments.

### **9.3.3 Time History Method**

The time history method has been previously described in Chapter 5 (Sections 5.2.5 for equivalent linear time history solution) and 5.3.2 for explicit nonlinear solution).

The method uses either nonlinear or equivalent linear properties for the isolators and is suitable for complex structures where modal methods are inappropriate, or where explicit modeling of the energy dissipators is required to better represent isolation systems that have high levels of damping (> 30%). In both approaches, ground motion time histories are required and these may be either site-specific or spectrum-compatible. In both cases, no less than three pairs (one N-S and one E-W component) of time histories should be used in the analysis. Each pair is applied simultaneously to a three-dimensional model of the bridge and the maximum displacement of the isolation system is obtained by the vectorial sum of the orthogonal displacements at each time step. Design actions of interest (e.g. a shear force at the base of a column) are calculated for each time history. If three time history analyses are performed, the maximum response of the action of interest is used in design. If seven or more time history analyses are performed, the average value is used.

If site-specific ground motions are not available, spectrum-compatible time histories may be generated by frequency-scaling recorded ground motions of past earthquakes such that their spectra closely match the design spectrum for the site (Figure 2-9). A procedure to obtain spectrum-compatible time histories is given in Section 2.8.

## 9.4 DESIGN

### 9.4.1 Design of Isolated Bridge Substructures and Foundations

As described in Section 9.3, the analysis of an isolated bridge is typically performed assuming elastic substructures and foundations, and nonlinear isolators, which are modeled either by a nonlinear hysteretic element or a linearized spring with equivalent viscous damping. Among several response quantities, the analysis determines the maximum lateral force in each isolator,  $F_{isol}$ , (Equation 9-16). Also available are the yield force of the isolation system ( $F_y$  in Figure 9-3), the friction force in a sliding isolation system ( $Q_d$  in Figure 9-3), and the ultimate capacity of a sacrificial service restraint system, if used. For the purpose of the explanation below, these last three forces are denoted as  $Q$ .

The substructures of seismically-isolated bridges in Seismic Zones 2, 3 and 4 should be designed for the effects of  $Q$  or  $F_{isol}/R$ , whichever is largest, where  $R$  is one-half of the response modification factor of Table 3.10.7.1-1 of AASHTO (2013), but need not be less than 1.5 (Art. 6.0 and 11.0, AASHTO, 2010). R-factors shall not be used if the provisions of AASHTO (2014) are being followed.

### 9.4.2 Design Properties of Isolation Systems

#### 9.4.2.1 Minima and Maxima

Isolator properties vary over time for a variety of reasons such as manufacturing differences, aging, wear, contamination, history of loading, and temperature. These variations may alter the effective period and equivalent damping of the isolation system, both of which will influence the dynamic response of the isolated structure. To adequately account for these variations, estimates should be made of minimum and maxima values for each quantity of interest and analyses made of bridge response with both sets of values. For example minimum and maximum values for effective stiffness should be calculated from minimum and maximum values of  $Q_d$  and  $K_d$  and the behavior of the bridge calculated using both values.

Minima and maxima for  $Q_d$  and  $K_d$  may be found using system property modification factors ( $\lambda$ ) as follows:

$$K_{d \max} = \lambda_{\max Kd} K_d \quad 9-17$$

$$K_{d \min} = \lambda_{\min K_d} K_d \quad 9-18$$

$$Q_{d \max} = \lambda_{\max Q_d} Q_d \quad 9-19$$

$$Q_{d \min} = \lambda_{\min Q_d} Q_d \quad 9-20$$

where  $Q_d$  and  $K_d$  are nominal values (see Section 9.4.2.2).

Development of values for  $\lambda_{\max}$  and  $\lambda_{\min}$  is discussed in the next section.

#### 9.4.2.2 System Property Modification Factors ( $\lambda$ -factors)

The minimum value of the system property modification factor  $\lambda_{\min}$ , and is less than or equal to unity. Due to the fact that most values of  $\lambda_{\min}$  proposed to date (Constantinou et al., 1999) are close to unity,  $\lambda_{\min}$  is taken as unity (AASHTO, 2010). That is, the lower bound of the system property factors are considered to be the same as their nominal values. These nominal values are defined to be those determined for fresh and scragged (where appropriate) specimens under normal temperature conditions.

The maximum value of the  $\lambda$ -factor ( $\lambda_{\max}$ ) is calculated as the product of six component factors as follows:

$$\lambda_{\max} = (\lambda_{\max,t}) (\lambda_{\max,a}) (\lambda_{\max,v}) (\lambda_{\max,tr}) (\lambda_{\max,c}) (\lambda_{\max,scrag}) \quad 9-21$$

where

$\lambda_{\max,t}$  = maximum value of factor to account for the effect of temperature

$\lambda_{\max,a}$  = maximum value of factor to account for the effect of aging (including corrosion)

$\lambda_{\max,v}$  = maximum value of factor to account for the effect of velocity (established by tests at different velocities)

$\lambda_{\max,tr}$  = maximum value of factor to account for the effect of travel and wear

$\lambda_{\max,c}$  = maximum value of factor to account for the effect of contamination (sliding isolators)

$\lambda_{\max,scrag}$  = maximum value of factor to account for the effect of scragging (elastomeric)

isolators)

Recommendations for  $\lambda_{max}$ -factors for elastomeric and sliding isolators are given in Sections 9.5.5 and 9.6.6 respectively.

### 9.4.2.3 System Property Adjustment Factors

Adjustment factors ( $f_a$ ) take into account the likelihood that maximum values for all of the component  $\lambda$ 's (Equation 9-16) will not occur at the same time. These are, in effect, reduction factors on the  $\lambda$ -factors and vary according to the importance of the bridge as shown in Table 9-4. The adjusted factor ( $\lambda_{adj}$ ) is given by

$$\lambda_{adj} = 1 + f_a (\lambda_{max} - 1) \quad 9-22$$

where  $\lambda_{max}$  is given by Equation 9-21.

**TABLE 9-4 - SYSTEM PROPERTY ADJUSTMENT FACTORS  
(Buckle, et. al., 2006)**

Bridge Importance	Adjustment Factor, $f_a$
Critical	1.00
Essential	0.75
Other	0.66

### 9.4.3 Minimum Restoring Force Capability

Seismic isolation systems that have been applied to buildings are characterized by strong restoring force capability. However, for bridge applications, two competing seismic isolation design strategies have been developed: (a) a strategy championed by engineers in New Zealand, the United States and Japan which requires strong restoring force in the isolation system, and (b) the Italian strategy in which the isolation system exhibits essentially elastoplastic behavior.

Specifications in the United States presume that the isolation system has, excluding any contribution from viscous devices, a bilinear hysteretic behavior characterized by the zero-force intercept or characteristic strength and the post-elastic stiffness.

The AASHTO *Guide Specification for Seismic Isolation Design* (AASHTO, 2010) specifies a minimum value for the post-elastic stiffness ( $K_d$ ) as follows:

$$K_d \geq 0.025 \frac{W}{D} \quad 9-23$$

This value for  $K_d$  is equivalent to requiring that the period  $T_d$ , based on the post-elastic stiffness  $K_d$ , satisfies:

$$T_d \leq 40 \sqrt{D/g} \quad 9-24$$

AASHTO (2010) caps  $T_d$  at 6.0 sec, and this limitation effectively restricts  $D$  to less than or equal to 9.0 in.

It is noted that the minimum stiffness given by Equation 9-23 is satisfied if the restoring force at displacement  $D$  is greater than the restoring force at displacement  $0.5D$  by at least  $W/80$ .

Isolation systems with a constant restoring force need not satisfy these requirements provided the force in the isolation system is at least 1.05 times the characteristic strength  $Q_d$ .

Forces that are not dependent on displacement, such as viscous forces, cannot be used to meet the above requirements.

The design strategy of requiring a strong restoring force is based on the experience that bridge failures in earthquakes have primarily been the result of excessive displacements. By requiring a strong restoring force, cumulative permanent displacements are avoided and the prediction of displacement demand is accomplished with less uncertainty. By contrast, seismic isolation systems with low restoring forces ensure that the force transmitted by the bearing to the substructure is predictable with some certainty. However, this is accomplished at the expense of uncertainty in the resulting displacements and the possibility for significant permanent displacements. Tsopelas and Constantinou (1997) have demonstrated the potential for significant permanent displacements in shake table testing of bridge models with seismic isolation systems having weak restoring force capability.

#### 9.4.4 Uplift, Restrainers and Tensile Capacity

Isolation bearings are subjected to varying axial loads during an earthquake due to the overturning effect of the resultant horizontal seismic load, which acts above the plane of the isolators in most bridges. Under certain conditions, these axial load variations may exceed the compression in the bearing due to the self weight of the bridge, and either uplift occurs (e.g., if sliding bearings and doweled rubber bearings are used) or the bearing experiences tension (e.g., if bolted rubber bearings are used).

Whereas this effect is present in all bridge superstructures, it is most pronounced when the depth : width ratio of the superstructure is high, such as in a long span, continuous, single cell, concrete box girder bridge with a high centroidal axis and relatively narrow cell width. In such cases, and especially over the pier, the centroidal axis (and center of mass) of the girder is sufficiently high that uplift may occur due to the lateral earthquake force. The likelihood of uplift is even greater if unfavorable vertical excitations are present.

The consequences of tension and uplift in isolation bearings may be one of the following:

- (1) *catastrophic*, when the isolators rupture, can no longer support the vertical load and the structure is unseated even though the uplift may be small (unless the designer provides an alternative load path), or
- (2) *problematic*, when significant uplift occurs without rupture, but the impact on the return half-cycle damages the isolator, or
- (3) *uneventful*, when both the uplift and tensile forces are minor and measures have been taken in the design of the isolator and substructure to resist the resulting axial loads and shear forces.

Nevertheless, it is preferred to avoid both uplift and tensile forces out of concern for the behavior of the isolators under conditions that are not well understood nor easily analyzed. Particularly, the tensile capacity of elastomeric bearings is not well understood.

#### 9.4.5 Clearances

Adequate clearances should be provided at the abutments to allow the superstructure to move freely during an earthquake. This clearance should be provided in two orthogonal directions and should not be less than the greater of:

- the calculated superstructure displacement,
- $8 S_{DI} T_{eff} / B_L$  (inches), or
- 1 inch

where  $S_{DI}$ ,  $T_{eff}$  and  $B_L$  are as defined for Equations 9-6 and 9-7.

The purpose of these minima is to ensure adequate capacity for movement regardless of the results of higher order analyses. They are a consequence of the many uncertainties in seismic design and particularly a lack of confidence in the frequency content, duration and intensity of the ground motions.

#### **9.4.6 Vertical Load Stability**

A high factor of safety against instability is recommended for all isolators when carrying dead plus live load but not laterally deformed (i.e. non-seismic load case). Article 12.3 AASHTO (2010) requires a factor of 3.0 in these conditions.

Stability is also required (Factor of Safety  $\geq 1.0$ ) under either:

- (1) 1.2 times dead load + axial load due to overturning caused by seismic loads while deformed to 1.5 times the total design displacement ( $D$ ) for a 1000-year event with  $S_{DI} > 0.3$ , or 2.0 times the total design displacement ( $D$ ) for a 1000-year event with  $S_{DI} \leq 0.30$  ( $S_{DI}$  is defined in Figure 2-9), or
- (2) 1.2 times dead load + axial load due to overturning caused by seismic loads while deformed to 1.1 times the total design displacement ( $D$ ) for the maximum considered event.

#### **9.4.7 Non-Seismic Requirements**

Isolation systems are required to resist all non-seismic lateral load combinations that are applied to the bridge superstructure. Resistance to forces such as wind, centrifugal acceleration, braking, and thermally induced effects should be provided by a rational means and be verifiable by test.

### **9.5 ELASTOMERIC ISOLATORS**

Elastomeric bearings have been used for more than 50 years to accommodate thermal expansion effects in bridges and allow rotations at girder supports. Extending their application to seismic isolation has been

attractive in view of their high tolerance for movement and overload and minimal maintenance requirements. Three types of elastomeric isolator have evolved over the years to meet different requirements. These are:

- Lead-rubber isolator: natural rubber elastomeric bearing fitted with a lead core for energy dissipation
- High-damping rubber isolator: natural rubber elastomeric bearing fabricated from high damping rubber for energy dissipation
- Low-damping rubber isolator: natural rubber elastomeric bearing fabricated from low damping rubber (standard natural rubber) and used alongside a mechanical energy dissipator such as a viscous damper for energy dissipation.

In bridge applications the most common elastomeric isolator is the lead-rubber isolator and this device is the focus of the material presented in this section. Example 9-3 in Section 9.7 illustrates the design process for Lead-Rubber Isolators that is described below.

### 9.5.1 Lead Rubber Isolators

Lead-rubber isolators are elastomeric bearings fitted with a central lead core to increase the dissipation of energy during lateral displacements. As with other bridge isolators, these devices are usually installed directly under the superstructure and are seated on the substructures, in place of conventional expansion bearings. A section through a typical circular lead-rubber bearing is shown in Figure 9-12.

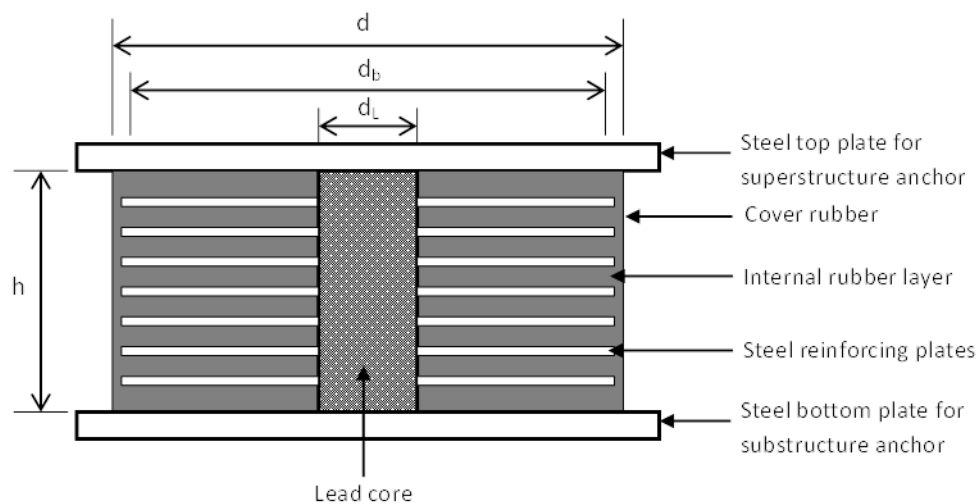


Figure 9-12 Cross section of Typical Lead-Rubber Isolator (Buckle et. al., 2006)

The bearing is made from layers of vulcanized rubber sandwiched together between thin layers of steel (shims). In the middle of the bearing is a solid lead-core. The core is inserted into a pre-formed hole in the bearing and is sized so that it is an interference fit after installation. Steel plates are fitted to the top and bottom of the bearing to attach to the masonry and sole plates on the sub- and super-structures respectively. The internal rubber layers provide flexibility in the lateral direction. The steel reinforcing plates provide confinement to the lead core, vertical stiffness and vertical load capacity. The lead core provides resistance to wind-induced and vehicle braking forces, to minimize the movement of the structure under service loads, but yields and dissipates energy under seismically-induced lateral movements. Creep in the lead permits slowly applied environmental movements (such as thermal expansion) to be accommodated with minimal effect on the substructures. The cover rubber protects the steel layers from environmental effects. The bearing is very stiff and strong in the vertical direction, but flexible in the horizontal direction (once the lead core yields).

#### 9.5.1.1 Mechanical Characteristics of Lead-Rubber Isolators

The mechanical characteristics of lead-rubber bearings with circular cross-section will be discussed here. The behavior of bearings with square or rectangular cross-section is similar. The combined lateral stiffness of the rubber layers and the lead core provide a large lateral elastic stiffness under service loads to control the movements of the structure. Under the effect of seismic loads the steel reinforcing plates force the lead-core to deform in shear. The lead yields at a low shear stress of about 1.3 ksi (9.0 MPa). Once the yielding takes place, the lateral stiffness of the bearing is considerably reduced. The rubber layers then easily deform in shear providing the lateral flexibility to elongate the period of the bridge. Figure 9-13 shows the deformation of the bearing under lateral load.

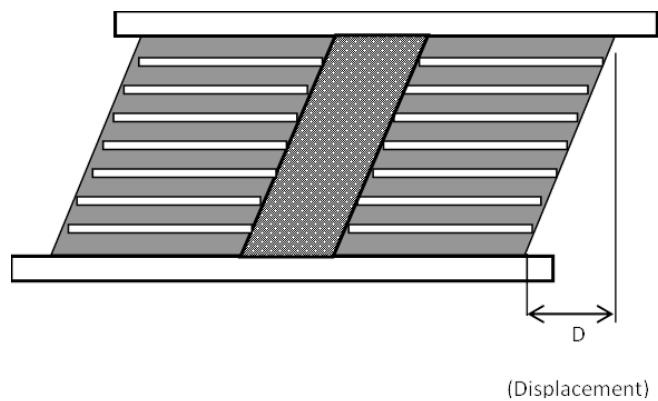


Figure 9-13 Shear Deformation in a Lead Rubber Isolator (Buckle et. al., 2006)

Figure 9-3 shows the idealized hysteretic behavior of the bearing. In the hysteresis loop of Figure 9-3,  $Q_d$  is the characteristic strength of the bearing and  $F_y$  is the yield strength. Since the elastomer is a low-damping natural rubber, both  $Q_d$  and  $F_y$  are determined by the lead core as follows:

$$F_y = \frac{1}{\psi} f_{yL} \frac{\pi d_L^2}{4} \quad 9-25$$

where  $f_{yL}$  = shear yield stress of the lead (1.3 ksi)

$d_L$  = diameter of the lead plug, and

$\psi$  = load factor accounting for creep in lead

= 1.0 for dynamic (seismic, wind and braking) loads

= 3.0 for slowly applied displacements (environmental effects such as thermal expansion/contraction).

The characteristic strength,  $Q_d$ , is then given by:

$$Q_d = F_y \left( 1 - \frac{K_d}{K_u} \right) \quad 9-26$$

where  $K_d$  = post elastic stiffness

$K_u$  = elastic loading and unloading stiffness

=  $n K_d$

$n$  = 10 for dynamic (seismic, wind and braking) loads

= 5 for slowly applied displacements (environmental effects such as thermal expansion/contraction)

For seismic loads, Equation 9- becomes:

$$Q_d = 0.9F_y \quad 9-27$$

It follows from Equations 9- and 9-, that for  $f_{yL} = 1.3$  ksi (9.0 MPa) and  $\psi = 1.0$

$$Q_d \approx 0.9d_L^2 \text{ K } (d_L \text{ in inches}) \quad 9-28$$

$$Q_d \approx 6.4d_L^2 \text{ N } (d_L \text{ in millimeters}) \quad 9-29$$

The post-elastic stiffness  $K_d$  is primarily due to the stiffness of the rubber but is also influenced by the post-yield stiffness of the lead core. Thus

$$K_d = fK_r \quad 9-30$$

where  $f$  is a factor to account for the contribution of the lead (generally taken equal to 1.1), and  $K_r$  is the elastic stiffness of the rubber material given by:

$$K_r = \frac{GA_b}{T_r} \quad 9-31$$

where  $G$  = shear modulus of rubber

$T_r$  = total thickness of rubber

$A_b$  = net bonded area of rubber

The net bonded area  $A_b$  is the gross area the bearing less the area of the lead core. Thus:

$$A_b = \frac{\pi(d_b^2 - d_L^2)}{4} \quad 9-32$$

where  $d_b$  is the diameter of bonded rubber.

The equivalent (linearized) properties of the lead-core isolator for use in elastic methods of analysis are the effective stiffness  $K_{eff}$  and the equivalent viscous damping ratio  $h$  as given by Equations 9-2 and 9-5.

An acceleration response spectrum with 5% damping is then modified for the actual damping,  $h$  and used for calculating the response of the isolated bridge (see Section 9.3).

### 9.5.1.2 Strain Limits in Rubber

The bearing must be designed with adequate dimensions to accommodate the gravitational loads and imposed shear displacements and rotations in both the service limit state (non-seismic load case) and the extreme event state (seismic load case). Accordingly the service limit states of AASHTO (2013) (Equations 14.7.5.3.3-1 and -2) and the extreme limit state of AASHTO (2010) (Equation 14.3-1), should be satisfied. The latter equation is as follows:

$$\gamma_c + \gamma_{s,eq} + 0.5\gamma_r \leq 5.5 \quad 9-33$$

where  $\gamma_c$ ,  $\gamma_r$  and  $\gamma_{s,eq}$  are the shear strains respectively due to the effect of vertical loads, lateral displacements, and rotations imposed by vertical loads and seismic loads as defined in Equations 9-, 9-, and 9- below.

#### 9.5.1.2.1 Compressive Strains

The maximum compressive strain in a rubber layer due to vertical load is given by:

$$\gamma_c = \frac{D_c \sigma_s}{GS} \quad 9-34$$

where  $D_c$  = shape coefficient for shear strains due to compression

= 1.0 for both circular and rectangular bearings

$\sigma_s$  = average compressive stress due to vertical load on the bearing

$G$  = shear modulus of elastomer

$S$  = layer shape factor, defined for circular lead plug rubber bearings as:

$$S = \frac{d_b^2 - d_L^2}{4d_b t_i} \quad 9-35$$

#### 9.5.1.2.2 Shear Strains

The shear strain,  $\gamma_{s,eq}$ , due to seismic lateral design displacement,  $D$ , is given by:

$$\gamma_{s,eq} = \frac{D}{T_r} \quad 9-36$$

The shear strain,  $\gamma_r$ , due to the design rotation,  $\theta$ , that include the rotational effects of dead load, live load and construction is given by:

$$\gamma_r = \frac{D_r d_b^2 \theta}{t_i T_r} \quad 9-37$$

where  $D_r$  = shape coefficient for shear strains due to rotation  
 = 0.375 for circular bearings  
 = 0.5 for rectangular bearings

In general, the torsional stiffness of individual bearings, and the stresses and strains resulting from torsion, are insignificant and may be neglected.

### 9.5.1.3 Stability of Lead-Rubber Isolators

Elastomeric bearings need to be checked against the possibility of instability in both the undeformed and deformed displaced states.

Instability is influenced by the installation details and there are two common types for these connections:

- (1) A moment-and-shear connection, such as a bolted connection to both the masonry and sole plates.
- (2) A shear-only connection, such as a doveled connection to the masonry and sole plates.  
 Alternatively, keeper bars welded to both plates may be used, or the bearing located within recesses in both plates

#### 9.5.1.3.1 Stability in Undeformed State

In the undeformed state and loaded only in the vertical direction, the critical load for bearings installed in either of the above two configurations is theoretically the same.

For a bearing with moment of inertia  $I$ , cross-sectional area  $A$ , and total rubber thickness  $T_r$ , this load,  $P_{cr}$ , is given by:

$$P_{cr} = \sqrt{\frac{\pi^2 E_c IGA}{3T_r^2}} \quad 9-38$$

where  $G$  is the shear modulus, and  $E_c$  is the modulus of elasticity of the rubber in compression and is given by:

$$E_c = \frac{1}{\left(\frac{1}{6GS^2} + \frac{4}{3\kappa}\right)} \quad 9-39$$

If the bulk modulus  $\kappa$ , is assumed to be infinite, then Equation 9-39 gives  $E_c = 6GS^2$  and for circular bearings with diameter  $d_b$  and layer thickness  $t$ , Equation 9-38 becomes:

$$P_{cr} = 0.218 \frac{Gd_b^4}{tT_r} \quad 9-40$$

For square bearings with side  $B$  and layer thickness  $t$ , Equation 9-38 becomes:

$$P_{cr} = 0.344 \frac{GB^4}{tT_r} \quad 9-41$$

The factor of safety against buckling in the undeformed state is calculated by dividing  $P_{cr}$ , by the total load due to dead plus live load.

### 9.5.1.3.2 Stability in Deformed State

In the deformed state the critical load depends on which of the above two configurations is used.

Case (1). For bolted connections, the critical load will be given by buckling as in the previous section, but modified to include the effect of the lateral deformation. However there is no simple rational theory that includes this effect and the following intuitive equation is used in lieu of a more rigorous solution (Buckle and Liu, 1994):

$$P'_{cr} = P_{cr} \frac{A_r}{A} \quad 9-42$$

where  $P'_{cr}$  = buckling load in deformed state

$A$  = bonded elastomer area, and

$A_r$  = effective column area defined as the area of the overlap between the top and bottom bonded areas of the deformed bearing (see Figure 9-14).

Using values for  $A_r$  given in Figure 9-14, it follows that:

$$P'_{cr} = P_{cr} \frac{(\delta - \sin \delta)}{\pi} \text{ for a circular bearing} \quad 9-43$$

and

$$P'_{cr} = P_{cr} \left(1 - \frac{d_t}{B}\right) \text{ for a square bearing} \quad 9-44$$

The factor of safety against instability due to buckling is calculated by dividing  $P'_{cr}$ , by the load due to dead plus seismic live load.

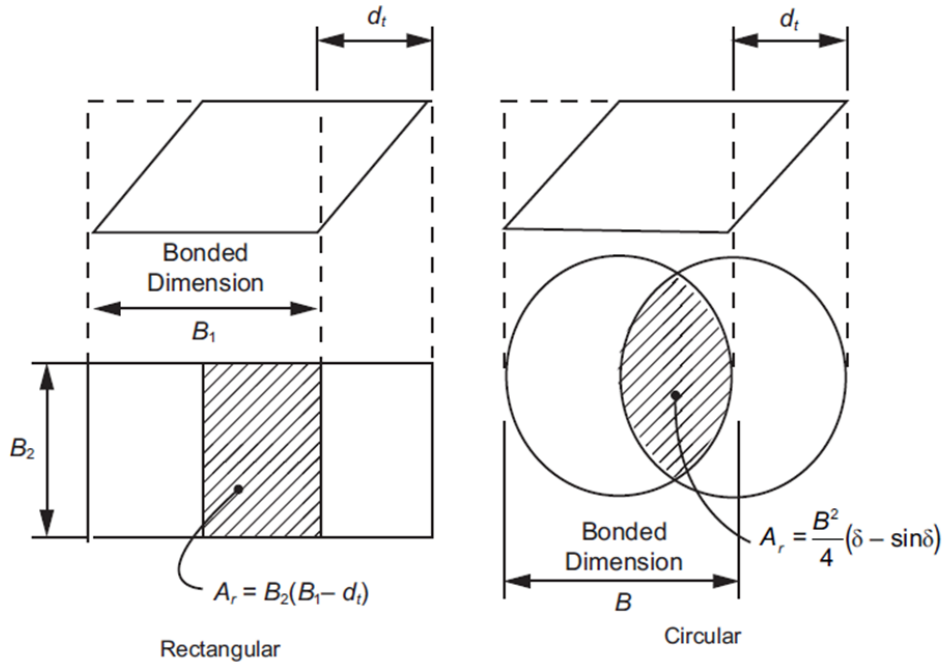


Figure 9-14 Overlap Area,  $A_r$ , Between Top-Bonded and Bottom-Bonded Areas of Elastomer in a Displaced Elastomeric Isolator (AASHTO, 2010)

Case (2) During large lateral deformation, dowelled bearings and bearings recessed in keeper plates may experience partial uplift. At some critical lateral displacement,  $D_{cr}$ , the bearings roll-over, i.e. overturn. The critical value of this displacement is given by:

$$D_{cr} = \frac{PB - Q_d H}{P + k_d H} \quad 9-45$$

where  $P$  = axial load on the bearing

$B$  = plan dimension (e.g. diameter)

$Q_d$  = characteristic strength

$k_d$  = post-elastic stiffness, and

$H$  = total height of bearing (total rubber thickness plus steel shims and end plates).

The factor of safety against instability due to rollover is given by dividing the rollover displacement  $D_{cr}$  by the design displacement  $D_d$ .

#### 9.5.1.4 Stiffness Properties of Lead-Rubber Isolators

In addition to the effective lateral stiffness,  $K_{eff}$ , the axial (compressive) and torsional stiffnesses of the isolators may be required for structural modeling of the bearings in a detailed seismic analysis. In the calculation of the axial stiffness of the bearing, the compressive stiffness of the steel reinforcing plates is neglected as it is much larger than that of the rubber. Thus, the axial stiffness,  $K_c$ , of the bearing, is determined by the stiffness of the rubber layers in compression and is given by:

$$K_c = \frac{E_c A_b}{T_r} \quad 9-46$$

where  $E_c$  is given by Equation 9-39 and  $A_b$  by Equation 9-32

The axial stiffness is assumed to be independent of axial strain, i.e. it is linear for the range of strains encountered in practice.

Similarly, the torsional stiffness,  $K_T$ , of the bearings is calculated based on the properties of the rubber portion of the bearing conservatively assuming that the entire bearing is made of rubber. Thus:

$$K_T = \frac{GJ}{T_r} \quad 9-47$$

where  $J$  is the polar moment of inertia of the entire bearing cross-section and for a circular section is given by:

$$J = \frac{\pi d_b^4}{32} \quad 9-48$$

The torsional stiffness is assumed to be independent of torsional strain, i.e. it is linear for the range of strains encountered in practice.

## 9.5.2 Properties of Natural Rubber

Elastomeric isolators use either natural or synthetic rubbers and in the United States, the most commonly-used elastomer in seismic isolators is natural rubber. Whereas neoprene (a popular synthetic rubber) has been used extensively in expansion bearings for bridges, there are few if any applications of neoprene to isolation bearings. This is because very high shear strains can occur in isolation bearings under extreme seismic loads and natural rubber performs better under these conditions than neoprene (it has higher elongation-at-break). Accordingly this section focuses on natural rubber. The notes below are adapted from Lindley (1978).

Natural rubber is a polyisoprene and as such, is a member of a high-polymer family that includes silk, cellulose, wool, resins and synthetic plastics and rubbers. The distinguishing feature of this family is the long length of the molecular chain and, for the subdivision which contains natural and synthetic rubbers, the flexible nature of this chain and its ability to deform elastically when cross-linked. Raw rubber occurs as a latex beneath the bark of certain trees, notable *Hevea brasiliensis*, which is cultivated in the plantations of Malaysia and other tropical countries. To make practical use of this material it is first vulcanized, which is a chemical and mechanical process involving mastication while adding sulfur and various fillers, and applying heat. During this process the long chain molecules are chemically linked, usually by sulfur, forming an elastic compound with properties that depend on the curing conditions (temperature and time) and the additives.

Mechanical and other properties of natural rubber are listed in Table 9-5 and discussed further below.

### 9.5.2.1 Elastic Modulus, $E$

Vulcanized rubber is a solid three-dimensional network of crosslinked molecules. The more crosslinks there are in the network, the greater the resistance to deformation under stress. Certain fillers, notably

reinforcing blacks (carbon), create a structure within the rubber which further increases both strength and stiffness. Load-deflection curves are approximately linear at small strains (less than a few percent) and values of the elastic modulus can be obtained from these linear regions. Values in tension and compression are approximately equal. Table 9-5 gives typical values for natural rubbers of varying hardness (amounts of carbon black filler).

#### **9.5.2.2 Bulk Modulus, $\kappa$**

Typical values for the bulk modulus of rubber range from 145 - 200 ksi and are many times larger than corresponding values for elastic modulus (130 - 1400 psi). These very high numbers mean that rubber is virtually incompressible and Poisson's Ratio may be taken as 0.5. Table 9-5 gives typical values for natural rubbers of varying hardness (amounts of carbon black filler).

#### **9.5.2.3 Shear Modulus, $G$**

Theoretically, with a Poisson's ratio of 0.5, the shear modulus is one-third the elastic modulus. Test results show this to be true for soft gum rubbers (un-filled rubbers), but for harder (filled) rubbers that contain a reasonable proportion of non-rubber constituents, thixotropic and other effects reduce the shear modulus to about one-fourth of the elastic modulus. This can be seen in Table 9-5 where the ratio of elastic to shear modulus increases from about 3 to more than 4 as the hardness increases from 30 to 75.

#### **9.5.2.4 Hardness**

Hardness measurements are generally used to characterize vulcanized rubber as seen in Table 9-5. For rubber, hardness is essentially a measurement of reversible elastic deformation produced by a specially shaped indenter under a specified load and is therefore related to the elastic modulus of the rubber, unlike metal hardness which is a measure of an irreversible plastic indentation. Readings using International Rubber Hardness degrees (IRHD) and the Shore Durometer A Scale are essentially the same. Hardness is a relatively simple and easy number to obtain but is subject to some uncertainty ( $\pm 2^0$  in Table 9-5). Values for shear modulus are more accurate but more difficult to measure.

**TABLE 9-5 HARDNESS AND MODULI FOR A CONVENTIONAL RUBBER COMPOUND<sup>1</sup>**

Hardness IRHD / Shore A	Elastic modulus, $E^2$		Shear modulus, $G^2$		Material constant, $k^3$	Bulk modulus, $K^4$	
	psi	MPa	psi	MPa		psi	MPa
30	133	0.92	44	0.30	0.93	145,000	1000
35	171	1.18	49	0.37	0.89	145,000	1000
40	218	1.50	65	0.45	0.85	145,000	1000
45	261	1.80	78	0.54	0.80	145,000	1000
50	319	2.20	93	0.64	0.73	149,350	1030
55	471	3.25	117	0.81	0.64	158,050	1090
60	645	4.45	152	1.06	0.57	166,750	1150
65	862	5.85	199	1.37	0.54	175,450	1210
70	1066	7.35	251	1.73	0.53	184,150	1270
75	1363	9.40	322	2.22	0.52	192,850	1330

- Notes:**
1. Data in table are for a conventional, accelerated-sulphur, natural rubber compound, using SMR 5 (highest grade Standard Malaysian Rubber) and reinforcing black filler for hardnesses above 45. Tensile strength is 3,770 psi. Elongation at break is 730% (Lindley, 1978).
  2. For an incompressible material (Poisson's ratio = 0.5), the elastic modulus is theoretically three times the shear modulus. Although rubber is virtually incompressible (Poisson's ratio = 0.4997), the ratio between these two moduli in the above table varies from 3.1 (at hardness= 30) to 4.2 (at hardness = 75). This is believed to be due to the effect of non-rubber fillers added to the compound to increase hardness (reinforcing black), improve resistance to environment (anti-oxidants), and assist with processing.
  3. Material constant,  $k$ , is used to calculate compression modulus ( $E_c$ ) of bonded rubber layers, i.e.,  $E_c = E(1 + 2kS^2)$ , where  $S$  is the layer shape factor.
  4. Bulk Modulus values are very sensitive to test method especially for samples with high shape factors. Other data (e.g., Wood and Martin (1964)) suggest values twice those listed above, particularly for parts with high shape factors.

### 9.5.2.5 Ultimate Strength and Elongation-at-Break

The tensile strength of a good quality natural rubber is in the range 2 - 4 ksi, based on the original cross-sectional area, and the strain at rupture (elongation-at-break) will be in the range 500 – 750 %. If the area-at-break is used to calculate the ultimate strength, it can be as high as 30 ksi. Compressive strengths are typically of the order of 25 ksi.

### 9.5.2.6 Fillers

Rubbers that contain only sulphur (and other chemicals necessary for vulcanization such as stearic acid and zinc oxide), protective agents, and processing aids, are known as gum rubbers, or un-filled rubbers.

By far the majority of rubbers used in engineering applications also contain fillers such as carbon black which may comprise up to one-third of the vulcanizate compound. These black fillers fall into two groups: (1) ‘reinforcing’ blacks, which improve tear and abrasion properties, and increase elastic modulus, hysteresis and creep, and (2) ‘non-reinforcing’ blacks, which have little effect on tear and abrasion and give only moderate increases in modulus, hysteresis and creep. They can however be used in greater volumes than reinforcing blacks.

#### **9.5.2.7 Hysteresis**

Natural unfilled rubbers exhibit very little hysteresis but, as noted above, fillers can be used to increase this effect. The High-Damping Rubber (HDR) isolator is device where fillers are added to increase the hysteresis to a level where the energy dissipation is sufficient to limit structure displacements in a cost-effective manner. However, uncertainty about creep and scragging effects has limited their application and few, if any, HDR isolators have been used in bridge applications. By contrast natural rubbers with minimal amounts of filler (just sufficient for hardness and abrasion resistance), are used almost exclusively in elastomeric bridge isolators in the U.S. In these cases, energy dissipation for displacement control is provided by a separate mechanical means, such as a lead core that yields or a friction device.

#### **9.5.2.8 Temperature Effects**

The physical properties of rubber are generally temperature dependent, but these effects are also fully reversible provided no chemical change has occurred within the rubber. Below  $-5^{\circ}\text{F}$ , the stiffness (hardness) of a typical natural rubber begins to increase until, at about  $-75^{\circ}\text{F}$ , it is glass-like and brittle. This glass-hardening phenomenon is fully reversible and elasticity is recovered as the temperature is increased. Natural rubber will also crystallize and lose elasticity if it is held for several days at its crystallization temperature (about  $-15^{\circ}\text{F}$  for a typical compound). Like glass-hardening, this effect also disappears quickly as the temperature is increased. The temperatures at which these two phenomena occur can be lowered by compounding the rubber specifically for low-temperature applications.

Typical rubbers can be used at sustained temperatures up to  $140^{\circ}\text{F}$  without any deleterious effect (but see note below about susceptibility to oxygen, UV and ozone). Specially compounded rubbers are available for applications up to  $212^{\circ}\text{F}$ . At temperatures approaching those used for vulcanizing (about  $285^{\circ}\text{F}$ ), further vulcanization may occur resulting in increased hardness and decreased mechanical strength. At very high temperatures (above say  $660^{\circ}\text{F}$ ), rubber first softens as molecular breakdown occurs and then becomes resin-like, i.e., hard and brittle.

### 9.5.2.9 Oxygen, Sunlight and Ozone

Exposure to oxygen, ultra-violet (UV) radiation, and ozone generally results in a deterioration of physical properties and an increase in creep and stress relaxation. These effects are more pronounced in parts with thinner cross-sections, and/or subject to tensile strain. Elevated temperatures may also accelerate these effects. As a result, antioxidants are almost always added to natural rubber compounds intended for engineering applications, along with carbon black fillers for UV protection, and waxes for ozone resistance.

### 9.5.2.10 Chemical Degradation

Natural rubber is remarkably resistant to a wide range of chemicals from inorganic acids to alkalies. However, if a large volume of a liquid is absorbed, rubber will swell and lose strength. The extent of this swelling depends on the liquid and the nature of the rubber compound. Typical natural rubbers have excellent swelling resistance to water, alcohol, and vegetable oils, but are very susceptible to low-viscosity petroleum products such as gasoline. Whereas the occasional splashing of a rubber part with gasoline is not likely to be serious, immersion should be avoided. Such a situation is not anticipated in isolators intended for bridge applications but in the unlikely event that it did occur, due say to an overturned gasoline tanker, the large physical size of these devices is expected to give adequate time for clean-up before swelling becomes significant.

### 9.5.3 Properties of Lead

Pure lead has a yield stress in shear of about 1.3 ksi which means that lead cores with reasonable sized dimensions can be designed such that wind and other service loads can be resisted within the elastic range. Nevertheless it is important that the core size is neither too small nor too large for the elastomeric bearing in which it is to be fitted. As a general rule, the core diameter ( $d_L$ ) should fall within the following range:

$$\frac{B}{6} < d_L < \frac{B}{3} \quad 9-49$$

where  $B$  = bonded diameter if a circular bearing, or side dimension if square.

It is also important that the lead be tightly confined within the bearing, which means that the rubber layer thickness should not exceed 3/8 in and the ends of the core be sealed by end caps in the cover plate. These

caps not only help confine the lead but also protect the ends of the core against damage during shipping and installation.

Pure lead recrystallizes at room temperature which means that after extrusion or shear deformation the elongated grains necessary to accommodate the deformation, regain their original shape almost instantaneously. Most metals exhibit recrystallization but few do so at room temperature. Lead therefore does not work-harden at room temperature and it is virtually impossible to cause lead to fail by fatigue. These characteristics apply only to chemically pure lead; the slightest contamination with antimony and other elements that occur naturally with lead, will elevate the recrystallization temperature leading to work-hardening at ambient temperatures.

Lead also has a relatively high creep coefficient which means that slowly applied deformations, such as expansion and contraction due to seasonal temperature changes in the superstructure, can occur without significant resistance. Loads imposed on substructures due to these effects are correspondingly small.

The mechanical properties of lead are very stable with time and the system property modification for lead is set equal to 1.0 (Table 9-7).

#### **9.5.4 Effects of Variability of Properties, Aging, Temperature and Load History**

The properties of isolators inevitably vary due to manufacturing differences, aging, wear, history of loading, temperature, and the like. These variations may alter the effective period and equivalent damping of the isolation system, both of which will influence the dynamic response of the isolated structure. The interested reader is referred to Constantinou et al. (1999) for a detailed description of these effects. They are briefly discussed below.

##### **9.5.4.1 Variability of Properties**

The mechanical properties of seismic isolation hardware exhibit variability in values as a result of natural variability in the properties of the materials used and as a result of the quality of manufacturing. It is not unusual to have properties, such as the post-elastic stiffness or the characteristic strength in a particular cycle of reversed loading, differ by  $\pm 25$  percent from the average values among all tested isolators.

##### **9.5.4.2 Aging**

Aging is the degradation or change of properties with time. Herein, a brief description of the aging

effects on the mechanical properties of characteristic strength and post-elastic stiffness of seismic isolation hardware is presented. Moreover, it should be recognized that aging may also have effects on the ability of the isolation hardware to sustain stress, strain, force or deformation, which also need to be considered in design.

Seismic isolation is a relatively new technology so that the field observation of performance of seismic isolation hardware is limited to about 25 years. Actual data on the mechanical properties of seismic isolation bearings removed from structures and re-tested after years of service are limited to a pair of bearings but the results are inclusive given that the original condition of the bearings was not exactly known. However, there is considerable information collected from the field inspection of seismic isolation and other similar bearings, from testing of field-aged bearings in non-seismic applications, from laboratory studies and from theoretical studies. While this information is indirect, it is very useful and may be summarized as follows:

- (1) Aging in elastomeric bearings is dependent on the rubber compound and generally results in increases in both the stiffness and the characteristic strength. These increases are expected to be small, likely of the order of 10-percent to 20-percent over a period of 30 years, for the standard low damping, high shear modulus compounds (shear modulus of 70 to 140 psi). However, the increases may be larger, and likely substantially larger, for improperly cured bearings and for materials compounded for either very high damping or very low shear modulus.
- (2) The continuous movement of bearings due to traffic loads in bridges may cause wear and fatigue. While AASHTO (2010) requires that tests be performed to evaluate the effects of cumulative movement of at least 1 mile, such tests have not been performed on elastomeric bearings. It is expected that such tests may reveal some but not significant change in properties.

#### **9.5.4.3 Temperature**

The effects of temperature on the mechanical properties of seismic isolation bearings may be discussed in two distinct ways: (a) the effect of heating (viscous, hysteretic or frictional) on the mechanical properties during cyclic movement of the bearings, and (b) the effect of ambient temperature (and particularly low temperature) and of the duration of exposure to this temperature on the mechanical properties.

#### **9.5.4.3.1 Heating During Cyclic Movement**

In elastomeric bearings without a lead core, heating results from energy dissipation in the entire volume of rubber. Constantinou et al. (1999) have shown that for typical conditions (pressure of 1 ksi, shear strain of 150-percent), the rise in temperature is about 2<sup>0</sup>F or less per cycle regardless of the speed of the cyclic movement. This figure is consistent with experimental results. The temperature rise is too small to have any significant effect on the mechanical properties of the bearings.

In lead-rubber bearings, the energy dissipation primarily takes place in the lead core which is substantially heated during cyclic movement. During the first couple of cycles, when the generated heat in the lead core is entirely consumed for the rise of its own temperature, rises in temperature of the order of 40 to 80<sup>0</sup>F per cycle have been calculated (Constantinou et al., 1999) for typical conditions (pressure of about 800 psi, shear strain of 120-percent, velocity of up to 40 in/sec). Under these conditions, the mechanical properties of lead (e.g., ultimate strength and effective yield stress) become smaller, resulting in a noted reduction of energy dissipated per cycle.

#### **9.5.4.3.2 Effect of Ambient Temperature**

Low temperatures generally cause an increase in stiffness and characteristic strength (or friction in sliding bearings). For elastomeric bearings this increase is depicted in Figure 9-15. As noted in Section 9.5.2.8, elastomers exhibit almost instantaneous stiffening when exposed to low temperatures, which is followed by further time-dependent stiffening (Constantinou et al., 1999; Roeder et al., 1987). As an example, Figure 9-16 compares loops recorded in testing of an elastomeric bearing (bonded area = 177 in<sup>2</sup>, rubber height = 7.68 in, natural rubber grade 3, shore A hardness 45, tested at peak shear strain of about 60%). The substantial increase in stiffness and energy dissipated per cycle are evident following conditioning for 48 hours in a chamber at -15<sup>0</sup> F temperature. Also, Figure 9-17 compares loops recorded in the testing of a lead-rubber bearing of identical construction as the previously described bearing but with a 2.75 in diameter lead core. Note that in this case the increases in stiffness and energy dissipation per cycle at low temperature are due primarily to changes in the properties of the elastomer and not of the lead core.

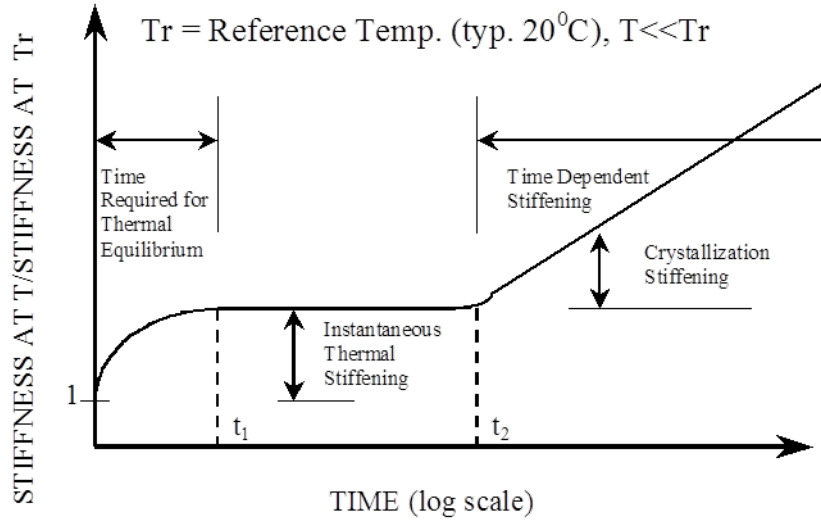


Figure 9-15 Time-Dependent Low-Temperature Behavior of Elastomers (Buckle et.al., 2006)

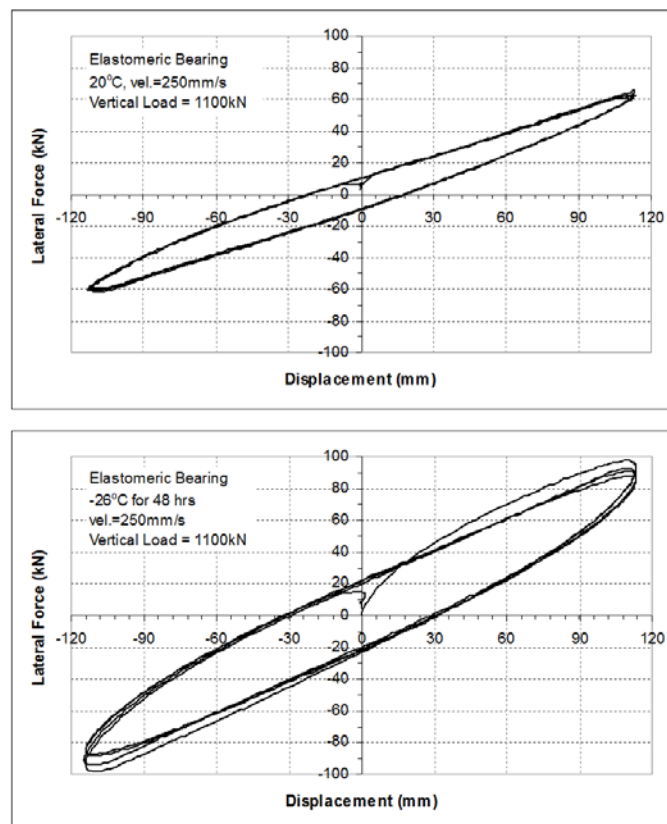


Figure 9-16 Force-Displacement Relation of an Elastomeric Isolator at 68°F (top) and -4°F (bottom) (Buckle et.al., 2006)

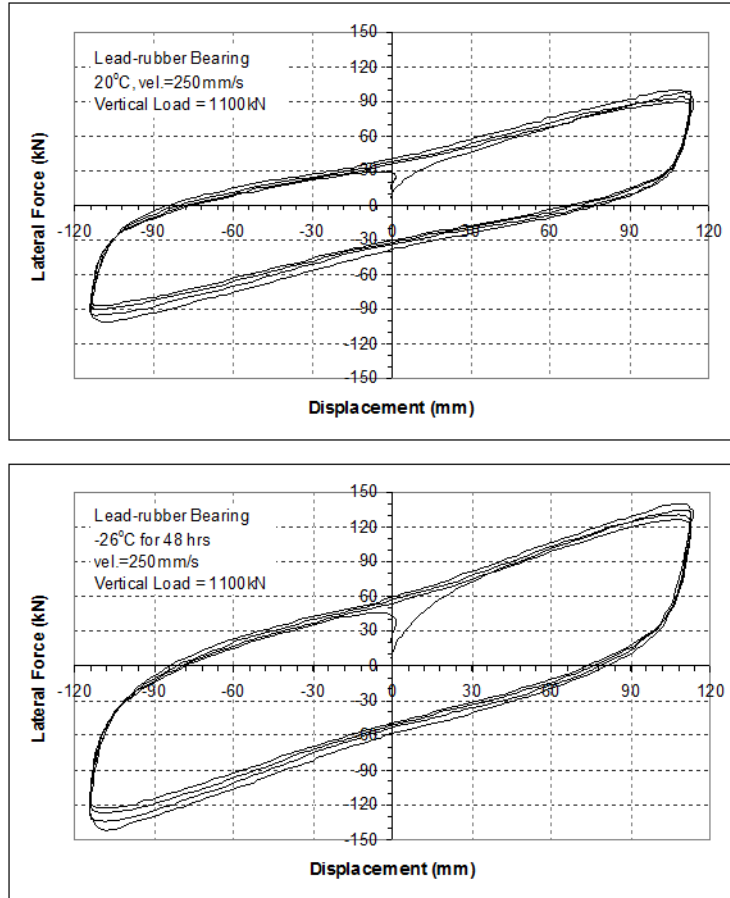


Figure 9-17 Force-Displacement Relation of a Lead-Rubber Isolator at 68<sup>0</sup>F (top) and -4<sup>0</sup>F (bottom) (Buckle et.al., 2006)

#### 9.5.4.4 Loading History

The history of loading can have a marked effect on the mechanical properties of all types of bearings. Some of these effects have a profound impact, leading to significant error if disregarded. Two examples are discussed below: scragging effects in rubber, and cyclic loading in lead-rubber isolators. Cyclic loading effects in friction pendulum isolators are discussed in Section 9.6.5.4.

Shown in Figure 9-18 is the force-displacement relation of a high damping elastomeric bearing (Thompson et al., 2000). The bearing exhibits a substantially higher stiffness during the initial cycle than during the subsequent cycles of motion. The initial stiffness occurs at the unscragged state of the elastomer, that is, under virgin conditions. Following stretching and fracture of molecules of the elastomer during deformation, the bearing reaches the scragged state with stable properties.

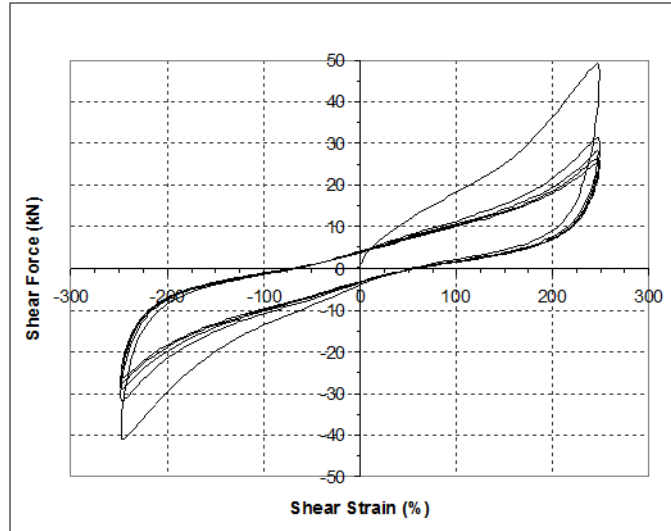


Figure 9-18 Force-Displacement Relation for a Virgin (Unscragged) High-Damping Elastomeric Isolator (Buckle et. al., 2006)

It has been assumed in the past that the elastomer cannot recover to the virgin state so that the initial high stiffness was disregarded in the analysis. However, recent experimental evidence (see Thompson et al., 2000 and Constantinou et al., 1999) demonstrated that recovery occurs within short period of time due likely to continuous chemical activity in the elastomer. Thompson et al. (2000) demonstrated that substantial differences between unscragged and scragged properties are possible in low shear modulus elastomers. It is essential that elastomeric bearings be tested in their virgin stage so that both the unscragged and scragged properties be determined.

Tests conducted on lead-core rubber isolators indicate that the characteristic strength  $Q_d$  of these isolators may deviate from the average by about 20%-25%. In a test involving 3-5 cycles of displacement, the characteristic strength of the bearing in the first cycle is generally about 25% larger than the average characteristic strength from all the cycles. The average characteristic strength from all the cycles represents the target design characteristic strength of the bearing. Accordingly, the initial lower characteristic strength,  $Q_L$ , is set equal to the target design characteristic strength. The initial upper bound characteristic strength,  $Q_U$ , is then initially set equal to  $1.25Q_L$  for design purposes. However, this should later be verified by the actual prototype testing of the bearings and the coefficient 1.25 may be modified accordingly. The initial lower and upper bound characteristic strengths of the bearing are then adjusted using the property modification factors defined below to obtain the minimum and maximum probable characteristic strengths for the isolators.

### 9.5.5 System Property Modification Factors for Elastomeric Isolators

As described in Section 9.4.2, system property modification factors are used to account for the likely variations in isolator properties over the life of an isolated bridge. In this approach, the minimum and maximum effective stiffness and equivalent damping of the isolation system are calculated using the minimum and maximum values of the post-elastic stiffness,  $K_d$ , and characteristic strength,  $Q_d$ , of each isolation bearing. These values of parameters are calculated as the product of (1) the nominal values of these parameters, and (2) the minimum and maximum values of the corresponding system property modification factors.

The minimum value of the system property modification factor ( $\lambda$ -factor) is denoted as  $\lambda_{min}$  and has values less than or equal to unity. Due to the fact that most values of  $\lambda_{min}$  proposed by Constantinou et al. (1999) are close to unity, the AASHTO *Guide Specifications* (AASHTO, 2010) sets  $\lambda_{min}$  equal to unity. That is, the lower bound values of properties of the isolation systems are considered to be the nominal values. These values are defined to be those determined for fresh and scragged specimens under normal temperature conditions.

As noted in Section 9.4.2.2 and shown in Equation 9-16, the maximum value of the  $\lambda$ -factor is calculated from the product of six component factors which account for the effects of temperature, aging, velocity, travel and wear, contamination, and scragging. Values for each of these factors are presented in Tables 9-6 to 9-8 (AASHTO, 2010, and Constantinou et al., 1999).

Recent studies on the scragging factor (Thompson et al., 2000) conclude that the scragging factor values in Table 9-8 should be increased and the shear modulus of the elastomer rather than the equivalent damping should be used to classify materials. Specifically, Thompson et al. (2000) recommend the following values of the  $\lambda$ -factor for scragging: (1) 1.5 for elastomers with shear modulus (at third cycle, at 100% strain) larger than 100 psi, and (2) 2.0 for elastomers with shear modulus less than 100 psi. This recommendation was based on experimental data from about 30 bearings with different elastomeric compounds which were produced by manufacturers in the United States, Japan, England and Italy. Figure 9-19 presents values of the scragging factor as reported by Thompson et al. (2000).

**TABLE 9-6 MAXIMUM VALUES FOR TEMPERATURE  $\lambda$ -FACTORS FOR ELASTOMERIC ISOLATORS,  $\lambda_{max,T}$  (AASHTO, 2010)**

Minimum Temperature For Design		$Q_d$			$K_d$		
°C	°F	HDRB-1	HDRB-2	LDRB	HDRB-1	HDRB-2	LDRB
21	70	1.0	1.0	1.0	1.0	1.0	1.0
0	32	1.3	1.3	1.3	1.2	1.1	1.1
-10	14	1.4	1.4	1.4	1.4	1.2	1.1
-30	-22	2.5	2.0	1.5	2.0	1.4	1.3

**Note:** HDRB-1 is High Damping Rubber Bearing with large difference (more than 25%) between scragged and unscragged properties

HDRB-2 is High Damping Rubber Bearing with small difference (less than or equal to 25%) between scragged and unscragged properties

LDRB is Low Damping Rubber Bearing (conventional natural rubber bearing)

**TABLE 9-7 MAXIMUM VALUES FOR AGING  $\lambda$ -FACTORS FOR ELASTOMERIC ISOLATORS,  $\lambda_{max,a}$  (AASHTO,2010)**

Material	$K_d$	$Q_d$
Low Damping Natural Rubber (LDRB)	1.1	1.1
High Damping Rubber with large differences (>25%) between scragged and unscragged properties (HDRB-1)	1.3	1.3
High Damping Rubber with small differences ( $\leq$ 25%) between scragged and unscragged properties (HDRB-2)	1.2	1.2
Lead	-	1.0
Neoprene	3.0	3.0

**TABLE 9-8 MAXIMUM VALUES FOR SCRAGGING  $\lambda$ -FACTORS FOR ELASTOMERIC ISOLATORS,  $\lambda_{max,scrag}$  (AASHTO, 2010)**

Material	$Q_d$	$K_d$
LDRB	1.0	1.0
HDRB-A	1.2	1.2
HDRB-B	1.5	1.8

**Note:** HDRB-A is High Damping Rubber Bearing with equivalent viscous damping ratio  $\leq 0.15$

HDRB-B is High Damping Rubber Bearing with equivalent viscous damping ratio  $> 0.15$

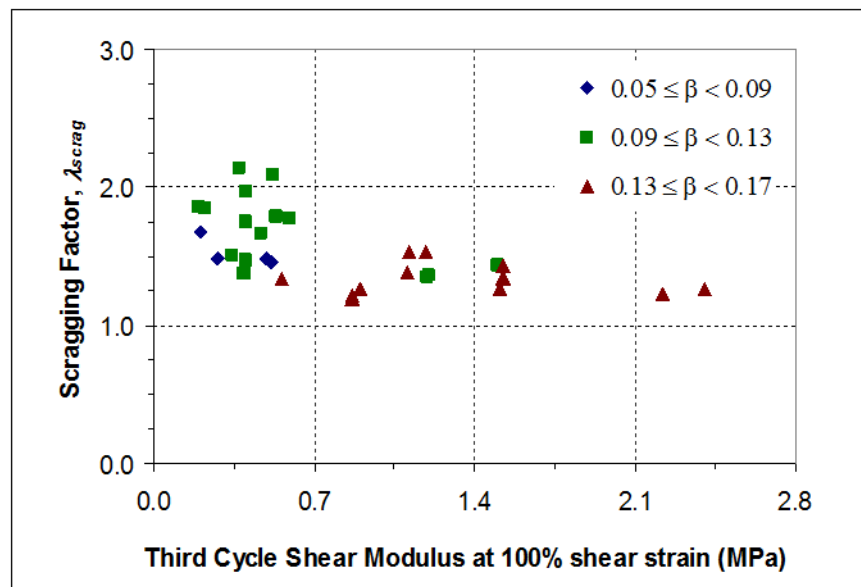


Figure 9-19 Values of the Scragging  $\lambda$ -Factor for Elastomeric Isolators (Buckle et. al., 2006)

## 9.6 SLIDING ISOLATORS

Contemporary sliding seismic isolation systems take a variety of forms but, in general, are of two types: (a) those with flat sliding surfaces, and (b) those with curved sliding surfaces.

Flat sliding bearings have been used for many years to accommodate expansion and contraction movements in bridges. Three basic types are shown in Figure 9-20, where they are seen to differ by the nature of the rotational element beneath the sliding surface: pot, disk, or ball and socket. This element allows the flat surface to rotate about a horizontal axis (simulating a pinned connection), with the ball and

socket having the least rotational resistance and hence the most favorable distribution of pressure on the sliding surface.

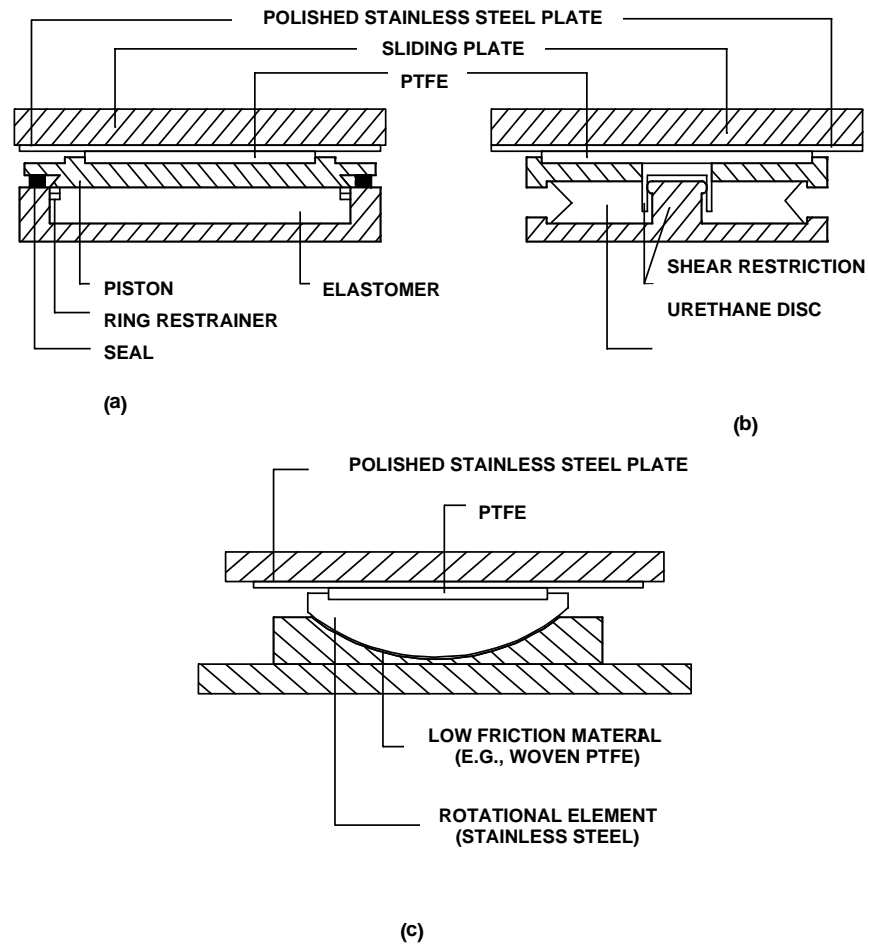


Figure 9-20 Flat Sliding Bearings: (a) Pot bearing, (b) Disc bearing, (c) Ball and socket (spherical) bearing (Buckle et. al., 2006)

Materials used for the sliding interface of these bearings are typically austenitic stainless steel (either type 304 or preferably the most corrosion-resistant type 316 which contains molybdenum) in contact with unfilled PTFE. To achieve significant energy dissipation capability, the PTFE needs to be non-lubricated.

Other materials have been used such as woven PTFE, PTFE-composites and bronze-lead composites, although bi-metallic interface are considered problematic (AASHTO,2010, Constantinou et al., 1999).

Flat sliding bearings may be combined with elastomeric bearings or mechanical energy dissipators to form hybrid isolation systems with a range of energy dissipation capabilities and stiffnesses. For example,

lubricated flat sliding bearings have been used in combination with yielding steel elastoplastic devices, such as those depicted in Figure 9-21 (Marioni, 1997), in bridge seismic isolation systems. In these systems, lock-up devices (or shock transmission devices) are used to allow for unobstructed thermal movement of the bridge on the lubricated bearings. The devices lock-up in seismic excitation and engage the yielding steel devices, which dissipated energy and limit the seismic movement. However, such systems lack sufficient restoring force capability and thus may develop significant permanent displacements.

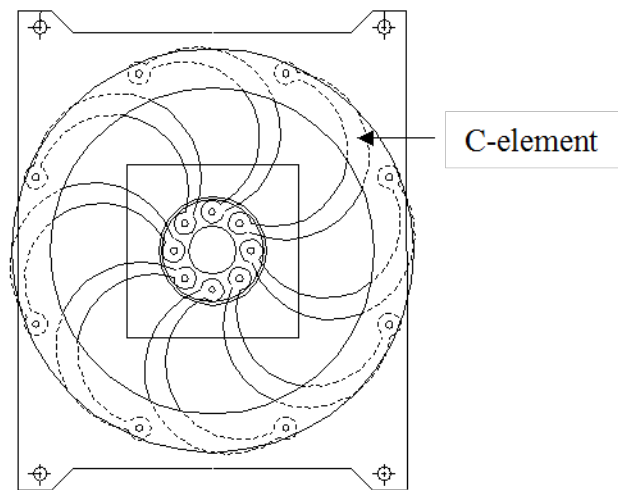


Figure 9-21 Elasto-Plastic Yielding Steel Device Used in Combination with Lubricated Sliding Isolators in Bridges (Buckle et.al., 2006)

Another example is the Eradquake Isolator shown in Figure 9-22. This isolator consists of a flat plate slider mounted on a disk bearing and fitted with orthogonally aligned, urethane springs as restoring force elements. Most of the applications to date of this type of isolator have been in the low-to-moderate seismic zones of the central and eastern United States.

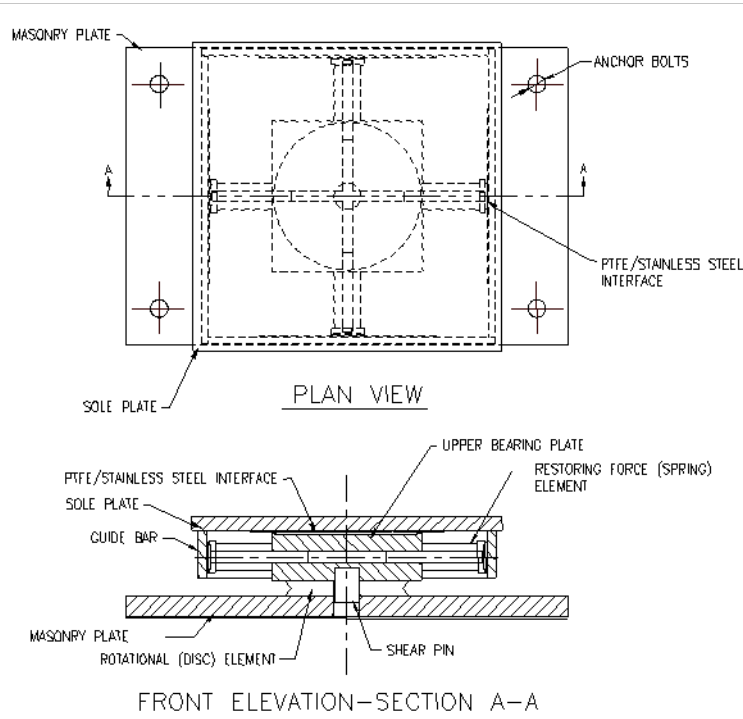


Figure 9-22 Eradiquake Isolator (Buckle et.al., 2006)

Curved sliding bearings are similar in construction to flat sliding bearings except the curvature of the surface provides stiffness to lateral load and a re-centering capability. These attributes make them attractive as seismic isolators and a typical concave friction isolator is shown in Figure 9-23.

These isolators are capable of carrying very large axial loads (see Table 9-3) and can be designed to have long periods of vibration (5 seconds or longer) with large capacities for lateral displacement. Section 9.6.1 describes these isolators in more detail. See also Example 9-3 in Section 9.7.

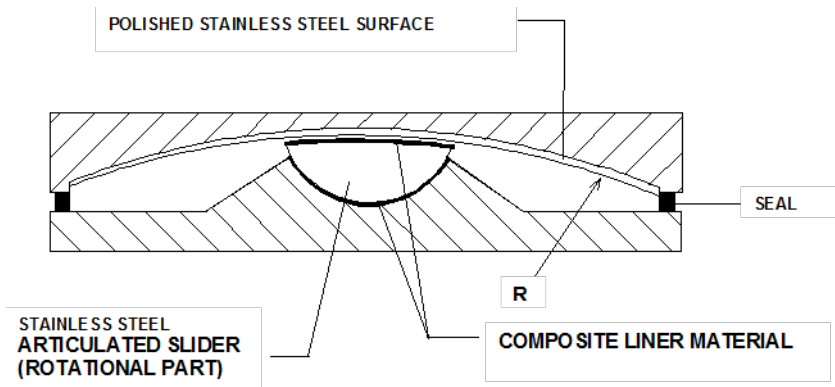


Figure 9-23 Concave Friction Isolator (Buckle et.al., 2006)

### 9.6.1 Concave Friction Isolators

As noted above, concave friction isolators are sliding-based isolators with lateral stiffness and re-centering capabilities not found in flat sliders. A typical concave friction bearing used in the Mississippi River Bridge in Ontario, Canada, is shown in Figure 9-24. Sectional and plan views of the same bearing are shown in Figure 9-25.

The main components of these isolators are a stainless steel concave spherical plate, an articulated slider and a housing plate as shown in Figure 9-25. In this figure, the concave spherical plate is facing down. The bearings may also be manufactured to have the spherical plate facing up. The side of the articulated slider in contact with the concave surface is coated with a low-friction composite material. The other side of the slider is also spherical but coated with stainless steel and sits in a spherical cavity also coated with low-friction composite material.



Figure 9-24 Concave Friction Isolator, Mississippi River Bridge, Ontario, Canada (Buckle et.al., 2006)

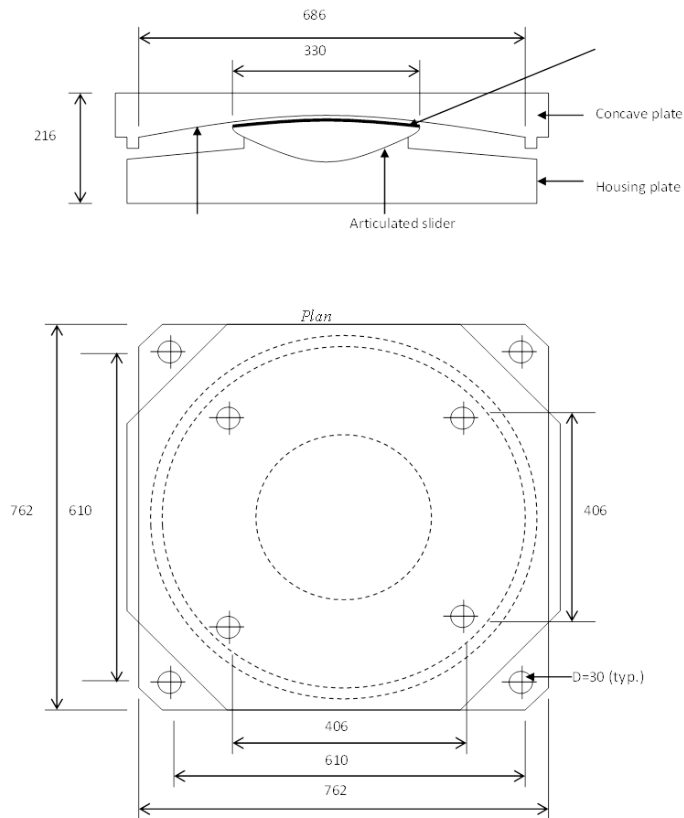


Figure 9-25 Section and Plan, Concave Friction Isolator, Mississippi River Bridge, Ontario, Canada (Buckle et.al., 2006)

### 9.6.1.1 Mechanical Characteristics of Concave Friction Isolators

Concave friction bearings are described by the same equation of motion as a conventional pendulum and their period of vibration is directly proportional to the radius of curvature of the concave surface. Long period shifts are therefore possible with surfaces that have large radii of curvature. Friction between the articulated slider and the concave surface dissipates energy and the weight of the bridge acts as a restoring force, due to the curvature of the sliding surface (Figure 9-26).

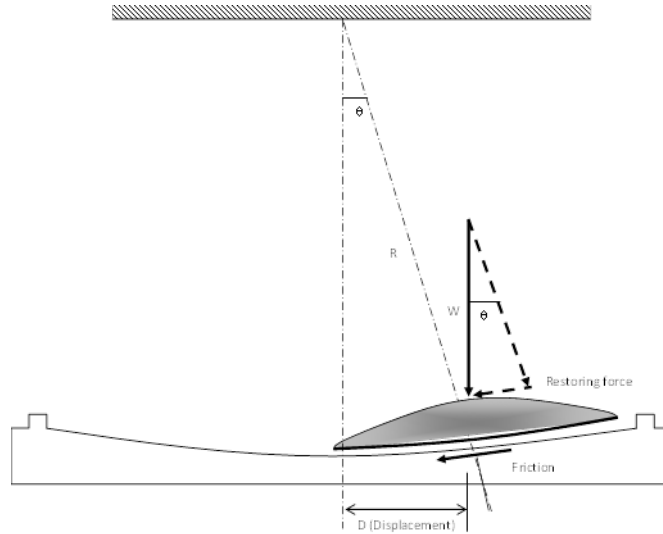


Figure 9-26 Forces Acting in Concave Friction Isolator when Sliding to Right - Not to Scale (Buckle et. al., 2006)

#### 9.6.1.1.1 Formulation of Isolator Behavior

The resistance of the bearing to horizontal forces that act to increase displacement, is provided by two different mechanisms. The first one is the frictional resistance,  $F_f$ , generated at the interface between the articulated slider and the concave surface as shown in Figure 9-26. This force is equal to the product of the dynamic friction coefficient,  $\mu$ , and the component of the weight normal to the concave surface.

Thus:

$$F_f = \mu W \cos \theta \quad 9-50$$

The second resistance mechanism is the restoring force generated by the tangential component of the weight acting on the bearing, also shown in Figure 9-26. This force is given by:

$$F_f = W \sin \theta \quad 9-51$$

If the displacement,  $D$ , of the bearing is small compared to the radius,  $R$ , of the concave surface, then:

$$\cos \theta = 1 \quad 9-52$$

and

$$\sin \theta = \frac{D}{R} \quad 9-53$$

Substituting Equations 9-52 and 9-53 into Equations 9-50 and 9-51 and summing up the results, the total horizontal resistance of the bearing to displacement is given by:

$$F = \mu W + \frac{W}{R} D \quad 9-54$$

Setting  $Q_d = \mu W$  and  $k_d = W/R$  and substituting into Equation 9-54 gives:

$$F = Q_d + k_d D \quad 9-55$$

which is identical to the expression used for in Equation 9-2.

It will be seen that the term  $W/R$  in Equation 9-54 is the lateral stiffness produced by the tangential component of the weight. Using this stiffness and the weight acting on the bearing, the period while sliding  $T_d$ , is given by:

$$T_d = 2\pi \sqrt{\frac{R}{g}} \quad 9-56$$

where  $g$  is the gravitational acceleration.

The sliding period is seen to be a function of the radius,  $R$ , alone.

The idealized force-displacement hysteresis loop for the concave friction isolator is shown in Figure 9-27. The envelope of the loop is defined by Equations 9-54 and 9-55.

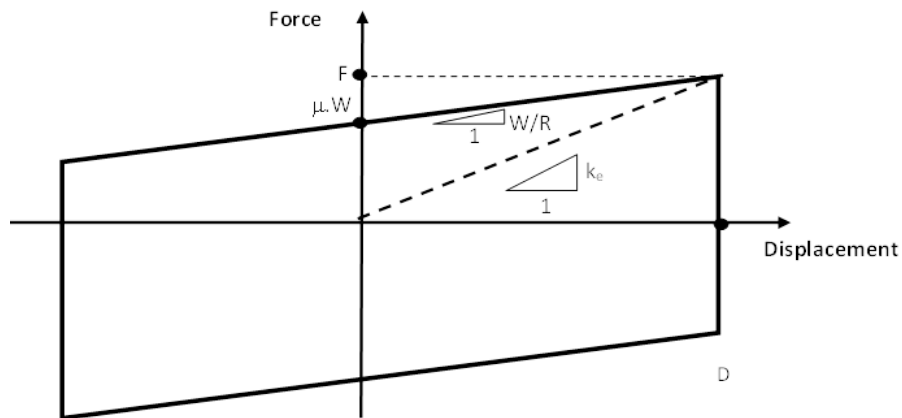


Figure 9-27 Idealized Force-Displacement Hysteretic Behavior of a Concave Friction Isolator (Buckle et.al., 2006)

Since the behavior of the isolator is non-linear, equivalent linearized properties are needed if elastic methods of analysis are to be used (Section 9.3). As with elastomeric isolators, these properties include the effective bearing stiffness and an equivalent viscous damping ratio to account for the effect of the hysteretic energy dissipation.

The effective bearing stiffness,  $K_{eff}$ , is shown in Figure 9-27, and is obtained by dividing the horizontal force,  $F$ , by the corresponding bearing displacement,  $D$ . Thus:

$$K_{eff} = \frac{\mu W}{D} + \frac{W}{R} \quad 9-57$$

Since the area of the hysteretic loop in Figure 9-24 is given by:

$$Area = 4\mu WD \quad 9-58$$

Substitution into Equation 9-1 gives the following expression for the equivalent viscous damping ratio,  $h$

$$h = \frac{2}{\pi} \left( \frac{\mu}{\mu + \frac{D}{R}} \right) \quad 9-59$$

This result can also be obtained from the damping ratio for elastomeric isolators by substituting  $D_y = 0$ ,  $Q_d = \mu W$ , and  $k_d = W/R$  into Equation 9-5.

An acceleration response spectrum with 5% damping is then modified for the actual damping,  $h$ , and used for calculating the response of the isolated bridge, as explained in Section 9.3.

## 9.6.2 Eradiquake Isolators

### 9.6.2.1 Mechanical Characteristics of Eradiquake Isolators

As noted above the essential components of the Eradiquake isolator include a pair of flat sliding plates, a disc bearing to accommodate rotation when required, and a set of urethane springs, called Mass Energy Regulators, to provide a restoring force to re-center the bridge after an earthquake.

### 9.6.2.1.1 Formulation of Bearing Behavior

As with the Friction Pendulum Isolator, the resistance of the bearing to horizontal forces is provided by two different mechanisms. The first is frictional resistance,  $F_f$ , generated at the interface between the flat PTFE and stainless steel as shown in Figure 9-22. The friction force is the product of the coefficient of friction,  $\mu$ , and the weight acting on the bearing:

$$F_f = \mu W \quad 9-60$$

The second mechanism is the restoring force generated by compression of the Mass Energy Regulators (MER) against the upper bearing plate. The MER is a polyether urethane cylinder that acts like a spring and provides a stiffness given as  $K_d$ . The restoring force  $F_r$ , is given by:

$$F_r = K_d D \quad 9-61$$

The total horizontal resistance of the bearing is obtained by summing the friction and MER resistances to give:

$$F = \mu W + K_d D \quad 9-62$$

The idealized force displacement hysteresis loop for an Eradquake bearing is the same as shown for the friction pendulum isolator in Figure 9-27, except that the second slope of the hysteresis loop is  $K_d$  instead of  $W/R$ .

Since the behavior of the isolator is non-linear, equivalent linearized properties are needed if elastic methods of analysis are to be used (Section 9.3). As with the CFB and elastomeric isolators, these properties include the effective bearing stiffness and an equivalent viscous damping ratio to account for the effect of the hysteretic energy dissipation.

The effective bearing stiffness,  $K_{eff}$ , is shown in Figure 9-27, and is obtained by dividing the horizontal force,  $F$ , by the corresponding bearing displacement,  $D$ . Thus:

$$K_{eff} = \frac{\mu W}{D} + K_d \quad 9-63$$

Since the area of the hysteretic loop in Figure 9-27 is given by:

$$Area = 4\mu WD \quad 9-64$$

Equation 9-1 gives the following expression for the equivalent viscous damping ratio,  $h$ :

$$h = \frac{2}{\pi} \left( \frac{\mu}{\mu + \frac{K_d D}{W}} \right) \quad 9-65$$

This result can also be obtained from the damping ratio for elastomeric isolators by substituting  $D_y = 0$ , and  $Q_d = \mu W$  into Equation 9-5.

An acceleration response spectrum with 5% damping is then modified for the actual damping and used as the input spectrum for calculating the response of the isolated bridge, as explained in Section 9.3.

### 9.6.3 Design of Sliding Isolators

The design of a sliding isolator involves the following steps:

- (1) Selection of the materials for the sliding interface and the contact pressure in order to achieve the desired frictional characteristics.
- (2) Selection of the thickness of the stainless steel plate in order to avoid uplift or bow waves that may lead to rupture.
- (3) Selection of the thickness of PTFE or other mating material in order to meet the desired wear characteristics for the application.
- (4) Selection of thickness of the end plates to safely sustain stresses and to provide sufficient stiffness in order to avoid distortion of the sliding surface.
- (5) Selection of the size and stiffness of the rotational part in order to minimize edge stresses on the sliding interface. These stresses may lead to excessive wear.

The following geometric and material specifications are recommended in AASHTO (2010) and should be used as guidance in the design of sliding isolation bearings:

- (1) The useful thickness (thickness of part projecting out of recess or thickness of part capable of wearing out) of sheet and woven PTFE should be at least 0.06 in after compression. By comparison, the European Standard EN 1337-1 (European 2000) relates the useful thickness (or protrusion) to the dimensions of the sheet and requires a minimum thickness of 0.08 in in the unloaded condition.
- (2) The useful thickness of other bearing liners should either be 0.06 in or be determined on the basis of wear tests for the conditions of application. For bridge applications, wear due to bearing movement caused by traffic may be the dominating factor for the selection of materials and thicknesses.
- (3) The stainless steel sliding surface should be polished to a high degree of reflectivity. AASHTO 2010 recommends a finish with an arithmetic average ( $R_a$ ) surface roughness of not more than 30 microinches. The commercially available mirror finish will result in an arithmetic average surface roughness ( $R_a$ ) of about 1.0 microinches per ANSI/ASME B46.1-1985 (ASME 1985).
- (4) The stainless steel should be austenitic and preferably of the 316 type conforming to ASTM A 240 (in the U.S.A.) or type 5 CrNiMo conforming to DIN 17440 (in Germany) or equivalent. Austenitic 304 type is also acceptable, although it is of lesser corrosion resistance.
- (5) The thickness of the stainless steel sliding plate should be at least 0.06 in for surfaces having a maximum dimension of less than 12 in, and at least 0.09 in for surfaces having a maximum dimension of less than 36 in. For larger dimensions the thickness of the stainless steel plate needs to be verified by testing of full size bearings at representative loads and velocities.
- (6) Materials other than corrosion-resistant austenitic stainless steel in contact with PTFE, woven PTFE, or other non-metallic liner materials are not recommended. Particularly, chrome-plated carbon steel and bi-metallic interfaces are known to either corrode or result in significant changes in friction (British Standards Institution, 1979; Constantinou et al. 1999).
- (7) Lubricated bearings should be of the sheet PTFE type and dimpled. The dimples should have diameter not more than 0.3 in and depth not more than 0.075 in. Dimples should cover 20 to 30-percent of the PTFE surface. The lubricant should be silicone grease effective to very low temperatures.

Sliding bearings must have rotational capability in order to accommodate rotation resulting from loading, construction tolerances and thermal effects. Furthermore, the concave friction bearing needs to accommodate rotation,  $\theta$ , resulting from lateral movement:

$$\theta = \sin^{-1}\left(\frac{D}{R}\right) \qquad 9-66$$

where  $D$  = lateral movement (displacement) and  
 $R$  = radius of curvature.

Since typically  $D/R \leq 0.2$ , the rotation is about 0.2 rad or less.

The rotational resistance of sliding bearings is important in calculating the moment acting on the bearing and the associated additional edge stresses on the sliding interface. Roeder et al. (1993) presented experimental data on the rotational resistance of pot, disk and spherical bearings that may be used as guidance in calculating the rotational stiffness of sliding bearings.

Sliding bearings have insignificant torsional resistance and can typically accommodate very large torsional rotations.

Torsional rotations of bridge superstructures are typically very small and may be estimated on the basis of the simple procedure recommended in the International Building Code (International Code Council, 2000), i.e.,

$$\phi \cong \frac{12eD}{b^2 + d^2} \quad 9-67$$

where  $e$  = eccentricity between the center of resistance of isolation and the center of mass  
 $D$  = displacement of isolation system at the center of resistance, and  
 $b, d$  = plan dimensions of superstructure.

Torsional rotations given by Equation 9-67 are usually of the order of 0.01 rad.

#### **9.6.4 Frictional Properties of Sliding Isolators**

An attempt to summarize the state of knowledge on the nature of friction in sliding structural bearings has been presented by Constantinou et al. (1999). Herein it is sufficient to present representative and informative data on the frictional properties of unlubricated sheet PTFE in contact with highly polished stainless steel. The behavior of other materials such as woven PTFE and PTFE-based, non-metallic composites is similar.

The coefficient of friction of PTFE-polished stainless steel interfaces depends on a number of factors, of which the apparent bearing pressure, the velocity of sliding, and the temperature are the most important. In general, the behavior of these interfaces may be described as follows:

- (1) At initiation motion and under quasi-static condition, the interfaces exhibit a high value of coefficient of friction. It is termed static or breakaway and it is denoted as  $\mu_B$ .
- (2) Following breakaway, and while moving at very low velocity, the coefficient of friction attains its minimum value,  $f_{min}$ , which is substantially less than the breakaway value.
- (3) The coefficient of friction increases with increasing velocity and attains a constant maximum value,  $f_{max}$ , at velocities beyond about 100 mm/sec.
- (4) In general,  $f_{min}$  is much less than  $\mu_B$  or  $f_{max}$  and  $f_{max}$  is larger than  $\mu_B$ , except for very low temperatures (about  $-40^\circ$  F and less) where  $\mu_B$  becomes larger than  $f_{max}$ . This behavior is depicted in Figure 9-28 and 9-29.
- (5) At intermediate values of velocity ( $v$ ), the coefficient of friction may be expressed in terms of  $f_{min}$  and  $f_{max}$  as follows (Zayas and Low, 1990):

$$\mu = f_{max} - (f_{max} - f_{min})e^{-av} \quad 9-68$$

- (6) The breakaway value of the coefficient of friction appears to be independent of the duration of loading without movement. Rather, it appears to be a maximum when the specimen is tested for the first time regardless of the duration of loading.

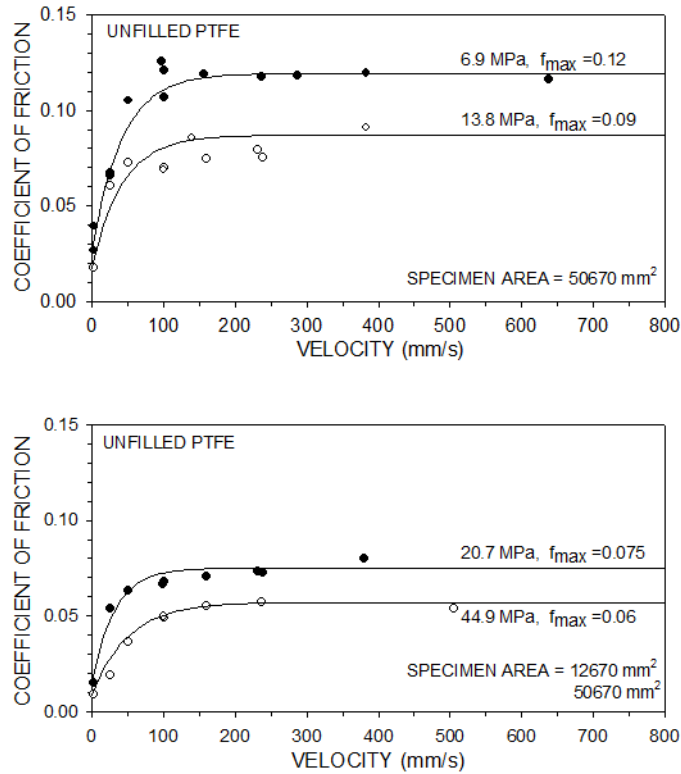


Figure 9-28 Coefficient of Sliding Friction of Unfilled PTFE-Polished Stainless Steel Interfaces - Surface Roughness 1.2 $\mu$ m Ra; Ambient Temperature about 68<sup>o</sup> F (Buckle et.al., 2006)

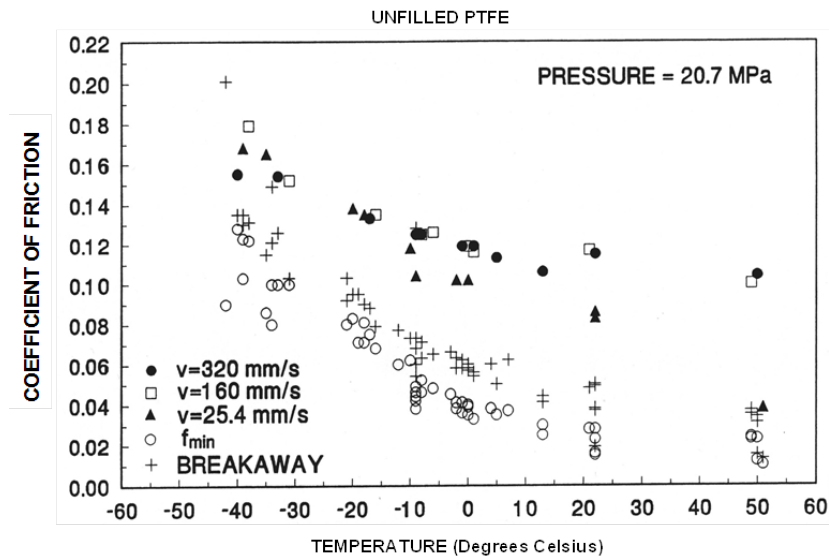


Figure 9-29 Coefficient of Friction of Unfilled PTFE-Polished Stainless Steel Interfaces as a Function of Temperature (Buckle et.al., 2006)

- (7) Temperature in the range of  $-22^{\circ}\text{F}$  to  $122^{\circ}\text{F}$  has a rather mild effect on the maximum value of the coefficient of friction ( $f_{max}$ ) as seen in Figure 9-29. This phenomenon is the result of frictional heating at the sliding interface (see also Section 9.6.5).
- (8) Cumulative travel has an effect on the coefficient of friction as shown in Figure 9-30. Following small travel, the coefficient of friction drops to stabilize at a lower value that is maintained for travel of at least 1600 ft.

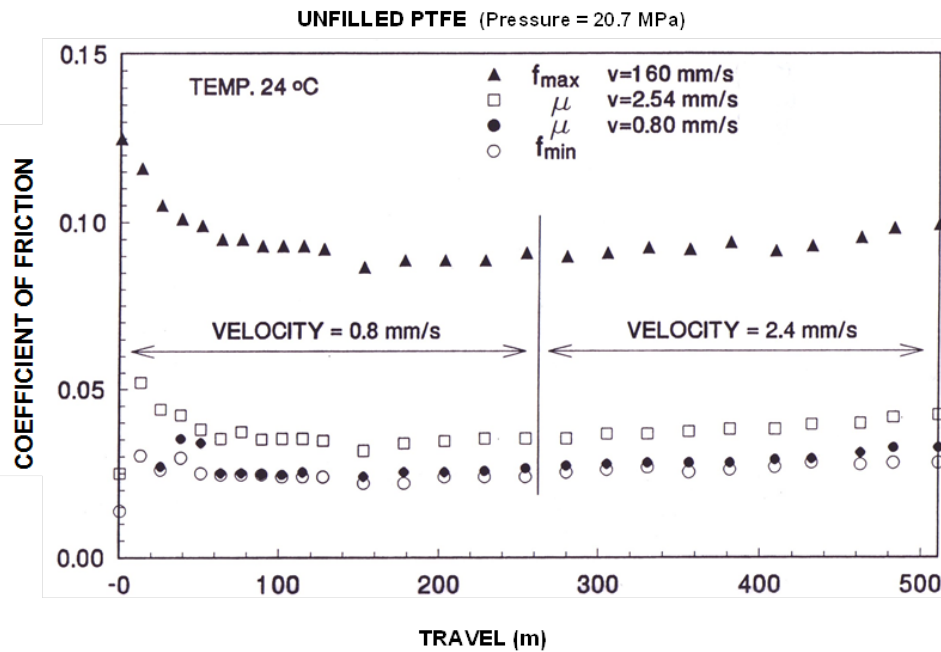


Figure 9-30 Effect of Cumulative Movement (Travel) on Sliding Coefficient of Friction of unfilled PTFE in Contact with Polished Stainless Steel (Buckle et. al., 2006)

- (9) The effect of the degree of roughness of the stainless steel surface on the coefficient of friction is presented in Figure 9-31. In this figure, data for roughness measured as arithmetic average of  $1.2\ \mu\text{m } R_a$  correspond to highly polished (mirror finish) surface. Data for roughness of  $12$  and  $20\ \mu\text{m } R_a$  correspond, respectively, to as-milled and to artificially roughened surfaces. They approximately represent the conditions at the surface of stainless steel following years of exposure that resulted in uniform rust stains. The results demonstrate substantial effects on the breakaway ( $\mu_B$ ) and the low velocity friction ( $f_{min}$ ) and rather insignificant effects on the high velocity friction ( $f_{max}$ ).

### 9.6.5 Effects of Variability of Properties, Aging, Temperature, and Load History

The properties of isolators inevitably vary due to manufacturing differences, aging, wear, history of

loading, temperature, etc. These variations may alter the effective period and effective damping of the isolation system, either of which will influence the dynamic response of the isolated structure. The interested reader is referred to Constantinou et al. (1999) for a comprehensive discussion on the effects of the environment, temperature, aging, history of loading, etc. on the mechanical properties of isolators. These effects are briefly discussed in the following sections.

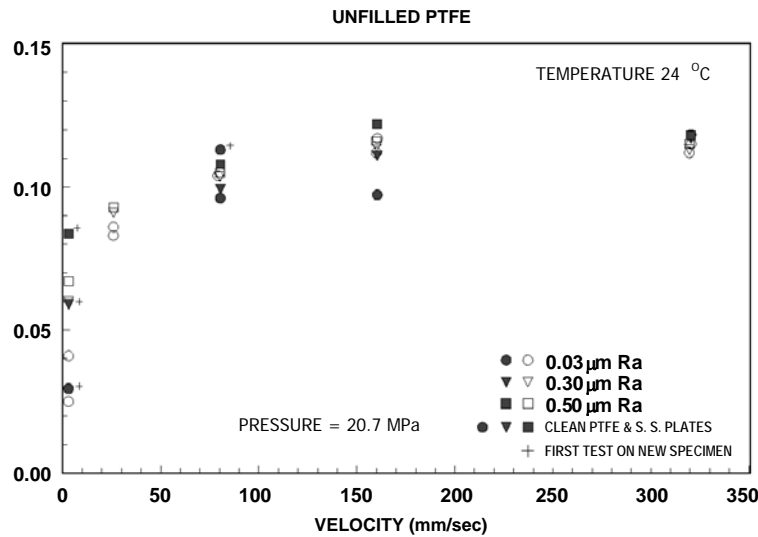


Figure 9-31 Effect of Surface Roughness of Stainless Steel on the Sliding Coefficient of Friction of Unfilled PTFE (Buckle et.al., 2006)

### 9.6.5.1 Variability of Properties

The mechanical properties of seismic isolation hardware exhibit variability in values as a result of natural variability in the properties of the materials used and as a result of the quality of manufacturing. It is not unusual to have properties, such as the sliding stiffness or the coefficient of friction in a particular cycle of reversed loading, differ by  $\pm 25$  percent from the average values among all tested isolators.

### 9.6.5.2 Aging

Aging is the degradation or change of properties with time. Herein, a brief description of the aging effects on the mechanical properties of characteristic strength and post-elastic stiffness of seismic isolation hardware is presented. Moreover, it should be recognized that aging may also have effects on the ability of the isolation hardware to sustain stress, strain, force or deformation, which also need to be considered in design.

Seismic isolation is a relatively new technology so that the field observation of performance of seismic isolation hardware is limited to about 15 years. Actual data on the mechanical properties of seismic isolation bearings removed from structures and re-tested after years of service are limited to a pair of bearings but the results are inclusive given that the original condition of the bearings was not exactly know. However, there is considerable information collected from the field inspection of seismic isolation and other similar bearings, from testing of field-aged bearings in non-seismic applications, from laboratory studies and from theoretical studies. While this information is indirect, it is very useful and may be summarized as follows:

- (1) Aging in sliding bearings generally results in increases in the coefficient of friction. However, the origins of the increase are complex to describe and interpret, and they depend on the nature of the sliding interface. Aging may be due to corrosion of stainless steel, an increase in the true contact area following prolonged loading without movement, contamination, or loss of material at the sliding interface or any combination.
- (2) Corrosion of stainless steel is typically limited to light rust stains over small part of the surface following several years of service. Data extend up to 25 years in urban, chemical, industrial and marine environments. Insignificant corrosion was observed in austenitic, type 316 stainless steel (which contains molybdenum). This type of stainless steel is mostly used in seismic isolation bearings.
- (3) Bi-metallic sliding interfaces tend to slowly creep under prolonged loading without movement, which results in an increase in the true contact area. This, in turn, results in substantial increases in friction even in the absence of corrosion. AASHTO (2010) severely penalizes the use of bi-metallic interfaces in sliding seismic isolation bearings. By contrast, experimental studies and theoretical considerations indicate that this phenomenon does not occur in interfaces consisting of PTFE, or PTFE composites in contact with highly polished stainless steel.
- (4) Contamination of sliding interfaces while under load (bearings in service) is preventable with proper installation and sealing of the bearings. AASHTO (2010) recommends installation of sealed bearings with the stainless steel surface facing down. All other types of installation are either penalized or prohibited. Moreover, it is important not to disassemble sliding bearings in the field. Also, grease-lubricated sliding bearings tend to be much more easily contaminated than non-lubricated bearings.
- (5) Continuous movement of sliding bearings due to primarily traffic loading in bridges results in wear and eventual loss of the softer material (PTFE or PTFE-composite) of the sliding interface. AASHTO (2010) requires evaluation of wear over the expected lifetime of the structure, including

testing for cumulative travel of at least 1 mile. Such tests have so far been performed only for friction pendulum bearings and PTFE / stainless sliding bearings.

### **9.6.5.3 Temperature**

The effects of temperature on the mechanical properties of seismic isolation bearings may be discussed in two distinct ways: (a) the effect of heating (viscous, hysteretic or frictional) on the mechanical properties during cyclic movement of the bearings, and (b) the effect of ambient temperature (and particularly low temperature) and of the duration of exposure to this temperature on the mechanical properties.

#### **9.6.5.3.1 Heating During Cyclic Movement**

For sliding bearings, frictional heating has been described by Constantinou et al. (1999), where analytical and experimental results are presented. Due to the fact that frictional heating occurs at the sliding interface, which is very small in volume, the temperature at the sliding interface increases substantially and in proportion to the velocity of sliding. While these high temperatures diffuse quickly in the surrounding medium, they cause wear and some reduction of the friction force. The reduction in the friction force is modest due to the fact that friction is due to a number of contributing mechanisms, each one of which is differently affected by elevated temperature. It appears that wear is the major result of frictional heating.

#### **9.6.5.3.2 Effect of Ambient Temperature**

Low temperatures generally cause an increase in friction in sliding bearings, as shown in Figure 9-32. In general, the coefficient of friction of PTFE or related materials in contact with highly polished stainless steel exhibits a variation with the velocity of sliding as shown in this figure. The maximum value of the coefficient of friction occurs at velocities of sliding that, in general, exceed about 4 in/sec (denoted as  $f_{max}$ ). As temperature reduces, the friction values substantially increase at the initiation of movement but increase much less at high velocities of sliding. At temperature below about -40° F, the maximum value of the coefficient of friction occurs at initiation of motion (denoted as  $\mu_B$ ). As an example, Figure 9-33 presents recorded normalized friction force vs. displacement loops of a sliding bearing (consisting of unfilled sheet PTFE in contact with highly polished stainless steel) at temperatures of 70°F and -36° F. Note that the tests were conducted with imposed sinusoidal displacement history of peak velocity equal to 5 in/sec. Despite the modest velocity and the extremely low temperature, frictional heating is substantial so that the low temperature effects are mitigated.

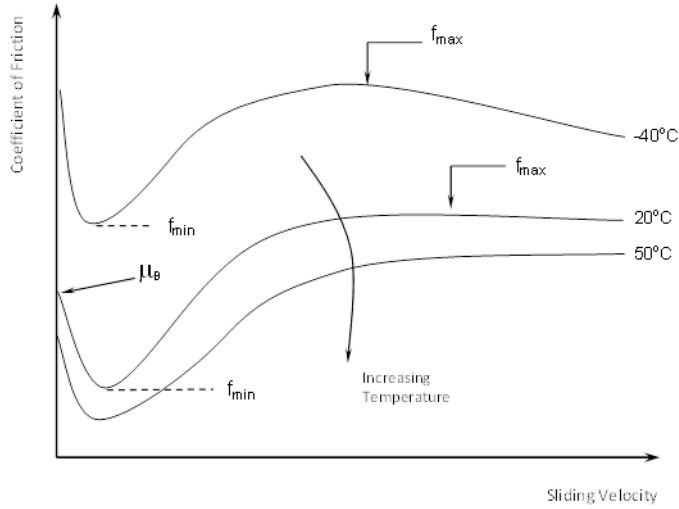
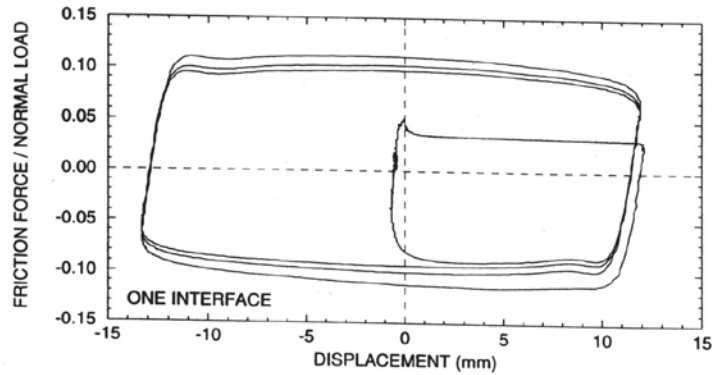


Figure 9-32 Effect of Temperature on the Frictional Properties of PTFE-Polished Stainless Steel Interfaces (Buckle et. al., 2006)

21°C, vel.=125mm/s, p = 21 MPa



-38°C, vel.=125mm/s, p = 21 MPa

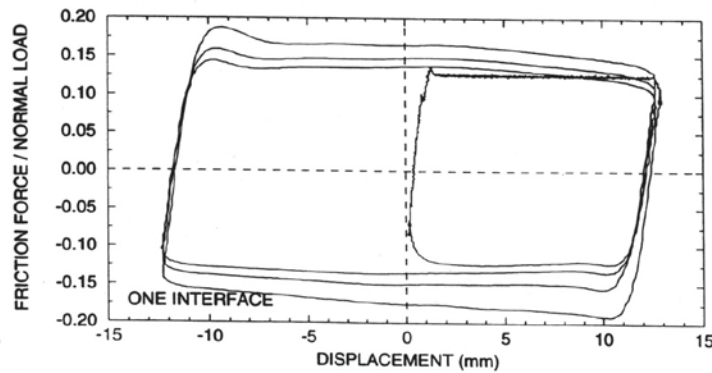


Figure 9-33 Normalized Force-Displacement Relation of a Flat Sliding Isolator at 70<sup>0</sup> F (top) and -36<sup>0</sup> F (bottom) (Buckle et. al., 2006)

#### 9.6.5.4 Loading History

The history of loading can have a marked effect on the mechanical properties of all types of bearings. Some of these effects have a profound impact, leading to significant error if disregarded. Loading history effects on elastomeric isolators are discussed in Section 9.5.4.4. In this section cyclic loading effects in friction isolators are presented.

Tests conducted on friction pendulum isolators indicate that the dynamic friction coefficient from tests of full-size isolators should fall within 20% of the specified value. For conventional design applications, in a test involving 3-5 cycles of displacement, the coefficient of friction in the first cycle is generally about 20% higher than the average coefficient of friction from all the cycles. The average coefficient of friction from all the cycles represents the target design coefficient of friction. Accordingly, the initial lower bound friction coefficient,  $\mu_L$ , is set equal to the target design coefficient of friction. The initial upper bound friction coefficient  $\mu_U$ , is then initially set equal to  $1.2\mu_L$  for design purposes. However, this should later be verified by the actual prototype testing of the bearings and the coefficient 1.2 may be modified accordingly. The initial lower and upper bound friction coefficients are then adjusted using the property modification factors to obtain the minimum and maximum probable friction coefficients for the isolators.

#### 9.6.6 System Property Modification Factors for Sliding Isolators

As described in Section 9.4.2 system property modification factors are used to account for the likely variations in isolator properties over the life of a bridge. In this approach, the minimum and maximum effective stiffness and effective damping of the isolation system are calculated using the minimum and maximum values of the post-elastic stiffness,  $K_d$ , and characteristic strength,  $Q_d$ , of each isolation bearing. These values of parameters are calculated as the product of (1) the nominal values of these parameters, and (2) the minimum and maximum values of the corresponding system property modification factors.

The minimum value of the system property modification factor ( $\lambda$ -factor) is denoted as  $\lambda_{min}$  and has values less than or equal to unity. Due to the fact that most values of  $\lambda_{min}$  proposed by Constantinou et al. (1999) are close to unity, the AASHTO *Guide Specifications* (AASHTO, 2010) sets  $\lambda_{min}$  equal to unity. That is, the lower bound values of properties of the isolation systems are considered to be the nominal values. These values are defined to be those determined for fresh and scragged specimens under normal temperature conditions.

As noted in Section 9.4.2.2 and shown in Equation 9-16, the maximum value of the  $\lambda$ -factor is calculated from the product of six component factors which account for the effects of temperature, aging, velocity, travel and wear, contamination, and scragging. Values for each of these factors are presented in Tables 9-9 to 9-12 (AASHTO 2010, Constantinou et al., 1999).

**TABLE 9-9 MAXIMUM VALUES FOR TEMPERATURE  $\lambda$ -FACTORS FOR SLIDING ISOLATORS ( $\lambda_{MAX,T}$ ) (AASHTO, 2010)**

Minimum Temperature for Design		Unlubricated PTFE	Lubricated PTFE	Bimetallic Interfaces
°C	°F			
21	70	1.0	1.0	To be established by test
0	32	1.1	1.3	
-10	14	1.2	1.5	
-30	-22	1.5	3.0	

**TABLE 9-10 MAXIMUM VALUES FOR AGING  $\lambda$ -FACTORS FOR SLIDING ISOLATORS ( $\lambda_{MAX,A}$ )<sup>1</sup> (AASHTO, 2010)**

Environment/ Condition	Unlubricated PTFE		Lubricated PTFE		Bimetallic Interfaces <sup>4</sup>	
	Sealed	Unsealed <sup>2</sup>	Sealed	Unsealed <sup>2</sup>	Sealed	Unsealed <sup>2</sup>
Normal	1.1	1.2	1.3	1.4	2.0	2.2
Severe <sup>3</sup>	1.2	1.5	1.4	1.8	2.2	2.5

- Notes:**
1. Values are for 30-year exposure of stainless steel. For chrome-plated carbon steel, multiply by 3.0.
  2. Unsealed conditions assumed to allow exposure to water and salt, thus promoting further corrosion.
  3. Severe environments include marine and industrial environments.
  4. Values for bimetallic interfaces apply to stainless steel - bronze interfaces.

**TABLE 9-11 MAXIMUM VALUES FOR TRAVEL AND WEAR  $\lambda$ -FACTORS FOR SLIDING ISOLATORS ( $\lambda_{MAX,TR}$ ) (AASHTO, 2010)**

Cumulative Travel		Unlubricated PTFE	Lubricated PTFE	Bimetallic Surfaces
ft	m			
<3300	<1005	1.0	1.0	To be established by test
≤6600	≤2010	1.2	1.0	To be established by test
>6600	>2010	To be established by test	To be established by test	To be established by test

**TABLE 9-12 MAXIMUM VALUES FOR CONTAMINATION  $\lambda$ -FACTORS FOR SLIDING ISOLATORS ( $\lambda_{max,c}$ ) (AASHTO, 2010)**

	<b>Unlubricated PTFE</b>	<b>Lubricated PTFE</b>	<b>Bimetallic Interfaces</b>
Sealed with stainless steel surface facing down	1.0	1.0	1.0
Sealed with stainless surface facing up <sup>1</sup>	1.1	1.1	1.1
Unsealed with stainless surface facing down	1.1	3.0	1.1
Unsealed with stainless surface facing up	Not allowed	Not allowed	Not allowed

**Note 1.** Use factor of 1.0 if bearing is galvanized or painted for 30-year lifetime.

## 9.7 EXAMPLES

Three examples are given in this section, which illustrate the simplified analysis of isolated bridges with and without flexible substructures, and the preliminary design of lead-rubber and concave friction isolators.

---

## EXAMPLE 9-1 ANALYSIS OF AN ISOLATED BRIDGE WITH STIFF SUBSTRUCTURES

---

### Problem Statement

The superstructure of a 2-span bridge weighs 533 K. and is supported on a total of 12 seismic isolators at the abutments and piers. The bridge is located on a rock site where  $S_{DI} = 0.55$ . Analyze the bridge for each situation described in (a) through (c) below. Neglect the flexibility of the center pier, i.e., assume a stiff substructure.

- (a) If  $Q_d = 0.075 W$  and  $K_d = 13.0$  K/in for the equivalent system isolator (sum of 12 individual isolators), calculate the total base shear (sum of all the isolator shears) and superstructure displacement in the longitudinal direction. ( $W =$  weight of superstructure  $= 533$  K.)
- (b) Calculate  $Q_d$  such that the displacement of the superstructure in the longitudinal direction does not exceed 5.0 ins ( $K_d = 13.0$  K/in).
- (c) Calculate  $Q_d$  and  $K_d$  such that the displacement in the longitudinal direction does not exceed 6.0 ins and the total base shear does not exceed 110 K.

Use the Simplified Method described above for these analyses and assume the isolators have negligible yield displacements ( $D_y = 0$ ).

### Solution

An excel spreadsheet may be constructed to solve these three problems. Such a spreadsheet is given below together with solutions to (a), (b), and (c). Results are summarized as follows:

- (a) When  $Q_d = 0.075W$  and  $K_d = 13.0$  K/in, the superstructure displacement is 5.98 in and the total base shear is 117.7 K (22.1% of the weight).
- (b) To reduce the superstructure displacement to less than 5.0 ins while keeping  $K_d = 13.0$  K/in,  $Q_d$  is increased to  $0.10W$ .
- (c) To reduce the base shear to less than 110.0 K while keeping the displacement less than 6.0 ins,  $K_d$  is reduced to 11.25 K/in and  $Q_d$  increased to  $0.08W$ .

Results are given in the spreadsheet below for four iterations for each problem. The final solution is the fourth trial in each case.

**(a) FIND BRIDGE RESPONSE FOR  $Q_d = 0.075W$  and  $K_d = 13.0 \text{ K/in}$** 

Step	Parameter	Trial 1	Trial 2	Trial 3	Trial 4
	Characteristic strength, $Q_d$	0.075	0.075	0.075	0.075
	Post-yield stiffness, $K_d$	13.00	13.00	13.00	13.00
1	Assumed displacement, D	5.00	5.60	6.00	5.98
2	Effective stiffness, $K_{eff}$	20.995	20.138	19.663	19.685
3	Effective period, $T_{eff}$	1.610	1.644	1.664	1.663
4	Viscous damping ratio, $\beta$	0.242	0.226	0.216	0.216
5	Damping factor, B	1.58	1.55	1.53	1.53
6	Displacement, D (eq 3-4)	5.61	5.83	5.98	<b>5.98</b> Answer
8	Total base shear, F	117.70	117.50	117.63	<b>117.69</b> Answer
	Base shear / weight				<b>22.08%</b> Answer

**(b) FIND  $Q_d$  for  $D < 5.0 \text{ ins}$  ( $K_d = 13.0 \text{ K/in}$ )**

Step	Parameter	Trial 1	Trial 2	Trial 3	Trial 4
	Characteristic strength, $Q_d$	0.075	0.090	0.120	<b>0.100</b> Answer
	Post-yield stiffness, $K_d$	13.00	13.00	13.00	13.00
1	Assumed displacement, D	5.00	5.00	5.00	5.00
2	Effective stiffness, $K_{eff}$	20.995	22.594	25.792	23.660
3	Effective period, $T_{eff}$	1.610	1.552	1.453	1.517
4	Viscous damping ratio, $\beta$	0.242	0.270	0.316	0.287
5	Damping factor, B	1.58	1.64	1.70	1.67
6	Displacement, D (eq 3-4)	5.61	5.21	4.70	5.00
8	Total base shear, F	117.70	117.63	121.25	118.21
	Base shear / weight				22.18%

**(c) FIND  $Q_d$  and  $K_d$  for  $D < 6.0 \text{ ins}$  and  $F < 110 \text{ K}$** 

Step	Parameter	Trial 1	Trial 2	Trial 3	Trial 4
	Characteristic strength, $Q_d$	0.050	0.075	0.075	<b>0.080</b> Answer
	Post-yield stiffness, $K_d$	13.00	10.00	11.00	<b>11.25</b> Answer
1	Assumed displacement, D	6.00	6.00	6.00	5.85
2	Effective stiffness, $K_{eff}$	17.442	16.663	17.663	18.539
3	Effective period, $T_{eff}$	1.767	1.808	1.756	1.714
4	Viscous damping ratio, $\beta$	0.162	0.255	0.240	0.250
5	Damping factor, B	1.35	1.61	1.58	1.60
6	Displacement, D (eq 3-4)	7.20	6.18	6.11	5.89
8	Total base shear, F	125.56	102.90	107.96	109.22
	Base shear / weight				20.49%

---

## EXAMPLE 9-2 ANALYSIS OF AN ISOLATED BRIDGE WITH FLEXIBLE SUBSTRUCTURES

---

### Problem Statement

The superstructure of a 2-span bridge weighs 533 K. and is supported on a total of 12 seismic isolators at the abutments and piers. The bridge is located on a rock site where  $S_{DI} = 0.55$ . The center pier is a single 36-inch diameter reinforced concrete column, 25 ft high, fixed at the base and pinned at the top. The elastic modulus for the concrete is 3,000 ksi. The lateral stiffness of the each abutment is 10,000 K/in. The bridge is isolated with bearings at the abutments and over the pier. Total values for  $Q_d$  and  $K_d$  summed over all the isolators are  $0.075W (= 40 \text{ K})$  and 13.0 K/in respectively. Isolator properties and the weight carried at each substructure are given in table below.

Substructure	Weight carried (K)	$Q_d$ (K)	$K_d$ (K/in)
North Abutment	100	7.50	2.44
Pier	333	25.00	8.12
South Abutment	100	7.50	2.44
<b>Totals</b>	<b>533</b>	<b>40.00</b>	<b>13.00</b>

- Calculate seismic response of the bridge. In particular find the displacement of the superstructure, the total base shear, and the distribution of this shear to the three substructures (two abutments and pier).
- If the shear capacity of the pier is only 5 percent of the weight of the bridge, redistribute the isolator properties between the abutments and pier to satisfy this limitation.

Use the displacement-based method described above for these analyses and assume the isolators have negligible yield displacements ( $D_y = 0$ ).

### Solution

As for the previous example, an excel spreadsheet may be constructed to solve these two problems. Such a spreadsheet is given below with solutions for (a) and (b). The approach is the same as for the Example 9-1 except that the calculation of the effective stiffness for the complete bridge system (Step 2

(a) FIND BRIDGE RESPONSE FOR  $Q_d = 0.075W$  and  $K_d = 13K/in$

Step	Parameter	Solution1	Step 2.	Effective stiffness of bridge Isolation system, $K_{eff}$											
	Characteristic strength, $Q_d$	0.075	<b>D</b>	<b>6.26</b>											
	Post-yield stiffness, $K_d$	13			<b>Substruc</b>	<b>Wsub</b>	<b>Qd</b>	<b>Kd</b>	<b>Ksub</b>	<b><math>\alpha</math></b>	<b>Keff</b>	<b>Disol</b>	<b>Dsub</b>	<b>Fsub</b>	<b>Fsub %</b>
1	Assumed displacement, D	6.26			N. Abut	100.00	7.50	2.44	10,000.00	0.0004	3.63	6.258	0.002	22.75	21.87%
2	Effective stiffness, $K_{eff}$	16.623			Pier	333.00	25.00	8.13	27.48	0.5159	9.35	4.129	2.131	58.55	56.27%
3	Effective period, $T_{eff}$	1.810			S. Abut	100.00	7.50	2.44	10,000.00	0.0004	3.63	6.258	0.002	22.75	21.87%
4	Viscous damping ratio, $\beta$	0.245			<b>Totals</b>	<b>533.00</b>	<b>40.00</b>	<b>13.00</b>			<b>16.62</b>			<b>104.06</b>	<b>100.00%</b>
5	Damping factor, B	1.59													
6	Displacement, D (eq 3-4)	<b>6.26</b>													
8	Total base shear, F	<b>104.13</b>													
	Base shear / weight	<b>19.54%</b>													

(b) REDISTRIBUTE  $Q_d$  and  $K_d$  such that maximum shear in center pier < 26.65K (5% total weight)

Step	Parameter	Solution1	Step 2.	Effective stiffness of bridge Isolation system, $K_{eff}$											
	Characteristic strength, $Q_d$	0.075	<b>D</b>	<b>6.04</b>											
	Post-yield stiffness, $K_d$	13			<b>Substruc</b>	<b>Wsub</b>	<b>Qd</b>	<b>Kd</b>	<b>Ksub</b>	<b><math>\alpha</math></b>	<b>Keff</b>	<b>Disol</b>	<b>Dsub</b>	<b>Fsub</b>	<b>Fsub %</b>
1	Assumed displacement, D	6.04			N. Abut	100.00	20.00	4.33	10,000.00	0.0008	7.64	6.035	0.005	46.15	40.16%
2	Effective stiffness, $K_{eff}$	19.025			Pier	333.00	0.00	4.33	27.48	0.1577	3.74	5.217	0.823	22.61	19.67%
3	Effective period, $T_{eff}$	1.692			S. Abut	100.00	20.00	4.33	10,000.00	0.0008	7.64	6.035	0.005	46.15	40.16%
4	Viscous damping ratio, $\beta$	0.221			<b>Totals</b>	<b>533.00</b>	<b>40.00</b>	<b>13.00</b>			<b>19.02</b>			<b>114.91</b>	<b>100.00%</b>
5	Damping factor, B	1.54													
6	Displacement, D (eq 3-4)	<b>6.03</b>													
8	Total base shear, F	<b>114.73</b>													
	Base shear / weight	<b>21.53%</b>													

requires the summation of the effective stiffnesses of each substructure. This is shown in the spreadsheet in a separate section of the sheet. This section is entered with an estimate of the displacement (6.26 in) and the effective stiffness is calculated for that displacement (16.62 K/in). This value is then used in Step 3 to calculate the effective period and the solution proceeds as before. The solution shown over the page is the final trial after convergence has been obtained. Intermediate trials are not shown. It will be seen that the section that calculates effective stiffness, also calculates the displacements in the isolators and substructures, and the shears in the substructures both in absolute terms and as a percentage of the total base shear.

Results for the two cases are summarized as follows:

(a) Superstructure displacement = 6.26 in

Total base shear = 104.1 K (19.5%  $W$ )

North abutment shear = 22.8 K (21.9% total base shear, 4.3%  $W$ )

Pier shear = 58.5 K (56.2% total base shear, 11.0%  $W$ )

South abutment shear = 22.8 K (21.9% total base shear, 4.3%  $W$ )

Isolator and substructure displacements:

- at north abutment: 6.26 in (isolator), 0 in (abutment)
- at pier: 4.13 in (isolator), 2.13 in (pier)
- at south abutment: 6.26 in (isolator), 0 in (abutment)

Comparing these results with those obtained for part (a) of Example 9-1 where the substructure was considered to be rigid, the effect of the flexible pier is to increase the displacements by about 5% (from 5.98 to 6.26 in) and to reduce the total base shear by about 12% (from 118 K to 104 K). It is seen that the assumption of a rigid substructure gives a conservative estimate of base shear but underestimates the superstructure displacement (slightly). The main reason for this behavior is the lengthening of the effective period due to the increased flexibility of the bridge when the single-column pier is introduced (from 1.66 sec to 1.81 sec).

(b) Since the strength of the pier is so low (5%  $W$ ), the strategy adopted in this solution is to soften the isolators above the pier and stiffen the ones at the abutments to draw lateral load away from the pier and to the abutments. Hence  $Q_d$  for the pier isolators is set to zero and the abutment values increased accordingly to maintain the total required value of  $0.075W$ . Also the  $K_d$  values at the pier are reduced and the abutment values increased to provide a total value of 13.0 K/in as required. In this solution it

will be seen that  $K_d$  has been equally divided between all three substructures but this is not the only approach that will lead to a successful result. There are in fact many solutions to this problem and the optimal one will be determined when actual isolators (lead-rubber, concave friction or Eradiquake) are designed to meet these  $Q_d$  and  $K_d$  values while simultaneously supporting the weight of the bridge and providing the period shift.

Superstructure displacement = 6.04 in

Total base shear = 114.9 K (21.5%  $W$ )

North abutment shear = 46.2 K (40.2% total base shear, 8.7%  $W$ )

Pier shear = 22.6 K (19.6% total base shear, 4.2%  $W$ )

South abutment shear = 46.2 K (40.2% total base shear, 8.7%  $W$ )

Isolator and substructure displacements:

- at north abutment: 6.04 in (isolator), 0.0 in (abutment)
- at pier: 5.22 in (isolator), 0.82 in (pier)
- at south abutment: 6.04 in (isolator), 0.0 in (abutment).

---

### **EXAMPLE 9-3 PRELIMINARY DESIGN OF ISOLATION HARDWARE FOR EXAMPLE 9-1a**

---

#### **Problem Statement**

The superstructure of a 2-span bridge weighs 533 K. and is supported on a total of 12 seismic isolators at the abutments and piers. The bridge is located on a rock site where  $S_{DI} = 0.55$ . The properties of the isolation system (total for all 12 isolators) are  $Q_d = 0.075W$  and  $K_d = 13.0$  K/in. In Example 9-1(a) it was found that the maximum displacement of the superstructure across the isolators is 5.98 ins and the maximum shear transmitted by the isolators is 117.7 K for the given seismic hazard ( $S_{DI} = 0.55$ ).

Design a set of lead-rubber isolators and a set of concave friction isolators that will have these properties and deliver this performance.

#### **Lead-Rubber Isolator Solution**

1. Summarize given data:

Number of isolators = 12, total weight ( $W$ ) = 533 K, total  $Q_d = 0.075W = 40K$ , total  $K_d = 13$  K/in

Weight /isolator =  $533/12 = 44.42K$ ,  $Q_d$  /isolator =  $3.33K$ ,  $K_d$  / isolator =  $1.08$  K/in

2. Size lead core using Equation 9-30:  $d_L = \sqrt{(Q_d/0.9)} = \sqrt{(3.33/0.9)} = 1.92$  ins
3. Size bearing plan dimension. Assume circular bearing and 800 psi allowable compressive stress for preliminary design purposes.

$$\text{Bonded area} = 44.42 / 0.8 = 55.52 \text{ in}^2 \text{ and corresponding diameter} = \sqrt{4(55.52)/\pi} = 8.4 \text{ in}$$

Assume a side cover layer of 0.5 in round perimeter, then overall diameter = 8.4 + 1.0 = 9.4 ins

4. Determine required thickness of elastomer using Equation 9-33. Assume shear modulus,  $G = 0.1$ ksi.

$$T_r = GA_b / K_d = 0.1 (55.52) / 1.08 = 5.14$$

5. Determine overall height of isolator assuming 0.5-inch thick layers, 0.125-inch thick shims, and 0.5-inch cover plates.

$$\text{Number of rubber layers} = T_r / 0.5 = 5.14 / 0.5 = 11, \text{ to nearest whole number}$$

$$\text{Number of internal shims} = 11 - 1 = 10$$

Number of cover plates = 2, and

$$\text{Overall height} = 11 \times 0.5 + 10 \times 0.125 + 2 \times 0.5 = 7.75 \text{ in}$$

6. Check maximum shear strain in rubber ( $\gamma_{max}$ ) against allowable (150%):

$$\gamma_{max} = \text{max. displacement across isolator} / \text{total rubber thickness}$$

$$= 5.98 / (11 \times 0.5) = 5.98 / 5.5 = 109\% < 150\% \text{ OK}$$

#### 7. Preliminary design solution:

Isolation system consists of 12 x 9.4-inch diameter x 7.75 in high circular elastomeric bearings each with a 1.92-inch lead core.

#### 8. Final solution

Checks are required and above design modified as necessary, for the following:

- System performance with actual bearing dimensions and properties (e.g., actual rubber layer thickness,  $T_r$ ) and minimum and maximum values determined by System Property Modification Factors (Sec 9.4.2.1 and Tables 9-6, 9-7, and 9-8)
- Minimum restoring force capability (Sec 9.4.3)
- Size limits on lead core (Equation 9-57)
- Strain limits in rubber (Equation 9-39)
- Vertical load stability (Sec. 9.4.6, Equations 9-46 and 9-50)
- Non-seismic requirements

#### Concave Friction Isolator Solution

1. Summarize given data:

$$\text{Number of isolators} = 12, \text{ total weight } (W) = 533 \text{ K}, \text{ total } Q_d = 0.075W = 40\text{K}, \text{ total } K_d = 13 \text{ K/in}$$

$$\text{Weight /isolator } (P) = 533 / 12 = 44.42\text{K}, Q_d / \text{isolator} = 3.33\text{K}, K_d / \text{isolator} = 1.08 \text{ K/in}$$

2. Determine friction coefficient:  $\mu = Q_d/P = 3.33/44.42 = 0.075$
3. Select glass-filled PTFE (15% by weight) and stainless steel for sliding surfaces and provide contact pressure ( $p$ ) of 3,000 psi to obtain  $\mu_{\max} = 0.085$ .
4. Determine contact area of PTFE slider =  $P/p = 44.42/3.0 = 14.80 \text{ in}^2$
5. Determine diameter of PTFE slider =  $\sqrt{4(14.80)/\pi} = 4.35 \text{ in}$
6. Determine radius of spherical surface ( $R$ ) from Equations 9-62 and 9-63 which give  
 $R = W/K_d = 44.42/1.08 = 41.13 \text{ ins.}$
7. Determine overall diameter of isolator (see Figures 9-25 and 9-26)  
 Overall diameter = slider diameter + 2 x max. displacement + 2 x shoulders  
 $= 4.35 + 2 \times 5.98 + 2 \times 1.0 = 18.31 = 18.5 \text{ ins, say}$   
 Overall height estimated at one-quarter of overall diameter =  $0.25 \times 18.5 = 4.75 \text{ ins, say}$

**9. Preliminary design solution:**

Isolation system consists of 12 x 18.5-inch diameter x 4.75-inch high circular bearings each with a 4.35-inch diameter PTFE slider and a stainless steel spherical surface of radius 41.13 in.

**10. Final solution**

Checks are required and above design modified as necessary, for the following:

- System performance with actual bearing dimensions and properties (e.g., actual coefficient of friction) and minimum and maximum values determined by System Property Modification Factors (Sec 9.4.2.1 and Tables 9-9, 9-10, 9-11, and 9-12)
- Minimum restoring force capability (Sec. 9.4.3)
- Vertical load stability (Sec. 9.4.6)
- Non-seismic requirements (Sec. 9.4.7)

**9.8 TESTING ISOLATION HARDWARE**

Rigorous testing of isolation hardware is generally required for each application. This is because these devices are required to perform under extreme loads without degradation under large earthquakes. Actual testing requirements vary from code to code but in general there are both generic requirements and isolator specific requirements.

Generally there are three categories of tests for seismic isolators. These are:

- (1) Characterization tests performed to establish databases of properties such as effect of velocity, effect of pressure, effect of cumulative travel, effect of temperature, etc. These tests may be used to establish system property modification factors, to characterize the longevity of the bearings, and to develop models of the bearings for analysis.
- (2) Prototype tests performed for each project prior to fabrication of production isolation bearings. These tests are used to establish key mechanical properties of the bearings for comparison to the values used by the engineer for the design of the isolation system. Typically, two full-size isolators of each type and size of isolation bearing proposed are tested.
- (3) Production tests performed on each produced bearing. These tests represent quality control tests and are typically performed together with other material quality control tests as specified by the engineer.

AASHTO requirements are described in Section 13 of AASHTO (2010).

## **9.9 SUMMARY**

This chapter has presented information on the principles of isolation, the benefits to be expected for new and existing bridges, a summary of applications to bridges in the United States, simplified methods of analysis for isolated bridges, detailed information on elastomeric and sliding isolators, and brief guidance on testing specifications for the manufacture of isolators.

The material in this chapter is based on the *Guide Specifications for Seismic Isolation Design* published by the American Association of State Highway and Transportation Officials, Washington DC (AASHTO 2010), and is intended to be compatible with these specifications. Additional detail is provided in the FHWA/MCEER Special Publication on *Seismic Isolation for Highway Bridges* (Buckle et.al., 2006).



## **CHAPTER 10**

### **SEISMIC RETROFITTING OF HIGHWAY BRIDGES**

#### **10.1 GENERAL**

Many bridges in the United States are inadequate for seismic loads and could be seriously damaged or suffer collapse in a small-to-moderate earthquake. Major structural damage has occurred in Alaska, California, Washington and Oregon due to earthquake ground shaking. Some of these failures occurred at relatively low levels of ground motion and although the risk of bridge collapse is lower in the central and eastern United States, it is believed that ground motions large enough to cause damage have a 10 percent chance of occurring within the next 50 years in 37 of the 50 states. In some states, this could lead to bridge collapse, and to remedy this situation, retrofitting or replacement of deficient structures is necessary. This is done by identifying bridges at risk, evaluating their vulnerability for collapse or major damage, and initiating a program to reduce this risk.

Retrofitting is the most common method of mitigating risks; however, the cost of this strengthening may be so prohibitive that abandoning the bridge (total or partial closure with restricted access) or replacing it altogether with a new structure may be favored. Alternatively, doing nothing and accepting the consequences of damage is another possible option. The decision to retrofit, abandon, replace, or do-nothing requires that both the importance and degree of vulnerability of the structure be carefully evaluated. Limited resources will generally require that deficient bridges be prioritized, with important bridges in high risk areas being given the first priority for retrofitting.

This chapter summarizes procedures for evaluating and upgrading the seismic resistance of existing highway bridges including:

- A screening process to identify and prioritize bridges that need to be evaluated for seismic retrofitting.
- A methodology for quantitatively evaluating the seismic capacity of a bridge and determining the overall effectiveness of alternative retrofitting measures, including cost and ease of installation.
- Retrofit approaches and corresponding techniques for increasing the seismic resistance of existing bridges.

This process is the same as that described in the FHWA *Seismic Retrofitting Manual for Highway Structures* (FHWA, 2006) and illustrated in Figure 10-1. A bridge may be exempt from retrofitting if it is located in the lowest seismic zone, or has limited remaining useful life. Temporary bridges and those closed to traffic, may also be exempt. Details are provided in Section 10.4.7.

This chapter does not prescribe rigid requirements as to when and how bridges are to be retrofitted. The decision to retrofit depends on a number of factors, several of which are outside the realm of engineering. These include, but are not limited to, the availability of funding, and a number of political, social, and economic issues. This chapter focuses on the engineering factors.

The recommendations in this chapter are intended for use on conventional steel and concrete highway bridges. Suspension bridges, cable-stayed bridges, arches, long-span trusses, and movable bridges are not covered. However, many of the procedures and techniques presented herein can be applied to these types of structures, if appropriate judgment is used.

## **10.2 BACKGROUND**

Within the United States, the first attempt to seismically retrofit bridges took place in the aftermath of the 1971 San Fernando earthquake in southern California. This earthquake has often been cited as a watershed event in bridge engineering since it demonstrated quite dramatically that the bridge design practices of the time did not guarantee that bridges would perform well during an earthquake, even if the earthquake was of moderate intensity.

Although bridge failures during this earthquake could be attributed to deficiencies in several types of structural components, initial retrofit measures focused on the potential for loss of support at bridge bearing seats. The principal retrofit strategy was to add restrainer cables or high strength bars within bridge superstructures in order to limit relative movements at expansion joints, and to tie individual spans to the bridge piers. A program was initiated in California to retrofit all bridges that had vulnerable expansion joints. Some believed at the time that this would prevent most, if not all, bridge failures at minimum cost, but experience has shown this not to be the case.

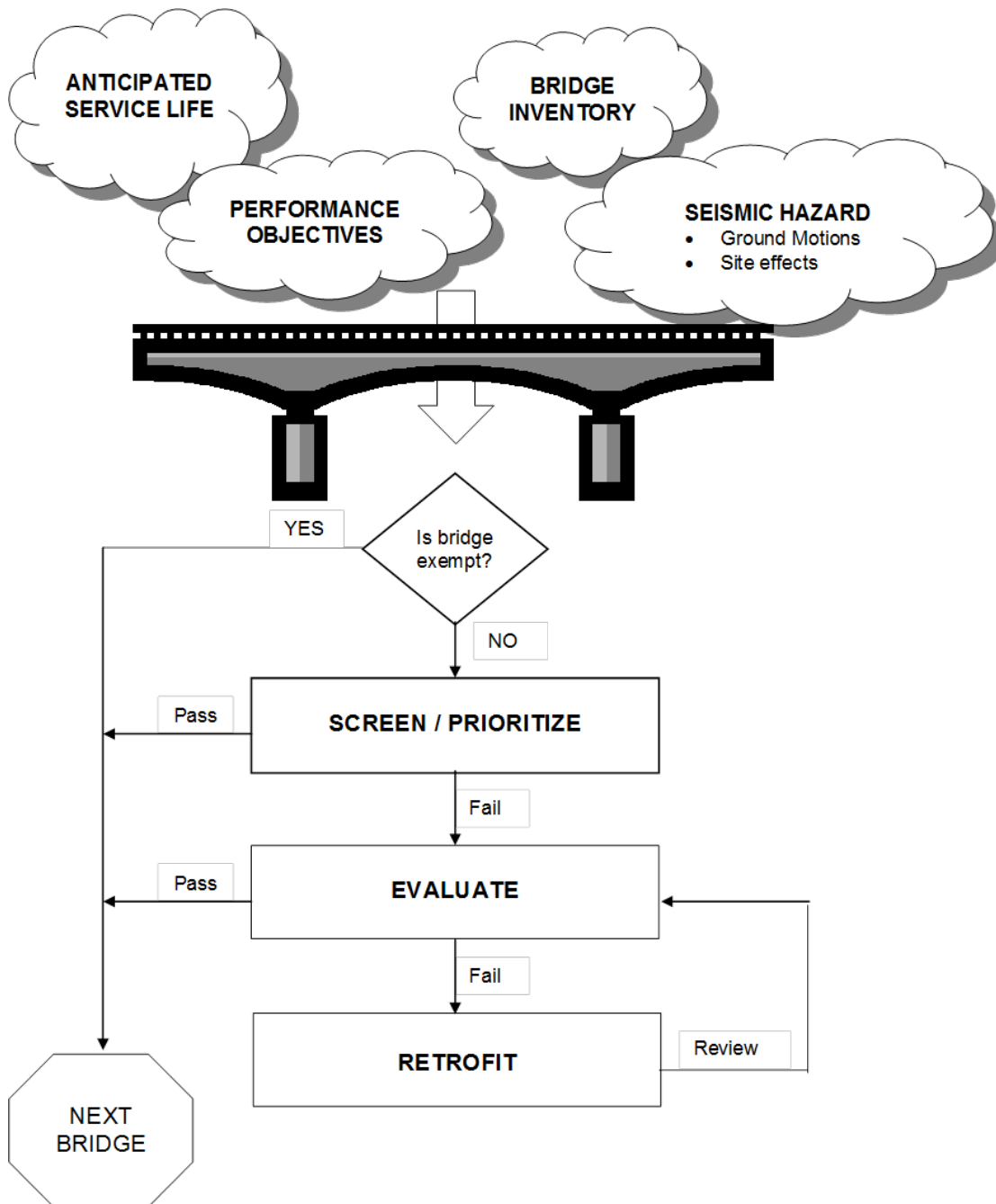


Figure 10-1 Overview of the Retrofitting Process for Highway Bridges (FHWA, 2006)

During the 1987 Whittier Narrows earthquake, a bridge that had been retrofitted with expansion joint restrainers suffered severe column damage, threatening the overall stability of the bridge (Wipf et al., 1997). This poor performance prompted renewed interest in column retrofitting, and research efforts were intensified to develop suitable methods for improving the seismic performance of existing reinforced concrete columns. Much of this research was conducted at the University of California at San Diego and was initially focused on the addition of steel shells (or jackets) to enhance confinement of the

reinforcing steel within the columns (Chai et al., 1992). Unfortunately, the 1989 Loma Prieta earthquake occurred before Caltrans could begin a state-wide column retrofitting program. The most dramatic failure during this earthquake was the collapse of the Cypress Viaduct in Oakland due to column joint failures. Although this two-level structure had been retrofitted with expansion joint restrainers prior to the earthquake, large portions of the upper deck collapsed onto the lower deck, crushing vehicles and resulting in a number of deaths (Housner, 1990).

The Loma Prieta earthquake also demonstrated that the early restrainer designs were inadequate. Many of these designs relied on too few restrainers while others caused failures to occur elsewhere in the structure, such as in the diaphragms at either side of expansion joints (Yashinsky, 1997). Many of these deficiencies had been identified through research and refined analysis (Selna and Malvar, 1987) and were not entirely unexpected. Still, it emphasized the need to review earlier bridge retrofits.

Since the Loma Prieta earthquake, there has been a major effort to perform comprehensive seismic retrofits on a large number of bridges in California. Initially, this effort was focused on bridges with single column piers, which were believed to be the most vulnerable to collapse. However, many bridges with multi-column piers collapsed or were severely damaged during the 1994 Northridge earthquake, and bridges of this type were subsequently added to the Caltrans retrofit program (Buckle, 1994).

Other states besides California now have active programs in seismic retrofitting. Washington and Nevada, for example, have sponsored research efforts and started seismic retrofit programs. Similarly, countries such as Japan and New Zealand have seismic retrofit programs. Due to these parallel efforts, significant progress has been made in the state-of-the-art of retrofitting bridge superstructures, columns, and foundations.

The Federal Highway Administration (FHWA) became a major sponsor of bridge seismic research shortly after the 1971 San Fernando earthquake, including research on the retrofitting of existing bridges. An early research project dealing with the retrofitting of bridges was conducted at the Illinois Institute of Technology (Robinson et al., 1979). The first known guidelines for retrofitting highway bridges were published by FHWA in 1981, in a report titled *Seismic Design Guidelines for Highway Bridges*, FHWA-RD-81-081. This was followed in 1983 by the publication of the FHWA *Retrofitting Guidelines for Highway Bridges*, which contained recommendations intended for national use (FHWA-RD-83-007, ATC, 1983). In addition to providing formal screening and evaluation procedures, these guidelines

presented retrofit concepts that in many cases had not been used in practice at that time. Measures were proposed for various bridge components in addition to expansion joints, such as columns, abutments and footings. Over the years, many of these concepts have been developed and refined into techniques that are commonly used today.

The principal pioneer and contributor to the state-of-the-practice in seismic retrofitting as known today, has been the California Department of Transportation (Caltrans). Following the 1989 Loma Prieta earthquake, the Highway Bridge Seismic Retrofit Program was established by Caltrans to address the more than 9,000 state-owned bridges built before 1971 and believed to be seismically-at-risk. Under this Program, and supported by an aggressive research effort, about 2,000 bridges have since been retrofitted. Much has been learned about the art and science of seismic retrofitting and this experience is reflected in the Caltrans Memo to Designers 20-4: *Seismic Retrofit Guidelines for Bridges in California* (Caltrans 2008).

In addition, the Federal Highway Administration sponsored a multi-year research program in 1992 to advance the state-of-practice in seismic retrofitting of bridges. This work was conducted at the National Center for Earthquake Engineering Research (NCEER), later to become the Multidisciplinary Center for Earthquake Engineering Research (MCEER). In 1995, a revision to the 1983 FHWA Guidelines was published under the title *Seismic Retrofit Manual for Highway Bridges* (FHWA-RD-94-052). This revision reflected advancements in the practice of retrofitting that had occurred since 1983. Other products of this research program included improved methods for restrainer design (Randall et al., 1999; DesRoches and Fenves, 1998); methods for improving the performance of older steel bridge bearings (Mander et al., 1998); improved methods of analysis and retrofit of reinforced concrete columns (Dutta, 1999); retrofit methods for multi-column reinforced concrete piers (Mander et al., 1996a and b); and a better understanding of the performance of retrofits that use both conventional and seismic isolation elastomeric bearings (Wendichansky et al., 1998). This program ended with the publication in 2006 of an updated version of the 1995 Manual, titled *Seismic Retrofitting Manual for Highway Structures: Part 1- Bridges* (FHWA-HRT-06-032). In addition to updating the retrofit techniques in the previous edition, based on research and field experience, this new edition introduced the concept of performance-based retrofitting for dual-level earthquake ground motions. This chapter is based on this edition of the FHWA Manual (FHWA, 2006).

### 10.3 PHILOSOPHY

It has been common practice to design new bridges and buildings for a single-level of earthquake ground motion. This ground motion, often called the *design earthquake*, represents the largest motion that can be reasonably expected during the life of the bridge. Implied in such a statement is the fact that ground motions larger than the *design earthquake* may occur during the life of the bridge, but the likelihood of this happening is small. This likelihood is usually expressed as the *probability of exceedance*, but it may also be described by an annual probability of occurrence, or a *return period* in years. When setting the seismic hazard level, most design specifications use the same probability of exceedance from one region to another. This ‘uniform hazard’ approach is considered to be more rational than using the maximum historical event for each region, which may have a very low probability of occurrence.

The *Standard Specification for Highway Bridges* (AASHTO, 2002) in the United States adopted a uniform hazard approach following the 1989 Loma Prieta earthquake, and chose a level of hazard that had a 10 percent probability of exceedance in a 50-year exposure period (the assumed life of a bridge). This corresponded to a ground motion with a return period of about 500 years. During the development of the *AASHTO LRFD Specification* in the mid-nineties, the life of the average highway bridge was reassessed at 75 years and the exposure period was adjusted accordingly (AASHTO, 1998). The probability of exceedance was then raised to 15 percent to maintain (approximately) the same return period (500 years).

At the same time as adopting this uniform hazard approach, a corresponding set of performance standards were included in the philosophy of the *AASHTO Standard Specifications for Highway Bridges* (AASHTO, 2002). These are given in Art. 1.1 of these Specifications and summarized below:

- Small to moderate earthquakes should be resisted within the elastic range, without significant damage.
- Realistic seismic ground motion intensities and forces be used in the design procedures.
- Exposure to shaking from large earthquakes should not cause collapse of all or part of the bridge. Where possible, damage that does occur should be readily detectable and accessible for inspection and repair.

A set of basic concepts for seismic design was derived from this philosophy for use in the *Standard Specifications*, and since embodied in the *AASHTO LRFD Bridge Design Specifications* (AASHTO 2007) and the *AASHTO Guide Specifications for LRFD Seismic Bridge Design* (AASHTO 2009). These concepts are:

- Hazard to life is minimized.
- Bridges may suffer damage but should have a low probability of collapse.
- Function of essential bridges is maintained.
- Ground motions used in design should have a low probability of being exceeded in the normal lifetime of the bridge.

In like manner, previous retrofit guidelines and manuals have also used a single-level of earthquake ground motion (a 500-year event) for representing the earthquake hazard, and adopted the same performance criteria as in the then current AASHTO Specifications for bridge design.

The assumption is made in single-level design and retrofit, that if performance under the *design earthquake* is satisfactory, it will be satisfactory at all other levels of ground motion, both smaller and larger. Such an assumption is generally not true as seen in recent earthquakes in California, Costa Rica, Japan, Turkey and Taiwan. It would be true for a smaller event if elastic performance was required at the design ground motion, and it may also be true for a larger event, if it exceeded the design ground motion by only a small margin (i.e., less than 50 percent), and there was a sufficient reserve of strength in the bridge to accommodate this higher demand.

However, in many areas of the United States, these larger ground motions can be three or four times the design ground motions and may cause instability and collapse. Although such ground motions rarely happen, their occurrence should be explicitly considered in the design and retrofit process and a ‘multi-level’ rather ‘single-level’ design process should be used. In addition, performance requirements should be adjusted for ground motions of different sizes, with higher levels of performance being expected for smaller motions and lesser levels of performance for larger motions.

*Performance-based design* provides a format for addressing these needs in a rational manner. It explicitly allows for different performance expectations for bridges of varying importance while subject to different levels of seismic hazard. Accordingly, the FHWA Manual (FHWA, 2006) recommends a performance-based approach to the seismic retrofitting of highway bridges in the United States.

This relationship is shown in Figure 10-2. Representation of the hazard and performance expectations by discrete zones (or levels) is necessary given the current state-of-the-art, and this leads to the bar chart

shown in this figure. Nevertheless, the trends are the same: high performance standards in high hazard zones imply higher costs.

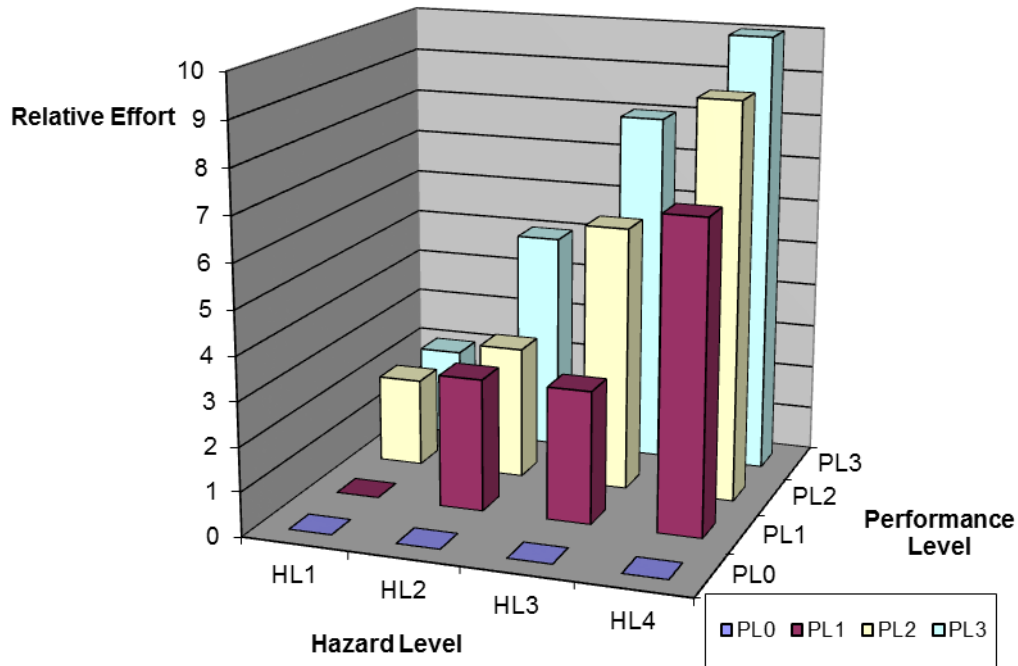


Figure 10-2 Conceptual Relationship Between Relative Effort, Increasing Hazard and Performance Level (FHWA, 2006).

## 10.4 SEISMIC PERFORMANCE CRITERIA

### 10.4.1 Performance Levels

As noted in the previous section, the FHWA Manual (FHWA, 2006) presents a performance-based approach to the seismic retrofitting of highway bridges. This means that the expected performance of the retrofitted bridge is explicitly recommended for different levels of earthquake ground motion. For this purpose, performance criteria are defined for four performance levels, as follows:

Performance Level 0 (PL0): No minimum level of performance is recommended.

Performance Level 1 (PL1): Life safety. Significant damage is sustained during an earthquake and service is significantly disrupted, but life safety is assured. The bridge may need to be replaced after a large earthquake.

Performance Level 2 (PL2): Operational. Damage sustained is minimal and full service for emergency vehicles should be available after inspection and clearance of debris. Bridge should be repairable with or without restrictions on traffic flow.

Performance Level 3 (PL3): Fully Operational. No damage is sustained and full service is available for all vehicles immediately after the earthquake. No repair is required.

The terms *minimal* damage and *significant* damage are used in the above performance criteria. These terms are explained below:

- Minimal damage includes minor inelastic response and narrow flexural cracking in concrete. Permanent deformations are not apparent and repairs can be made under non-emergency conditions with the possible exception of superstructure expansion joints which may need removal and temporary replacement.
- Significant damage includes permanent offsets and cracking, yielded reinforcement, and major spalling of concrete, which may require closure to repair. Partial or complete replacement of columns may be required. Beams may be unseated from bearings but no span should collapse. Similarly, foundations are not damaged except in the event of large lateral flows due to liquefaction, in which case inelastic deformation in piles may be evident.

Higher levels of performance may be specified by the owner. For example, the following criteria might be used for extremely important bridges:

- Sustained damage is negligible and full service to all traffic is available after inspection and clearance of debris. Damage that does occur is repairable without interruption to traffic flow. Negligible damage includes evidence of movement, and/or minor damage to nonstructural components, but no evidence of inelastic response in structural members or permanent deformations of any kind.

Generally, the performance criteria vary with level of earthquake ground motion, bridge importance and anticipated service life. In this chapter, these objectives are defined for two ground motion levels (a *lower* and an *upper* level), two importance classifications (*standard* and *essential*), and three service life categories (ASL 1, 2 and 3), as discussed below.

#### 10.4.2 Earthquake Ground Motion Levels

The *lower level* (LL) earthquake ground motion is a motion that has a reasonable likelihood of occurrence within the life of the bridge (assumed to be 75 years), i.e., it represents a relatively small but likely ground motion<sup>1</sup>. Rather than assign a probability of occurrence to this motion, it is common practice to use a probability of exceedance to characterize the motion, as noted in Section 10.3. Accordingly, the lower level motion has a relatively high probability of exceedance within the life of a bridge, and a figure of 50 percent is recommended for retrofit design. A 50 percent probability of exceedance in 75 years corresponds to a return period of about 100 years.

By contrast, the *upper level* (UL) earthquake ground motion is a motion that has a finite, but remote, probability of occurrence within the life of the bridge; i.e., it represents a large but unlikely ground motion<sup>2</sup>. Just as for the lower level motion, it is common practice to use a probability of exceedance to characterize this motion. Thus the upper level earthquake ground motion has a relatively low probability of exceedance within the life of a bridge. In this chapter, the upper level motion has a 7 percent probability of exceedance in 75 years, which corresponds to a return period of about 1,000 years.

Spectral ordinates and peak ground accelerations for both the lower and upper level ground motions may be found as explained in Chapter 2. For this purpose bridge sites are identified by zip code or, more accurately, by latitude and longitude.

#### 10.4.3 Bridge Importance

Classification of bridge importance based on traffic counts and detour lengths has been proposed in the past and importance indices developed. But such quantitative methods do not usually include many non-technical issues that directly affect importance and are loosely called socio- economic factors. Instead, a

---

<sup>1</sup> This ground motion is sometimes called the *frequent* earthquake. In the *NCHRP 12-49 Recommended LRFD Guidelines for Seismic Design* (ATC/MCEER, 2003) it is called the *expected* earthquake, and in the *Caltrans Seismic Design Methodology* (Caltrans, 1999) it is called the *functional evaluation earthquake (FEE)*.

<sup>2</sup> This ground motion is sometimes called the *rare* earthquake. In the *NCHRP 12-49 Recommended LRFD Guidelines for Seismic Design* (ATC/MCEER, 2003) it is the *maximum considered earthquake (MCE)*, and in the *Caltrans Seismic Design Methodology* (Caltrans, 1999) it is the *safety evaluation earthquake (SEE)*.

broad classification based on engineering judgment is preferred, and in this chapter two such classes are recommended: essential and standard. *Essential* bridges are those that are expected to function after an earthquake or which cross routes that are expected to remain open immediately following an earthquake. All other bridges are classified as *standard*. The determination of importance is therefore subjective and consideration should be given to societal/survival and security/defense requirements when making this judgment.

An *essential* bridge is therefore one that satisfies one or more of the following conditions:

- A bridge that is required to provide secondary life safety; e.g., one that provides access to local emergency services such as hospitals. This category also includes those bridges that cross routes that provide secondary life safety, and bridges that carry lifelines such as electric power and water supply pipelines.
- A bridge whose loss would create a major economic impact; e.g., one that serves as a major link in a transportation system, or one that is essential for the economic recovery of the affected region.
- A bridge that is formally defined by a local emergency plan as critical; e.g., one that enables civil defense, fire departments, and public health agencies to respond immediately to disaster situations. This category also includes those bridges that cross routes that are defined as critical in a local emergency response plan and those that are located on identified evacuation routes.
- A bridge that serves as a critical link in the security and/or defense roadway network. Security and defense requirements may be evaluated using the 1973 Federal-aid Highway Act, which required that a plan for defense highways be developed by each state. Now called STRAHNET, this defense highway network provides connecting routes to military installations, industries, and resources and is part of the National Highway System.

#### **10.4.4 Anticipated Service Life**

An important factor in deciding the extent to which a bridge should be retrofitted is the anticipated service life (ASL). Retrofitting a bridge with a short service life is difficult to justify in view of the very low likelihood that the design earthquake will occur during the remaining life of the structure. On the other hand, a bridge that is almost new or being rehabilitated to extend its service life, should be retrofitted for the longer remaining service life.

Estimating remaining life is not an exact science and depends on many factors such as age, structural

condition, specification used for design, and capacity to handle current and future traffic. Nevertheless, estimates can be made, at least within broad ranges, for the purpose of determining a bridge’s remaining service life and, subsequently, a retrofit category. Three such categories are used in this chapter, as defined in Table 10-1. When setting these categories, it was noted that new bridges are assumed to have a service life of 75 years in the *AASHTO LRFD Specifications* (AASHTO, 2007), and this life span was then divided into three categories for the purpose of assigning retrofit levels (retrofit categories) according to age and remaining life. It is recognized that many long-span bridges have service lives far greater than 75 years, but these are outside the scope of this chapter. Bridges in benign climates and those located on low-density routes may also have service lives in excess of 75 years.

**TABLE 10-1 – SERVICE LIFE CATEGORIES (FHWA, 2006)**

SERVICE LIFE CATEGORY	ANTICIPATED SERVICE LIFE	AGE (if not rehabilitated) <sup>1</sup>
ASL 1	0 - 15 yrs	60 - 75 yrs
ASL 2	16 - 50 yrs	25 - 60 yrs
ASL 3	> 50 yrs	< 25 yrs
<p><b>Note:</b> 1. Age is calculated assuming total service life is 75 years and the bridge has not been rehabilitated in its lifetime to date.</p>		

Bridges in category ASL 1 are considered to be near the end of their service life and retrofitting may not be economically justified. Thus, these bridges need not be retrofitted and are assigned to the lowest seismic retrofit category, i.e., category A (see Section 10.8). Bridges in category ASL 3 are almost new, and retrofitting to the standard of a new design may be justified. Those in category ASL 2 fall between these two extremes and a lesser standard is acceptable. However, the owner may always choose to retrofit to a higher standard as circumstances permit.

Bridges are often rehabilitated toward the end of their service life to address deficiencies that have accumulated over time (e.g., deteriorated deck slabs, frozen bearings and damaged expansion joints), improve safety, and to accommodate increased traffic volume. As a consequence, a bridge with 15 years, or less, of life may, after rehabilitation, have a new service life of 35 years, and in so doing, the service life category (ASL) for the bridge has been lifted from ASL 1 to ASL 2 (Table 10-1). The bridge should

now be reevaluated for seismic performance, which should be done at the same time as planning the other rehabilitation. In this way, retrofit measures (if needed) can be implemented at the same time. By taking advantage of the contractor being on site, the cost of the seismic retrofit may be significantly reduced.

#### **10.4.5 Selection of Performance Level**

Recommended minimum performance levels are given in Table 10-2 according to the level of earthquake ground motion, bridge importance and service life category, as defined above. If retrofitting to these levels cannot be justified economically, the owner may choose a lower level. On the other hand, for certain classes of bridges, the owner may choose a higher level than that recommended here. An example of such a case is the bridges on STRAHNET, which are critically important to the operation of national or regional transportation routes. Suggested criteria for these special structures are given in Section 10.4.1, but it is also likely that these bridges are of sufficient importance to justify site-specific and structure-specific performance criteria.

#### **10.4.6 Retrofitting Process for Dual Level Ground Motions**

As noted in Section 10.3, retrofitting is only one of several courses of action when faced with a bridge that is seismically vulnerable. Others include bridge closure, bridge replacement, and acceptance of the damage and its consequences. Bridge closure or replacement is usually not justified by seismic deficiency alone and will generally only be an option when other deficiencies exist. Therefore, for all practical purposes, a choice is made between strengthening and accepting the risk. This decision often depends on the importance of the bridge and on the cost and effectiveness of the proposed retrofit.

Budget constraints and limited resources prevent the simultaneous retrofit of all of the deficient bridges on the highway system, and the most critical bridges should be upgraded first. The selection and prioritizing of bridges for retrofitting requires an appreciation of not just the engineering issues but also the economic, social, and practical aspects of the situation.

Since it is recommended above that the seismic performance of a bridge be checked for two levels of earthquake ground motion (lower level and upper level), the overall retrofitting process has two distinct stages:

- Stage 1. Screening, evaluation and retrofitting for the lower level earthquake ground motion, and
- Stage 2. Screening, evaluation and retrofitting for the upper level earthquake ground motion.

**Table 10-2 MINIMUM PERFORMANCE LEVELS FOR RETROFITTED BRIDGES  
(FHWA, 2006)**

EARTHQUAKE GROUND MOTION	BRIDGE IMPORTANCE and SERVICE LIFE CATEGORY					
	Standard			Essential		
	ASL 1	ASL 2	ASL 3	ASL 1	ASL 2	ASL 3
<b>Lower Level Ground Motion</b> 50 percent probability of exceedance in 75 years; return period is about 100 years.	PL0 <sup>4</sup>	PL3	PL3	PL0 <sup>4</sup>	PL3	PL3
<b>Upper Level Ground Motion</b> 7 percent probability of exceedance in 75 years; return period is about 1,000 years.	PL0 <sup>4</sup>	PL1	PL1	PL0 <sup>4</sup>	PL1	PL2
<b>Notes:</b> <ol style="list-style-type: none"> <li>Anticipated Service Life categories are:                             <ul style="list-style-type: none"> <li>ASL 1: 0 – 15 years</li> <li>ASL 2: 16 – 50 years</li> <li>ASL 3: &gt; 50 years</li> </ul> </li> <li>Performance Levels are:                             <ul style="list-style-type: none"> <li><b>PL0: No minimum</b> level of performance is recommended.</li> <li><b>PL1: Life safety.</b> Significant damage is sustained and service is significantly disrupted, but life safety is preserved. The bridge may need to be replaced after a large earthquake.</li> <li><b>PL2: Operational.</b> Damage sustained is minimal and service for emergency vehicles should be available after inspection and clearance of debris. Bridge should be repairable with or without restrictions on traffic flow.</li> <li><b>PL3: Fully Operational.</b> No damage is sustained and full service is available for all vehicles immediately after the earthquake. No repairs are required.</li> </ul> </li> <li>Spectral ordinates and peak ground accelerations may be found as described in Chapter 2.</li> <li>Bridges assigned a Performance Level of PL0 have 15 years, or less, anticipated service life (ASL) and are candidates for replacement or rehabilitation. If the bridge is replaced or rehabilitated, the ASL category will change and so will the required Performance Level.</li> </ol>						

It is not possible to combine these two stages into one, since the performance criteria for each is very different. For example, the criteria for the lower level ground motion includes no damage and no repair (i.e., elastic behavior is expected) whereas for the upper level ground motion, damage is acceptable provided collapse does not occur and, for some bridges, access for emergency vehicles is available (i.e., inelastic behavior is expected).

Each stage comprises the three steps discussed in Section 10.1 and is shown schematically in Figure 10-1, i.e., screening, evaluation, and retrofitting for the relevant ground motion. The breakdown of each stage into these steps is illustrated in Figure 10-3, and discussed in Sections 10.6 and 10.7.

#### **10.4.7 Exempt Bridges**

A bridge is exempt from retrofitting for both levels of ground motion if it satisfies any one of the following criteria:

- The bridge has 15 years or less of anticipated service life (Section 10.4.4)
- The bridge is ‘temporary’ (i.e., anticipated service life is 15 years or less)
- The bridge is closed to traffic and does not cross an active highway, rail or waterway

A bridge is exempt from retrofitting for the upper level ground motion if it meets the criteria for Seismic Retrofit Category A (Section 10.6) for this level of motion.

### **10.5 SEISMIC HAZARD LEVELS**

Each bridge is assigned a Seismic Hazard Level (SHL) as indicated in Table 10-3, based on  $S_{DS}$  and  $S_{DI}$ , which are defined in Chapter 2. In the event that two different hazard levels are indicated by Table 10-3 for the same site, the higher level should be used.

The two footnotes to Table 10-3 effectively limit boundaries for Site Classes E and F in Hazard Levels I and II to those of site class D. This is because of the greater uncertainty in the values of  $F_v$  and  $F_a$  for class E and F soils when ground shaking is relatively low ( $S_I < 0.10$  and  $S_s < 0.25$ ).

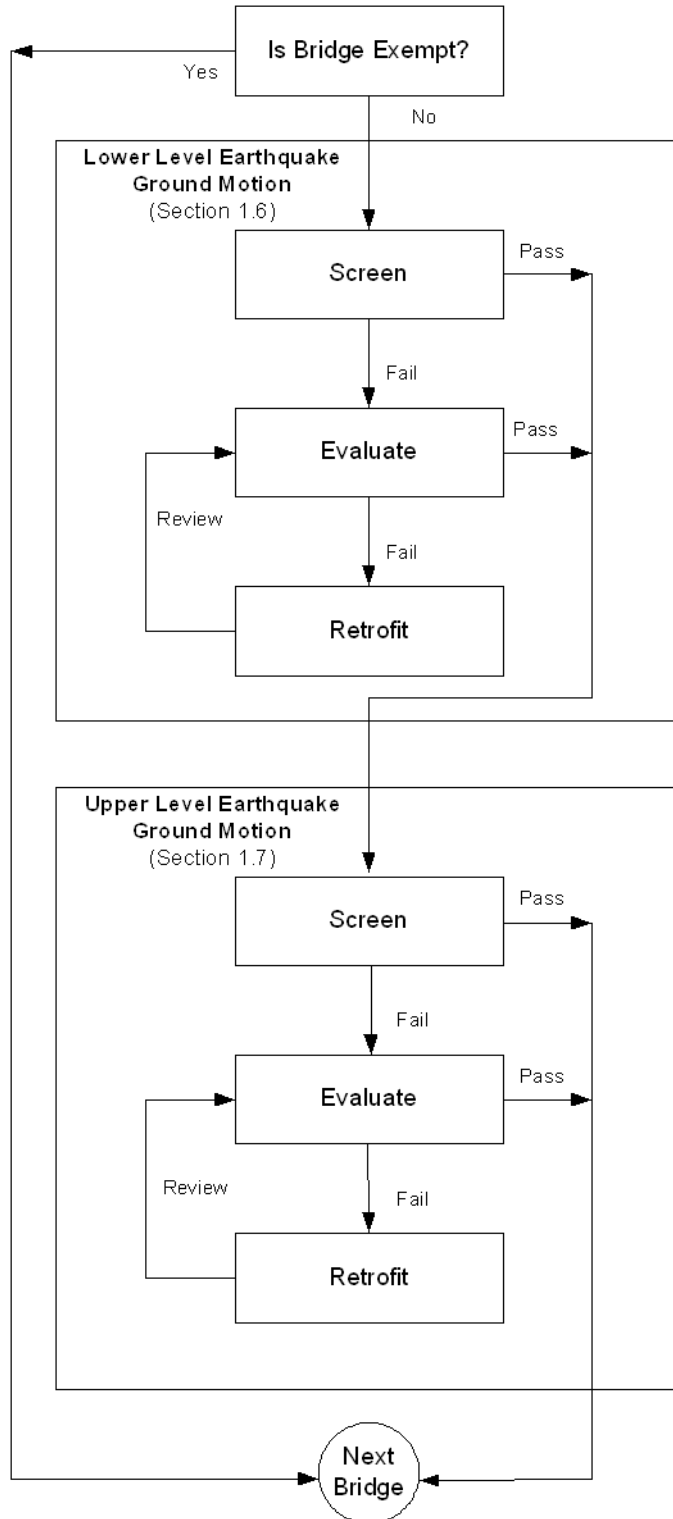


Figure 10-3 Retrofit Process for Dual Level Earthquake Ground Motions (FHWA, 2006)

**TABLE 10-3 SEISMIC HAZARD LEVEL (FHWA, 2006)**

HAZARD LEVEL	Using $S_{DI} = F_v S_I$	Using $S_{DS} = F_a S_s$
I	$S_{DI} \leq 0.15$	$S_{DS} \leq 0.15$
II	$0.15 < S_{DI} \leq 0.25$	$0.15 < S_{DS} \leq 0.35$
III	$0.25 < S_{DI} \leq 0.40$	$0.35 < S_{DS} \leq 0.60$
IV	$0.40 < S_{DI}$	$0.60 < S_{DS}$
<p><b>Notes:</b></p> <ol style="list-style-type: none"> <li>1. For the purposes of determining the Seismic Hazard Level for Site Class E soils, the value of <math>F_v</math> and <math>F_a</math> need not be taken larger than 2.4 and 1.6 respectively, when <math>S_I</math> is less than or equal to 0.10 and <math>S_s</math> is less than 0.25.</li> <li>2. For the purposes of determining the Seismic Hazard Level for Site Class F soils, <math>F_v</math> and <math>F_a</math> values for Site Class E soils may be used with the adjustment described in Note 1 above.</li> </ol>		

**10.6 PERFORMANCE-BASED SEISMIC RETROFIT CATEGORIES**

Seismic retrofit categories (SRC) are used to identify minimum screening requirements, evaluation methods and retrofitting measures for deficient bridges. They are determined by the anticipated service life, importance, and the seismic hazard exposure of the bridge. There are four categories, A through D, in increasing order of rigor and complexity. SRC A is a default category, which means that bridges in this category do not need to be screened, evaluated or retrofitted. SRC D is the highest category requiring the most rigorous screening, evaluation, and retrofitting measures.

Seismic retrofit categories are given in Table 10-4 where they are determined by the performance level (PL) required, and the seismic hazard level (SHL) at the site. The steps required to determine an SRC are shown in Figure 10-4 and are as follows:

Step 1: From the bridge records and other sources determine the:

- Importance of the bridge: either *standard* or *essential*,
- Anticipated service life of the bridge, and assign a service category: ASL 1 through ASL 3 (Table 10-1), and
- Site class based on soil type and profile (Chapter 2).

**TABLE 10-4 PERFORMANCE-BASED SEISMIC RETROFIT CATEGORIES (FHWA, 2006)**

HAZARD LEVEL	PERFORMANCE LEVEL				
	During Upper Level Earthquake			During Lower Level Earthquake	
	PL0: No Minimum Level	PL1: Life Safety	PL2: Operational	PL0: No Minimum Level	PL3: Fully Operational
I	A	A	B	A	C
II	A	B	B	A	C
III	A	B	C	A	C
IV	A	C	D	A	D

Step 2: Determine the performance level for the bridge (PL0 through PL3), based on the anticipated service life and bridge importance (Table 10-2).

Step 3: Obtain the spectral accelerations  $S_s$  and  $S_I$ , the soil factors  $F_a$  and  $F_v$  from Chapter 2, and determine the hazard level using Table 10-3. Determine the seismic retrofit category required to satisfy the performance objective for this event, using Table 10-4. These steps are summarized as follows:

Step 3.1: Obtain the spectral ordinates,  $S_s$  and  $S_I$ , from Chapter 2

Step 3.2. Obtain the soil factors,  $F_a$  and  $F_v$ , for the site (Chapter 2).

Step 3.3. Determine the seismic hazard level (SHL) based on  $F_a S_s$  and  $F_v S_I$  (Table 10-3).

Step 3.4. Obtain the SRC for the required performance level from Table 10-4.

This process is illustrated in Example 10.1.

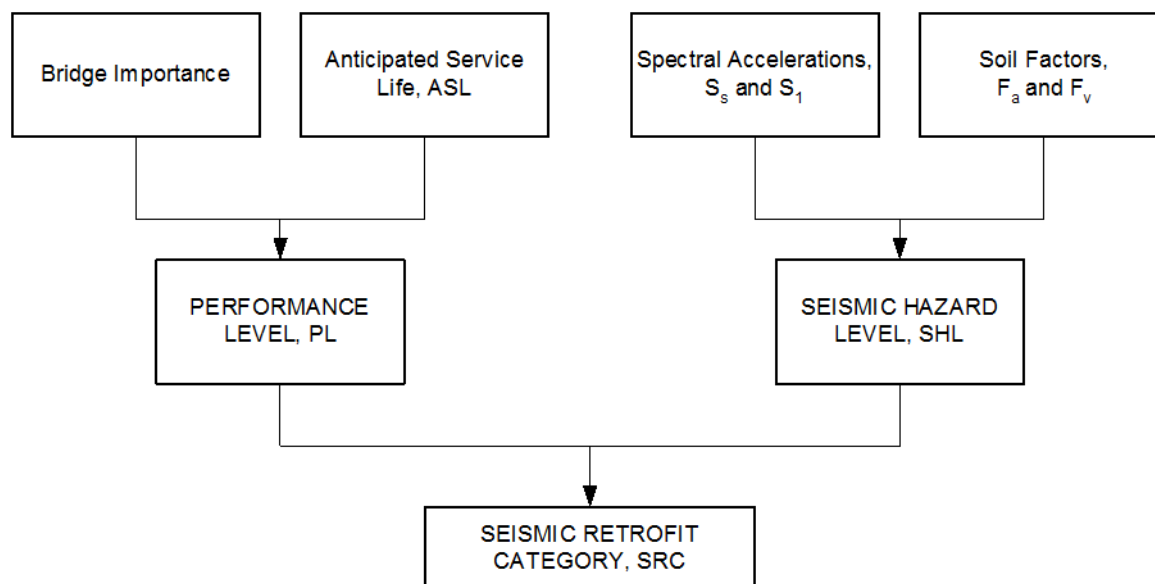


Figure 10-4 Determination of Seismic Retrofit Category (FHWA, 2006)

---

**EXAMPLE 10.1: DETERMINATION OF SEISMIC RETROFIT CATEGORIES  
FOR BOTH UPPER AND LOWER LEVELS OF GROUND MOTION**

---

An *essential* bridge in Salt Lake City, UT (zip code 84112) has an anticipated service life of 30 years, and is founded on very dense soils with an average shear wave velocity, in the upper 100 ft, of 1,350 ft/sec. Determine the seismic retrofit categories (SRC) for this bridge for both the upper and lower levels of ground motion.

**Step 1. Importance, Anticipated Service Life, and Site Class**

- 1.1 Bridge is stated to be *essential*.
- 1.2 For an anticipated service life of 30 years, the service life category is ASL 2 (Table 10-1)
- 1.3 For the given soil description and shear wave velocity, the site class is C (Chapter 2)

**Step 2. Performance Criteria**

- 2.1 From Table 10-2, for the lower level ground motion, the performance level is PL3.
- 2.2 From Table 10-2, for the upper level ground motion, the performance level is PL1.

### Step 3. Seismic Retrofit Category for Upper Level Ground Motion

3.1 For zip code = 84112,  $S_S = 1.11$  and  $S_I = 0.39$  (Chapter 2)

3.2 For site class C and the values obtained for  $S_S$  and  $S_I$ :  $F_a = 1.0$  and  $F_v = 1.4$  (Chapter 2)

3.3  $F_a S_S = 1.0 (1.11) = 1.11$

$F_v S_I = 1.4 (0.39) = 0.55$

Seismic Hazard Level (SHL) = IV (Table 10-3)

3.4 Seismic retrofit category for PL1 and SHL = IV, is C (Table 10-4, upper level motion).

This is the SRC for the upper level ground motion.

### Step 4. Seismic Retrofit Category for Lower Level Ground Motion

4.1 For zip code = 84112,  $S_S = 0.18$  and  $S_I = 0.05$  (Chapter 2)

4.2 For site class C and the values obtained for  $S_S$  and  $S_I$ :  $F_a = 1.2$  and  $F_v = 1.7$  (Chapter 2)

4.3  $F_a S_S = 1.2 (0.18) = 0.22$

$F_v S_I = 1.7 (0.05) = 0.09$

Seismic Hazard Level (SHL) = II (Table 10-3)

Seismic retrofit category for PL3 and SHL = II, is C (Table 10-4, lower level motion).

This is the SRC for the lower level ground motion.

---

## 10.7 RETROFITTING PROCESS FOR LOWER LEVEL GROUND MOTION

The lower level earthquake ground motion has a return period of about 100 years and is therefore a relatively small motion. The performance required of any bridge for these motions (Table 10-2) is elastic behavior, which is similar to the requirements for wind and braking loads. Indeed, in many parts of the United States, wind and braking loads may be larger than the earthquake loads for this return period and may govern for this stage.

The process of retrofitting bridges for the lower level earthquake ground motion is divided into three parts. These are:

- Preliminary screening of bridge inventory
- Detailed evaluation of an existing bridge

- Selection of retrofit strategy and design of retrofit measures

Note that decisions are made at each step, based on the results obtained thus far, that determine the next step in the process. Bridges are passed through a series of checkpoints to assure that only those structures actually in need of retrofit will be strengthened.

As described in Section 10.6, seismic retrofit categories (SRC) are used to recommend minimum requirements for evaluation and retrofitting. These requirements for the lower level ground motion are given in Table 10-5.

The retrofitting process for this level of ground motion is described in the following sections where it will be seen to be a force-based approach. Displacements are not explicitly considered since they are assumed to be small and within the default capacity of the structure. This is a reasonable expectation provided yielding does not occur, bearing restraints do not fail, and soils do not soften at this level of ground motion.

### **10.7.1 Screening and Prioritization for the Lower Level Ground Motion**

All bridges in the inventory should be checked for their lateral strength in both the transverse and longitudinal directions. This strength should be based on the elastic capacities of the members and foundations. Previous design calculations for wind and braking loads may be useful here. This capacity should then be checked against the seismic force ( $F$ ) on the bridge, which can be conservatively estimated as:

$$F = S_{DS}W \quad 10-1$$

where  $S_{DS}$  is defined in Chapter 2 and  $W$  is the weight of the superstructure. If the capacity is greater than the demand ( $F$ ), the bridge passes the screen and the process moves to the second stage (Section 10.8). If the capacity is less than the demand, the bridge should be considered for retrofitting at this earthquake level.

As noted above, a quick estimate of the elastic capacity of a bridge in the transverse direction is obtained by applying the factored wind load used in the design of the bridge. In the longitudinal direction, the factored braking load may be used for this purpose. If the seismic demand ( $F$ ) is greater than either of these two service loads, a more detailed evaluation is necessary, as described in Section 10.7.2.

**TABLE 10-5 - MINIMUM REQUIREMENTS (FHWA, 2006).**

ACTION		SEISMIC RETROFIT CATEGORY FOR THE LOWER LEVEL EARTHQUAKE				SEISMIC RETROFIT CATEGORY FOR THE UPPER LEVEL EARTHQUAKE			
		A	B <sup>1</sup>	C	D	A	B	C	D
<b>Screening</b> Components to be screened:		NR <sup>2</sup>	-	seat widths, connections, columns, walls, footings and liquefaction	seat widths, connections, columns, walls, footings, abutments and liquefaction	NR	seat widths, connections and liquefaction	seat widths, connections, columns, walls, footings and liquefaction	seat widths, connections, columns, walls, footings, abutments and liquefaction
<b>Evaluation</b> Evaluation methods to be used <sup>3,4</sup> . See table 1-9.		Nr	-	C	C	NR	A1/A2	B/C/D1/D2	C/D1/D2/E
<b>Retrofitting</b> Components to be retrofitted, if deficient:	Seats and Connections	NR	-	Yes	Yes	NR	Yes	Yes	Yes
	Columns, walls, footings	NR	-	Yes	Yes	NR	NR	Yes	Yes
	Abutments	NR	-	Yes	Yes	NR	NR	NR	Yes
	Liquefaction	NR	-	Yes	Yes	NR	Yes	Yes	Yes
<p><b>Notes:</b></p> <ol style="list-style-type: none"> <li>Seismic Retrofit Category B is not used when evaluating and/or retrofitting bridges for lower level ground motions.</li> <li>NR = Not Required.</li> <li>A1/A2 = No analysis; minimum capacity checks B = No analysis; component capacity checks C = Component C/D method using elastic dynamic analysis methods D1 = Capacity spectrum method. D2 = Structure C/D method; also called Nonlinear Static Procedure, or Displacement Capacity Evaluation E = Nonlinear dynamic method using inelastic time history analysis</li> <li>Selection of evaluation method also depends on bridge geometry: for irregular (complex) bridges, use Methods A, C, D2 and E as appropriate.</li> </ol>									

## 10.7.2 Evaluation for the Lower Level Ground Motion

The seismic demand given by Equation 10-1 is very conservative since it makes two simplifying assumptions. First, the period of the bridge is assumed to be very short (less than  $T_s$ , Figure 2.9), in both the longitudinal and transverse directions, and second, the entire weight of the superstructure is assumed to be mobilized during an earthquake in both the longitudinal and transverse directions.

Therefore, a two-step process is recommended for the detailed evaluation of a bridge for the lower level ground motion. These steps are:

Step 1. Revise the estimate of the seismic demand using improved values for the period of vibration.

Step 1.1. Calculate the period of the bridge in both the longitudinal and transverse directions using any of the elastic methods described in Method C (Section 10.11). These include the Uniform Load Method and the Multi-mode Spectral Method.

Step 1.2. Obtain the response spectral accelerations in the longitudinal and transverse directions ( $S_{aL}$  and  $S_{aT}$ , respectively), using the periods found in step 1.1 and the response spectra in Figure 2.9.

Step 1.3. Calculate the longitudinal and transverse seismic demands ( $F_L$  and  $F_T$ ) from:

$$F_L = S_{aL}W \quad 10-2$$

$$F_T = S_{aT}W \quad 10-3$$

Step 1.4. Compare  $F_L$  and  $F_T$  against total longitudinal braking load, and total transverse wind load respectively, and if either one is greater than the corresponding service load, a more rigorous evaluation is required. Go to step 2. If, however, both  $F_L$  and  $F_T$  are less than the corresponding service loads, no further evaluation is necessary. Proceed to Section 10.8.

Step 2. Revise the estimate of bridge capacity using explicit member strengths.

Use Method C (Section 10.11) to calculate capacity/demand ratios for each member and component in the lateral load path. Members and components with capacity/demand ratios less than unity are flagged for further consideration under Section 10.7.3.

### **10.7.3 Retrofitting for the Lower level Ground Motion**

Once a bridge has been found to be vulnerable to the lower level ground motion, the next step is to decide what, if anything, should be done to correct the deficiencies. Decision-making may be formalized by exploring retrofit options and associated cost implications using the same process described for the upper level motion in Section 10.12. In most instances, these deficiencies will be a lack of sufficient elastic strength, in which case component strengthening will be the most practical approach. The first column of Table 10-9 lists a number of strengthening approaches that may be applicable. These approaches are described in detail in FHWA (2006).

## **10.8 RETROFITTING PROCESS FOR UPPER LEVEL GROUND MOTION**

The process of retrofitting bridges for the upper level earthquake ground motion involves an assessment of many variables and requires the use of considerable judgment. Just as for the lower level ground motion, it helps to divide the process into three parts. These are:

- Preliminary screening of bridge inventory
- Detailed evaluation of an existing bridge
- Selection of retrofit strategy and design of retrofit measures

Figure 10-1 illustrates this three-step process and Figure 10-5 shows the process in greater detail for the upper level ground motion. Note that decisions are made at each step, based on the results obtained thus far, that determine the next step in the process. Bridges are passed through a series of checkpoints to assure that only those structures actually in need of retrofit will be strengthened.

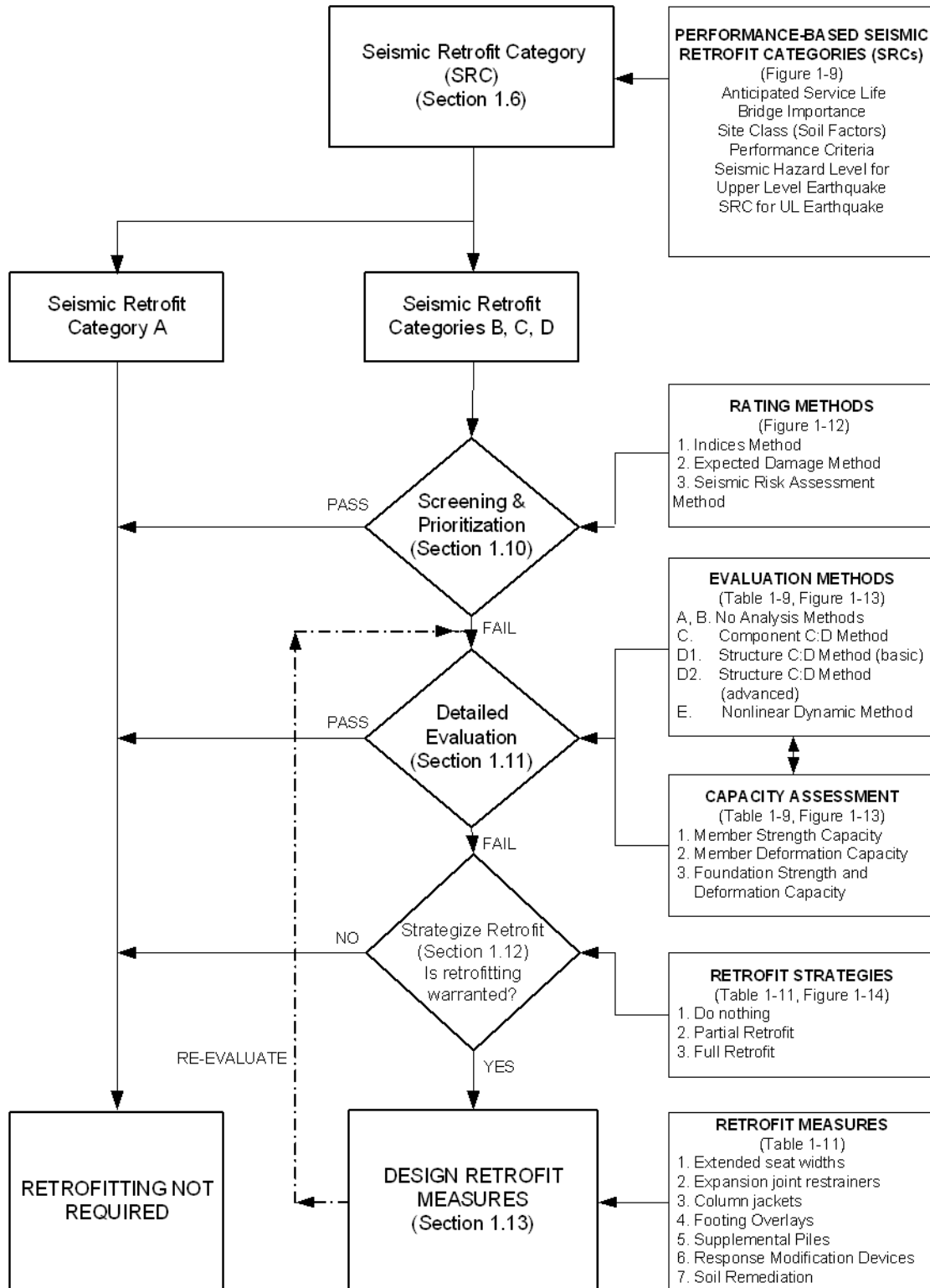
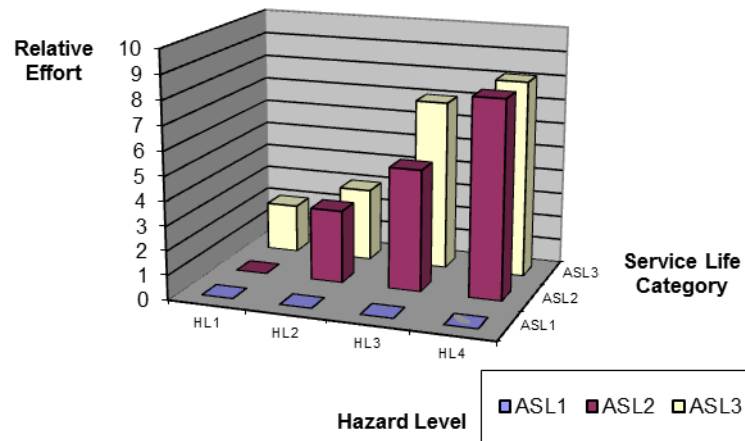
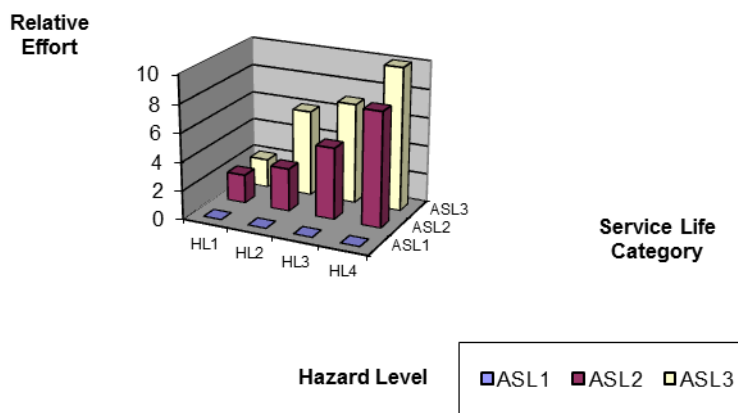


Figure 10-5 Seismic Retrofitting Process for Highway Bridges Subject to Upper Level Ground Motion (FHWA, 2006)

As described in greater detail in Sections 10.6 and 10.9, seismic retrofit categories (SRC) are used to recommend minimum requirements for evaluation and retrofitting. The SRC assigned to a bridge dictates the level of effort required to screen, analyze and retrofit a bridge, should strengthening be necessary. The SRC is determined by the importance of the bridge, its anticipated service life, and the seismic hazard level. Using these three factors, it is possible to schematically illustrate the relative effort required to retrofit bridges of different importance, in different hazard zones, and with different service lives. Figure 10-6 shows this relationship for both ‘standard’ and ‘essential’ bridges.



(a) ‘Standard’ Bridge



(b) ‘Essential’ Bridge

Figure 10-6 Relative Effort to Retrofit (a) ‘Standard’ and (b) ‘Essential’ Bridges with Varying Service Life and Hazard Level (FHWA, 2006).

## **10.9 MINIMUM REQUIREMENTS FOR UPPER LEVEL GROUND MOTION**

Minimum requirements for screening, evaluation and retrofitting are determined by the Seismic Retrofit Category (SRC), as recommended in Table 10-5. As noted above, bridges in SRC A need not be retrofitted due to their short anticipated service life, or the fact that they are located in the lowest seismic zone with minimum performance objectives (life safety only). Minimum screening, evaluation and retrofitting requirements are therefore given only for SRCs B, C and D. In general, the higher the category, the more rigorous the requirements, as seen in Table 10-5.

The screening requirements in Table 10-5 list those components of a bridge that should be examined when setting priorities for retrofitting. Since insufficient seat width and inadequate connections are common reasons for bridge failures, the minimum screening requirements (SRC B) start with seats and connections. Other components are added in the higher categories.

The evaluation requirements in Table 10-5 give permissible methods of evaluation depending on the SRC. They range from the ‘no analysis’ option and simplified elastic methods for SRC B, up to the rigorous, nonlinear dynamic analysis methods for bridges in SRC D.

Table 10-5 lists those components of a bridge that should be retrofitted if found to be deficient. Inadequate seats and connections are common reasons for bridge failures and minimum requirements (SRC B) start with restrainers, seat width extensions and connection strengthening. More extensive retrofit measures such as column jacketing, footing overlays, cap beam prestressing, ground remediation and the like, are added in the higher categories.

Finally, it is noted that the requirements in Table 10-5 are the minimum, and the owner may at any time exceed these and impose more rigorous requirements than those recommended here, at any stage of the retrofit process.

## **10.10 SCREENING AND PRIORITIZATION FOR UPPER LEVEL GROUND MOTION**

### **10.10.1 General**

Bridge inventories are screened to identify structures that are seismically deficient and to prioritize them in order of need for retrofitting. Such a process is intended to be rapid, easy to apply and conservative.

Bridges found to be deficient at this stage are subject to detailed evaluation at the next step (Section 10.11), and any that are later found to be satisfactory are excluded from further study at that time. An overview of the recommended process for screening and prioritizing an inventory of bridges for retrofitting is illustrated in Figure 10-7. Details are given in FHWA (2006).

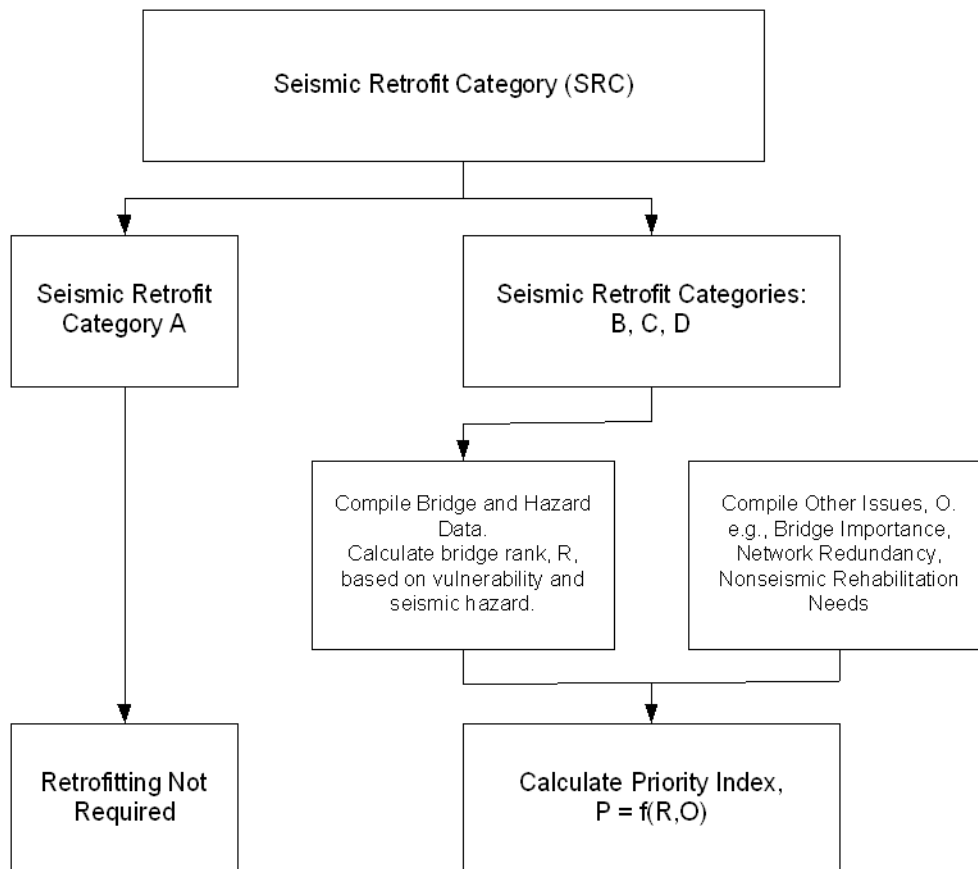


Figure 10-7 Screening and Prioritization Process (FHWA, 2006)

Three screening and prioritization methods are described in this chapter, two are presented in depth, and the third is only briefly noted. Screening programs for bridges in Seismic Retrofit Category A need not be conducted beyond the initial determination of SRC, since bridges in this category are not required to be retrofitted, regardless of their structural deficiencies or level of hazard.

Many screening and prioritization methods have been proposed in the past (Buckle, 1991). Most develop a Seismic Rating System first, and then use the results of this rating exercise to prioritize the inventory.

Factors considered in the rating exercise usually include structural vulnerabilities, and prevailing seismic and geotechnical hazards. Some also include bridge importance and network redundancy at this stage, but others use these factors only when prioritizing the list of deficient structures. Another important factor to be considered is the political, social, and economic context in which the retrofit program is being conducted. Regardless of the process used to develop the final prioritized list, all bridges should be subject to detailed evaluation before actual retrofitting is undertaken, to confirm the identified structural deficiencies and determine the cost-benefits of retrofitting.

### **10.10.2 Factors to be Considered**

The objective of a screening and prioritization program is to determine which bridge (or set of bridges) should be retrofitted first. Factors affecting such a program are the structural and soil vulnerabilities, the level of the seismic hazard and several other factors which include:

- Bridge importance. See Section 10.4.3.
- Network redundancy. This is a measure of route availability and is used to calculate bridge importance. Whereas redundancy implies resiliency in the network, and should lessen the need for retrofitting, setting priorities based on redundancy alone is not so straightforward. For example, the likelihood that alternative routes will be damaged in the same earthquake must be considered. Suppose a freeway overpass is highly vulnerable but it can be bypassed using adjacent access ramps. Since a convenient detour is nearby, a lower seismic rating might be assigned. But this assumes that the ramps remain operational, which may not be the case if there is strong ground motion in the area. If, on the other hand, the structure is a vulnerable river crossing, and the nearest detour several miles away, the redundancy of the network will be low. However, the possibility of the alternate crossing being damaged will be low and an alternate route may be available. The length of the detour then becomes the issue when deciding priority for retrofitting. Other examples where network redundancy leads to unexpected results are given in Example 10.2.
- Age and physical condition. It is generally not wise to spend a large sum retrofitting a bridge with relatively few years of service life remaining. This is one reason why bridges in SRC A do not need to be retrofitted. It is also true that an unusually high seismic vulnerability may be justification to accelerate closure or replacement of such a bridge. Also, a bridge in poor physical condition, or one that is already scheduled for structural or functional rehabilitation, may be given a higher priority for seismic retrofitting, since cost savings can be achieved by performing the non-seismic and seismic work simultaneously.

The above factors are not an exhaustive list, but illustrate some of the principles involved in assigning priorities. In most cases, seismic ratings are used to guide decision-making but are not the final word. Common sense and engineering judgment are necessary when weighing the actual costs and benefits of retrofitting against the risks of doing nothing.

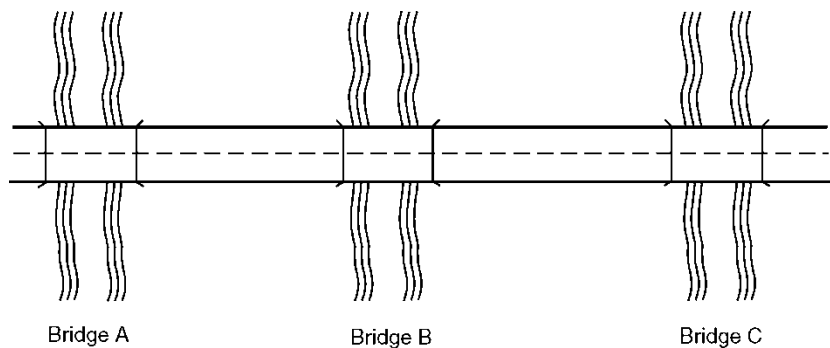
---

### EXAMPLE 10.2: IMPACT OF NETWORK REDUNDANCY ON BRIDGE PRIORITIZATION (FHWA 2006)

---

#### Example 10.2(a).

In the figure at right, assume that Bridge A is a seismically vulnerable bridge and has a high seismic vulnerability rating. It is located on a major route in series with lower-rated Bridges B and C, which are also vulnerable to earthquakes, but to a lesser degree than Bridge A.



Assume that no convenient detour to this route exists and that each bridge can be economically retrofitted. What priority should be given to Bridges B and C?

*Answer:* Since retrofitting Bridge A alone would improve only one point on the route and do nothing to prevent the failure of Bridges B or C, and because construction and administration savings can be realized by retrofitting more than one bridge in the same geographical area at a time, Bridges B and C, although lower rated than A, should also be considered for retrofitting.

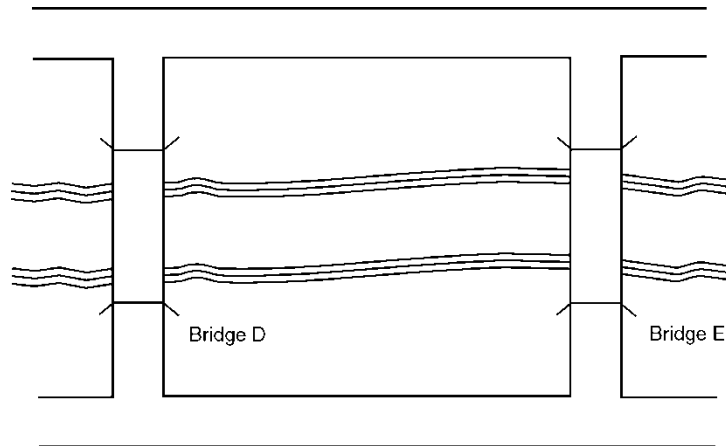
#### Example 10.2(b).

Suppose in the Example above, Bridge B has a high vulnerability rating but cannot be economically retrofitted. What priority should now be given to Bridges A and C?

*Answer:* Because Bridge B is in series with Bridges A and C, the route would be closed if Bridge B were to collapse. Therefore, unless Bridge B can be replaced at the same time, it may be advisable to give Bridges A and C a lower retrofit priority because strengthening of these two bridges alone may not prevent closure of the route.

**Example 10.2(c).**

Consider two bridges that have parallel functions, such as Bridges D and E in the figure at right. If Bridge D has a lower vulnerability rating than Bridge E, which bridge should be retrofitted first?



*Answer:* Since Bridge D has the lower rating, it is possible that it could be more economically retrofitted than Bridge E,

since less strengthening is required. If this is true, and the collapse of one bridge is preferred over the loss of both bridges, then it might be more logical to retrofit Bridge D before Bridge E, even though Bridge E had the higher vulnerability rating.

---

### 10.10.3 Seismic Vulnerability Rating Methods

Most vulnerability rating methods assign a structure vulnerability index (from Figure 10-5) and a hazard index (Figure 10-5), and combine these in various ways to obtain an overall seismic rating. Some methods also develop an importance index (Figure 10-5) to address daily traffic flow, redundancy and the socioeconomic climate. Others use qualitative measures to include these factors. This last approach was recommended in the 1995 *FHWA Retrofitting Manual* (FHWA, 1995) and is also included in the current edition (FHWA, 2006). Recent progress in seismic risk assessment methods has led to the development of fragility functions for specific classes of bridges. These in turn have led to loss estimation methodologies for highway systems. These methodologies have many potential applications in highway design and retrofitting, including planning for emergency response and recovery. They may be used for screening bridge inventories with more rigorous results than possible with the above methods, since they quantify the uncertainties surrounding bridge and site vulnerability, network redundancy and importance factors.

The three methods summarized below have increasing complexity, but decreasing conservatism. Two of these are further described in later sections of this chapter. These methods are differentiated by the manner in which structure vulnerability, seismic and geotechnical hazards, importance, redundancy and various socioeconomic factors are treated.

The methods are:

1. Indices Method (FHWA, 1995)

Indices are used to characterize the structure vulnerability and hazard level and are then combined to give a single rating for each bridge. Indices range from 0 to 10 and are based on conservative, semi-empirical rules. Prioritization is determined by this rating together with a qualitative assessment of importance, redundancy, non-seismic issues, and socioeconomic factors. This is the simplest of the three methods, but it is also the most conservative, since it uses arbitrary rules to allow for inherent uncertainties.

2. Expected Damage Method

This method compares the severity of expected damage for each bridge in the inventory, for the same earthquake. Severity of damage is measured either by sustained damage state(s) or by estimating direct economic losses. Bridges with the highest expected damage (and/or loss) are given the highest priority for retrofitting. Uncertainty in ground motions, and randomness in soil and structure properties, are explicitly addressed by using fragility functions to estimate damage-state probabilities. A qualitative assessment of indirect losses, network redundancy, and non-seismic issues is required and the ranking, based on fragility, is modified accordingly.

3. Seismic Risk Assessment Method

Explicit analysis of the highway network is performed for a given hazard level and the resulting damage states used to estimate the effect on system performance as measured by traffic flow (e.g., increased travel times). Sensitivity of this performance to bridge condition is subsequently used to determine bridge retrofit needs and priorities. Independent qualitative assessment of non-seismic issues and socioeconomic factors is required. This is the most complex of the three methods, but it is also the most rigorous with the least conservatism in the final result.

Methods 1 and 2 are summarized in Sections 10.10.4 and 10.10.5 below and in detail in FHWA (2006). Method 3 is considered outside the scope of this chapter and is not discussed further. A full description may be found in Werner et al., 2000.

### **10.10.3.1 Minimum Screening Requirements**

Minimum requirements for screening bridge inventories, based on Seismic Retrofit Categories, are recommended in Table 10-5.

### **10.10.3.2 Seismic Inventory of Bridges**

The first step in implementing any of the above methods is to compile a bridge inventory with the objective of obtaining the following basic information:

- The structural characteristics of each bridge to determine either the vulnerability rating or to select the fragility function, and
- The seismicity and soil conditions at each bridge site to determine the seismic hazard rating or select the fragility function.

This information may be obtained from the bridge owner's records, the National Bridge Inventory (<http://www.fhwa.dot.gov/bridge/nbi.htm>), “as-built” plans, maintenance records, the regional disaster plan, on-site bridge inspection records, and other sources. A form, such as the sample shown in Table 10-6, should be used for recording this information and filed with the bridge records.

Much of the information used to assign the required performance level for the retrofitted bridge in Section 10.4 will also be necessary when making assessments of importance, redundancy, and socioeconomic issues in the sections that follow.

### **10.10.4 Indices Method**

In this method, the seismic rating of a bridge is determined by its structural vulnerability, the seismic and geotechnical hazards at the site, and the socioeconomic factors affecting the importance of the structure. Ratings of each bridge are first found in terms of vulnerability and hazard, and then modified by importance (societal and economic issues) and other issues (redundancy and non-seismic structural issues) as necessary to obtain a final, ordered determination of retrofitting priority (Buckle, 1991; FHWA, 1995).

**TABLE 10-6 - SAMPLE BRIDGE SEISMIC INVENTORY FORM (FHWA, 2006).**

**BRIDGE SEISMIC INVENTORY DATA FORM**

Bridge Name \_\_\_\_\_ BIN Number \_\_\_\_\_

Location \_\_\_\_\_

Year Built \_\_\_\_\_ ADT \_\_\_\_\_ Detour Length \_\_\_\_\_

Total Length \_\_\_\_\_ Feature Carried \_\_\_\_\_

Overall Width \_\_\_\_\_ Feature Crossed \_\_\_\_\_

Importance: essential / standard      Alignment: straight / skewed/ curved      Geometry: regular / irregular

Seismic Hazard (100-year event):  $S_s =$  \_\_\_\_\_ g     $S_1 =$  \_\_\_\_\_ g    Soil Site Class: A / B / C / D / E \_\_\_\_\_  
 (1000-year event):  $S_s =$  \_\_\_\_\_ g     $S_1 =$  \_\_\_\_\_ g    Soil Site Class: A / B / C / D / E \_\_\_\_\_

**SUPERSTRUCTURE:** Material and Type \_\_\_\_\_

Number of spans \_\_\_\_\_ Continuous: yes / no      Number of expansion joints \_\_\_\_\_

**BEARINGS:** Type \_\_\_\_\_ Condition: functioning / not functioning \_\_\_\_\_

Type of restraint: Longitudinal: \_\_\_\_\_ Transverse: \_\_\_\_\_

Actual support length \_\_\_\_\_ Minimum required length \_\_\_\_\_

**COLUMNS AND PIERS:** Material and Type \_\_\_\_\_

Cross-section: Min. transverse dimension \_\_\_\_\_ Min. longitudinal dimension \_\_\_\_\_

Height range (low – high): \_\_\_\_\_ Fixity: Top \_\_\_\_\_ Bottom \_\_\_\_\_

Longitudinal reinforcement (%) \_\_\_\_\_ Splices in end zones ? yes / no \_\_\_\_\_

Transverse confinement steel \_\_\_\_\_

**FOUNDATIONS AND ABUTMENTS:** Type: spread footings / pile footings / pile bent / single shaft / other \_\_\_\_\_

Abutment type: seat / integral / other \_\_\_\_\_ On Piles: yes / no other \_\_\_\_\_

Abutment height \_\_\_\_\_ Wingwalls: yes / no      Liquefaction: susceptibility low / moderate / high

This rating system has two parts: quantitative and qualitative. The quantitative part produces a seismic rating ('bridge rank') based on structural vulnerability and site hazard. The qualitative part modifies the rank in a subjective way that accounts for importance, network redundancy, non-seismic deficiencies, remaining useful life, and similar issues to arrive at an overall priority index. Engineering and societal judgment are key to the second stage of the screening process. This leads to a priority index,  $P$ , which is a function of rank, importance, and other issues:

$$P = f(R, \text{importance, non-seismic, and other issues}) \quad 10-4$$

where  $P$  is the priority index, and  $R$  is the rank based on structural vulnerability and seismicity.

In summary, *bridge rank* is based on structural vulnerability and seismic hazard, whereas *retrofit priority* is based on bridge rank, importance, non-seismic deficiencies, and other factors such as network redundancy. A methodology for calculating bridge rank ( $R$ ) and the assignment of the priority index ( $P$ ) is given by FHWA (2006).

#### 10.10.5 Expected Damage Methods

The Expected Damage Method compares the severity of expected damage for each bridge in the inventory for the same earthquake, and ranks each bridge accordingly. Severity of damage is measured either by the sustained damage state(s) or the estimated direct economic loss. Bridges with the highest expected damage (and/or loss) are given the highest priority for retrofitting.

In its present form, the method does not include indirect economic losses due to loss of life, injuries, business disruption, traffic congestion, denial of access to emergency responders and the like. These losses will probably exceed the direct losses (i.e., repair costs) but the state-of-the-art of loss estimation is currently unable to quantify these costs with any certainty.

As in the Indices Method, this method has two parts: quantitative and qualitative. The quantitative part is based on expected damage and direct economic losses, and is used to obtain a bridge rank,  $R$ . The qualitative part modifies the rank in a subjective way that takes into account such factors as indirect losses, network redundancy, non-seismic deficiencies, remaining useful life, and other issues, to obtain an overall priority index. As in the previous method, engineering and societal judgment are the key to the

second stage of the process. This leads to a priority index,  $P$ , which is a function of rank, indirect losses, redundancy, and other issues, as follows:

$$P = f(R, \text{indirect losses, redundancy and various non-seismic issues}) \quad 10-5$$

where  $P$  is the priority index, and  $R$  is the rank based on expected damage and direct losses.

It is seen that *bridge rank* is based on expected damage and direct losses for a given earthquake, whereas *retrofit priority* is based not only on bridge rank, but also on expected indirect losses, network redundancy and non-seismic factors, estimated in a subjective way. Although Equation 10-5 has the same form as Equation 10-4, the terms are calculated in different ways. A particular advantage of this method is that it provides a template by which indirect losses may be rationally included, as the state-of-the-art improves.

The estimation of expected damage is a critical step in this method and due to uncertainty in earthquake ground motions, and randomness in soil and structure properties, this step is a probabilistic one. Fragility functions are used to estimate the probability of a bridge being in one or more specified damage states, after a given earthquake.

As noted in Section 10.10.3, fragility functions are also essential elements in the Seismic Risk Assessment Method for screening and prioritizing bridges. These functions are also used in most loss-estimation methodologies, including HAZUS, which is under development by the National Institute of Building Sciences for the Federal Emergency Management Agency (HAZUS, 1997).

In order to simplify the method as much as possible, input data requirements are kept to a minimum. In particular, all structure attributes may be found in the NBI. Ground motions and soils data are based on spectral accelerations and soil types as described in Chapter 2.

A methodology is given by FHWA (2006) for calculating bridge rank ( $R$ ) and the assignment of the priority index ( $P$ ), based on expected damage.

## 10.11 METHODS FOR EVALUATION OF UPPER LEVEL GROUND MOTION

Bridges found to be deficient during screening and prioritization (Section 10.10) are subject to detailed evaluation using one or more of the methods described in this section. Since the screening procedures described above are necessarily conservative, it is likely that a bridge identified as deficient during screening will be found satisfactory upon a more detailed evaluation.

The seismic evaluation of a bridge is explicitly or implicitly a two-part process. A demand analysis is first required to determine the forces and displacements imposed on the bridge by an earthquake; this is then followed by an assessment of capacity to withstand this demand. Most evaluation methods express their results as capacity/demand ratios calculated on a component-by-component basis, or for the bridge as a whole (i.e., as a single structural system).

Six evaluation methods are described in this chapter, which are all based, to varying degrees, on capacity-demand principles. They are listed below in order of increasing sophistication and rigor, and are summarized in Table 10-7. All six methods are described in detail in FHWA (2006). These methods emphasize the calculation of *demand* on a member or component of a bridge. Methods for calculating the *capacity* of a member or component are described in detail in FHWA (2006). The relationships between these methods for demand analysis and capacity assessment are shown schematically in Figure 10-8.

Method A1/A2: Connection forces and seat width checks. Seismic demand analysis is not required but the capacity of connections and seat width adequacy is checked against minimum values. The method is suitable for all single span bridges and others in low hazard zones. The method is divided into two categories, A1 and A2. If the short-period spectral ordinate  $S_s < 0.10$ , Method A1 may be used. Otherwise, Method A2 must be used, which requires higher minimum connection capacities than Method A1 (FHWA, 2006).

Method B: Component capacity checks. Seismic demand analysis is not required, but the relative strength of the members and the adequacy of certain key details are checked against recommended minima. This method is suitable for regular bridges in SRC C, subject to restrictions on  $F_v S_1$  as explained in FHWA (2006).

**TABLE 10-7 - EVALUATION METHODS FOR EXISTING BRIDGES (FHWA, 2006)**

METHOD		CAPACITY ASSESSMENT	DEMAND ANALYSIS	APPLICABILITY		COMMENTS
				SRC-UL <sup>1</sup>	Bridge Type	
A1 A2	Connection and Seat Width Checks	Uses default capacity due to non-seismic loads for connections and seat widths.	Not required	A – D B	All single span bridges. Bridges in low hazard zones.	Hand method, spreadsheet useful.
B	Component Capacity Checks	Uses default capacity due to non-seismic loads for connections, seats, columns and foundations.	Not required	C	Regular bridges, but subject to limitations on $F_v S_1$ .	Hand method, spreadsheet useful.
C	Component Capacity/Demand Method	Uses component capacities for connections, seat widths, column details, footings, and liquefaction susceptibility (11 items).	Elastic Methods <sup>2</sup> : • ULM • MM • TH	C & D	Regular and irregular bridges that respond almost elastically, such as those in low-to-moderate seismic zones and those with stringent performance criteria.	Calculates capacity/demand (C/D) ratios for individual components. Software required for demand analysis.
D1	Capacity Spectrum Method	Uses bilinear representation of structure capacity for lateral load, subject to restrictions on bridge regularity.	Elastic Methods <sup>2</sup> : • ULM	C & D	Regular bridges that behave as single-degree-of-freedom systems and have ‘rigid’ in-plane superstructures.	Calculates C/D ratios for complete bridge, for specified limit states. Spreadsheet useful.
D2	Structure Capacity/Demand Method	Uses pushover curve from detailed analysis of superstructure, individual piers and foundation limit states.	Elastic Methods <sup>2</sup> : • ULM • MM • TH	C & D	Regular and irregular bridges.	Calculates C/D ratios for bridge superstructure, individual piers, and foundations. Also known as <i>Nonlinear Static Procedure</i> or <i>Displacement Capacity Evaluation Method</i> . Software required.
E	Nonlinear Dynamic Method	Uses component capacities for connections, seat widths, columns and footings.	Inelastic Methods <sup>2</sup> • TH	D	Irregular complex bridges, or when site specific ground motions are to be used such as for bridges of major importance.	Most rigorous method, expert skill required. Software essential.
<p><b>Notes:</b> 1. SRC-UL = Seismic Retrofit Category for upper level earthquake ground motion                  2. ULM = Uniform Load Method; MM = Multi-Mode Spectral Method; TH = Time History Method</p>						

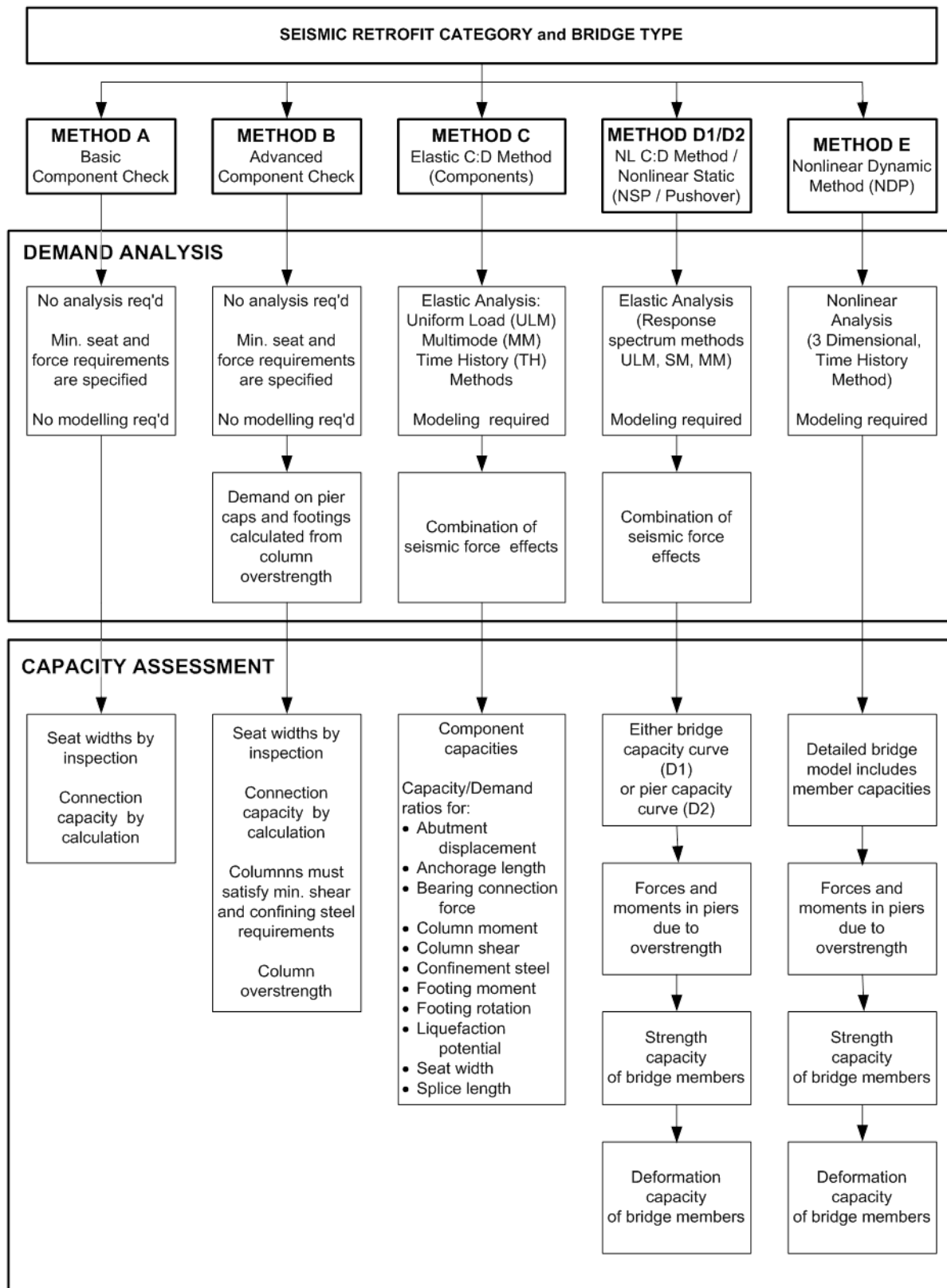


Figure 10-8 Evaluation Methods for Existing Bridges Showing Relationship Between Demand Analysis and Capacity Assessment (FHWA, 2006)

Method C: Component capacity/demand method. Seismic demands are determined by an elastic analysis such as the uniform load method, multi-mode response spectrum method, or an elastic time history method (Section 5.2). The uniform load method is adequate for bridges with regular configurations; otherwise, the multi-mode method is used as a minimum. Capacity/demand ratios are calculated for all relevant components. This method is suitable for all bridges in SRC C and D, but gives best results for bridges that behave elastically or nearly so.

Method D1: Capacity spectrum method. Seismic demands are determined by simple models such as the uniform load method, and capacity assessment is based on a simplified bilinear lateral strength curve. A capacity spectrum is used to calculate the capacity/demand ratio for the bridge, for each limit state. This method is suitable for regular bridges in SRC C and D (Section 5.3.1.2).

Method D2: Structure capacity/demand method. Seismic demands are determined by elastic methods such as the multi-mode response spectrum method, or an elastic time history method. Capacity assessment is based on the displacement capacity of individual piers as determined by a ‘pushover’ analysis, which includes the nonlinear behavior of the inelastic components. A capacity spectrum is used to calculate the capacity/demand ratio for each pier, bearing, and foundation of the bridge, for each limit state. This method is suitable for all bridges in SRC C and D. It is also known as the *Pushover Method* or alternatively the *Nonlinear Static Procedure* (Section 5.3.1.1).

Method E: Nonlinear dynamic procedure (time history analysis). Seismic demands are determined by a nonlinear dynamic analysis using earthquake ground motion records to evaluate the displacement and force demands. Capacities of individual components are explicitly modeled in the demand analysis. This method is suitable for irregular complex bridges, or when site specific ground motions are to be used for a bridge of major importance (Section 5.3.2).

In summary, Methods A and B are based on default minima with no demand analysis required. Methods C and D are capacity-demand methods of varying rigor, and Method E is the most rigorous of all the methods and is based on inelastic time history analysis.

The choice of method to be used for an evaluation is determined by the minimum requirements in Table 10-5 and the regular/irregular requirements summarized above and in Table 10-4. The minima in Table 10-5 are related to the Seismic Retrofit Category of the bridge under consideration, and are based on two principles. First, as the seismic hazard increases, improved modeling and analysis for the seismic

demands is necessary, because bridge response is sensitive to increasing demand. Second, as the complexity of the bridge increases, more sophisticated models are required to capture both the demand and capacity with certainty. Note that a higher level of analysis may always be used in place of a lower-level method.

## **10.12 RETROFIT STRATEGIES FOR UPPER LEVEL GROUND MOTION**

### **10.12.1 General**

Once a bridge is found to be seismically deficient, the next step is to decide what, if anything, should be done to correct the deficiencies. Decision-making may be formalized by exploring retrofit options and the associated cost implications. This section revisits the objectives of retrofitting and discusses the selection of a retrofit strategy (including cost considerations), developing a retrofit approach, and identifying retrofit measures.

A *Retrofit Strategy* is the overall plan for the seismic retrofit of a bridge. This plan can employ more than one retrofit approach and thus several different retrofit measures. Retrofit strategies are discussed in Section 10.12.2.

A *Retrofit Approach* is the philosophy of seismic enhancement adopted for a bridge. Strengthening is an example of a retrofit approach. One or more retrofit approaches can be employed in the seismic retrofit of a bridge. Various approaches are discussed in Section 10.12.3.

A *Retrofit Measure* is the physical modification of a component in a bridge for the purpose of upgrading overall seismic performance. For example, the addition of a steel shell to a reinforced concrete column is a retrofit measure. Retrofit measures for superstructure, substructure, and foundation components are summarized in Section 10.13, and described in detail in FHWA (2006).

### **10.12.2 Retrofit Strategy Selection**

#### **10.12.2.1 Objective of Retrofitting and Acceptable Damage**

The objective of retrofitting a bridge is to ensure that it will perform satisfactorily when subjected to the design earthquake. Specifically, bridges should be retrofitted to meet the performance criteria given in

Section 10.4 and Table 10-2, which are determined by the importance of a bridge and its anticipated service life.

Performance criteria for both new and existing bridges permit considerable structural damage as long as collapse is prevented, and the amount of acceptable damage in existing bridges may be greater than for new designs.

There are at least two reasons why accepting some level of damage is an essential ingredient of almost all retrofit strategies. These are:

- Retrofitting is usually more complex and more expensive than providing adequate resistance in a new bridge. In some cases, the added cost of preventing damage could be as much, or more, than the cost of repairing the damage in the un-retrofitted bridge (neglecting indirect losses).
- Existing bridges may have a reduced useful or remaining life due to normal ‘wear and tear,’ and increasing traffic volume and/or load capacity requirements. This shortened life reduces the likelihood that such a structure will experience a damaging earthquake, and increases the annualized cost of every dollar spent to prevent earthquake damage.

There are exceptions to this rule. These include very important bridges, and where the societal cost of any damage that disrupts serviceability, or reduces traffic capacity, is unacceptable.

#### **10.12.2.2 Cost Considerations of Seismic Retrofit**

Cost is a major consideration in seismic retrofitting. As noted above, the average cost of seismic retrofitting is much higher than of incorporating seismic resistance into the design of a new bridge. In fact, it has been estimated that in extreme cases, seismic retrofitting may be two to three times more expensive.

Data giving the actual cost of retrofitting is hard to find because very few States have completed extensive retrofit programs from which cost databases may be compiled. However, Table 10-8 gives some data based on Caltrans’ experience in retrofitting 165 bridges during 1993 and 1994. In this table, retrofit costs are expressed as a fraction of the cost of new construction and the average cost is seen to be about 15 percent of the cost of building a new bridge in the same time period. Also, as might be expected,

retrofit costs strongly depend on the strategy employed. When only the superstructure is retrofitted (cable restrainers and seat width extenders), the average construction cost is about 3.1 percent of new construction. When the substructure is also retrofitted, but not the foundation, the average cost rises to 15.4 percent. When the foundation is included, the average cost rises further to 28.8 percent. Table 10-8 also shows a significant variation in cost when the same strategy is applied to different bridges, due to differences in the extent of retrofitting required. Although this data reflects prevailing conditions in the California construction market at the time of these retrofits, the trends are believed applicable elsewhere in the country.

**TABLE 10-8 - COST OF VARIOUS RETROFIT STRATEGIES AS PERCENTAGE OF NEW CONSTRUCTION COSTS<sup>1,2</sup> (FHWA, 2006)**

RANGE	RETROFIT STRATEGY			TOTAL <sup>4</sup>
	Superstructure Only <sup>3</sup>	Superstructure and Substructure	Superstructure, Substructure and Foundations	
Low	1.3	0.7	2.3	0.7
Average	3.1	15.4	28.8	15.1
High	13.2	64.8	232.9	232.9

**Notes:** 1. Caltrans data for 165 bridges retrofitted in 1993 and 1994.  
2. Costs expressed as percentage of new construction for same time frame.  
3. Superstructure includes restrainers and seat width extensions.  
4. Weighted sum of all retrofits in California 1993 and 1994.

Engineering costs for retrofit design are also generally higher than for new construction. It is not unrealistic to expect that these costs will be twice the cost of the engineering required for a new bridge of similar value. This is because many bridges are unique and often require customized retrofit strategies. Standardization of design and retrofit details is therefore difficult to achieve. In addition, the detailed seismic evaluation of a bridge and identification of the most appropriate retrofit strategy is a time-consuming process that may involve a detailed dynamic analysis and potentially, many trial designs investigating possible strategies.

In addition to higher initial costs, the fact that the life of a retrofit should not exceed the remaining service life of the bridge means that the annualized cost of retrofitting is further increased over the cost of seismic resistance in new construction. This requires that the benefits of retrofitting, particularly for damage prevention, be weighed against these higher costs when selecting a retrofit strategy for the bridge.

### 10.12.2.3 Other Considerations and Non-seismic Issues

Many existing bridges within the United States are either structurally deficient or functionally obsolete, in addition to being seismically vulnerable. Either one of these two conditions could result in a bridge being rehabilitated, which might present an opportunity for improving the seismic resistance of a bridge at the same time. If retrofitting is required immediately, it may be advisable for the designer to consider the additional demands that will be placed on the structure when the future widening is finally accomplished. A designer should therefore consider both the present condition and possible future service that will be required of the bridge.

Bridge inspection and maintenance needs should also be considered when designing a seismic retrofit. This includes access for inspection as well as maintenance activities. The retrofit measure itself should not become a maintenance problem. The designer should be aware of the needs of maintenance personnel and include them in the selection process of the retrofit strategy.

Retrofit measures can dramatically alter the appearance of the bridge. The designer should therefore be sensitive to the aesthetics of the retrofit design. This could be particularly important if the original design has notable aesthetic value or if it is desirable or required to preserve the appearance of the bridge for other reasons (e.g., if the bridge is a historic structure). There may be alternative retrofit measures that are just as effective, but more aesthetically acceptable.

It is often not possible to close a bridge to traffic while retrofitting is performed, but some retrofit measures require access to portions of the bridge that will disrupt traffic. Rerouting of traffic and staged construction will then be necessary, and when this is difficult to achieve, a strategy that limits disruption to traffic must be found. Similar constraints may exist with respect to utilities on or near the bridge. If they cannot be easily relocated, it may be necessary to redesign the retrofit to avoid damage or disruption to these utilities.

Constructability is always an issue for the bridge designer, but potentially more so in the case of seismic retrofitting. The main problem is access to the work area on and around the existing bridge and surrounding facilities. Some examples include driving or drilling piles under an existing structure with limited headroom, placing concrete under an existing horizontal surface, and excavating near other adjacent facilities. The designer must carefully think through the steps required for construction, and verify that the proposed retrofit can indeed be built.

Political and environmental constraints often arise during retrofitting and should be identified as far ahead as possible during selection of the preferred strategy. For example, the bridge may be listed on an historical register, which could limit the types of modifications that can be performed. The bridge may be located in an environmentally sensitive area that limits access to certain critical elements such as columns or foundations. The bridge may be located in a highly urban or residential environment, which may limit certain types of construction activities such as pile driving because of vibration and noise. Hazardous wastes are likely to be present around bridges in urban environments and, if disturbed, will require remediation. Political opposition to certain solutions such as bridge replacement, may also limit the options of the designer. It is important that the designer be sensitive to these and other issues early in the retrofit process with a view to finding the best solution given the constraints.

#### **10.12.2.4 Identification and Evaluation a Retrofit Strategy**

Selecting the preferred retrofit strategy can be complicated. Not only is it often a challenge to find the right technical solution, it is also a challenge to satisfy a multitude of socio-economic constraints. A systematic process should therefore be followed to assure an appropriate strategy is selected. A flowchart for such a process is shown in Figure 10-9. The various steps are discussed below.

Step 1: Conduct a detailed as-built evaluation. The first step in seismic retrofitting is to perform a detailed analytical evaluation of the existing bridge, as it exists in the field. Procedures for this step are discussed in Section 10.11. The goal of this step is to assess the response of the bridge to the design earthquake and to identify weaknesses that can be addressed by retrofitting. A formal field review of the bridge should be performed as part of this step. This is needed to verify the as-built condition of the bridge and to identify any constraints on retrofitting. Structural and geotechnical specialists and the owner should be involved in this effort.

Step 2: Identify alternative retrofit strategies. Frequently, there is more than one way to improve the performance of an existing bridge, and it is important to identify as many options as possible. Many will be quickly eliminated because of excessive cost, constructability or other problems as noted in Section 10.12.2.3. Solutions that appear viable should be further considered in Step 3. Table 10-9 (see Section 10.13.2) identifies alternative retrofit approaches that might be used to address common deficiencies and directs the designer to possible retrofit measures for each approach. This table may therefore be helpful when looking for potential retrofit strategies.

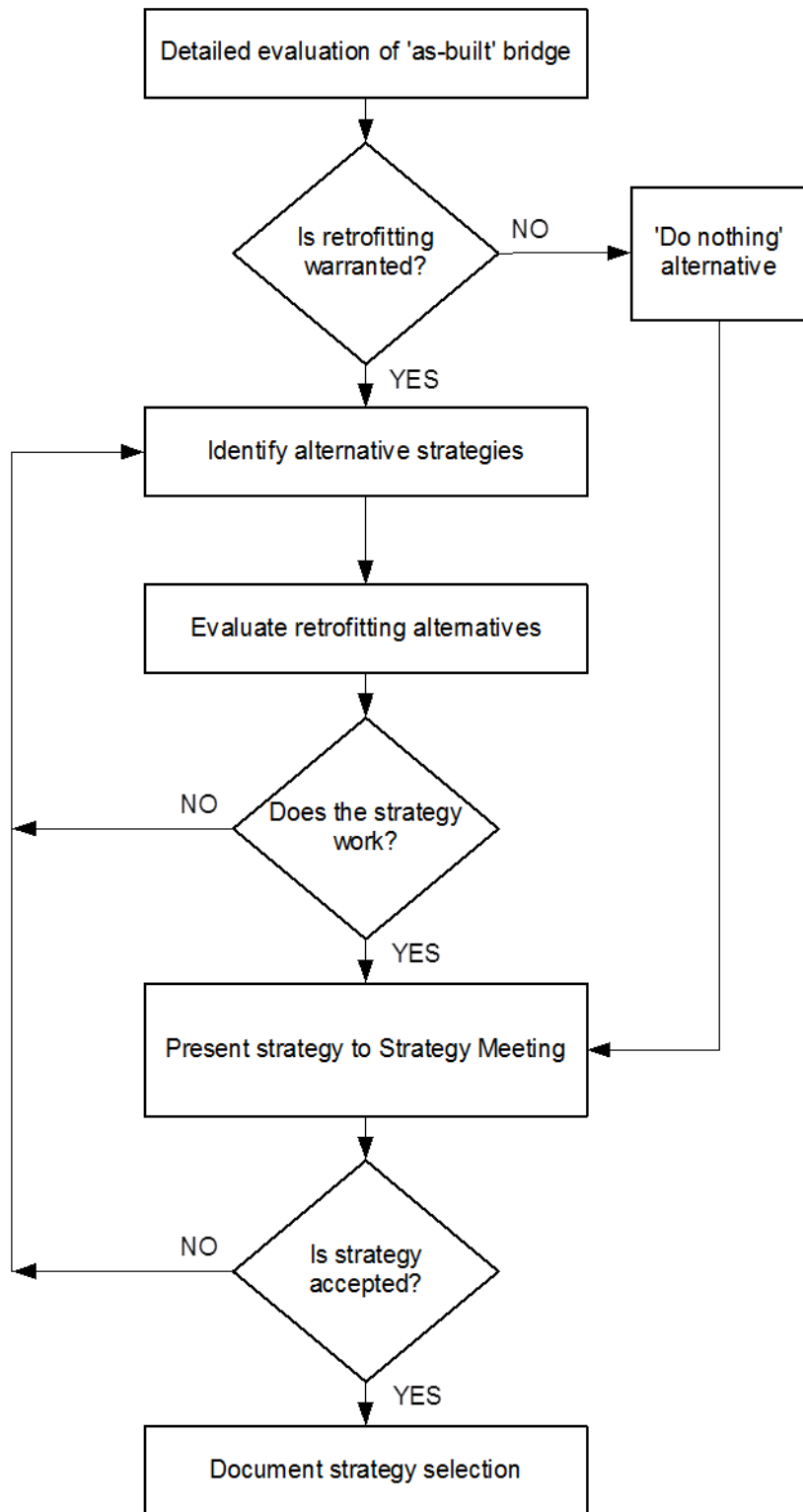


Figure 10-9 Identification and Evaluation of a Retrofit Strategy (FHWA, 2006)

Step 3: Evaluate alternative retrofit strategies. Detailed analytical evaluations of each viable retrofit strategy should be performed using the methods described in Section 10.11. This step should also include the preliminary design of the elements of the proposed retrofit so that a preliminary cost estimate may be prepared for each alternative.

Step 4: Conduct a strategy meeting. Since seismic retrofitting involves many complex issues, consensus must be achieved on the most appropriate strategy. This may be accomplished through a strategy meeting where the designer presents recommendations and cost estimates for retrofitting. Representatives of all agencies that have an interest in the project should attend this meeting, including the bridge owner, utility companies, Federal, state and local government agencies, structural and geotechnical engineering specialists, and environmental and citizens groups.

Step 5: Document the strategy selection. The retrofit decision should be documented in a strategy report that becomes part of the permanent record for the project. This report should include all the calculations of the as-built and as-retrofitted evaluations, preliminary plans and sketches showing the proposed retrofit, a summary of conclusions and recommendations, preliminary cost estimates, and a summary of the discussions from the strategy meeting.

#### **10.12.2.5 Do-nothing and Full-replacement Options**

When retrofitting a seismically deficient bridge, two possible solutions, at opposite ends of the spectrum, should be kept in mind: the ‘do-nothing’ and ‘full-replacement’ options.

The ‘do-nothing’ option requires the acceptance of damage during a future earthquake. This will be a relatively straightforward decision if life safety is the only performance requirement, and the expected damage is not a threat to life safety. The most likely cause of loss of life is total collapse of a span, but this is a relatively rare event. For example, the toppling or failure of individual bearings will not necessarily lead to collapse if the bearing seats are wide enough to catch the superstructure. Similarly, foundation failures are unlikely to cause collapse, unless the ground deformations are extremely large due to widespread liquefaction or massive ground failure such as fault rupture. Fortunately, these occurrences are rare. Nevertheless, judgment should be used when assessing collapse potential and, to the extent possible, this potential should be carefully evaluated using a detailed analysis.

The ‘full-replacement’ option may also be an attractive option, particularly when the cost of retrofit is on the same order of magnitude as the replacement cost of the bridge. Full replacement is generally considered whenever the retrofit costs approach 60 to 70 percent of a new bridge and may become even more attractive if the structure has non-seismic structural deficiencies and is functionally obsolete. However, in making this recommendation, the designer should also consider the cost of demolition and any costs associated with control and rerouting of traffic as part of the cost of the replacement alternative. These costs can be significant and may tip the scales back toward the retrofit alternative.

### **10.12.3 Seismic Retrofit Approaches**

#### **10.12.3.1 General**

Seismic retrofit approaches may be used alone or in combination to develop a seismic retrofit strategy for a given bridge. Some of the more common approaches are listed below and discussed in Sections 10.12.3.1 through 10.12.3.7.

- Strengthening.
- Improvement of Displacement Capacity.
- Force Limitation.
- Response Modification.
- Site Remediation by Ground Improvement.
- Acceptance or Control of Damage to Specific Components.
- Partial Replacement.

#### **10.12.3.2 Strengthening**

Strengthening is intended to increase the force or moment capacity of one or more deficient elements of a bridge. This approach should also take into account any significant increase in stiffness due to the strengthening, and its likely effect on structural response.

It is generally not feasible to economically retrofit a bridge for a major earthquake within the elastic range of the members, and therefore, yield is to be expected in many locations. In cases where the force or moment demands on a structural element are limited by yielding elsewhere in the structure, the strength of the element should be sufficient to resist the demands placed on it without damage. Such is usually the case with superstructure and foundation elements where forces are controlled by column yielding. When

these elements are not strong enough to resist the forces or moments generated by the existing or retrofitted column, they must then be strengthened.

Strengthening of a ductile component can reduce the ductility demand on the component and thus improve seismic performance. However, it will usually increase the forces or moments in adjacent components, which will then also need to be strengthened.

The addition of restrainer cables or high strength bars at hinges and seats is also considered to be a form of strengthening. The added strength and stiffness of restrainers will limit the relative movement between superstructure spans or frames, with the goal of preventing failure due to loss of support.

### **10.12.3.3 Improvement of Displacement Capacity**

Displacement capacity is generally a better indicator of structural performance than member strength. A common retrofit approach, therefore, focuses on improving displacement capacity. This can be achieved in one of two ways.

The first technique extends the length of bearing seats to permit greater relative movement at bearing locations without loss of support. This is an alternative method to the use of restrainer cables or bars, which is a strengthening approach intended to reduce the displacement demand on the bearing seat. In many cases, both approaches are used in combination, i.e., both restrainers and seat extenders are used to prevent loss of support at the same location.

The second technique increases the ductility capacity of columns and piers. Large inelastic deformations may be required of columns and piers during a major earthquake and ductility capacity is a measure of their ability to sustain this deformation without collapse or fracture. A ductile column or pier can therefore accommodate large imposed deformations, and any technique which increases this capacity is considered to be a form of displacement capacity enhancement.

### **10.12.3.4 Force Limitation**

Forces in critical structural components can be limited by using yielding elements as a structural ‘fuse’, i.e., a sacrificial element. If one member in a bridge is deliberately designed to yield and thus limit the forces that can be transmitted to an adjoining member, the second member is ‘capacity-protected’ by the first member. If, for example, a column is intended to yield and develop plastic hinges, the maximum

moment that can be transmitted from the column to the foundation is limited by the yield moment of the hinges. In such a case, the foundation is ‘capacity-protected’ by the column.

Although force limitation occurs naturally in many structures, several force-limiting retrofit methods have been developed to reduce the cost of strengthening of components, particularly those that are structurally difficult to implement.

One method of force limitation uses seismic isolation bearings. Although these bearings can be used to modify the dynamic response of a bridge, as discussed in Section 10.12.3.4, they can also be used as ‘fuses’ that limit the amount of shear force that can be transmitted to a substructure or foundation.

Another example of force limitation is the link-beam concept that has been used for retrofitting multi-column piers. With this technique, shear forces are limited by plastic hinging in the beams, which in turn limits the magnitude of the moments that can be transmitted to bent caps and footings.

The ductile end diaphragm method described by FHWA (2006) also utilizes the force limitation approach.

#### **10.12.3.5 Response Modification**

The dynamic response of a bridge to earthquake ground motion determines the force and displacement demands that will be placed on various components. It is often possible to retrofit the bridge in such a way that the dynamic response will be significantly altered. This could reduce force and displacement demands and thus eliminate or reduce the need for retrofitting by strengthening or enhancing displacement capacity. An example of this approach is seismic isolation, in which the fundamental period of the structure is deliberately increased to reduce the force demands. In this case, however, the displacement demands in the isolators may be very large and additional damping is usually provided to reduce these demands. Energy dissipators and dampers also modify dynamic response and may be used to reduce the need for strengthening or improving displacement capacity.

Another method of response modification is to modify the load path for horizontal inertia forces. Retrofitting to strengthen or stiffen an alternative load path may be used to attract forces away from vulnerable components, and thus reduce or eliminate the need to retrofit them. An example is a continuous bridge in which the abutment stiffness and strength are increased. Inertial forces are then redistributed to the abutments, which relieve or reduce the forces on the interior columns or piers. This approach can be very effective for simply supported spans if the retrofit also includes provision for

making the deck continuous for live load. Shock transmission units can also be used to modify a load path.

Response modification is a powerful retrofit approach but it requires careful consideration of possible side effects, such as changes in the way a bridge responds to service loads.

#### **10.12.3.6 Site Remediation by Ground Improvement**

Bridges can suffer significant damage when large permanent ground movements occur during an earthquake. Liquefaction, lateral spreading, landslides, and fault rupture are some of the more common causes of this damage. There are two possible approaches to this problem.

The first approach is to give the structure the capacity to resist the loading and/or accommodate the displacements created by the moving soil without collapse. A critical step in this approach is the quantification of the loads and/or the expected ground movement or fault rupture, which is a difficult problem to solve.

The second approach is to modify the soil using ground improvement techniques, such as those discussed by FHWA (2006). Site remediation often involves treatment of large areas of soil and can be expensive. In the case of river or stream crossings, improvements may be subject to flooding and require protection from scour. Nevertheless, there will be cases where this approach is a viable option and should be considered. It is not, however, applicable to sites where fault rupture is expected.

#### **10.12.3.7 Acceptance or Control of Damage to Specific Components**

When collapse prevention is the main goal of retrofitting, it is often acceptable to allow component damage as long as this does not jeopardize the overall stability of the structure. Often this will mean that no retrofit is required for the members in question. In some cases, however, damage must be controlled to prevent collapse. An example of this is the “P” column retrofit commonly used by Caltrans (Caltrans, 1996). This retrofit method is intended to preserve the vertical load carrying capacity of the column while the column sustains considerable damage. It is common to ignore the lateral load carrying capacity of such a retrofit when conducting an analysis of the structural response.

### **10.12.3.8 Partial Replacement**

There are cases where the required retrofitting of a bridge component may be so extensive that partial replacement is the most economical solution. Partial replacement may have several goals, such as increasing strength and ductility when a column is replaced. In some cases, the type of retrofit performed on an adjacent element may mandate partial replacement. When load-bearing elements are replaced, temporary shoring will be required.

## **10.13 RETROFIT MEASURES FOR UPPER LEVEL GROUND MOTION**

### **10.13.1 General**

In the last decade, the range of available retrofit measures has increased markedly. Measures have now been developed for deficient superstructures, bearings, beam seats, piers and columns, including weak cap beams and column-to-cap beam joints. In addition, techniques for improving the behavior of abutments and foundations have been developed, including measures for bridges on hazardous sites. This progress is the result of an aggressive research program in California and elsewhere and field experience, mainly in California.

These measures includes:

- Diaphragm strengthening
- Energy dissipating ductile diaphragms
- Provision of longitudinal continuity in simply supported spans
- Replacement of bearings
- Seismic isolation bearings
- Energy dissipators
- Seat width extensions and catcher blocks at girder supports and intermediate hinges
- Restrainers at girder supports and intermediate hinges
- Column replacement
- Concrete shells, steel and fiber-composite jackets for columns
- Infill shear walls in bents
- Cap beam strengthening using prestressing
- Supergirders

- Anchor slabs behind abutments
- Soil and gravity anchors
- Abutment shear keys
- Footing replacement
- Footing overlays
- Pile tie-down enhancement
- Supplemental piles
- Articulation for fault crossings
- Site remediation for unstable slopes and liquefaction
- Vibro-replacement of soils and stone columns

Figure 10-10 illustrates some of the above measures as below. Details may be found in FHWA (2006).

- Restrainers (Figure 10-10(a))
- Bearing replacement and strengthening (Figure 10-10(b))
- Superstructure strengthening (Figure 10-10(c))
- Seismic isolation (Figure 10-10(d))
- Steel jackets (Figure 10-0(e))
- Infill walls (Figure 10-10(f))
- Footing overlays and piled extensions (Figure 10-10(g))
- Site remediation(Figure 10-10(h))

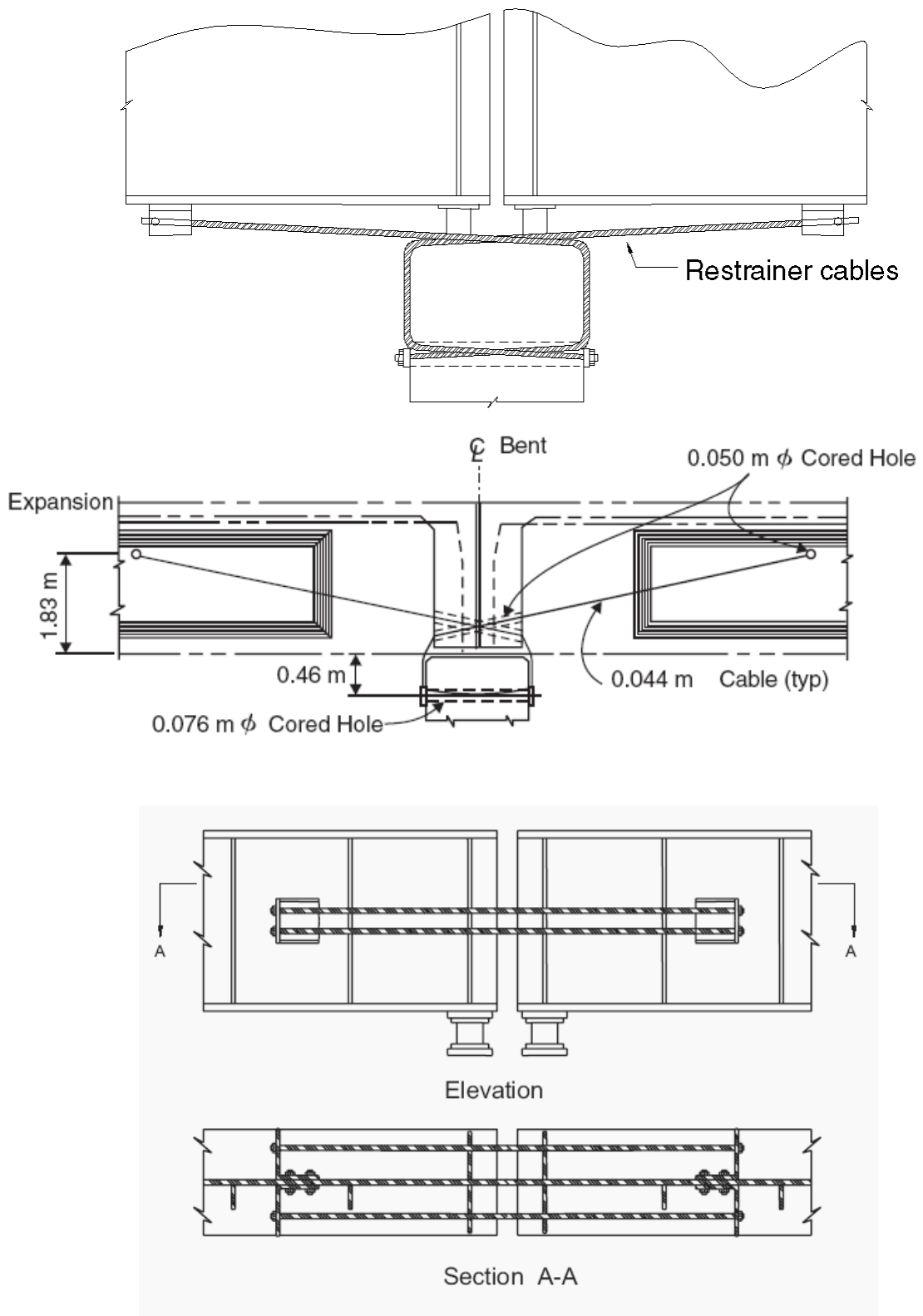


Figure 10-10(a) Restrainers at Piers for Steel Girders (top and bottom) and Concrete Girders (upper center)

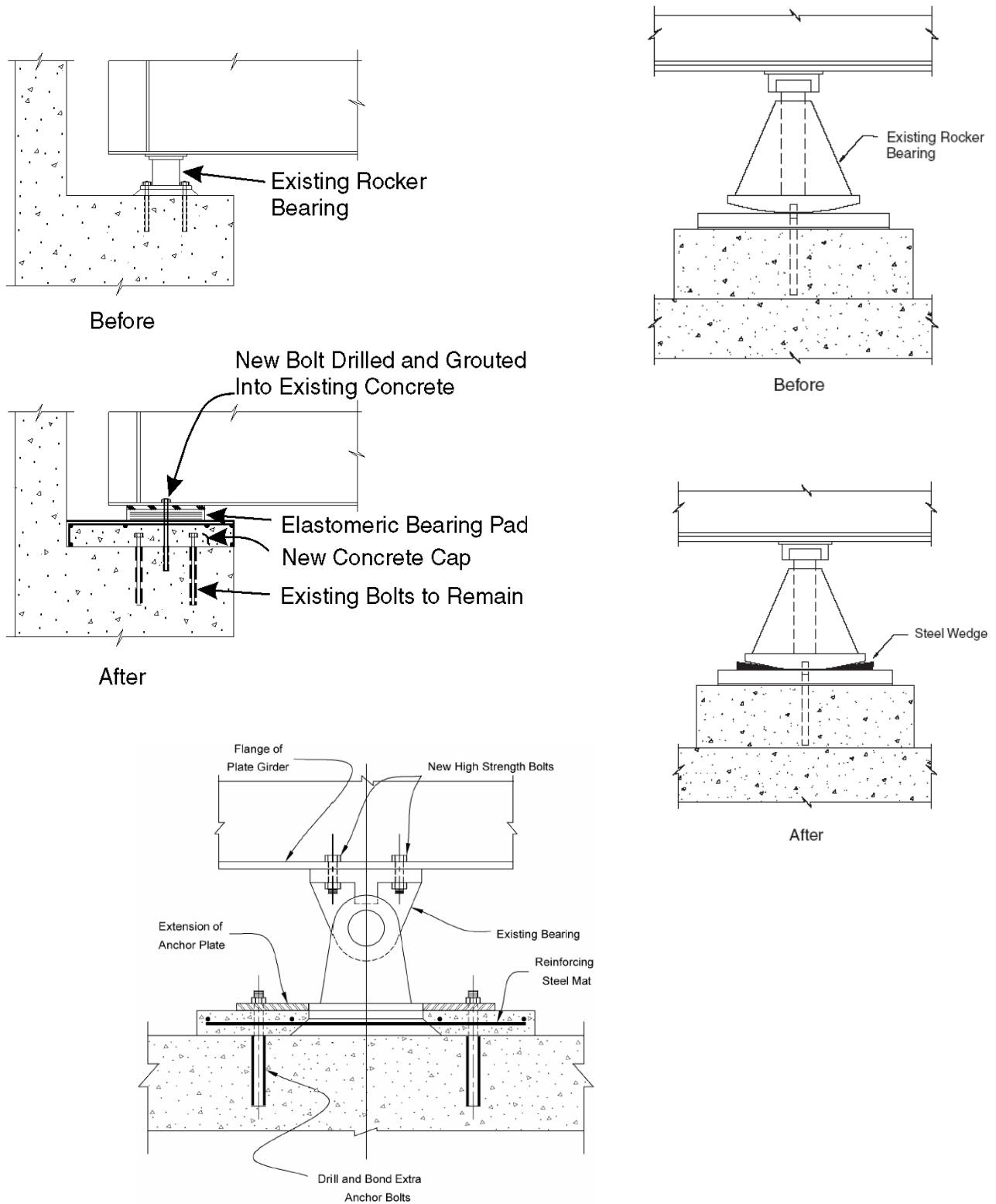


Figure 10-10(b) Bearing Strengthening and Replacement: Bearing Replacement with Elastomeric Pad (upper left), Improving Stability of Rocker Bearing (upper right), and Anchor Bolt Replacement (lower left)

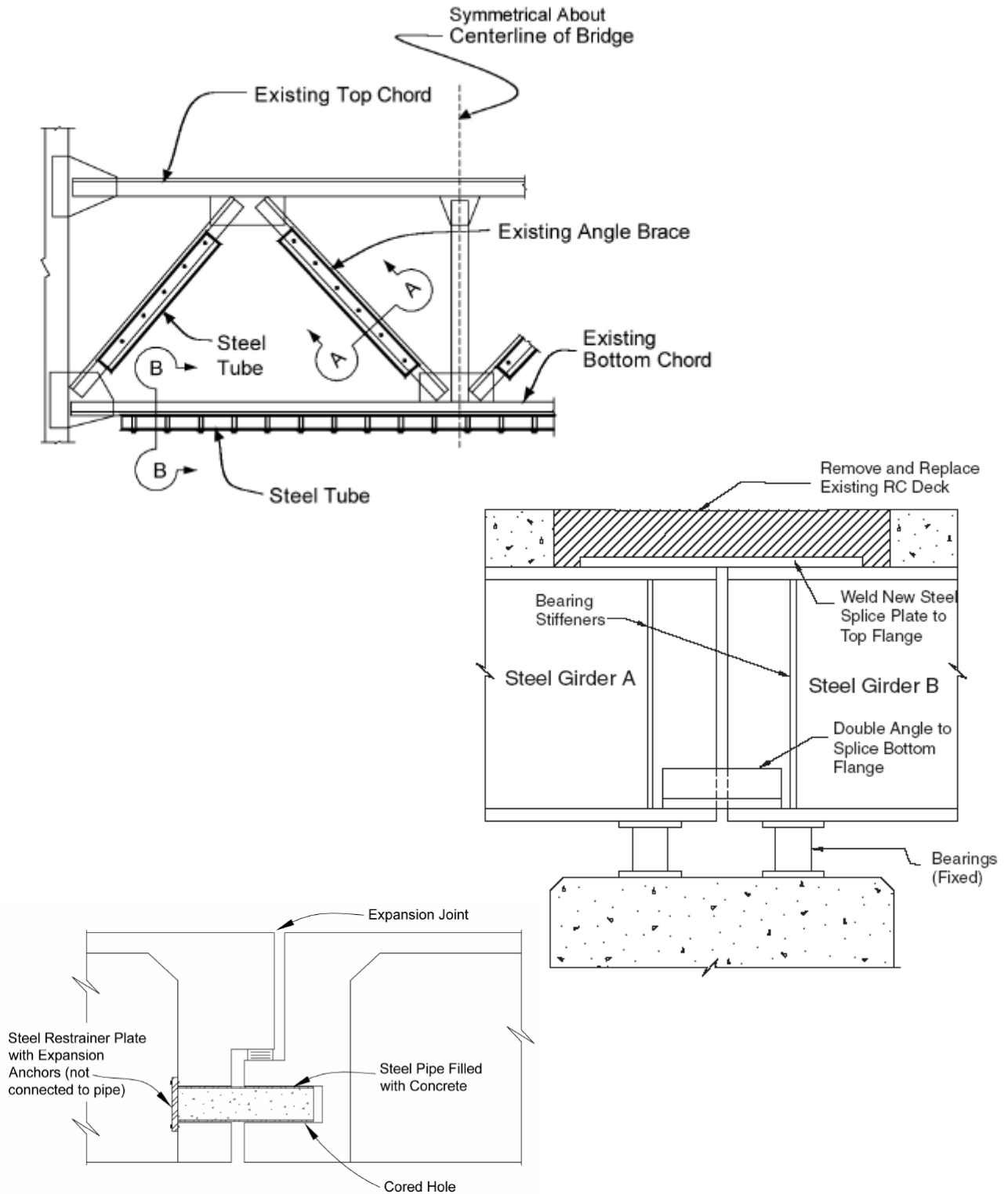


Figure 10-10(c) Superstructure Strengthening: Cross Brace Strengthening (top), Making Simple Spans Continuous (center), and Seat Extension at Intermediate Hinge (bottom)

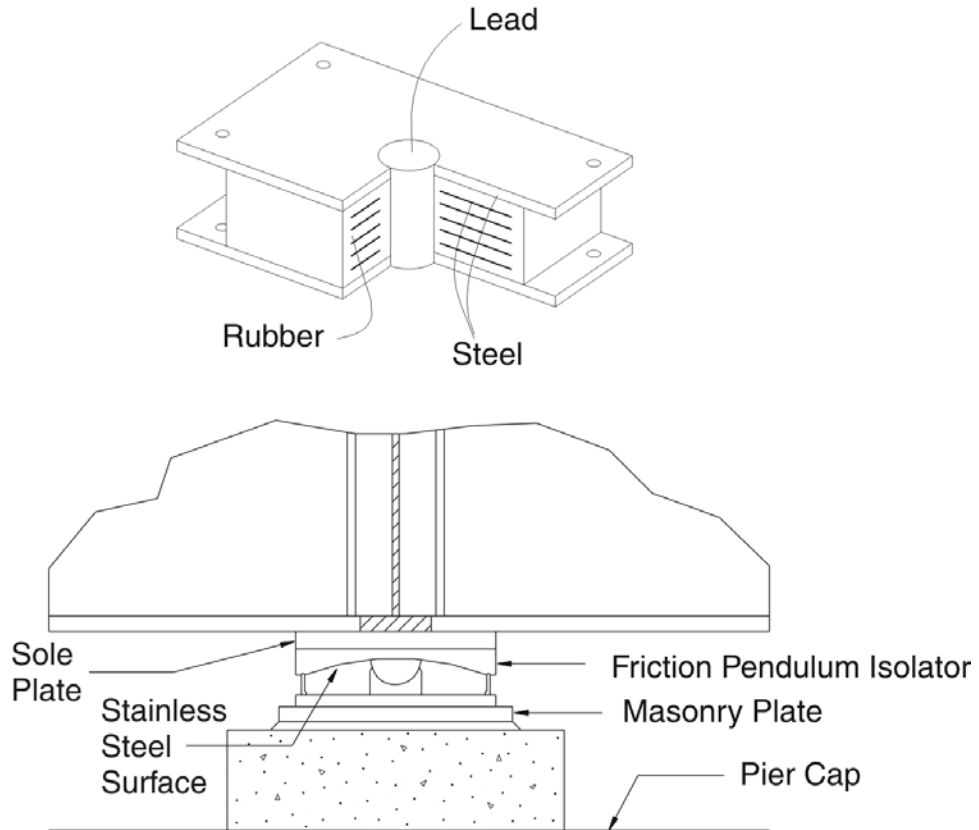


Figure 10-10(d) Lead-Rubber Isolator (top), Friction-Pendulum Isolator (center), and Installation of Friction Pendulum Isolator on I-40 Crossing Mississippi River, Memphis (bottom)

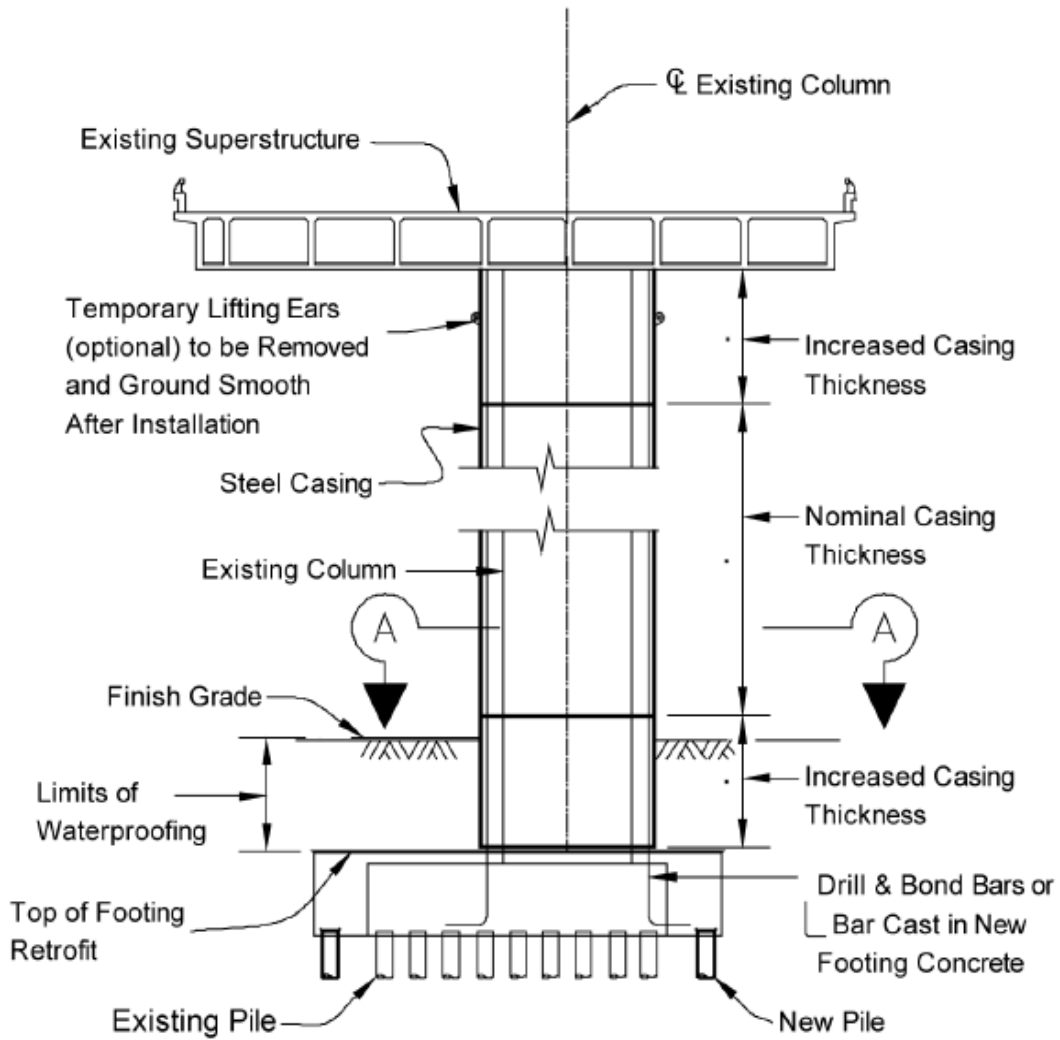


Figure 10-10(e) Steel Jackets for Concrete Columns (top) and Installation on Hernando Desoto Bridge, I-40 Retrofit, photo R.A. Imbsen (bottom)

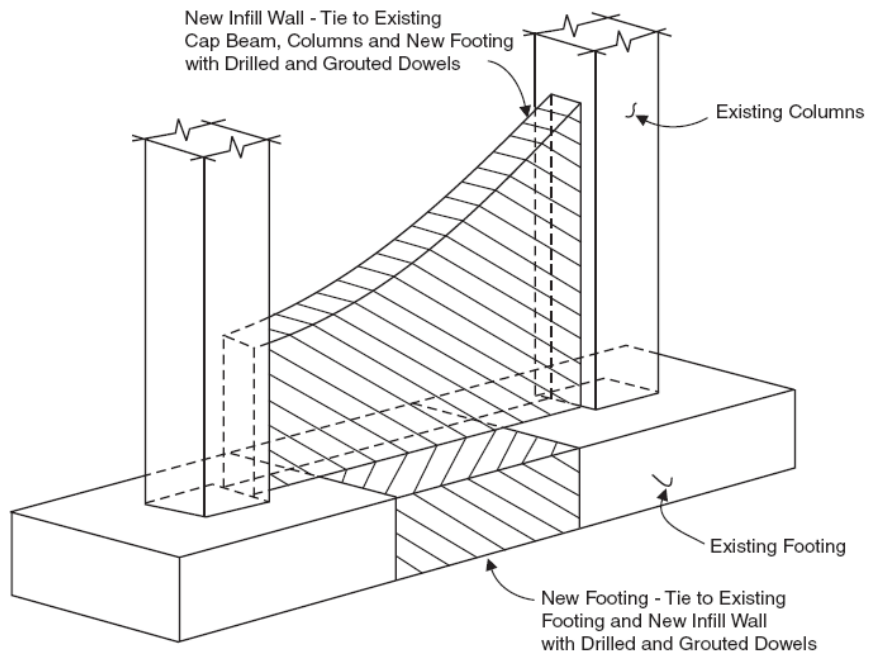


Figure 10-10(f) Infilled Walls for Concrete Piers (top) and Installation on West Lake Sammish Parkway, I-90 Retrofit, photo L.M. Marsh (bottom)

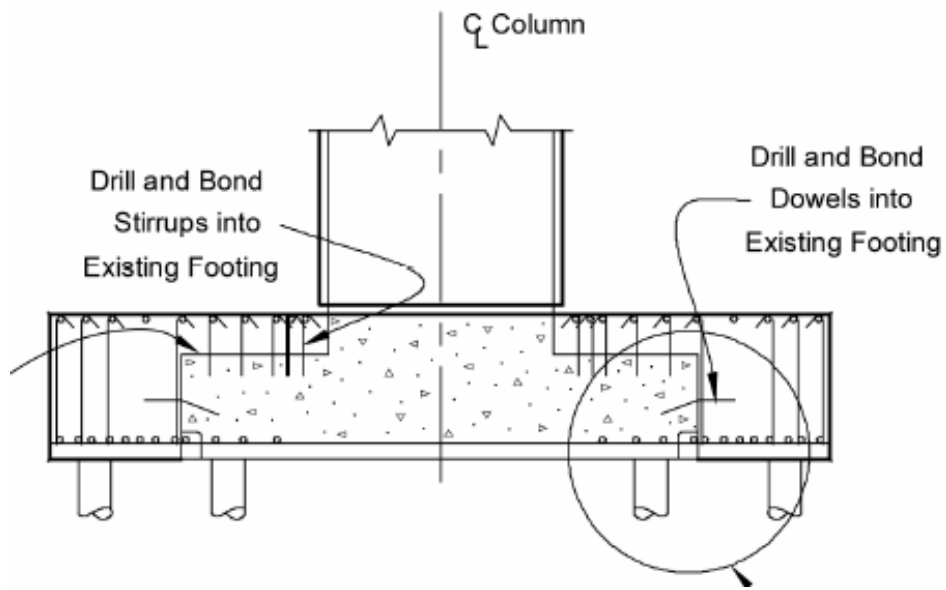


Figure 10-10(g) Footing Overlay with Piled Extension (top) and Installation on Hernando-Desoto Bridge, I-40 Retrofit, photo R.A. Imbsen (center and bottom)

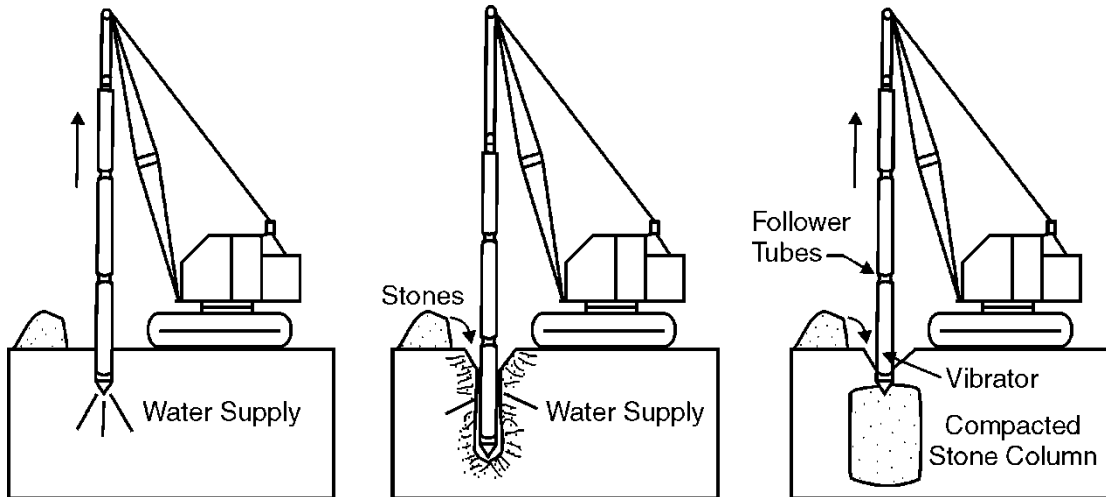


Figure 10-10(h) Vibro-Replacement Site Remediation

### 10.13.2 Seismic Retrofit Matrix

The matrix presented in Table 10-9 is a roadmap for the above list of retrofit measures. It shows the relationship between the seven retrofit approaches in Section 10.12.3 and the retrofit measures necessary to make them work.

For example, if the *strengthening* approach is chosen to address *insufficient seat length*, then the following measures are recommended in Table 10-9 for consideration:

- Providing Longitudinal Continuity, Web and Flange Plates, and
- Installing Longitudinal Joint Restrainers.

Although Table 10-9 presents a comprehensive list of approaches and measures it is not intended to preclude other retrofit approaches or measures that are not specifically mentioned in this chapter.

**TABLE 10-9 - MATRIX OF SEISMIC RETROFIT APPROACHES AND ASSOCIATED RETROFIT MEASURES (FHWA, 2006).**

SEISMIC DEFICIENCY	RETROFIT APPROACH						
	Strengthening	Displacement Capacity Enhancement	Force Limitation	Response Modification	Site Remediation	Damage Acceptance or Control	Partial Replacement
Superstructure deficiencies	Strengthening of Deck to Girder Connection Girder Strengthening Strengthening of Continuous Superstructures						
Structurally deficient diaphragms	Diaphragm Strengthening or Stiffening		Energy Dissipating Ductile Diaphragms				
Structurally deficient bearings/connections	Strengthening of Existing Bearings Strengthening of Superstructure to Substructure Connections Transverse Restrainers Vertical Motion Restrainers			Replacement with Seismic Isolation Bearings Energy Dissipation Devices Shock Transmission Units			Replacement with Conventional Bearings
Insufficient seat length	Web and Flange Plates Longitudinal Joint Restrainers	Concrete Seat Extensions and Catcher Blocks Pipe Extenders		Superstructure Joint Strengthening Reduction of Dead Load			
Flexurally deficient columns or piers	Column Flexural Strengthening Supplemental Column Shear Walls Braced Frames Built-up Compression Members Concrete Wall Piers	Column Ductility Improvement and Shear Strengthening Built-up Compression Members	Limitation of Column Forces Braced Frames			Preservation of the Vertical Load Capacity of Columns	Column Replacement
Shear deficient columns or piers	Column Ductility Improvement and Shear Strengthening Supplemental Column Shear Walls						

Table 10-9 Continued Next Page

**TABLE 10-9 CONTIUED - MATRIX OF SEISMIC RETROFIT APPROACHES AND ASSOCIATED RETROFIT MEASURES  
(FHWA, 2006).**

SEISMIC DEFICIENCY	RETROFIT APPROACH						
	Strengthening	Displacement Capacity Enhancement	Force Limitation	Response Modification	Site Remediation	Damage Acceptance or Control	Partial Replacement
Structurally deficient pier caps	Pier Cap Strengthening		Reduction of Pier Cap Forces	Supergirders			Partial Replacement at a Joint Total Replacement
Structurally deficient column-to-cap joints	Strengthening of Column and Beam Joints			Supergirders			Partial Replacement at a Joint
Structurally deficient column-footing joints	Strengthening of Footings			Limiting Forces Transmitted to the Footings			Footing Replacement
Unstable footings	Strengthening of Footings Pile Tie-downs			Limiting Forces Transmitted to the Footings	Site Remediation Using Ground Improvement		Footing Replacement
Structurally deficient footings	Strengthening of Footings			Limiting Forces Transmitted to the Footings			
Abutment fill settlement		Approach Slabs			Site Remediation Using Ground Improvement		
Unstable abutments	Anchor Slabs Transverse Abutment Anchors Soil and Gravity Anchors			Anchor Slabs			

Table 10-9 Continued Next Page

**TABLE 10-9 CONTIUED - MATRIX OF SEISMIC RETROFIT APPROACHES AND ASSOCIATED RETROFIT MEASURES  
(FHWA, 2006).**

SEISMIC DEFICIENCY	RETROFIT APPROACH						
	Strengthening	Displacement Capacity Enhancement	Force Limitation	Response Modification	Site Remediation	Damage Acceptance or Control	Partial Replacement
Structurally deficient abutments	Diaphragm Walls Transverse Abutment Shear Keys						
Excessive ground movement	Web and Flange Plates Longitudinal Joint Restrainers Concrete Wall Piers Strengthening of Footings	Concrete Seat Extensions and Catcher Blocks Pipe Extenders Column Ductility Improvement and Shear Strengthening Built-up Compression Members	Limitation of Column Force		Site Remediation Using Ground Improvement	Preservation of the Vertical Load Capacity of Columns	Column Replacement

## 10.14 SUMMARY

Retrofitting is the most common method of mitigating seismic risk. However, the cost of strengthening may be so prohibitive that abandoning the bridge (total or partial closure with restricted access) or replacing it altogether with a new structure may be favored. Alternatively, doing nothing and accepting the consequences of damage is another possible option. The decision to retrofit, abandon, replace, or do-nothing requires that both the importance and degree of vulnerability of the structure be carefully evaluated. Limited resources will generally require that deficient bridges be prioritized, with important bridges in high risk areas being given the first priority for retrofitting.

This chapter has presented a procedure for evaluating and upgrading the seismic resistance of existing highway bridges including:

- A screening process to identify and prioritize bridges that need to be evaluated for seismic retrofitting
- A methodology for quantitatively evaluating the seismic capacity of a bridge and determining the overall effectiveness of alternative retrofitting measures, including cost and ease of installation, and
- Retrofit approaches and corresponding techniques for increasing the seismic resistance of existing bridges. Such techniques include restrainers, bearing replacements, seat extensions, column jackets, infill walls, footing overlays and extensions, seismic isolation, and site remediation.

This procedure has been taken from the FHWA *Seismic Retrofitting Manual for Highway Structures* (FHWA 2006). Rigid requirements as to when and how bridges are to be retrofitted are not prescribed. The decision to retrofit depends on a number of factors, several of which are outside the realm of engineering. These include, but are not limited to, the availability of funding, and a number of political, social, and economic issues. This chapter has focused on the engineering factors.

The recommendations in this chapter are intended for use on conventional steel and concrete highway bridges. Suspension bridges, cable-stayed bridges, arches, long-span trusses, and movable bridges are not covered. However, many of the procedures and techniques presented herein can be applied to these types of structures, if appropriate judgment is used.



## CHAPTER 11

### REFERENCES

- AASHTO (American Association of State Highway and Transportation Officials) (1983), “Guide Specifications for Seismic Design of Highway Bridges”, AASHTO, Washington DC, 106 pp.
- AASHTO (American Association of State Highway and Transportation Officials) (1998) “LRFD Bridge Design Specifications”, Second Edition, AASHTO, Washington, DC.
- AASHTO (American Association of State Highway and Transportation Officials) (2002) “Standard Specifications for Highway Bridges, Division I-A Seismic Design,” 17<sup>th</sup> Edition, AASHTO, Washington, D.C.
- AASHTO (American Association of State Highway and Transportation Officials) (2004), “LRFD Bridge Design Specifications, Customary U.S. Units” Third Edition with 2005 and 2006 Interims, American AASHTO, Washington, D.C.
- AASHTO (American Association of State Highway and Transportation Officials) (2007) “LRFD Bridge Design Specifications, Customary U.S. Units” Fourth Edition with 2008 and 2009 Interims, AASHTO, Washington, D.C.
- AASHTO (American Association of State Highway and Transportation Officials) (2013) “LRFD Bridge Design Specifications, Customary U.S. Units” Sixth Edition with 2013 Interim, AASHTO, Washington, D.C.
- AASHTO (American Association of State Highway and Transportation Officials) (2009) “Guide Specifications for LRFD Seismic Bridge Design,” AASHTO, Washington, D.C.
- AASHTO (American Association of State Highway and Transportation Officials) (2014) “Guide Specifications for LRFD Seismic Bridge Design” Second Edition with 2014 Interim, AASHTO, Washington, D.C.
- AASHTO (American Association of State Highway and Transportation Officials) (2010) “Guide Specification for Seismic Isolation Design” Third Edition, AASHTO, Washington, D.C.
- AASHTO and AWS (American Association of State Highway and Transportation Officials and American Welding Society) (2010), “Bridge Welding Code”, AASHTO/AWS D1.5M/D1.5 or BWC-5, Washington, D.C.
- Abrahamson, N.A. (1992), “Generation of Spatially Incoherent Strong Motion Time Histories,” Proceedings of the Tenth World Conference on Earthquake Engineering, Madrid, Spain, July 19-24, pp. 845-850.
- Abrahamson, N.A., Atkinson, G., Boore, D., Bozorgnia, Y., Campbell, K., Chiou, I., Idriss, I., Silva, W., and Young, R. (2008) “Comparisons of the NGA Ground- Motion Relations.” Earthquake Spectra, Vol. 24, No. 1, Earthquake Engineering Research Institute, pp. 45-66.

- Aiken, I.D. and A. S. Whittaker, (1993) "Development and application of passive energy dissipation techniques in the U.S.A.," Proceedings, International Post-SMiRT Conference Seminar on Isolation, Energy Dissipation, and Control of Vibrations of Structures, Capri, Italy, August 1993.
- ASTM (American Society for Testing and Materials) (1998). "Soil and Rock", ASTM, v.4.08, March.
- ASME (American Society of Mechanical Engineers) (1985), "Surface Texture (Surface Roughness, Waviness and Lay)", ANSI/ASME B46.1-1985, ASME, New York.
- Astaneh-Asl, A. (1996). "Seismic Design, Evaluation and Retrofit of Steel Bridges", Proceedings of the Second U.S. Seminar, San Francisco, CA.
- ATC (Applied Technology Council) (1981) "Seismic Design Guidelines for Highway Bridges", ATC, Report ATC-6, Redwood City, CA
- ATC (Applied Technology Council) (1983) "Seismic Retrofitting Guidelines for Highway Bridges", Report ATC-6-2, ATC, Redwood City, CA.
- ATC (Applied Technology Council) (1996) "Improved Seismic Design Criteria for California Bridges", ATC-32, ATC, Redwood City, CA.
- ATC (Applied Technology Council) (1998). "Recommended LRFD Guidelines for the Seismic Design of Highway Bridges", ATC-49, ATC, Redwood City, CA.
- ATC (Applied Technology Council) (2003) "Liquefaction Study Report, Recommended LRFD Guidelines for the Seismic Design of Highway Bridges", MCEER/ATC 49-1, MCEER/ATC Joint Venture, Redwood City, CA
- ATC/MCEER (Applied Technology Council/Multidisciplinary Center for Earthquake Engineering Research) (2003), "Recommended LRFD Guidelines for the Seismic Design of Highway Bridges, Specifications and Commentary", MCEER-ATC 49, ATC/MCEER Joint Venture, University at Buffalo, Buffalo NY.
- Bardet, J.P., Idriss, I.M., O'Rourke, T.D., Adachi, N., Hamada, M. and Ishihara, K. (1997). "North America-Japan Workshop on the Geotechnical Aspects of the Kobe, Loma Prieta and Northridge Earthquakes," University of Southern California, February.
- Berrill, J.B., Christensen, S.A., Keenan, R.J., Okada, W. and Pettinga, J.R. (1997). "Lateral-spreading Loads on a Piled Bridge Foundation," Seismic Behavior of Ground and Geotechnical structures, Proc. Special Technical Session on Earthquake Engineering, 14th ICSMFE, A.A.A. Balkema, Rotterdam, 173-183.
- Berry, M. and Eberhard, M. (2003), "Estimating Flexural Damage in Reinforced Concrete Columns", University of Washington, Seattle, WA.
- Berry, M. and Eberhard, M. (2003a), "Performance Models for Flexural Damage in Reinforced Concrete Columns", Pacific Earthquake Engineering Research Center, PEER, August.
- Boore, D. M., Joyner, W. B., and Fumal, T. E. (1997). "Equations for Estimating Horizontal Response Spectra and Peak Acceleration from Western North American Earthquakes: A summary of recent work", Seism. Res. Letters, v. 68, p. 128-153.

- Bozorgzadeh, A., Megally, S.H., Ashford, S., and Restrepo, José L. (2007) “Seismic Response of Sacrificial Exterior Shear Keys in Bridge Abutments”, Report No. SSRP-04/14, Structural Systems Research Project, University of California, San Diego, CA.
- Bowles, J.E. (1982) “Foundation Analysis and Design”, McGraw-Hill Book Company, Third Edition.
- British Standards Institution (1979) “Commentary on Corrosion at Bi-metallic Contacts and Its Alleviation,” BSI Standard PD 6484, Confirmed March 1990, British Standards Institution, London.
- Buckle, I.G. (1991) “Screening Procedures for the Retrofit of Bridges”, *Proceedings of the Third U.S. Conference on Lifeline Earthquake Engineering*, ASCE, Monograph Number 4, Technical Council of Lifeline Earthquake Engineering, pp. 156-165
- Buckle, I.G. (1994) “The Northridge, California Earthquake of January 17, 1994: Performance of Highway Bridges”, Technical Report NCEER-94-0008, National Center for Earthquake Engineering Research, University at Buffalo, Buffalo, NY
- Buckle, I.G. Mayes, R.L. and Button, M.R.(1986) “Seismic Design and Retrofit Manual for Highway Bridges”, Federal Highway Administration Report FHWA-IP-87-6, Washington, D.C., 290 pp.
- Buckle, I.G. and Mayes, R.L. (1990) “Seismic Retrofit of Bridges Using Mechanical Energy Dissipators”, Proc. Fourth U.S. National Conference on Earthquake Engineering, Vol. 3, Earthquake Engineering Research Institute, Oakland, CA, pp 305-314.
- Buckle, I.G., and Liu, H. (1994) “Critical Loads of Elastomeric Isolators at High Shear Strain”, Proc. 3<sup>rd</sup> US-Japan Workshop on Earthquake Protective Systems for Bridges”, Report NCEER-94-0009, National Center for Earthquake Engineering Research, Buffalo, NY
- Buckle, I.G., Constantinou, M., Dicleli, M., and Ghasemi, H. (2006) “Seismic Isolation of Highway Bridges”, Multidisciplinary Center for Extreme Events Research, Special Publication MCEER-06-SP07, Buffalo NY.
- Caltrans (1999) “Seismic Design Methodology”, Memo to Designers 20-1, California Department of Transportation, Sacramento, CA, 14 pp.
- Caltrans (2001) “Splices in Bar Reinforcing Steel”, Memo to Designers 20-9, California Department of Transportation, Sacramento, CA.
- Caltrans (2008) “Visual Inspection & Capacity Assessment of Earthquake Damaged Reinforced Concrete Bridge Elements”, Report CA08-0284, Final Report, Sacramento, CA.
- Caltrans (2013). “Seismic Design Criteria”, Version 1.7, Office of Earthquake Engineering, California Department of Transportation, Sacramento, CA,
- Caltrans (2008) “Seismic Retrofit Guidelines for Bridges in California”, Memo to Designers 20-4, California Department of Transportation, Sacramento, CA, 13pp.
- Caltrans Seismic Advisory Board Ad Hoc Committee on Soil-Foundation-Structure Interaction (CSABAC), (1999), “Seismic Soil-Foundation-Structure Interaction”, Final Report Prepared for California Department of Transportation, February.

- Carden, L.P., Itani, A.M., and Buckle I. (2006) "Seismic Performance of Steel Girder Bridges with Ductile End Cross Frames Using Single Angle X Braces," *Journal of Structural Engineering*, American Society of Civil Engineers, Reston, VA.
- Carden, L.P., Buckle, I., and Itani, A.M., (2007) "Transverse Displacement Capacity and Stiffness of Steel Plate Girder Bridge Superstructures for Seismic Loads," *Journal of Constructional Steel Research*, Vol. 63, 1546-1559.
- Chai, Y.H., Priestley, M.J.N., and Seible, F. (1992) "Retrofit of Bridge Columns for Enhanced Seismic Performance," *Seismic Assessment and Retrofit of Bridges*, Report Number SSRP-91/03, Department of Applied Mechanics and Engineering Sciences, University of California San Diego, CA.
- Chan, W.W.L. (1955) "The Ultimate Strength and Deformation of Plastic Hinges in Reinforced Concrete Frameworks," *Magazine of Concrete Research*, Vol. 7, No. 21, pp. 121-132.
- Chang, C.-Y, Mok, C.M., Power, M.S., Tang, Y.K., Tang, H.T., and Stepp, J.C. (1990) "Equivalent Linear Versus Nonlinear Ground Response Analyses at Lotung Seismic Experiment Site," *Proceedings, Fourth U.S. National Conference on Earthquake Engineering*, Palm Springs, CA, May 20-24, 1990, Earthquake Engineering Research Institute, El Cerrito, CA, Vol 1, pp327-336
- Chopra, A. (2012) "Dynamics of Structures", Fourth Edition, Pearson/Prentice Hall, NJ.
- CERC (Civil Engineering Research Center) (1992), "Temporal Manual of Design Method for Base-Isolated Highway Bridges", Japan (in Japanese).
- Clough, R. and Penzien, J. (1993) "Dynamics of Structures" Second Edition, McGraw Hill, Singapore.
- Constantinou, M.C. (1998) "Application of Seismic Isolation Systems in Greece", *Proceedings of '98 Structural Engineers World Congress*, Paper T175-3, San Francisco, CA.
- Constantinou, M.C., Tsopelas, P., Kasalanati, A. and Wolff, E.D. (1999) "Property Modification Factors for Seismic Isolation Bearings", Report No. MCEER-99-0012, Multidisciplinary Center for Earthquake Engineering Research, Buffalo, NY.
- Coppersmith, K.J. and Youngs, R.R., (1990) "Earthquakes and Tectonics" *Demonstration of a Risk-Based Approach to High-Level Nuclear Waste Repository Evaluation*, Report EPRI NP-7057, Electric Power Research Institute, Palo Alto, CA
- Coppersmith, K.J. and Youngs, R.R., (2000) "Data Needs for Probabilistic Fault Displacement Hazard Analysis" *Journal of Geodynamics*, Volume 29, pp. 329-343
- Correal, J., Saiidi, S., and Sanders, D. (2004) "Seismic Performance of RC Bridge Columns Reinforced with Two Interlocking Spirals", California Department of Transportation (Caltrans), University of Nevada, Reno, NV.
- CSI (Computers and Structure, Inc.) (1998) "SAP2000 Three Dimensional Static and Dynamic Finite Element Analysis and Design of Structures", Berkeley, CA.
- DesRoches, R. and Fenves, G. (1997) "New Design and Analysis Procedures for Intermediate Hinges in Multiple-Frame Bridges", Earthquake Engineering Research Center, University of California, Berkeley, CA.

- DesRoches, R., and Fenves, G.L. (1998) “Design Procedures for Hinge Restrainers and Hinge Seat Width for Multiple-Frame Bridges”, Technical Report MCEER-98-0013, Multidisciplinary Center for Earthquake Engineering Research, University at Buffalo, Buffalo, NY.
- Dutta, A. (1999) “On Energy-based Seismic Analysis and Design of Highway Bridges”, Ph.D. Dissertation, State University of New York at Buffalo, Buffalo, NY.
- EERI (1990) “Loma Prieta Earthquake Reconnaissance Report”, Earthquake Spectra, Supplement to Volume 6, Earthquake Engineering Research Institute, Oakland, CA.
- EERI (Earthquake Engineering Research Institute) (1995a) “Northridge Earthquake Reconnaissance Report, Volume 1”, Earthquake Spectra, Supplement C to Volume 11, EERI, Oakland, CA.
- EERI (Earthquake Engineering Research Institute) (1995b) “The Hyogo-Ken Nanbu Earthquake, January 17, 1995, Preliminary Reconnaissance Report”, EERI, Oakland, CA.
- European Committee for Standardization (2000) “Structural Bearings”, European Standard EN 1337-1, Brussels.
- FEMA (Federal Emergency Management Agency) (2000a) “Recommended Seismic Design Criteria for New Steel Moment-Frame Buildings”, FEMA 350, SAC Joint Venture, Federal Emergency Management Agency, Washington, D.C.
- FEMA (Federal Emergency Management Agency) (2000b) “Recommended Specifications and Quality Assurance Guidelines for Steel Moment-Frame Construction for Seismic Applications”, FEMA 353, SAC Joint Venture, Federal Emergency Management Agency, Washington, D.C.
- FHWA (Federal Highway Administration) (1981), “Seismic Design Guidelines for Highway Bridges”, FHWA-RD-81-081, FHWA, Washington, DC.
- FHWA (Federal Highway Administration) (1983) “Seismic Retrofitting Guidelines for Highway Bridges”, FHWA-RD-83-007, Federal Highway Administration, Washington, DC.
- FHWA (Federal Highway Administration) (1995) “Seismic Retrofitting Manual for Highway Bridges”, FHWA-RD-94-052, Federal Highway Administration, Research and Development, Turner-Fairbank Highway Research Center, McLean, VA.
- FHWA (Federal Highway Administration) (1997). “Geotechnical Engineering Circular No. 3 - Earthquake Engineering for Highways, Design Principles, Volume 1” FHWA-SA-97-076, FHWA, Washington DC, May.
- FHWA (Federal Highway Administration) (1998). “Geotechnical Earthquake Engineering,” FHWA HI-99-012, FHWA, Washington, DC, December.
- FHWA (Federal Highway Administration) (1998a). “Rock Slopes”, FHWAHI-99-007, FHWA, Washington, DC, October.
- FHWA (Federal Highway Administration) (2006), “Seismic Retrofitting Manual for Highway Structures: Part 1-Bridges”, FHWA-HRT-06-032, Federal Highway Administration, Turner-Fairbank Highway Research Center, McLean, VA, January.

- FHWA (Federal Highway Administration) (2011). "Geotechnical Engineering Circular No. 3 – LRFD Seismic Analysis and Design of Transportation Geotechnical Features and Structural Foundations" FHWA-NHI-11-032, FHWA, Washington DC, March.
- Gazetas, G. and Mylonakis, G. (1998) "Seismic Soil-Structure Interaction: New Evidence and Emerging Issues," *Proceedings of an ASCE Specialty Conference on Geotechnical Earthquake Engineering and Soil Dynamics III*, Seattle, August 3-6, ASCE Special Publication No. 75, pp. 1119-1174.
- GeoMotions, LLC (2007). "D-MOD2000 User's Manual."
- Hanks TC, and Kanamori H (1979). "A moment magnitude scale". *Journal of Geophysical Research* 84 (B5): 2348–50
- Haroun, M.A., Pardoen, G.C., Shepherd, R. (1993) "Cyclic Behavior of Bridge Pier Walls for Retrofit", Final Report to the California Department of Transportation, RTA No. 59N974, University of California, Irvine, CA.
- Haroun, M.A., Pardoen, G.C., Shepherd, R., Haggag, H.A., and Kazanjy, R. (1994) "Assessment of Cross-Tie Performance in Bridge Pier Walls", Final Report to the California Department of Transportation, RTA No. 59S986, University of California, Irvine, CA.
- Harp, E.L., and Jibson, R.W., (1995), "Inventory of landslides triggered by the 1994 Northridge, California earthquake" U.S. Geological Survey Open-File Report 95-213, 17 p., 2 plates.
- HAZUS (1997) "Earthquake Loss Estimation Methodology", Technical Manual, National Institute of Building Sciences for Federal Emergency Management Agency, Washington, DC.
- Hodge, P.G. (1981) "Plastic Analysis of Structures", Revised Edition, Robert E. Krieger Publishing Co, Malabar, FL.
- Housner, G.W. (1941) "Calculating the Response of an Oscillator to Arbitrary Ground Motion", *Bulletin of the Seismological Society of America*, Vol. 31, No. 2.
- Housner, G.W. (1956) "Limit Design of Structures to Resist Earthquakes", *Proceedings of World Conference on Earthquake Engineering*, Berkeley, CA.
- Housner, G. (1990) "Competing Against Time", Report to Governor George Deukmejian from Governor's Board of Inquiry on the 1989 Loma Prieta Earthquake, Department of General Services, North Highlands, CA.
- Hynes, M.E. and Franklin, A.G. (1984). "Rationalizing the Seismic Coefficient Method," Miscellaneous Paper GL-84-13, U.S. Army Waterways Experiment Station, Vicksburg, MS, 21 pp.
- Idriss, I.M. (1999). "An Update to the Seed-Idriss Simplified Procedure for Evaluating Liquefaction Potential" in *Proceedings, TRB Workshop on New Approaches to Liquefaction*, Publication No. FHWA-RD-99-165, Federal Highway Administration, January.
- Idriss, I. M., and Boulanger, R. W. (2007), "SPT- and CPT-based relationships for the residual shear strength of liquefied soils." *Earthquake Geotechnical Engineering*, 4th International Conference on

Earthquake Geotechnical Engineering – Invited Lectures, K. D. Pitilakis, ed., Springer, The Netherlands, 1-22

Idriss, I. M., and Boulanger, R. W. (2008) “ Soil liquefaction during earthquakes” Monograph MNO-12, Earthquake Engineering Research Institute, Oakland, CA, 261 pp.

Idriss, I.M. and Sun, J.I. (1992), "User's Manual for SHAKE91," Center for Geotechnical Modeling, Department of Civil and Environmental Engineering, University of California, Davis, California, 13p. (plus Appendices).

Imbsen & Associates, Inc. (2006). Task 6 Report for Updating “Recommended LRFD Guidelines for the Seismic Design of Highway Bridges”, NCHRP 20-07/Task 193, Sacramento, CA.

International Code Council (2000) “International Building Code”, Falls Church, Virginia.

Lindley, P.B. (1978) “ Engineering Design with Natural Rubber”, Malaysia Rubber Producers Research Association, now Tun Abdul Razak Laboratory, Hertford, England, 48pp.

Imbsen & Associates, Inc. (2006). Task 6 Report for Updating “Recommended LRFD Guidelines for the Seismic Design of Highway Bridges”, NCHRP 20-07/Task 193, Sacramento, CA.

Itasca Consulting Group, Inc. (2006). “FLAC – Fast Lagrangian Analysis of Continua, User’s Manual.”

Keaton, J.R., and Currey, D.R., (1989), “Earthquake hazard evaluation of the West Valley fault zone in the Salt Lake City urban area, Utah” Salt Lake City, Dames and Moore, Final Technical Report for U.S. Geological Survey, Contract No. 14-08-001-G1397, 69 p.; published as Utah Geological Survey Contract Report 93-7, 1993.

Keaton, J.R., Currey, D.R., and Olig, S.J., (1987), “Paleoseismicity and earthquake hazards evaluation of the West Valley fault zone, Salt Lake City urban area, Utah” Salt Lake City, Dames and Moore, Final Technical Report for U.S. Geological Survey, Contract No. 14-08-0001-22048, 55 p.; published as Utah Geological Survey Contract Report 93-8, 1993.

Keever, M. (2008) “Impact of Research on Seismic Design”, Seismic Performance of Bridge Systems with Conventional and Innovative Designs, NEES Webinar, National Science Foundation, Washington, DC.

Lam, I.P., and Law, H. (2000) “Soil Structure Interaction of Bridges for Seismic Analysis”, Technical Report MCEER-00-0008, Multidisciplinary Center for Earthquake Engineering Research, University at Buffalo, Buffalo, NY, September 25, 2000

Lee, M.K.W. and Finn, W.D.L. (1978), "DESRA-2, Dynamic Effective Stress Response Analysis of Soil Deposits with Energy Transmitting Boundary Including Assessment of Liquefaction Potential," Soil Mechanics Series No. 36, Department of Civil Engineering, University of British Columbia, Vancouver, Canada, 60 p.

Li, X.S., Wang, Z.L. and Shen, C.K. (1992), "SUMDES - A Nonlinear Procedure for Response Analysis of Horizontally-Layered Sites Subjected to Multi-Directional Earthquake Loading," Department of Civil Engineering, University of California, Davis, California.

- Lilhanand, K. and Tseng, W.S. (1988), "Development and Application of Realistic Earthquake Time Histories Compatible with Multiple-Damping Design Spectra," Proceedings of the 9th Work Conference of Earthquake Engineering, Tokyo-Kyoto, Japan, August 2-9.
- MacRae, G., Priestley, M.J.N., and Tao, J. (1993) "P- $\Delta$  Design in Seismic Regions, Report SSRP-93/05, Structural Systems Research Project, University of California, San Diego, CA.
- Makdisi, F.I. and Seed, H.B. (1978). "Simplified Procedure for Estimating Dam and Embankment Earthquake-Induced Deformation," *Journal of Geotechnical Engineering*, ASCE, Vol. 104, GT7, pp 849-867.
- Mander, J.B., Priestley, M. J. N., and Park, R (1988a), "Theoretical Stress-Strain Model for Confined Concrete", *Journal of Structural Engineering*, ASCE, Vol. 114, No. 8, pp. 1804-1826.
- Mander, J.B., Priestley, M. J. N., and Park, R (1988b), "Observed Stress-Strain Behavior of Confined Concrete", *Journal of Structural Engineering*, ASCE, Vol. 114, No. 8, pp. 1827-1849.
- Mander, J.B., Mahmoodzadegan, B., Bhadra, S. and Chen, S.S. (1996a), "Seismic Evaluation of a 30-Year Old Non-Ductile Highway Bridge Pier and Its Retrofit", Technical Report NCEER-96-0008, National Center for Earthquake Engineering Research, University at Buffalo, Buffalo, NY.
- Mander, J.B., Kim, J.H., and Ligozio, C.A. (1996b), "Seismic Performance of a Model Reinforced Concrete Bridge Pier Before and After Retrofit", Technical Report NCEER-96-0009, National Center for Earthquake Engineering Research, University at Buffalo, Buffalo, NY.
- Mander, J.B., Dutta, A. and Goel, P. (1998) "Capacity Design of Bridge Piers and the Analysis of Overstrength", Technical Report MCEER-98-0003, Multidisciplinary Center for Earthquake Engineering Research, University at Buffalo, Buffalo, NY.
- Marioni, A. (1997), "Development of a New Type of Hysteretic Damper for the Seismic Protection of Bridges," Proc. Fourth World Congress on Joint Sealants and Bearing Systems for Concrete Structures, SP-1-164, Vol. 2, American Concrete Institute, 955-976.
- Marsh, M.L. and Stringer, S.J. (2013) "Performance-Bases Seismic Bridge Design", NCHRP Synthesis 440, National Cooperative Highway Research Program, Transportation Research Board, Washington, D.C.
- Martin, G.R. and Qiu, P. (1994). "Effects of Liquefaction on Vulnerability Assessment," NCEER Highway Project on Seismic Vulnerability of New and Existing Highway Construction, Year One Research Tasks, Technical Research Papers.
- Martin, G.R., and Lam, I.P. (1995), "Seismic Design of Pile Foundations: Structural and Geotechnical Issues," *Proceedings, Third International Conference on Recent Advances in Geotechnical Earthquake Engineering and Soil Dynamics*, St. Louis, Volume 3, pp. 1491-1515.
- Martin, G.R. and Qiu, P., (2000), "Site Liquefaction Evaluation: The Application of Effective Stress Site Response Analyses, Multidisciplinary Center for Earthquake Engineering Research," NCEER Task Number 106-E-3.1 (A), Buffalo.

- Matasovic, N. (1993) "Seismic Response of Composite Horizontally-Layered Soil Deposits," Ph.D. Dissertation, Civil and Environmental Engineering Department, University of California, Los Angeles.
- Matasovic, N., and Hashash, Y. (2012) "Practices and Procedures for Site-Specific Evaluation of Earthquake Ground Motions," National Cooperative Highway Research Program (NCHRP) Synthesis Report 428, Transportation Research Board, Washington, DC, 78 p.
- Matlock, H., Foo, S.H.C., and Bryant, L.M. (1978) "Simulation of Lateral Pile Behavior Under Earthquake Motion," *Proceedings, Earthquake Engineering and Soil Dynamics*, ASCE Specialty Conference, Pasadena, California, pp. 601-619.
- Matlock, H., Martin, G.R., Lam, I.P. and Tsai, C.F. (1981) "Soil-Pile Interaction in Liquefiable Cohesionless Soils During Earthquake Loading," *Proceedings, International Conference on Recent Advances in Geotechnical Earthquake Engineering and Soil Dynamics*, St. Louis, Missouri, Volume 2, April 1981.
- MCEER/ATC (2003) "Recommended LRFD Guidelines for the Seismic Design of Highway Bridges", MCEER/ACT 49, Multidisciplinary Center for Earthquake Engineering/Applied Technology Council Joint Venture, University at Buffalo, Buffalo, NY.
- McLean, D.I. and Buckingham, G.C. (1994) "Seismic Performance of Bridge Columns with Interlocking Spiral Reinforcement", Washington State Transportation Center, WA-RD 357.1.
- Megally, S.H., Silva, P.F., and Seible, F. (2002) "Seismic Response of Sacrificial Shear Keys in Bridge Abutments", Report No. SSRP-2001/23, Structural Systems Research Project, University of California, San Diego, CA.
- Miranda, E., and Bertero, V.V. (1996) "Seismic Performance of an Instrumented Ten-Story Reinforced Concrete Building", *Earthquake Engineering and Structural Dynamics*, Vol. 25, pp 1041-1059.
- Mirza, S.A., and MacGregor, J.G. (1979) "Variability of Mechanical Properties of Reinforcing Bars", *Journal of the Structural Division, ASCE*, 105 (ST5), pp. 921-937.
- Muto, K., et al. (1960) "Non-linear Response Analyzers and Application to Earthquake-Resistant Design", *Proceedings of the Second World Conference on Earthquake Engineering*, Vol. 2, Japan.
- Mylonakis, G., Gazetas, G., Nikolaou, A, and Chauncey, A. (2002) "Development of Analysis and Design Procedures for Spread Footings", Technical Report MCEER-02-0003, Multidisciplinary Center for Earthquake Engineering Research, University at Buffalo, Buffalo, NY.
- Nada, H., Sanders, D., and Saiid, M.S. (2003) "Seismic Performance of RC Bridge Frames with Architectural-Flared Columns," Report No. CCEER 03-01, Department of Civil and Environmental Engineering, University of Nevada Reno, NV.
- NBS (National Bureau of Standards) (1971) "Engineering Aspects of the 1971 San Fernando Earthquake", NBS BSS-40, NBS, US Department of Commerce, Washington, D.C.
- NCHRP (National Cooperative Highway Research Program) (2001). "NCHRP Project 12-49: Comprehensive Specification for the Seismic Design of Bridges," NCHRP Report 472, ATC/MCEER Joint Venture.

- NCHRP (National Cooperative Highway Research Program) (2003). “ NCHRP Project 12-49, Recommended LRFD Guidelines for the Seismic Design of Highway Bridges, Part I, Specifications, Part II, Commentary and Appendices, Submitted by MCEER/ATC, Report MCEER/ATC 49, and Liquefaction Study Report, Report MCEER/ATC 49-1.
- NCHRP (National Cooperative Highway Research Program) (2005) “NCHRP 20-07/Task 193-Task 8 Report for Updating ‘Recommended LRFD Guidelines for the Seismic Design of Highway Bridges”, Imbsen and Associates, Sacramento, CA.
- NCHRP (National Cooperative Highway Research Program) (2008),” NCHRP Project 12-70, Seismic Analysis and Design of Retaining Walls, Buried Structures, Slopes and Embankments, Recommended Specifications, Commentaries and Example Problems, NCHRP Report 611, Transportation Research Board, Washington, DC.
- Novak, M. (1991) “Piles Under Dynamic Loads,” *Proceeding, Second International Conference on Recent Advances on Geotechnical Earthquake Engineering and Soil Dynamics*, Rolla, Missouri, Volume 3, pp. 2433-2456.
- NUREG (2001) “Technical Basis for Revision of Regulatory Guidance on Design Ground Motion: Hazard- and Risk-Consistent Ground Motion Spectra Guidelines (2001)” NUREG report CR-6728, prepared for the Nuclear Regulatory Commission by Risk Engineering, Inc., Boulder, Colorado
- Olsen and Stark (2002) Olson, S. M., and Stark, T. D. \_2002\_. “Liquefied strength ratio from liquefaction flow failure case histories.” *Can. Geotech. J.*, 39, 629–647
- Paulay, T., and Priestley, M.J.N. (1992) “Seismic Design of Reinforced Concrete and Masonry Buildings”, John Wiley & Sons, NY.
- Pecker, A. and Pender, M. (2000) “Earthquake Resistant Design of Foundations: New Construction,” *Proceedings, GeoEng 2000 Conference*, Melbourne, Australia.
- Pender, M.J. (1993) “Aseismic Pile Foundation Design and Analysis,” *Bulletin of the New Zealand National Society for Earthquake Engineering*, Volume 26, Number 1, pp. 49-160.
- Popov, E.P., Bertero, V.V., and Chandramouli, S. (1975) “Hysteretic Behavior of Steel Columns”, UCB/EERC-75-11, Earthquake Engineering Research Center, University of California, Berkeley, CA.
- Port of Long Beach (2009) “Wharf Design Criteria”, Version 2.0, Long Beach, CA.
- Priestley, M.J.N, Sieble, F., and Chai, Y.H. (1992) “Design Guidelines for Assessment Retrofit and Repair of Bridges for Seismic Performance”, Report No. SSRP-92/01, Structural Systems Research Project, University of California, San Diego, CA.
- Priestley, M.J.N., Seible, F., and Calvi, G.M. (1996) “Seismic Design and Retrofit of Bridges”, John Wiley & Sons, NY.
- Pyke, R. M. (2000) “*TESS: A computer program for nonlinear ground response analyses*”, TAGA Engineering Systems and Software, Lafayette, Calif.

- Qiu, P. (1998) "Earthquake-Induced Nonlinear Ground Deformation Analyses," Ph.D. Dissertation, University of Southern California, Los Angeles
- Randall W. Jibson, Edwin L. Harp, and John A. Michael. (1998) "A Method for Producing Digital Probabilistic Seismic Landslide Hazard Maps: An Example from the Los Angeles, California, Area" Open-File Report 98-113, USGS.
- Randall, M.J., Saiidi, M.S., Maragakis, E.M. and Isakovic, T. (1999) "Restrainer Design Procedures for Multi-Span Simply-Supported Bridges", Technical Report MCEER-99-0011, Multidisciplinary Center for Earthquake Engineering Research, University at Buffalo, Buffalo, NY.
- Robinson, R.R., Longinow, A., and Chu, K.H. (1979) "Seismic Retrofit Measures for Highway Bridges", Volumes I and II, Federal Highway Administration, Department of Transportation, Washington, DC.
- Roeder, C.W., Stanton, J.F., and Taylor, A.W. (1987) "Performance of Elastomeric Bearings", Report No. 298, National Cooperative Highway Research Program, Transportation Research Board, Washington, D.C.
- Roeder, C.W., Schneider, S.P. and Carpenter, J.E., (1993) "Seismic behavior of momentresisting steel frames - analytical study", Journal of Structural Division, ASCE. Vol 119, No. 6, New York, pgs 1866-84.
- Roeder, C.W., Stanton, J.F. and Campbell, T.I. (1995) "Rotation of High Load Multirotational Bridge Bearings", Journal of Structural Engineering, ASCE, Vol. 121, No. 4, pp. 746-756.
- Sanchez, A., Seible, F., Priestley, N. (1997) "Seismic Performance of Flared Bridge Columns", Report No. SSRP 97/06, Structural Systems Research Project, University of California, San Diego, CA.
- SCEC (Southern California Earthquake Center) (1999). "Recommended Procedures for Implementation of DMG Special Publication 117 Guidelines for Analyzing and Mitigating Liquefaction Hazards in California", SCEC, March.
- SCEC (Southern California Earthquake Center) (2002), "Recommended Procedures for Implementation of DMG Special Publication 117 Guidelines for Analyzing and Mitigating Landslide Hazards in California," SCEC, February.
- Schneider, S.P., Roeder, C.W., and Carpenter, J.E. (1992) "Seismic Behavior of Moment-Resisting Steel Frames: Experimental Study", ASCE Structural Journal, Volume 119, No. 6, American Society of Civil Engineers, Reston, VA.
- Schwartz, D.P. and Coppersmith, K.J. (1984). "Fault Behavior and Characteristic Earthquake: Examples from the Wasatch and San Andreas Faults", J. Geophysical Research, Vol. 89, pp.5681-5698.
- Seed, H.B. (1987). "Design Problems in Soil Liquefaction", *J. Geotechnical Eng.*, ASCE 113(8), 827-845.
- Seed, H.B. and Idriss, I.M. (1970), "Soil Moduli and Damping Factors for Dynamic Response Analyses," Report No. EERC 70-10, Earthquake Engineering Research Center, University of California, Berkeley, California, 40 p.
- Seed, H.B., and Idriss, I.M. (1971). "Simplified Procedure or Evaluating Soil Liquefaction Potential," *Journal of the Soil Mechanics, and Foundations Division*, American Society of Civil Engineers,

Volume 97, Number SM9, September, pp. 1249-1273.

- Seed, H.B. and Silver, M.L. (1972). "Settlement of dry sands during earthquakes." *J. Soil Mech. Found. Div.*, ASCE, 98(4), 381-397.
- Seed, H.B. and Idriss, I.M. (1982), "*Ground Motions and Soil Liquefaction During Earthquakes*", Monograph Series, Earthquake Engineering Research Institute, 134 pp.
- Seed, R.B. and Harder, L.F. (1990). "SPT-based analysis of Cyclic Pore Pressure Generation and Undrained Residual Strength", in *Proceedings, Seed Memorial Symposium*, J.M. Duncan, ed., BiTech Publishers, Vancouver, British Columbia, pp. 351-76.
- Selna, L.G., and Malvar, L.J. (1987) "Full Scale Testing of Retrofit Devices Used for Reinforced Concrete Bridges," Report No. 87-01, University of California Earthquake Engineering Structural Laboratory, Los Angeles, CA.
- Shimazaki, K. and Sozen, M.A. (1984) "Seismic Drift of Reinforced Concrete Structures", Research Reports, Hazama-Gumi Ltd., Tokyo, (in Japanese) and draft research report (in English).
- Silva, W.J. and Lee, K., (1987). "WES RASCAL code for synthesizing earthquake ground motions". State-of-the-art for assessing earthquake hazards in the U.S. Report 24, Miscellaneous Paper S-73-1. U.S. Army Engineers Waterways Experimental Station. Vicksburg, M.S.
- Silver M.L. and Seed H.B. (1971). "Volume changes in sands due to cyclic loading", *J. Soil Mech. & Foundations Div.*, ASCE, 97(9), 1171-1182.
- Somerville, P.G., N.F. Smith, R.W. Graves, and N.A. Abrahamson (1997). "Modification of Empirical Strong Ground Motion Attenuation Relations to include the Amplitude and Duration Effects of Rupture Directivity", *Seismological Research Letters* 68, 199-222.
- Sugita, H. and Mahin, S.A. (1994) "Manual for Menshin Design of Highway Bridges: Ministry of Construction, Japan", Report No. UCB/FERC-94/10, Earthquake Engineering Research Center, University of California Berkeley.
- Taylor, A.W., Kuo, C., Wellenius, K., and Chung, D. (1997) "A Summary of Cyclic Lateral Load Tests on Rectangular Reinforced Concrete Columns", NISTIR 5984, Building and Fire Research Laboratory, National Institute of Standards and Technology, Gaithersburg, Maryland.
- Thompson, A.C.T., Whittaker, A.S., Fenves, G.L. and Mahin, S.A. (2000) "Property Modification Factors for Elastomeric Seismic Isolation Bearings", Proc. 12<sup>th</sup> World Conference on Earthquake Engineering, New Zealand.
- Tokimatsu, K. and Seed, H.B. (1987). "Evaluation of Settlements in Sands Due to Earthquake Shaking," *Journal of the Geotechnical Engineering Division*, ASCE, Volume 113, Number 8, pp. 861-878.
- Tokimatsu, K. and Asaka, Y. (1998). "Effects of Liquefaction-Induced Ground Displacements on Pile Performance in the 1995 Hyogoken-Nambu Earthquake," *Special Issue of Soils and Foundation*, pp. 163-177.
- Tsopelas, P. and Constantinou, M.C., (1997) "Study of Elastoplastic Bridge Seismic Isolation System", *Journal of Structural Engineering*, ASCE, 123 (4) pp 489-498.

- TRB (Transportation Research Board) (1996), "Landslides: Investigation and Mitigation," A.K. Turner and R.L. Schuster, editors, National Research Council Special Report 247, 673 pp.
- Trochalakis, P., Eberhard, M.O., and Stanton, J.F. (1997) "Design of Seismic Restrainers for In-Span Hinges", *Journal of Structural Engineering*, ASCE, Vol. 123, No. 4, pp. 469-478.
- Veletsos, A.S., and Newmark, N.M. (1960) "Effect of Inelastic Behavior on the Response of Simple Systems to Earthquake Motions", *Proceedings of Second World Conference on Earthquake Engineering*, Vol. 2, Japan.
- Wells, D.L. and Coppersmith, K.J. (1994). "Empirical Relationships Among Magnitude, Rupture Length, Rupture Area, and Surface Displacement," *Bulletin of the Seismological Society of America*, Volume 84, pp. 974-1002.
- Wendichansky, D.A., Chen, S.S. and Mander, J.B. (1998) "Experimental Investigation of the Dynamic Response of Two Bridges Before and After Retrofitting with Elastomeric Bearings", Technical Report NCEER-98-0012, Multidisciplinary Center for Earthquake Engineering Research, University at Buffalo, Buffalo, NY
- Werner, S.D., Taylor, C.E., Moore, J.E., Walton, J.S., and Cho, S. (2000) "A Risk-based Methodology for Assessing the Seismic Performance of Highway Systems", Technical Report MCEER-00-0014, Multidisciplinary Center Earthquake Engineering Research, University at Buffalo, 265 pp.
- Wieczorek, G.F., Wilson, R.C., and Harp, E.L., (1985), "Map showing slope stability during earthquakes in San Mateo County California: U.S. Geological Survey Miscellaneous Investigations Map I-1257-E, scale 1:62,500".
- Wilson, R.C., and Keefer, D.K., (1983), "Dynamic analysis of a slope failure from the 6 August 1979 Coyote Lake, California, earthquake" *Bulletin of the Seismological Society of America*, v. 73, p. 863-877.
- Wilson, R.C., and Keefer, D.K., (1985), "Predicting areal limits of earthquake-induced landsliding, in Ziony, J.I., ed., *Evaluating Earthquake Hazards in the Los Angeles Region-An Earth-Science Perspective*" U.S. Geological Survey Professional Paper 1360, p. 316-345.
- Wipf, T.J., Klaiber, F.W. and Russo, F.M. (1997) "Evaluation of Seismic Retrofit Methods for Reinforced Concrete Bridge Columns", Technical Report NCEER-97-0016, National Center for Earthquake Engineering Research, University at Buffalo, Buffalo, NY.
- Wood, L.A., and Martin, G.M. (1964) "Compressibility of Natural Rubber at Pressures Below 500 kg/cm<sup>2</sup>", *Rubber Chemistry and Technology*, 37, pp 850-85.
- WSDOT (2008). "Bridge Design Manual", M 23-50.03, Bridge and Structures Office, Washington State Department of Transportation. Olympia, WA.
- Yashinsky, M. (1997) "Caltrans' Bridge Restrainer Retrofit Program," *Second U.S.-Japan Workshop on Seismic Retrofit of Bridges*, Report No. UCB/EERC-97/09, University of California Berkeley, CA
- Yashinsky, M and M.J. Karshenas (2003) "Fundamentals of Seismic Protection for Bridges", *Earthquake Engineering Research Institute, Monograph MNO-9*, Oakland, CA.

- Youd, T.L. (1993). "Liquefaction-induced Damage to Bridges," Transportation Research Record No. 14311, National Research Council, *National Academy Press*, Washington, D.C. 35-41.
- Youd, T.L. (1998). *Screening Guide for Rapid Assessment of Liquefaction Hazard at Highway Bridge Sites*, Technical Report MCEER-98-0005, Multidisciplinary Center for Earthquake Engineering Research, University at Buffalo.
- Youd, T.L. and Perkins, D.M. (1978). "Mapping of Liquefaction-Induced Ground Failure Potential," *Journal of the Geotechnical Engineering Division*, American Society of Civil Engineers, Volume 104, Number 4, April, pp. 433-446.
- Youd, T.L. and Idriss, I.M., (1997). *Proceedings of the NCEER Workshop on Evaluation of Liquefaction Resistance of Soils*, Salt Lake City, UT, January 5-6, 1996, Technical Report NCEER-97-0022, National Center for Earthquake Engineering Research, University at Buffalo.
- Youd, T.L., Idriss, I.M., Andrus, R.D., Arango, I., Castro, G., Christian, J.T., Dobry, R., Finn, W.D.L., Harder, L.F. Jr., Hynes, M.E., Ishihara, K., Koester, J.P., Liao, S.S.C., Marcuson, W.F., III, Martin, G.R., Mitchell, J.K., Moriwaki, Y., Power, M.S., Robertson, P.K., Seed, R.B., and Stokoe, K.H., II (2001). "Liquefaction Resistance of Soils: Summary Report from the 1996 NCEER and 1998 NCEER/NSF Workshops on Evaluation of Liquefaction Resistance of Soils," *Journal of Geotechnical Geoenvironmental Engineering*, ASCE, Volume 127, No. 10, p. 817-833.
- Zayas, V.A., and Low, S.S., (1990) "A Simple Pendulum Technique For Achieving Seismic Isolation." *Earthquake Spectra*, Professional Journal of the Earthquake Engineering Research Institute, May 1990.